Binding Patterns in Main-Chain Phosphorus-Containing Polymers

Dissertation

zur Erlangung des Grades

`Doktor rerum naturalium (Dr. rer. nat.)´ im Promotionsfach Chemie

Fachbereich Chemie, Pharmazie und Geowissenschaften (FB 09),

der Johannes Gutenberg-Universität Mainz

Mark Steinmann

geboren in Bremen, Deutschland

Mainz 2016

JOHANNES GUTENBERG UNIVERSITÄT MAINZ

Max-Planck-Institut für Polymerforschung

Max Planck Institute for Polymer Research

Diese Arbeit wurde in der Zeit

Von Oktober 2013 bis September 2016

am Max-Planck-Institut für Polymerforschung und

des Fachbereiches Chemie, Pharmazie und Geowissenschaften

der Johannes Gutenberg-Universität Mainz

unter der Betreuung von

Herrn Priv.-Doz. Dr. Frederik Wurm

und

Frau Prof. Dr. Katharina Landfester

durchgeführt.

Die vorliegende Arbeit wurde im Zeitraum von Oktober 2013 bis September 2016 am Max-Planck-Institut für Polymerforschung in Mainz im Arbeitskreis von Prof. Dr. Katharina Landfester angefertigt unter der Betreuung von Dr. habil. Frederik R. Wurm.

1. Gutachter: Dr. habil. Frederik R. Wurm

2. Gutachter: Prof. Dr. Holger Frey

Tag der mündlichen Prüfung:

Erklärung

Hiermit erkläre ich, dass ich diese Arbeit eigenständig und nur unter Verwendung der angegebenen Hilfsmittel angefertigt habe. Alle Stellen, die im Sinn oder Wortlaut anderen Arbeiten entnommen wurden, sind durch entsprechende Quellenangaben kenntlich gemacht.

meinen Eltern und meinen Großeltern gewidmet

„Vollendet ist das große Werk, der Schöpfer sieht's und freuet sich."

Joseph Haydn: Die Schöpfung (1798)

Acknowledgements

I would like to thank my project leader Dr. Frederik Wurm for admitting me in his group, for the interesting subject of this thesis, his strong support and enabling an attractive and exciting research stay at the Max-Planck Institute of Polymer Research in Mainz.

I would also like to thank Prof. Dr. Katharina Landfester for the welcome in her group and the excellent working conditions.

My special thanks go also to Dr. Frederik Wurm for his encouragement, guidance and support from the initial to the final level of this thesis which enabled me to develop a deep understanding of the subject. I esteem their excellent teaching and supervising skills not only during the lab work but also during many helpful and insightful discussions about my work, future projects and polymer science.

I would like to thank all members of the groups of Prof. Dr. Katharina Landfester for their assistance. Especially, Jens Markwart, who was helping me with the 2nd chapter of this thesis and to evaluate flame retardant properties. Additionally, I would like to thank Filippo Marsico for the great introduction to the field of poly(phosphoester) synthesis and Rose Soskind for the English corrections, which helped improve a lot of my writings.

I especially extend my sincere thanks to the polymer and the NMR analytics group at the Max-Planck Institute for Polymer Research in Mainz for measuring numerous samples using various techniques.

This thesis would not have been possible without the support from my friends, fellow students, my parents and my grandparents, to whom I am indebted to the tremendous support and for their help without which my studies would not have been possible.

Table of Contents

A Abstract

Phosphorus-containing polymers are ubiquitous in nature. All life on earth is based on deoxyribonucleic acid (DNA) and ribonucleic acid (RNA), which are both poly(phosphoester)s (PPEs). However, besides some commercial flame retardants additives, few other consumer products have been realized to date. This is mainly due to the limited availability of polymerization methods during the past decades. Instead modern synthetic techniques enable the controlled synthesis of new phosphorus-containing polymers. This thesis is dedicated to extending the family of phosphorus-containing polymers via novel synthetic techniques in order to introduce well-designed polymers for a far greater scope of applications than just as flame retardants. Particularly, novel PPEs, poly(phosphorodiamidate)s (PPDAs) and poly(phosphorodithiolate)s (PPDTs) were investigated in this work.

Chapter 1 provides an introduction to phosphorus-containing polymers. An overview of phosphorus in nature, traditional and modern synthesis techniques, and important classes of polymers are presented. Furthermore, a selection of important properties and applications are reviewed in the respective chapters. Here, the unique position of phosphorus in nature but also in synthetic chemistry is displayed. The pentavalence of phosphorus makes it to a versatile tool for manufacturing polymers. While two ester groups can build up a polymer backbone, the third pendant group features an easy access to side-chain modifications. The biocompatibility and degradability of phosphorus-containing polymers, as well as the possibility to adjust the properties to individual needs, are presented. Besides several modern synthetic routes to phosphorus-containing polymers, the acyclic diene metathesis (ADMET) polymerization is the main tool of this thesis and is also discussed in detail in **Chapter 1**.

Chapter 3.1 displays the synthesis of poly(alkylidene chlorophosphate)s via olefin metathesis polymerization and the subsequent post-modification. Here, it is shown that the ADMET approach in olefin metathesis has accomplished the task of polymerizing reactive alkylidene chlorophosphates. Two novel monomers are introduced, namely di-(buten-3-yl)

chlorophosphate and di-(undecen-10-yl) chlorophosphate. The molecular weights of the resulting polymers can be manufactured in a controlled manner by ADMET polymerization. The ADMET approach is able to, for the first time, polymerize chlorophosphates as highly electrophilic monomers. Post-modifications with nucleophiles, i.e. alcohols, amines, or water have been successfully conducted. Moreover, it was demonstrated that up to three different functional groups can be introduced to one polymer to result in a multifunctional copolymer which may be of interest for many applications. In addition in **Chapter 3.1.2** different ratios of hydroxyethyl methacrylate (HEMA), 2-methoxyethanol and hydroxyl groups have been introduced as side-chains to optimize the adhesive properties, accordingly.

In **Chapter 3.2**, novel PPDAs were synthesized by ADMET polymerization with two amidate-linkages in the main-chain and either a third pendant hydroxyl (P-OH) or methoxy (P-OCH_3) group. Structurally analogous polymers based on phosphotriesters were prepared for comparison with PPDAs. The unsaturated polymers were hydrogenated to yield saturated counterparts with different properties. The monomers and polymers were studied with respect to hydrolytic degradability. Controlled degradation by adjusting the pH value was observed. It was found that phosphoramidate bonds inside the backbone are easily cleavable at acidic conditions to degrade the polymer completely but in basic environment the bonds are rather stable. Also different enzymes (lipase, phosphodiesterase and alkaline phosphatase) were not able to cleave the P-N bonds under the investigated conditions. In contrast, the P-O linkage is remarkably stable in acidic milieu but the cleavage of the side-chain under basic conditions makes the system selective to different pH values and their enzymatic degradation was reported earlier in the literature.[1-2] In order to verify flame retardant properties, the thermal properties and thermooxidative stability were analyzed. An increased degradation temperatures and enhanced glass transition and/or melting temperatures of PPDAs compared to analogous PPEs were detected. This makes these novel materials to potential flame retardant additives and promising properties for biomedical applications such as for the controlled release of drugs or for tissue engineering scaffolds.

The focus in **Chapter 3.3** lies in introducing the radical thiol-ene polyaddition as a versatile tool to polymerize PDAs and PEs. The radical polyaddition circumvents the use of heavy metals and in addition thioether functionalities are introduced (by thiol groups of the

comonomer) into the backbone of the polymers. PPDAs exhibited continuously higher thermal stability and glass transition temperatures when compared to the PPEs. In addition, the side-chain had a crucial influence on thermal behavior and hydrolytic stability. Glass transition temperatures are increasing by changing the third pendant group from methoxy to hydroxyl functionalities for PPEs and PPDAs. The use of 2-(2-methoxyethoxy)ethanethiol as comonomer resulted in amorphous polymers, due to the flexible ether bonds, without any melting points. The comparison of the all-alkyl backbone of the polymers generated by ADMET polymerization in **Chapter 3.2**, shows that the properties shift from crystalline, with partly high melting points to amorphous materials in case of polymers with the dithiol monomer. The comonomer used in the synthesis not only introduced thioethers, but also allows a further adjustment of the hydrophilicity of the polymers. More precisely, the thioethers were transformed to sulfones by oxidation which increased their glass transition temperature and further leads to an increased hydrophilicity. Hydrolytic stability experiments for such fully water-soluble polymers revealed that the P-N bonds degrade at acidic conditions. More precisely, PPEs with hydroxyl groups are hydrolytically stable in basic environment at least for several months on the contrary to polymers with methoxy side-chain, which degrade rapidly under basic conditions. The PPDAs with pendant hydroxyl group are stabile in basic environment, but the backbone is easily degradable in acidic milieu. In contrast, the PPDAs with methoxy side-chain can be cleaved in basic conditions to release the methoxy group, while the polymer backbone is degradable only in acidic conditions.

In **Chapter 3.3.2** various phosphorus-based monomers from **Chapter 3.2.1** and a second comonomer (1,2-ethanedithiol) beside 2-(2-methoxyethoxy)ethanethiol were linked by thiol-ene polyaddition. By introduction of 1,2-Ethanedithiol as comonomer and phosphorus-based monomers with longer alkyl-chains polymers with partly high melting points are observed.

Chapter 3.4 shows the synthesis of PPDTs, i.e. PPEs carrying two P-S-bonds instead of P-O linkages along the main chain. The introduced procedure to yield ω-diene monomers could not be applied in order to obtain phosphorodithiolates. Instead, a new approach was developed to synthesize polymerizable monomers. In order to observe high yields the thiol were transformed to a thiolate to react with a phosphoric acid chloride. ω-Diene

phosphorodithiolates have been prepared for the first time by this new synthetic approach. It was observed that modern synthetic routes such as ADMET polymerizations have made it possible to change the binding motifs of monomers to P-S linkages, which means to polymerize compounds with sulfur, a well-known catalyst poison.

B Zusammenfassung

Phosphorhaltige Polymere sind einzigartig in der Natur. Das gesamte Leben auf der Erde basiert auf Desoxyribonukleinsäure (DNS) und Ribonukleinsäure (RNS), welche beide zur Klasse der Poly(phosphoester) (PPEs) gehören. Jedoch gibt es heutzutage, mit Ausnahmen von einigen kommerziellen Flammschutzadditiven nur wenige Produkte die in größerem Maßstab hergestellt werden. Der Grund dafür liegt größtenteils in den einschränkten Synthesetechniken, die in den letzten Jahrzehnten verfügbar waren. Dagegen ermöglichen moderne Syntheserouten die gezielte Herstellung neuer phosphorhaltiger Polymere. Daher trägt diese Arbeit dazu bei, die Familie der phosphorhaltigen Polymere mithilfe neuer Synthesetechniken zu vergrößern. Daraus resultieren genau konzipierte Polymere die für weit mehr geeignet sind, als nur als Flammschutzmittel. Insbesondere neuartige PPEs, Poly(phosphordiamidate) (PPDAs) und Poly(phosphordithiolate) (PPDTs) werden in dieser Doktorarbeit untersucht.

Kapitel 1 liefert eine Einführung in phosphorhaltige Polymere. Es wird ein Überblick über Phosphor in der Natur, traditionelle sowie moderne Syntheseverfahren und wichtige Klassen von Polymeren präsentiert. Zudem werden ausgewählte Eigenschaften und Anwendungen in den jeweiligen Kapiteln besprochen. Dabei wird die einzigartige Position von Phosphor in der Natur aber auch in der Synthesechemie hervorgehoben. Die Fünfwertigkeit des Phosphors macht es zu einem vielseitigen Werkzeug zur Herstellung von Polymeren. Während zwei Ester-Gruppen das Polymerrückrat aufbauen, weist die dritte Gruppe am Phosphor einen leichten Zugang zu Seitenkettenmodifikationen auf. Die Biokompatibilität und Abbaubarkeit von phosphorhaltigen Polymeren, aber auch die Möglichkeit der gezielten Justierung von Eigenschaften für individuelle Bedürfnisse werden vorgestellt. Von mehreren modernen Synthesewegen zu phosphorhaltigen Polymeren, ist die acyclische Dien Metathese (ADMET) Polymerisation das wichtigste Werkzeug in dieser Abhandlung und wird in **Kapitel 1** ausführlich besprochen.

Kapitel 3.1 zeigt die Synthese von Poly(alkyliden chlorphosphat)en via Olefinmetathese Polymerisation und der anschließenden Post-Modifikation. Dabei kann gezeigt werden, das die ADMET Polymerisation, eine Olefin Metathese Reaktion, für die Aufgabe der

Polymerisation von reaktiven Chlorphosphaten prädestiniert ist. Mit Di-(buten-3-yl)-chlorphosphat und Di-(undecen-10-yl)-chlorphosphat werden zwei neue Monomere eingeführt. Das Molekulargewicht des resultierenden Polymers kann durch die ADMET Polymerisation genau kontrolliert werden. Die ADMET Technik ist zum ersten Mal in der Lage Chlorophosphate als hoch-elektrophile Monomere zu polymerisieren. Post-Modifikationen mit Nukleophilen, wie z.B. Alkohole, Amine oder Wasser konnten erfolgreich durchgeführt werden. Außerdem wird demonstriert, dass bis zu drei funktionelle Gruppen in ein Polymer eingeführt werden können, um ein multifunktionales Copolymer zu erhalten, das für viele Anwendungen interessant sein könnte. Weiterhin wurden in **Kapitel 3.1.2** verschiedene Verhältnisse an Hydroxyethylmethacrylat (HEMA), Methoxyethanol und Hydroxylgruppen als Seitenketten am Polymer eingeführt, um die Klebstoffeigenschaften zu optimieren.

In **Kapitel 3.2** werden neue PPDAs durch ADMET Polymerisation synthetisiert, wo sich beide Phosphordiamidat Funktionalitäten in der Hauptkette befinden und entweder eine Hydroxyl- (P-OH) oder eine Methoxygruppe (P-OCH_3) als dritte Gruppe am Phosphor vorhanden ist. Strukturanaloge Polyphosphortriester wurden für Vergleichszwecke mit den PPDAs hergestellt. Die ungesättigten Polymere wurden hydriert um gesättigte Gegenstücke mit anderen Eigenschaften zu erhalten. Die Monomere und die Polymere wurden im Hinblick auf ihre hydrolytische Stabilität untersucht. Es kann eine kontrollierte Abbaubarkeit durch die Einstellung des pH-Wertes erreicht werden. Es konnte gezeigt werden, dass Phosphoramid Bindungen in saurem Medium innerhalb der Hauptkette des Polymers leicht zu spalten während sie in basischer Umgebung stabil sind. Auch verschiede Enzyme (Lipase, Phosphodiesterase und alkalische Phosphatase) waren nicht in der Lage die P-N Bindungen unter den untersuchten Bedingungen zu spalten. Im Gegensatz dazu ist die P-O-Bindung bemerkenswert stabil in saurem Milieu aber die Spaltung der Seitenkette unter basischen Bedingungen macht das System selektiv zu verschiedenen pH-Werten. Von deren enzymatischer Abbaubarkeit wurde schon zuvor in der Literatur berichtet. Um Flammschutzeigenschaften zu evaluieren wurden die thermischen und thermooxidativen Eigenschaften analysiert. Eine erhöhte Zersetzungstemperatur und eine höhere Glasübergangstemperatur und/oder Schmelztemperatur von PPDAs im Vergleich zu

strukturanalogen PPEs wurde festgestellt. Diese Eigenschaften machen diese neuartigen Materialien zu potentiellen Flammschutzadditiven und auch interessant für biomedizinische Anwendungen, wie für die kontrollierte Freisetzung von Medikamenten oder für Materialien als Tissue Engineering.

Der Fokus in **Kapitel 3.3** liegt auf der Einführung von radikalischen Thiol-en Polyadditionen als vielseitiges Werkzeug zum Polymerisieren von PDAs und PEs. Die radikalische Polyaddition umgeht die Benutzung von Schwermetallen und darüber hinaus werden Thioether Gruppen (durch das Dithiol Comonomer) in das Polymer Rückgrat eingeführt. PPDAs weisen kontinuierlich höhere thermische Stabilität und Glasübergangstemperaturen auf, wenn sie mit den PPEs verglichen werden. Zusätzlich haben die Seitenketten einen wesentlichen Einfluss auf das thermische Verhalten und die hydrolytische Stabilität. Glasübergangstemperaturen steigen durch das Austauschen von Methoxy zu Hydroxylgruppen als Seitenkette am Phosphor für PPEs und PPDAs. Die Verwendung von 2-(2-Methoxyethoxy)ethanethiol als Comonomer resultiert in amorphen Polymeren ohne Schmelzpunkte durch die flexiblen Etherbindungen. Der Vergleich mit einer reinen Alkylkette als Rückgrat des Polymers, dargestellt durch ADMET Polymerisation in **Kapitel 3.2**, zeigt, dass es von kristallinen Polymeren, mit teils hohen Schmelzpunkten, zu amorphen Materialien übergeht. Das eingesetzte Comonomer führt nicht nur zu Thioethergruppen im Polymerrückgrat, sondern erlaubt auch eine weitere Justierbarkeit der Hydrophilie des Polymers. Genauer betrachtet wurden die Thioethergruppen durch Oxidation in Sulfone umgewandelt, welche eine erhöhte Glasübergangstemperatur und eine gesteigerte Hydrophilie aufweisen. Experimente zur hydrolytischen Stabilität für diese vollständig wasserlöslichen Polymere zeigen, dass die P-N Bindung unter sauren Bedingungen gespalten werden kann. Genauer konnte gezeigt werden, dass der PPE und das PPDA mit Hydroxylgruppe mehrere Monate in basischer Umgebung stabil bleibt. Im Gegensatz zu Polymeren mit Methoxyseitenkette, welche leicht abbaubar sind. Die PPDAs mit Hydroxylseitengruppe sind in basischer Umgebung stabil, aber das Rückgrat ist leicht spaltbar unter sauren Bedingungen. Im Gegensatz dazu, spalten die PPDAs mit Methoxyseitenkette unter basischen Bedingungen Methanol ab und die Hauptkette ist nur in saurem Milieu spaltbar.

In **Kapitel 3.3.2** werden verschiedene Monomere aus **Kapitel 3.2.1** via Thiol-en Polyaddition nicht nur mit einem Copolymer zur Reaktion gebracht, sondern auch mit einem zweiten Copolymer (1,2-Ethandithiol). Durch die Einführung von 1,2-Ethandithiol als Comonomer und phosphorhaltigen Monomeren mit längerer Alkylkette treten zum Teil Polymere mit hohen Schmelzpunkten auf.

Kapitel 3.4 zeigt die Synthese von Poly(phosphordithiolat)en (PPDTs), d.h. PPEs welche P-S-Bindungen innerhalb der Hauptkette tragen. Das eingeführte Protokoll von ω-Dien-Monomeren kann nicht eingesetzt werden zur Phosphordithiolat Synthese. Stattdessen ist eine neue Methode entwickelt worden, um die polymerisierbare Monomere darzustellen. Die Reaktion wird ermöglicht, durch die eingesetzten Thiolate statt der bisher verwendenten Thiole, damit diese dann mit Phosphorsäurechloriden reagieren können. ω-Dien Phosphordithiolate werden zum ersten Mal durch diese neue Synthesemethode synthetisiert. Es kann gezeigt werden, dass moderne Synthesewege, wie ADMET Polymerisationen, es möglich gemacht haben, den Wechsel zum P-S Bindungsmotiv zu ermöglichen. D.h. Verbindungen zu polymerisieren die Schwefel beinhalten, welches ein bekanntes Katalysatorgift ist.

1 Introduction

The chemical element phosphorus is the 15th element in the periodic table of elements. It can be found in the third period between silicon (element 14) and sulfur (element 16). Phosphorus is nestled in the group of pnictogens, beneath nitrogen (element 7) and above arsenic (element 33). Phosphorus occurs in two major forms: white and red. However, these elemental forms of phosphorus have never been found in nature. This is due to the fact that free elemental phosphorus is highly reactive in the presence of many other elements. The most stable phosphorus-based compounds are produced by reaction with its neighbors in the periodic table, especially oxygen. This is why nature chooses phosphoesters as the preferred form of phosphorus. The reason for the strong affinity to oxygen can be found in the strength of the P-P bond compared to the C-C bond. These linkages have to be broken before an oxide can form. The enthalpy for the formation of phosphorous oxides is ca. 540 kJ · mol^{-1}. But it is less than 400 kJ · mol^{-1} for the formation of carbon dioxide from graphite. That is the reason why phosphorus occurs in nature usually linked to oxygen. Phosphorus can also connect to other elements such as nitrogen or sulfur by amidate or thioester linkages. In nature they are some examples of phosphoramidates as Phosphocreatine[3] or Histidine kinase.[4] However, as mentioned above, phosphorus is able to bind to a variety of elements in the periodic table. This chapter reviews phosphorus-containing polymers with P(V) in the polymer backbone.

1.1 Phosphorus in Nature

Phosphorus is essential for life. It occurs as a building block in deoxyribonucleic acid (DNA) and ribonucleic acid (RNA), adenosine triphosphate (ATP) and nicotinamide adenine dinucleotide (NAD) to store chemical energy, and in phospholipids to form cell membranes. In nature, phosphorus plays an important role in minerals found in the Earth's crust or in living organisms. Phosphorus almost always occurs in the form of phosphate (PO_4^{3-}) or pyrophosphate (anhydrides of phosphates). In addition inorganic phosphates in living organism are for example responsible for regulating inflammation, regenerating bone, and coagulating blood. Besides phosphates, phosphonates are found in nature as well. They are

not as important as phosphates, yet they can be found in various living organism.[5] Evidently up to 30 % of phosphorus in the sea is from phosphonic acid derivatives.[6]

In nature, phosphorus occurs in the form of phosphate esters. In a seminal article from 1987, Westheimer provided a background on phosphoesters in nature and compared them to commonly synthesized polymers of carbon based esters and amides. Its use of a third pendant group and its importance as a leaving group in reactions within living organisms makes organophosphates essential to the biology of life. The ability of the P-O-C bond to be highly robust under physiological conditions yet readily cleavable under other types of conditions makes organophosphates a valuable tool in biochemistry, but also interesting in the design of novel synthetic reagents or polymers.

DNA/RNA. DNA and RNA are the carriers of genetic information.[7] All known living organisms need DNA and RNA for instructions on growth, development, functioning, and reproduction of cells. The structures, illustrated in **Figure** 1, consist of two nucleosides connected by a phosphate unit to form a poly(phosphodiester). This alternating carbohydrate-phosphate backbone is stabilized by the negative charge at the third oxygen atom linked to the phosphate.

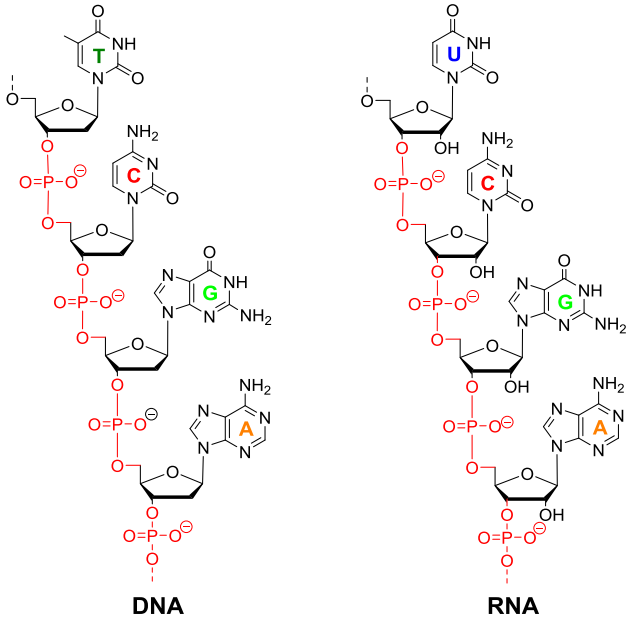

Figure 1: Chemical structures of DNA and RNA with red highlighted phosphate groups and labeled nucleobases (C = cytosine, A = adenine, G = guanine, T = thymine (in DNA), U = uracil (in RNA)).

ATP. Another phosphorus bearing compound in nature is ATP, which is responsible for a large part of energy transfer in living cells,[8] and is used as a coenzyme. ATP consists of adenine linked to a ribose sugar which is connected to a phosphoester anhydride (pyrophosphate) of three phosphate units (**Figure 2**). These phosphoester anhydride structures, a less stable form of phosphate, are easily cleavable to transfer energy. This mechanism is reversible to restore energy by binding energy between phosphate units. Here, energy-rich storage units are necessary and can be found in the form of pyrophosphates.

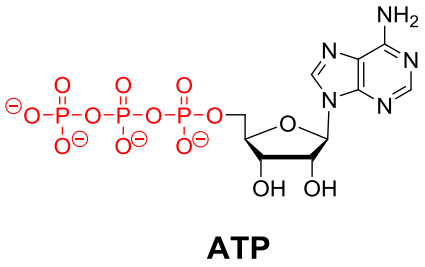

Figure 2: Chemical structure of adenosine triphosphate (ATP) with red highlighted pyrophosphate groups.

NAD. The second energy transfer agent in living organisms is NAD, which is also based on a pyrophosphate consisting of two phosphate units. One of the phosphates is linked to adenine, and the other phosphate unit is connected to nicotinamide (**Figure 3**). In contrast to ATP, NAD can be oxidized to NADH and reduced again to transfer energy. Here, an electron transfer process is the mechanism of action.

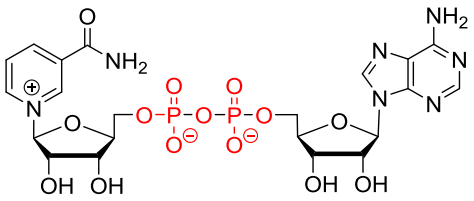

NAD$^+$

Figure 3: Chemical structure of nicotinamide adenine dinucleotide (NAD) with the red highlighted phosphate groups.

Phospholipids. Another essential phosphate-based biomaterial is the phospholipid.[9] Phospholipids are amphiphilic molecules because of a hydrophobic tail and a hydrophilic head. Generally, two hydrophobic fatty acids (tail) and a hydrophilic phosphate unit (head) are connected by a glycerol molecule (**Figure 4**). The hydrophilic character is generated by a negatively-charged phosphate unit. Phospholipids are the major components of cell membranes that separate the content of cells from the outside environment. Without these cell membranes, cell interiors would not be arranged properly and would thus be unable to ensure optimal functionality of biochemical systems. Cell membranes are composed of the phospholipid bilayer. Two layers of phospholipids (tail-to-tail) form a bilayer (**Figure 4**). Hence, this forms a barrier to water-soluble molecules which, for the most part, is impermeable to ions. They are robust because of the stable negatively charged phosphate unit within the molecule. The stability of this ionic structure has already been shown in the previously-introduced polymers and molecules from nature. This advantage, as well as the fascinating structure of phospholipids, are used in this work to manufacture amphiphilic polymers with a phosphate linker between alkyl chains in order to observe unique properties useful for various applications similar to those of the phospholipids.

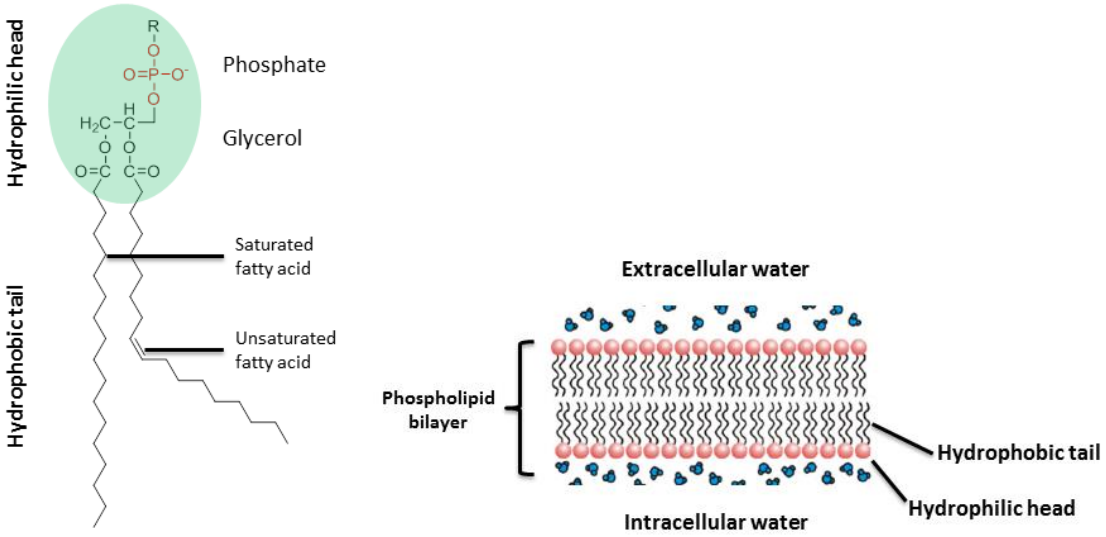

Figure 4: Left: Chemical structure of a phospholipid with the red highlighted phosphate group. Right: Phospholipid bilayer. Reproduced from Ref.[10] with permission from Elsevier.

The last subsection of this chapter is dedicated to artificially-produced phosphate-containing materials, which are commonly used for improving growth in agriculture, and even against nature and living organisms. Phosphate-containing fertilizers are by far the highest-selling commercial products with phosphorus. Organophosphorus compounds are another important class of phosphorus-containing products. They can be found in detergents and pesticides, but also in nerve agents such as sarin or venomous agent X (VX) (**Figure 5**).

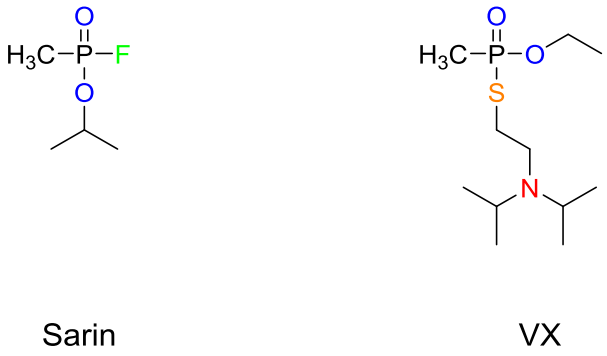

Sarin VX

Figure 5: Left: Chemical structure of sarin; Right: Chemical structure of VX.

Overall, the phosphate group is perfectly suitable for many applications in nature and serves as one of the most versatile elements.

1.2 Synthetic Approaches to Main-Chain Phosphorus-Containing Polymers

Phosphorus-containing polymers are interesting for flame retardancy, biomedical applications and in regards to biocompatibility as well as (bio)degradability. Several approaches have been realized to introduce phosphorus into polymeric materials. The majority of publications use side-chain modification of polymers to realize flame retardant and dental applications, protein absorption resistance as well as bioconjugation etc.[11]

In contrast, PPEs with the phosphorus atoms along the polymer backbone were studied with much less focus. The variation of the binding pattern or the oxidation number of the phosphorus in the backbone would be ideal handles for synthetic materials.

In contrast to nature, where the phosphate is the most stable derivative of phosphorus, synthetic chemistry allows the formation of many more phosphorus -derivatives to build up polymers with various properties. Today, only phosphate-based flame retardant plastics or additives are produced on an industrial scale, while all other possibilities remained rather unexplored so far. The change of the binding motif around the central phosphorus in the polymer backbone is a straightforward handle to materials properties, such as thermal properties, which are interesting for flame retardant potential, but also hydrophilicity or degradation profiles.

The importance of phospholipids in nature is due to the amphiphilic character. The polymers introduced in this chapter exhibit usually a long hydrophobic part and a hydrophilic phosphorus-containing group just like phospholipids and are important for many applications. The stability of P-O bonds as well as the flame retardant properties of P-N linkages and the option to use three binding sites as desired contribute to this variety of applications. **Figure 6** provides all binding motifs of phosphorus-(V)-containing polymers with either oxygen and/or nitrogen connected to phosphorus. These binding motifs are addressed in this chapter.

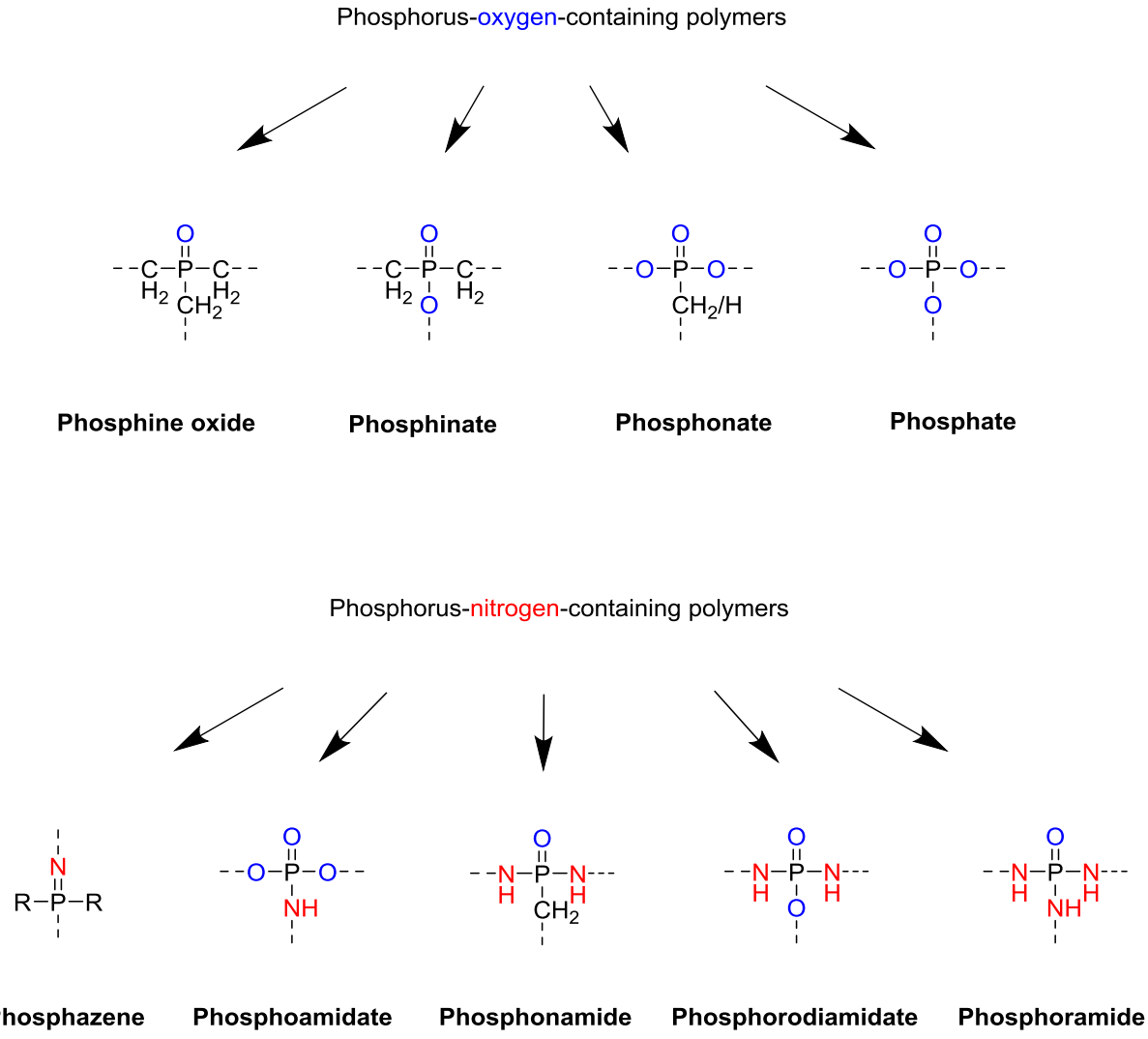

Figure 6: Subclasses of phosphorus-containing polymers.

Nature uses only PPEs as binding motifs, while in contrast, modern research uses a pool of different elements connected to phosphorus (see **Figure 6**) to allow adjustment of properties of synthesized compounds. A short introduction about sulfur-phosphorus binding motifs is given in this introduction as well. The next chapters of this thesis provide an overview of suitable reactions to obtain phosphorus-containing polymers and classes of phosphorus-based polymers with different binding motifs and their properties and potential applications. By changing the binding motif, the mechanical and chemical properties of the polymer backbone and side-chains can be tailored as desired to obtain features such as changing from amorphous to crystalline, from water soluble to insoluble, and from elastic to stiff materials.

1.2.1 Polycondensation

Polycondensation is the technical approach for phosphorus-containing polymers. The first report on PPEs by Arvin presented the treatment of bisphenol-A with phosphorus oxychloride.[12] Generally, phosphonic dihalides and diols are the reagents of typical polycondensation reactions (**Scheme 1**).

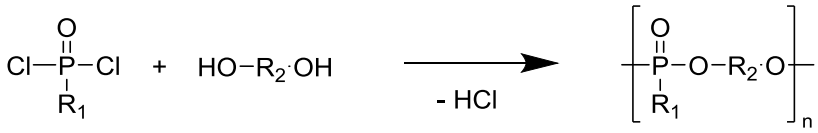

R_1 = H, O-alkyl, O-aryl, NH_2, etc.

R_2 = alkyl, aryl, etc.

Scheme 1: General polycondensation of phosphorus dichloride with diols.

As polycondensations are step-growth polymerizations, the side-products have to be removed, to generate high molecular weight polymers. Due to problems in shifting of this equilibrium or other side-reactions with such high reactive compounds, often low molecular weights polymers are obtained.[13] Furthermore, the introduction of functional groups is difficult to realize due to harsh reaction conditions such as high reaction temperatures, vacuum environment, and formation of acidic side products. However, polycondensations are one of the most commonly used methods to produce phosphorus-based materials due to the ready availability of the reagents, typically low costs, which allow some modularity of the polymer backbone.

Research by Cass and coworkers revealed that phosphorus-based polymers exhibit flame retardant properties.[14] However, until recently halogenated carbon based materials have dominated flame retardant materials. The reason for this can be found in high costs. Nowadays, phosphorus-containing polymers are considered safer compared to halogenated materials when it comes to fire safety. This has been evaluated by REACH[15] (registration, evaluation, authorization and restriction of chemicals) and the EU-funded collaborative research project ENFIRO.[16]

Polycondensations can be carried out by traditional melt and solution polymerizations, under Lewis acid catalysis, aqueous interfacial[17], or phase transfer catalyzed polycondensation.[18] The latter can build up polymers with high molecular weights (above 40,000 g · mol^{-1}). Phase transfer catalyzed polycondensation is carried out under relatively mild conditions. Even structures like phenolphthalein or ferrocene groups can be introduced.[19]

1.2.2 Ring-opening polymerization (ROP)

Ring-opening polymerization (ROP) is a chain-growth polymerization technique and probably one of the most versatile polymerization methods in general. Usually, well-defined polymers have been synthesized with low molecular weight distribution and controlled microstructure. However, due to a complex monomer synthesis, the consequence is that ROP is thus far only of interest in academic research. Nevertheless, polymers that are both water-soluble[20] or hydrophobic[21] are accessible by changing the pendant group on the cyclic phosphorus-containing monomer (**Scheme 2**).

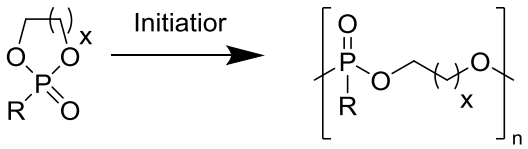

R = alkyl, aryl, Oalkyl, Oaryl, etc.

x = 1, 2

Scheme 2: Ring-opening polymerization of cyclic phosphoesters.

ROP is accessible by anionic, cationic, or metal-catalyzed insertion mechanisms, but anionic is the most used mechanism. The anionic ROP can also follow characteristics of a “living” polymerization.[22] As a result, the reaction will take place as long as monomer is available and the reaction will carry out in a very controlled manner. Features include low molecular weight distributions and high molecular weights (above 30,000 g · mol^{-1}), and the adjusting of molecular weights as desired by varying the ratio between initiator and monomer concentration.[23] As a consequence, linear[24], branched[25] and hyperbranched[26], grafted[27], or cross-linked[28] polymers are attainable.

Strained cyclic phosphoesters are perfectly suitable to polymerize via ROP. Here, tri- and pentavalent phosphorus can be used. Polymers derived from trivalent phosphorus-containing monomers have been investigated by Kobayashi et al.[29-31] In the case of trivalent phosphorus monomers, only cationic ROP is possible. This approach is limited mostly to low molecular weights. Five and six membered ring systems are widely used as monomers for ROP. Lucas et al. introduced the synthesis of cyclic alkylene phosphites by condensation of suitable diols and phosphorus trichloride,[32] which were transformed by oxidation to the respective cyclic phosphoester, also known as phospholane oxide. This method allows for the last chlorine atom at the phosphorus to be exchanged by various functional groups. The introduced group is the third pendant group (**Scheme 3**).

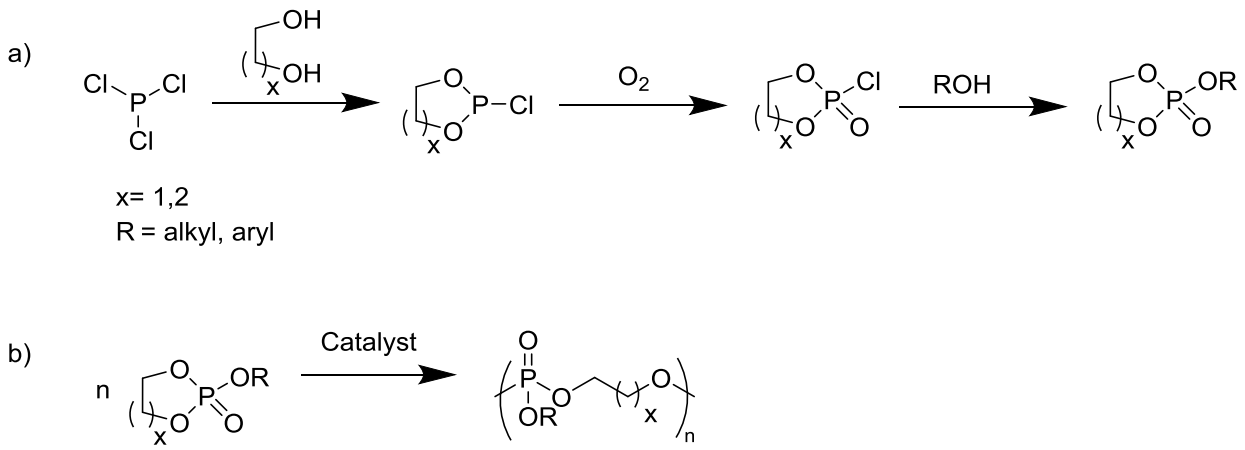

Scheme 3: a) Most cited synthetic approach to cyclic phosphoester monomers, b) ROP of PPEs.

Nowadays, ROP with six-membered cyclic phosphoesters is rather seldomly used. The efficacy when compared to five-membered ring counterparts is much lower due to smaller ring-strain. Polymerizations of five-membered rings have been realized by cationic ROP, but mostly only low molecular weights are obtained and side-reactions occur in the process.[33] However, after the discovery of efficient polymerization strategies for anionic ROP, very high molecular weights can be reached.[20] Here, the important step that was needed was to find appropriate nucleophiles to support the reaction. First catalysts to reach high molecular weights are n-butyllithium or certain Grignard reagents. Under the right conditions, five-membered ring systems have been carried out as living polymerizations as a consequence of

ring-strain. Nevertheless many functional groups have to be protected. Otherwise, the reactive chain-end might react with the introduced moiety. Besides deprotonation of the monomer through strong bases and unintended side-reactions, the bases and initiators often contain metals which make it difficult to apply these materials to biocompatible applications.

ROP by use of insertion polymerization is mostly catalyzed by metal carboxylates. Some work has done by Xiao et al. to investigate the mechanism of reactions with tin(II) 2-etyhlhexanoate ($Sn(Oct)_2$) as a catalyst for phosholanes.[34] However, one of the problems in polymer chemistry is the need for metal catalysts which are usually toxic to living organisms. Hence, new catalyst systems have been investigated. Strong organobases such as 4-dimethylaminopyridine (DMAP) were introduced[35] and the first satisfying results have been realized with so-called "superbases". Important representatives are the amidine 1,8-diazabicyclo[5.4.0]undec-7-ene (DBU) and guanidines such as 1,5,7-triazabicyclo[4.4.0]dec-5-ene (TBD).[36] Here, molecular weight distributions of < Mw/Mn < 1.10 and molecular weights of up to 100,000 g mol^{-1} are achievable.

1.2.3 Polytransesterification

Transesterification is used in many fields of organic chemistry. Even for industrial applications, this is an adequate method to manufacture esters. Several advantages can be applied. Transesterification simply means the exchange of alkoxy groups between different esters (**Scheme 4**).

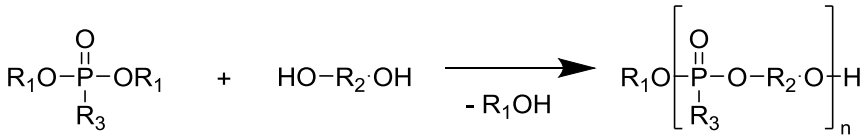

R_1, R_2 = $(CH_2)_n$, 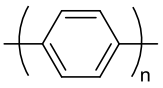 , etc.

R_3 = Alkyl, Aryl, H, etc.

Scheme 4: General polytransesterfication of PPEs.

In the case of polymers as products, the reaction is called polytransesterification. This approach has also found its way into the industrial process. Poly(phosphite)s and poly(phosphonate)s are synthesized by this approach. Poly(phosphate)s are difficult to obtain by polytransesterification because of three pendant groups on the phosphorus atom. There is always unwanted branching. However, poly(phosphite)s can be altered to phosphates by post polymerization reactions.[37] Limited molecular weights are observed by postesterifications due to several side reactions that might occur such as intramolecular formation of cyclic adducts or dealkylation of the PE.[38]

1.2.4 Olefin metathesis polymerization

Olefin metathesis polymerization was used to obtain phosphorus-containing polymers with high molecular weights. Well-defined catalysts introduced by Grubbs make it possible to obtain highly functional polymers due to the high functional group tolerance given by metal carbenes (mostly Grubbs catalysts). Olefin metathesis polymerization can be applied in either step-growth or chain-growth polymerizations. Metathesis polymerizations with a step-growth mechanism are called acyclic diene metathesis (ADMET) polymerizations and feature advantages as inexpensive and readily available monomers. Ring-opening metathesis polymerization (ROMP) represents the chain-growing equivalent of metathesis reactions. It distinguishes itself by the ability to easily introduce different functional end groups and to form block copolymers by other approaches. Both ADMET and ROMP, can be used to manufacture in a controlled manner a broad range of polymers with tailored properties.

1.2.5.1 Ring-opening metathesis polymerization

For ROMP, cyclic unsaturated monomers are needed. Esterification of phosphoric or phosphonic acid with appropriate unsaturated diols leads either to a 7-membered phosphate or a phosphonate monomer (**Scheme 5**).[39] The driving force of this polymerization is the release of ring-strain. The 7-membered ring is the smallest system possible and the only one investigated so far. Due to a low ring-strain for a 7-membered ring, the homopolymerization ROMP polymers show rather low molecular weights even at longer reaction times.[40-41] However, high molecular weights are accessible by ROMP copolymerization with e.g. cyclooctene (**Scheme 5**).

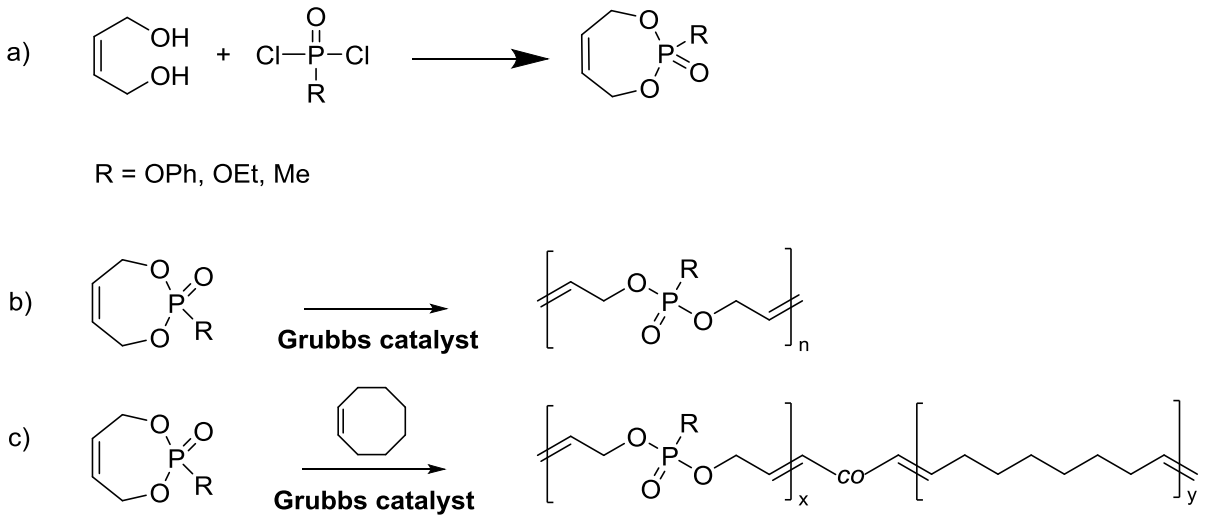

Scheme 5: a) Monomer synthesis of 7-membered unsaturated cyclic phosphates or phosphonates; b) Homopolymerization of different ROMP monomers; c) Copolymerization of different ROMP monomers. Reproduced from Ref.[22] with permission from John Wiley and Sons.

1.2.5.1 Acyclic diene metathesis polymerization

In contrast to ROMP, ADMET (and acyclic triene metathesis (ATMET)) polymerizations are step-growth reactions. However, the same type of catalyst is used. Suitable monomers need to have two (or three) terminal double bonds and can be synthesized by esterification of phosphoric acid or phosphonic acid (or derivatives which are preferably chlorides) and ω-unsaturated alcohols, amines, thiols. Different lengths of the spacer between double bonds and phosphorus, as well as di- or trifunctional monomers, can be adjusted (**Scheme 6**). The spacer has to be at least two carbon atoms long. Otherwise reasonable polymer length cannot be observed due to the "negative neighboring effect".[42]

The driving force of this reaction is the release of ethylene as a volatile side-product. By removing ethylene at reduced pressure, the equilibrium can be shifted to the product side very effectively even at moderate temperatures (**Scheme 6**).

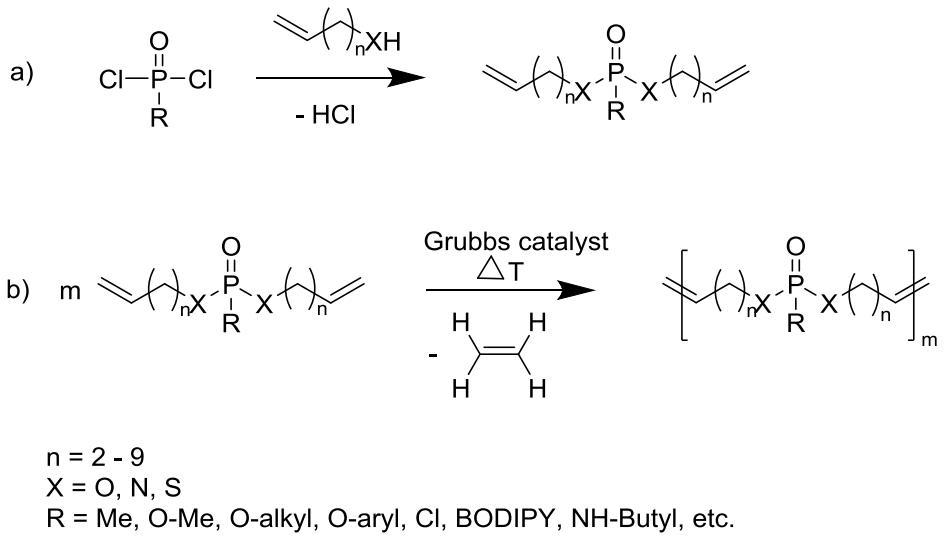

Scheme 6: a) General synthesis for ADMET of PPE monomers; b) ADMET polymerization of difunctional monomers.

ATMET polymerizations with trifunctional monomers provide perfect conditions for preparing hyperbranched systems which are already applied for scavenging singlet oxygen to protect the triplet-triplet annihilation photon upconversion process.[43] Recent research is investigating flame retardant properties of these structures as additives of other polymers.[44]

1.2.6 Polyaddition

Another step-growth reaction is the polyaddition reaction. However, there are significant differences when compared to the polycondensation reaction. Precisely, the removal of side products is not essential to influence the equilibrium of the reaction. Typical reactions to obtain phosphorus-containing polymers are reactions of phosphoric and phosphonic acid dichlorides with bis(epoxides)s[45] or bisoxetanes[46].

1.2.6.1 Thiol-ene polyaddition

A thiol-ene polyaddition is a radical step-growth reaction. It has been known for more than 100 years, and can be described as the hydrothiolation of a double bond (**Scheme 7**).[47] Some consider it as a "click" reaction because it is a highly efficient reaction which tolerates a lot of functional groups. Furthermore, thiol-ene polyaddition is simple to execute under mild conditions with no other side products. The yields are usually high and the reaction time is relatively short, but the disadvantage of oxidation-prone thiols as reagents has to be

considered.[48] Moreover, no metal-based catalyst is needed. This is a great advantage in order to avoid metals which are toxic to living organisms. Potential applications in medicine or biomedical applications can be explored. In order to investigate thiol-ene polyaddition, various research has been conducted.[49-50] In this way polymers for different applications such as new materials for optical components, adhesives, or high-impact energy absorbing materials has been manufactured.[48]

Phosphorus-containing polymers made by thiol-ene polyadditions will be introduced in this thesis. The thiol-ene approach to obtain linear polymers is new for phosphorus based polymers. It was only used to crosslink macromonomers to a network so far.[51] Applicable monomers are phosphorus based dienes (the same monomers as for ADMET polymerizations) and a dithiol as comonomer. Two different comonomers have been used, namely 1,2-Ethanedithiol and 2-(2-methoxyethoxy)ethanethiol. Because of the radical mechanism, a remarkable functional group tolerance and a wide range of dithiols are possible (**Scheme 7**). Hereby this thesis is introducing high-molecular weight polymers with adjustable properties such as hydrophilicity or thermal properties.

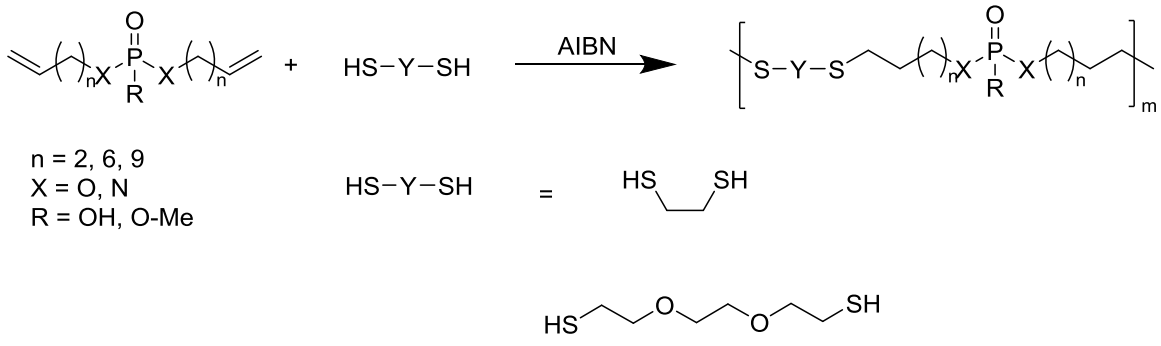

Scheme 7: Thiol-ene polyaddition of phosphorus-containing diene monomers with dithiol comonomers.

1.3 Main-Chain Phosphorus-Containing Polymers

Different kinds of phosphorus-based polymers will be presented in order to outline already synthesized polymers and their properties. This introduction will beginning with oxygen-phosphorus polymers which are the closest class to phosphorus-containing polymers in nature, then continue with nitrogen-phosphorus polymers, and close with sulfur-phosphorus polymers where the monomers are often used against nature as pesticides. By solely changing the binding motif, high variability of phosphorus-based materials can be observed.

1.3.1 Phosphorus-oxygen-containing polymers

The oxygen-phosphorus polymers are subdivided by the number of oxygen atoms around the phosphorus. Because of the pentavalence of phosphorus always a P=O bond is present. There are other elements which can connect to phosphorus via double bond but this will not be subject of this thesis. Possibilities ranging from one P=O bond to the phosphorus (**phosphine oxide**), to one ester bond besides the P=O bond, (**phosphinate**), to two ester bonds (**poly(phosphite)s, poly(phosphonate)s, poly(chlorophosphoester)s**), and finally to three ester bonds on the phosphorus in **poly(phosphate)s**.

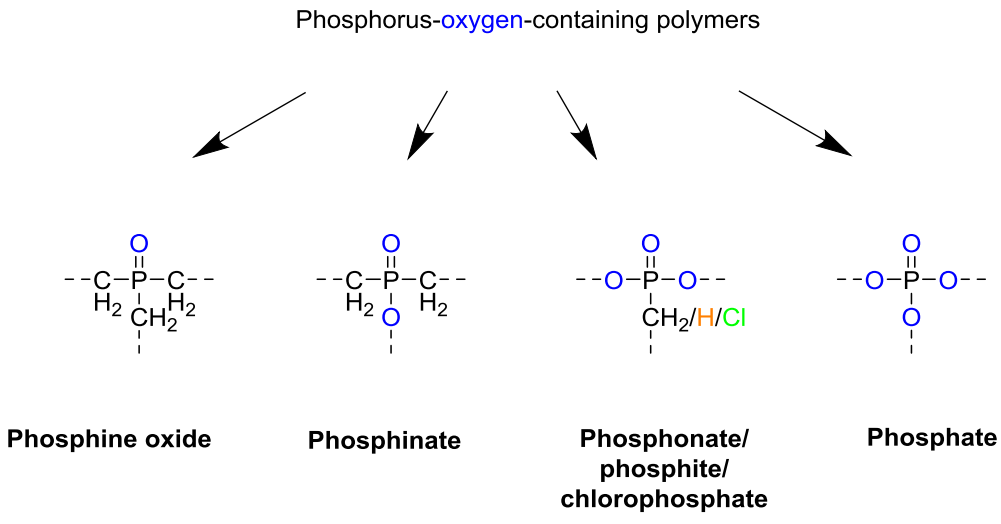

Figure 7: Subclasses of phosphorus-oxygen-containing polymers.

1.3.1.1 Polymers with a single P=O bond

Phosphine oxide-containing polymers. Though different classes of polymers will be introduced, all of them exhibit the same phosphine oxide group. Here, one oxygen atom is linked to the phosphorus atom via double bond. Phosphine oxides in a ring generally exhibit better flame retardant properties than linear counterparts.[52] Many of these linear and ring phosphine oxide-containing polymers can be found in literature.[53-56]

A typical field of application of phosphorus-containing polymers are flame retardant additives. In general, the flame retardant properties exhibit a strong dependency on the amount of phosphorus within the polymer, the position of phosphorus inside the structure, and the architecture of the polymer itself. It can be summarized that cyclic architectures present higher thermooxidative stability and enhanced flame retardancy. Therefore, they are used as additives in plastics or coatings to lower the flammability of commonly plastics which usually display high flammability.

The chosen ring system is called phenoxaphosphine and has a binding motif which consists of oxygen linked by a double bond to phosphorus and three P-C bonds. Examples for polyamides containing phenoxaphosphine are given by the reaction of 2,8-(chloroformyl)-10-phenoxaphosphine-10-oxide and aromatic diamines in dimethylacetamide (DMA) by polycondensation (**Chapter 1.2.1**) in solution with triethylamine to remove the formed acid (**Scheme 8**).[57] The cyclodehydration of polyhydrazides yields Poly(1,3,4-oxadiazole)s. These polymers demonstrate stability at up to 400 °C and are self-extinguishing.[58]

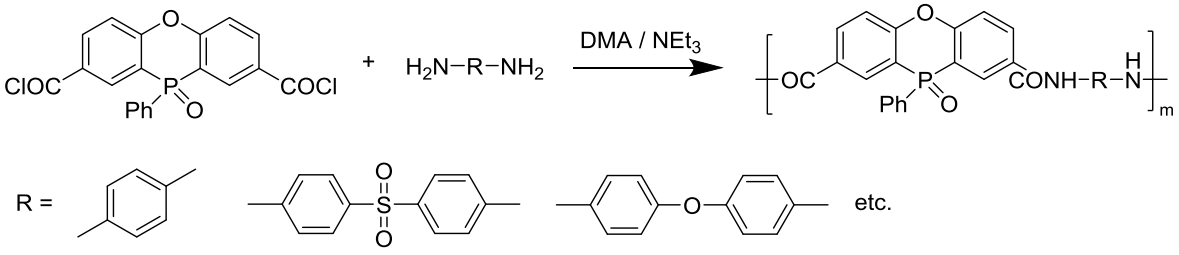

Scheme 8: Polycondensation of 2,8-(chloroformyl)-10-phenoxaphosphine-10-oxide and aromatic diamines.

In similar reactions, other polymers containing phenoxaphosphine or phenothiophoshine have been synthesized and studied in regards to flame-resistance behavior. They all show analogous properties as mentioned above.[52] However, these polymers have not been previously studied with regards to other features.

1.3.1.2 Polymers with a single P-O and P=O bond

Phosphinate-containing polymers. 9,10-Dihydro-9-oxa-10-phosphaphenanthrene 10-oxide (DOPO) is a well-known molecule because of its good flame retardant properties. Interestingly, DOPO cannot be polymerized in the main-chain. It is usually mixed to polymers such as epoxy resin to improve the flame retardancy. However it can be directly connected to the backbone of e.g. polyesters (**Figure 6**).[59-60] These DOPO-modified polymers provide improved flame retardant behavior such as higher thermal stability when compared to the blank ester or epoxy resin. Besides flame retardant behavior, no consideration to other possible properties has been shown thus far.

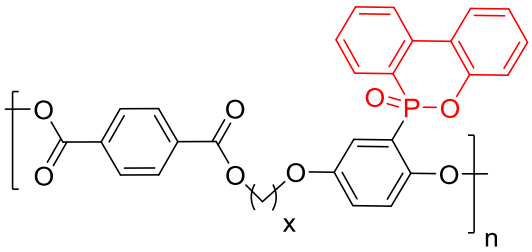

Figure 8: Common example of DOPO-containing polyester. The DOPO group is highlighted in red.

1.3.1.3 Polymers with two P-O and one P=O bond

Poly(phosphite)s (poly(H-phosphonate)s). Poly(phosphite)s already exhibit two ester groups around the phosphorus and a hydrogen atom directly linked to phosphorus. These polymers are a good example of reactive polymers. This can be used as an advantage in order to exchange the hydrogen with a variety of elements or functional groups. Nitrogen and oxygen can easily replace the hydrogen and provide stability against moisture.[37, 61] These reactive polymers have proved challenging but also highly interesting and important to polymer chemists for a long time.[62] Reactive polymers show high potential for new materials and for

medicine. The idea is to link drugs or biopharmaceuticals under mild conditions to these reactive structures. Different techniques can be used to synthesis high molecular-weight reactive polymers. Surprisingly, reactive P-H bonds in poly(phosphite)s are inert and obtainable with high molecular weights by postesterification (**Chapter 1.2.3**) of phosphonic acid esters with diols[37] and by introducing five- as well as six-membered cyclic phosphorus-containing monomers (as 5-2-hydro-2-oxo-1,2,3-dioxaphosphorinane to cationic (Arbuzov-type reaction)[30, 52] and anionic ROP (**Chapter 1.2.2**).[52, 63-64] The advantage of reactive polymers can be used for postmodification reactions to gain a broad variety of functional materials. Modifications towards phosphate derivatives can be accomplished by chlorination or oxidation (**Scheme 9**).[37]

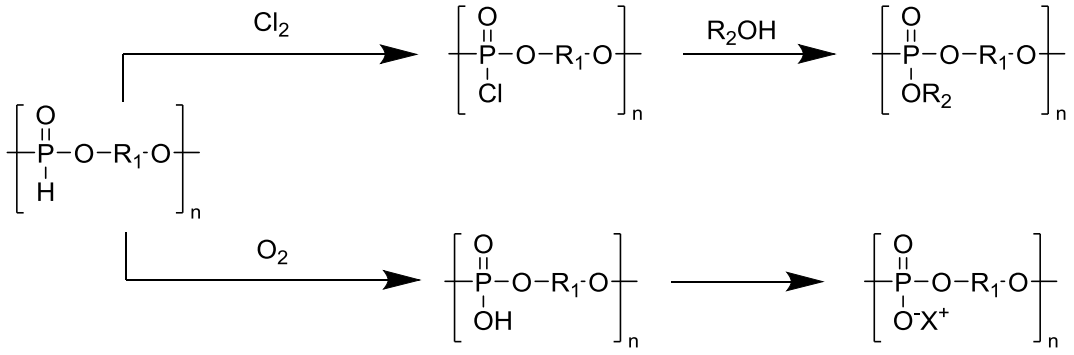

R_1 = $(-CH_2-)_5$, $(-CH_2-)_8$, etc.

R_2 = Alkyl, etc.

X^+ = Na, NR_4,NHR_3, etc.

Scheme 9: Oxidation and chlorination of poly(phosphite)s and subsequent modifications.

Atterton-Todd reactions are another type of effective post-modification reaction to introduce amine functionalities with various primary and secondary amines (**Scheme 10**).[65-66] Also anticancer drugs could be linked to the polymer without losing the function of the drug.[67]

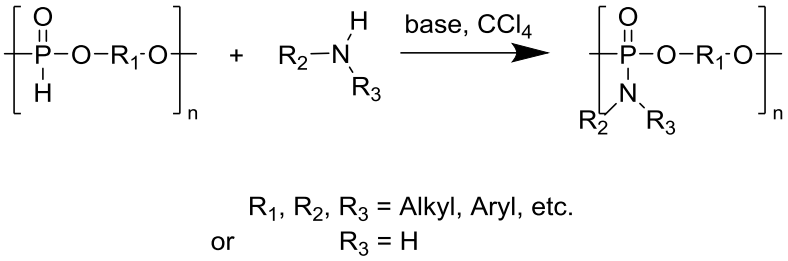

Scheme 10: Atherton-Todd reaction of poly(phosphite)s to poly(phosphoramidate)s.

It can be shown that poly(phosphite)s are excellent reactive polymers for post-modifications. However, it is difficult to use them directly for various applications because of reactivity. For comparison of post modified polymers, see **Chapter 1.3.2.1** for phoshoramidates and **Chapter 1.3.1.4** for phosphates.

Poly(phosphonate)s. Poly(phosphonate)s can be prepared by polycondensation reaction[68] (**Chapter 1.2.1**) and polyadditions[69] (**Chapter 1.2.4**). ROP can be applied, as well (**Chapter 1.2.2**). The investigation of flame retardant properties display for Poly(phosphonate)s even higher thermal stability and hydrolytic stability because of the P-C bond as for PPEs. In this area, some progress was recently reported with the first living polymerization of cyclic five-membered phosphonates. To generate a cyclic phosphonate monomer, the protocol described in **Chapter 1.2.2** has to be modified. The polymerization is carried out with an alcohol initiator and DBU catalyst.[70] In the meantime, different kinds of pendant groups are introduced by living ROP with interesting properties for the field of biomedicine.[71] ADMET of unsaturated phosphonates are also accessible to produce polymers due to the high intrinsic functional group tolerance of the Grubbs catalysts. Monomer and polymer synthesis is explained in **Chapter 1.2.4**. Relatively high melting points of up to 70 °C have been discovered for poly(icos-10-en-1,20-dioxy methylphosphonate).[40] One of the most interesting applications is the introduction of a benzaldehyde modified poly(phosphonate) for use as an agent to promote Horner-Wadsworth-Emmons (HWE) reactions. The advantage is that the byproduct is a polymer and is easy to remove (**Scheme 11**).[72]

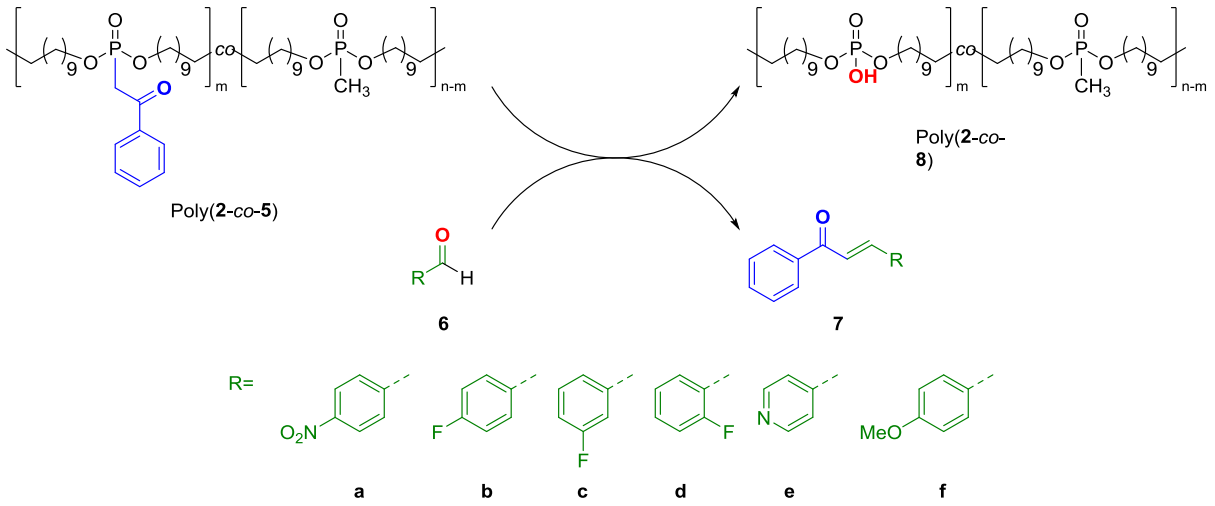

Scheme 11: HWE reaction with different aldehydes labelled *6a-f* yielding corresponding chalcones *7a-f*. Reproduced from Ref. [72] with permission from The Royal Society of Chemistry.

ROMP completes the list of synthesis methods. Examples are shown in **Chapter 1.2.5.1**. Homopolymerization leads to amorphous materials with rather high PDIs and small molecular weights. However, copolymerization with cis-cyclooctene has been shown to be a good alternative for producing small PDIs and high molecular weights.[40-41, 73]

(Reactive) Poly(chlorophosphoester)s. Poly(alkylidene chlorophosphate)s are not as reactive as carboxylic acid chlorides, but nevertheless are still reactive enough to undergo post-polymerization reactions with several groups. Similar to poly(phosphite)s (**Chapter 1.3.1.3**), this class of material can be considered as reactive polymers. Diunsaturated chlorophosphate monomers are polymerizable by ADMET reaction and will be discussed later in detail in this thesis (**Chapter 2**).[74] In comparison, poly(phosphite)s cannot be polymerized by ADMET. In addition, to generate different kinds of phosphates from poly(chlorophosphoester)s, just one step is needed instead of two as in the case of poly(phosphite)s.

1.3.1.4 Polymers with three P-O and one P=O bond

Poly(phosphate)s. Probably the most important phosphorus-containing polymer class are poly(phosphate)s, which exhibit three ester groups around the phosphorus. Advantages such as high biocompatibility, biodegradability and low toxicity are attractive features of PPEs.

Furthermore, the use of three equivalent pendant groups makes PPEs a versatile tool to adjust the main-chain and the side-chains as desired. This adaptability is not found in other common structures in polymer science such as carbon-based polyesters and polyamides. PPEs have been synthesized by polycondensation (**Chapter 1.2.1**), polyaddition (**Chapter 1.2.6**), ROP (**Chapter 1.2.2**) and olefin metathesis polymerization (**Chapter 1.2.4**). A great variety of PPEs can be formed using these methods.[70, 75] The molecular structure is easy to change due to the third pendant group. Hence linear, hyperbranched,[76] homo-, and copolymers[77] have been manufactured. Thiol-ene polyadditions (**Chapter 1.2.6.1**) can be used to synthesize PPEs, as well, which will be a subject discussed in this thesis.

Besides flame retardancy attractive applications such as linking boron-dipyrromethene (BODIPY) molecules on the phosphate as a dye for fluorescence microscopy makes PPEs a versatile tool for many research fields.[78] PPEs have been successfully introduced in nanoparticles generated by miniemulsion which exhibit a strong binding affinity to bone tissue. This may make these nanoparticles a valuable option for drug delivery to bones.[79] Moreover, due to the possibility to link functional groups to the ROP monomers, post-modifications have been conducted such as atom-transfer radical-polymerization (ATRP) with 2-methacryloyloxyethyl phosphorylcholine.[80] Hence, it is possible to change a hydrophobic polymer after grafting into a hydrophilic species. Other groups such as 2-((2,2-dimethyl-1,3-dioxolan-4-yl)methoxy)-1-dioxaphospholane-2-oxide have been introduced to release hydroxyl groups after cleavage for further modifications or vinyl ether side-chains to conduct thiol-ene polyadditions afterwards for several applications in the biomedical field. Many other groups can be applied as side-chains.[81] Many experiments have shown that PPEs exhibit high potential in the biomedical field. A lot of investigations with respect to drug delivery, gene delivery, protein absorption resistance, or tissue engineering have been documented.[79, 82-87] Properties such as biocompatibility, controlled degradability, and low toxicity *in vitro* make these polymers very promising materials.

Phosphorus-containing polymers can potentially be applied to the biomedical sector. Degradability is a valuable property of these polymers, which may allow for release of an active agent from a polymer-based nanocarrier. However, biodegradability is not only based on the nature of the binding motif of phosphorus, but also properties such as crystallinity,

hydrophobicity, glass transition temperature, and structure of the polymer. Generally, pH-values and enzymes can be used as triggers in order to degrade biopolymers. Kinetic experiments with PPEs[88-89] have been conducted by several workgroups. It has been shown that PPEs are degrading faster in basic as in acidic conditions. Furthermore, the side-chain is faster at degrading than the backbone because the phosphorus is less sterically hindered for the attack of the α-C atom in acidic environment. In contrast, basic conditions lead to similar degradation rates for the side- and main-chains. Here, the nucleophilic attack is directly at the central phosphorus atom. It has been taken into account that PPEs are remarkably stable under acidic pH values.[90-91] It has also been shown that spontaneous hydrolysis or the use of certain enzymes can slowly degrade the polymer.[92-94]

1.3.2 Phosphorus-nitrogen polymers

Another class of materials of great interest is polymers with P-N binding motifs inside the structure. This starts from one P=N linkage found in **poly(phosphazene)s** continuing to one P-N bond + two ester group and one P=O bond in **poly(phosphoramidate)s**. Two different binding motifs for two P-N linkages must be considered: **poly(phosphonamide)s** with a P-C bond beside two P-N linkages and **poly(phosphorodiamidate)s** with a P-O bond instead of a P-C bond. **Poly(phosphoramide)s** with three P-N connections besides one P=O bond are the polymers with the most nitrogen atoms connected to phosphorus.

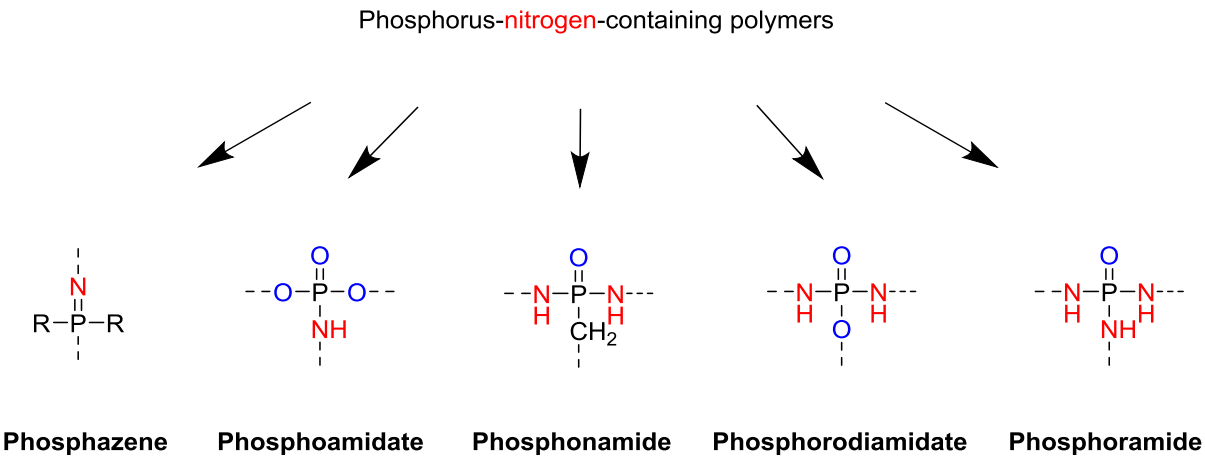

Figure 9: Subclasses of phosphorus-nitrogen-containing polymers.

1.3.2.1 Polymers with a single P-N and P=O bond

Polyphosphazenes. Polyphosphazenes are one of the first synthetically-produced phosphorus-containing polymers. Because of the absence of hydrocarbons within the backbone, polyphosphazenes are considered as inorganic polymers.[52] There are different kinds of reaction to yield polyphosphazenes but the thermal ROP (**Chapter 1.2.2**) of hexachlorocyclotriphosphazene is the most common one (**Scheme 12**). Hexachlorocyclotriphosphazene is synthesized by mixing ammonium chloride with phosphorus pentachloride in a boiling solvent as chlorobenzene (**Scheme 12**). The problem is that the reaction yields a mixture of linear and cyclic oligophosphazenes. Purification has to be done by sublimation at 60 °C to obtain pure hexachlorocyclotriphosphazene.[95]

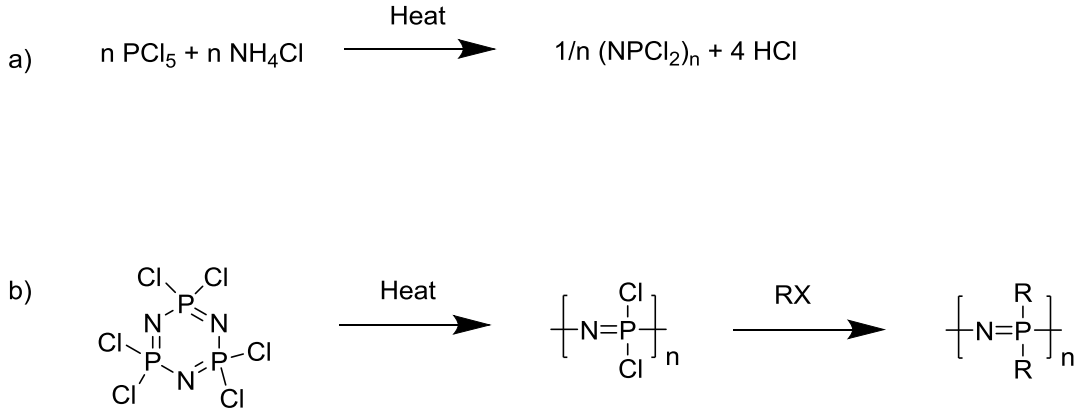

Scheme 12: a) Synthesis of hexachlorocyclotriphosphazene monomers; b) Polymerization to Polyphosphazenes and subsequent post-modification.

Although temperatures of 250 °C and higher are needed to polymerize hexachloro-cyclotri-phosphazene to polyphosphazene, an advantage of this reaction is that very high molecular weights can be achieved. Polymerization degrees of up to 15,000 can be attained, but because of harsh reaction conditions, control over the reaction is difficult. Low molecular weights are difficult to obtain, as well as narrow molecular weight distributions.[96-97]

The resulting polyphosphazene still has reactive chlorine atoms attached to the backbone. Post-modification reactions by replacing the chlorine atom with reactive amines, aryloxides,

alkyloxides, or organometallic reagents have been accomplished. The unmodified polymer is sensitive to water. In this state, the polymer is an elastomer. However by changing the water soluble side-chain of poly(dichlorophosphazene), hydrophobic polymers as well as film- and fiber-forming polymers have been prepared.[98] For example, poly(fluoralkoxyphosphazene)s show exceptional fuel and oil resistance and low temperature properties. If the modification is aryl-containing, excellent flame retardant properties are obtained.

In the meantime, new synthetic routes to control molecular weights have been established. For example, Ian Manners, Harry Allcock, and coworkers introduced "living" cationic polymerizations of phosphoranimines. By altering the ratio of monomer and initiator (PCl_5, $SbCl_5$, PBr_5, etc.) calculated molecular weight with narrow PDIs were observed (**Scheme 13**).[99]

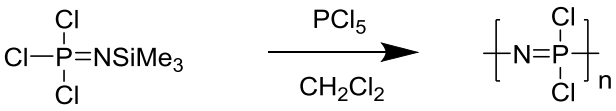

Scheme 13: "Living" cationic polymerization of phosphoranimines to polyphosphazenes in the presence of an initiator (i.e. PCl_5) in dichloromethane.

Poly(phosphoramidate)s. Poly(phosphoramidate)s carry one nitrogen connected to phosphorus, in addition to two ester groups and one P=O bond. Polycondensation reactions (**Chapter 1.2.1**) of *N*-arylphosphoramidic dichlorides and several aromatic diols have been synthesized. Properties such as good flame retardancy and thermo-oxidative stability were observed.[87, 100-102]

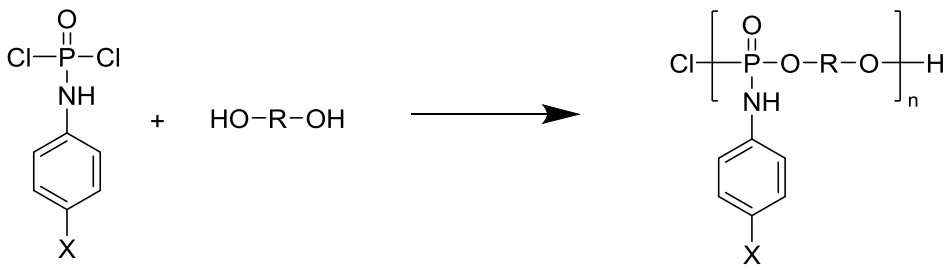

X = NO_2, Cl, Br, H, etc.

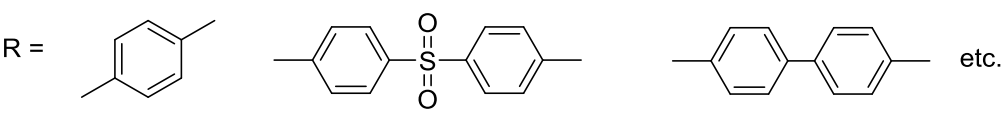

Scheme 14: Polycondensation reactions of *N*-arylphosphoramidic dichlorides and aromatic diols.

Aside from phosphorus, nitrogen exhibits excellent flame resistance behavior. Moreover, synergetic effects of both elements with even higher thermal stabilities has been found. Simultaneously, the charcoal residue for phosphorodiamidates (PDAs) is increased as compared to residue for PPEs.[103-104] This is important because the charcoal acts as a protective layer to inhibit heat transfer from the flame to the condensed phase. They are very promising materials with lower toxicity compared to also applied halogenated polycyclic aromatic compounds.[105]

Poly(phosphite)s can also be modified to yield poly(phosphoramidate)s. Moreover, groups such as imidazole have been introduced as side-chains.[106-107] Atherton-Todd reactions of poly(phosphite)s can lead to poly(phosphoramidate)s (see **Chapter 1.3.1.3**). Only very recently, ROP (**Chapter 1.2.2**) was introduced as a method to generate poly(phosphoamidate)s directly by polymerization of a cyclic phospholane amidate.[90] It has been shown that the amidate linkage is acid labile. The cleavage of the side-chain leads to phosphate ionomers (**Scheme 14**).[90]

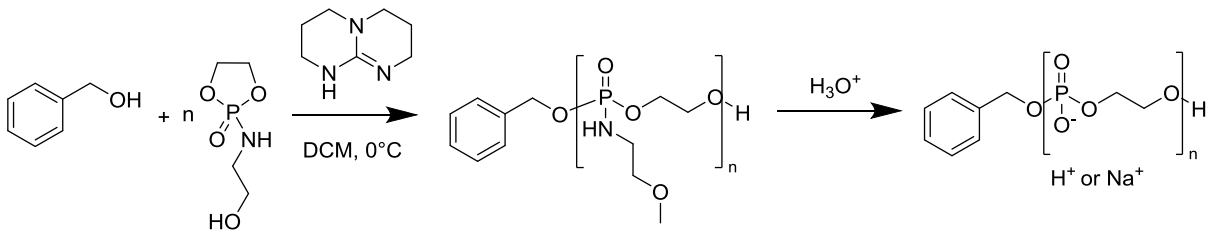

Scheme 14: Polymerization of cyclic phospholane amidate monomer with TBD as catalyst and benzyl alcohol as initiator and subsequent cleavage of the side chain to yield polyphosphoester ionomer. Reprinted with permission from Ref. [90]. Copyright 2013 American Chemical Society.

Phosphoramidates as the third pendant group accelerate the degradation of the polymer in acidic conditions.[108-109] In addition, phosphoramidate functionalities are stable in basic environments for several days.[90] This makes PDAs great examples for selective degradation

or as protective groups.[110] However phosphoramidate groups in the polymer backbone have never been investigated with regard to hydrolytic degradation.

Very recently, the first ADMET approach to synthesize poly(phosphoamidate)s has been reported.[110] Experiments with poly(phosphoramidate)s have been conducted to investigate the main-chain cleavage in basic conditions by preserving the side-chain degradation. Hereby, the side-chain exhibits the phosphoramidate linkage and not the main-chain. Experiments show the cleavage of the side-chain under acidic conditions (**cf. Appendix**). Interestingly, no degradation could be observed in basic conditions. As a consequence, polymers with phosphoramidate side-chains are controlled degradable under acidic conditions but stable in basic milieu in contrast to the basic labile PPDA side-chains.

Poly(phosphoramidate)s can also be formed by reactive chlorophosphates and modification with benzylamine, which will be explained in detail later in **Chapter 2**.

1.4.2.2 Polymers with two P-N and one P=O bond

Poly(phosphonamide)s. In 1962, poly(phosphonamide)s were prepared by polycondensation (**Chapter 1.2.1**) of the respective phosphonic dichloride and a diamine.[111]

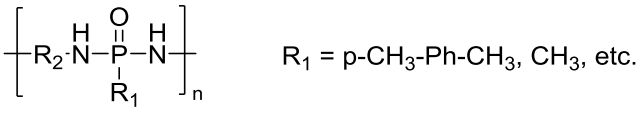

Figure 10: General form of poly(phosphonamide)s.

Since then, many poly(phosphonamide)s[17, 112] (poly(phosphonylurea)s[113]) by several techniques such as interfacial[113], solution polymerization have been presented.[114-115], or high temperature – high pressure synthesis polycondensation[116]

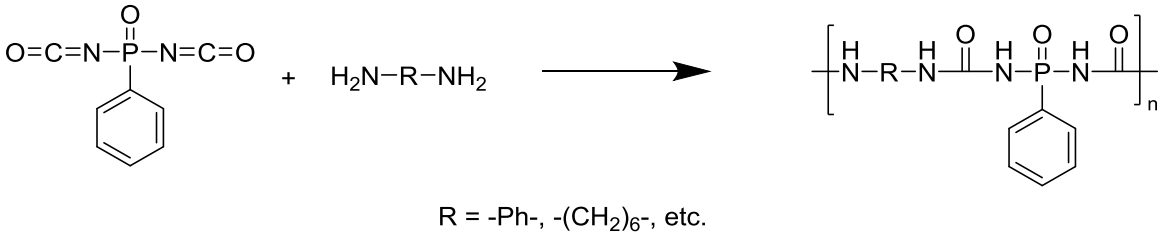

Scheme 15: Polycondensation reactions of phenylphosphonic diisocyanate with diamines to poly(phosphonylurea)s.

Polyphosphonamides exhibit flame retardancy, but further investigations have not been conducted to evaluate other potential properties. A lot of research has been done to prove their fire resistance behavior.[102, 117-119]

Poly(phosphorodiamidate)s have shown to be promising materials for flame retardancy. Synthesized by polycondensation (**Chapter 1.2.1**)[102] and low-temperature solution polycondensation[117] of different phosphorodichlorides with various diamines, which show high thermal stability and residual char up to 66 %.

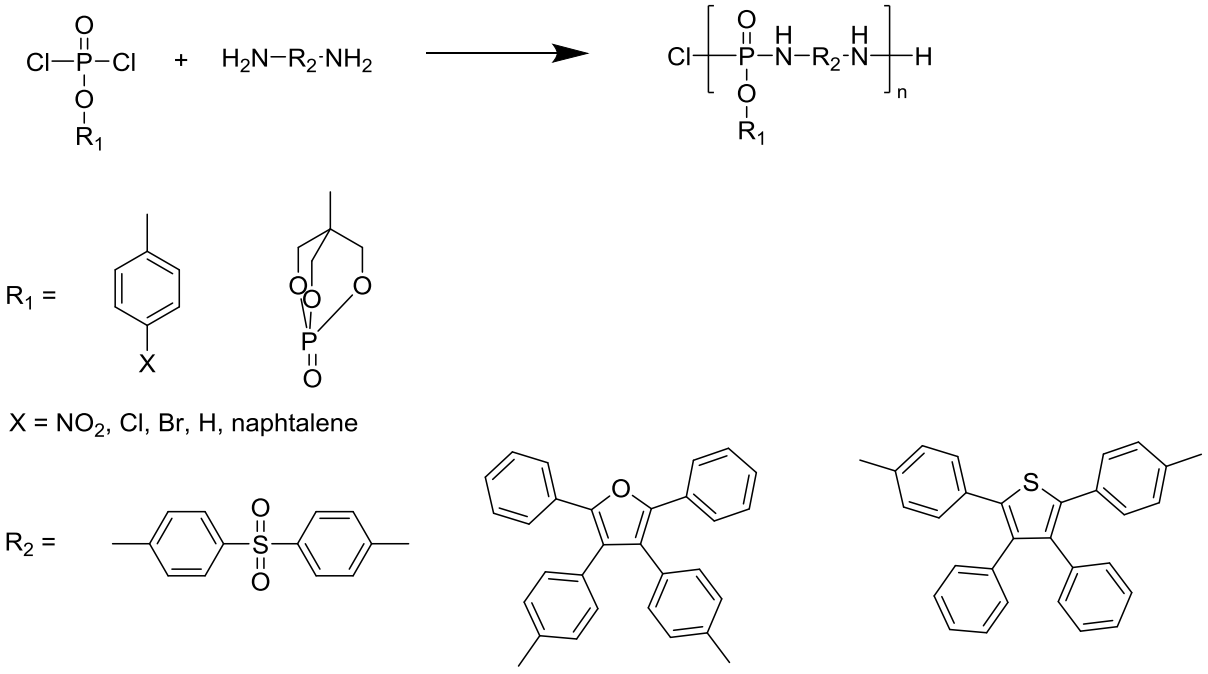

Scheme 16: Polycondensation reactions of diamines with phosphorodichlorides.

This thesis shows that ADMET reactions (**Chapter 1.2.4**) and thiol-ene polyadditions (**Chapter 1.2.6.1**) are valuable tools for preparing poly(phosphorodiamidate)s with fascinating properties.. In this thesis, it is presented that poly(phosphorodiamidate)s not only indicate promising flame retardant behavior, but also properties such as controlled degradation by various triggers (**Chapter 3** and **Chapter 4**). Surprisingly, these properties have never been studied before on this binding motif.

1.3.2.3 Polymers with three P-N and one P=O bond

1.3.2.3.1 Poly(phosphoramide)s

Poly(phosphoramide)s. Similar to polyphosphonamides, poly(phosphoramide)s have been generated by polycondensation (**Chapter 1.2.1**) of e.g. *N,N*-bis(p-chloroformylphenyl) phosphoric triamidate with several aromatic diols for evaluating the flame retardant behavior.[115]

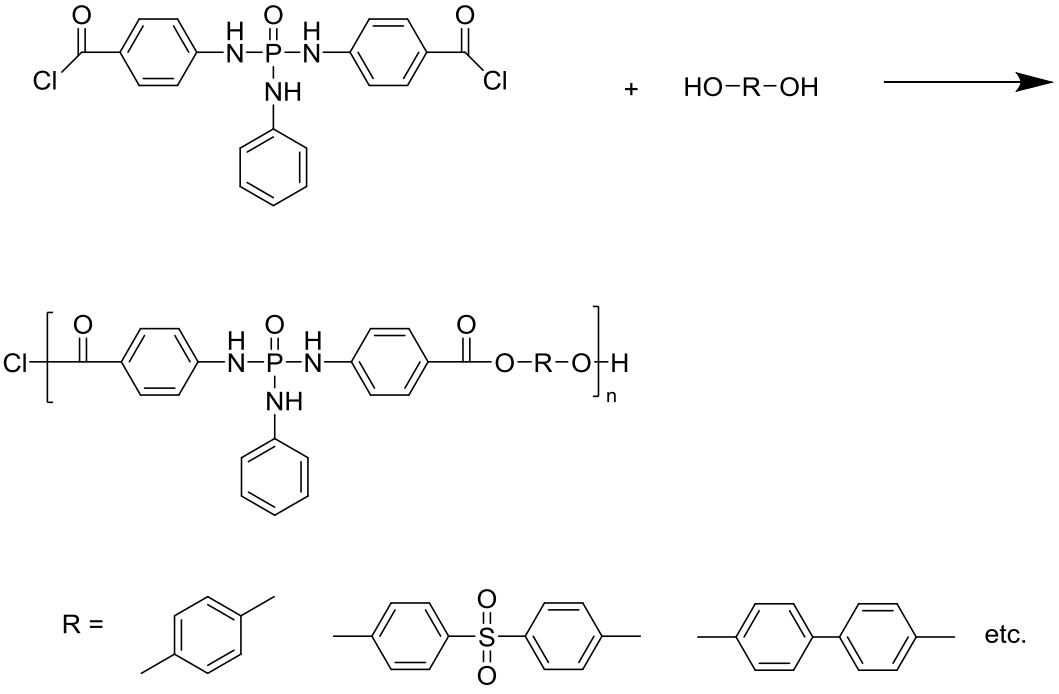

Scheme 17: Polycondensation reactions of *N,N*-bis(p-chloroformylphenyl) phosphoric triamidate with aromatic diols.

1.3.3 Sulfur-phosphorus polymers

The binding motive of P-S within the main-chain of polymers is rare. Literature known are modifications of oligo-DNA/RNA by substitute one or two oxygen atom with sulfur to yield 3'-*S*-phosphorothiolate or 5'-*S*-phosphorothiolate oligo-DNA/RNA (**Figure 11**).[120-122]

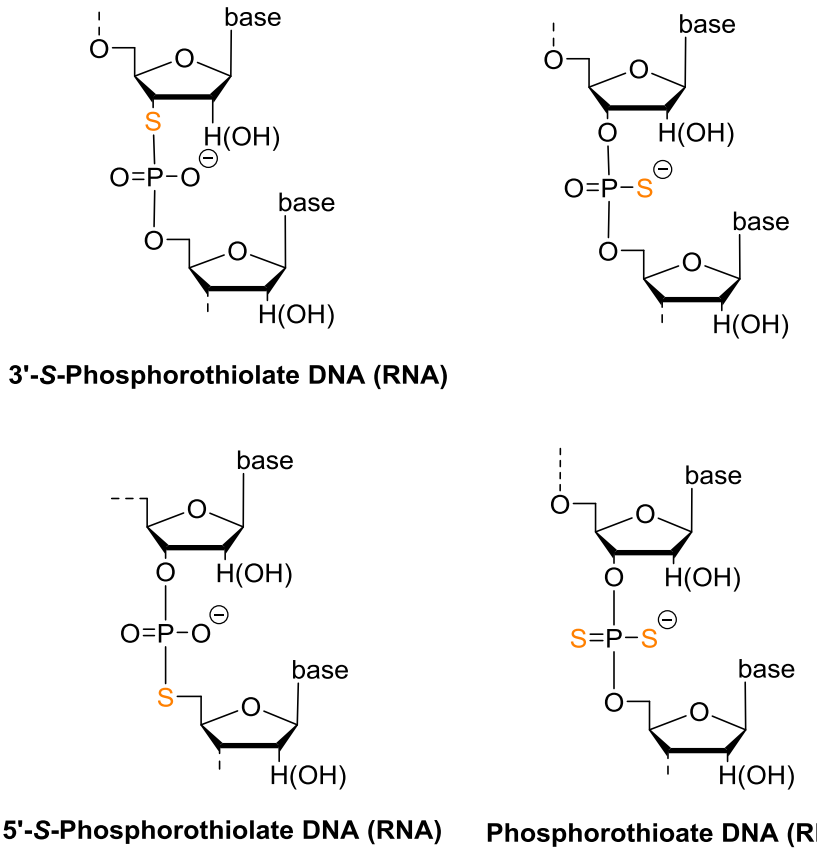

Figure 11: Chemical structures of 3'-*S*-phosphorothiolate and 5'-*S*-phosphorothiolate oligo-DNA (RNA; left) and phosphorothioate oligo-DNA (RNA; right) with orange highlighted sulfur atoms.

By replacing one or two of the oxygens around the phosphorus with a sulfur atom changes the overall chemical properties to make it resistant against nucleases and other molecular and cell biology research applications.[123]

However, besides modified oligo-DNA/RNA molecules with one, two, or three P-S linkages as binding motifs are a well-investigated class of materials due to application in agriculture as pesticides.[124]

In order to extend the knowledge of Polymers with the binding motif of P-S, this thesis shows the first attempt to synthesize poly(phosphorodithiolate)s with two P-S bonds in the main-chain in **Chapter 5**. ADMET polymerization has been used to synthesize poly(phosphorodithiolate)s for the first time. The reaction Scheme is exhibit in **Chapter 1.2.4**.

2 Motivation and Objectives

The mimicry of nature often promotes research. Phosphorus builds the basis of the living world in the form of phosphate groups which can be found in various polymers and molecules in living organisms, starting with the stabilization of the DNA or RNA backbone by the negative charge at the third oxygen atom linked to the phosphate group. Another important class of phosphates are phospholipids because they exhibit amphiphilic character. This pattern is introduced by the same advantage of the third pendant group of phosphates which can stabilize a negative charge, leading to a hydrophilic head next to hydrophobic tails of fatty acids. The amphiphilic structure of phospholipids from nature offers interesting properties. The third pendant group and its importance as a leaving group in reactions and in stabilizing negative charges within living organisms make organophosphates unique to nature. Due to the three pendant groups, phosphorus chemistry is unique for developing novel polymers and polymer architectures. However, the manufacture of precise polymers with useful properties similar to those found in nature has thus far been largely unsuccessful. This is why nowadays PPEs are not as important as other common polymers and are mainly used as flame retardant additives. Inspired by versatile properties, there has been an increased interest of phosphorus-containing polymers in recent years. The ability of the P-O-C bond to be highly robust under physiological conditions, yet readily cleavable under other types of conditions, makes organophosphates a valuable tool in biochemistry, but also interesting in the design of novel synthetic reagents or polymers.

A key feature of P-containing materials is the versatility of the phosphorus chemistry. Notably, studies in flame resistance behavior have produced the most promising materials for flame retardancy to date, and certain newly generated binding motifs of phosphorus-based materials have recently been applied to more sophisticated applications. Although binding motifs with neighboring elements in the periodic table have been accomplished, most of these compounds are usually not used in their polymerized form. Prominent examples are pesticides and nerve agents. P-O, P-N, and P-S binding motifs have been established to obtain novel properties and applications. Nature's closest relatives include the poly(phosphoester)s (PPEs) with only phosphoester bonds, i.e. P-O binding motifs. Modern

synthetic routes to adjust properties as desired have been explored for modern biomedical applications. However, poly(phosphoramidate)s (PPAs) from P-N binding motifs are thus far mainly used only as flame retardant materials. In contrast, phosphorothiolates from P-S binding motifs are mainly applied as pesticides and have never before been used within a polymeric structure in order to study their behavior.

The P-O binding motif has already proven to be a valuable tool in polymer chemistry by several publications in the last few years. PPEs exhibit high potential in the biomedical field. A lot of investigations with respect to drug delivery, gene delivery, protein adsorption resistance, or tissue engineering have been documented. Properties such as biocompatibility, controlled degradability, and low toxicity *in vitro* make these polymers very promising materials.

The P-N binding motif is well-known for flame retardant additives, because of improved flame retardant behavior by synergetic effects between phosphorus and nitrogen. Simultaneously, the char residue for phosphorodiamidates (PDAs) is increased as compared to the residue for PPEs. These are promising materials with lower toxicity as compared to halogenated polycyclic aromatic compounds used for similar purpose. However, other properties of these PPEs have scarcely been investigated. In 2012, Wooley and co-workers published a controlled degradation by adjusting the pH value of a phosphoramidate bond in a PPE. These two features, plus the biocompatibility and non-toxicity, make the P-N binding motif another promising new field of interest for polymers. Degradability may allow for the release of an active agent from a polymer-based nanocarrier. Generally, pH-values and enzymes can be used as triggers in order to degrade biopolymers. Phosphoramidates accelerate the degradation of the polymer in acidic conditions. However, phosphoramidate functionalities are stable in basic environments for several days. This makes PDAs great examples for selective degradation or as protective groups. However phosphoramidate groups in the polymer backbone have never been investigated with regard to hydrolytic degradation.

Reactive polymers have proved challenging but also highly interesting and important to polymer chemists for a long time. Reactive polymers show high potential for new materials

and for medicine. One idea is to link drugs or biopharmaceuticals under mild conditions to these reactive structures. Reactive polymers can be used for postmodification reactions to gain a broad variety of functional materials.

Polycondensation reactions have been the polymerization method of choice for a long time. However, in recent years, it was shown that there are several other ways to synthesize desired phosphorus-containing polymers which are strongly dependent on the monomer and help determine the properties of resulting polymers. Rather recently developed synthesis techniques make it possible to access controlled polymerization methods and a high functional group tolerance. Prominent examples are organocatalyzed ring-opening polymerization and olefin metathesis polymerization. In addition, many functionalities are now accessible within the polymeric structure. Hence, many post-modification reactions can now be established due to the tolerance of many functional groups during the synthesis. The ADMET approach has been proven to be a suitable candidate for tolerating many functional groups. It was already used for many PPE polymerizations in a very controlled manner. Furthermore, the thiol-ene polyaddition is a promising technique to polymerize phosphorus-containing materials. A comonomer is needed, which introduces thioether functionalities inside the backbone and allows further adjustment of thermal properties and hydrophilicity of the polymer by oxidation to sulfones.

This thesis is dedicated to extending the family of phosphorus-containing polymers via novel synthetic techniques (ADMET and thiol-ene polymerizations) in order to introduce well-designed polymers for a far greater scope of applications than just as flame retardants. Hereby, there is a focus on the synthesis of main-chain phosphorus containing polymers with the precise variation of the binding pattern around the central phosphorus. Such new polymers, especially with amide and thioester linkages, have only scarcely been reported to date. Thus, fundamental characterization of these polymers is needed. Because of the versatility of phosphorous, this thesis is focused on developing phosphorus-containing polymers by changing the third pendant group (side chain), backbone, or binding motif in order to attain exceptional properties.

The objectives of this thesis are:

I. Synthesis and post-modification of reactive PPE by polymerizing chlorophosphates via ADMET reaction and subsequently altering the polymer to gain novel (co)polymers for e.g. adhesive applications.

II. Extending the synthesis techniques for phosphorus-containing polymers by introducing thiol-ene polyadditions as a promising new polymerization method for phosphorus-containing monomers.

III. The development of suitable PDA monomers to polymerize them by ADMET reactions and thiol-ene polyadditions to PPDAs.

IV. Establishing the synthesis and polymerization of PDTs for the first time via ADMET reaction in order to fill this lack of binding motifs in phosphorus-containing polymers.

V. Investigation of the thermal behavior and thermo-oxidative stability of several synthesized polymers in order to present novel features and promising new flame-retardant materials.

VI. Studying the hydrolytic and enzymatic degradation behavior of hydrophilic as well as hydrophobic monomers and polymers in order to investigate the (controlled) cleavage of various binding motifs of phosphorus for biomedical applications and to analyze the degradation in natural environment.

3 Results and Discussion

3.1 Reactive Poly(phosphate)s via ADMET polymerization

Reactive polymers have been of great interest to polymer scientists for many years. The ability to alter side-chains after polymerization under mild conditions has revealed a high variety of post-modification options. Poly(phosphite)s are a class of reactive phosphorus-containing polymers. After polymerization, poly(phosphite)s are able to undergo a post-modification reaction by exchanging the hydrogen directly linked to phosphorus (**Chapter 1.3.1.3**). One option is by chlorination of the poly(phosphite)s to yield polychloro-phosphates. This allows nucleophiles to attack the phosphorus center to alter the polymer accordingly. However, two synthesis steps are necessary to modify the polymer as desired. Therefore, this chapter introduces a new approach of directly manufacturing polychlorophosphates by acyclic diene metathesis (ADMET) polymerization of chlorophosphates monomers. For which only one step is needed to modify the polymer structure after polymerization. In addition to potential modifications with alkoxides or amines, it is even possible to modify the polychlorophosphates with up to three different nucleophiles at one polymer chain. Completely different properties can be adjusted at this one polymer chain for use in many applications such as for making adhesives. For linking thiols on the internal double bonds or silyl groups on the terminal double bonds, or for use as macroinitiators of controlled radical polymerizations. Polychlorophosphates can also be used in biomedical applications as potential tissue engineering scaffold materials, and in materials science as flame-retardants.

Herein the synthesis of reactive chlorophosphates by olefin metathesis polymerization will be presented. Simultaneously, the scope of ADMET reactions will be extended by introducing the ability to polymerize highly reactive chlorophosphates. Published in Macromolecules 2014 and reprinted with permission from Ref. [74]. Copyright 2014 American Chemical Society.

3.1.1 *Poly(alkylidene chlorophosphate)s via acyclic diene metathesis polymerization: A general platform for the post-polymerization modification of poly(phosphoester)s*

*Mark Steinmann, Jens Markwart, Frederik R. Wurm**

Max-Planck-Institut für Polymerforschung, Ackermannweg 10, 55128 Mainz, Germany.

Contact address: wurm@mpip-mainz.mpg.de

Abstract

Reactive poly(phosphoester)s (PPEs) have been prepared via the acyclic diene metathesis polymerization of the monomers di-(buten-3-yl) chlorophosphate and di-(undecen-10-yl) chlorophosphate. Molecular weights can be adjusted from 1,000 to ca. 50,000 g/mol and have been prepared and characterized in detail. This is the first report on olefin metathesis polymerization of highly electrophilic phosphochlorides, which were post-modified with different nucleophiles, i.e. alcohols, amines, water, and thus allowing the synthesis of side chain polyphosphoamidates, -esters, and free acids from the same starting polymer. High side-chain functionality was found in all cases.

Keywords. Polyphosphoester, reactive polymer, postpolymerization modification, polyphosphoamidate

Introduction

Reactive polymers and reactions with polymers have a long history ranging back to Schönbein's nitration of cellulose[125-126] or the vulcanization process of natural rubbers.[127] Today, modern polymer chemistry offers a large toolbox to design novel and (poly)functional materials.[128-129] Controlled radical polymerization methods[130] and very tolerant catalytic polymerization techniques allow the introduction of a variety of functional groups into polymers, which was previously limited with "classical" methods such as polycondensation[131] or living ionic polymerization.[132] The direct polymerization of functional monomers is an attractive strategy. However, this is often hampered by interference with the polymerization conditions or -in copolymerizations- due to incompatible copolymerization parameters, especially in radical polymerization. These factors limit the synthesis of functional polymers, and moreover the access to materials having a precisely defined molecular weight, composition and architecture. Especially when several functional materials should be compared to establish structure-property relationships, the influence of the degree of polymerization or the molecular weight distribution in different batches of the "same" material are dominating problems. To overcome these issues, reactive polymers have been studied intensively in recent years.[133-134] These materials can be generated with various polymerization techniques and subsequently post-modified to generate the functional material of choice. The precursor polymers are soluble and the activated group is inert towards the polymerization conditions. This allows the facile generation of a diverse library of functional polymers with identical average chain length, molecular weight distribution, and architecture (e.g. degree of branching).[135]

Post-polymerization modification has been applied to almost every polymer class, however, degradable polymers have rarely been investigated.[136] This is probably attributed to the typically applied ring-opening polymerization (ROP) of cyclic esters or amides,[137] for which the synthesis of functional lactones/lactames, regardless if it should carry the final functionality or a reactive intermediate, can be challenging.

This work helps to fill the gap by the presentation of an approach for the synthesis of diverse functional and degradable polyesters: The approach uses metathesis polymerization to generate reactive and degradable poly(phosphoester)s (PPEs) that can be modified to create

highly functional materials which are only accessible via post-modification. PPEs have found increasing attention during the last years due to different synthetic methods via ring-opening polymerization and polycondensation or polytransesterification methods and the straightforward preparation of water-soluble or temperature-responsive polymers.[70, 77, 138-141] Recently, the Wooley lab used anionic ring-opening polymerization to synthesize reactive PPEs carrying reactive olefins or alkynes in the side chain with subsequent postmodification and assembly to degradable drug-carriers, for example.[142-145] Troev and coworkers used in a series of papers reactive Poly(H-phosphonate)s for the introduction of various pendant groups.[146-147] The metathesis platform already tolerates many reactive groups, such as anhydrides,[148-149] however, highly nucleophilic groups, acrylates, and others are either difficult to introduce or hamper the removal of the catalyst.[150] With the approaches presented herein, potentially biocompatible materials will be accessible and may find applications in polymer-therapeutics or adhesives.

Experimental section

Chemicals. 10-undecen-1-ol 98%, potassiumhydride 30 wt% dispersion in mineral oil, 2-methoxyethanol 99.8%, HEMA (2-Hydroxyethyl methacrylate) 97%, 1-chloronaphthalene 90%, Benzylamine 99% and 3-buten-1-ol 96 % were purchased from Sigma Aldrich and used as received. $POCl_3$ (Phosphoryl chloride) 99%, was purchased from Acros and used as received. Dichloromethane (CH_2Cl_2), toluene, tetrahydrofuran (THF) and triethylamine (Et_3N) were dried and stored under argon. Grubbs catalyst 1st generation was purchased from Sigma Aldrich and stored under argon. Ferrocenylmethanol was synthesized according to a previously published procedure.[151]

Tris(hydroxymethyl)phosphine 90%, was purchased from Sigma Aldrich, and used as receive for the polymer`s purification in order to remove the Grubbs Catalyst from the reaction with a similar already reported efficient procedure.[152]

Methods. Gel-permeation chromatography (GPC) measurements were carried out in THF, with samples of the concentration of 1 g L^{-1}. Sample injection was performed by a 1260-ALS auto sampler (Waters) at 30 °C (THF). The flow was 1 mL min^{-1}. In THF, three SDV columns (PSS) with dimensions of 300 × 80 mm, 10 µm particle size and pore sizes of 106, 104 und 500 Å were employed. Detection was accomplished with a DRI Shodex RI-101 detector (ERC) and UV-Vis 1260-VWD detector (Agilent). Calibration was achieved using poly(styrene) standards provided by Polymer Standards Service.

^{1}H NMR spectra were recorded on a Bruker avance 250 MHz or 300 MHz spectrometer. All spectra were recorded at room temperature. The proton, carbon and phosphorous spectra were measured in $CDCl_3$ and CD_2Cl_2 at 298.3K and the spectra were referenced as follows: for the residual $CHCl_3$ at $\delta(^1H)$ = 7.26 ppm, CD_2Cl_2 at $\delta(^1H)$ = 5.28 ppm, $CDCl_3$ $\delta(^{13}C$ triplett) = 77,0 ppm and triphenylphosphine (TPP) $\delta(^{31}P)$ = - 6.00 ppm.

^{13}C{H} and ^{31}P({H}) NMR experiments were recorded with a 5 mm BBI 1H/X z-gradient on the 700 MHz spectrometer with an Bruker Avance III system. For a ^{1}H NMR spectrum 64 transients were used with an 11 µs long 90° pulse and a 12600 Hz spectral width together with a recycling delay of 5 s. The ^{13}C{H} NMR (176 MHz) and ^{31}P({H}) NMR (283 MHz) measurements were obtained with an ^{1}H powergate decoupling method using 30° degree

flip angle, which had a 14,5 µs long 90° pulse for carbon and an 27,5 µs long 90° pulse for phosphor. Additionally carbon spectra were kept with a J-modulated spin-echo for ^{13}C-nuclei coupled to ^{1}H to determine number of attached protons with decoupling during acquisition. The spectral widths were 41660 Hz (236 ppm) for ^{13}C and 56818 Hz (200 ppm) for ^{31}P, both nuclei with a relaxation delay of 2s.

Similar 1D (^{13}C{H} and ^{31}P({H}) NMR's) measurements (^{1}H-NMR (500 MHz), ^{31}C{H}-NMR (125,77 MHz) and ^{31}P({H})-NMR (202 MHz)) were done on a Bruker Avance III 500 NMR spectrometer with a 5 mm BBFO probe equipped with a z-gradient. The spectra were obtained with π/2-pulse lengths of 11,9 µs (^{1}H), 13,2 µs (^{13}C) and 11 µs (^{31}P) and a sweep width of 10330 Hz (20,6 ppm) for ^{1}H, 29700 Hz (236 ppm) for ^{13}C and 40000 Hz (200 ppm) for ^{31}P, all nuclei with a relaxation delay of 2s.

Di-(but-3-en-1-yl) chlorophosphate (1). To a stirred solution of $POCl_3$ (6.57 g, 4.00 mL, 42.78 mmol, 1.0 eq) in toluene (20 mL) at 0 °C was added a mixture of 3-buten-1-ol (5.55 g, 6.63 ml, 77.01 mmol, 1.8 eq) and Et_3N (7.79 g, 10.74 mL, 77.01 mmol, 1.8 eq). After stirring overnight, $Et_3N{\cdot}HCl$ was removed as a white solid by filtration. The filtrate containing the dialkylene chlorophosphate in toluene was concentrated at reduced pressure. Pure **1** was obtained as colorless oil (Yield: 5.75 g, 25,7 mmol; 60 %) after distillation at 90°C ($5{\cdot}10^{-2}$ mbar). ^{1}H NMR (300 MHz, 298 K, $CDCl_3$, δ/ppm): 5.89-5.72 (ddt, *J* = 17.0, 10.1, 6.7 Hz, 2H), 5.29-5.05 (m, 4H), 4.41-4.03 (m, 4H), 2.64-2.39 (tdt, *J* = 6.7, 5.4, 1.3 Hz, 4H). ^{13}C{H} NMR (126 MHz, 298 K, $CDCl_3$, δ/ ppm): 132.52, 118.29, 68.61, 68.55, 34.13, 34.07**.** ^{31}P{H} NMR (202 MHz, 298 K, $CDCl_3$, δ/ ppm): 4.52. ESI-MS *m/z* 153.20 $[M+2K]^{2+}$, 261.20 $[M+K]^{+}$, (Calculated for $C_8H_{14}ClO_3P$: 224.04).

Di-(undec-10-en-1-yl) chlorophosphate (2). To a stirred solution of $POCl_3$ (6.57 g, 4.00 mL, 42.78 mmol, 1.0 eq) in toluene (20 mL) at 0 °C was added a mixture of 10-undecen-1-ol (13.1 g, 15.4 ml, 77.01 mmol, 1.8 eq) and Et_3N (7.79 g, 10.74 mL, 77.01 mmol, 1.8 eq). After stirring overnight, $Et_3N{\cdot}HCl$ was removed as a white solid by filtration. The filtrate containing the dialkylene chlorophosphate in toluene was concentrated at reduced pressure. **2** was obtained as yellow oil (Yield: 14.4 g, 34.2 mmol; 80 %) 2. The compound was used without further purification. ^{1}H NMR (300 MHz, 298 K, $CDCl_3$, δ/ ppm): 5.84 – 5.63 (ddt, *J* = 16.9, 10.2,

6.7 Hz, 2H), 4.99 – 4.80 (m, 4H), 4.32 – 4.00 (m, 2H), 2.04 – 1.89 (tdd, *J* = 6.6, 5.3, 1.4 Hz, 4H), 1.80 – 1.54 (m, 4H), 1.40 – 1.18 (m, 24H). ^{13}C{H} NMR (126 MHz, 298 K, $CDCl_3$, / ppm): 139.15, 114.15, 114.13, 69.79, 67.72, 45.18, 33.79, 32.65, 29.36, 29.11, 28.90, 26.88, 25.31. ^{31}P{H} NMR (202 MHz, 298 K, $CDCl_3$, δ/ ppm): 4.85. ESI-MS *m/z* 443.26 $[M+Na]^+$, 459.24 $[M+K]^+$, 863.52 $[2M+Na]^+$ (Calculated for $C_{22}H_{42}ClO_3P$: 420.26).

General procedure for the ADMET bulk polymerization to poly[hex-3-en-1-yl chlorophosphate] (Poly(1)) and poly[icos-10-en-1-yl phosphate] (Poly(2)). In a glass Schlenk tube the respective monomer (250 mg, 1.12 mmol (**1**), 0.60 mmol (**2**) and the Grubbs catalyst 1st generation (1 mol%) were mixed under an argon atmosphere. Polymerization was carried out at reduced pressure (to remove the ethylene gas evolving during the metathesis reaction) at temperatures between 25 and 50 °C for 1-8 h. the polymer was obtained as brownish viscous oil in quantitative yield. The compound was used without further purification.

General procedure for the ADMET solution polymerization to poly[hex-3-en-1-yl chlorophosphate] (Poly(1)) and poly[icos-10-en-1-yl chlorophosphate] (Poly(2)). The respective monomer (250 mg, 1.12 mmol (**1**), 0.60 mmol (**2**) and Grubbs catalyst 1st generation (1 mol%) were dissolved in 250 mg of 1-chloronaphthalene under an argon atmosphere. Polymerization was carried out at reduced pressure to remove ethylene gas evolving during the metathesis reaction at temperatures between 25 and 50 °C for 1-8 h. The crude polymer solution was used without further purification.

Poly(1). ^{1}H NMR (250 MHz, 298 K, $CDCl_3$, δ/ ppm): 5.97 – 5.70 (ddt, *J* = 17.0, 10.2, 6.7 Hz), 5.70 – 5.47 (m), 5.27 – 5.09 (m), 4.39 – 4.03 (m), 2.63 – 2.36 (m). ^{13}C{H} NMR (126 MHz, 298 K, $CDCl_3$, δ/ ppm): 132.52, 128.03, 127.05, 118.33, 68.82, 68.58, 34.13, 33.03, 28.11. ^{31}P{H} NMR (202 MHz, 298 K, $CDCl_3$, δ/ ppm): 4.57.

Poly(2). ^{1}H NMR (250 MHz, 298 K, $CDCl_3$, δ/ ppm): 5.93 – 5.70 (m), 5.52 – 5.36 (m), 5.07 – 4.84 (m), 4.25 – 4.06 (m), 2.12 – 1.87 (m), 1.87 – 1.61 (m), 1.50 – 1.16 (m). ^{13}C{H} NMR (126 MHz, 298 K, $CDCl_3$, δ/ ppm): 139.15, 130.84, 130.32, 129.85, 129.03, 128.22, 125.29, 114.16, 72.48, 69.93, 33.79, 32.61, 32.08, 29.85, 29.76, 29.41, 29.07, 28.20, 27.22, 25.65, 25.22, 21.46. ^{31}P{H} NMR (284 MHz, $CDCl_3$, δ/ ppm): 4.84.

General procedure for the postpolymerization modification of poly[hex-3-en-1-yl chlorophosphate] with various nucleophiles. The crude reaction mixture of **poly(1)** (250 mg, 1.12 mmol of monomer **1**) was dissolved in CH_2Cl_2 in a dry Schlenk tube equipped with a magnetic stir bar. The still active Ru-catalyst was deactivated by the addition of a few droplets of ethyl vinyl ether. Then, the appropriate nuleophile (see below) was mixed with Et_3N (112.93 mg, 154.7 µl, 1.12 mmol, 1 eq) and added to the **poly(1)** solution. The reaction was allowed to react under an argon atmosphere at room temperature for 24 h. When water was used as one of the nuclephiles, it was added after stirring for 24 h in excess and the solution was stirred for an additional 24 h. The modified polymer was treated with tris-(hydroxymethyl) phosphine (ca. 50 eq with respect to the catalyst) and washed twice with aqueous 10% HCl and finally twice with brine to remove the catalyst. The organic layer was separated, dried over sodium sulfate ($NaSO_4$), filtered and concentrated at reduced pressure. When the solvent 1-chloronaphthalene was used, the polymers were additionally precipitated into cold hexane and collected after decanting of the supernatant, and finally dried (yields typically: 70 %).

Synthesis of poly[hex-3-en-1-yl *N*-benzylphosphoamidate] (3). The reaction was carried out following the general procedure above with benzylamine (134.5 mg, 136.8 µl, 1.00 mmol, 0.9 eq) as nucleophile. The following spectral properties were observed: ^{1}H NMR (250 MHz, 298 K, $CDCl_3$, δ/ ppm): 7.53 – 7.15 (m), 5.84 – 5.67 (m), 5.63 – 5.38 (m), 5.20 – 5.03 (m), 4.35 – 3.80 (m), 2.60 – 2.12 (m). ^{13}C{H} NMR (298 K, $CDCl_3$, δ/ ppm): 139.79, 133.74, 128.50, 128.20, 127.33, 117.47, 65.69, 65.44, 53.46, 45.26, 33.61, 28.60. ^{31}P{H} NMR (284 MHz, 298 K, $CDCl_3$, δ/ ppm): 8.93.

Poly[hex-3-en-1-yl ferrocenylmethylphosphate] (4). The reaction was carried out following the general procedure above with potassium-ferrocenylmethanolate as nucleophile, which was previously produced by adding potassium hydride into a solution of ferrocenemethanol (241.1 mg, 1.12 mmol, 1eq) in THF. THF was used instead of CH_2Cl_2 as solvent for the reaction. The following spectral properties were observed: ^{1}H NMR (250 MHz, 298 K, $CDCl_3$, δ/ ppm): 5.63 – 5.38 (m), 5.35 – 5.14 (m), 4.74 – 4.62 (m), 4.58 – 4.46 (m), 4.28 – 3.95 (m), 2.58 – 2.25 (m). ^{31}P{H} NMR (284 MHz, 298 K, $CDCl_3$, δ/ ppm): 3.98.

Poly[hex-3-en-1-yl methoxyethylphosphate] (5). The reaction was carried out following the general procedure above with methoxymethanol (84.9 mg, 88.0 µl, 1,12 mmol, 1 eq) as nucleophile. The following spectral properties were observed: ^{1}H NMR (700 MHz, 298 K, $CDCl_3$, δ/ ppm): 5.77 – 5.67 (m), 5.54 – 5.40 (m), 5.11 – 5.00 (m,), 4.19 – 4.05 (m), 4.04 – 3.89 (m), 3.59 – 3.48 (m), 3.36 – 3.27 (m), 2.48 – 2.26 (m). ^{13}C{H} NMR (176 MHz, $CDCl_3$, 298 K, δ/ ppm): 133.36, 128.08, 127.13, 117.72, 71.34, 68.34, 67.05, 66.54, 58.96, 34.61, 33.44, 28.53. ^{31}P{H} NMR (284 MHz, 298 K, $CDCl_3$, δ/ ppm): -0.98.

Poly[hey-3-en-1-yl ethylmethacrylatephosphate] (6). The reaction was carried out following the general procedure above with HEMA (145,8 mg, 136.2 µl, 1,12 mmol, 1 eq) as nucleophile. The following spectral properties were observed: ^{1}H NMR (250 MHz, 298 K, $CDCl_3$, δ/ ppm): 6.16 – 5.99 (m), 5.64 – 5.32 (m), 4.38 – 3.77 (m), 2.54 – 2.05 (m), 1.94 – 1.80 (m). ^{13}C{H} NMR (126 MHz, 298 K, $CDCl_3$, δ/ ppm): 167.00, 135.80, 135.77, 128.53, 128.07, 126.34, 76.79, 67.19, 66.25, 65.39, 63.28, 63.22, 63.13, 33.52, 31.94, 30.67, 30.31, 29.72, 29.68, 29.38, 28.53, 26.91, 22.71, 18.35, 18.31, 18.29, 16.20, 16.15, 15.69, 14.16. ^{31}P{H} NMR (202 MHz, 298 K, $CDCl_3$, δ/ ppm): -1.29.

Poly[icos-10-en-1-yl phenylphosphate co poly[icos-10-en-1-yl phosphate] (7). The reaction was carried out following the general procedure above with potassium-phenolate as nucleophile, which was previously produced by adding potassium hydride into a solution of phenol (79.1 mg, 0.84 mmol, 0.75 eq) in THF. THF was used instead of CH_2Cl_2 as solvent for the reaction. After one night water (excess) was added to complete the modification. The following spectral properties were observed: ^{1}H NMR (300 MHz, $CDCl_3$, 298 K, δ/ ppm): 7.38 – 7.27 (m), 7.25 – 7.11 (m), 5.88 – 5.73 (m), 5.48 – 5.23 (m), 5.04 – 4.88 (m), 4.28 – 4.06 (m), 4.06 – 3.85 (m), 2.11 – 1.80 (m), 1.80 – 1.53 (m), 1.53 – 0.98 (m). ^{13}C{H} NMR (126 MHz, $CDCl_3$, 298 K, δ/ ppm): 150.86, 139.14, 130.31, 129.63, 124.88, 119.95, 114.13, 68.53, 67.64, 33.78, 32.61, 30.25, 29.77, 29.41, 29.10, 27.23, 25.46. ^{31}P{H} NMR (202 MHz, 298 K, $CDCl_3$, δ/ ppm): 1.22, -6.13.

Results and Discussion

Synthesis of reactive poly(phosphoalkenyl chloride)s. The synthesis of reactive poly(phosphoester)s (PPEs) was accomplished by metathesis polymerization of unsaturated phosphate monomers as recently introduced by our group.[40-41, 153] The versatile monomer synthesis starts from $POCl_3$ that is esterified sequentially with the alcohols of choice.[78] Two unsaturated alcohols are necessary to introduce the polymerizable units, while the third pendant ester is free to introduce functional groups. Herein, in contrast to previous works,we chose to leave the pendant group a phosphoric acid chloride in order to generate highly electrophilic PPEs that can readily react with various nucleophiles. To generate the reactive poly(alkenyl chlorophosphate)s, different monomers were prepared and investigated with respect to their polymerization behavior and efficiency in post polymerization modifications. It was expected that the highly reactive P-Cl-bond is inert to olefin metathesis conditions via Ruthenium catalysis. However, subsequent replacement with nucleophiles is possible to generate esters, amidates, etc. (Scheme 1). The first monomer is di-(buten-3-yl) chlorophosphate (with X = CH_2 in Scheme 1); this monomer is available in a single reaction step from $POCl_3$ and 3-buten-1-ol and can be distilled to achieve a high purity of the starting material, and with the rather short alkyl chains between the phosphates, the phosphorus content of the resulting polymer is relatively high. The polymeric acid chloride is expected to be well soluble in organic solvents, and processing of the polymer is possible (and removal of the catalyst after postmodification, see below). Based on previous and recent investigations on poly(phosphate)s synthesized via ADMET, it was expected and found that the glass transition temperature of the resulting poly(alkylidene chlorophosphate) (**poly(1)**) is low (ca. -60 °C; Supporting Information). This is an attractive property for ADMET polycondensation, as high molecular weights can be achieved for low-T_g materials, while are often difficulties arise in bulk polymerizations due to the high viscosity of the reaction mixture for polymers with high T_g. Even if metathesis polymerization tolerates many functional groups, solid monomers (or polymers) with a high melting point will typically lower the molecular weights that can be achieved with this method as solvents have to be used.[154] The second monomer synthesized herein is di-(undecen-10-yl) chlorophosphate (with X= $(CH_2)_8$ in Scheme 1). It has rather long alkyl chains

between the phosphates, therefore the phosphorus content of the resulting polymer is lower but the larger hydrophobic part leads to new interesting properties. The second polymer also features a rather low glass transition temperature (ca. -60 °C; Supporting Information). Furthermore, due to the longer alkyl chains between the phosphate groups this unsaturated polymer exhibits a melting point at -9 °C.

Postpolymerization modification. The postmodification should be investigated with several nucleophiles, from which alcohols (or the respective alkoxide) are to be used in order to generate poly(phosphate)s. Using this strategy, other graft-copolymers are also accessible, which would not be possible via direct copolymerization as molecular weights of grafting-through polymerizations are usually low.[155] The postmodification of this polymer class with amines is also very attractive. First, amines are highly nucleophilic and thus a high conversion is very likely. Second, the resulting side-chain poly(phosphoamidate)s are interesting due to their faster hydrolysis compared to phosphoesters.[90] This property could be used to reversibly attach drugs or labels to the polymeric carrier that can be released by acidic hydrolysis.

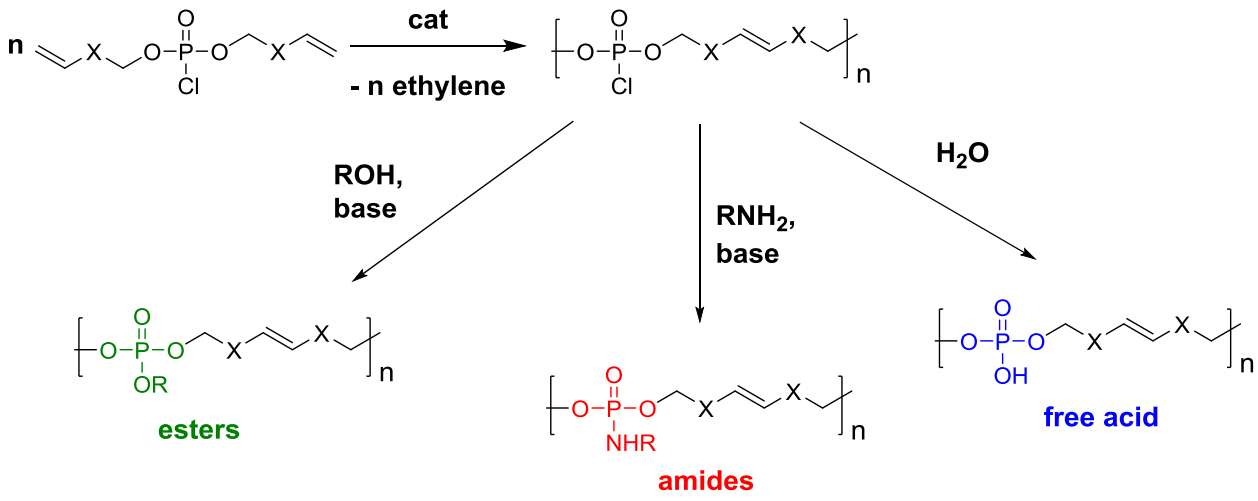

Scheme 1. Possible postpolymerization of poly(alkenyl phosphochloride)s (X = CH_2 or $(CH_2)_8$)

Di-(buten-3-yl) chlorophosphate **1** and the di-(undecen-10-yl) chlorophosphate **2** were used to generate reactive PPEs, which can be modified after the polymerization by the reactive acid chloride functionality. The protocol of the ADMET polymerization of the "chloro

monomers" **1** and **2** is described in Scheme 2 and in detail in the Supporting Information. Direct mixing of the monomer with Grubbs 1st generation catalyst (G1) in bulk or in 1-chlornaphthalene produces the polymer which is directly used for post-polymerization modifcation.

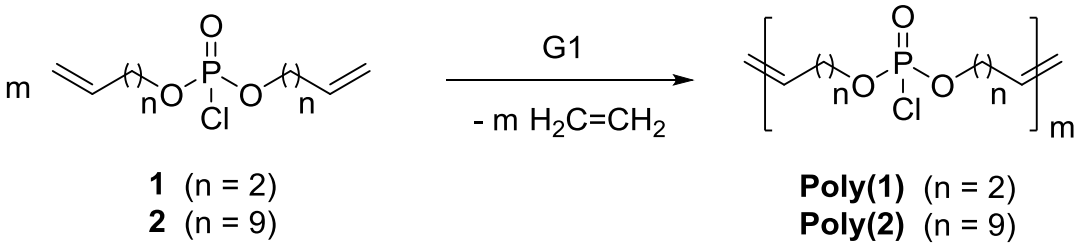

1 (n = 2)
2 (n = 9)

Poly(1) (n = 2)
Poly(2) (n = 9)

Scheme 2. ADMET polymerization of monomers **1** and **2**.

Table 1 lists the reaction conditions and the results of the polymerizations by Scheme 2. Noticeably, the solution polymerization produces higher molecular weights in shorter time periods, probably due to a better mixing of the reagents. Furthermore the polymerization of monomer 2 leads consistently to polymers with higher molecular weights as monomer 1 at the same reaction conditions (Table 1). This is based on the higher molecular weight of monomer 2 compared to monomer 1 which leads to polymers with higher molecular weights for the same number of repeating units.

Table 1. Conditions for the ADMET polycondensation (general representative procedure) of "chloro monomers" **1** and **2** and molecular weight data of the resulting polymers.

run	catalyst / mol%	monomer	reaction time / h	temperature / °C	conditions	DP_n [a]	M_n [a] / g·mol^{-1}
1	1.0	1	8	r.t	bulk [b]	13	3,000
2	1.0	2	8	r.t	bulk [b]	20	5,000
3	1.0	1	2	45 °C	bulk [b]	22	5,000
4	1.0	2	2	45 °C	bulk [b]	39	16,500
5	1.0	1	4	r.t	solution [c]	27	6,000
6	1.0	2	4	r.t	solution [c]	30	12,500
7	1.0	1	2	45 °C	solution [c]	47	10,500
8	1.0	2	2	45 °C	solution [c]	126	53,000

[a] Determined from endgroup analysis in ^{1}H NMR spectroscopy.
[b] Performed in bulk.
[c] Performed in 1-chloronaphthalene (50 wt%).

After addition of the Grubbs 1st generation catalyst, the reaction mixture immediately turned red with a gradual increase of the viscosity (only visible at bulk polymerizations) to give polymers with a broad range of molecular weights depending on the reaction conditions (Table 1). The polymeric materials isolated were in the range of 3,000-50,000 (M_n) g·mol^{-1}. Fig. 1 (and Fig. S1 – S12) shows the NMR spectra of polymers **poly(1)** and **poly(2)** as well as monomers **1** and **2**, respectively. The polymerization of monomer **1** is monitored by ^{1}H DOSY NMR spectroscopy: after polymerization the resonances of the terminal double bond protons (a and b) at 5.1 and 5.8 ppm are detected as the end groups of the polymers with a distinct lower diffusion coefficient compared to the monomer. Moreover, as expected, a new peak (c,c') appeared at 5.4 ppm due to formation of internal double bonds. Further, the methylene group next to the phosphorus (d: 4.25 ppm) and the methylene group next to the double bond can be distinguished. Also the ^{31}P{H} NMR (compare Fig. 2) shows a single resonance at ca. 4.5 ppm and ca. 4.8 ppm before and after polymerization of **1** and **2**, respectively (also see Fig. S3, S6, S9 and S12 in the Supporting Information) for the poly(alkylidene chlorophosphat)s.

As ADMET produces only linear polymers that possess terminal double bonds as the respective end groups, NMR spectroscopy allows the calculation of the absolute molecular

weight by integration of the terminal olefinic resonances in comparison with the internal double bonds (Table 1). For high molecular weights the method is limited, of course, as the noise to end group signal ratio increases.

In summary by variation of the reaction conditions the degree of polymerization for both **poly(1)** and **poly(2)** can be adjusted empirically (Table 1). GPC analysis of these polymers is not possible on our setup, as the polymer would react with the column material. The formation of high molecular weight polymers shows the highly stable catalyst system which is even stable in the presence of the electrophilic phosphoric acid chlorides.

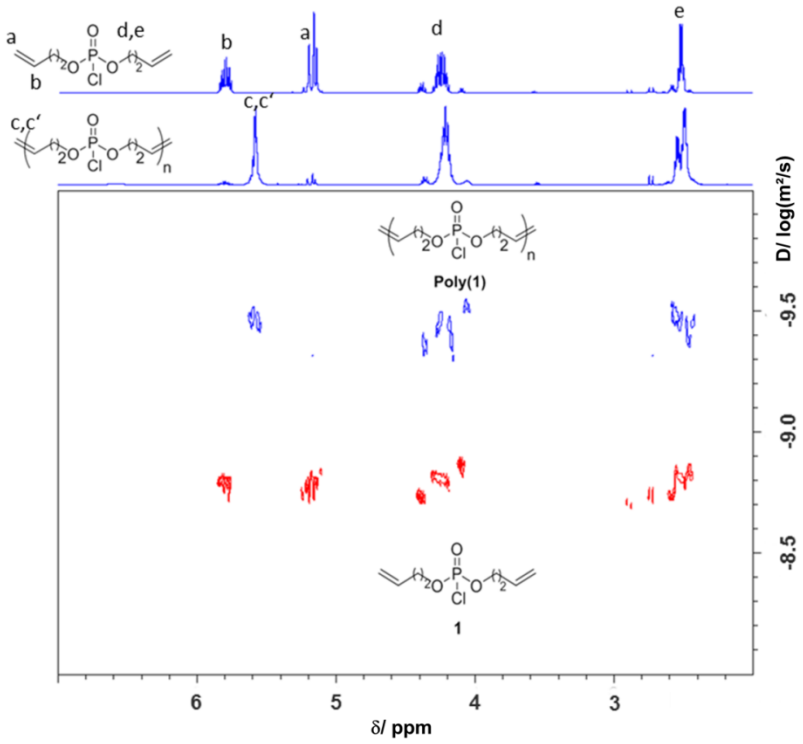

Figure 1. ^{1}H NMR spectrum of monomer 1 (top spectrum of the ^{1}H NMR axis; red signals in the DOSY spectrum) and the respective polymer poly(1) (bottom spectrum of the ^{1}H NMR axis; blue signals of DOSY spectrum) proving the formation of internal double bonds at 5.4 ppm (500 MHz in $CDCl_3$ at 25 °C).

The reactive poly(alkenyl chloro phosphate)s are a valuable platform for the post-polymerization modification with several nucleophiles. A similar strategy was presented by Allcock and coworkers in several elegant works on poly(dichloro phosphazene)s that are postmodified with various alcohols, amines, etc. for a great variety of applications.[156-157]

However, the herein presented polymers allow a higher variation: the combination of the phosphate chemistry and olefin metathesis is an ideal platform to adjust polymer properties. Poly(dichlorophosphazene) is typically synthesized from ammonium chloride with phosphorus pentachloride at 250 °C.[156-157] The polymerization is hard to control, and usually leading to high molecular weights polymers with high molecular weight distributions. Further, the backbone of polyphosphazenes is extremely hydrolysis sensitive while the phosphate linkages are more stable and can carry additional functionalities.[156-157]

Motivated by these facts, it was feasible to synthesize reactive PPEs with a decent stability in the presence of water and air. In order to confirm these properties, the poly(alkylidene chlorophosphate)s were exposed to different nucleophiles such as 2-methoxyethanol ($MeO(CH_2)_2OH$), as well as 2-hydroxyethylmethacrylate (HEMA), phenol (PhOH), ferrocenemethanol ($fcCH_2OH$), water (H_2O) and benzylamine ($BnNH_2$) in the presence of a base in order to remove the hydrogen chloride byproduct. The polymer modification was conducted by adding the respective reagent to polymer **poly(1)** dissolved in dichloromethane (CH_2Cl_2) in the presence of triethyl amine or after deprotonation the respective alkoxide in case of the $fcCH_2OH$-modified polymer. Reactions were mostly realized with polymer **poly(1)**, as it has a higher density of substitutable chloride atoms at the same length as the polymer **poly(2),** so it has more potential functionalization points per length unit.

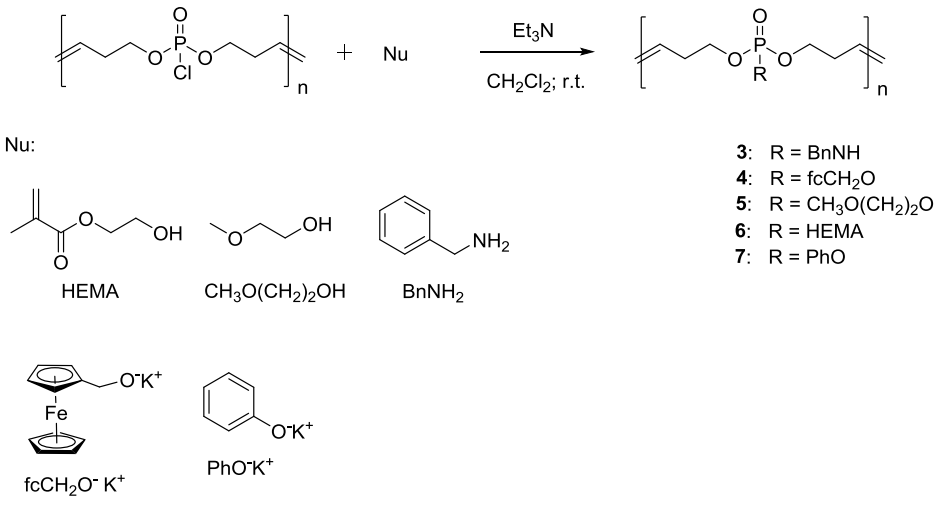

Scheme 3. Postmodification of poly[di-(buten-3-yl) chlorophosphate] (**poly(1)**) with a respective reagent.

^{31}P{H} NMR spectroscopy was used to prove the complete conversion of the polymer **poly(1)** since it is known that the ^{31}P{H} NMR resonance appears at a chemical shift of 4.57 ppm (compare above). ^{31}P{H} NMR spectroscopy was used to prove the complete conversion of the polymer **poly(1)**, since the chemical shift for the P-Cl resonances at 4.57 ppm disappeared after the reaction completely and new phosphorus resonances can be detected. It is shown in the spectra of the modified polymers (Fig. 2) that there are no signals of phosphorus next to chloride atoms at 4.57 ppm left instead new signals emerge at different chemical shifts respectively to the new neighbor to the phosphorus. Fig. 2 shows the shift of the ^{31}P{H} NMR signal to higher or lower chemical shifts according to the nucleophile. The ^{31}P{H} NMR resonances for polyphosphates are detected at lower chemical shifts than the phosphochlorides (between 4 and 1 ppm depending on the nature of the pendant ester). The poly(phosphoamidate) which is easily accessible via this route is detected at a characteristic ^{31}P{H} resonance at 8.85 ppm.[90] Additional NMR spectra can be found in the Supporting Information.

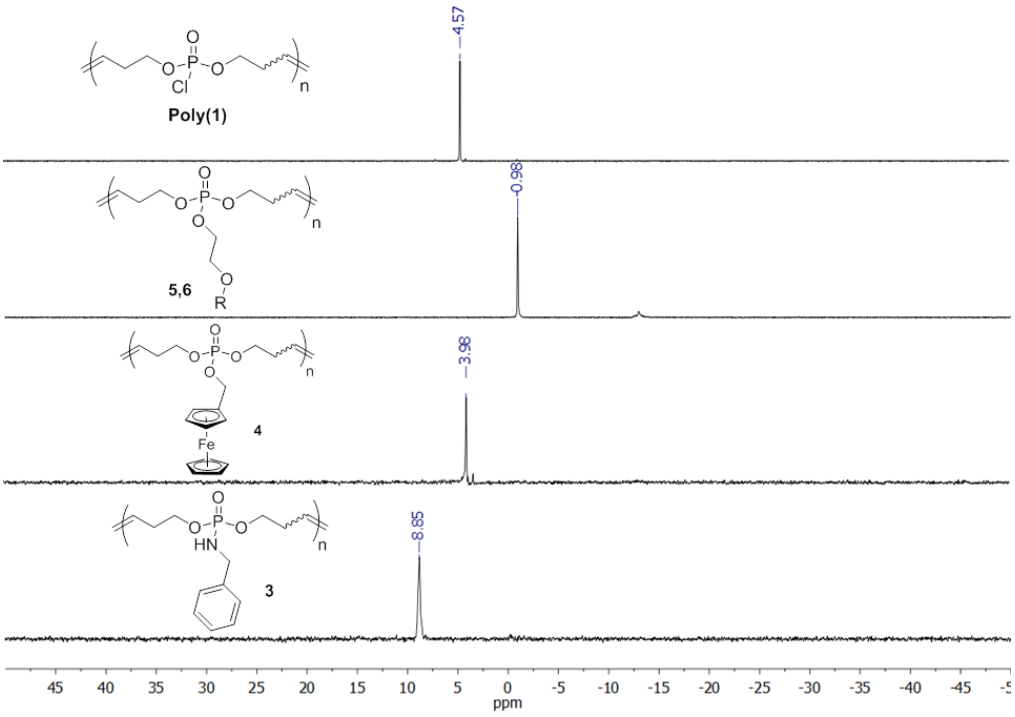

Figure 2: ^{31}P{H} NMR spectra of polymers poly(1), 3, 4, 5, 6 (284 MHz, 25 °C).

A crucial point for post polymerization modification of degradable polyesters with nucleophiles is the integrity of the polymer backbone during the reaction. Both nucleophilic reagents and the HCl side product could degrade the polymer or cause transesterification reactions. A clear and straightforward proof that the polymer backbone remains intact is given by ^{1}H DOSY NMR (and GPC, compare Supporting Information); Figure 3 shows an overlay of the 1H NMR spectra and the 1H DOSY spectra of poly(1) and polymer **3** proving a successful modification with benzylamine to the poly(phosphoamidate) without any degradation of the polymer backbone as no signals with higher diffusion coefficient (i.e. lower molecular weight) are detected.

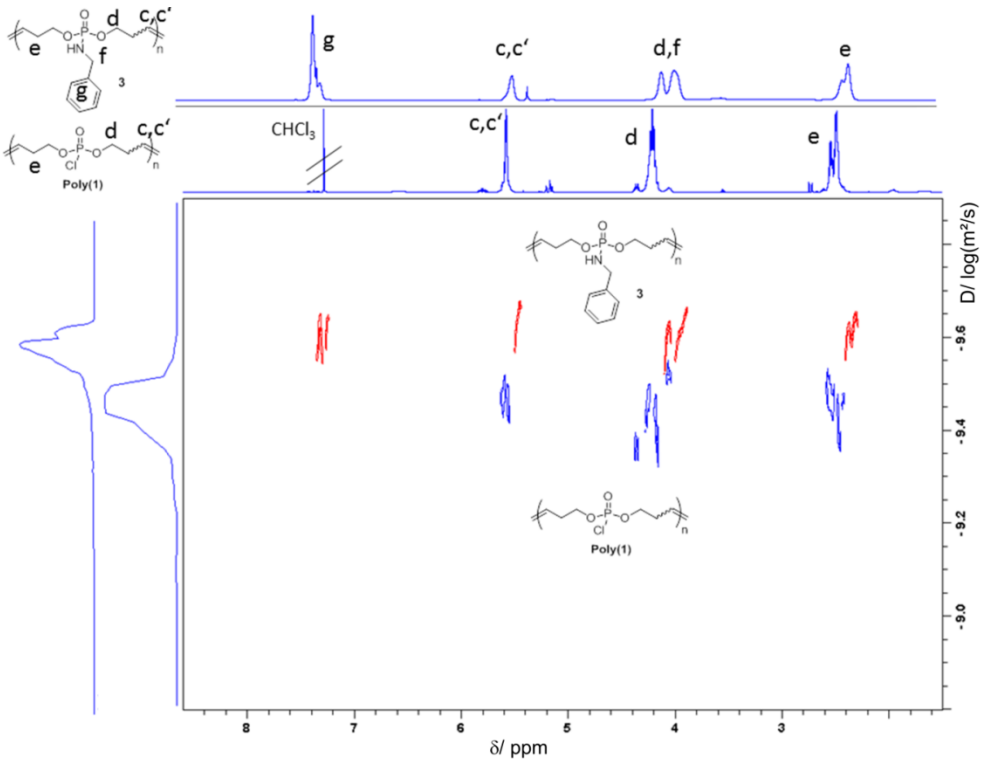

Figure 3. Overlay of ^{1}H DOSY NMR spectra of **poly(1)** and polymer **3** proving the efficient post-polymerization functionalization of **poly(1)** to polymer **3** and no degradation. (500 MHz in $CDCl_3$ at 25 °C).

Conclusions

A novel approach was developed for the synthesis of highly reactive poly(alkenyl chlorophosphate)s via acyclic diene metathesis polymerization. This is the first report on the synthesis of a poly(alkenyl phosphochloride) via olefin metathesis and its subsequent postpolymerization modification with various nucleophiles.

The reactive PPEs were synthesized via bulk and solution polymerization using Grubbs 1st generation catalyst. The molecular weights depending on the different reaction conditions can be adjusted from an oligomer to a high molecular weight polymer with molecular weights up to 50,000 g/mol which is probably not an upper limit. The polymers were reacted with different alcohols/alkoxides, water or amines to polyphosphates and poly(phosphoamidate)s. This general platform is highly interesting to access materials which are not accessible via conventional polycondensation or metathesis polymerization such as side-chain olefins or acrylates.

Applications like main chain adhesives or other possibilities according to the high variety of the functional groups are imaginable for these materials. With phosphate linkages along the unsaturated backbone, various properties of these unsaturated polyesters could be altered in future applications. Many post-polymerization reactions might be carried out in order to link thiols on the internal double bonds, silyl groups on the terminal double bonds, or to use them as macroinitiator for controlled radical polymerization for example. The unsaturated PPEs are also interesting candidates for biomedical applications and as potential tissue engineering scaffold materials[79], as well as in materials science due to their flame-retardant properties[158].

Acknowledgements

The authors thank Prof. Dr. Katharina Landfester for her support. F.R.W. thanks the Max Planck Graduate Center (MPGC) for support.

3.1.2 Cross-linkable poly(phosphoester)s carrying methacrylate side chains

As seen in the previous section of the chapter, multiple simultaneous modifications of a functional group can be achieved by using reactive poly(chlorophosphate)s. This advantage can be used to prepare well-designed polymers and obtain desired properties such as adhesive features. However, the installation of polymerizable acrylate groups is not possible directly by ADMET; thus, hydroxyl ethyl methacrylate was used to postmodify the reactive poly(chlorophosphate)s. Therefore, 30 % of HEMA and 35 % of 2-methoxyethanol modified polymers were produced which were soluble in water/alcohol mixtures (**Scheme 1**).

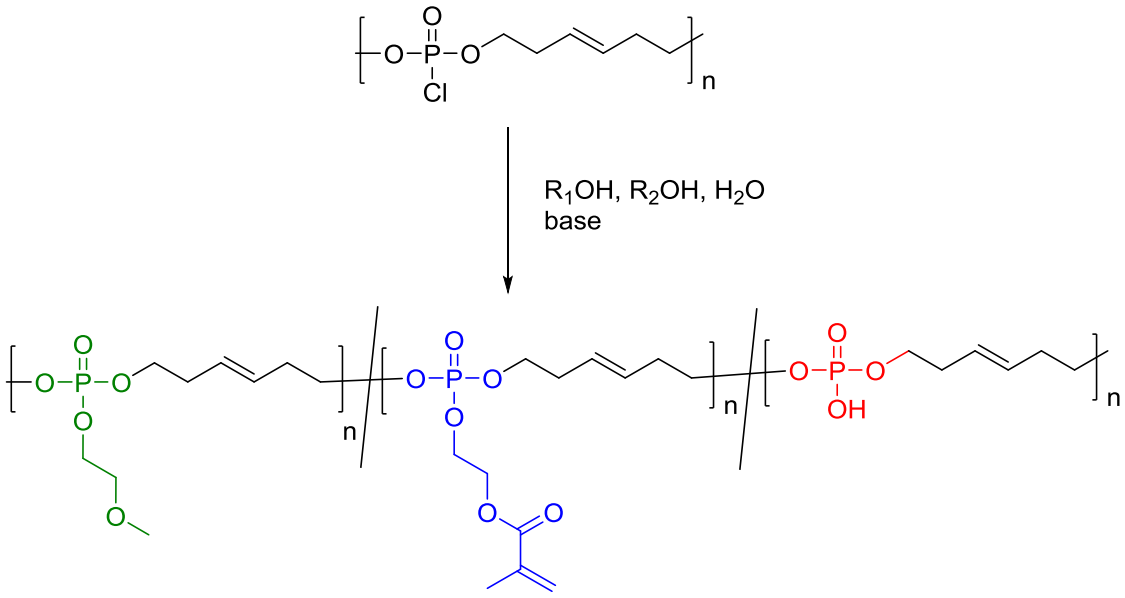

Scheme 1: Functionalization of poly(chlorophosphate) by HEMA, 2-methoxyethanol, and H_2O.

The simultaneous functionalization was accomplished by dissolving poly(chlorophosphate) with HEMA and 2-methoxyethanol in toluene with triethylamine. After 24 hours, an excess of water was added to the mixture and stirring again for 24 hours. Purification by washing the organic phase leads to pure product.

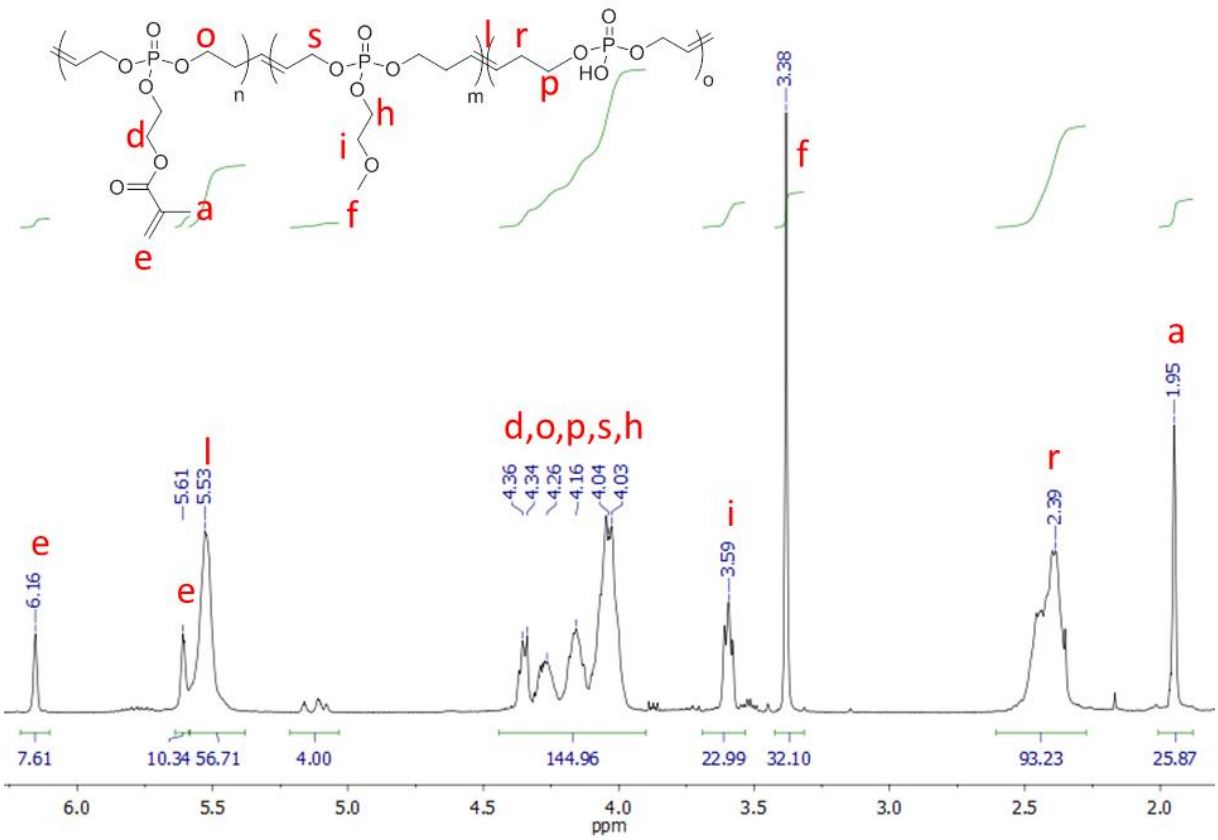

Figure 1: ^{1}H NMR spectrum of functionalized poly(dialkylene chlorophosphate) by HEMA, 2-methoxyethanol and H_2O (300 MHz, 298 K, $CDCl_3$).

All resonance signals by ^{1}H NMR are assigned to the copolymer in **Figure 1**. Clearly detectable are the acrylate protons (e) and the methyl group (a) of HEMA, as well as the methyl group (f) and the methylene group (i) of 2-methyoxyethanol. By integration of these signals and comparing with the integral of the internal double bond (l), the ratio of HEMA and 2-methoxyethanol has been calculated. The resulting ratio at this example batch is: 30 % of HEMA and 38 % of 2-methoxyethanol substituted copolymer. Moreover, ^{1}H NMR end group analysis reveals a molecular weight of 6,300 g mol^{-1}.

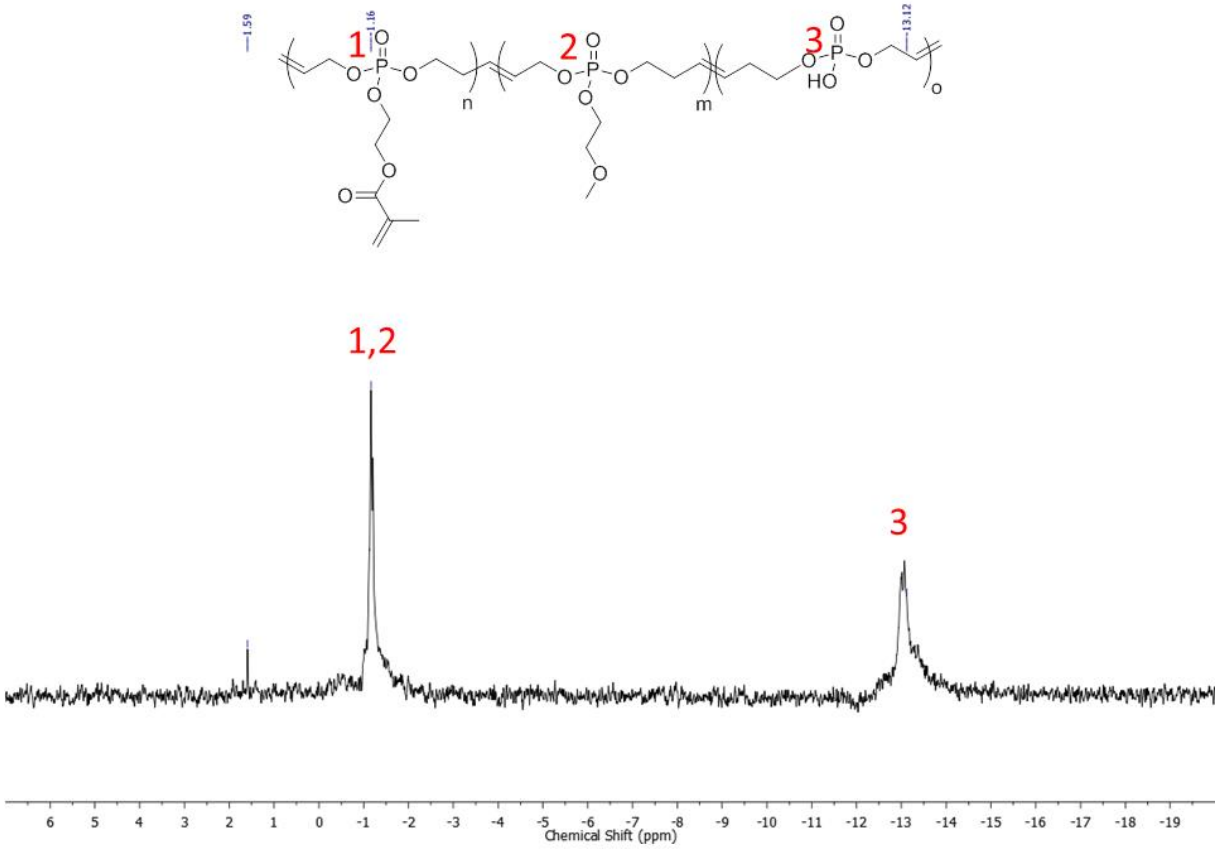

Figure 2: $^{31}P\{H\}$ NMR spectrum of functionalized poly(dialkylene chlorophosphate) by HEMA, 2-methoxyethanol and H_2O (176 MHz, 298 K, $CDCl_3$).

The $^{31}P\{H\}$ NMR spectrum of the modified polymer displays the different environments of phosphorus based on various binding motifs. Phosphate species 1 and 2 are very similar because of the same environment directly next to the phosphorus. This is why signals 1 and 2 cannot be detected separately. However, the phosphoric acid diester represented by signal 3 is clearly detectable at lower chemical shifts.

Conclusion

The simultaneous modification by three different nucleophiles has been accomplished. NMR data confirms the successful transformation to a copolymer and can be used to calculate the ratio of modification. These materials will be further investigated as adhesive materials, e.g. for tissue engineering.

Experimental section

For chemicals and methods see Experimental section of Chapter 3.1.1.

Monomer synthesis of di-(but-3-en-1-yl) chlorophosphate (1). and the subsequent ADMET bulk polymerization to poly[hex-3-en-1-yl chlorophosphate] (Poly(1)) has been shown in the Experimental section of Chapter 3.1.1.

General procedure for the postpolymerization modification of poly[hex-3-en-1-yl chlorophosphate] with various nucleophiles is also indicated in the Experimental section of Chapter 3.1.1.

Synthesis of polymer modified with HEMA, 2-methoxyethanol and hydroxyl groups. The reaction was carried out following the general procedure in **Chapter 3.1.1** by using 250 mg (1.12 mmol) poly[hex-3-en-1-yl chlorophosphate] with HEMA (29.2 mg, 27.2 µl, 0.224 mmol, 0.2 eq), 2-methoxyethanol (17.0 mg, 17.6 µl, 0.224 mmol, 0.2 eq), and subsequent an excess of water as nucleophiles. The following spectral properties were observed: ^{1}H NMR (300 MHz, 298 K, $CDCl_3$, δ / ppm): 6.19 – 6.12 (m), 5.64 – 5.58 (m), 5.56 – 5.49 (m), 4.39 – 4.30 (m), 4.19 – 4.12 (m), 4.07 – 3.99 (m), 3.63 – 3.56 (m), 3.42 – 3.35 (m), 2.42 – 2.35 (m), 1.98 – 1.92 (m). ^{13}C{H} NMR (176 MHz, 298 K, $CDCl_3$, δ / ppm): 167.0, 135.8, 127.1, 126.3, 71.3, 67.2, 67.0, 66.7, 66.6, 65.3, 63.2, 58.9, 33.5, 28.5, 18.3. ^{31}P{H} NMR (284 MHz, 298 K, $CDCl_3$, δ / ppm): -1.16, -13.12.

Supporting Information for

Poly(alkylidene chlorophosphate)s via acyclic diene metathesis polymerization: A general platform for the post-polymerization modification of poly(phosphoester)s

*Mark Steinmann, Jens Markwart, Frederik R. Wurm**

Max Planck Institut für Polymerforschung, Ackermannweg 10, 55128 Mainz, Germany.

Contact address: wurm@mpip-mainz.mpg.de

GPC

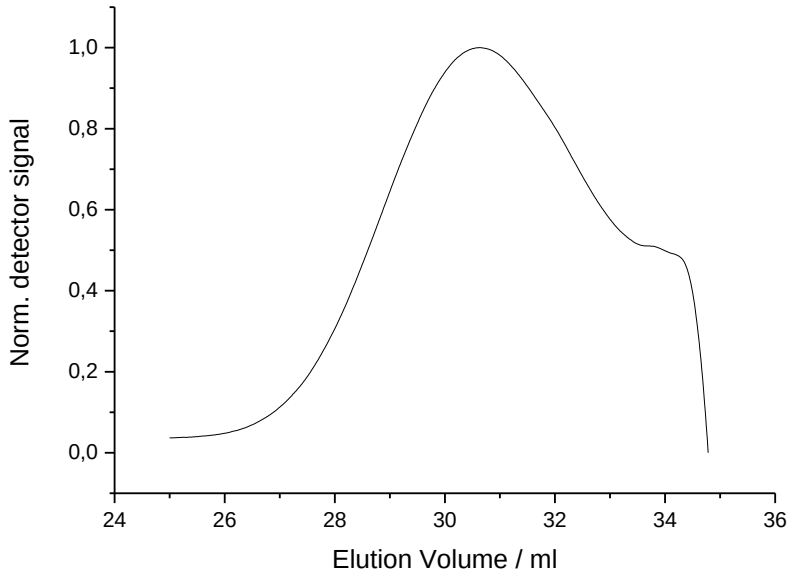

Figure S1: GPC-elugram of polymer **3** vs. polystyrene standards in DMF. This is a representative example for all polymers synthesized herein (with a molecular weight dispersity of 2.0).

NMR

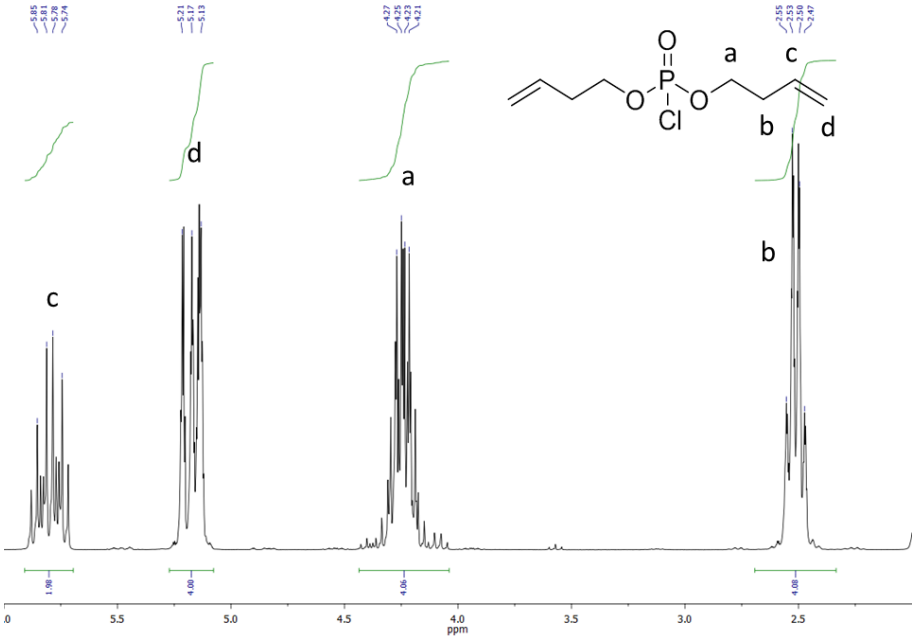

Figure S2: ^{1}H NMR of **1** (250MHz, 298 K, $CDCl_3$)

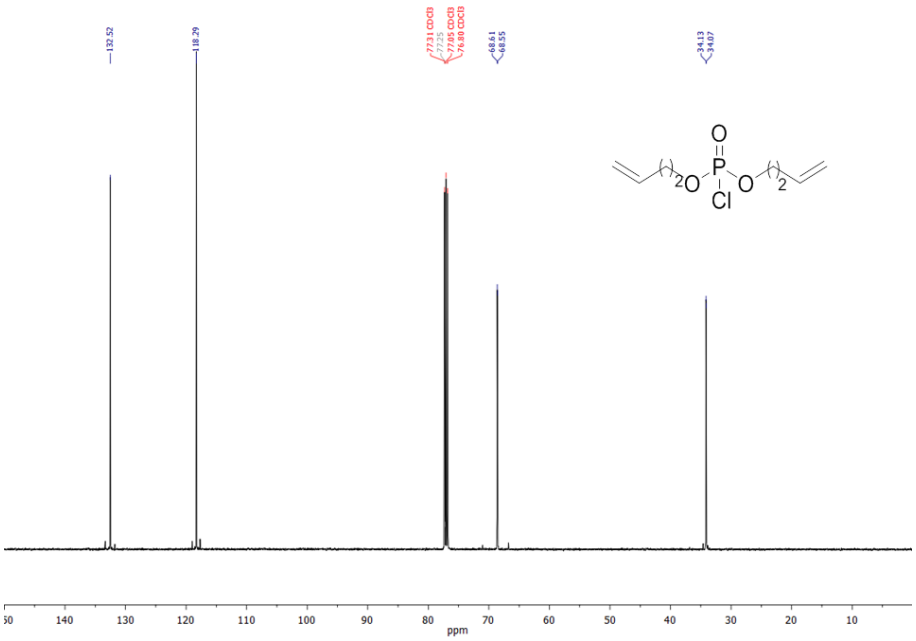

Figure S3: ^{13}C{H} NMR of **1** (126MHz, 298 K, $CDCl_3$)

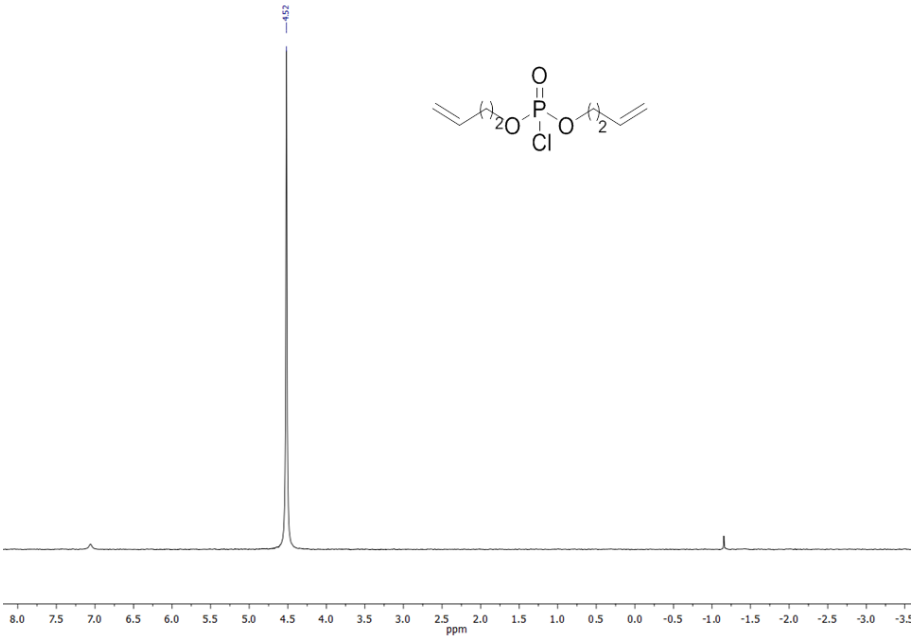

Figure S4: $^{31}P\{H\}$ NMR of **1** (202MHz, 298 K, $CDCl_3$)

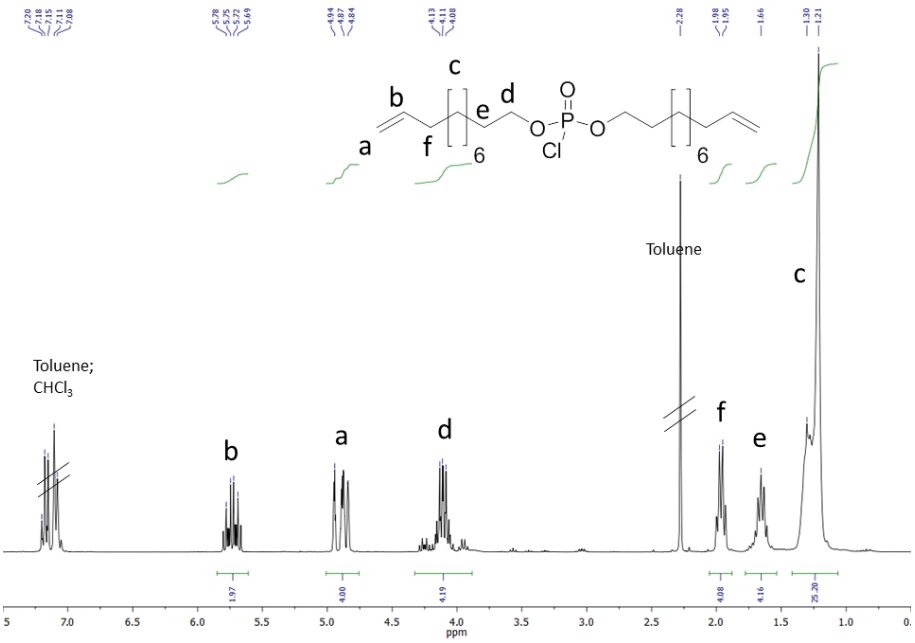

Figure S5: ^{1}H NMR of **2** (300MHz, 298 K, $CDCl_3$)

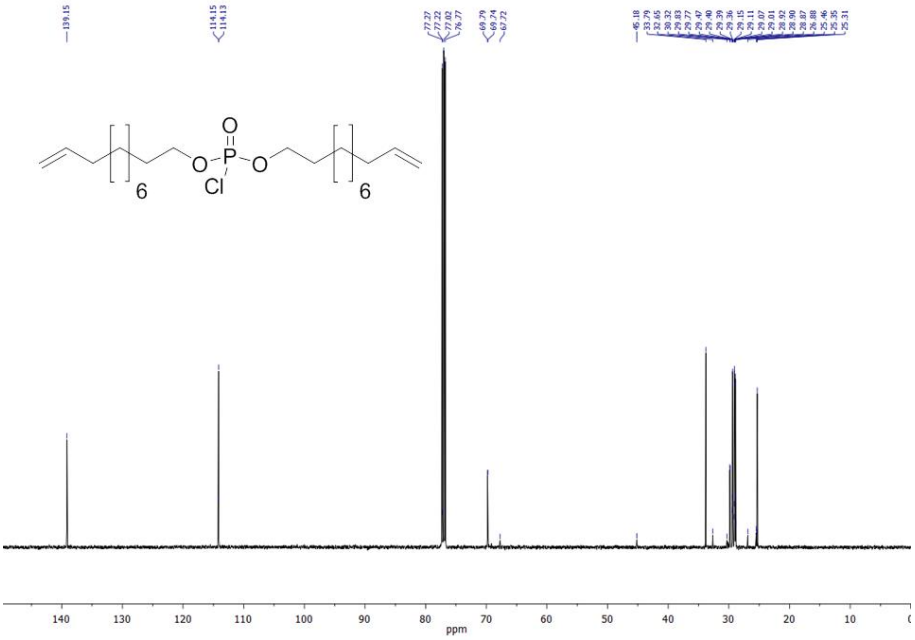

Figure S6: $^{13}C\{H\}$ NMR of **2** (126MHz, 298 K, $CDCl_3$)

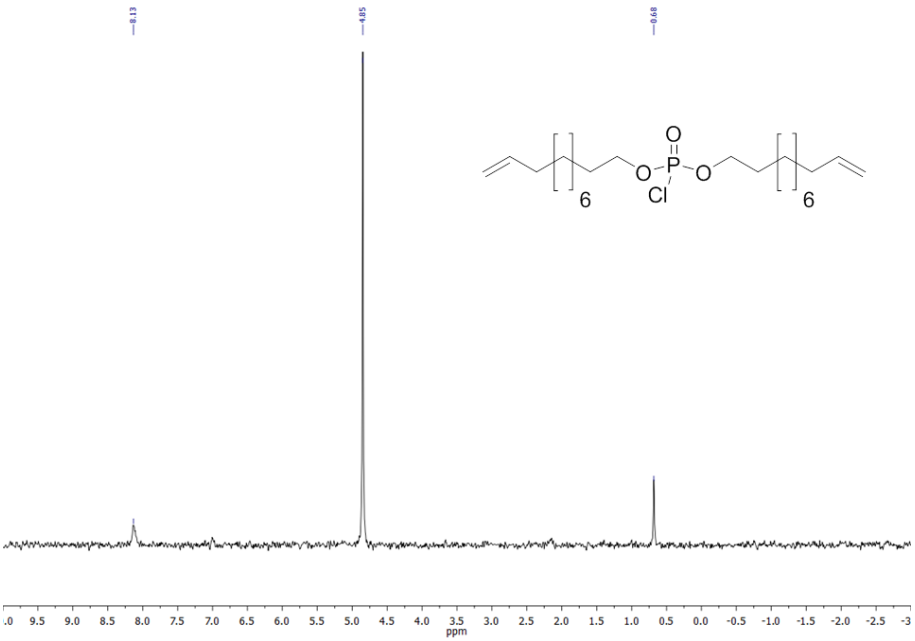

Figure S7: $^{31}P\{H\}$ NMR of **2** (202MHz, 298 K, $CDCl_3$)

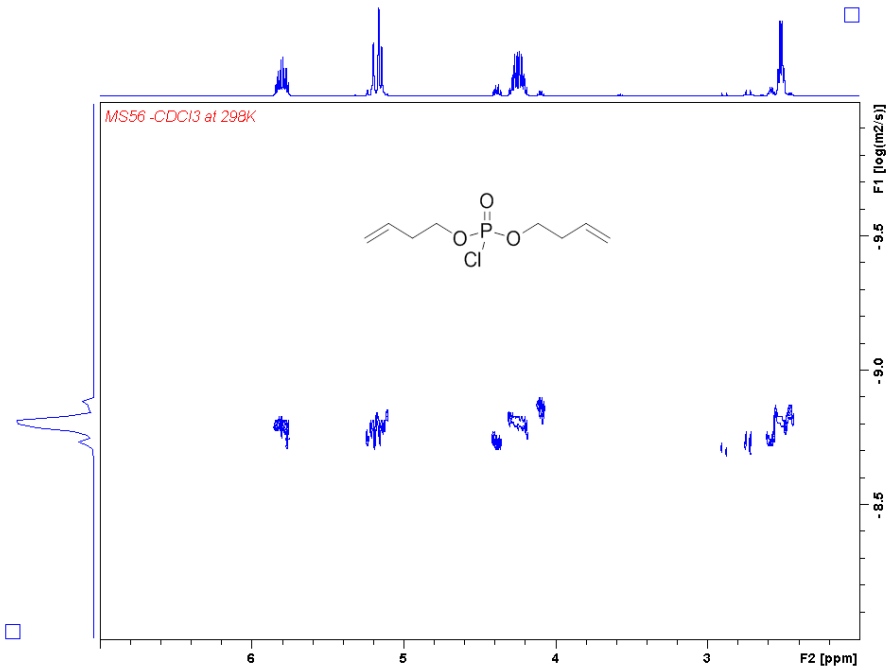

Figure S8: H DOSY of **2** (500 MHz, 298 K, $CDCl_3$)

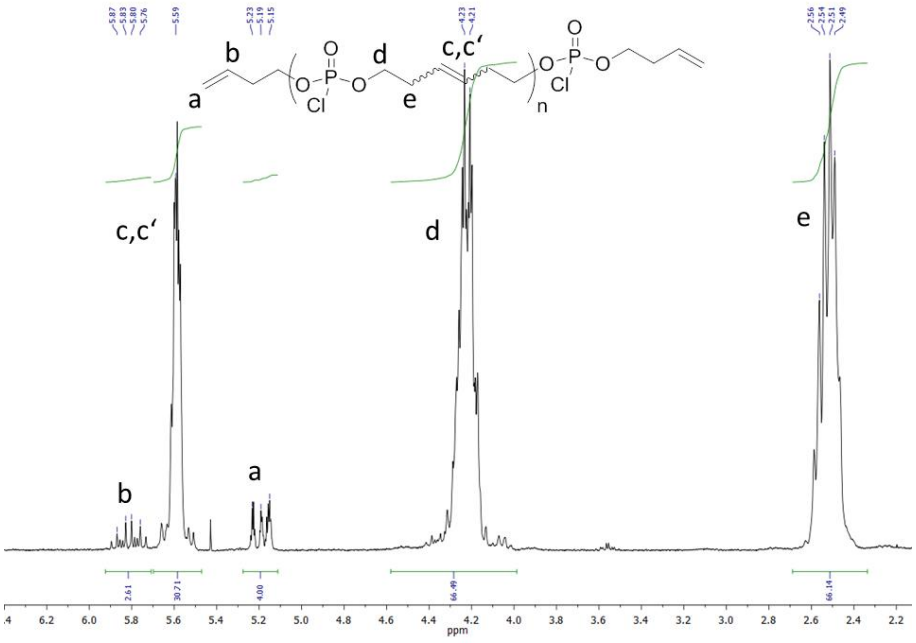

Figure S9: ^{1}H NMR of **Poly(1)** (250MHz, 298 K, $CDCl_3$)

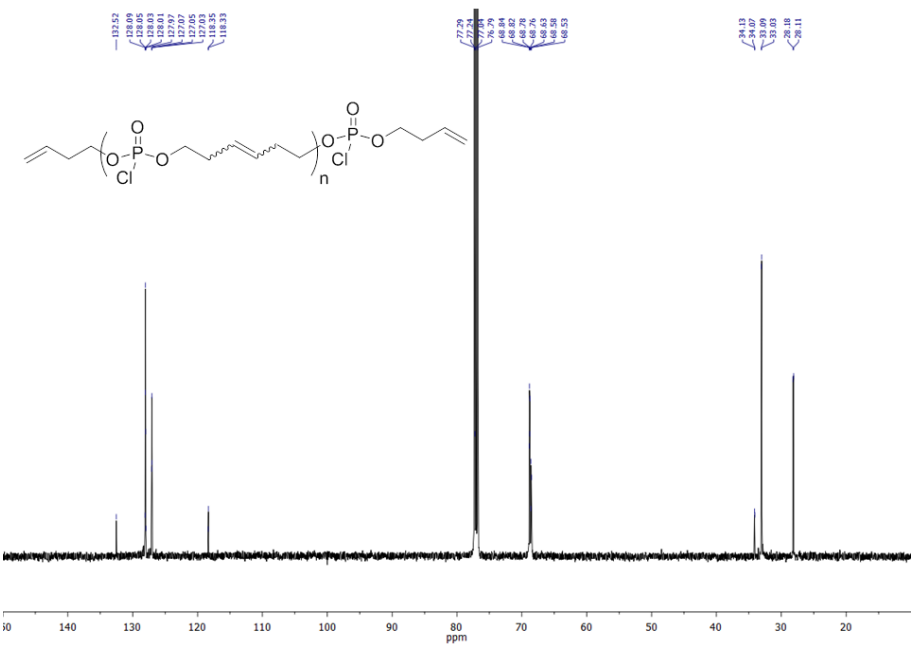

Figure S10: $^{13}C\{H\}$ NMR of **Poly(1)** (126MHz, 298 K, $CDCl_3$)

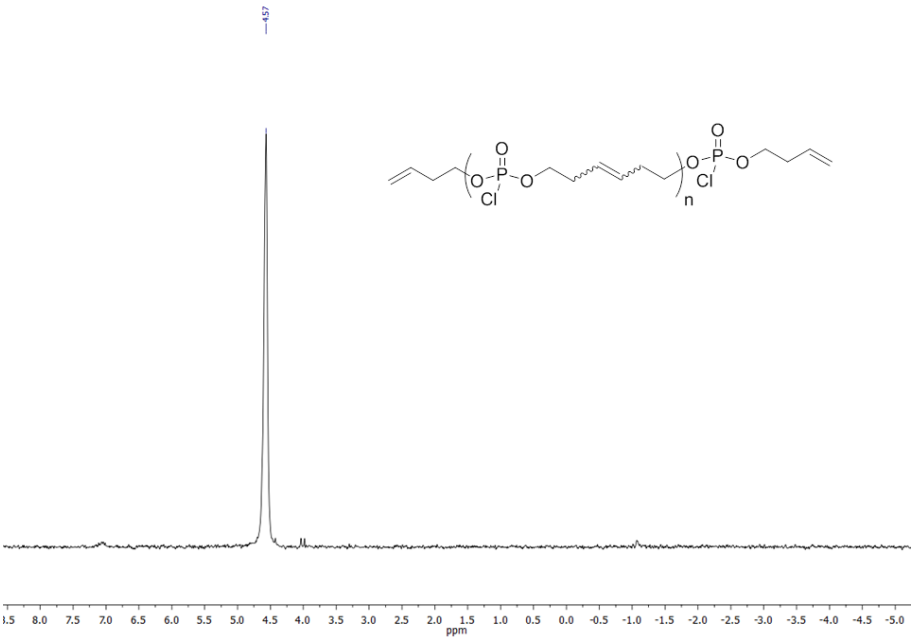

Figure S11: $^{31}P\{H\}$ NMR of **Poly(1)** (202MHz, 298 K, $CDCl_3$)

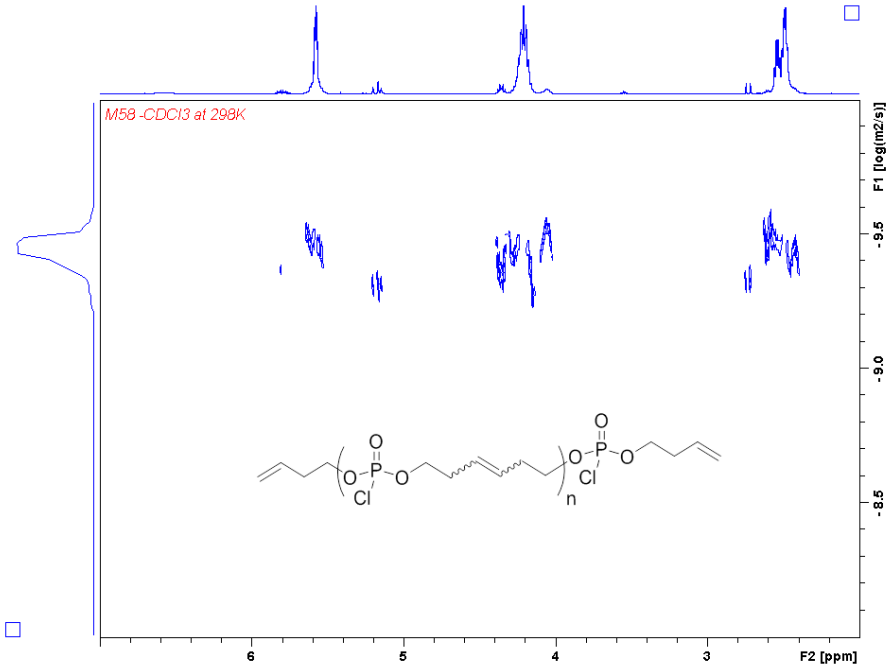

Figure S12: H DOSY of **Poly(1)** (500 MHz, 298 K, $CDCl_3$)

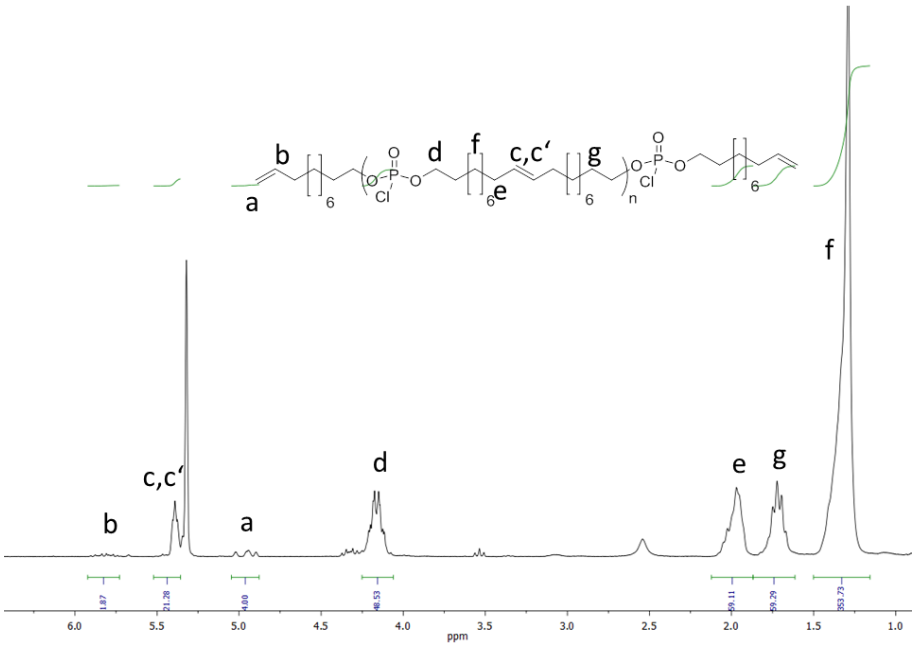

Figure S13: ^{1}H NMR of **Poly(2)** (250MHz, 298 K, $CDCl_3$)

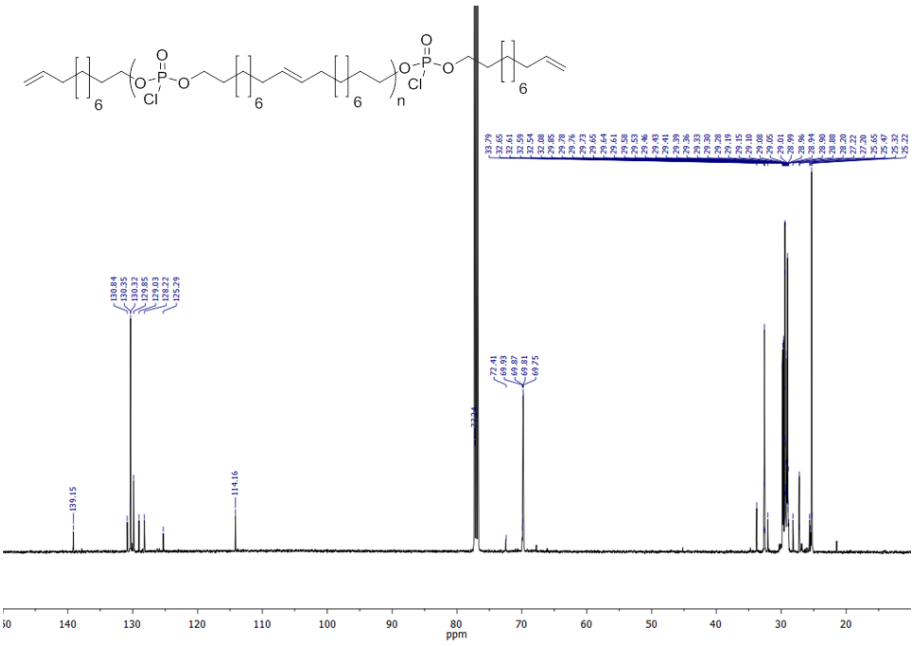

Figure S14: ^{13}C{H} NMR of **Poly(2)** (126MHz, 298 K, $CDCl_3$)

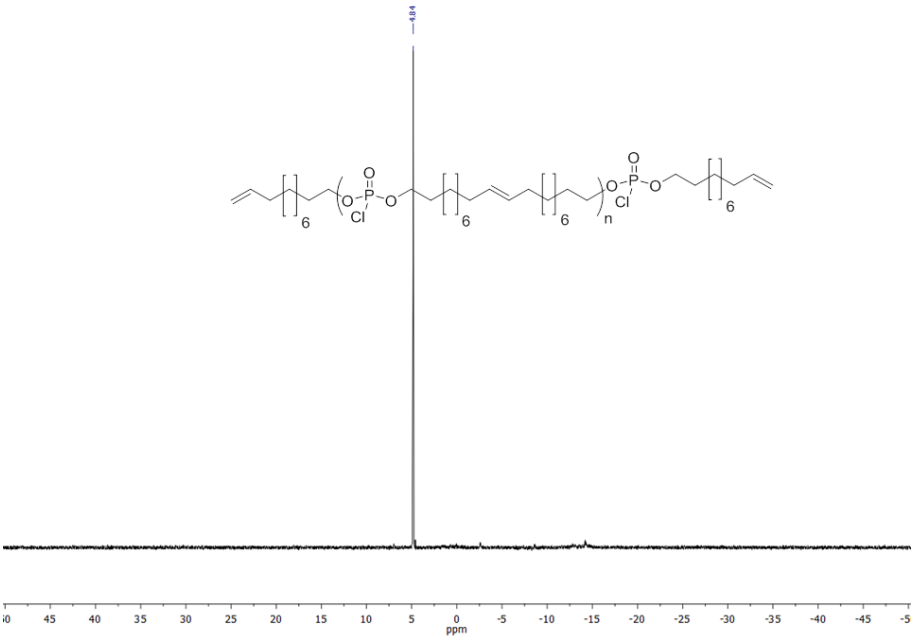

Figure S15: $^{31}P\{H\}$ NMR of **Poly(2)** (284 MHz, 298 K, $CDCl_3$)

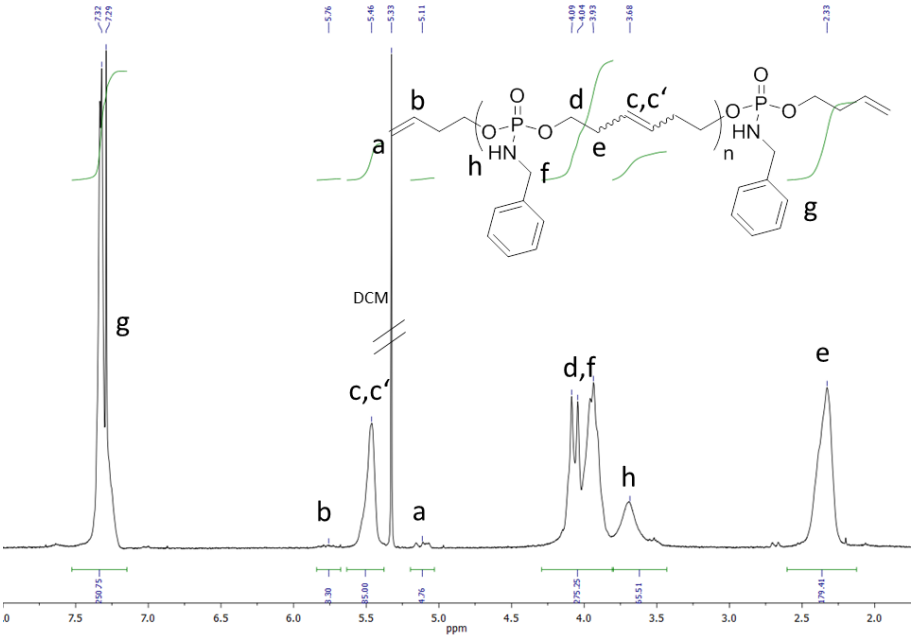

Figure S16: ^{1}H NMR of **3** (250MHz, 298 K, $CDCl_3$)

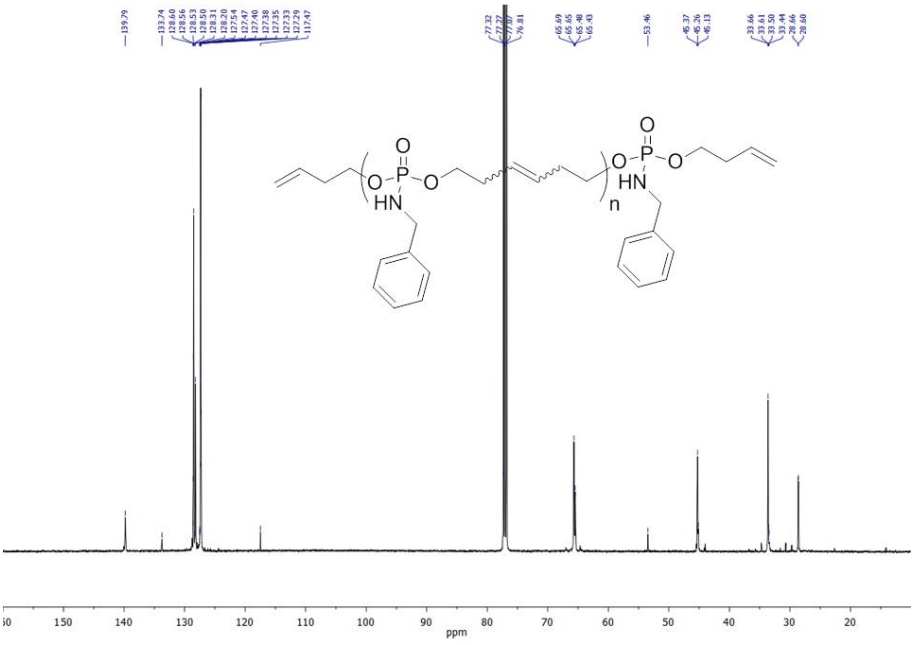

Figure S17: $^{13}C\{H\}$ NMR of **3** (126MHz, 298 K, $CDCl_3$)

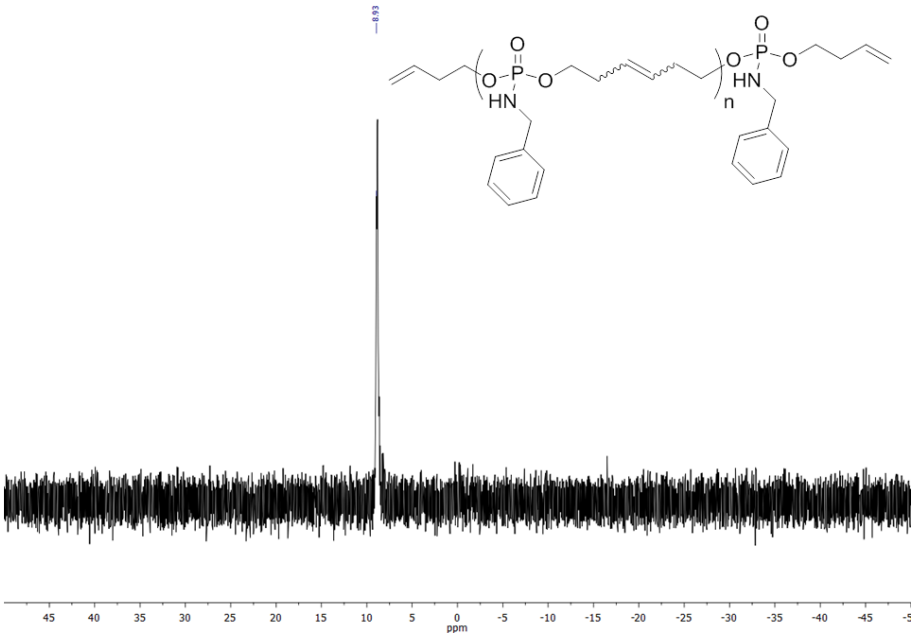

Figure S18: $^{31}P\{H\}$ NMR of **3** (284MHz, 298 K, $CDCl_3$)

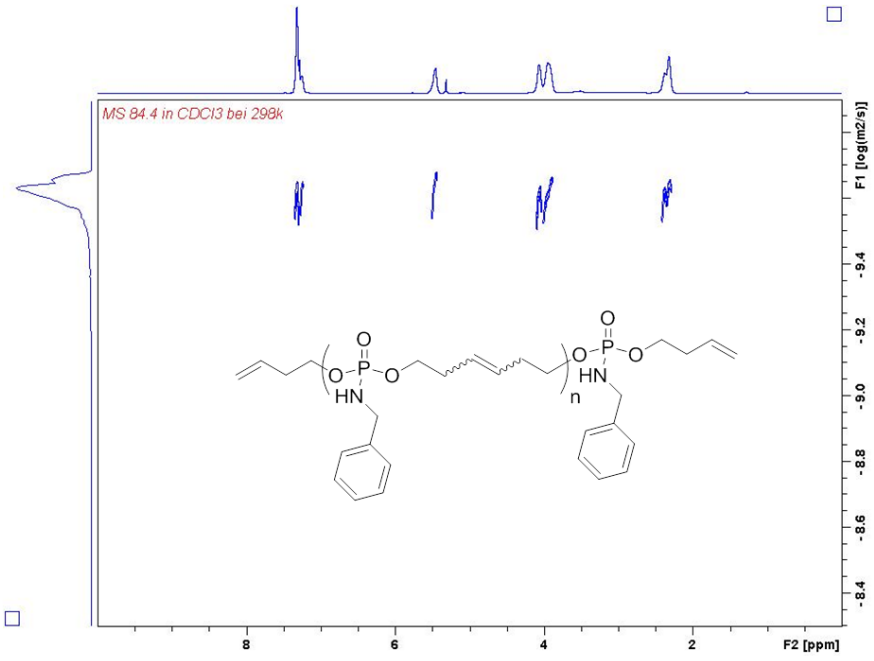

Figure S19: ^{1}H DOSY of **3** (500 MHz, 298 K, $CDCl_3$)

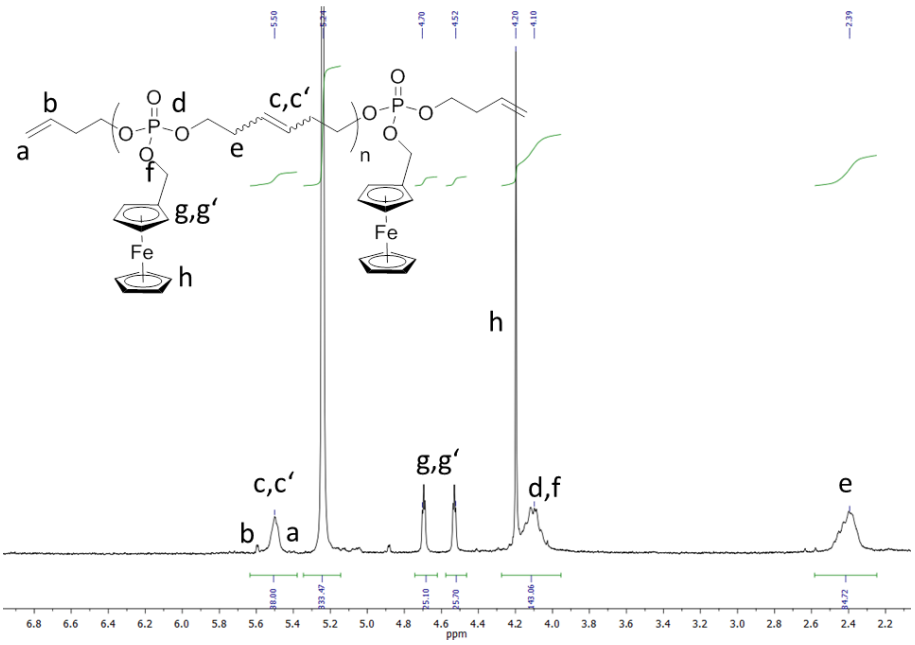

Figure S20: ^{1}H NMR of **4** (250MHz, 298 K, CD_2Cl_2)

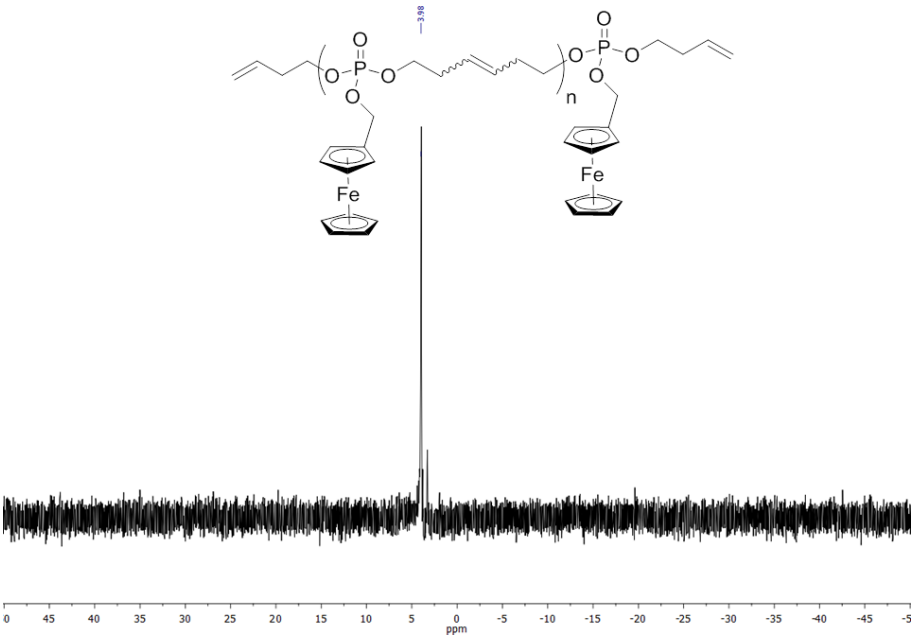

Figure S21: $^{31}P\{H\}$ NMR of **4** (284MHz, 298 K, CD_2Cl_2)

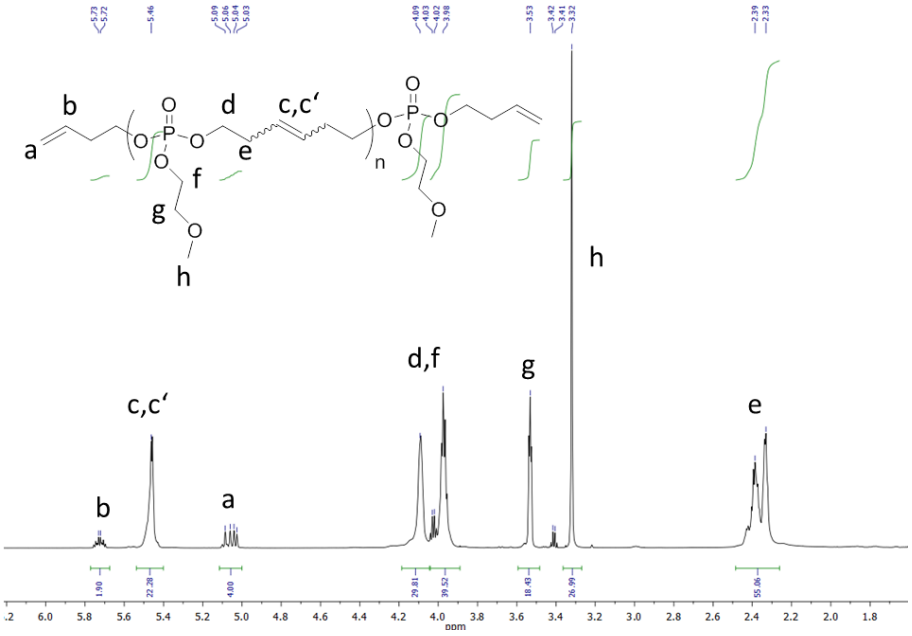

Figure S22: ^{1}H NMR of **5** (700MHz, 298 K, $CDCl_3$)

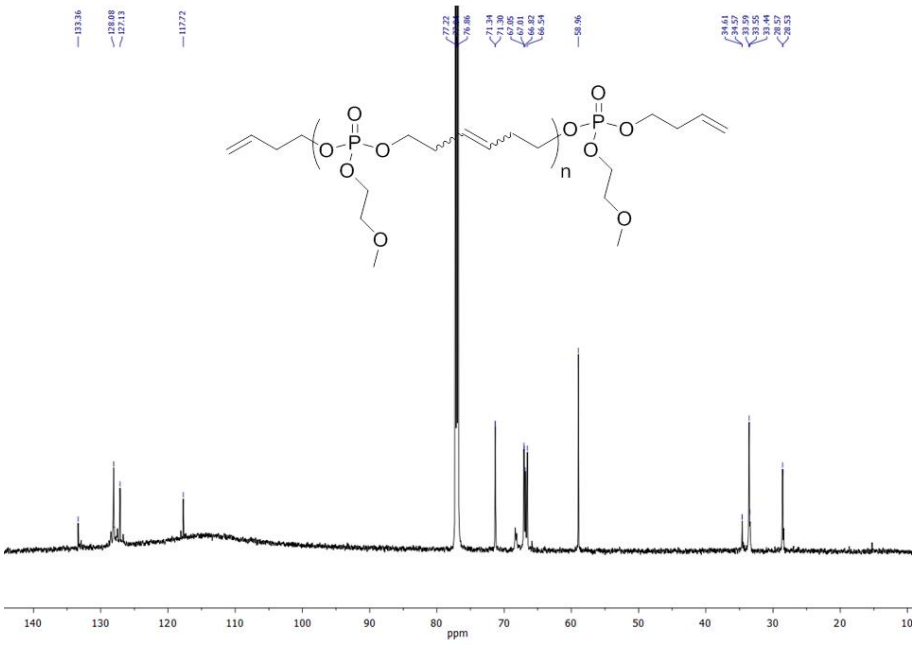

Figure S23: $^{13}C\{H\}$ NMR of **5** (176MHz, 298 K, $CDCl_3$)

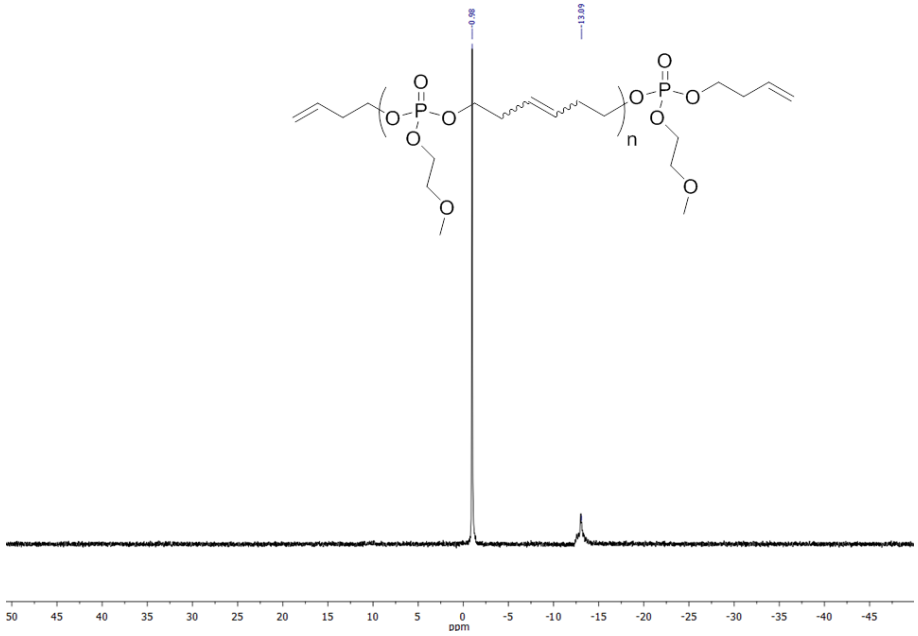

Figure S24: $^{31}P\{H\}$ NMR of **5** (284MHz, 298 K, $CDCl_3$)

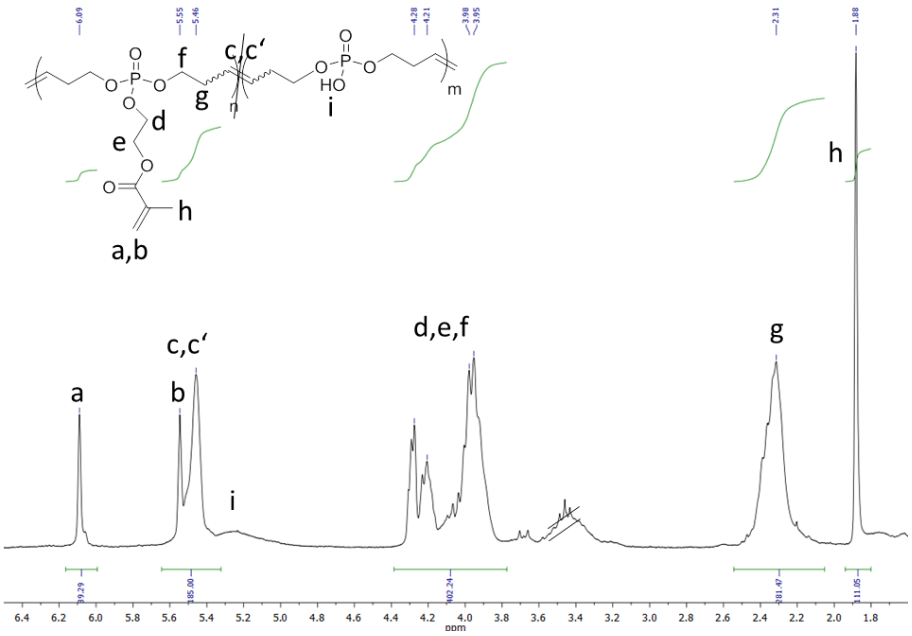

Figure S25: ^{1}H NMR of **6** (250 MHz, 298 K, $CDCl_3$)

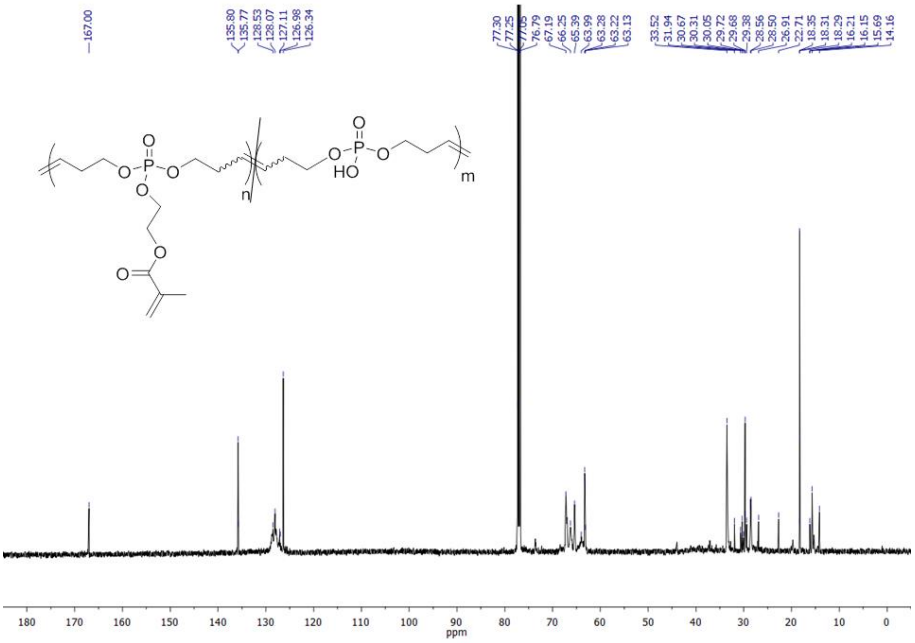

Figure S26: ^{13}C{H} NMR of **6** (126 MHz, 298 K, $CDCl_3$)

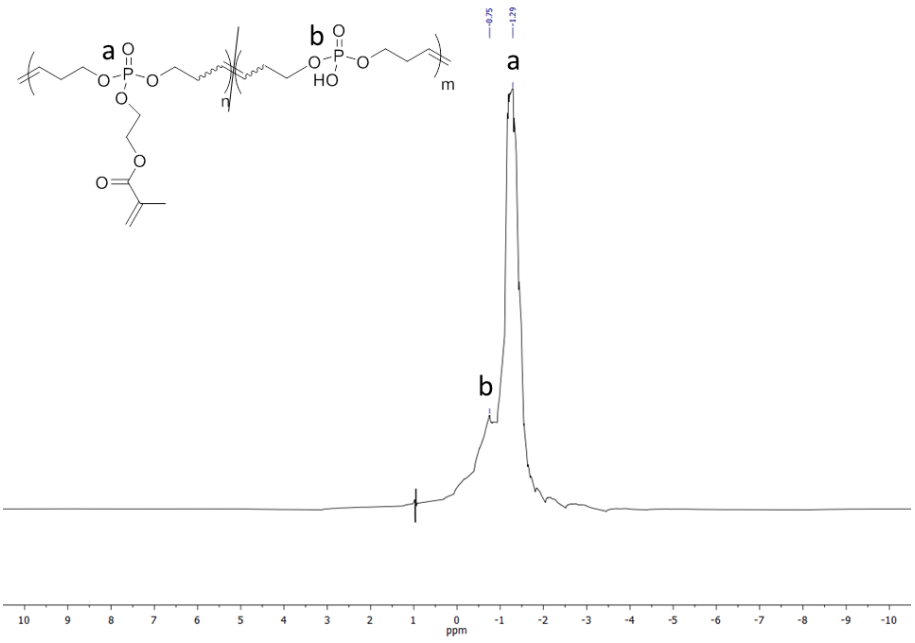

Figure S27: $^{31}P\{H\}$ NMR of **6** (202 MHz, 298 K, $CDCl_3$)

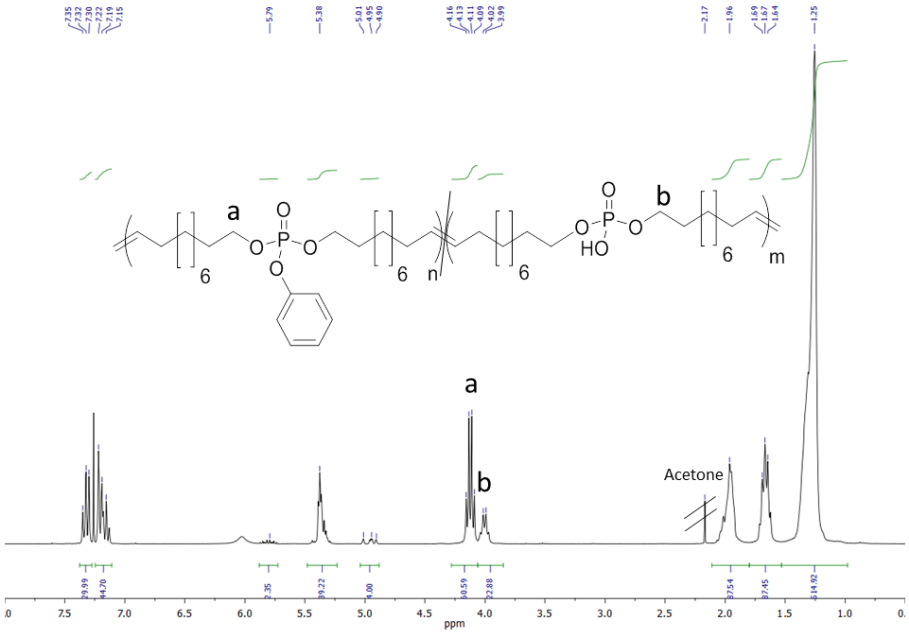

Figure S28: ^{1}H NMR of **7** (300 MHz, 298 K, $CDCl_3$)

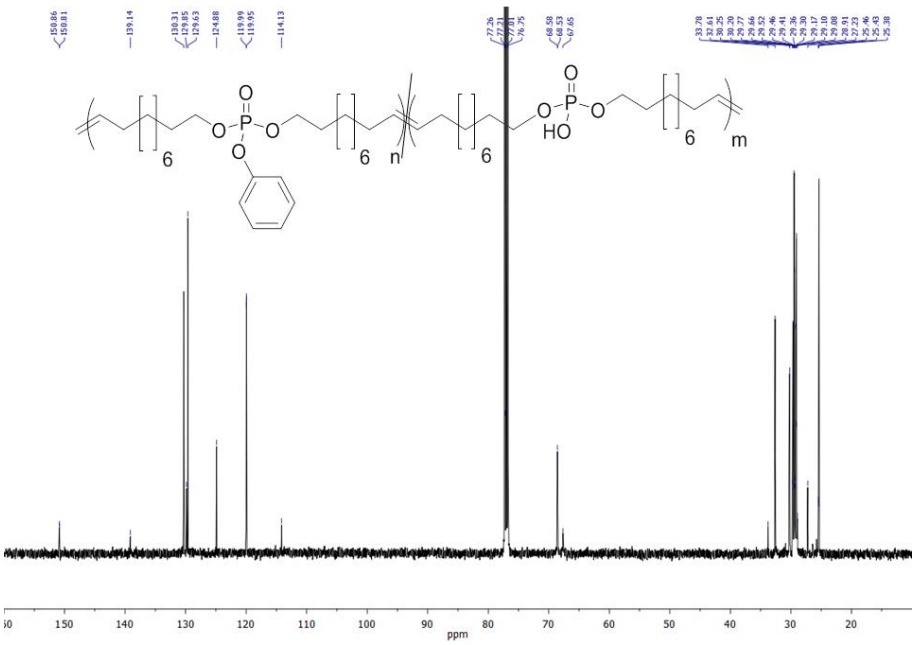

Figure S29: $^{13}C\{H\}$ NMR of **7** (26 MHz, 298 K, $CDCl_3$)

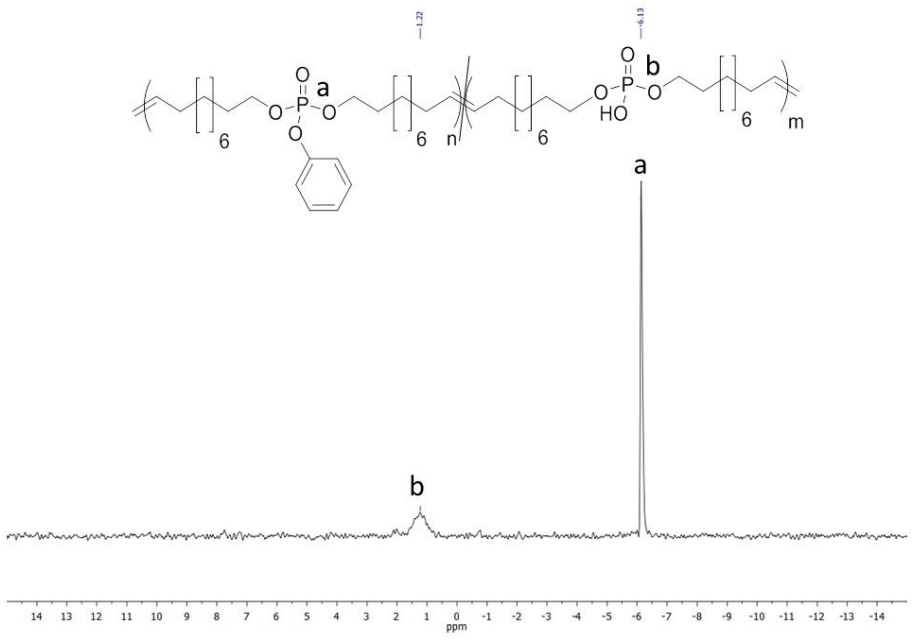

Figure S30: $^{31}P\{H\}$ NMR of **6** (202 MHz, 298 K, $CDCl_3$)

DSC

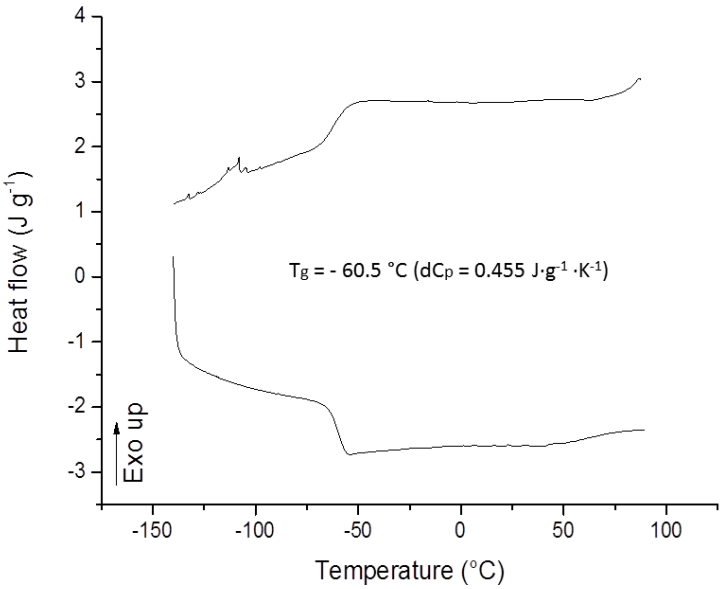

Figure S31: DSC thermogram of **poly(1)**

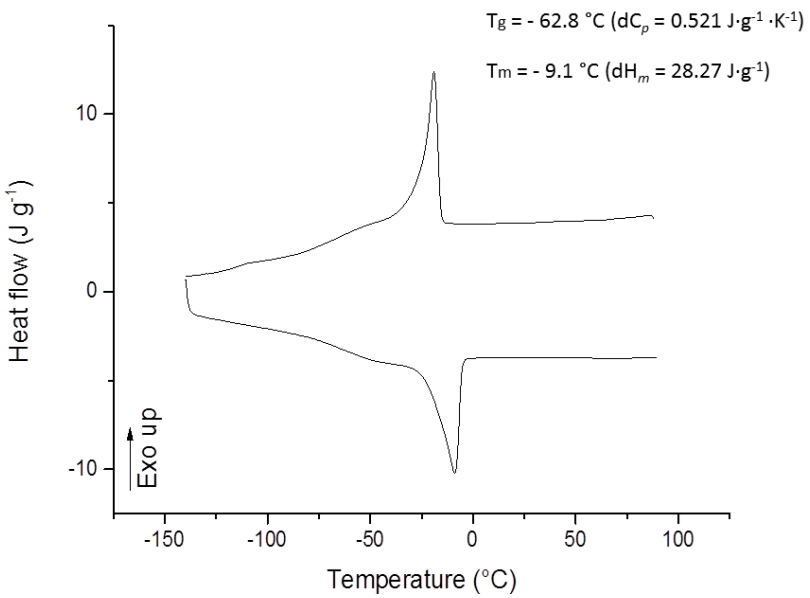

Figure S32: DSC thermogram of **poly(2)**

3.2 Poly(phosphorodiamidate)s via ADMET

Phosphorus-nitrogen binding motifs in polymers have already been known for a long time. Motivated by exceptional flame retardant properties, these polymers are well investigated (**Chapter 1.3.2**). However, till very recently, no other applications of these polymers were of interest. Perhaps modern polymerization techniques have contributed to recent investigations of these interesting materials. Wooley and coworkers investigated polymers with phosphoramidate bonds in 2013, with a focus on the selective degradation of the polymer side-chains under acidic conditions.[90] The results of these studies are expanded upon in this chapter with the exploration of phosphorodiamidates (PPDAs) also used for degradation of the polymer backbone itself. Controlled degradations are attractive for biomedical applications and polymer degradation in a natural environment. Nondegradable plastics in the environment have led to serious waste problems in nature. New alternatives are urgently needed. In contrast to other common polymers, the advantages of biocompatibility and degradability can easily be established for PPEs and PPAs and their degradation products.[159]

Herein, novel PPDAs have been investigated. Those polymers exhibit excellent adjustable degradation properties, besides flame resistance behavior. Combined with high thermal stabilities and melting points, degradable PPDA polymers may find application in novel biocompatible materials for tissue engineering or drug delivery, or as flame retardant materials.

This chapter is accepted for publication at Chemistry – A European Journal by Wiley-VCH (September 2016); it was altered at some parts for this thesis.

3.2.1 Poly(phosphorodiamidate)s by Olefin Metathesis Polymerization with Precise Degradation

*Mark Steinmann, Manfred Wagner, Frederik R. Wurm**

Max-Planck-Institut für Polymerforschung, Ackermannweg 10, 55128 Mainz, Germany.

Contact address: wurm@mpip-mainz.mpg.de

Abstract

Degradable polymers are a currently growing field of research for biomedical and materials science applications. The majority of such compounds is based on polyesters and polyamides. In contrast, their phosphorus-containing counterparts are much less studied, in spite of their potential precise degradation profile and biocompatibility. Herein, the first library of poly(phosphorodiamidate)s (PPDAs) with two P-N-bonds forming the polymer backbone and a pendant P-OR-group are prepared via acyclic diene metathesis polymerization. They are designe to vary in their hydrophilicity and are compared to structural analogues poly(phosphoester)s (PPEs) with respect to thermal properties and degradation profiles. The degradation of PPDAs can be controlled precisely by the pH: under acidic conditions the P-N-linkages in the polymer backbone are cleaved, while under basic conditions the pendant ester is cleaved selectively and almost no backbone degradation occurs. The PPDAs exhibit distinctively higher thermal stability (from TGA) and higher glass transition and/or melting temperatures (from DSC) compared to analogues PPEs. This renders this exotic class of phosphorus-containing polymers as highly promising for the development of future drug carriers or tissue engineering scaffolds.

Keywords: poly(phosphorodiamidate), poly(phosphoester), acyclic diene metathesis, degradation, phosphorus.

Introduction

P-N-linkages in polymers have been only scarcely investigated to date. The typical example for such compounds are poly(organophosphazene)s (POPs, **1**), going back to pioneering works from the 1960s.[156] Their general structure $(N=PR_2)_n$, with R as halogen, organic, or organometallic units, is usually prepared by the thermal ring-opening polymerization of hexachlorocyclotriphosphazene.[156] To date POPs with different properties such as hydrophilicity or crystallinity depending on the nature of the side group has been reported.[160] [161-162] [97, 99] POPs have been discussed as potential alternatives to conventional polymers and have become to probably one of the most famous "inorganic polymers" to date.[161]

However, the structural versatility of the main-chain is limited with only P=N-bonds forming the backbone. Herein, we prepare the first poly(phosphorodiamidate)s (PPDAs, **2**) with two P-N-linkages and different alkyl chains in the backbone to vary their hydrophilicity and crystallinity. In recent works, we and other research groups, studied poly(phosphoester)s (PPEs, **3**) as a promising class of materials for applications from bio to materials science.[70-71, 74, 141, 144, 163] Our group introduced the functional group tolerant olefin metathesis polymerization to the preparation kit of PPEs.[78, 164-165] Together with the chemical versatility of the phosphotriester repeat units, linear or branched polymers with a wide range of functional groups can be prepared.[73, 145, 163, 166] Wooley and coworkers reported recently on acid-labile poly(phosphoramidate)s (PPA, **4**): PPA and PPE share the same polyphosphodiester backbone (Scheme 1), but PPAs have an acid-labile phosphoramidate bond as side group.[90]

What is scarcely studied are polymers with phosphoramidate linkages in the main chain,[87] so called main-chain poly(phosphorodiamidate)s (PPDAs) have mostly been reported in aromatic flame-retardant oligomers.[102, 117-118]

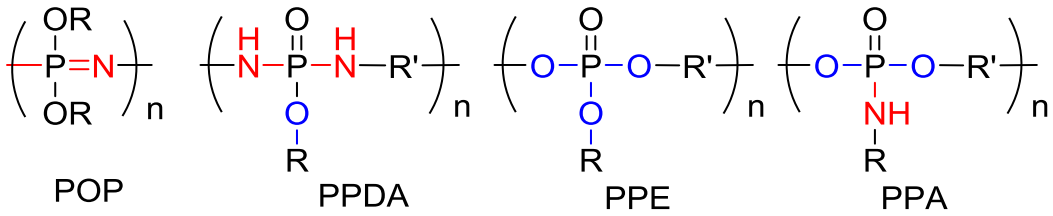

Scheme 1: General structures of poly(organophosphazene)s (POP, **1**), poly(phosphorodiamidate)s (PPDA, **2**), poly(phosphoester)s (PPE, **3**) vs. poly(phosphoramidates) (PPA, **4**).

Phosphorus-containing flame retardants show attractive properties compared to the previously used halogenated flame retardants as they prevent toxic gases during combustion and bioaccumulation[167-168] or in general exhibit low toxicity, which opens future possibilities for novel polymers with P-N-linkages.[169-170]

The acyclic diene metathesis polycondensation was used to prepare a library of novel PPDAs of variable hydrophilicity. These new compounds have been characterized and compared to structurally analogues (also novel) PPEs with respect to thermal stability and hydrolysis. Monomers and polymers were extensively investigated by ^{1}H NMR, ^{13}C NMR, ^{31}P NMR, ^{1}H DOSY, and ESI-MS (only monomers). The thermal properties reveal glass temperatures and/or melting points depending on the microstructure. The degradation of the water-soluble monomers and polymers was investigated by variation of the pH. Under basic conditions the pendant P-O bond is cleaved selectively, while under acidic conditions the backbone of PPDAs is degraded. In contrast, PPEs show a statistical cleavage of side or main chain under those conditions.

These PPDAs broaden the scope of P-containing polymers as future biodegradable materials with adjustable hydrophilicity and precise degradation profile, or with additional potential for flame-retardant polymer additives.

Experimental Section

Materials and Methods can be found in the Supporting Information.

Monomer syntheses:

8-Azide-1-octene (1). 8-Azide-1-octene **1** was synthesized similar to the literature procedure by Li et al.[171] To a stirred solution of 8-bromo-1-octene (5.00 g, 26.2 mmol, 1.0 eq.) in dry DMF (50 mL) was added NaN_3 (3.4 g, 52.3 mmol, 2.0 eq.) in 1 portion at 80 °C. After 16 h of stirring at 80 °C, the solution was poured into H_2O (200 ml). The reaction mixture was extracted with ethyl acetate (3 x 50 mL) and the combined organic phases were washed with brine. The organic phase was dried over anhydrous $MgSO_4$, and concentrated in vacuo. The crude 8-azide-1-octene **1** (3.8 g, 95 %) was used in the next step without further purification.

11-Azide-1-decene (2). 11-Azide-1-decene **2** was prepared from 11-bromo-1-decene as reported by Tsai et al with modifications.[172] 11-bromo-1-decene (5.00 g, 21.4 mmol, 1.0 eq.) was added in a solution of dry DMF (50 mL) and NaN_3 (2.8 g, 42.9 mmol, 2.0 eq.) in 1 portion at 80 °C. The reaction mixture was stirred for 16 h at 80 °C and filtered. The organic phase was extracted with hexane (3 x 25 ml) separated and combined, dried over anhydrous MgSO4, and concentrated in vacuo. The crude 11-Azide-1-decene **2** (3.9 g, 93 %) was used in the next step without further purification.

7-Octen-1-amine (3) and 10-decen-1-amine (4). 7-Octen-1-amine and 10-decen-1-amine **3** and **4** were synthesized by following the reported procedure with modifications.[173] A mixture of the azide **1** or **2** (26.2 mmol, 1.0 eq.) and Ph_3P (78.5 mmol, 3.0 eq.) in a 10:1 solution of H_2O (8 ml) in THF (80 ml) was stirred at 60 °C for 16 h. Subsequently, THF was removed under reduced pressure. The aqueous residue was dissolved in acetonitrile (100 ml) with 10 ml 10 w% HCl. After 1 h of stirring the acetonitrile was removed. To the mixture was added 150 ml H_2O and the aqueous phase was once extracted with DCM (1 x 25 ml). The aqueous phase was freeze dried. Amine **3** (90 %) or **4** (87 %) was obtained and used in the next step without further purification.

Representative procedure for synthesis of the "hydroxy- and methylphosphate monomers"

Bis-(but-3-en-1-yl)-methylphosphate (8). A mixture of 3-buten-1-ol (11.1 g, 13.3 ml, 0.154 mol, 1.8 eq.) and Et_3N (15.6 g, 21.4 ml, 0.154 mol, 1.8 eq.) in toluene (20 ml) was added to a stirred solution of $POCl_3$ (13.1 g, 8.0 ml, 0.0856 mol, 1.0 eq.) in toluene (50 ml) at room temperature. The resulting dispersion was stirred overnight at room temperature. Subsequently, $Et_3N{\cdot}HCl$ was removed by filtration. The filtrate was dried at reduced pressure to remove solvents and excess $POCl_3$. 40 ml diethylether was added to dissolve the dialkenyl chlorophosphate intermediate. The solution was stirred vigorously with water (ca. 25 mL) for 48h with exchanging the water phase several times.

The following purification was carried out with the water-soluble monomer **5**: The combined water phases were extracted with ethyl acetate (3 x 50 ml), combined and concentrated at reduced pressure to yield pure di-(but-3-en-1-yl) phosphate **5** (Yield: 15.5 g, 0.075 mol; 88 %).

The following purification was carried out with water-insoluble monomers **6** and **7**: The diethyl ether phase was dried and the solvent was removed at reduced pressure. The residue containing the dialkylene phosphates (**6** and **7**) was used without further purification.

5 (7.0 g, 0.0340 mol, 1.0 eq.) was mixed and stirred with trimethyl orthoacetate (8.2 g, 8.4 ml, 0.0679 mol, 2.0 eq.) at 80 °C. After stirring overnight, water was added to deactivate excess trimethyl orthoacetate. The water phase was extracted with CH_2Cl_2 (3 x 50 ml) and the extract was dried. After distillation at 90°C ($5{\cdot}10^{-2}$ mbar) pure **8** was obtained as colorless oil (Yield: 5.5 g, 0.0250 mmol; 74 %). ^{1}H NMR (500 MHz, 298 K, $CDCl_3$, δ/ ppm): 5.88 – 5.67 (ddt, J = 17.0, 10.3, 6.7 Hz, 2H), 5.19 – 5.01 (m, 4H), 4.17 – 3.97 (q, J = 6.9 Hz, 4H), 3.85 – 3.61 (d, J = 11.1 Hz, 3H), 2.53 – 2.32 (q, J = 6.7 Hz, 4H). ^{13}C{H} NMR (126 MHz, 298 K, $CDCl_3$, δ/ ppm): 133.4, 117.8, 66.9, 66.9, 54.3, 54.3, 34.7, 34.7. ^{31}P{H} NMR (202 MHz, 298 K, $CDCl_3$, δ/ ppm): 0.03. ESI-MS *m/z* 243.04 $[M+Na]^+$ (Calculated for $C_9H_{17}O_4P$: 220.09). Calcd C 49.09. H 7.78; found C 49.23. H 7.61.

Bis-(but-3-en-1-yl)-phosphate (5). Following the representative procedure described above, **5** was obtained as yellowish oil (Yield: 15.5 g, 0.0750 mol; 88 %). ^{1}H NMR (500 MHz, 298 K, $CDCl_3$, δ/ ppm): 11.84 – 11.30 (s, 1H), 5.96 – 5.67 (ddt, J = 17.0, 10.3, 6.7 Hz, 2H), 5.33 – 4.91

(m, 4H), 4.27 – 3.89 (q, J = 7.0 Hz, 4H), 2.59 – 2.40 (q, J = 6.7 Hz, 4H). ^{13}C{H} NMR (126 MHz, 298 K, $CDCl_3$, δ / ppm): 133.4, 133.4, 117.8, 117.8, 67.0, 67.0, 66.9, 66.8, 34.7, 34.7, 34.6, 34.6. ^{31}P{H} NMR (202 MHz, 298 K, $CDCl_3$, δ / ppm): 0.20. ESI-MS *m/z* 657.08 $[3M+K]^+$, 863.11 $[4M+K]^+$, 1069.17 $[5M+K]^+$ (Calculated for $C_8H_{15}O_4P$: 206.07). Calcd C 46.60, H 7.33; found C 46.45, H 7.27.

Bis-(oct-7-en-1-yl)-phosphate (6). Following the representative procedure described above until the synthesis steps of **5** using 7-octen-1-ol, **6** was obtained as yellowish oil (Yield: 54 %). ^{1}H NMR (300 MHz, 298 K, $CDCl_3$, δ / ppm): 5.97 – 5.57 (m, 2H), 5.08 – 4.82 (m, 4H), 4.52 – 4.15 (s, 5H), 4.13 – 3.89 (d, J = 6.8 Hz, 4H), 2.22 – 1.89 (d, J = 6.8 Hz, 4H), 1.82 – 1.49 (m, 4H), 1.52 – 0.97 (m, 15H). ^{13}C{H} NMR (126 MHz, 298 K, $CDCl_3$, δ / ppm): 137.1, 137.0, 112.4, 112.3, 75.4, 75.1, 74.9, 65.6, 65.6, 44.1, 31.8, 31.7, 28.3, 28.2, 26.9, 26.8, 26.8, 26.7, 23.4, 6.7. ^{31}P{H} NMR (202 MHz, 298 K, $CDCl_3$, δ / ppm): -1.15. ESI-MS *m/z* 319.17 $[M+H]^+$, 637.31 $[2M+H]^+$, 955.47 $[3M+H]^+$ (Calculated for $C_{16}H_{31}O_4P$: 318.20). Calcd C 60.36, H 9.81; found C 60.13, H 9.93.

Bis-(undec-10-en-1-yl)-phosphate (7). Following the representative procedure described above until the synthesis steps of **5** using 10-decen-1-ol, **7** was obtained as yellowish oil (Yield: 60 %). ^{1}H NMR (500 MHz, 298 K, $CDCl_3$, δ / ppm): 8.89 – 8.70 (s, 2H), 5.93 – 5.68 (ddt, J = 16.9, 10.2, 6.7 Hz, 2H), 5.09 – 4.82 (m, 4H), 4.17 – 3.78 (q, J = 6.7 Hz, 4H), 2.12 – 1.94 (q, J = 6.9 Hz, 4H), 1.79 – 1.60 (p, J = 6.7 Hz, 4H), 1.49 – 1.14 (d, J = 44.5 Hz, 26H). ^{13}C{H} NMR (126 MHz, 298 K, $CDCl_3$, δ / ppm): 139.3, 114.3, 76.9, 67.9, 67.9, 34.0, 30.4, 30.3, 29.6, 29.6, 29.6, 29.3, 29.3, 29.1, 25.6. ^{31}P{H} NMR (202 MHz, 298 K, $CDCl_3$, δ / ppm): 1.18. ESI-MS *m/z* 403.26 $[M+H]^+$, 805.48 $[2M+H]^+$, 1207.73 $[3M+H]^+$ (Calculated for $C_{22}H_{43}O_4P$: 402.29). Calcd C 65.64, H 10.77; found C 65.65, H 10.88.

Bis-(oct-7-en-1-yl)-methylphosphate (9). Following the representative procedure described above (without purification by distillation) using 7-octen-1-ol, **9** was obtained as yellowish oil (Yield: 92 %). ^{1}H NMR (500 MHz, 298 K, $CDCl_3$, δ / ppm): 5.91 – 5.67 (ddt, J = 16.9, 10.2, 6.7 Hz, 2H), 5.12 – 4.83 (m, 4H), 4.11 – 3.96 (q, J = 6.7 Hz, 4H), 3.83 – 3.70 (dd, J = 11.1, 6.4 Hz, 3H), 2.14 – 1.97 (q, J = 7.8, 7.3 Hz, 4H), 1.80 – 1.60 (p, J = 6.7 Hz, 4H), 1.52 – 1.28 (dd, J = 19.2, 7.2 Hz, 13H). ^{13}C{H} NMR (126 MHz, 298 K, $CDCl_3$, δ / ppm): 139.0, 114.4, 114.4, 67.9,

67.9, 67.8, 67.7, 54.2, 54.2, 33.7, 30.4, 30.4, 30.3, 28.8, 28.8, 28.7, 28.7, 28.7, 28.7, 28.7, 25.4, 25.4, 25.4. ^{31}P{H} NMR (202 MHz, 298 K, $CDCl_3$, δ / ppm): 0.33. ESI-MS *m/z* 333.18 $[M+H]^+$, 355.15 $[M+Na]^+$, 687.32 $[2M+Na]^+$, (Calculated for $C_{17}H_{33}O_4P$: 332.21). Calcd C 61.42, H 10.01; found C 61.68, H 10.17.

Bis-(undec-10-en-1-yl)-methylphosphate (10). Following the representative procedure described above (without purification by distillation) using 10-undecen-1-ol, **10** was obtained as yellowish oil (Yield: 86 %). ^{1}H NMR (500 MHz, 298 K, $CDCl_3$, δ/ ppm): 5.94 – 5.66 (ddt, J = 13.5, 10.1, 6.7 Hz, 2H), 5.11 – 4.80 (dd, J = 30.3, 13.4 Hz, 4H), 4.14 – 3.93 (q, J = 6.6 Hz, 4H), 3.86 – 3.64 (d, J = 11.0 Hz, 3H), 2.17 – 1.91 (q, J = 6.8, 6.3 Hz, 4H), 1.76 – 1.50 (m, 6H), 1.46 – 1.15 (d, J = 43.3 Hz, 27H). ^{13}C{H} NMR (126 MHz, 298 K, $CDCl_3$, δ/ ppm): 139.2, 114.2, 67.9, 67.9, 54.2, 54.1, 33.9, 30.4, 30.4, 29.5, 29.5, 29.2, 29.2, 29.0, 25.5. ^{31}P{H} NMR (202 MHz, 298 K, $CDCl_3$, δ/ ppm): -1.51. ESI-MS *m/z* 417.25 $[M+H]^+$, 439.23 $[M+Na]^+$, 833.51 $[2M+H]^+$, 855.46 $[2M+Na]^+$ (Calculated for $C_{23}H_{45}O_4P$: 416.31). Calcd C 66.31, H 10.89; found C 66.37, H 10.81.

Representative procedure for synthesis of the phosphorodiamidate monomers:

***N,N`*-Bis-(but-3-en-1-yl)-phosphorodiamidate (11).** A mixture of 3-buten-1-amine (1.5 g, 1.9 ml, 0.0211 mol, 2.0 eq.) and Et_3N (2.2 g, 3.1 ml, 0.0222 mol, 2.1 eq.) in toluene (20 ml) was added to a stirred solution of $POCl_3$ (1.6 g, 1.0 ml, 0.0106 mol, 1.0 eq.) in toluene (50 ml) at room temperature. The resulting dispersion was stirred overnight at room temperature and then filtered to remove $Et_3N{\cdot}HCl$. The solvent of the filtrate was removed at reduced pressure. Ethyl acetate (50 mL) was added to dissolve the dialkenyl chlorophosphorodiamidate intermediate and DMAP (100 mg, 0.819 mmol) was added. The resulting mixture was stirred vigorously with water for 48h with exchanging the water several times. The ethyl acetate phases were combined and washed with 10% HCl solution and brine. After removing the solvent at reduced pressure pure di-(but-3-en-1-yl) phosphorodiamidate **11** was obtained as yellowish oil (Yield: 0.86 g, 0.00424 mmol; 73 %). ^{1}H NMR (300 MHz, 298 K, $CDCl_3$, δ/ ppm): 5.94 – 5.44 (td, J = 17.1, 6.9 Hz, 2H), 5.28 – 4.90 (m, 4H), 3.19 – 2.81 (m, 4H), 2.42 – 2.11 (q, J = 6.7 Hz, 4H). ^{13}C{H} NMR (176 MHz, 298 K, $CDCl_3$, δ / ppm): 135.1, 117.4, 77.2, 77.1, 76.9, 40.3, 35.8. ^{31}P{H} NMR (202 MHz, 298 K, $CDCl_3$, δ/

ppm): 8.84. ESI-MS *m/z* 391.21 $[2M-H_2O+H]^+$, 803.36 $[3M-2H_2O+Na]^+$, (Calculated for $C_8H_{17}N_2O_2P$: 204.10). Calcd C 47.05, H 8.39, N 13.72; found C 47.14, H 8.39, N 13.58.

***N,N`*-Bis-(oct-7-en-1-yl)-phosphorodiamidate (12).** Following the representative procedure described above using 7-octen-1-amine **3**, **12** was obtained as yellowish oil (Yield: 62 %). ^{1}H NMR (300 MHz, 298 K, D_2O, δ/ ppm): 6.08 – 5.70 (ddt, J = 17.0, 10.2, 6.7 Hz, 2H), 5.14 – 4.90 (m, 4H), 3.10 – 2.84 (t, J = 7.5 Hz, 4H), 2.21 – 1.89 (q, J = 7.0, 6.3 Hz, 3H), 1.78 – 1.51 (p, J = 7.1 Hz, 4H), 1.51 – 1.19 (m, 12H). ^{13}C{H} NMR (126 MHz, 298 K, $CDCl_3$, δ/ ppm): 142.6, 116.6, 42.0, 41.9, 35.4, 30.3, 30.2, 30.1, 29.2, 29.1, 29.1, 28.1, 27.9, 27.9, 27.9, 27.1. ^{31}P{H} NMR (202 MHz, 298 K, $CDCl_3$, δ / ppm): 8.26. ESI-MS *m/z* 637.44 $[2M-H_2O+Na]^+$, 915.55 $[3M-2H_2O+H]^+$, 1251.89 $[4M-3H_2O+K]^+$, (Calculated for $C_{16}H_{33}N_2O_2P$: 316.23). Calcd C 60.73, H 10.51, N 8.85; found C 60.59, H 10.56, N 8.81.

Representative procedure for synthesis of the methylphosphorodiamidate monomers

***N,N`*-Bis-(but-3-en-1-yl)-methylphosphorodiamidate (13).** A mixture of 3-buten-1-amine (1.787 g, 2.300 ml, 25.12 mmol, 2.0 eq.), DBU (4.015 g, 3.944 ml, 26.38 mmol, 2.1 eq.) and DMAP (384 mg, 3.14 mmol, 0.25 eq.) in CH_2Cl_2 (10 ml) was added to a stirred solution of methyl dichlorophosphate (1.871 g, 1.260 ml, 12.56 mmol, 1.0 eq.) in CH_2Cl_2 (20 ml) at room temperature. The resulting solution was stirred overnight at room temperature. The solvent of the filtrate was removed at reduced pressure. The resulting residue was dissolved in diethyl ether. The diethyl ether phase was washed with 10% HCl solution, $NaHCO_3$ solution and brine. After removing the solvent at reduced pressure pure **13** was obtained as yellowish oil (Yield: 1.92 g, 8.79 mmol; 70 %). ^{1}H NMR (500 MHz, 298 K, $CDCl_3$, δ/ ppm): 5.81 – 5.67 (ddt, J = 17.1, 10.2, 6.9 Hz, 2H), 5.13 – 5.07 (m, 4H), 3.67 – 3.63 (d, J = 11.2 Hz, 3H), 3.02 – 2.94 (ddq, J = 13.0, 6.5, 3.1, 2.0 Hz, 4H), 2.66 (s, 2H), 2.28 – 2.21 (q, J = 6.7 Hz, 4H). ^{13}C{H} NMR (126 MHz, 298 K, $CDCl_3$, δ/ ppm): 135.4, 117.3, 51.8, 40.3, 36.2, 36.1. ^{31}P{H} NMR (202 MHz, 298 K, $CDCl_3$, δ/ ppm): 16.67. ESI-MS *m/z* 219.11 $[M+H]^+$, 241.08 $[M+Na]^+$, (Calculated for $C_9H_{19}N_2O_2P$: 218.12). Calcd C 49.33, H 8.78, N 12.84; found C 49.11, H 8.70, N 12.96.

***N,N`*-Bis-(oct-7-en-1-yl)-methylphosphorodiamidate (14).** Following the representative procedure described above using 7-octen-1-amine **3**, **14** was obtained as yellowish oil (Yield: 84 %). ^{1}H NMR (500 MHz, 298 K, $CDCl_3$, δ/ ppm): 5.75 – 5.71 (td, J = 16.9, 6.7 Hz, 2H), 4.93 –

4.86 (m, 4H), 3.58 – 3.57 (d, J = 11.2 Hz, 3H), 2.82 (m, 4H), 2.34 – 2.33 (d, J = 6.8 Hz, 2H), 1.98 – 1.97 (q, J = 6.8, 6.4 Hz, 4H), 1.42 – 1.18 (m, 23H). ^{13}C{H} NMR (176 MHz, 298 K, $CDCl_3$, δ/ ppm): 138.9, 132.1, 132.1, 131.9, 128.5, 128.5, 114.3, 70.6, 51.7, 41.2, 41.1, 33.7, 32.0, 31.9, 29.7, 28.8, 28.8, 28.7, 26.6. ^{31}P{H} NMR (202 MHz, 298 K, $CDCl_3$, δ/ ppm): 16.87. ESI-MS *m/z* 331.28 $[M+H]^+$, 683.47 $[2M+Na]^+$, 1013.76 $[3M+Na]^+$, (Calculated for $C_{17}H_{35}N_2O_2P$: 330.24). Calcd C 61.79, H 10.68, N 8.48; found C 61.67, H 10.57, N 8.32.

***N,N`*-Bis-(undec-10-en-1-yl)-methylphosphorodiamidate (15).** Following the representative procedure described above using 10-undecen-1-amine **4**, **15** was obtained as yellowish oil (Yield: 73 %). ^{1}H NMR (500 MHz, 298 K, $CDCl_3$, δ/ ppm): 5.88 – 5.65 (td, J = 16.9, 6.7 Hz, 2H), 5.05 – 4.83 (m, 4H), 3.79 – 3.43 (d, J = 11.2 Hz, 3H), 2.97 – 2.74 (t, J = 7.9 Hz, 4H), 2.57 – 2.30 (d, J = 8.0 Hz, 2H), 2.13 – 1.89 (m, 4H), 1.53 – 1.38 (m, 4H), 1.38 – 1.09 (d, J = 46.7 Hz, 27H). ^{13}C{H} NMR (176 MHz, 298 K, $CDCl_3$, δ / ppm): 139.2, 132.1, 132.1, 131.9, 128.5, 128.5, 114.1, 53.6, 51.7, 51.7, 41.6, 41.2, 39.8, 33.8, 32.0, 32.0, 29.5, 29.4, 29.4, 29.3, 29.2, 29.1, 28.9, 27.7, 26.7. ^{31}P{H} NMR (202 MHz, 298 K, $CDCl_3$, δ/ ppm): 17.03. ESI-MS *m/z* 415.37 $[M+H]^+$, 437.35 $[M+Na]^+$, 829.72 $[2M+H]^+$, 851.69 $[3M+Na]^+$, 1266.03 $[3M+H]^+$, (Calculated for $C_{23}H_{47}N_2O_2P$: 414.34). Calcd C 47.05, H 8.39, N 13.72; found C 47.14, H 8.39, N 13.58.

Representative procedure for the ADMET polymerization of the methylphosphate and methylphosphorodiamide monomers.

Poly(8). Bis-(but-3-en-1-yl)-methylphosphate **8** (1.0 g, 4.54 mmol) and Grubbs catalyst 1st generation (37.4 mg, 0.0454 mmol, 1 mol%) (or Hoveyda-Grubbs catalyst 2nd generation (2 mol% and 2 mol% after 2 h) for PPDAs) were placed in a glass Schlenk tube equipped with a magnetic stir bar under an argon atmosphere. The reaction was carried out at reduced pressure (to remove the ethylene gas evolving during the metathesis reaction) in bulk or solution at temperatures between r.t. and 50 °C for 16 h. **Poly(8)** was obtained in bulk as brownish viscous oil in quantitative yield. Purification: Tris-(hydroxymethyl) phosphine (ca. 50 eq. with respect to the catalyst) was added to a solution of CH_2Cl_2 and the polymer. After the addion of water, the emulsion was stirred for several hours until the CH_2Cl_2 phase was almost colorless. The CH_2Cl_2 phase was washed with aqueous 10% HCl and finally with brine to remove residues of catalyst. The CH_2Cl_2 phase was separated, dried over magnesium

sulfate ($MgSO_4$), filtered and concentrated at reduced pressure (Yield: 920 mg, 4.18 mmol; 92 %). ^{1}H NMR (500 MHz, 298 K, $CDCl_3$, δ/ ppm): 5.64 – 5.41 (m), 4.18 – 3.92 (m), 3.84 – 3.63 (m), 2.53 – 2.25 (m). ^{13}C{H} NMR (126 MHz, 298 K, $CDCl_3$, δ/ ppm): 128.2, 127.3, 67.2, 67.1, 67.1, 67.1, 66.9, 66.9, 54.4, 54.3, 54.3, 54.3, 33.7, 33.7, 28.7, 28.7. ^{31}P{H} NMR (202 MHz, 298 K, $CDCl_3$, δ/ ppm): 0.08.

Representative procedure for catalytic hydrogenation.[153]

100 mg of polymer **poly(8)**, 5 mL of CH_2Cl_2, and 5 mg of 10% Pd/C catalyst were charged into a reactor and flushed with argon. Hydrogenation was then performed with vigorous stirring under a hydrogen pressure of 25 bar at room temperature for 16 h. The solution was filtered over Celite® and polymer **poly-H(8)** isolated after solvent evaporation in a yield of 80 %.

Poly-H(8). Hydrogenation of **poly(8)**: yield: 82 %. ^{1}H NMR (300 MHz, 298 K, $CDCl_3$, δ/ ppm): 4.12 – 3.84 (m), 3.84 – 3.48 (m), 1.76 – 1.50 (m), 1.50 – 1.10 (m). ^{13}C{H} NMR (126 MHz, $CDCl_3$, δ/ ppm): 67.9, 67.6, 67.0, 54.2, 33.6, 33.5, 31.3, 30.2, 30.1, 25.0, 22.5, 14.0. ^{31}P{H} NMR (202 MHz, 298 K, $CDCl_3$, δ/ ppm): 0.38.

Poly(9). The reaction was carried out following the general procedure above with bis-(oct-7-en-1-yl)-methylphosphate **9** (150.0 mg, 0.451 mmol) as monomer for 16 h (yield: 85 %).. ^{1}H NMR (250 MHz, 298 K, $CDCl_3$, δ/ ppm): 5.42 – 5.14 (m), 4.11 – 3.82 (m), 3.78 – 3.59 (m), 2.07 – 1.78 (m), 1.74 – 1.45 (m), 1.45 – 1.07 (m). ^{13}C{H} NMR (126 MHz, 298 K, $CDCl_3$, δ/ ppm): 138.87, 130.90, 130.25, 130.0, 129.8, 114.3, 67.8, 67.8, 67.4, 67.3, 54.08, 54.1, 54.1, 33.6, 32.5, 32.4, 31.7, 30.3, 30.2, 29.6, 29.5, 28.7, 27.6, 27.1, 26.1, 25.3, 25.0, 24.8.^{31}P{H} NMR (202 MHz, 298 K, $CDCl_3$, δ/ ppm): 0.39.

Poly-H(9). Hydrogenation of **poly(9)**. Yield: 78 %. ^{1}H NMR (300 MHz, 298 K, $CDCl_3$, δ/ ppm): 4.06 – 3.85 (m), 3.76 – 3.61 (m), 1.72 – 1.44 (m), 1.44 – 1.06 (m). ^{13}C NMR (126 MHz, $CDCl_3$, δ / ppm): 67.9, 67.8, 54.1, 54.0, 31.9, 30.3, 30.3, 29.6, 29.6, 29.5, 29.2, 27.6, 27.3, 26.6, 26.5, 26.4, 25.4, 24.7, 22.7, 22.6, 14.1. ^{31}P NMR (202 MHz, 298 K, $CDCl_3$, δ/ ppm): 0.37.

Poly(10). The reaction was carried out following the general procedure above with Bis-(undec-10-en-1-yl)-methylphosphate **10** (250.0 mg, 0.600 mmol) as monomer for 8 h (yield: 78 %). ^{1}H NMR (700 MHz, 298 K, $CDCl_3$, δ/ ppm): 5.91 – 5.66 (m), 5.44 – 5.23 (m), 5.04 – 4.85

(m), 4.07 – 3.94 (m), 3.79 – 3.67 (m), 2.08 – 1.87 (m), 1.76 – 1.55 (m), 1.47 – 1.08 (m). ^{13}C{H} NMR (176 MHz, $CDCl_3$, δ/ ppm): 130.4, 130.0, 69.0, 68.0, 54.2, 54.2, 32.7, 30.5, 30.4, 29.8, 29.6, 29.6, 29.3, 27.4, 25.6. ^{31}P{H} NMR (284 MHz, 298 K, $CDCl_3$, δ/ ppm): 0.83.

Poly-H(10). Hydrogenation of **poly(10)**. Yield: 84 %). ^{1}H NMR (500 MHz, 298 K, $CDCl_3$, δ/ ppm): 4.17 – 3.97 (m), 3.86 – 3.68 (m), 1.77 – 1.52 (m), 1.47 – 1.08 (m). ^{13}C{H} NMR (126 MHz, $CDCl_3$, δ/ ppm): 67.9, 67.8, 54.1, 54.0, 31.9, 30.3, 30.3, 29.7, 29.7, 29.7, 29.6, 29.5, 29.5, 29.3, 29.2, 25.4, 25.4, 22.7, 14.1. ^{31}P{H} NMR (202 MHz, 298 K, $CDCl_3$, δ/ ppm): 0.38.

Poly(13). The reaction was carried out following the general procedure above with Hoveyda-Grubbs catalyst 2nd generation (11.4 mg, 0.00908 mmol, 2 x 2 mol%) as catalyst and *N,N`*-bis-(but-3-en-1-yl)-methylphosphorodiamidate **13** (100.0 mg, 0.458 mmol) as monomer in bulk in 16 h and in a 50w% 1-chlornaphthalin solution for 20 h (yield: 75 %).. ^{1}H NMR (300 MHz, 298 K, $CDCl_3$, δ/ ppm): 5.62 – 5.53 (m), 5.15 – 5.07 (m), 3.62 – 3.59 (m), 3.53 – 3.32 (m), 2.91 – 2.89 (m), 2.25 – 2.10 (m). ^{13}C{H} NMR (126 MHz, 298 K, $CDCl_3$, δ/ ppm): 135.4, 131.2, 129.8, 128.7, 127.0, 117.3, 117.3, 117.3, 115.6, 51.9, 43.1, 43.0, 40.6, 40.2, 36.1, 34.9, 34.5, 17.6. ^{31}P{H} NMR (202 MHz, 298 K, $CDCl_3$, δ/ ppm): 16.98.

Poly[*N,N`*-hexan-1-yl methylphosphorodiamidate] (Poly-H(13)). Hydrogenation of **poly(13)**. Yield: 70 %. ^{1}H NMR (300 MHz, 298 K, $CDCl_3$, δ/ ppm): 3.69 – 3.59 (m), 2.94 – 2.87 m), 1.60 – 1.40 (m), 1.39 – 1.30 (m). ^{13}C{H} NMR (126 MHz, $CDCl_3$, δ/ ppm): 51.7, 45.5, 41.2, 40.9, 34.1, 34.1, 29.7, 19.9, 13.7. ^{31}P{H} NMR (202 MHz, 298 K, $CDCl_3$, δ/ ppm): 17.20 – 16.91 (m).

Poly(14). The reaction was carried out following the general procedure above with Hoveyda-Grubbs catalyst 2nd generation (6.0 mg, 0.00964 mmol, 2 x 2 mol%) as catalyst and *N,N`*-Bis-(oct-7-en-1-yl)-methylphosphorodiamidate **14** (100.0 mg, 0.241 mmol) as monomer in a 50w% 1-chlornaphthalin solution for 16 h (yield: 73 %). ^{1}H NMR (500 MHz, 298 K, $CDCl_3$, δ/ ppm): 5.55 – 5.24 (m), 5.11 – 4.85 (m), 3.78 – 3.53 (m), 3.05 – 2.68 (m), 2.14 – 1.80 (m), 1.72 – 1.01 (m). ^{13}C{H} NMR (176 MHz, 298 K, $CDCl_3$, δ/ ppm): 130.5, 130.3, 130.1, 53.4, 53.1, 51.7, 41.2, 32.5, 32.0, 29.5, 29.3, 28.8, 27.1, 26.7, 26.3. ^{31}P{H} NMR (121.5 MHz, 298 K, $CDCl_3$, δ/ ppm): 17.05 (m).

Poly-H(14). Hydrogenation of **poly(14)**. Yield: 67 %. ^{1}H NMR (300 MHz, 298 K, $CDCl_3$, δ / ppm): 3.70 – 3.59 (m), 2.97 – 2.83 (m), 1.50 – 1.35 (m), 1.36 – 1.23 (m). ^{13}C{H} NMR (75 MHz, CD_2Cl_2, δ / ppm): 41.5, 32.5, 32.4, 32.2, 30.08, 30.0, 29.7, 27.2, 23.1, 14.3. ^{31}P{H} NMR (202 MHz, 298 K, $CDCl_3$, δ / ppm): 16.63 (m).

Poly(15). The reaction was carried out following the general procedure above with Hoveyda-Grubbs catalyst 2nd generation (6.0 mg, 0.00964 mmol, 2 x 2 mol%) as catalyst and *N,N`*-Bis-(undec-10-en-1-yl)-methylphosphorodiamidate **15** (100.0 mg, 0.241 mmol) as monomer in a 50w% 1-chlornaphthalin solution for 16 h (yield: 71 %). ^{1}H NMR (500 MHz, 298 K, $CDCl_3$, δ / ppm): 5.38 – 5.34 (m), 3.66 – 3.60 (m), 2.89 – 2.85 (m), 2.50 – 2.26 (m), 1.97 – 1.93 (m), 1.47 – 1.43 (m), 1.28 – 1.24 (m). ^{13}C{H} NMR (176 MHz, $CDCl_3$, δ / ppm): 130.3, 129.9, 51.7, 51.7, 41.2, 32.6, 32.6, 32.0, 32.0, 29.8, 29.6, 29.6, 29.5, 29.5, 29.3, 29.2, 29.1, 27.2, 26.8. ^{31}P{H} NMR (202 MHz, 298 K, $CDCl_3$, δ / ppm): 17.00 (m).

Poly-H(15). Hydrogenation of **poly(15)**. Yield: 81 %. ^{1}H NMR (500 MHz, 298 K, $CDCl_3$, δ / ppm): 3.67 – 3.56 (m), 2.97 – 2.78 (m), 2.53 – 2.41 (m), 1.53 – 1.37 (m), 1.37 – 1.10 (m). ^{13}C{H} NMR (75 MHz, CD_2Cl_2, δ / ppm): 41.5, 32.3, 30.1, 29.8, 27.2, 23.1, 14.3. ^{31}P{H} NMR (202 MHz, 298 K, $CDCl_3$, δ / ppm): 17.19.

Representative procedure for the ADMET copolymerization of methylphosphate monomers and methylphosphorodiamidate monomers

Copolymer of monomer 5 and 10 (Poly(5-10)). Bis-(undec-10-en-1-yl)-methylphosphate **10** (200 mg, 0.480 mmol, 3 eq), bis-(but-3-en-1-yl)-phosphate **5** (33 mg, 0.160 mmol, 1 eq) Grubbs catalyst 1st generation (5.3 mg, 0.0064 mmol, 1 mol%) (or Hoveyda-Grubbs catalyst 2nd generation (2 mol% and 2 mol% after 2 h) for PPDAs) were placed in a glass Schlenk tube equipped with a magnetic stir bar under an argon atmosphere. The reaction was carried out at reduced pressure at a temperature of 50 °C for 16 h for phosphate based polymers and **Poly(11-13)**. For polymer **Poly(12-15)** the reaction was carried out in a 50w% 1-chloronaphthalin solution at reduced pressure at room temperature. **Poly(5-10)** was obtained as an off-white viscous oil in quantitative yield after 16 h. Purification: see above. (91 %). ^{1}H NMR (300 MHz, 298 K, $CDCl_3$, δ / ppm): 5.64 – 5.21 (m), 4.15 – 3.89 (m), 3.82 – 3.61 (m), 2.55 – 2.24 (m), 2.10 – 1.84 (m), 1.78 – 1.54 (m), 1.51 – 1.11 (m). ^{13}C{H} NMR (75

MHz, 298 K, $CDCl_3$, δ/ ppm): 130.3, 129.8, 67.9, 54.1, 32.6, 30.3, 30.2, 29.7, 29.5, 29.4, 29.2, 27.2, 25.4. $^{31}P\{H\}$ NMR (121.5 MHz, 298 K, $CDCl_3$, δ/ ppm): 1.38 - 0.50, 0.50 - 0.25.

Copolymer of monomer 6 and 10 (Poly(6-10)). The reaction was carried out following the general procedure above with bis-(oct-7-en-1-yl)-phosphate **6** (51 mg, 0.160 mmol, 1 eq) as hydroxyl monomer for 16 h. (Yield: 86 %). ^1H NMR (300 MHz, 298 K, $CDCl_3$, δ/ ppm): 5.49 – 5.23 (m), 4.15 – 3.90 (m), 3.84 – 3.68 (m), 2.15 – 1.86 (m), 1.82 – 1.52 (m), 1.53 – 1.14 (m). $^{13}C\{H\}$ NMR (75 MHz, 298 K, $CDCl_3$, δ/ ppm): 130.5, 130.3, 130.1, 129.8, 67.9, 67.8, 54.1, 54.0, 32.6, 32.5, 30.3, 30.2, 29.7, 29.5, 29.4, 29.2, 27.2, 25.4. $^{31}P\{H\}$ NMR (121.5 MHz, 298 K, $CDCl_3$, δ/ ppm): 1.45 - 0.58, 0.57 - 0.20.

Copolymer of monomer 7 and 10 (Poly(7-10)). The reaction was carried out following the general procedure above with bis-(undec-10-en-1-yl)-phosphate **7** (51 mg, 0.160 mmol, 1 eq) as hydroxyl monomer for 16 h. (Yield: 93 %). ^1H NMR (300 MHz, 298 K, $CDCl_3$, δ/ ppm): 5.49 – 5.25 (m), 4.21 – 3.90 (m), 3.86 – 3.66 (m), 2.13 – 1.83 (m), 1.81 – 1.49 (m), 1.49 – 1.14 (m). $^{13}C\{H\}$ NMR (75 MHz, 298 K, $CDCl_3$, δ/ ppm): 130.3, 129.8, 67.9, 67.8, 54.1, 54.0, 53.4, 32.6, 30.3, 30.2, 29.7, 29.5, 29.2, 27.2, 25.4. $^{31}P\{H\}$ NMR (121.5 MHz, 298 K, $CDCl_3$, δ/ ppm): 1.40 – 0.75, 0.39 – 0.19.

Copolymer of monomer 11 and 13 (Poly(11-13)). The reaction was carried out following the general procedure above with Hoveyda-Grubbs catalyst 2nd generation (14.4 mg, 0.0229 mmol, 2 x 2 mol%) as catalyst, N,N`-bis-(but-3-en-1-yl)-phosphorodiamidate **11** (23.4 mg, 0.115 mmol, 1 eq) as hydroxyl monomer and N,N`-Bis-(but-3-en-1-yl)-methylphosphorodiamidate **13** as methyl monomer (100 mg, 0.458 mmol, 8 eq) for 16 h. (Yield: 88 %). ^1H NMR (300 MHz, 298 K, $CDCl_3$, δ/ ppm): 5.62 – 5.14 (m), 3.71 – 3.50 (m), 3.50 – 3.33 (m), 3.14 – 2.65 (m), 2.36 – 2.01 (m). $^{13}C\{H\}$ NMR (75 MHz, 298 K, CD_2Cl_2, δ/ ppm): 136.2, 134.3, 131.5, 130.3, 129.2, 117.9, 117.0, 43.3, 40.9, 40.7, 39.6, 36.5, 35.2, 34.8, 32.1, 23.0, 21.2, 18.3, 17.8, 14.3. $^{31}P\{H\}$ NMR (121.5 MHz, 298 K, CD_2Cl_2, δ/ ppm): 17.28, 8.68.

Copolymer of monomer 12 and 15 (Poly(12-15)). The reaction was carried out following the general procedure above with Hoveyda-Grubbs catalyst 2nd generation (8.0 mg, 0.0128 mmol, 2 x 2 mol%) as catalyst, N,N`-bis-(but-3-en-1-yl)-phosphorodiamidate **11** (23.4 mg, 0.080 mmol, 1 eq) as hydroxyl monomer and N,N`-Bis-(but-3-en-1-yl)-

methylphosphorodiamidate **13** as methyl monomer (100 mg, 0.241 mmol, 3 eq) for 16 h. (82 %). ^{1}H NMR (300 MHz, 298 K, $CDCl_3$, δ/ ppm): 5.58 – 5.22 (m), 3.82 – 3.54 (m), 3.05 – 2.76 (m), 2.14 – 1.84 (m), 1.71 – 1.43 (m), 1.43 – 1.03 (m).^{13}C{H} NMR (75 MHz, 298 K, CD_2Cl_2, δ/ ppm): 130.7, 41.5, 33.0, 32.4, 30.0, 30.0, 29.7, 29.5, 27.2, 18.1. ^{31}P{H} NMR (121.5 MHz, 298 K, CD_2Cl_2, δ/ ppm): 17.88, 12.76, 9.44.

Procedure for hydrolytic degradation.

11, **13** or **poly(13)** (6.0 mg) were dissolved into 0.6 ml deuterated buffer solution (pH = 1.0: 0.136 mM hydrogen chloride - potassium chloride solution, pH = 3.0: 0.088 mM hydrogen chloride - potassium hydrogen phthalate solution, pH = 5.0: 0.100 mM sodium acetate - acetic acid solution, pH = 7.0: 0.01 mM PBS buffer solution, pH = 8.0: 0.015 mM borax - hydrogen chloride solution, pH = 13: 0.145 mM sodium hydroxide - potassium chloride solution). The mixtures were poured in NMR tubes and measured during the degradation.

Preparation of PPDA nanoparticles

30 mg of **poly(15)** was dissolved in 1 g (846 µg) of chloroform and added to a aqueous solution of Lutensol AT50 (30 mg) in 5 g of water. The two layer system was sonicated with a Brandon W450-D sonifier with a ¼ tip at 70 % amplitude in a pulsed regime (30 s sonication, 10 s pause) under ice cooling. The obtained miniemulsion was stirred open at 40 °C for 16 h to evaporate the organic solvent. The obtained nanoparticles (ca. 240 nm from DLS) were divided into volumes of 500 µL and 40 µL of concentrated HCl was added to each vial. Every other day one of those suspensions was freeze dried, dissolved in deuterated chloroform and measured by ^{31}P{H} NMR spectroscopy.

Acknowledgements

The authors thank Prof. Dr. Katharina Landfester (MPIP) for continuous support. The Deutsche Forschungsgemeinschaft (WU750/ 8-1) is acknowledged for funding.

Results and Discussion

Monomer Synthesis. For the comparison between PPEs and PPDAs, a library of different monomers was prepared (Scheme 2): the phosphate monomers **5-10** carry either a P-OH or

a P-OCH_3 side group with two unsaturated alkyl chains of different length attached via P-O-bonds. Monomers **11-15** have analogue structures, but instead of phosphoesters, two phosphoramidate linkages attach the polymerizable groups.

The reasoning for these monomer structures is their expected stability profiles: it is well-known that phosphodiesters are resilient to hydrolysis, while phosphotriesters can be cleaved hydrolytically. Such structures are compared with our novel PDAs.

The monomers with P-OH functionality are accessible by esterification or amidation with 3-butene-1-amine, 3-butene-1-ol, 7-octene-1-amine, 7-octene-1-ol, 10-undecene-1-amine and 10-decene-1-ol, followed by careful hydrolysis (Scheme 2). The phosphate monomers carrying a methyl ester side chain (**8**, **9**, **10**) can be prepared either by the direct coupling of methyl dichlorophosphate with the respective unsaturated alcohol or by treating $POCl_3$ with two equivalents of the respective alcohol, followed by hydrolysis. The intermediate monomer (i.e. with the pendant hydroxyl group) is then reacted with trimethyl orthoacetate as previously reported.[174]

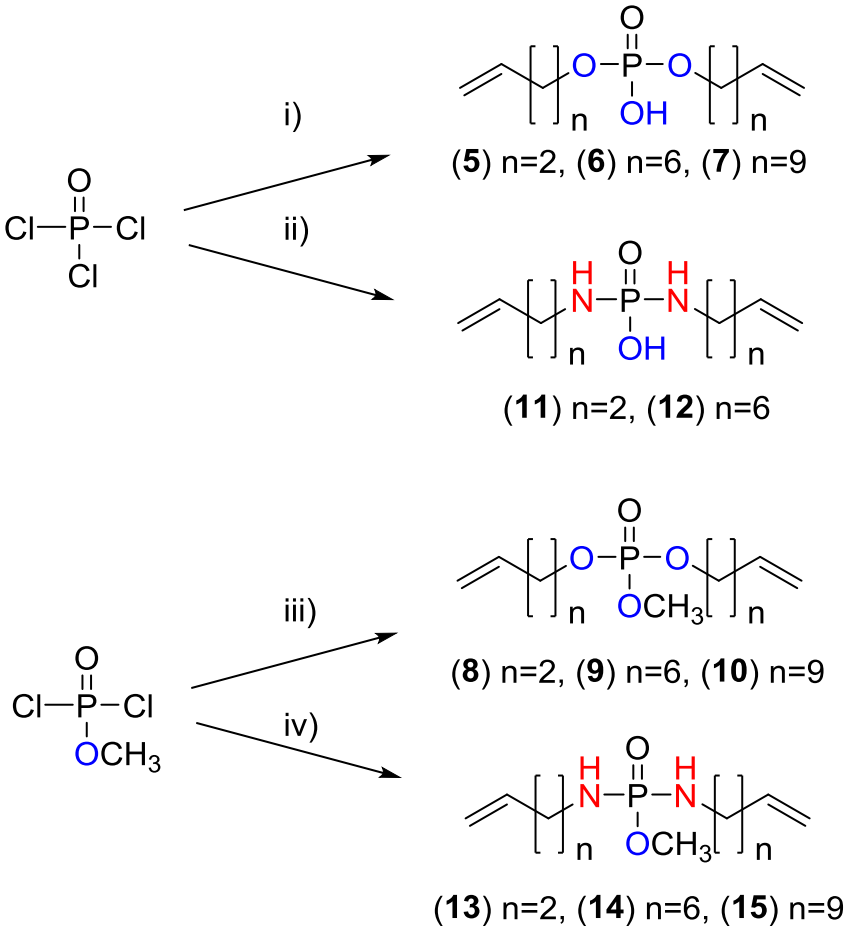

Scheme 2: Synthetic strategy for phosphate and phosphorodiamidate monomers for the ADMET polymerization (i) a) alcohol, pyridine, b) water; ii) amine, pyridine, b) water; iii) alcohol, pyridine; iv) amine, pyridine).

^{1}H NMR, ^{13}C{H} NMR, elemental analysis, and ESI MS confirmed the successful synthesis of all monomers (Supporting Information). Monomer **5** is the only one water-soluble of the phosphate based monomers, while for the phosphorodiamidates both "butenyl" monomers (**11** and **13**) are water-soluble due to the more polar P-N-bonds. Figure 1 shows the NMR spectra of monomers **11** and **13**. The ^{1}H NMR spectrum of **13** exhibits the characteristic doublet of a methoxy phosphoester at ca. 3.6 ppm (J= 11,2 Hz), due to coupling with the NMR-active phosphorus. The ^{31}P{H} NMR spectra exhibit single resonances at ca. 8.7 ppm for **11** and ca. 17.0 ppm for **13**, respectively, consistent with the ^{31}P NMR chemical shifts of other reported phosphorodiamidates.[90]

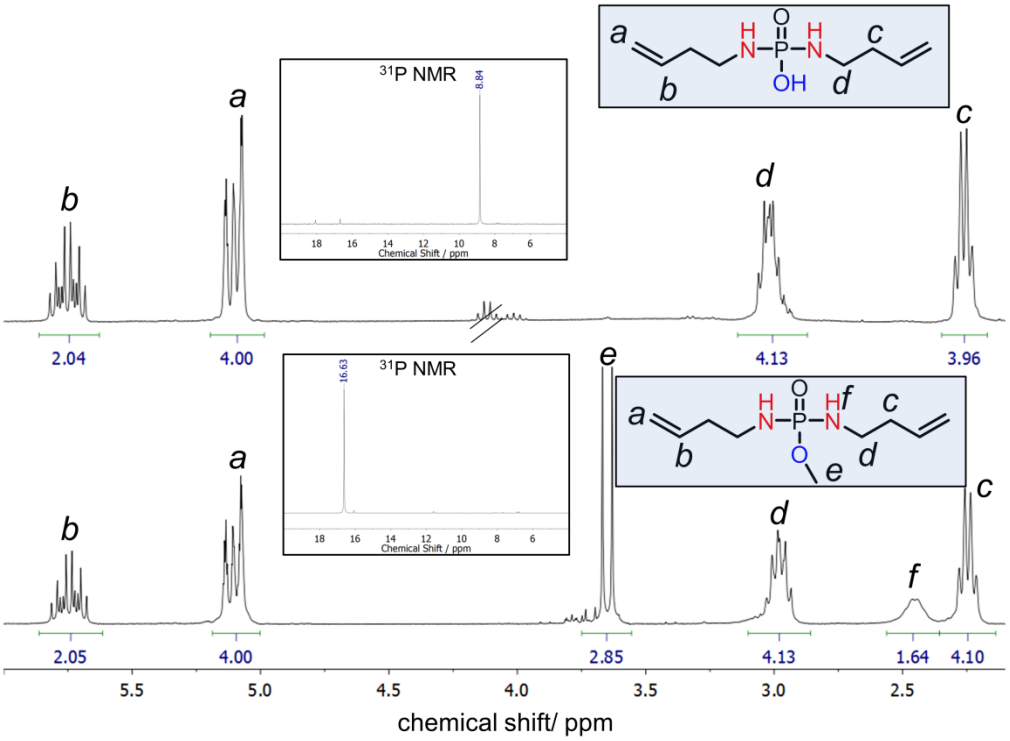

Figure 1: ^{1}H NMR (300 MHz, $CDCl_3$, 298K) of **11** (top) and **13** (bottom) (the Inset shows the ^{31}P{H} NMR (202 MHz)).

Polymerization. The synthesis of PPEs and PPDAs was accomplished by acyclic diene metathesis (Scheme 3).[70, 153, 175] For PPEs, typically Grubbs catalyst 1st generation leads to polymers with high molecular weights,[74] but produced only oligomers for phosphorodiamidates. When Hoveyda-Grubbs 2nd generation catalyst was used, successful polymerization for PPDAs was observed either in bulk (if the monomer is liquid) or in solution (50 wt% in 1-chloronaphtalin) and with 1 mol% of Hoveyda-Grubbs 2nd generation catalyst at r.t. to 60 °C at reduced pressure. The phosphate monomers are liquids with low viscosity; during the polymerization the viscosity increases and the temperature was increased (to 50 °C) to ensure efficient stirring for 8 to 16 h until the reaction mixture solidified. Due to the higher viscosity of the phosphorodiamidates their polymerization was conducted in solution and an additional 1 mol% catalyst was added to the mixture to promote the polymerization after 2 h until the solution was too viscous to allow efficient stirring (ca. 24h). Catalyst deactivation occurred during the reaction, which was visible as the color changed during the polymerization in case of Grubbs 1st generation from purple to red

and eventually to brown; in case of Hoveyda-Grubbs 2nd generation catalyst the color changed from green to brown.

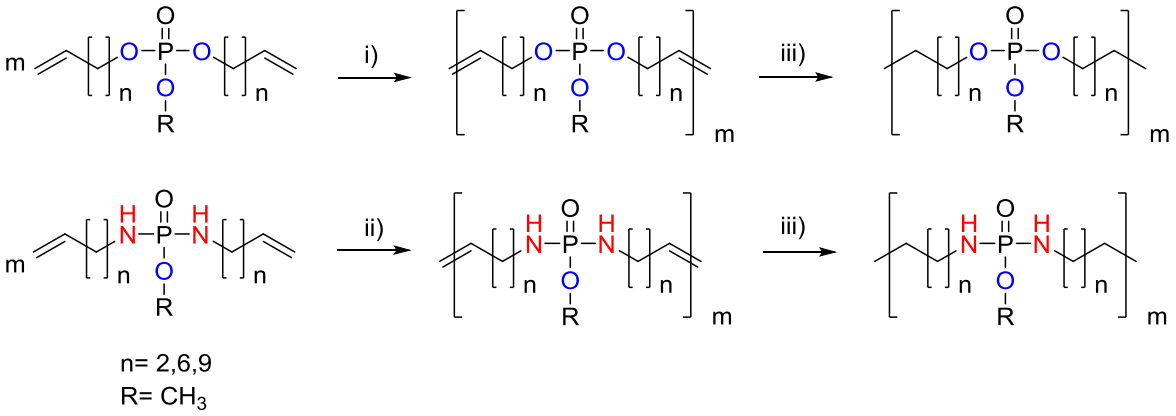

Scheme 3: ADMET polycondensation of unsaturated phosphates and phosphorodiamidates (i) Grubbs 1st generation, 50 °C, bulk ii) Grubbs Hoveyda 2nd generation, r.t., 1-chloronaphtalin iii) Pd/C, r.t., CH_2Cl_2).

PPEs can be obtained with higher molecular weights compared to the PPDAs (Table 1). This is probably due to the polymerization of the PDAs at room temperature and in solution. In order to generate higher molecular weight PPDAs the solution polymerization was conducted at 50°C at a controlled reduced pressure of 100 mbar (Method E in **Table 1**). **Poly(8)** and **poly(13)**, which is water-soluble, exhibit lower molecular weights probably due to the negative neighboring effect described earlier.[153] The successful polymerization can be detected easily from the ^{1}H NMR spectra as the terminal double bonds (at ca. 5 ppm and 6 ppm in the monomers, cf. Figure 1 and Figure 2) are transformed into internal double bonds during the polymerization showing a broad resonance at ca. 5.5 ppm (Figures 2 and 3). The overlay of the ^{1}H DOSY spectra of **14** and **poly(14)** proves successful polymerization as the diffusion coefficient is shifted to lower values after the reaction (Figure 2 and Supp. Info. for other monomers). In contrast to all monomers bearing a methoxy side chain, which undergo successful ADMET, the monomers with OH side chain did not undergo efficient homopolymerization under these conditions and only oligomers were obtained. This is probably attributed to interactions of the P-OH-groups with the catalyst. However, it was possible to generate copolymers of the "OH-series" with monomers carrying methoxy side

chains. PPEs and PPDAs in the range of 1,000 - 30,000 g/mol have been synthesized (Table 1 and Supp. Info. for further details).

In addition to the unsaturated polymers that are obtained directly after the metathesis, catalytic hydrogenation produces the saturated analogues. The hydrogenation was carried out at room temperature with palladium (10 % Pd/C) at 25 bar (compare Experimental Section for details). Figure 3 shows the comparison of **poly(15)** and the hydrogenated **poly-H(15)**. After hydrogenation, the double bond resonances at ca. 5. ppm disappear producing the saturated materials.

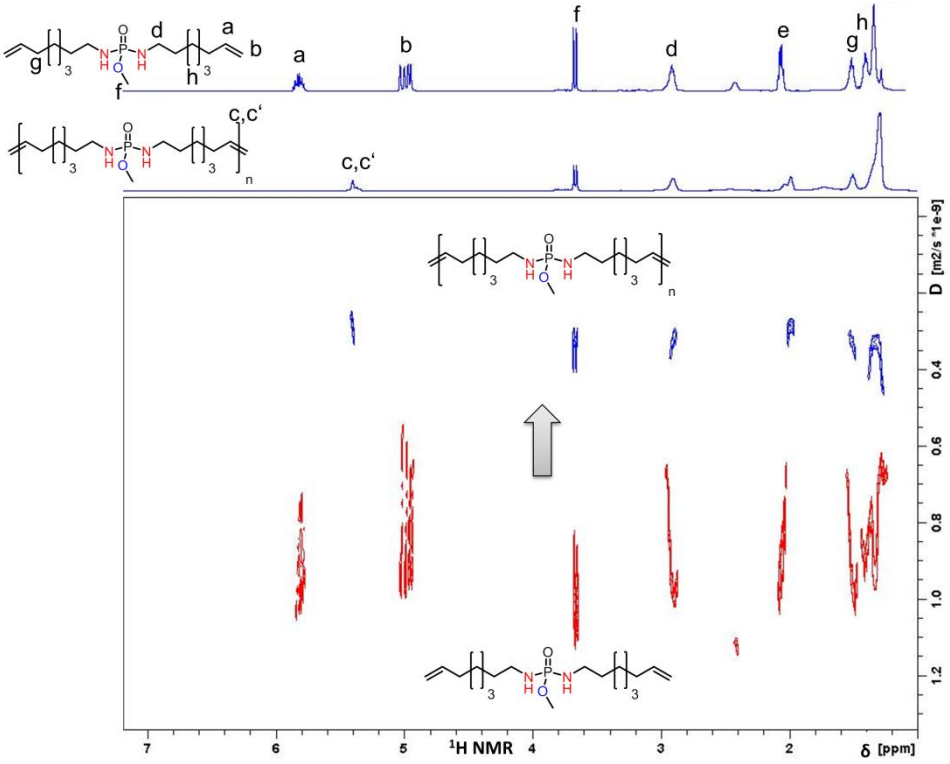

Figure 2: ^{1}H DOSY NMR spectrum of monomer **14** (red signals of DOSY spectrum) and the respective polymer **poly(14)** (blue signals of DOSY spectrum), proving the formation of internal double bonds at 5.4 ppm and the diffusion coefficient shift (500 MHz, 298 K, $CDCl_3$).

Molecular weight determination of phosphorus-containing materials by GPC is often difficult due to possible column interactions.[70-71] GPC measurements were only successful for the PPEs on our setup (Supp. Info.); for PPDAs, GPC was not applicable. To estimate the molecular weights of the polymers, ^{1}H DOSY NMR calibrated with PS standards of different

molecular weights was used instead. The measurements revealed the diffusion coefficients of the polymers which can be calibrated to polymer standards (the calibration curve is shown in the Supp. Info.) allowing the determination of an apparent M_w of unknown polymers in solution without any column material (Table 1). This method has been previously used to study polymerization kinetics and to determine polymer molecular weights.[176]

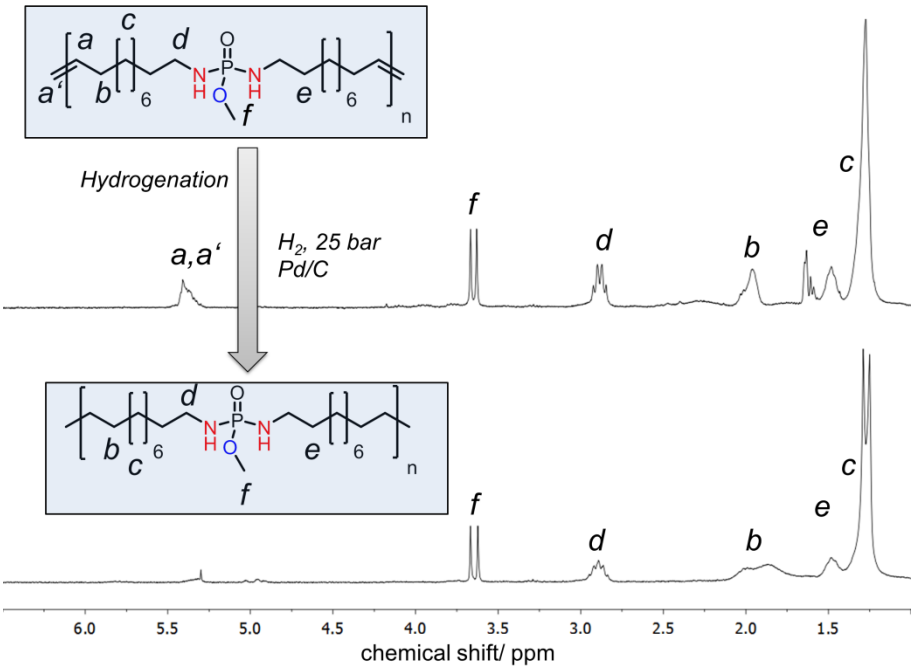

Figure 3: Comparison of the ^{1}H NMR spectra (300 MHz, $CDCl_3$, 298K) of **poly(15)** (top) and **poly-H(15)** (bottom).

Table 1. Molecular weight results for the ADMET polycondensation of phosphates and phosphorodiamidates.

Polymer	Conditions[a]	M_{wGPC}[b] (g/mol)	M_{wNMR}[c] (g/mol)	Đ
Poly(8)	A	1,400	-	1.23
Poly-H(8)	D	1,200	-	1.20
Poly(13)	A	-	1,100	-
Poly-H(13)	C	-	1,000	-
Poly(9)	A	19,700	-	4.32
Poly-H(9)	D	21,300	-	5.46
Poly(14)	B	-	2,800	-
Poly-H(14)	C	-	2,400	-
Poly(10)	A	19,900		2.41
Poly-H(10)	D	16,400	-	3.19
Poly(15)	B	-	6,500	-
Poly(15)	E	-	12,000	-
Poly-H(15)	C	-	5,800	-
Poly(5-10)	A	9,500	-	1.75
poly(6-10)	A	13,900	-	1.92
Poly(7-10)	A	12,000	-	2.49
Poly(11-13)	B	-	1,000	-
Poly(12-15)	B	-	8,000	-

[a] Conditions: A = bulk, 50 °C, 16h; B = 50 wt% solution of 1-chloronaphtalin, r.t.; C = CH_2Cl_2, r.t., 16h; D = toluene, r.t., 16h; E = 50 wt% Solution of 1-chloronaphtaline, 50 °C.

[b] Determined by GPC in THF measured by RI-detector.

[c] Determined by ^{1}H DOSY NMR.

Thermal properties

PPEs are interesting compounds as flame retardant additives: In addition to the phosphorus, PP(D)As have shown a synergistic effect of P and N with high thermal stabilities.[103, 177-178] Furthermore, the charring is relatively high compared to PPEs which leads to the decreasing of pyrolysis gases.[104] The thermal properties of the polymers were examined by thermal gravimetric analysis (TGA) and differential scanning calorimetry (DSC) under nitrogen atmosphere. The PPEs exhibited glass transition temperatures of -30 to -70 °C. For unsaturated PPEs with 6 and 14 methylene groups in the backbone no melting was observed, while **poly(10)** with 20-methylene groups exhibited a melting of ca. 17 °C.

In comparison to PPEs, the thermal properties of PPDAs differ strongly: all PPDAs exhibit higher glass transitions and/or melting temperatures (**Figure 4** and **Table 2**).

In Figure 4 (a) and (b) the DSC traces of PPDAs **poly(13)** and **poly(15)** were compared to their phosphate analogues **poly(8)** and **poly(13)**. The main- and the side-chain of those polymers are kept the same except that the two “ester-oxygens” were exchanged by amidate linkages (“NH instead of O”). For the amorphous materials **poly(8)** and **poly(13)** the glass transition temperatures of the PPDA **poly(13)** are more than 40°C higher than for the PPE analogue **poly(8)** (Figure 4a). Furthermore, the PPDA **poly(15)** (T_m ca. 50.4 °C) shows an increase of the melting point of more than 30°C compared to its PPE equivalent **poly(10)** (T_m = 17.2 °C). The melting enthalpy is rather similar for both materials (ΔH_m(PPE) = 26.42 J·g^{-1}; ΔH_m(PPDA) = 23.94 J·g^{-1}). For PPDA **poly(15)** the glass transition cannot be detected from the DSC curve.

Table 2: Thermal properties of polymers measured by DSC and TGA

Polymer	T_g / °C	ΔC_p / $Jg^{-1}K^{-1}$	T_m / °C	ΔH_m / Jg^{-1}	T_{on} /°C	$T_{50\%}$ /°C
Poly(8)	-65.4	0.438	-	-	212	364
Poly-H(8)	-67.9	0.369	-	-	211	272
Poly(9)	-49.6	0.439	-	-	287	314
Poly-H(9)	-	-	13,8	-37.22	259	314
Poly(10)	-52.4	0.317	17.2	-26.42	282	300
Poly-H(10)	-45.0	0.389	57.7	-61.79	288	314
Poly(13)	-22.3	0.521	-	-	142	368
Poly-H(13)	-27.1	0.498	-	-	185	343
Poly(14)	37.2	0.0746	-	-	194	393
Poly-H(14)	-	-	22.4	-2.73	231	373
Poly(15)	-	-	50.4	-23.94	267	441
Poly-H(15)	-	-	77.3	-52.20	217	395
Poly(5-10)	-50.4	0.474	10.0	-25.40	247	279
Poly(6-10)	-46.9	0.316	9.9	-29.67	278	292
Poly(7-10)	-43.9	0.400	21.1	-39.00	287	296
Poly(11-13)	-33.4	0.531	-	-	107	482
Poly(12-15)	-9.1	0.296	-	-	220	449

After hydrogenation, higher melting points and higher melting enthalpy values for both polymers are observed. The saturated PPDA **poly-H(15)** exhibit the highest melting point of P-containing polymer prepared by ADMET to date: 77.3 °C (ΔH_m = -52.20 $J \cdot g^{-1}$) compared to 50.4 °C (ΔH_m = 23.94 $J \cdot g^{-1}$) for the unsaturated **poly(15)** due to the disappearance of the double bonds which act as a defect during the crystallization of the polymer (Table 2). The PPE-equivalent **poly-H(10)** shows a melting endotherm at ca. 57.7 °C (ΔH_m = 61.79 $J \cdot g^{-1}$).

The PPDAs exhibit strongly different thermal stabilities compared to PPEs as detected by TGA measurements (Figure 4, Table 2). The starting degradation temperature of PPDAs is lower compared to PPEs, however, the temperature range in which the degradation occurs is much broader with several degradation steps (Figure 4c, and Table 2 lists the onset of the mass loss (T_{on}) and the 50% weight loss temperature ($T_{50\%}$)). The phosphorodiamidate unit degrades first at ca. 375 °C and afterwards the carbon backbone at ca. 450 °C. Furthermore, the residue obtained after TGA (under N_2) up to 600 °C remains ca. 30 wt%, rendering the PPDAs interesting for future flame retardant materials.

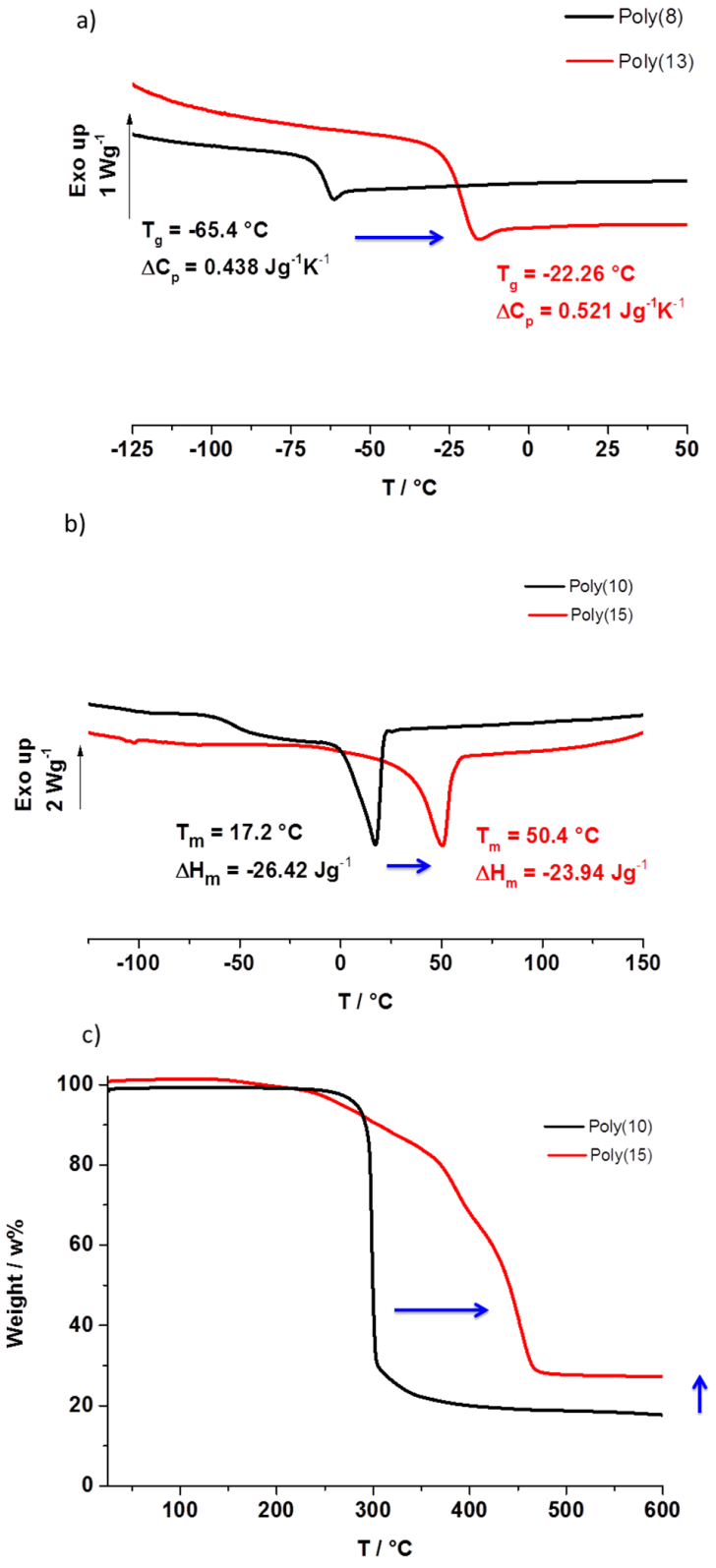

Figure 4. DSC thermograms of a) **poly(8)** vs. **poly(13),** b) **poly(10)** vs. **poly(15)** and c) TGA of **poly(10)** vs. **poly(15)**.

Hydrolytic stability. In contrast to poly(phosphazene)s, only few reports on the hydrolytic stabilities of low molecular weight phosphorodiamidates,[88, 108-109] PPAs,[87] or PPDAs[102, 117-118] have been conducted. Compared to polyamides based on carboxylic acids and amines, the phosphoramidate bond is relatively labile and can be hydrolyzed under mild acidic conditions,[90] while they are rather stable under basic conditions (at pH =13).

The hydrolytic stabilities of PPDAs have been investigated at different pH-values. Hydrolysis kinetics by ^{1}H NMR spectroscopy of the water-soluble monomers **11** and **13** and their respective polymers were conducted. The hydrolysis of **11** and **13** was studied in aqueous buffer solutions at different pH-values (based on deuterium oxide the conversion of pD = pH + 0.4 was assumed[179]) and monitored by ^{1}H NMR spectroscopy. Two separate resonances can be used to analyze the degradation. The signal of the methylene group next to the amidate linkage (ca. 3.0 ppm) is detected as a multiplet and the pendant methoxy group shows up as a double due to the coupling with phosphorus (3.65 ppm, J = 11,2 Hz; cf. Supp. Info. shows the degradation in aqueous buffer solutions at pH = 1.0, 3.0, 5.0, 7.0, 8.0, and 13.0). Monomer **13** was degraded at a pH of 1.0 (Figure 5). The degradation was monitored in the ^{1}H NMR spectrum by following the integral values of the methoxy resonance.

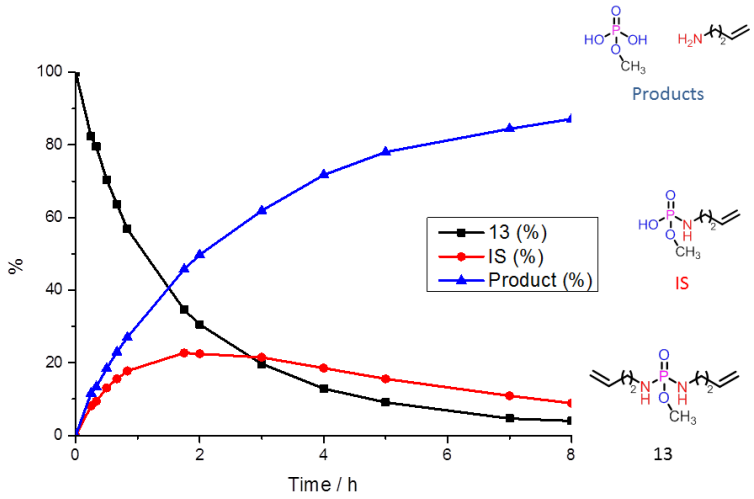

Figure 5. Monitoring the degradation of the P-N-bonds in **13** at pH=1.0 by ^{1}H NMR spectroscopy.

In general, the cleavage of the P-N bonds is strongly pH-dependent and shows the highest degradation rate at pH = 1.0, reaching full completion after 10 h. The cleavage at pH = 3.0, 5.0 is significantly slower than at pH = 1.0. At pH = 7.0, 8.0 and 13.0 the PPDA main chain remained stable over at least 70 days. However, under basic conditions, the P-OCH_3 ester hydrolyzes selectively and no further backbone degradation is observed (Figures 6 and S16). The degradation for **poly(13)** was also compared to the degradation of the monomer **13**: as expected the degradation kinetics are very similar (Figure 5 and Supp. Info.).

All other polymers were water-insoluble. To study the degradation of the hydrophobic polymers, **poly(15)** was converted into polymer nanoparticles by a miniemulsion solvent evaporation process.[79] A chloroform solution of **poly(15)** was dispersed by ultrasonication in an aqueous Lutensol solution with subsequent evaporation of the organic solvent. A stable PPDA-nanoparticle dispersion (diameter ca. 240 nm determined from dynamic light scattering) was obtained. After the addition of HCl (to pH = 1.0) the degradation of the nanoparticles was studied. Due to the hydrophobicity of the polymer complete backbone degradation was achieved after 7 days at room temperature. The ^{31}P-NMR spectra prove the polymer degradation partly after 3 days and completely after 7 days (Supp. Info.).

These properties make that material capable for a specific cleavage of the side-chain at basic conditions or the total degradation of the polymer backbone at acidic conditions. PPDAs would consequently present a new class of (bio)degradable polymers for various applications, especially because of the specific degradation of side- or main-chain. These results indicate a selective cleavage or control of the degradation profile of PPDAs by adjusting of the pH-value.

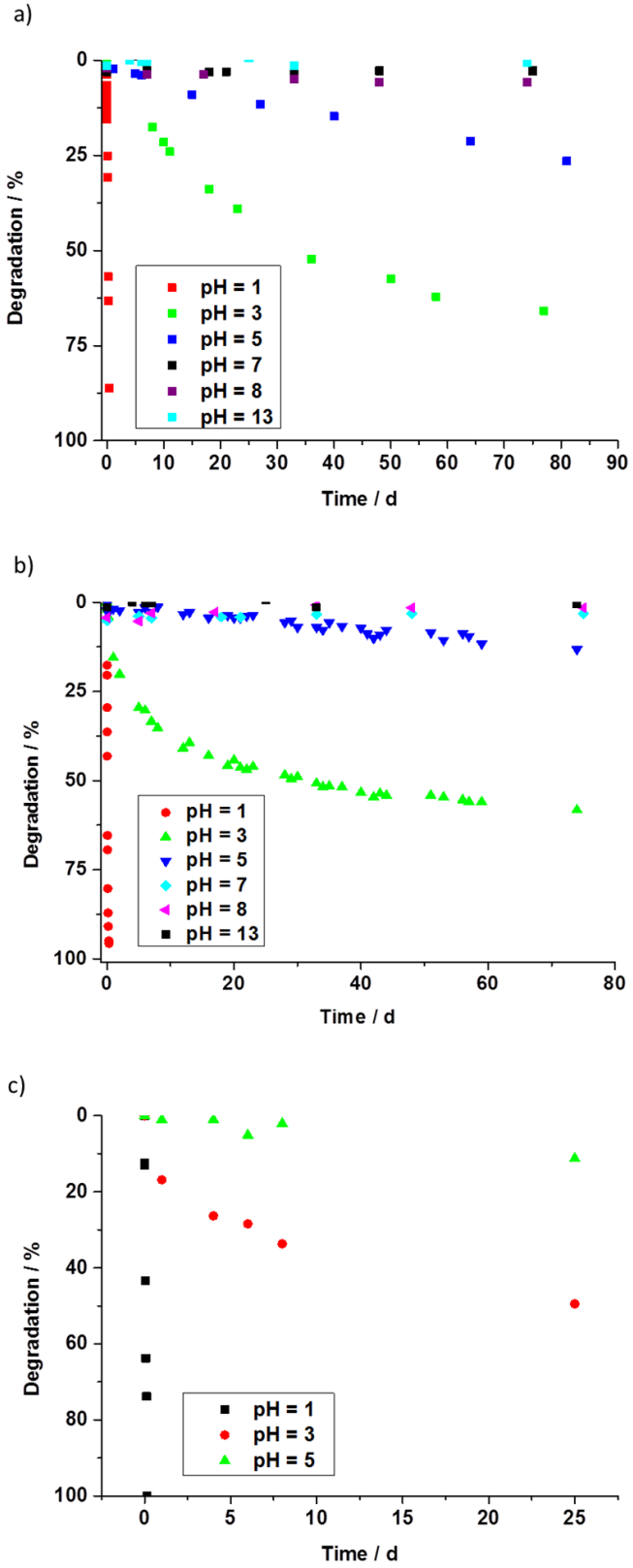

Figure 6. Degradation of phosphoramidate bonds in monomers **11 (a), 13 (b)** and **poly(13) (c)** at different pH values monitored by ^{1}H NMR spectroscopy.

Enzymatic degradation. Additionally, the enzymatic degradability of the water-soluble monomers **11** and **13** was investigated in order to investigate the general cleavability of phosphordiamidate-linkages by enzymes. Lipase from pseudomonas cepacia, alkaline phosphatase from bovine intestinal mucosa, and phosphodiesterase I from crotalus adamanteus venom were chosen as potential candidates for the degradation of **11** and **13** at their optimal conditions. The kinetics of the enzymatic hydrolysis of the monomers was monitored by $^{31}P\{H\}$ NMR spectroscopy (in phosphate buffered saline at pH = 7.4 for lipase and at pH = 9.0 with added $MgCl_2$ and NaCl for alkaline phosphatase and phosphodiesterase I according to the literature[1, 180]). In order to exclude a hydrolytic decomposition under these conditions, a control sample at pH = 9.0 with $MgCl_2$ and NaCl and without enzyme was measured. Interestingly, **13** was not degraded under these conditions with all enzymes. In contrast, **11** shows low degradation in the presence of phosphodiesterase I (Figure S7): the resonance of **11** ca. 8.8 ppm decreases and a new signal at ca. 2.3 ppm slowly emerges.

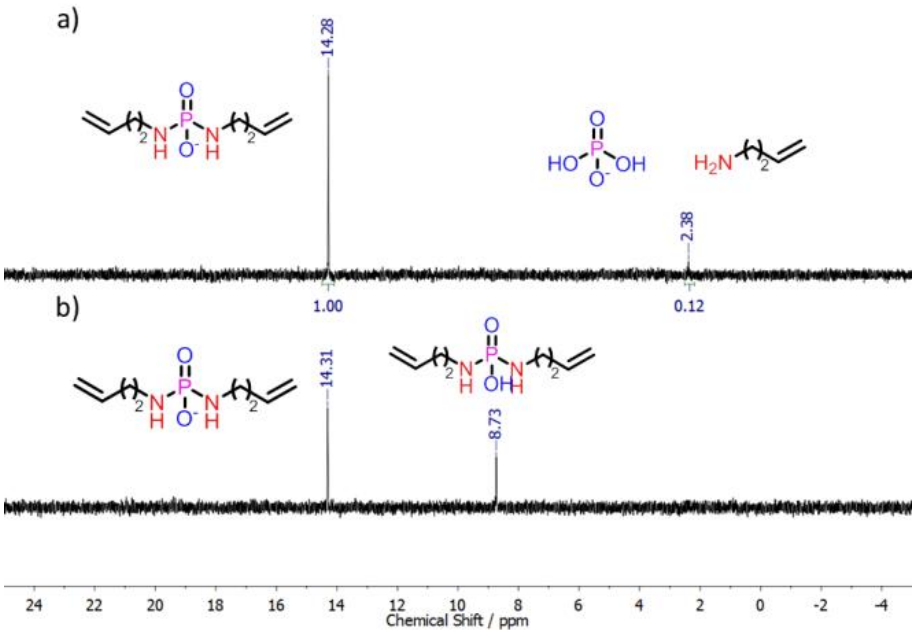

Figure 7: a) $^{31}P\{H\}$ NMR spectra of the degradation of the P-N-bond in **11** by phosphodiesterase I at pH = 9 in the presence of $MgCl_2$ and NaCl b) Control sample at pH = 9 without enzyme after 30 days. (Note: The signal at ca. 14 ppm belongs to the anion of **11** and can also be observed at the degradation of **13** and **11** by basic conditions.)

These results indicate a slow enzymatic response for PPDAs, however, their hydrolytic degradation profile is much more controllable. As we did not refresh the enzyme during the curse of this experiment, further *in vivo* studies are needed in order to fully confirm their enzymatic response.

Conclusions

A library of novel poly(phosphorodiamidate)s (PPDAs) and structural analogues poly(phosphoester)s (PPEs) was prepared by ADMET polycondensation. Polymers of variable hydrophilicity were generated, carrying either a pendant methylester or a free P-OH-group. Both unsaturated and saturated (after hydrogenation) polymers were realized and characterized. The monomers with the methoxy side chains can be polymerized in all cases, while the monomers carrying pendant P-OH groups only undergo copolymerization under these conditions. Their molecular weights were determined either by GPC or by ^{1}H DOSY NMR spectroscopy. The polymers of both series were compared with respect to thermal behavior (stability, T_g, T_m) and hydrolytic degradation. Glass transitions and melting points are typically higher in the case of PPDAs compared to structural analogues PPEs. The P-N bond in PPDAs can be degraded by acidic hydrolysis, but are rather stable under basic conditions. In contrast, the pendant P-O bond in PPDAs hydrolyses selectively under basic conditions without the degradation of the backbone. Hydrophobic polymers were transformed into aqueous nanoparticle dispersions by a miniemulsion protocol: they show a slow hydrolysis under acidic conditions over a period of several days. The specific degradation might be an interesting feature for future applications. Combined with the high thermal stabilities and melting points, PPDAs might find application in novel biodegradable materials for tissue engineering or drug delivery or also as flame retardant materials.

Acknowledgments

The authors thank Prof. Dr. Katharina Landfester for continuous support and the Deutsche Forschungsgemeinschaft (WU750/ 8-1) for funding.

Supporting Information for

Poly(phosphorodiamidate)s by Olefin Metathesis Polymerization with Precise Degradation

*Mark Steinmann, Manfred Wagner, Frederik R. Wurm**

Max-Planck-Institut für Polymerforschung, Ackermannweg 10, 55128 Mainz, Germany.

Contact address: wurm@mpip-mainz.mpg.de

Table of content

Materials and Methods

Chemicals. 10-undecen-1-ol 98%, 1-chloronaphthalene 90%, Benzylamine 99%, trimethyl orthoacetate 99%, 8-bromo-1-octene 97 %, sodium azide 99 % (NaN_3), 11-bromo-1-decene 95 %, hydrochloric acid >37 % p.a. (HCl), Celite® 545, Phosphate buffered saline (BioPerformance Certified, pH 7.4; PBS buffer), potassium chloride >99 %, sodium acetate >99 %, sodium hydroxide p.a., sodium chloride p.a., magnesium chloride >98 %, magnesium sulfate >99,5 % ($MgSO_4$), Sodium hydrogencarbonate >95 % ($NaHCO_3$), Sodium tetraborate decahydrate >99,5 % (Borax), Tris base >99,9 %, 4-(Dimethylamino)pyridine >99 % (DMAP), Phosphatase (Alkaline from bovine intestinal mucosa), Lipase from Pseudomonas cepacia, and 3-buten-1-ol 96 % were purchased from Sigma Aldrich and used as received. $POCl_3$ (Phosphoryl chloride) 99%, diethylether, toluene, ethyl acetate, Dichloromethane (CH_2Cl_2) and tetrahydrofuran (THF) were purchased from Acros and used as received. 3-Buten-1-amine 97% was purchased from Alfa Aesar and used as received. Methyl dichlorophosphate 85% and 1,8-Diazabicyclo[5.4.0]undec-7-ene 98 % (DBU) were purchased from Sigma Aldrich and purified by distillation before use. Triphenyl phosphine 99 % (Ph_3P), Toluene, 99.8%, extra dry, trimethylamine 99.7%, extra pure (Et_3N) were purchased from Acros and stored under argon. Hexane 95 %, acetonitrile (HPLC grade) and acetic acid glacial (analytical grade) were purchased from fisher chemical. Grubbs catalyst 1st generation and Hoveyda-Grubbs Catalyst 2nd Generation 97% were purchased from Sigma Aldrich and stored under argon. Potassium hydrogen phthalate and palladium/charcoal activated (10 % Pd) were purchased from Merck Millipore. Dry DMF was purchased from Appli Chem Panreac. 7-Octenol >96 % was purchased from TCI. Phosphodiesterase I (E.C. 3.1.4.1) from *Crotalus adamanteus* venom was purchased from affymetrix. Tris(hydroxymethyl)phosphine 90%, was purchased from Sigma Aldrich, and used as received for the polymer`s purification in order to remove the Grubbs Catalyst from the reaction with a similar already reported efficient procedure.[152]

Methods. Gel-permeation chromatography (GPC) measurements were carried out in THF, with samples of the concentration of 1 g L^{-1}. Sample injection was performed by a 1260-ALS auto sampler (Waters) at 30 °C (THF). The flow was 1 mL min^{-1}. In THF, three SDV columns (PSS) with dimensions of 300 × 80 mm, 10 µm particle size and pore sizes of 106, 104 und 500 Å were employed. Detection was accomplished with a DRI Shodex RI-101 detector (ERC)

and UV-Vis 1260-VWD detector (Agilent). Calibration was achieved using poly(styrene) standards provided by Polymer Standards Service.

The glass transition temperature was measured by differential scanning calorimetry (DSC) on a Mettler Toledo DSC 823 calorimeter. Three scanning cycles of heating–cooling were performed (in a N2 atmosphere 30 mL min^{-1}) with a heating rate of 10 °C min^{-1}.

Thermogravimetric analysis (TGA) measurements were performed on a Mettler-Toledo 851 (Mettler-Toledo, USA) thermobalance with temperatures ranging from 35 °C to 600 °C at a heating rate of 10 °C min^{-1} under nitrogen flow (30 mL min^{-1}).

For ultrasonication, a Branson Sonifier W-450-Digital was used with a 1/4" tip, operating under ice cooling for 2 min at 70% amplitude with pulse cycles of 30 s sonication and 10 s pauses. The average size and size distribution of the PNCs were measured via dynamic light scattering (DLS) at 25 °C using a Nicomp 380 submicron particle sizer (Nicomp Particle Sizing Systems, U.S.A.) at an angle of 90°.

^{1}H NMR, ^{13}C NMR, and ^{31}P NMR spectra were either recorded on a Bruker Avance 250 MHz or 300 MHz or 500 MHz or 700 MHz spectrometer (Details of several measurements by different spectrometers see below). The proton, carbon and phosphorous spectra were measured in $CDCl_3$, D_2O and CD_2Cl_2 at 298.3K and the spectra were referenced as follows: for the residual $CHCl_3$ at δ (^{1}H) = 7.26 ppm, CH_2Cl_2 at δ (^{1}H) = 5.28 ppm, H_2O (^{1}H) = 4.79 ppm, $CHCl_3$ δ (^{13}C triplett) = 77,0 ppm and triphenylphosphine (TPP) δ (^{31}P) = - 6.00 ppm.

^{1}H, ^{13}C,^{31}P NMR and ^{1}H DOSY experiments were recorded with a 5 mm BBI 1H/X z-gradient on the 700 MHz spectrometer with an Bruker Avance III system. For a ^{1}H NMR spectrum 64 transients were used with an 11 µs long 90° pulse and a 12600 Hz spectral width together with a recycling delay of 5 s. The ^{1}H NMR (700 MHz), ^{13}C NMR (176 MHz), and ^{31}P NMR (283 MHz) measurements were obtained with an ^{1}H powergate decoupling method using 30° degree flip angle, which had a 14,5 µs long 90° pulse for carbon and an 27,5 µs long 90° pulse for phosphor. Additionally carbon spectra were kept with a J-modulated spin-echo for ^{13}C-nuclei coupled to ^{1}H to determine number of attached protons with decoupling during

acquisition. The spectral widths were 41660 Hz (236 ppm) for ^{13}C and 56818 Hz (200 ppm) for ^{31}P, both nuclei with a relaxation delay of 2s.

Similar 1D (^{1}H, ^{13}C and ^{31}P NMR's) measurements (^{1}H-NMR (500 MHz), ^{31}C-NMR (125,77 MHz) and ^{31}P-NMR (202 MHz)) and 2D experiments ^{31}P, HSQC and ^{1}H HMBC were conducted on a Bruker Avance III 500 NMR spectrometer with a 5 mm BBFO probe equipped with a z-gradient. The spectra were obtained with π/2-pulse lengths of 11,9 µs (^{1}H), 13,2 µs (^{13}C) and 11 µs (^{31}P) and a sweep width of 10330 Hz (20,6 ppm) for ^{1}H, 29700 Hz (236 ppm) for ^{13}C and 40000 Hz (200 ppm) for ^{31}P, all nuclei with a relaxation delay of 2s.

For the diffusion measurements a 2D sequence (DOSY[181], dstebgp3s[182]) with a double stimulated echo for convection compensation and LED using bipolar gradient pulse for diffusion was used additionally.The temperature was kept at 298.3 K and regulated by a standard ^{1}H methanol NMR sample using the topspin 3.2 software (Bruker). The control of the temperature was realized with a VTU (variable temperature unit) and an accuracy of +/- 0,1K.

GPC

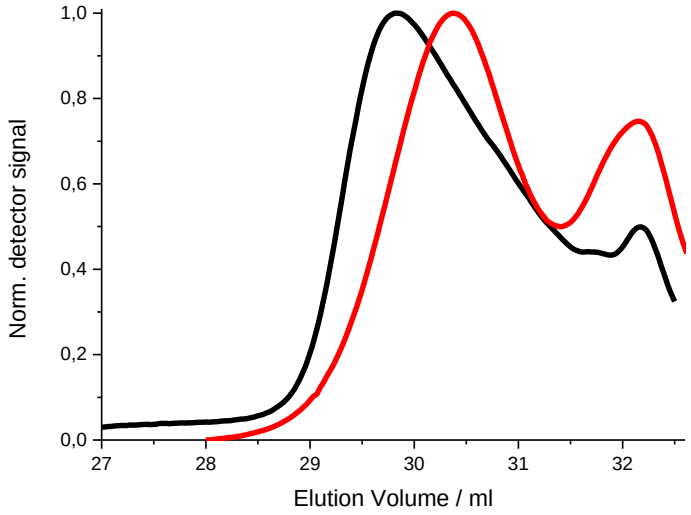

Figure S1: GPC-elugram of polymer **poly(8)** (black curve; M_w = 1,400 g·mol^{-1}) and **poly-H(8)** (red curve; M_w = 1,200 g·mol^{-1}) in THF measured by RI-detector.

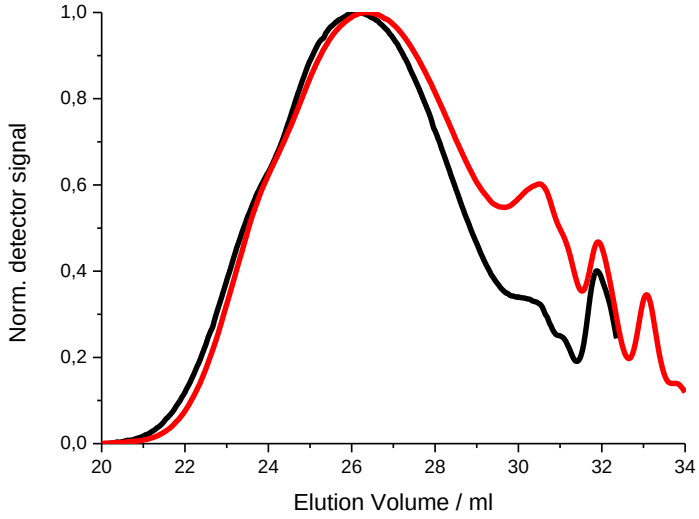

Figure S2: GPC-elugram of polymer **poly(9)** (black curve; M_w = 19,700 g·mol^{-1}) and **poly-H(9)** (red curve; M_w = 21,300 g·mol^{-1}) in THF measured by RI-detector.

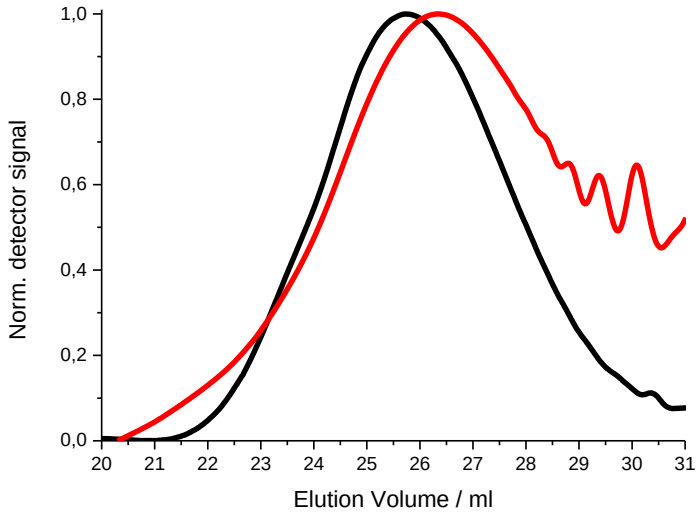

Figure S3: GPC-elugram of polymer **poly(10)** (black curve; M_w = 19,900 g·mol^{-1}) and **poly-H(10)** (red curve; M_n = 16,400 g·mol^{-1}) in THF measured by RI-detector.

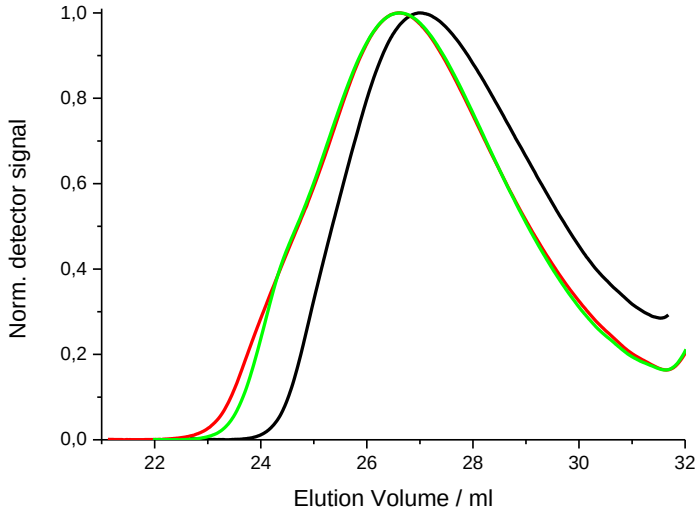

Figure S4: GPC-elugram of polymer **poly(5-10)** (black curve; M_n = 5,400 g·mol^{-1}), **poly(6-10)** (red curve; M_n = 7,200 g·mol^{-1}) **poly(7-10)** (green curve; M_n = 4,800 g·mol^{-1})in THF measured by RI-detector.

Calibration for DOSY-NMR

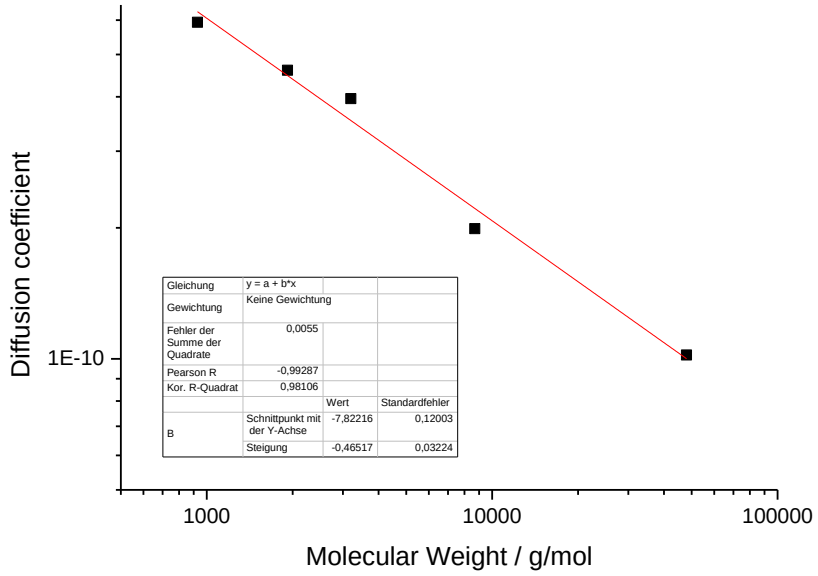

Figure S5: Calibration curve of DOSY-NMR molecular weight determination (700 MHz, 298 K, CD_2Cl_2).

Degradation

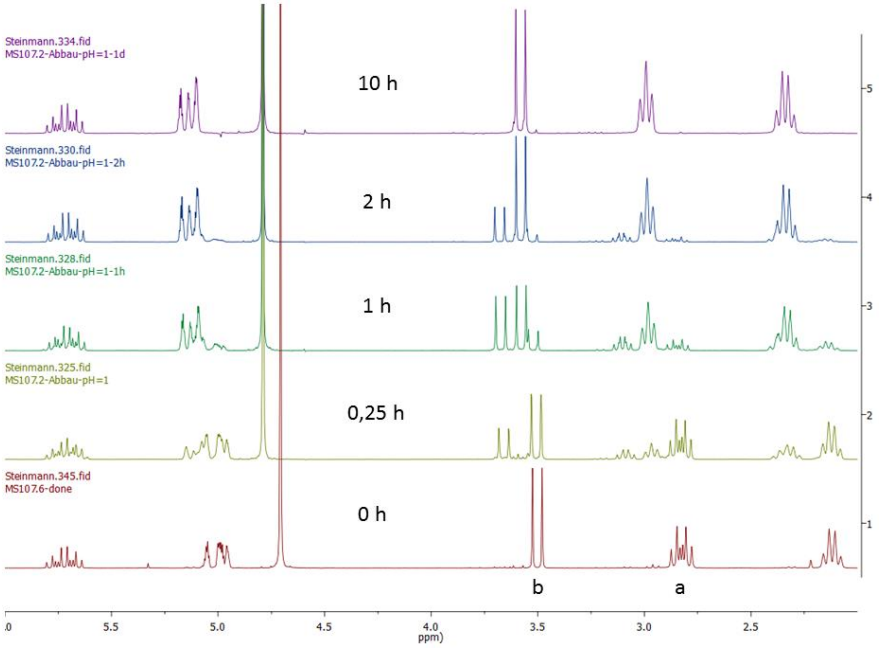

Figure S6: ^{1}H NMR spectra of degradation of **13** from 0 to 10 hours at pH = 1(300 MHz, 298 K, D_2O).

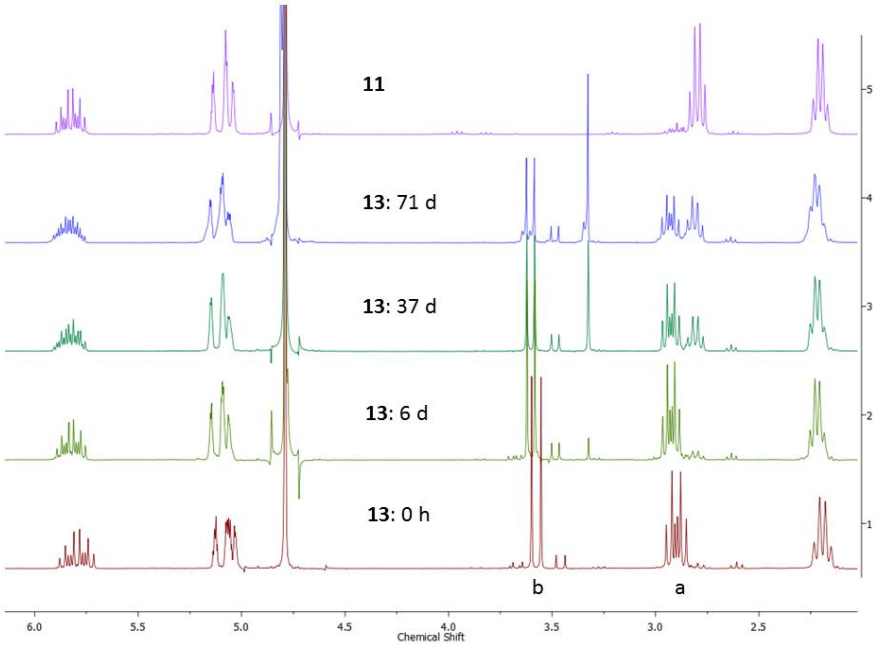

Figure S7: ^{1}H NMR spectra of degradation of **13** from 0 to 71 days pH = 13 compared to resulting structure of **11** (300 MHz, 298 K, D_2O).

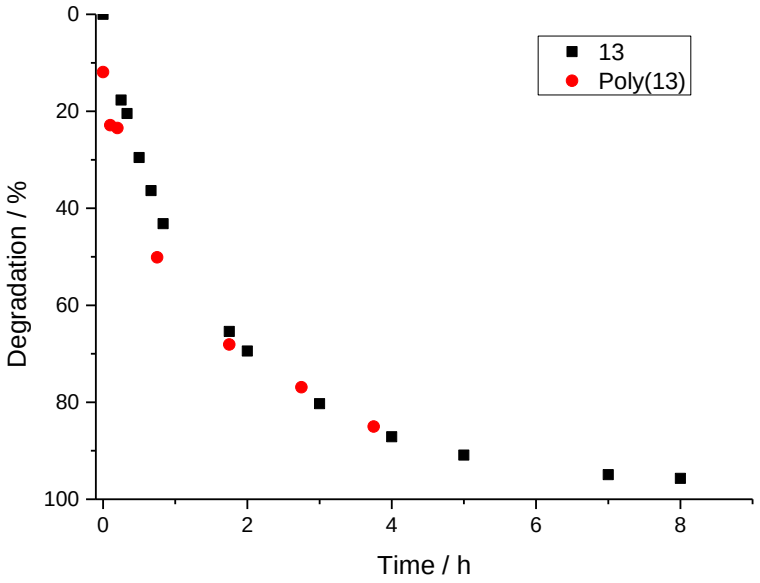

Figure S8: Comparison of degradation of **13** and **poly(13)** at pH = 1 monitored by ^{1}H NMR (300 MHz, 298 K, D_2O).

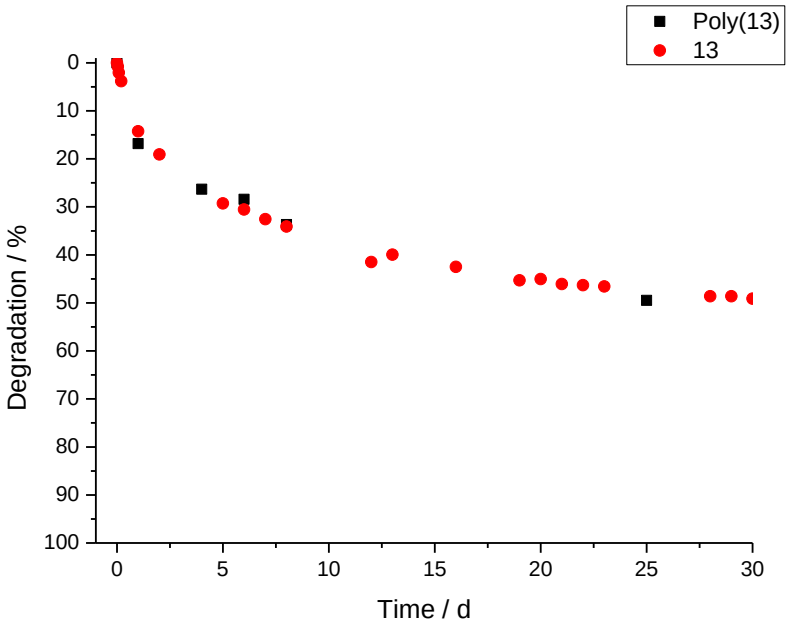

Figure S9: Comparison of degradation of **13** and **poly(13)** at pH = 3 monitored by ^{1}H NMR (300 MHz, 298 K, D_2O).

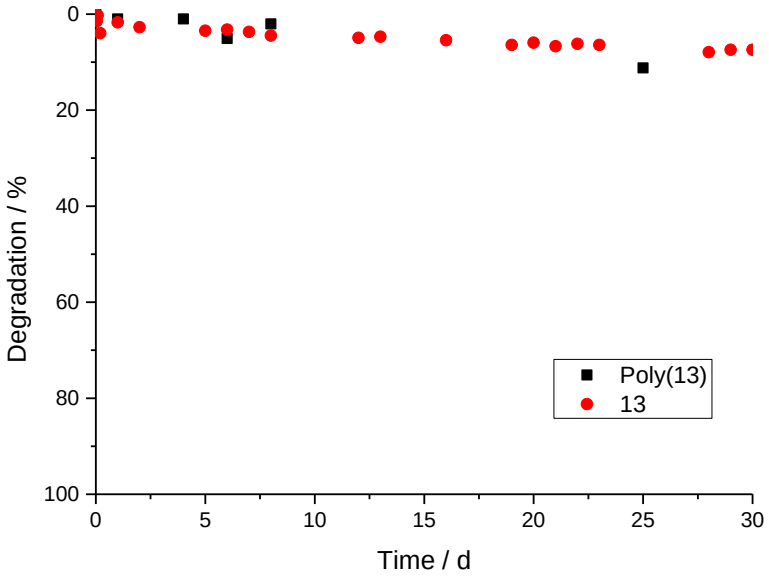

Figure S10: Comparison of degradation of **13** and **poly(13)** at pH = 5 monitored by ^{1}H NMR (300 MHz, 298 K, D_2O).

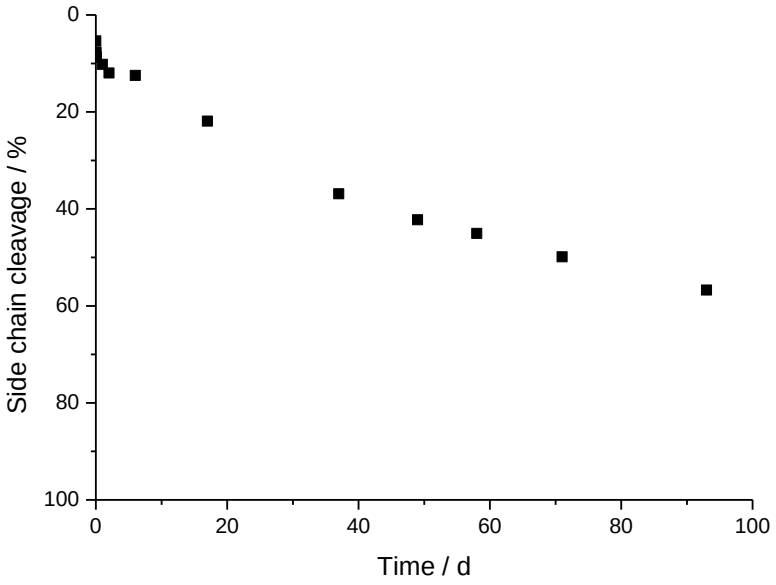

Figure S11: Side chain cleavage of **13** at pH = 13 monitored by ^{1}H NMR (300 MHz, 298 K, D_2O).

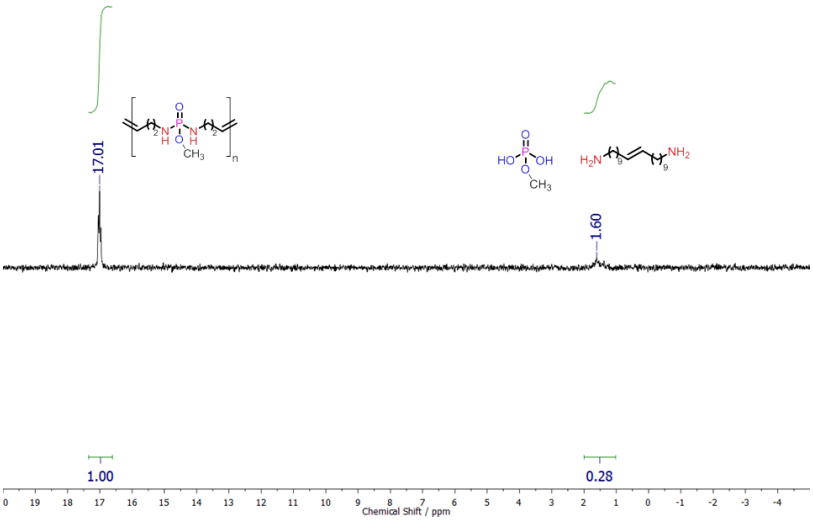

Figure S12: a) $^{31}P\{H\}$ NMR spectra of the main-chain degradation of **poly(15)** at pH = 1.0 after 3 days. Both the polymer signal at ca. 10 ppm and the methyl phosphate at 1.6 ppm are detectable (121.5 MHz, 298 K, D_2O).

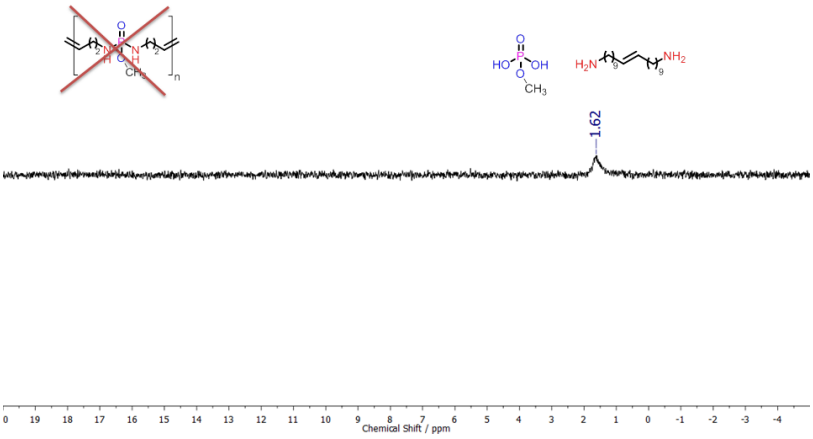

Figure S13: a) $^{31}P\{H\}$ NMR spectra of the main-chain degradation of **poly(15)** at pH = 1.0 after 7 days. Only the methyl phosphate signal at 1.6 ppm is detectable (121.5 MHz, 298 K, D_2O).

NMR spectra: Monomers:

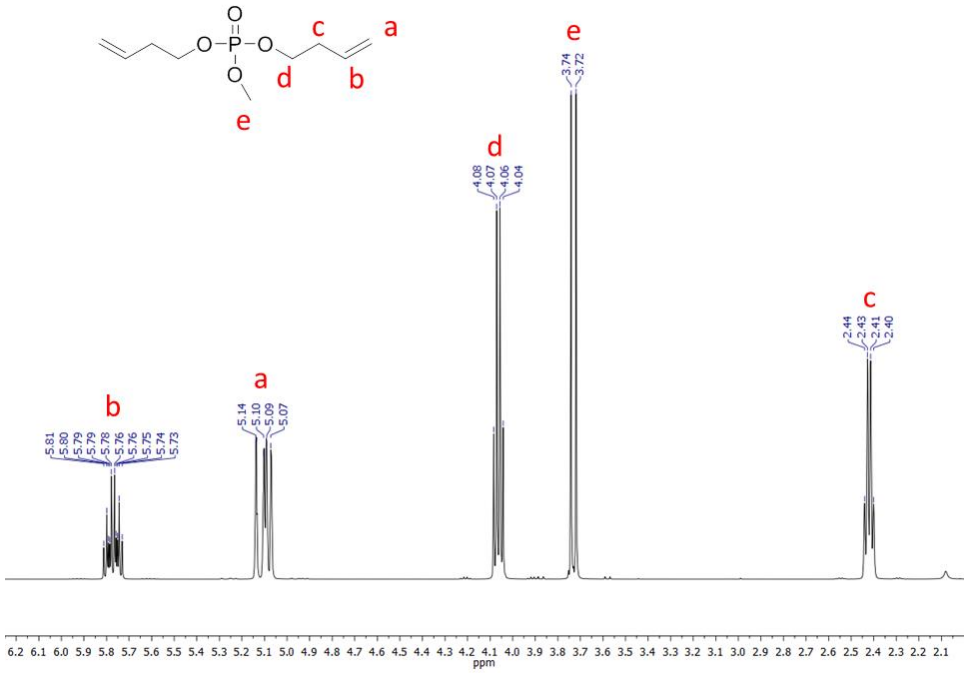

Figure S14: ^{1}H NMR of **8** (500 MHz, 298 K, $CDCl_3$).

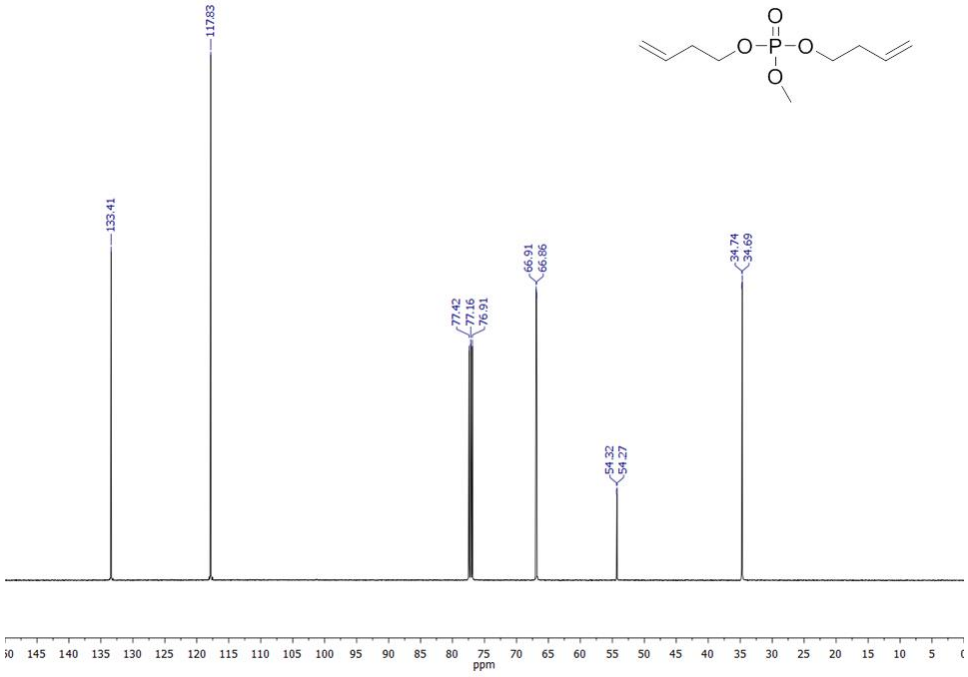

Figure S15: ^{13}C{H} NMR of **8** (126 MHz, 298 K, $CDCl_3$).

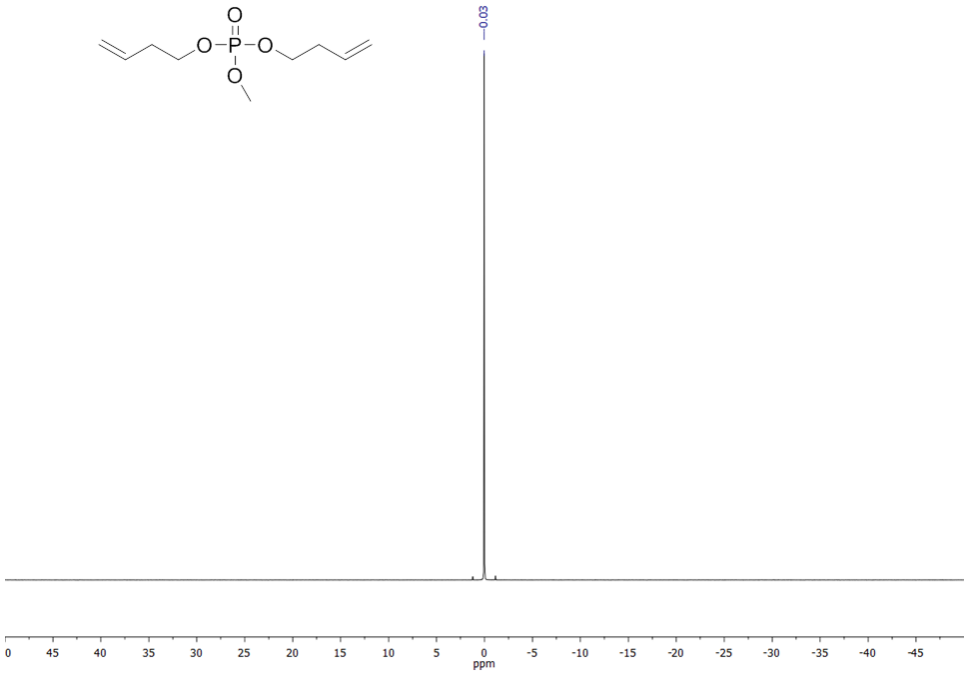

Figure S16: $^{31}P\{H\}$ NMR of **8** (202 MHz, 298 K, $CDCl_3$).

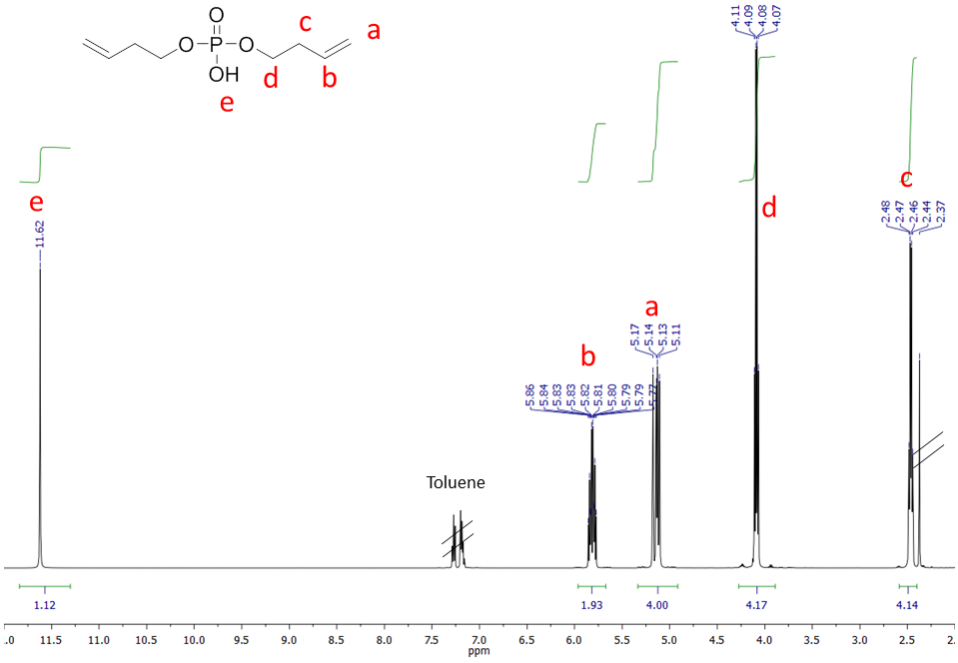

Figure S17: ^{1}H NMR of **5** (500 MHz, 298 K, $CDCl_3$).

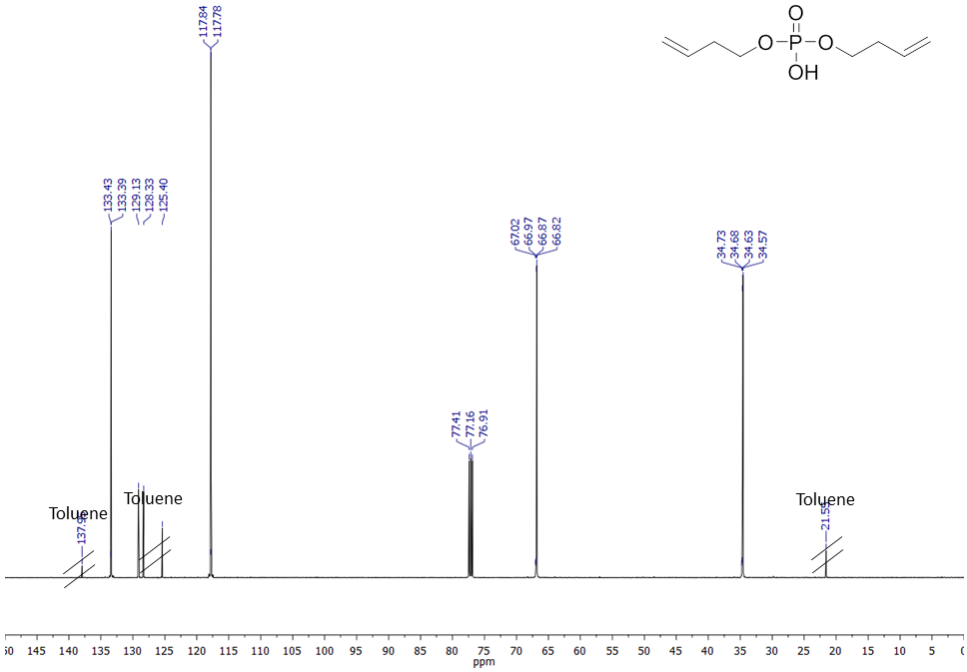

Figure S18: $^{13}C\{H\}$ NMR of **5** (126 MHz, 298 K, $CDCl_3$).

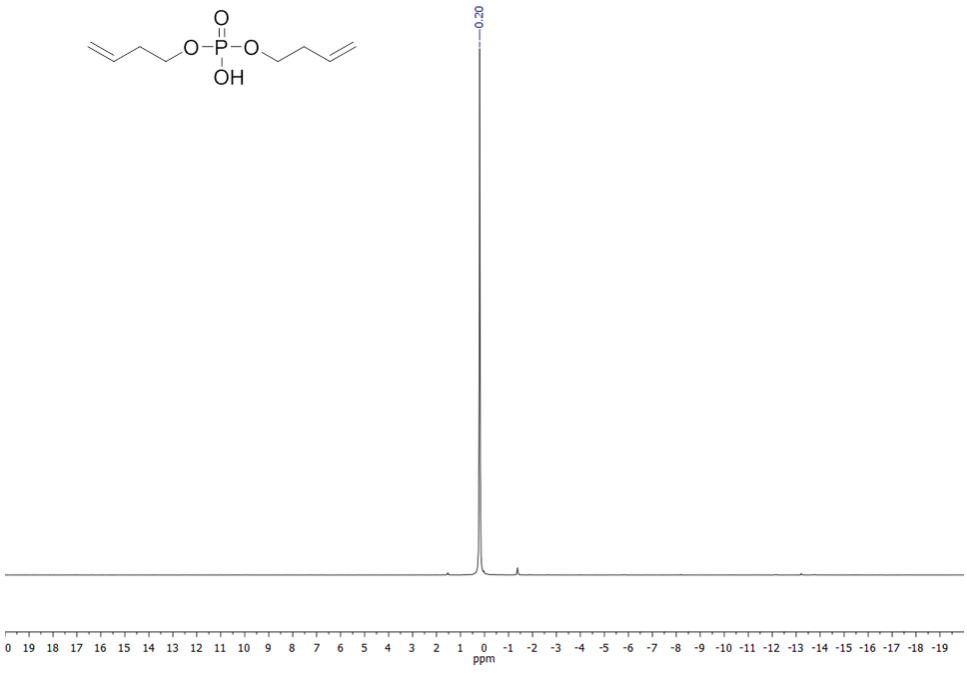

Figure S19: $^{31}P\{H\}$ NMR of **5** (202 MHz, 298 K, $CDCl_3$).

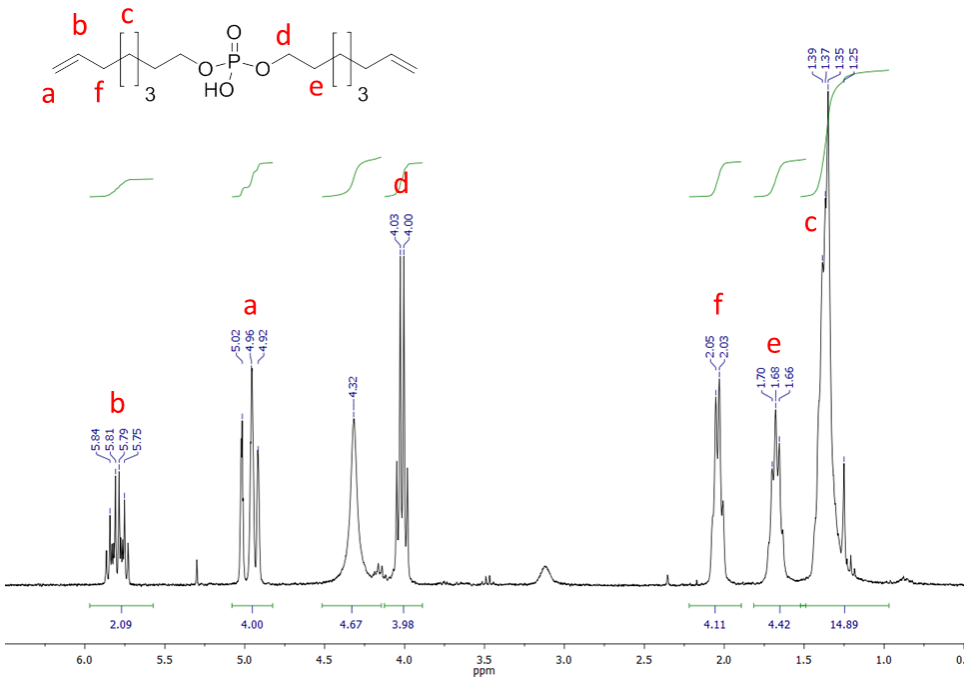

Figure S20: ^{1}H NMR of **6** (300 MHz, 298 K, $CDCl_3$).

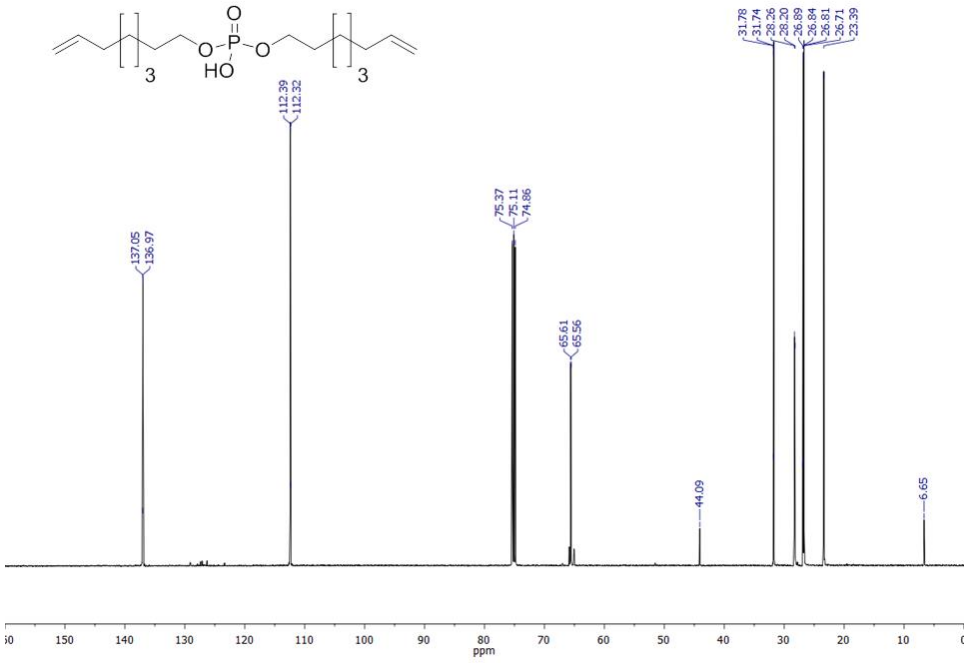

Figure S21: ^{13}C{H} NMR of **6** (126 MHz, 298 K, $CDCl_3$).

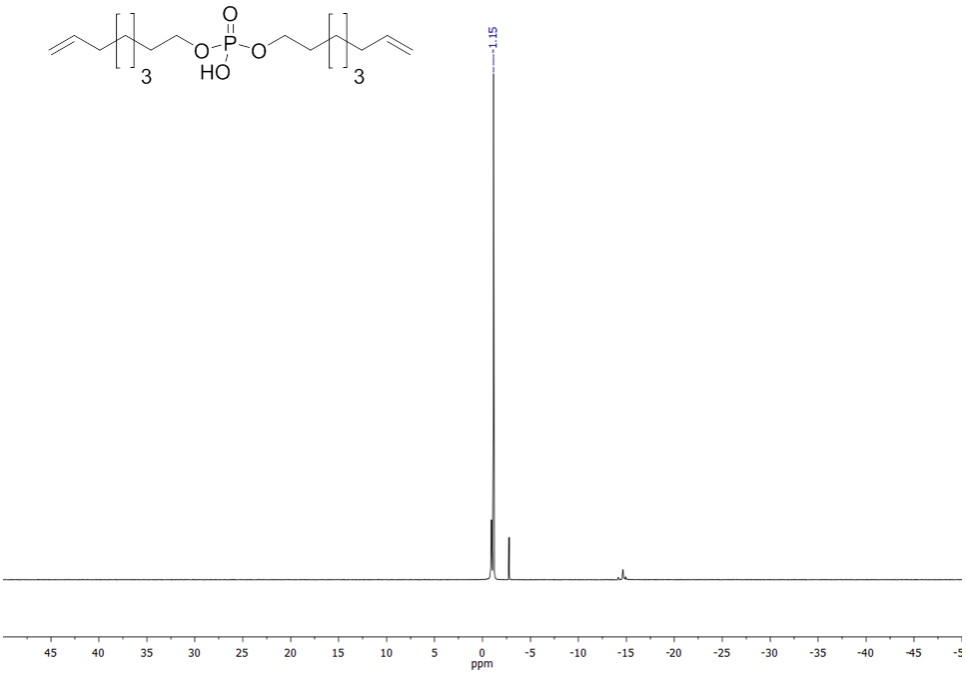

Figure S22: $^{31}P\{H\}$ NMR of **6** (202 MHz, 298 K, $CDCl_3$).

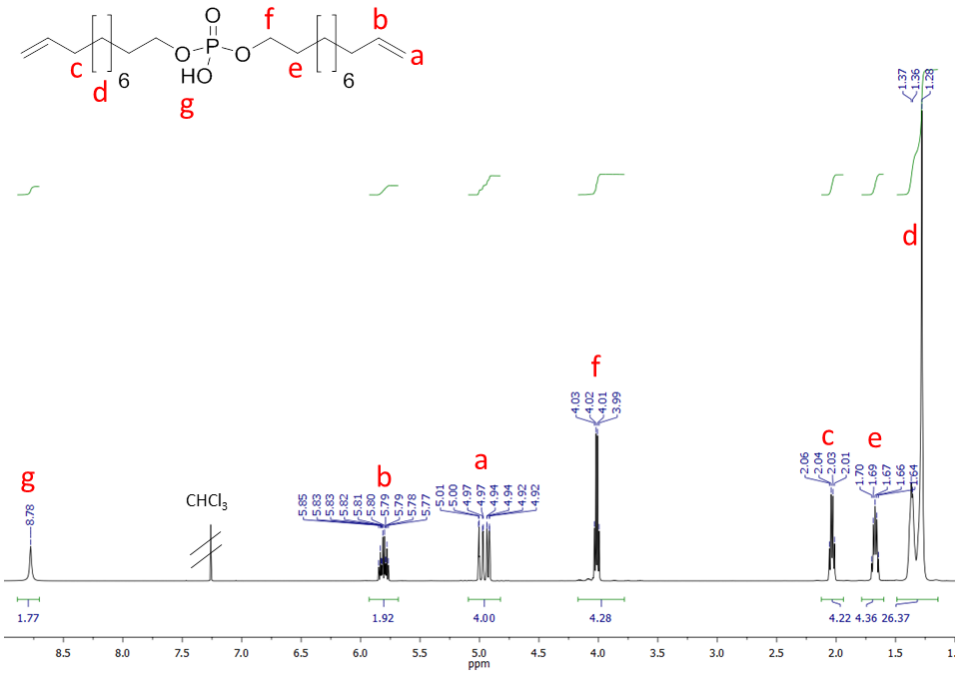

Figure S23: ^{1}H NMR of **7** (500 MHz, 298 K, $CDCl_3$).

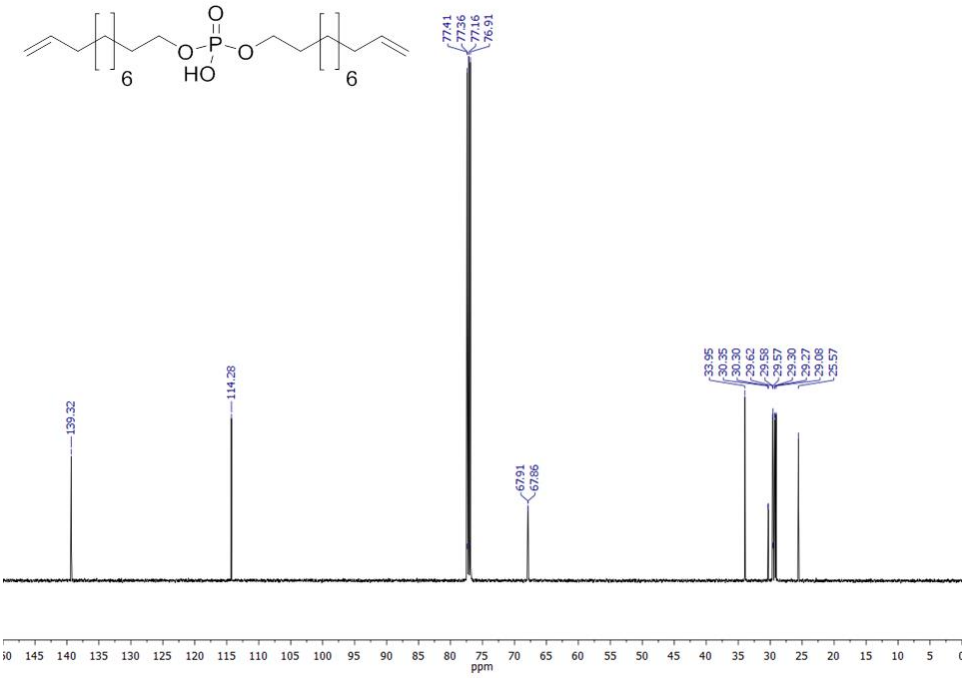

Figure S24: $^{13}C\{H\}$ NMR of **7** (126 MHz, 298 K, $CDCl_3$).

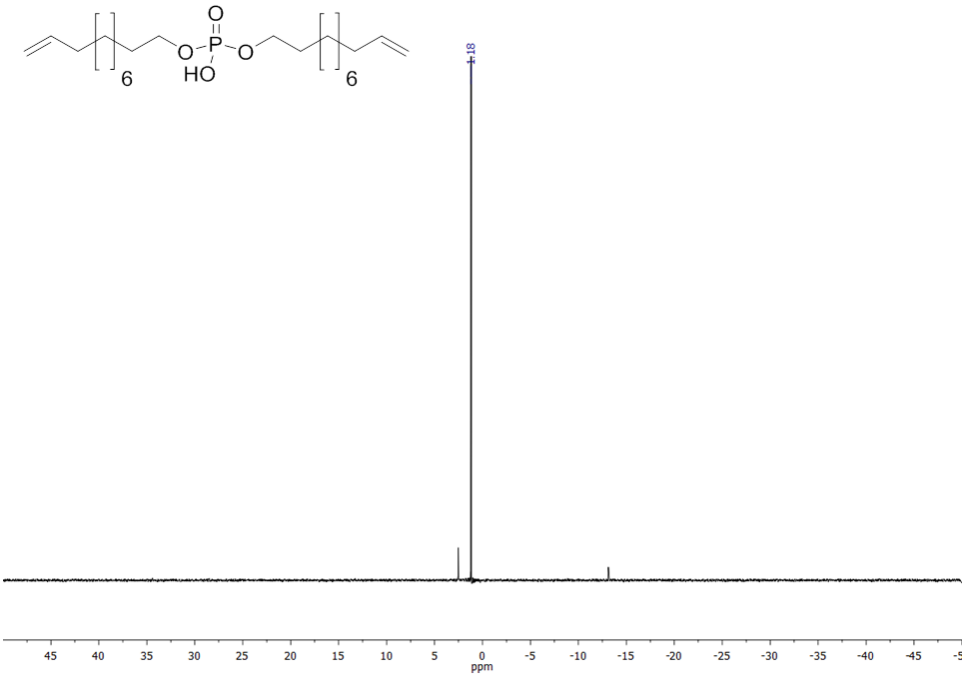

Figure S25: $^{31}P\{H\}$ NMR of **7** (202 MHz, 298 K, $CDCl_3$).

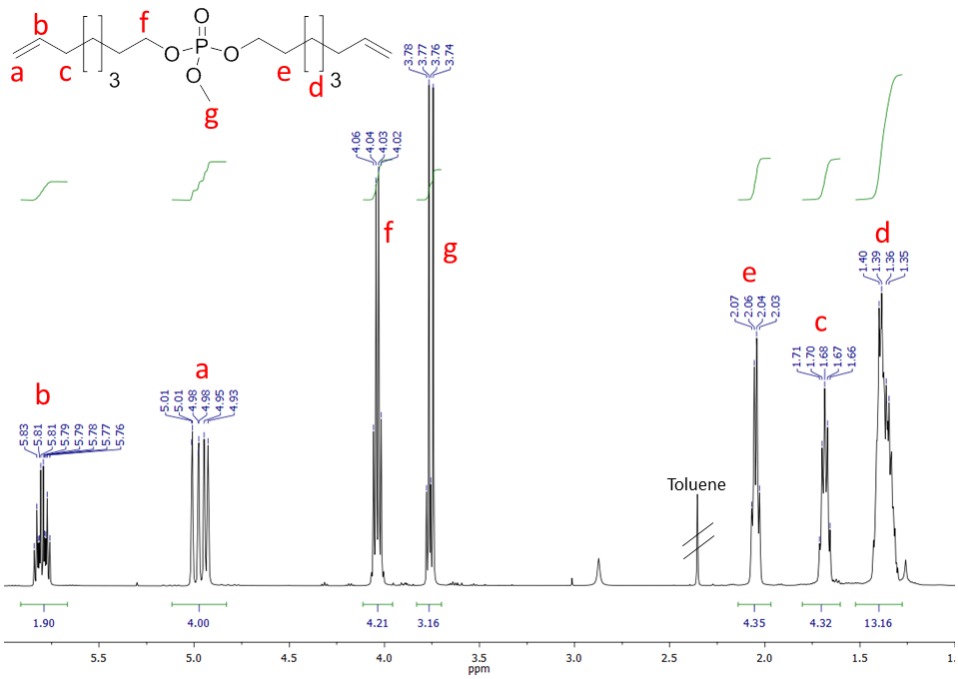

Figure S26: ^{1}H NMR of **9** (500 MHz, 298 K, $CDCl_3$).

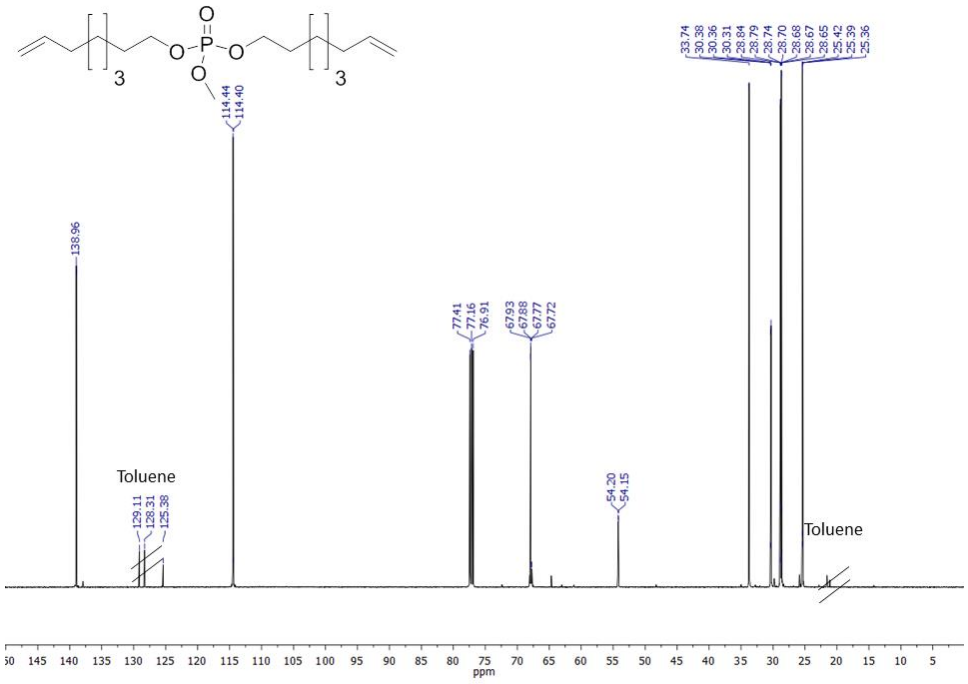

Figure S27: ^{13}C{H} NMR of **9** (126 MHz, 298 K, $CDCl_3$).

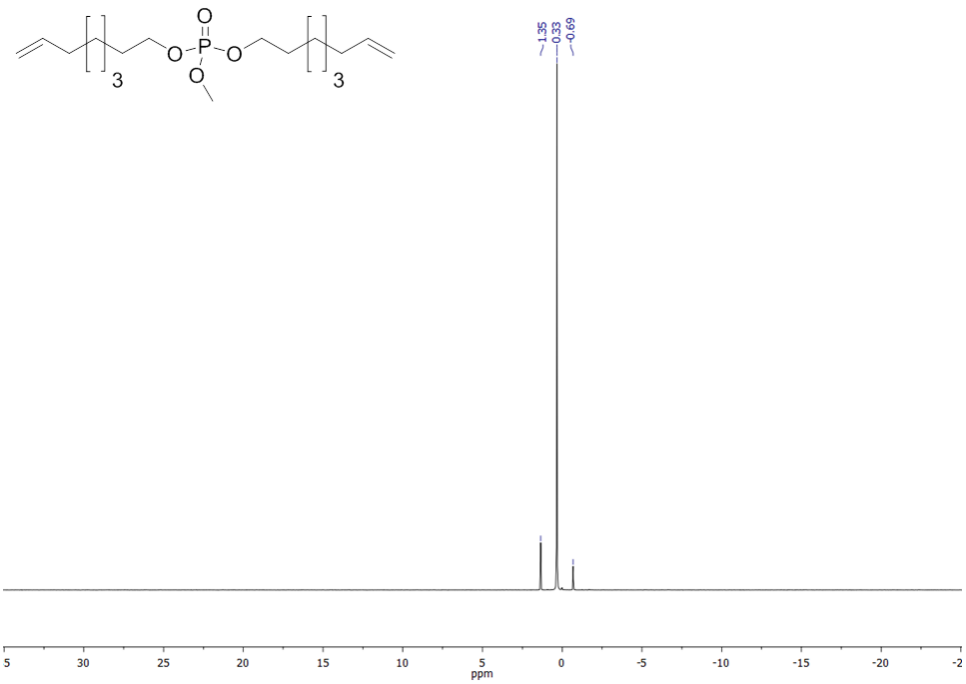

Figure S28: $^{31}P\{H\}$ NMR of **9** (202 MHz, 298 K, $CDCl_3$).

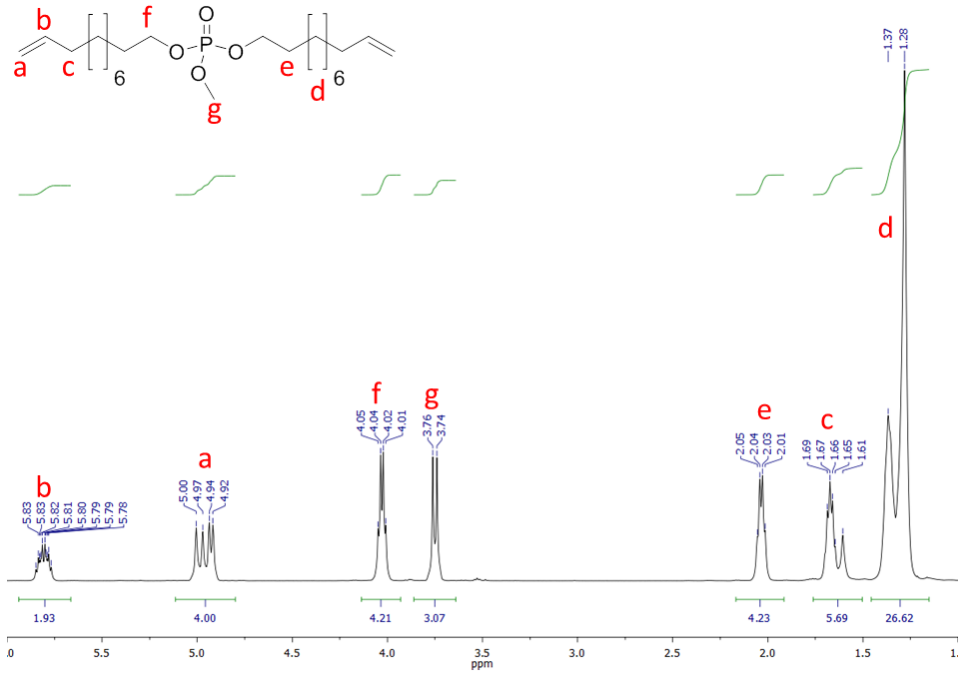

Figure S29: ^{1}H NMR of **10** (500 MHz, 298 K, $CDCl_3$).

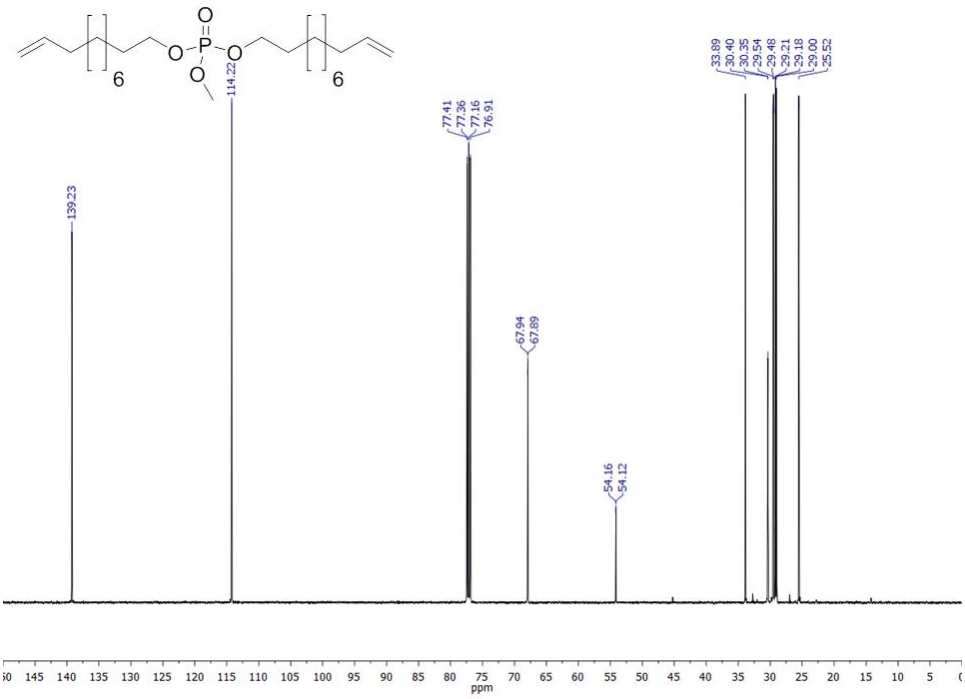

Figure S30: $^{13}C\{H\}$ NMR of **10** (126 MHz, 298 K, $CDCl_3$).

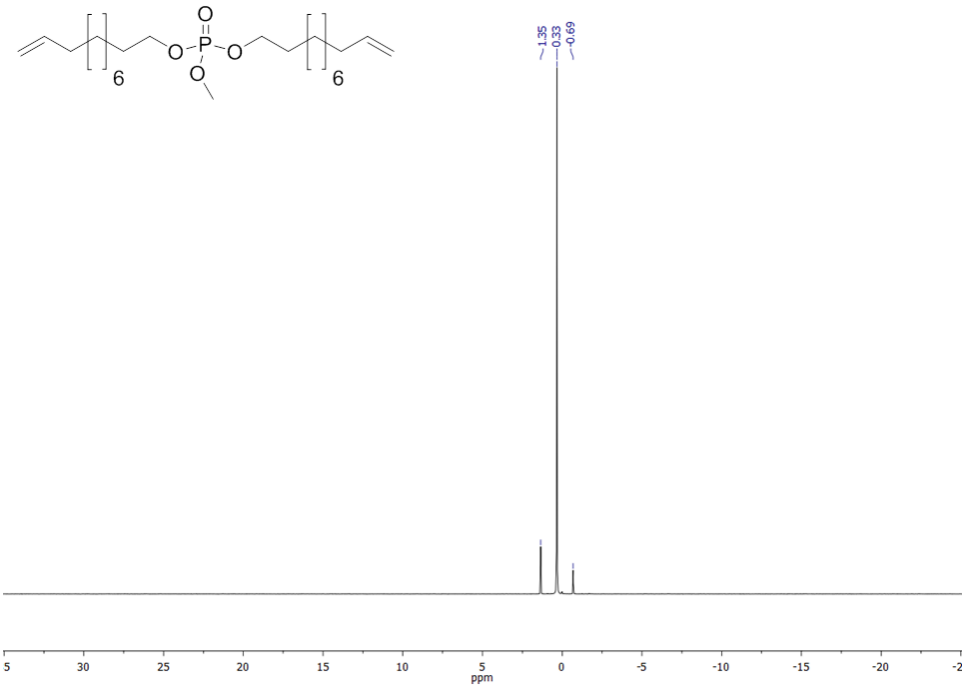

Figure S31: $^{31}P\{H\}$ NMR of **10** (202 MHz, 298 K, $CDCl_3$).

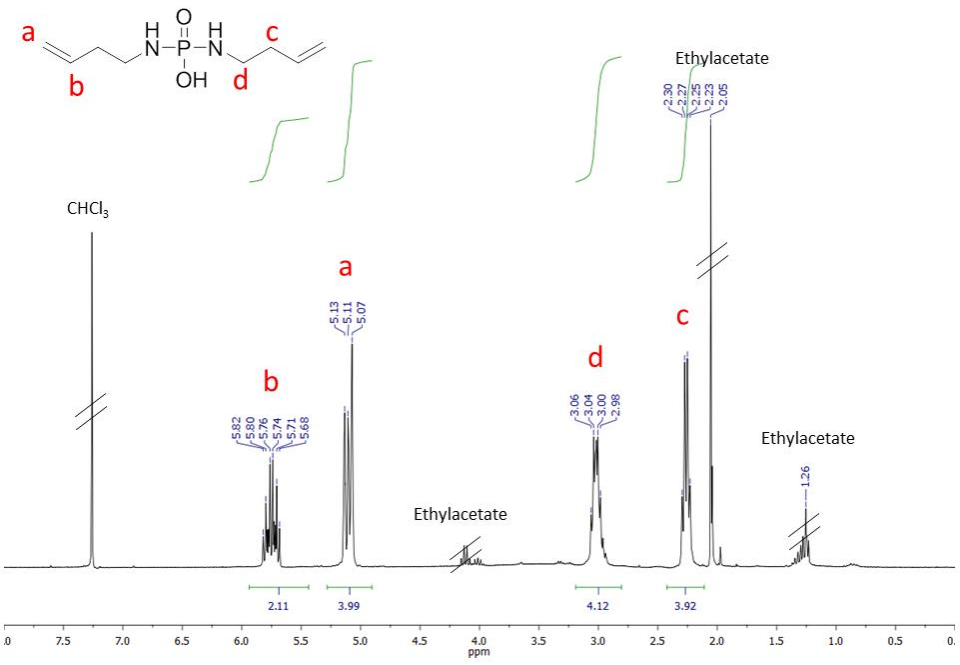

Figure S32: ^{1}H NMR of **11** (300 MHz, 298 K, $CDCl_3$).

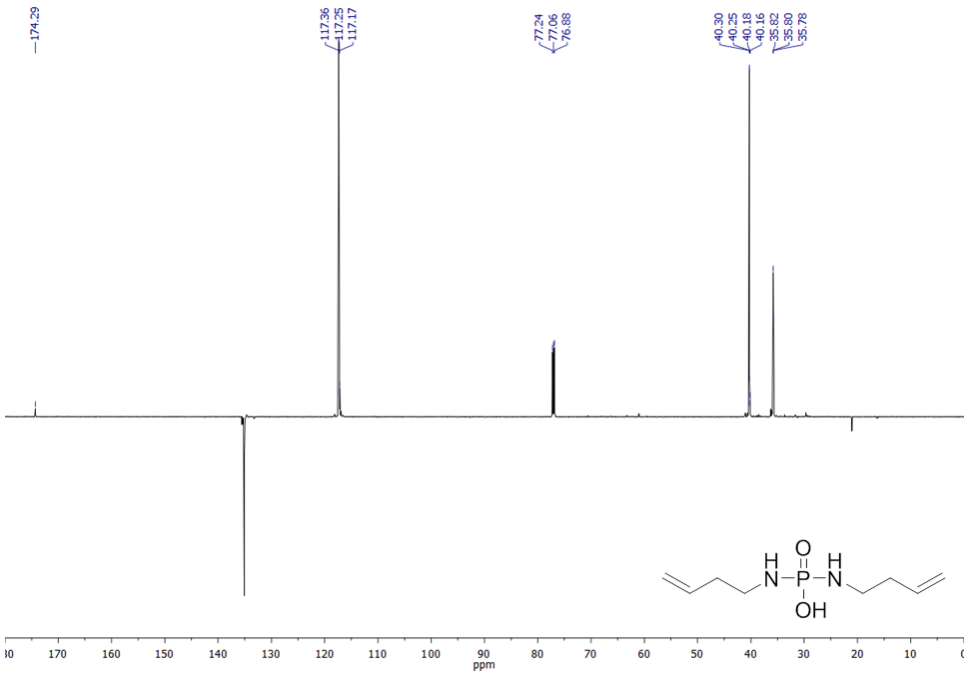

Figure S33: DEPT-135 ^{13}C{H} NMR of **11** (176 MHz, 298 K, $CDCl_3$).

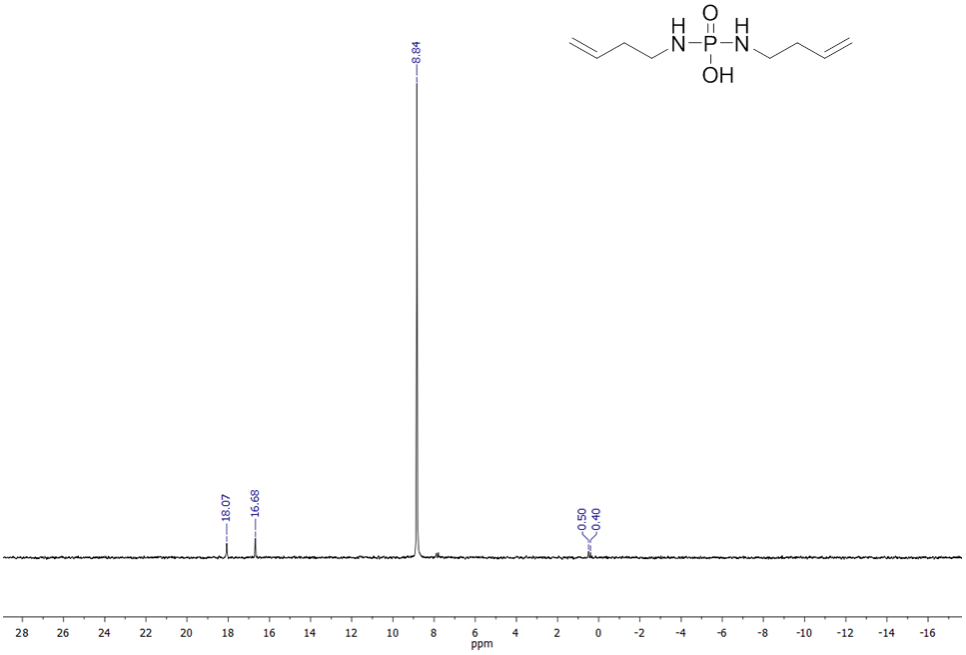

Figure S34: $^{31}P\{H\}$ NMR of **11** (202 MHz, 298 K, $CDCl_3$).

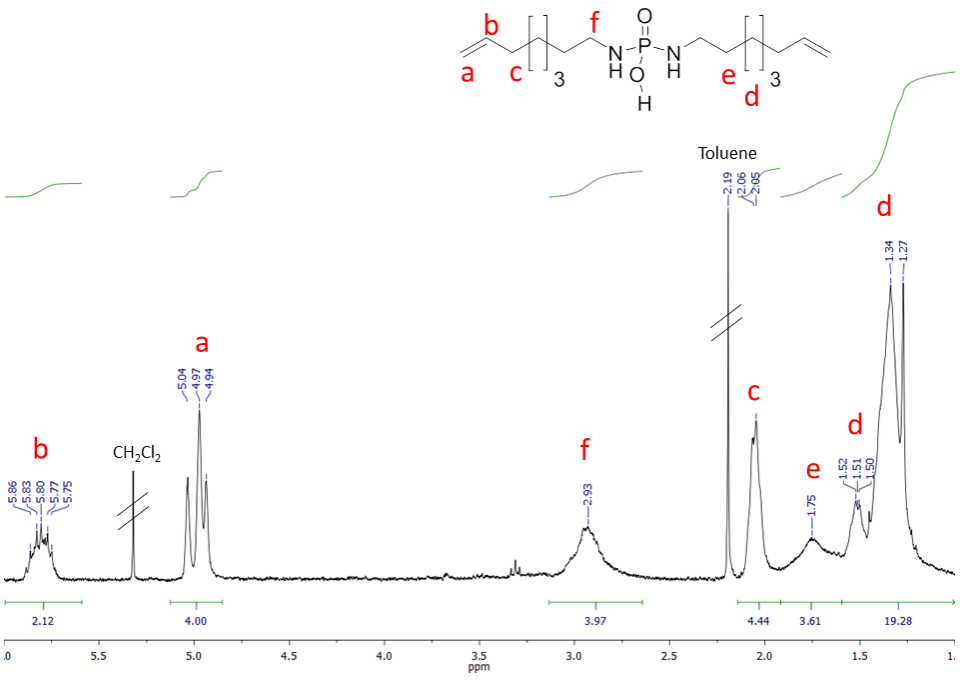

Figure S35: ^{1}H NMR of **12** (300 MHz, 298 K, $CDCl_3$).

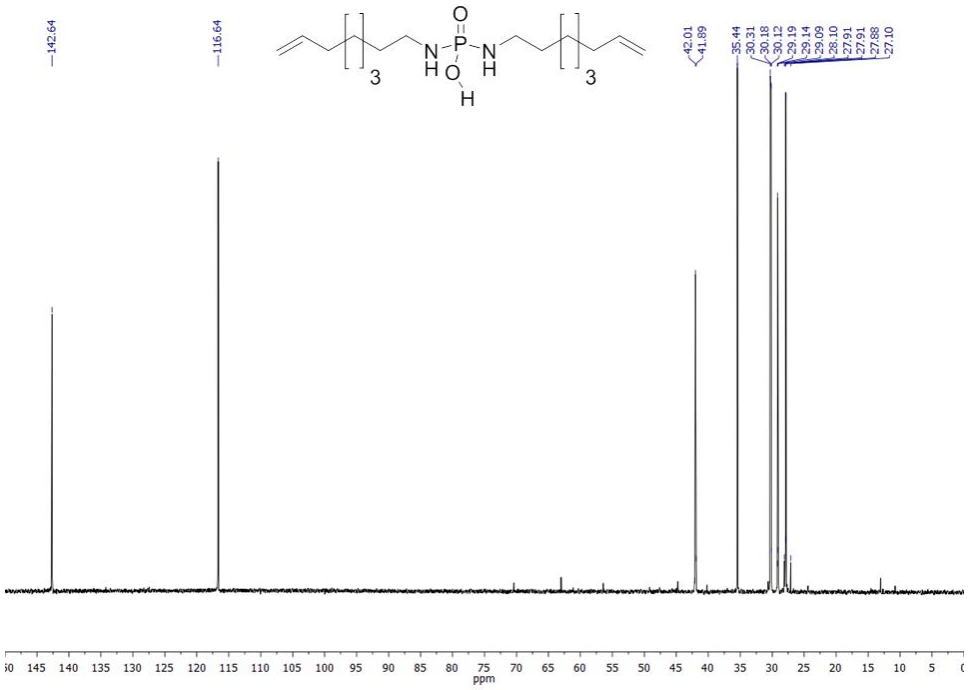

Figure S36: $^{13}C\{H\}$ NMR of **12** (126 MHz, 298 K, $CDCl_3$).

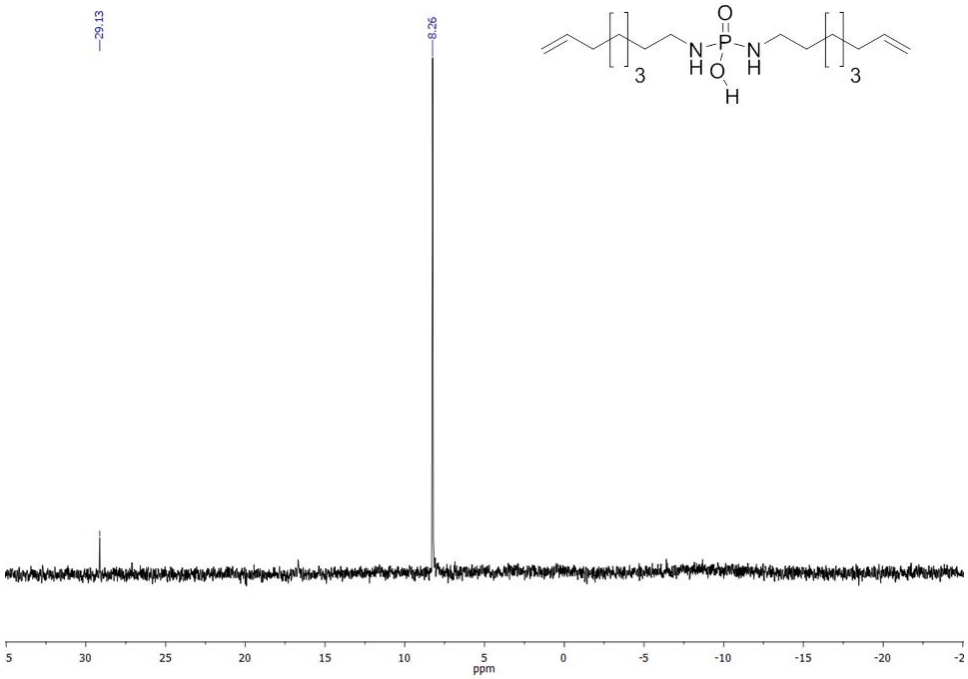

Figure S37: $^{31}P\{H\}$ NMR of **12** (202 MHz, 298 K, $CDCl_3$).

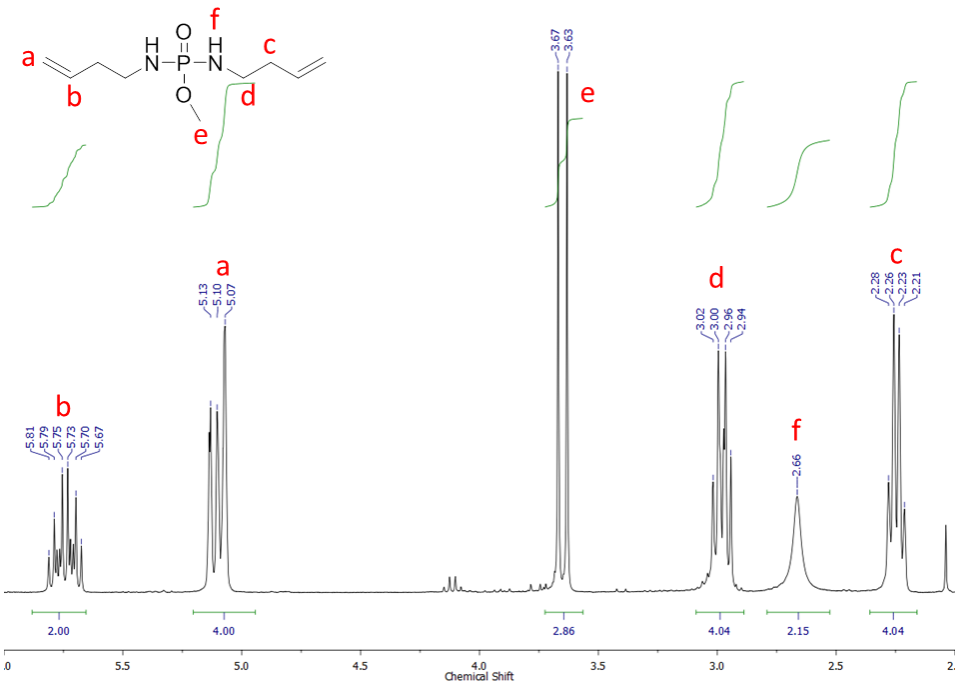

Figure S38: ^{1}H NMR of **13** (500 MHz, 298 K, $CDCl_3$).

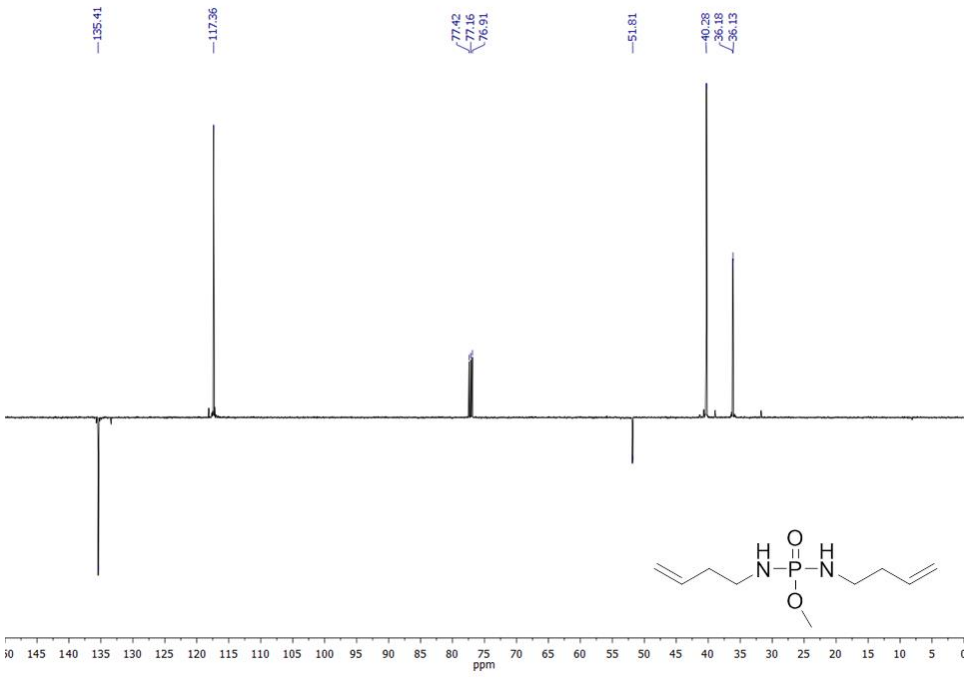

Figure S39: DEPT-135 ^{13}C{H} NMR of **13** (126 MHz, 298 K, $CDCl_3$).

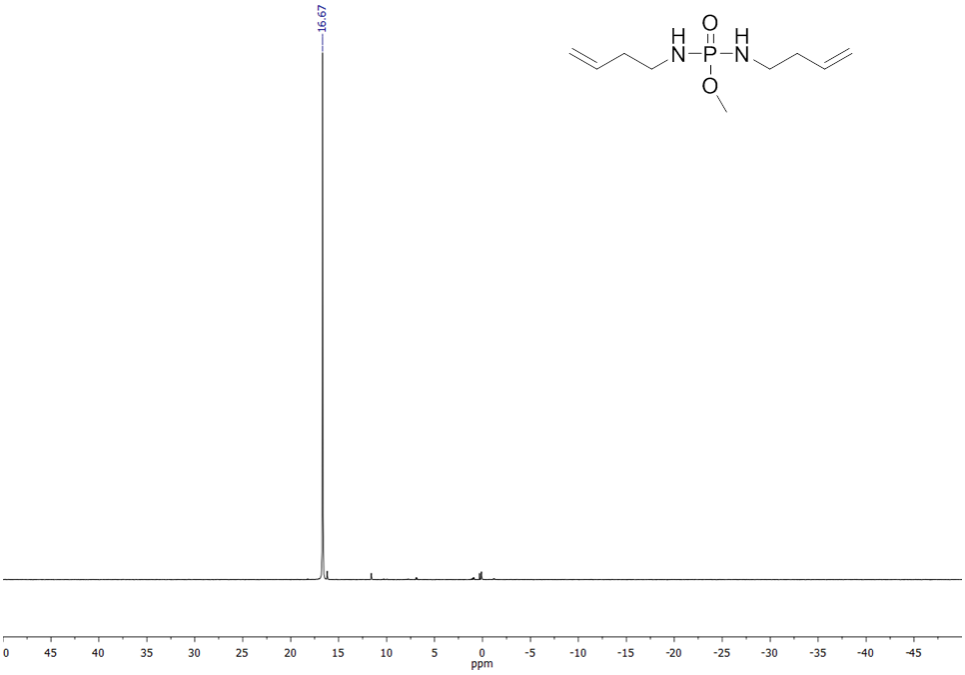

Figure S40: $^{31}P\{H\}$ NMR of **13** (202 MHz, 298 K, $CDCl_3$).

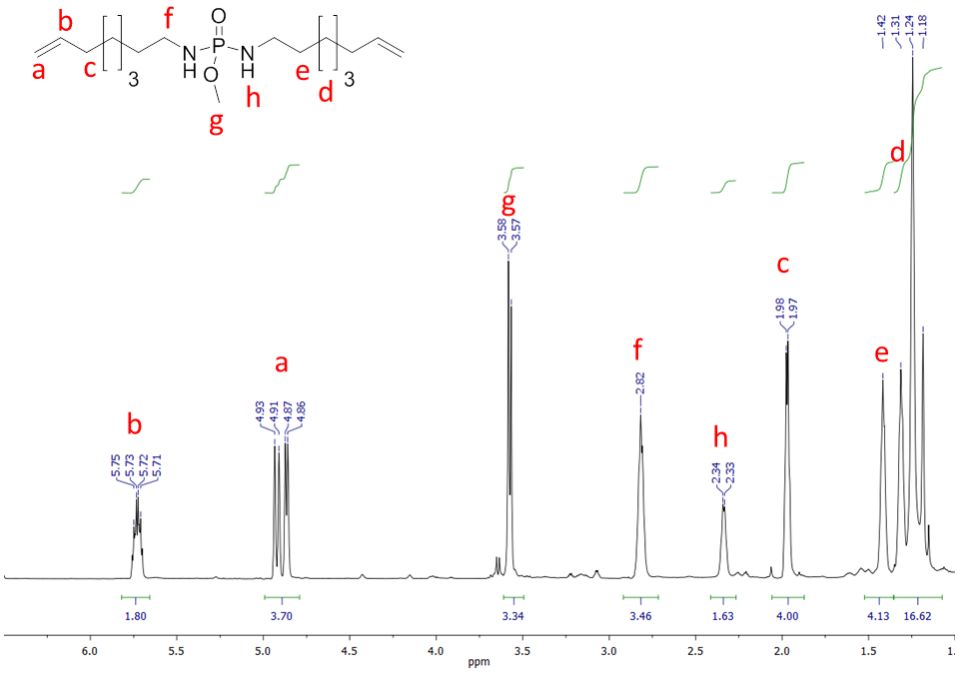

Figure S41: ^{1}H NMR of **14** (500 MHz, 298 K, $CDCl_3$).

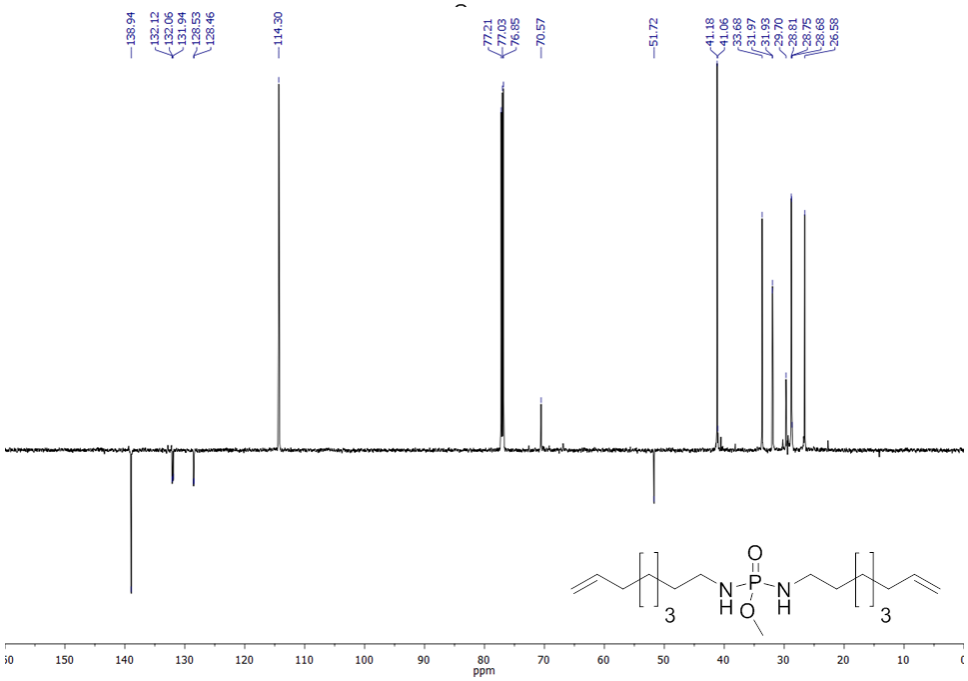

Figure S42: DEPT-135 $^{13}C\{H\}$ NMR of **14** (176 MHz, 298 K, $CDCl_3$).

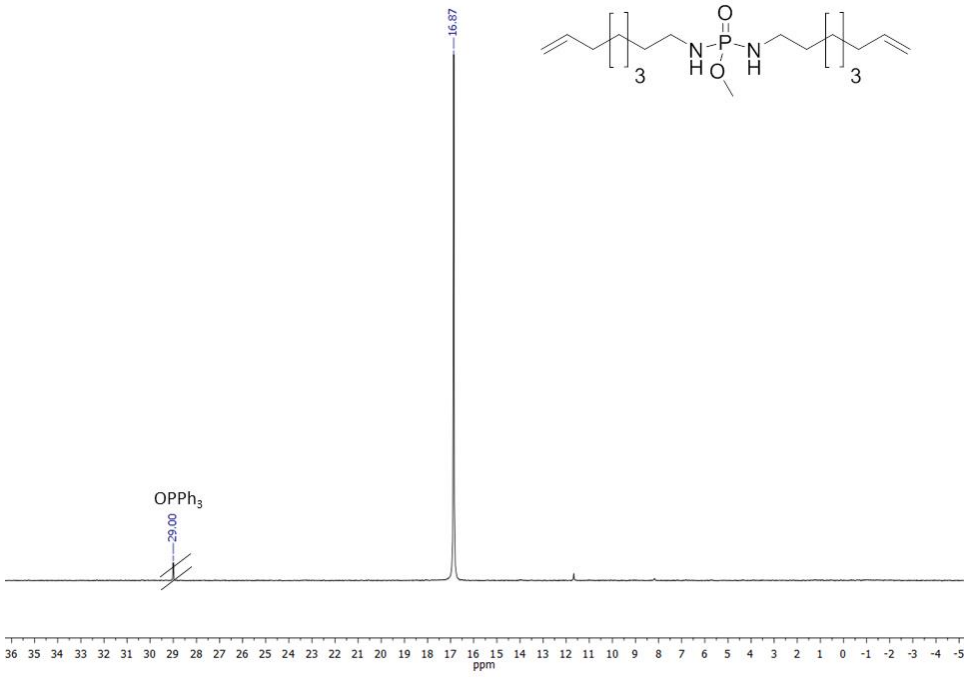

Figure S43: $^{31}P\{H\}$ NMR of **14** (202 MHz, 298 K, $CDCl_3$).

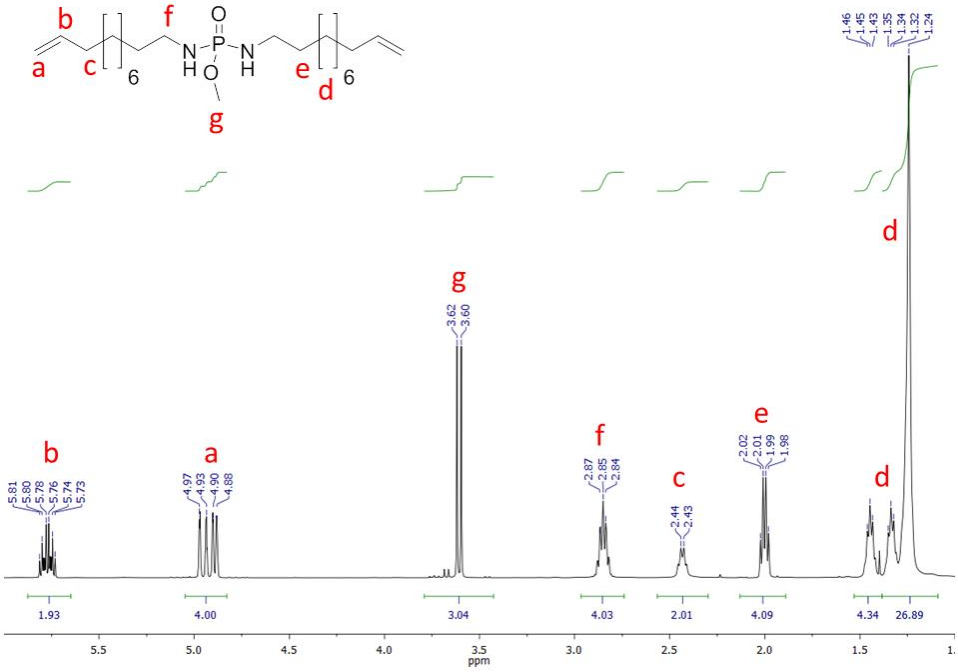

Figure S44: ^{1}H NMR of **15** (500 MHz, 298 K, $CDCl_3$).

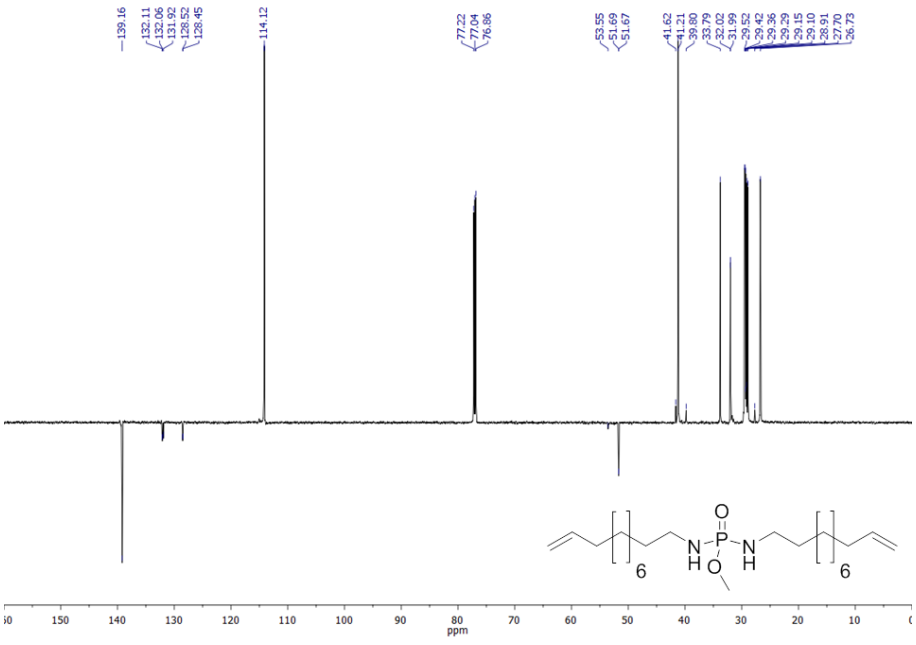

Figure S45: DEPT-135 ^{13}C{H} NMR of **15** (176 MHz, 298 K, $CDCl_3$).

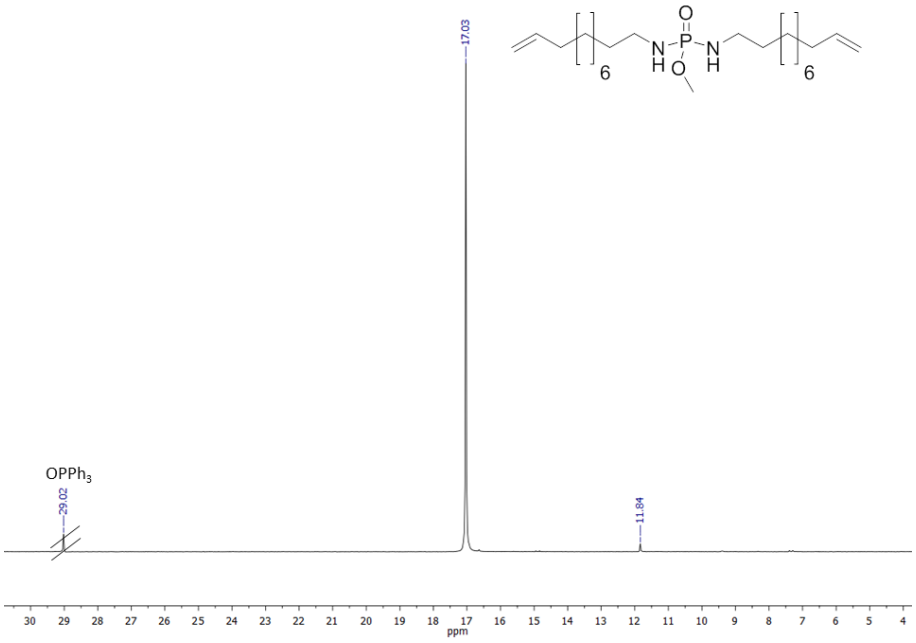

Figure S46: $^{31}P\{H\}$ NMR of **15** (202 MHz, 298 K, $CDCl_3$).

Polymers

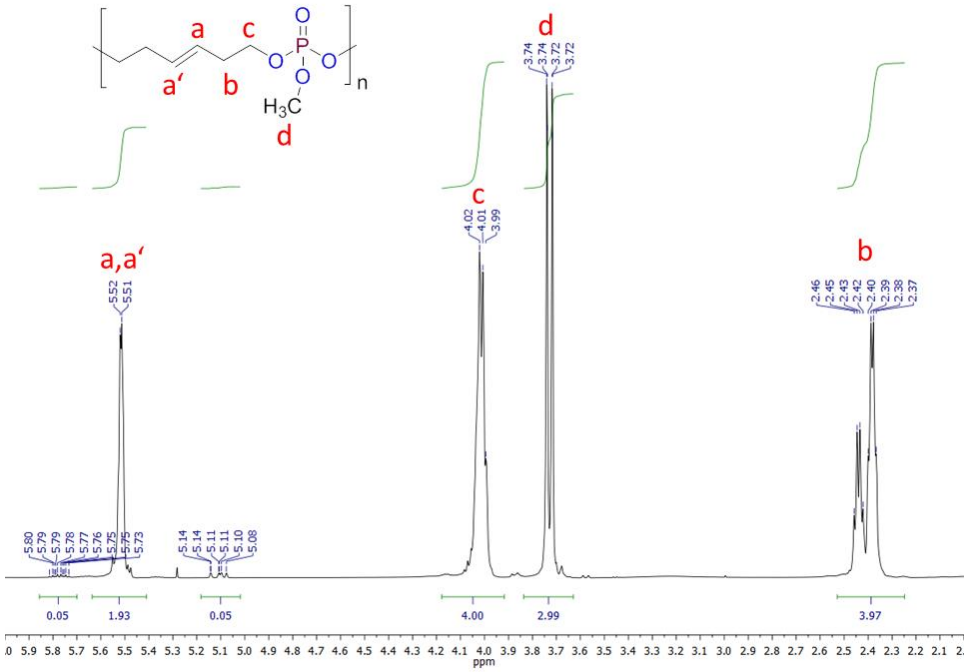

Figure S47: ^{1}H NMR of **poly(8)** (500 MHz, 298 K, $CDCl_3$).

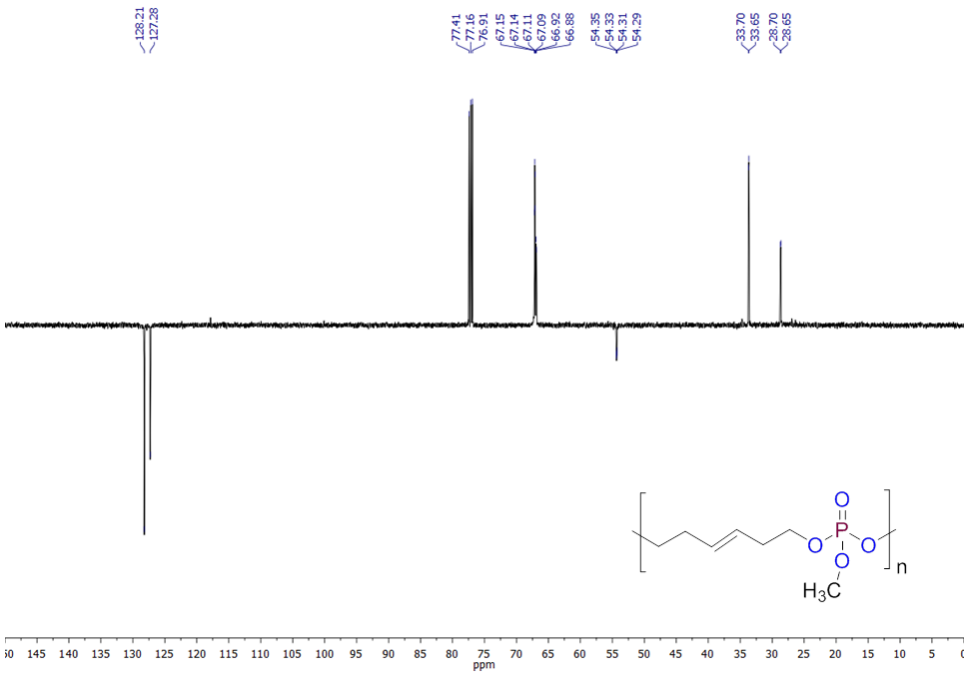

Figure S48: DEPT-135 ^{13}C{H} NMR of **poly(8)** (126 MHz, 298 K, $CDCl_3$).

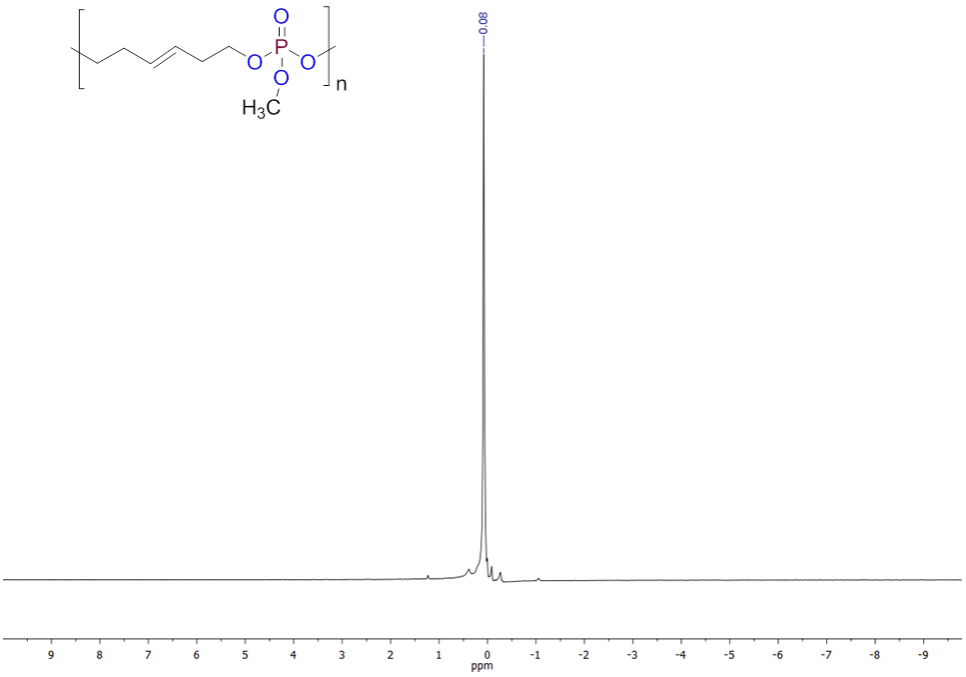

Figure S49: $^{31}P\{H\}$ NMR of **poly(8)** (202 MHz, 298 K, $CDCl_3$).

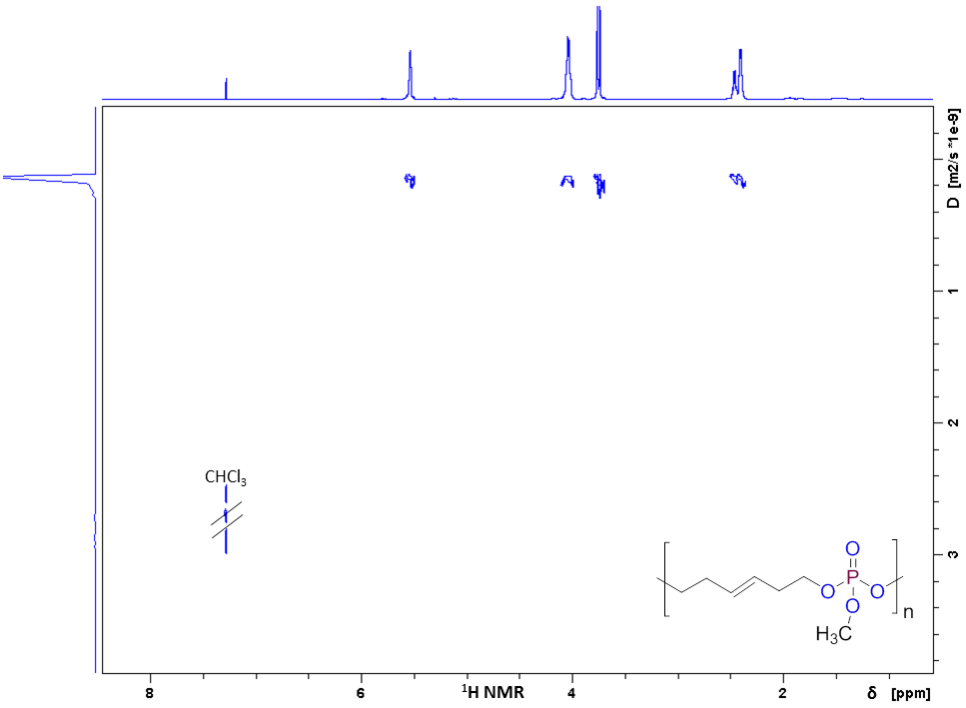

Figure S50: ^{1}H DOSY of **poly(8)** (500 MHz, 298 K, $CDCl_3$).

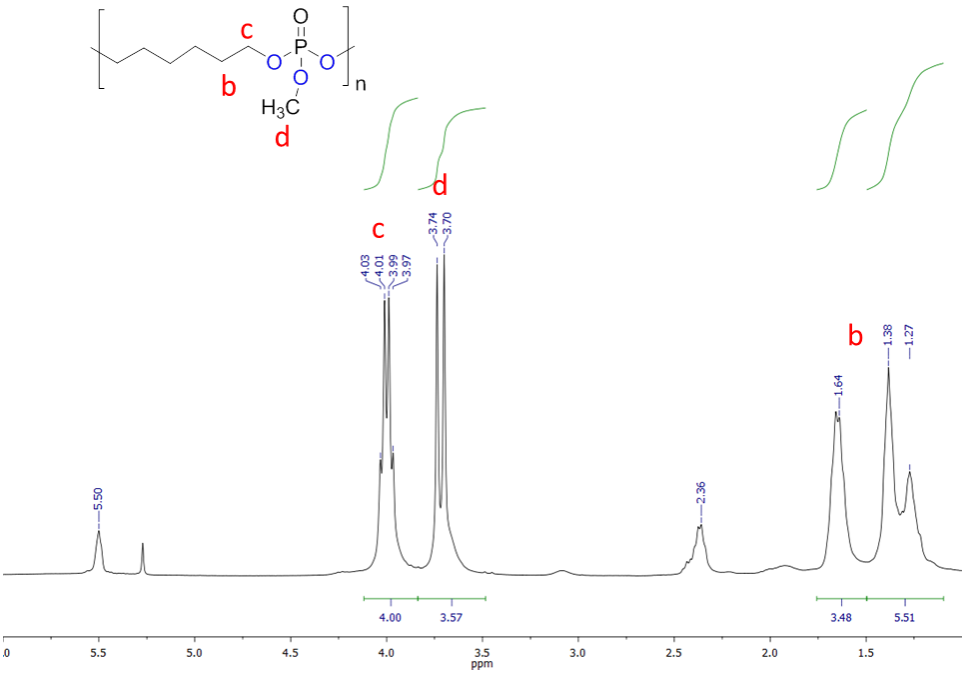

Figure S51: ^{1}H NMR of **poly-H(8)** (300 MHz, 298 K, $CDCl_3$).

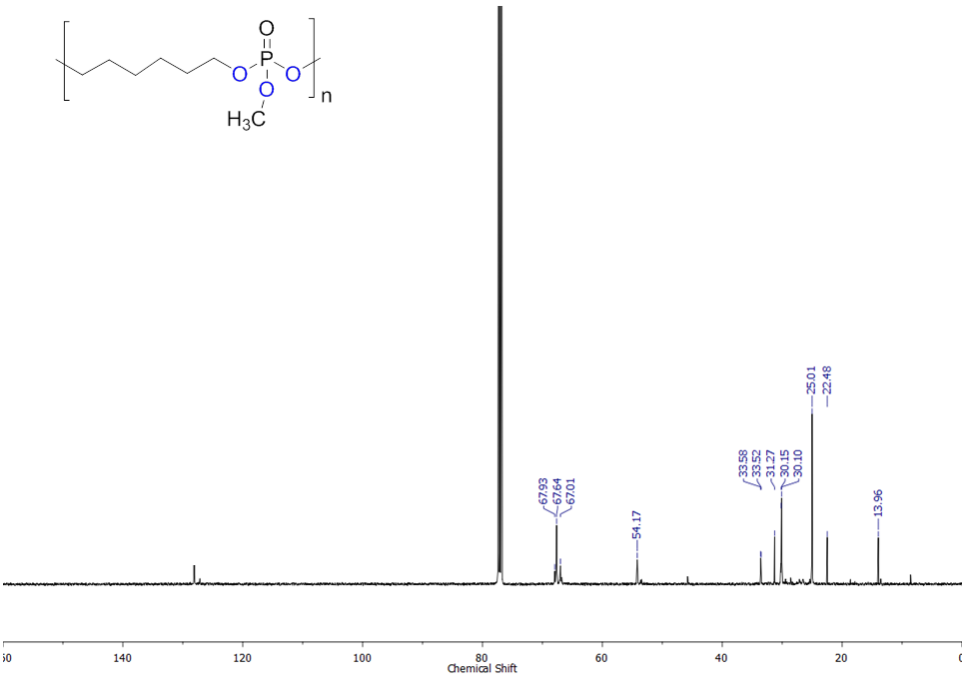

Figure S52: ^{13}C{H} NMR of **poly-H(8)** (126 MHz, 298 K, $CDCl_3$).

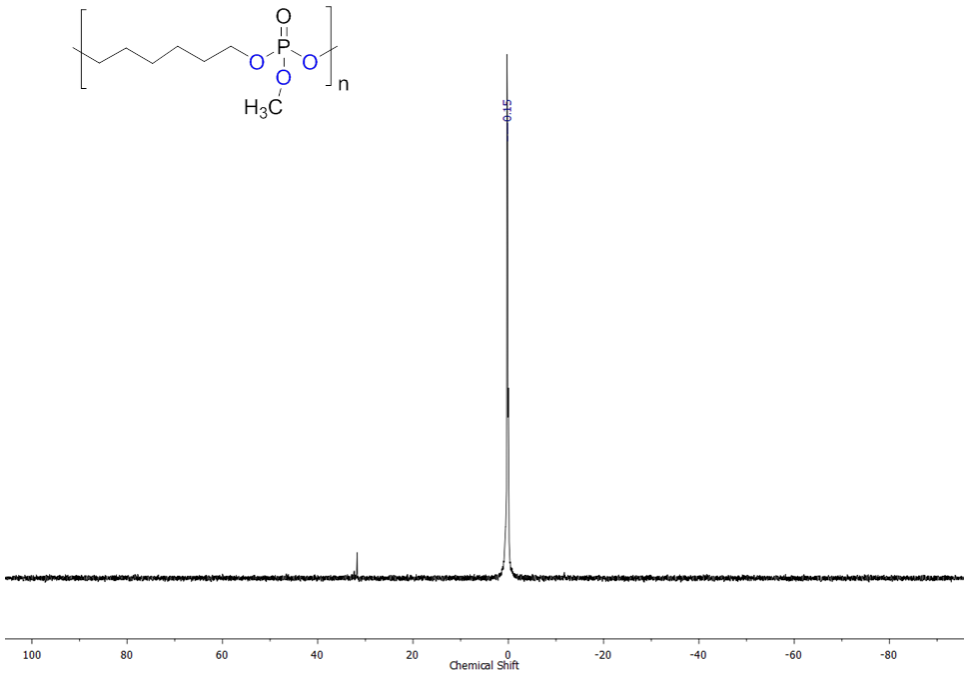

Figure S53: $^{31}P\{H\}$ NMR of **poly-H(8)** (202 MHz, 298 K, $CDCl_3$).

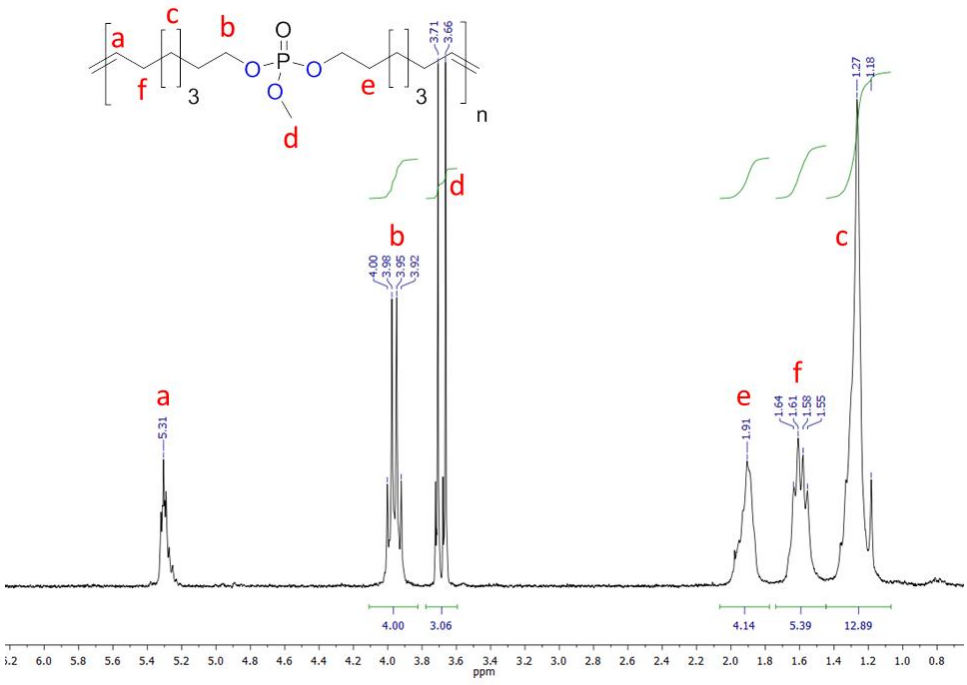

Figure S54: ^{1}H NMR of **poly(9)** (500 MHz, 298 K, $CDCl_3$).

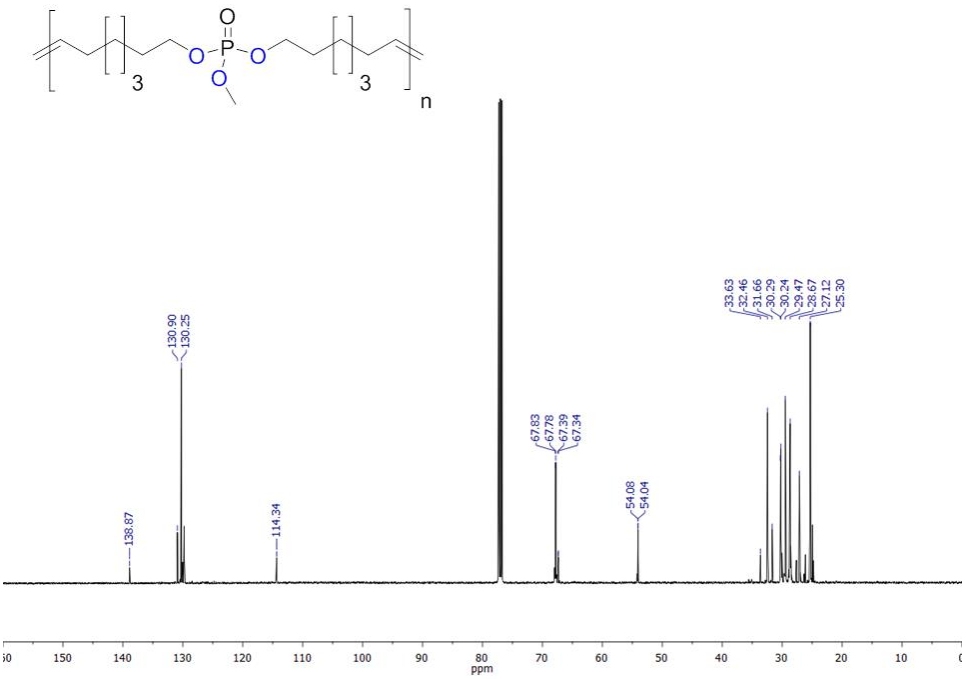

Figure S55: $^{13}C\{H\}$ NMR of **poly(9)** (126 MHz, 298 K, $CDCl_3$).

Figure S56: $^{31}P\{H\}$ NMR of **poly(9)** (202 MHz, 298 K, $CDCl_3$).

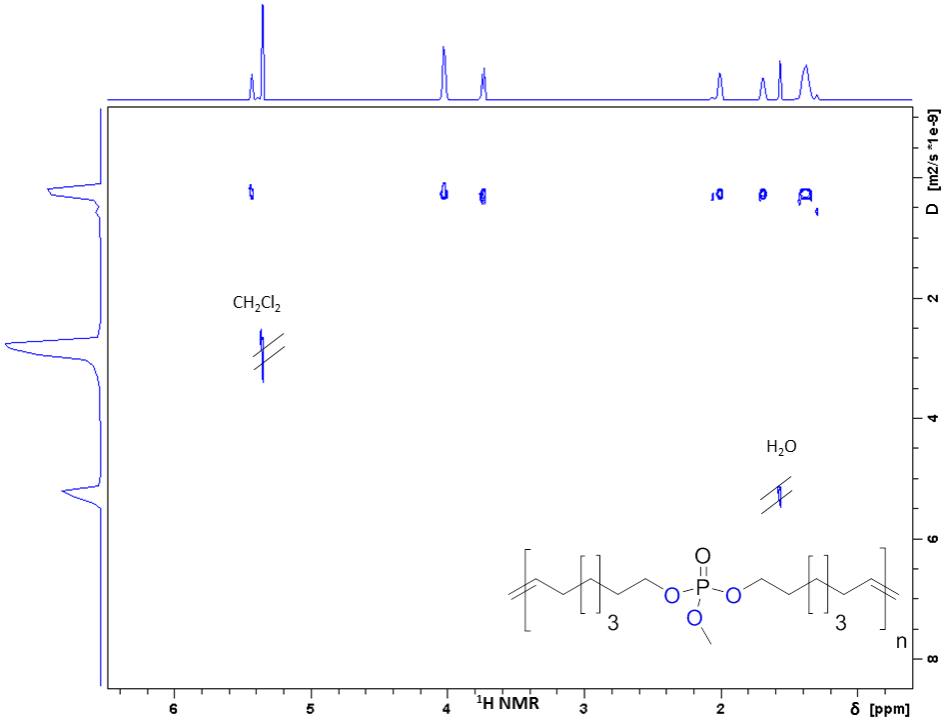

Figure S57: ^{1}H DOSY of **poly(9)** (700 MHz, 298 K, CD_2Cl_2).

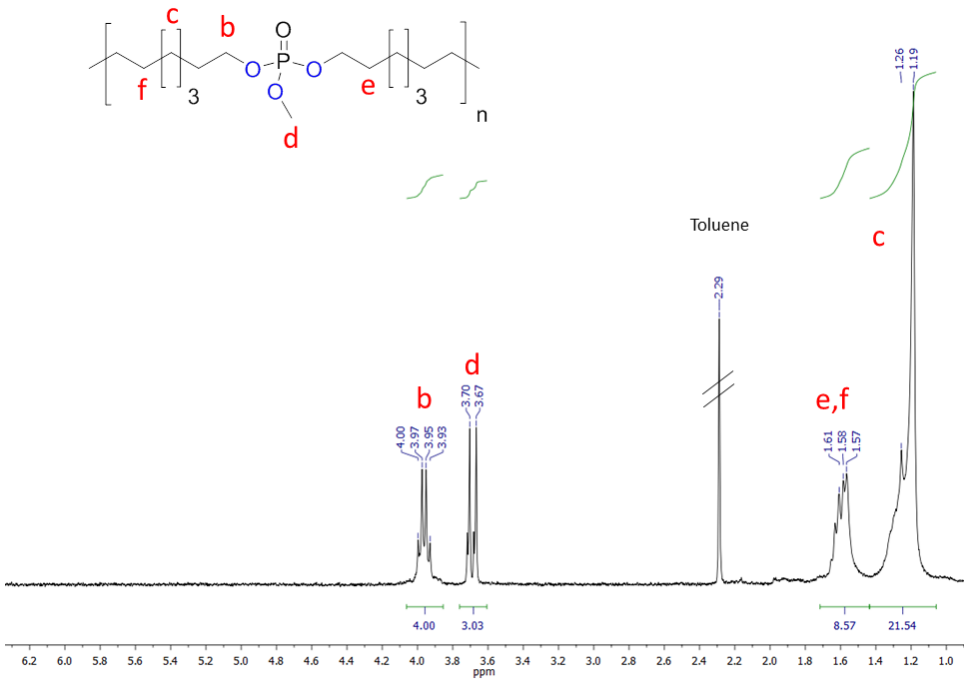

Figure S58: ^{1}H NMR of **poly-H(9)** (300 MHz, 298 K, $CDCl_3$).

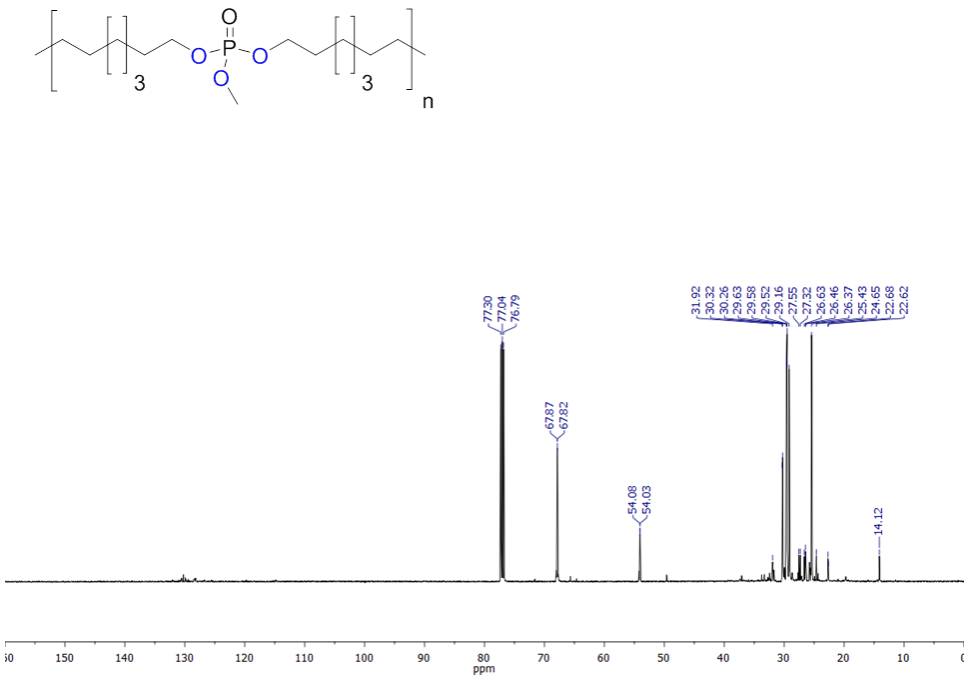

Figure S59: $^{13}C\{H\}$ NMR of **poly-H(9)** (126 MHz, 298 K, $CDCl_3$).

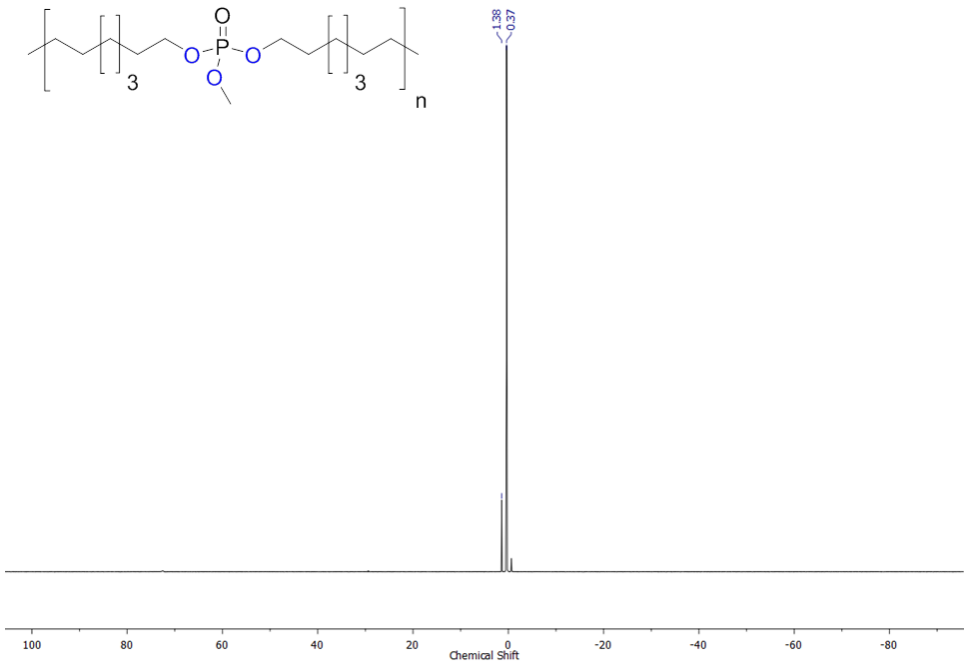

Figure S60: $^{31}P\{H\}$ NMR of **poly-H(9)** (202 MHz, 298 K, $CDCl_3$).

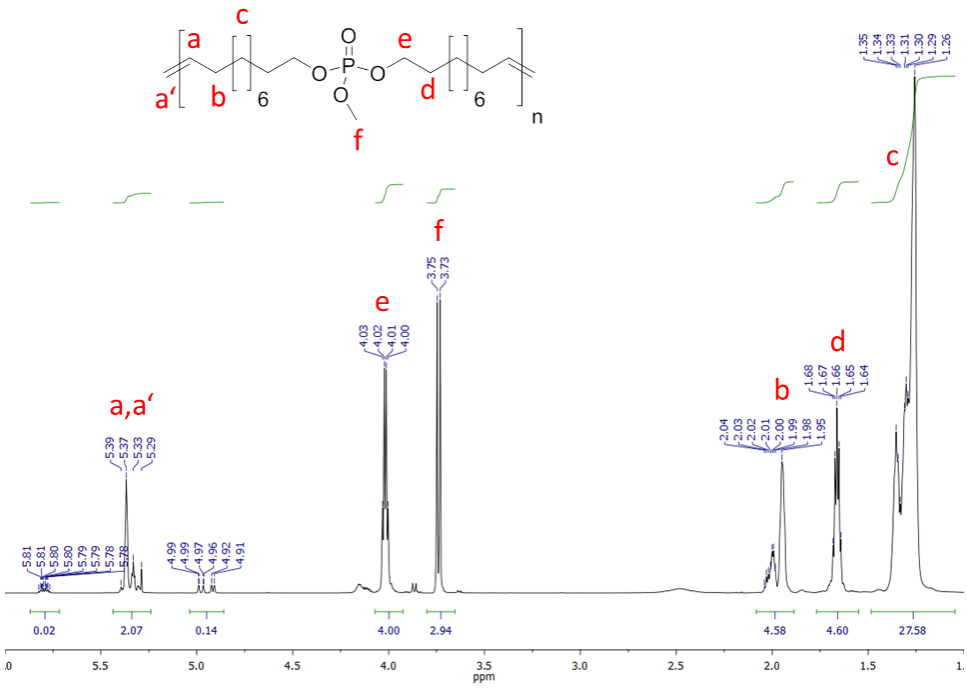

Figure S61: ^{1}H NMR of **poly(10)** (700 MHz, 298 K, $CDCl_3$).

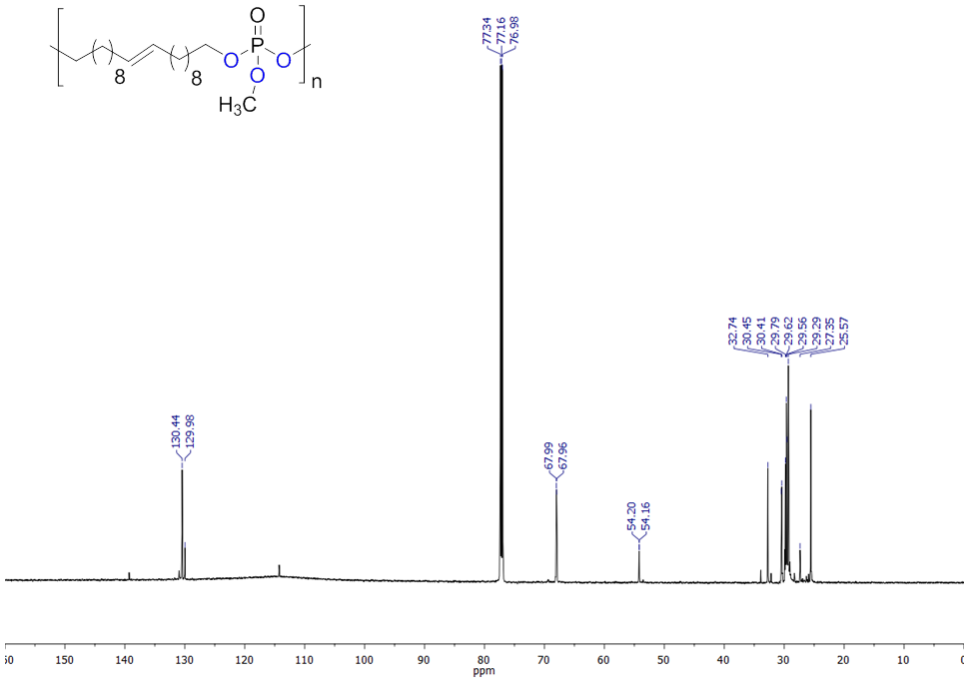

Figure S62: ^{13}C{H} NMR of **poly(10)** (176 MHz, 298 K, $CDCl_3$).

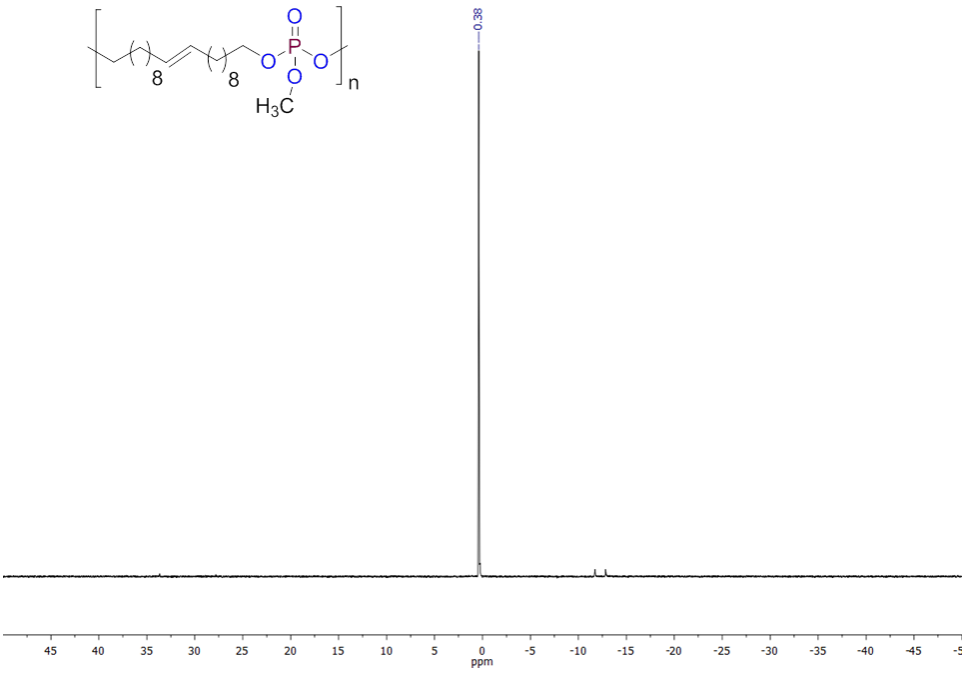

Figure S63: $^{31}P\{H\}$ NMR of **poly(10)** (284 MHz, 298 K, $CDCl_3$).

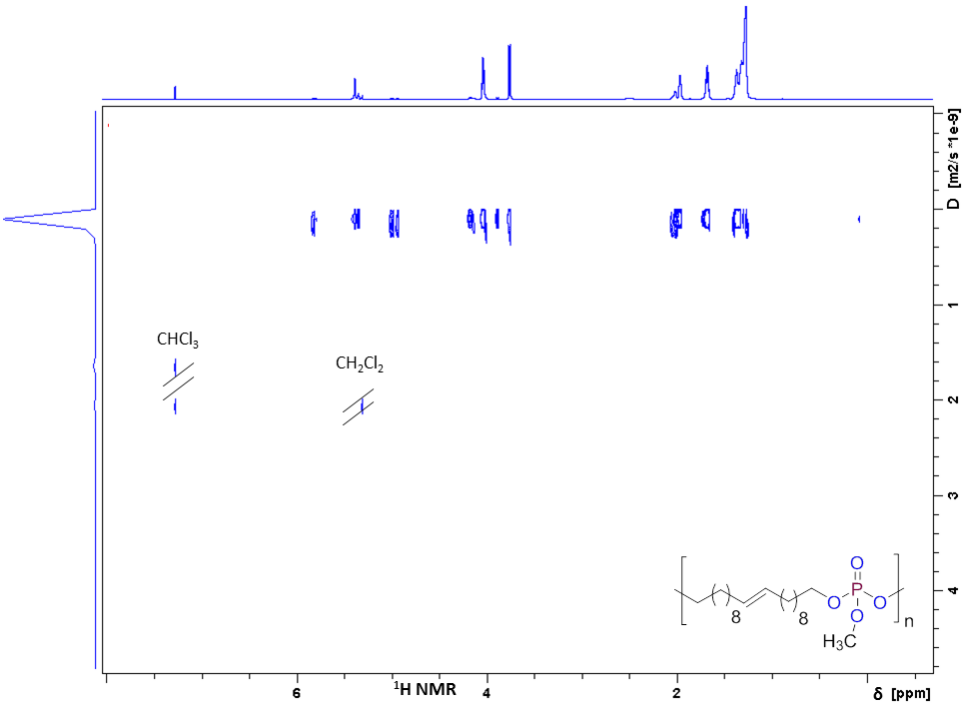

Figure S64: ^{1}H DOSY of **poly(10)** (700 MHz, 298 K, $CDCl_3$).

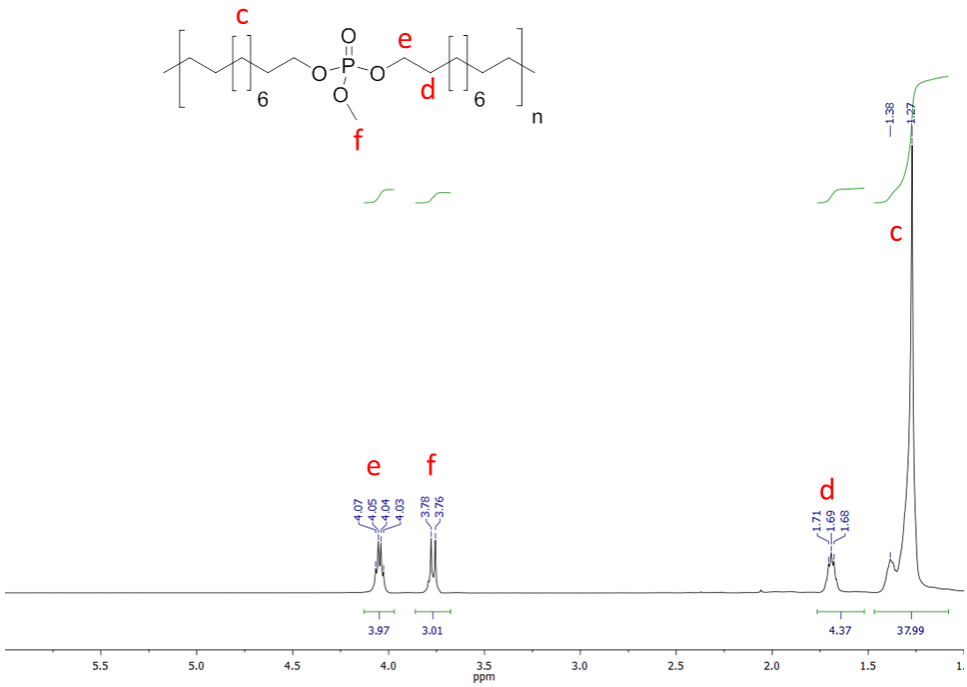

Figure S65: ^{1}H NMR of **poly-H(10)** (500 MHz, 298 K, $CDCl_3$).

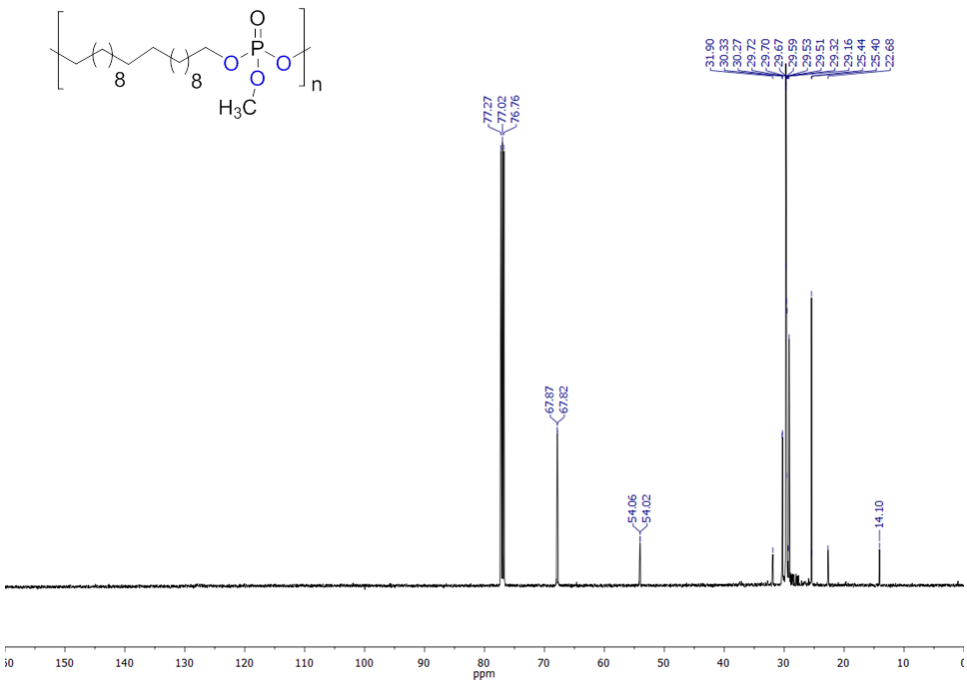

Figure S66: ^{13}C{H} NMR of **poly-H(10)** (126 MHz, 298 K, $CDCl_3$).

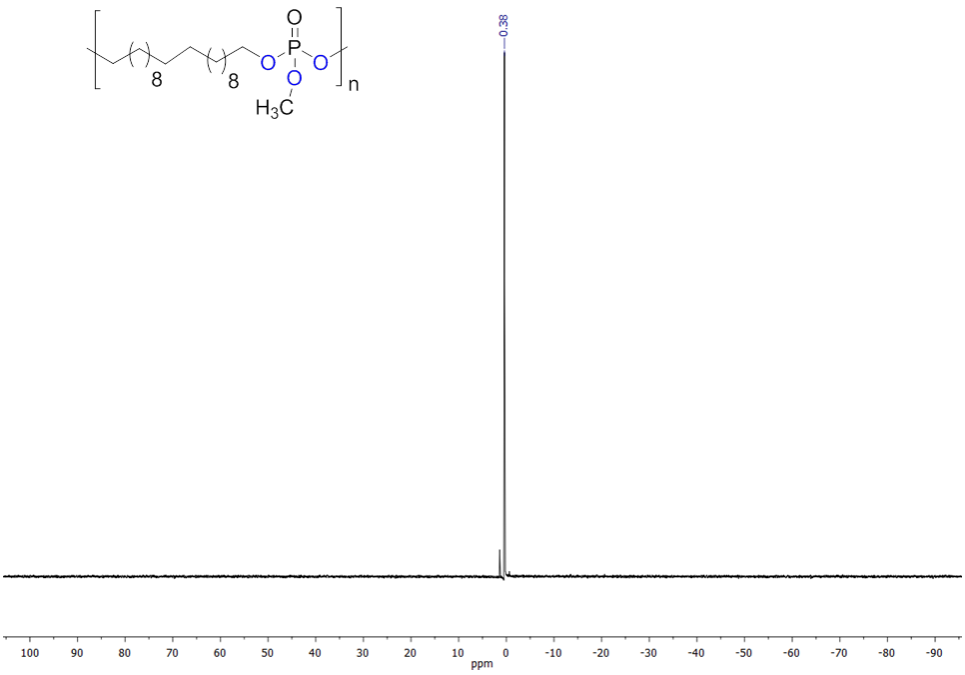

Figure S67: $^{31}P\{H\}$ NMR of **poly-H(10)** (202 MHz, 298 K, $CDCl_3$).

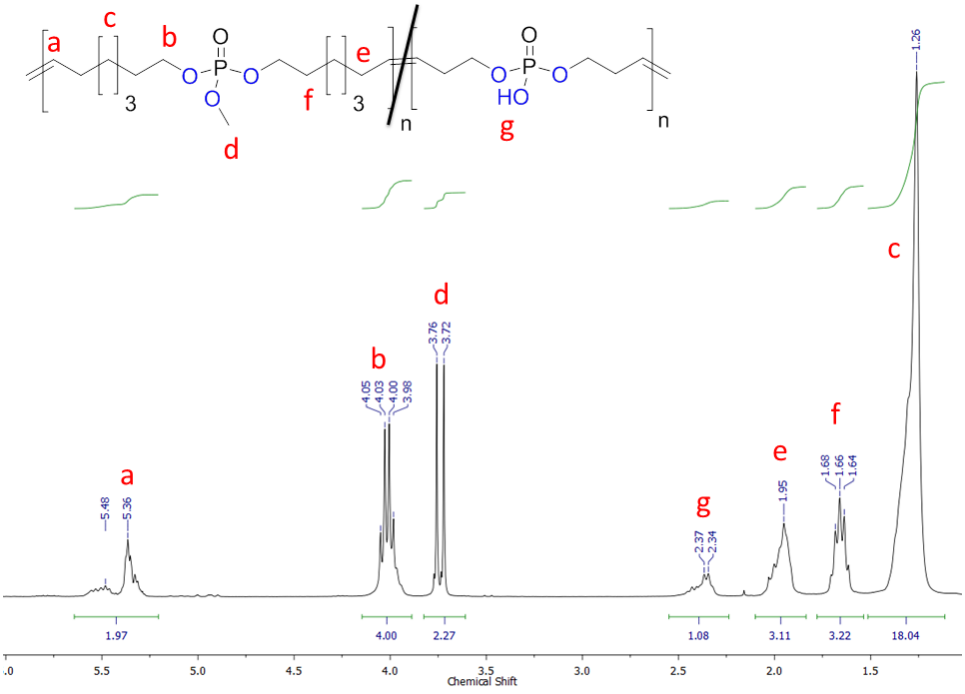

Figure S68: ^{1}H NMR of copolymer **poly(5-10)** (300 MHz, 298 K, $CDCl_3$).

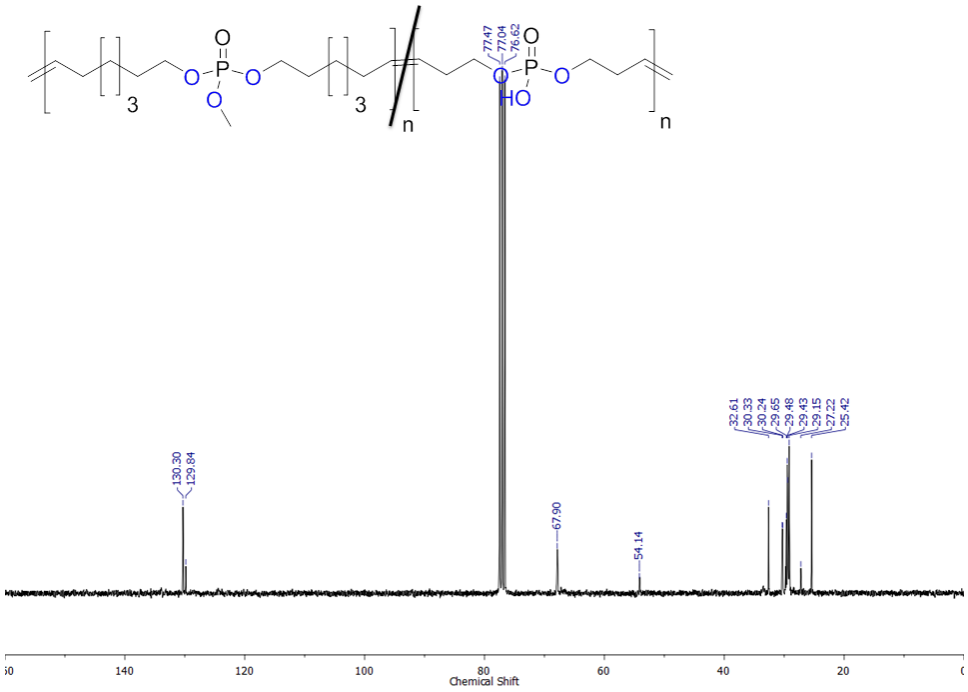

Figure S69: $^{13}C\{H\}$ NMR of copolymer **poly(5-10)** (75 MHz, 298 K, $CDCl_3$).

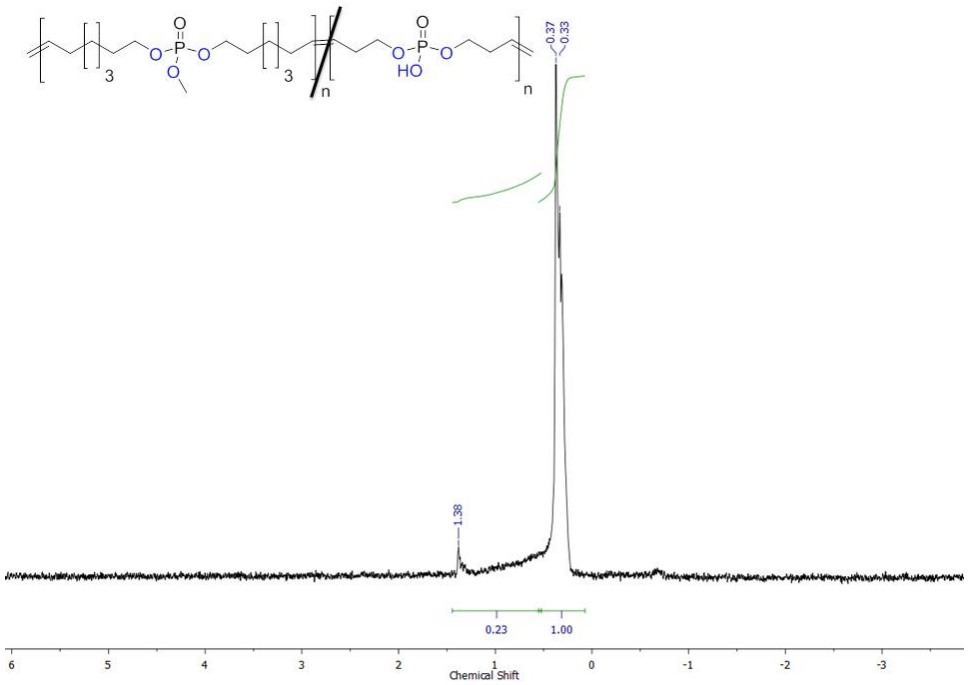

Figure S70: $^{31}P\{H\}$ NMR of copolymer **poly(5-10)** (121.5 MHz, 298 K, $CDCl_3$).

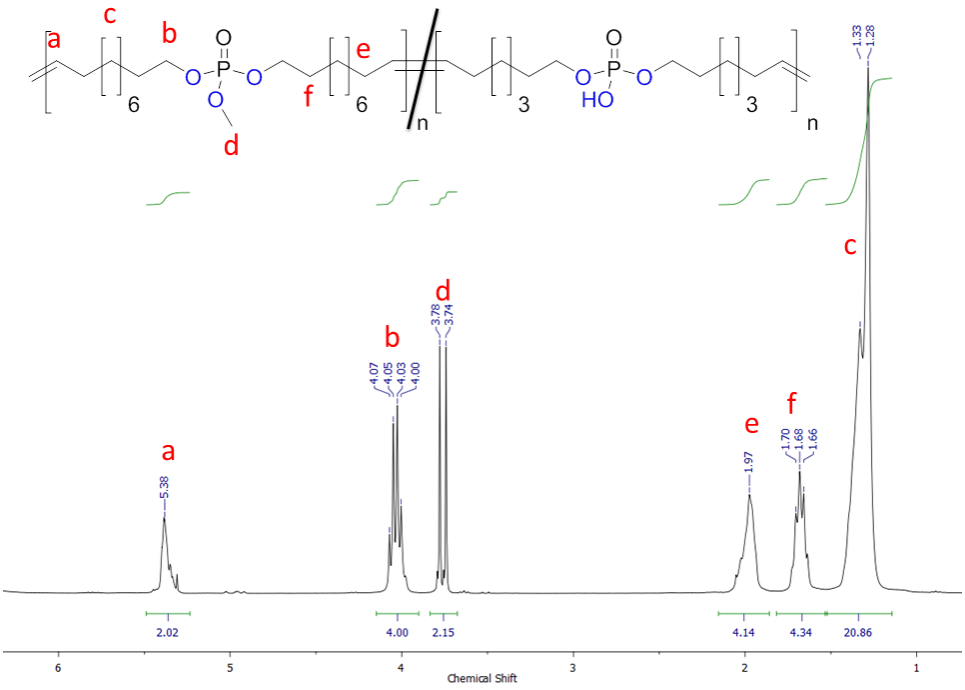

Figure S71: ^{1}H NMR of copolymer **poly(6-10)** (300 MHz, 298 K, $CDCl_3$).

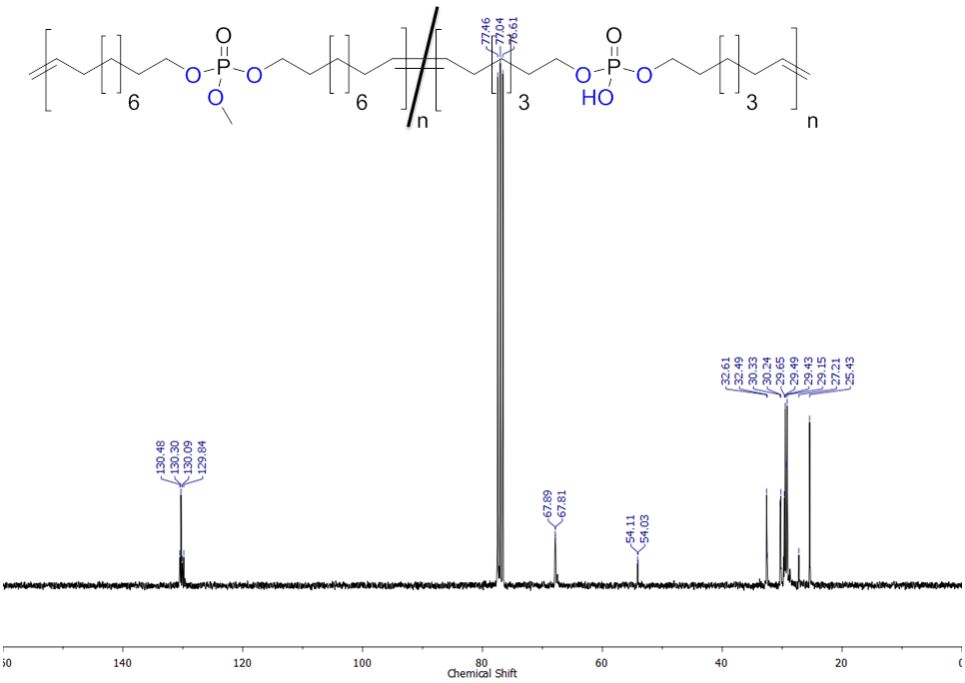

Figure S72: ^{13}C{H} NMR of copolymer **poly(6-10)** (75 MHz, 298 K, $CDCl_3$).

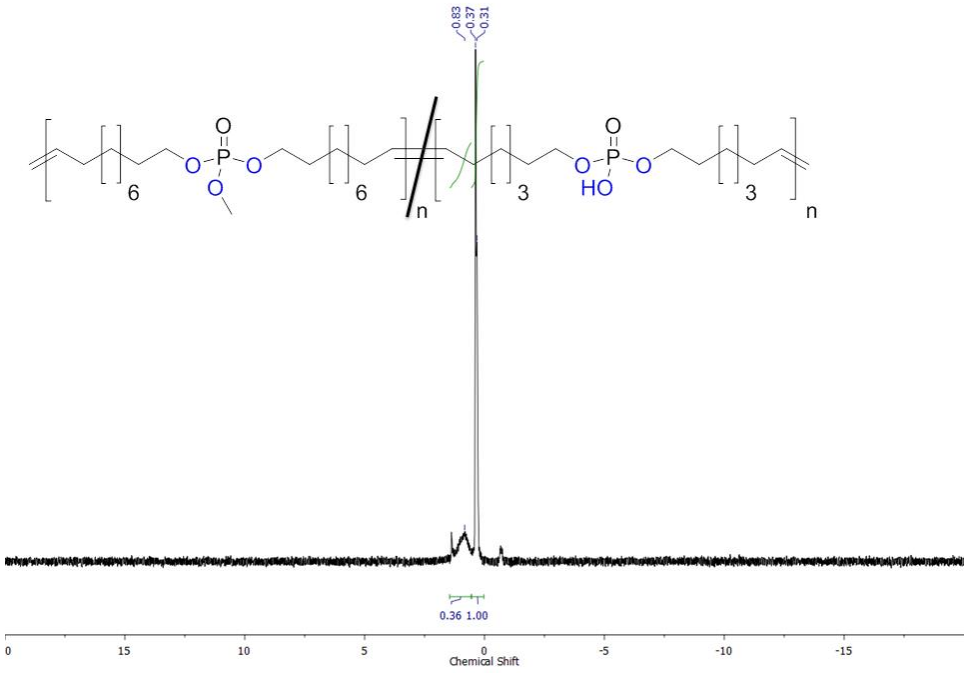

Figure S73: $^{31}P\{H\}$ NMR of copolymer **poly(6-10)** (121.5 MHz, 298 K, $CDCl_3$).

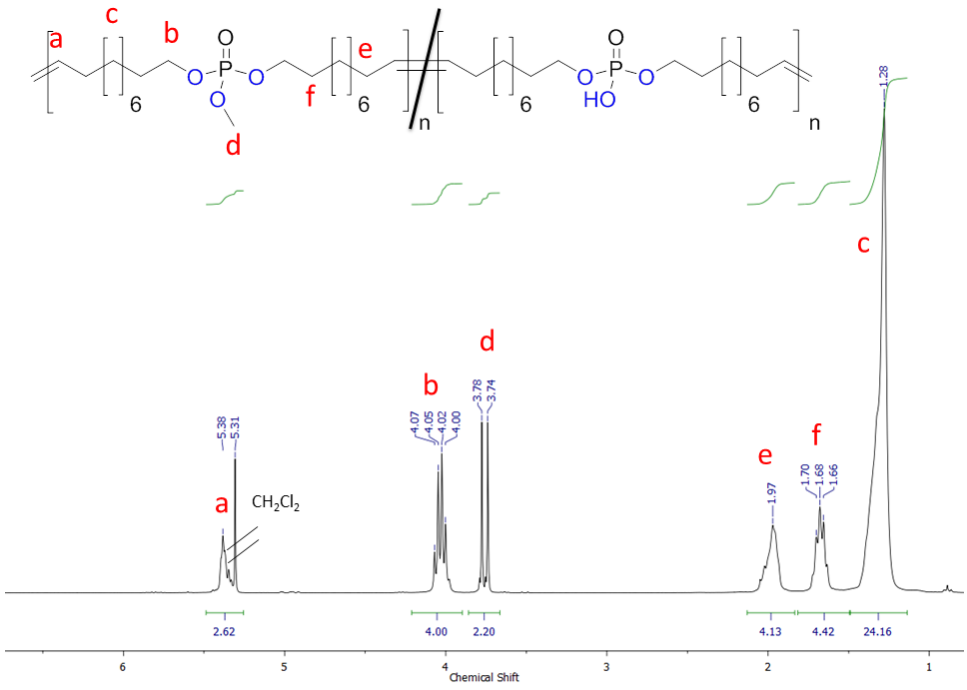

Figure S74: ^{1}H NMR of copolymer **poly(7-10)** (300 MHz, 298 K, $CDCl_3$).

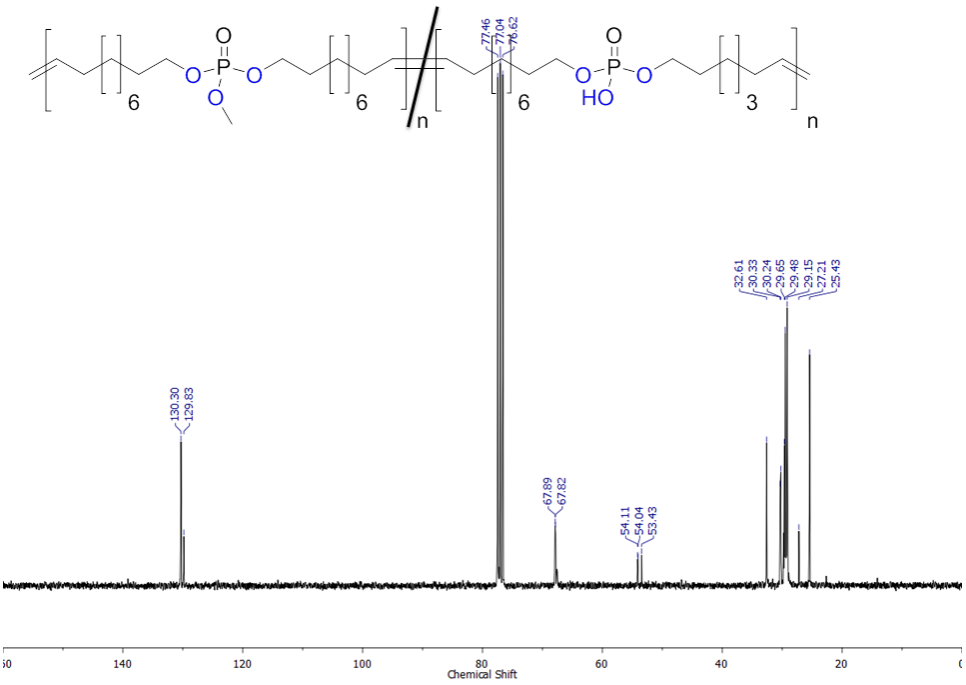

Figure S75: $^{13}C\{H\}$ NMR of copolymer **poly(7-10)** (75 MHz, 298 K, $CDCl_3$).

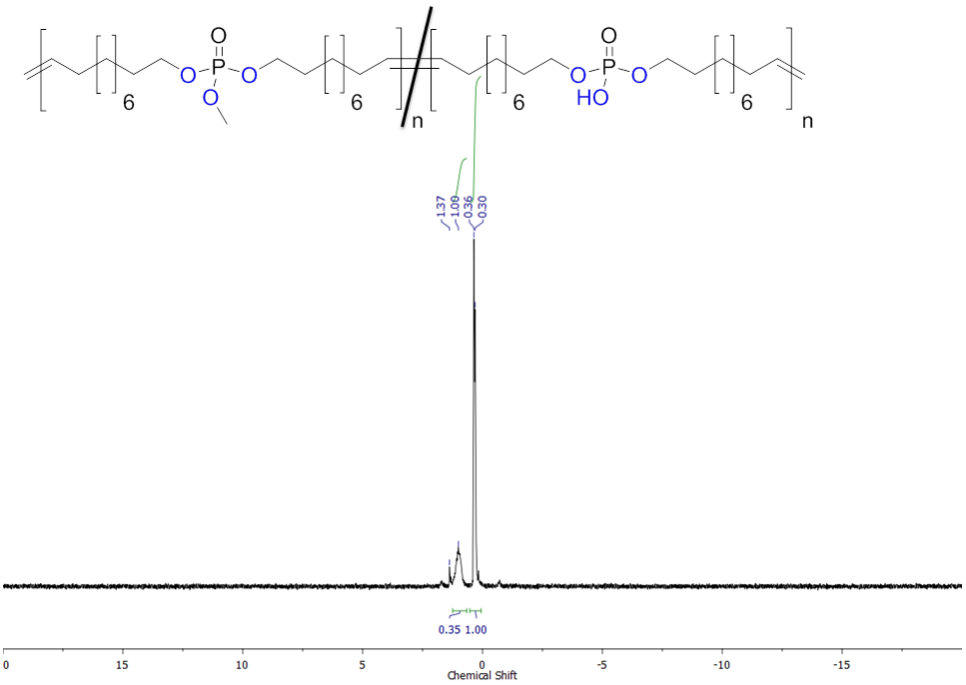

Figure S76: $^{31}P\{H\}$ NMR of copolymer **poly(7-10)** (121.5 MHz, 298 K, $CDCl_3$).

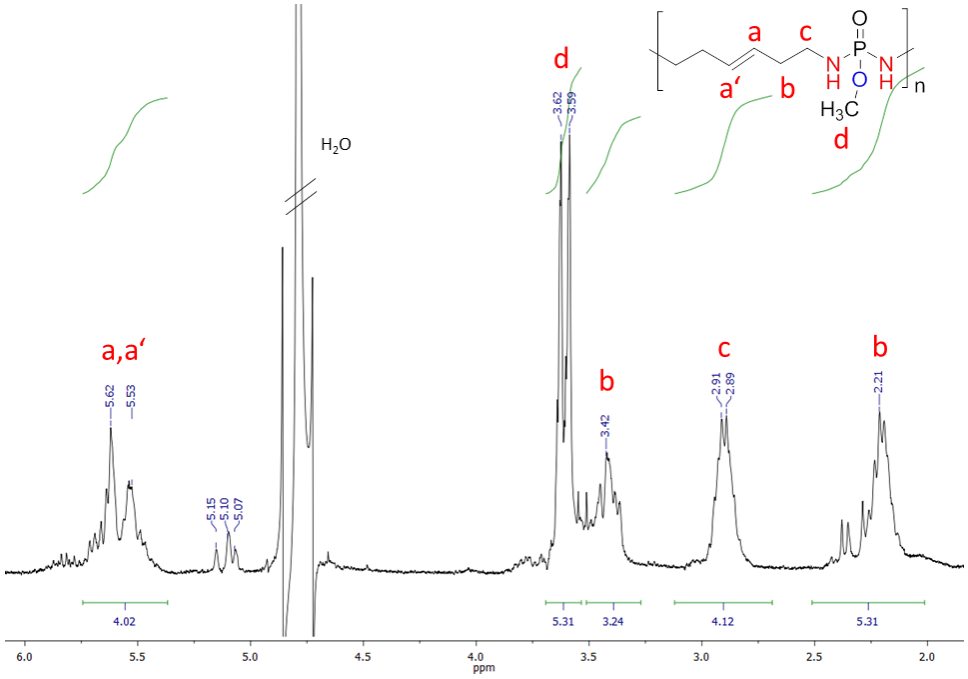

Figure S77: ^{1}H NMR of **poly(13)** (500 MHz, 298 K, $CDCl_3$).

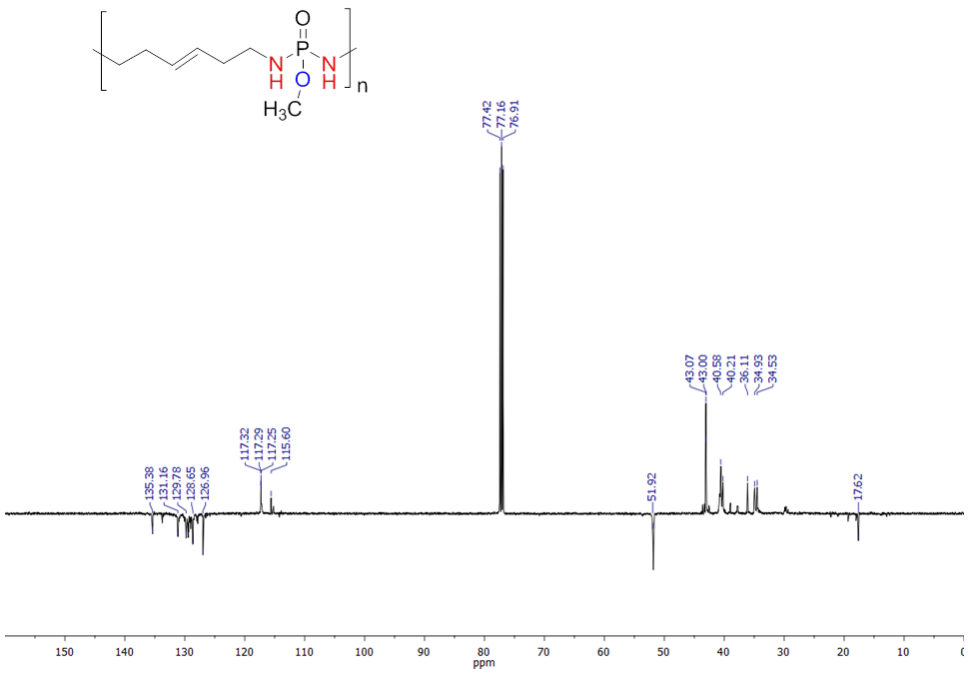

Figure S78: DEPT-135^{13}C{H} NMR of **poly(13)** (126 MHz, 298 K, $CDCl_3$).

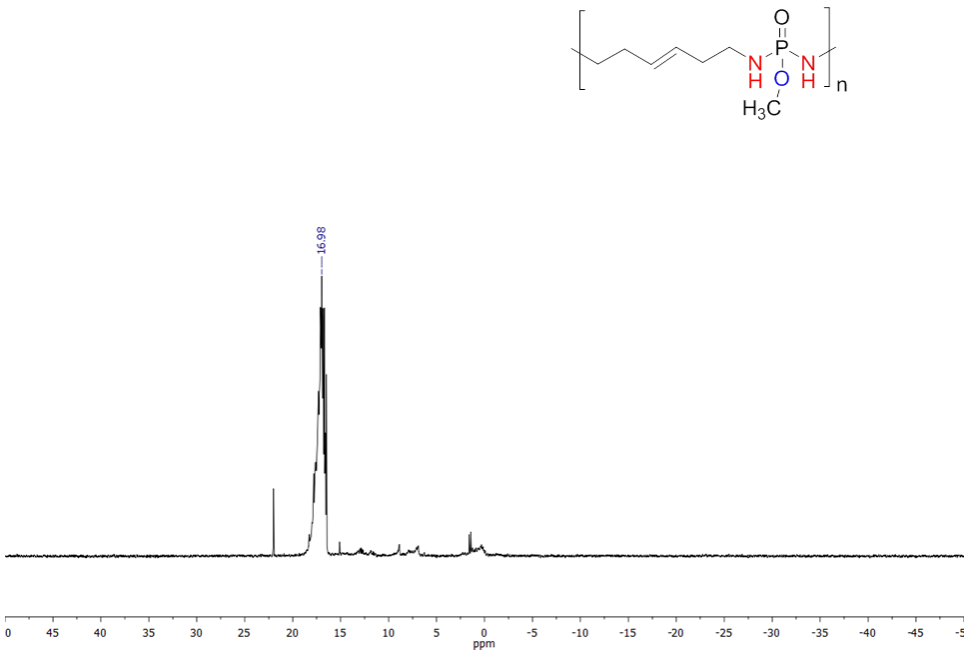

Figure S79: $^{31}P\{H\}$ NMR of **poly(13)** (202 MHz, 298 K, $CDCl_3$).

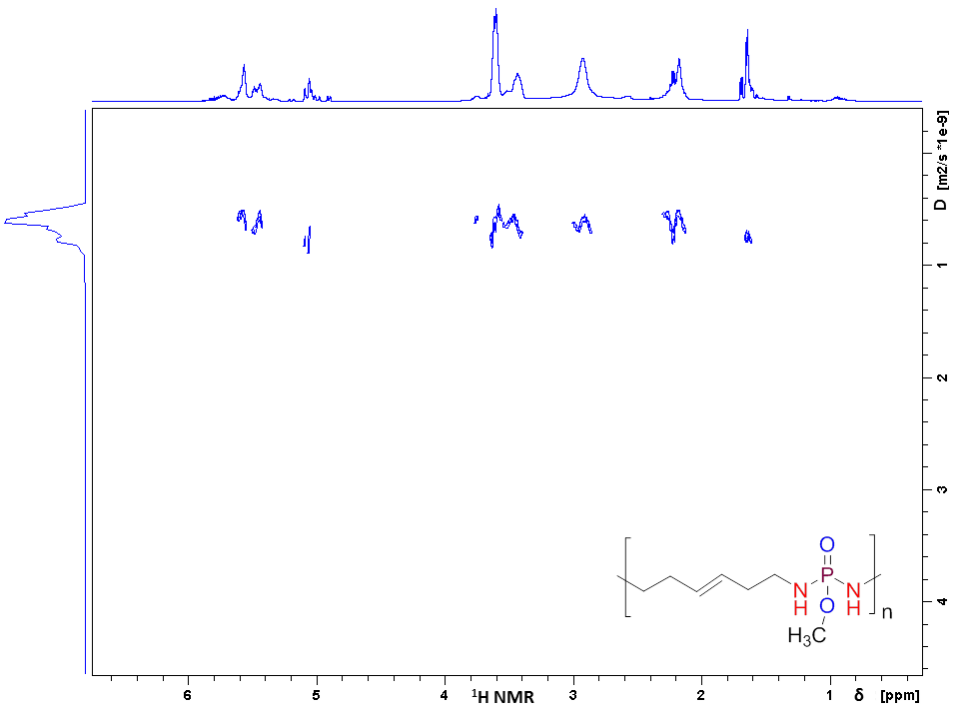

Figure S80: ^{1}H DOSY of **poly(13)** (500 MHz, 298 K, $CDCl_3$).

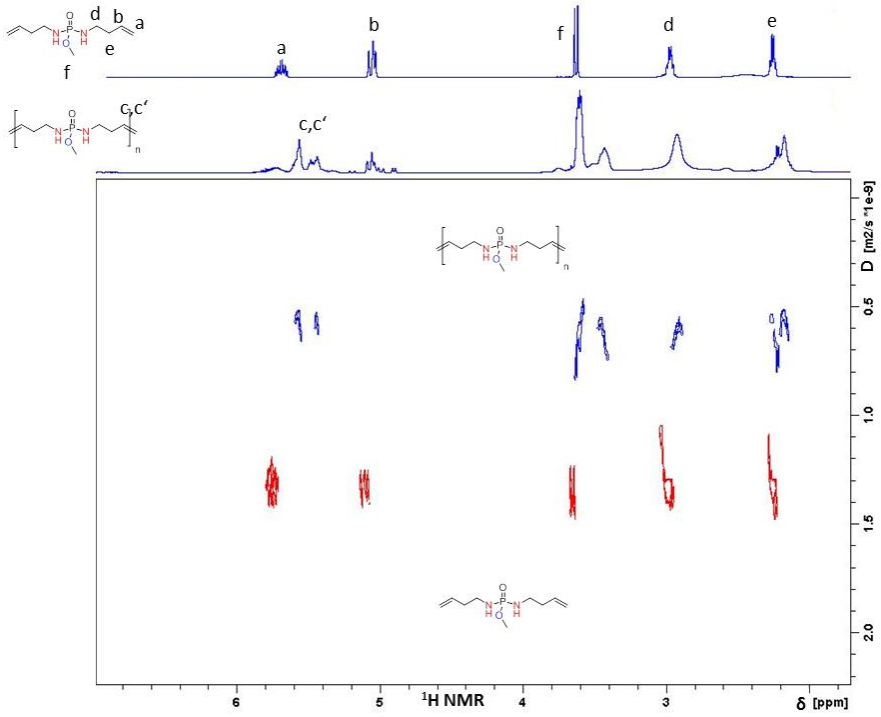

Figure S81: ^{1}H NMR spectrum of monomer **13** (top spectrum of ^{1}H NMR spectra; red signals of DOSY spectrum) and the respective polymer **poly(13)** (bottom spectrum of ^{1}H NMR spectra; blue signals of DOSY spectrum), proving the formation of internal double bonds at 5.4 ppm and the diffusion coefficient shift (500 MHz, 298 K, $CDCl_3$).

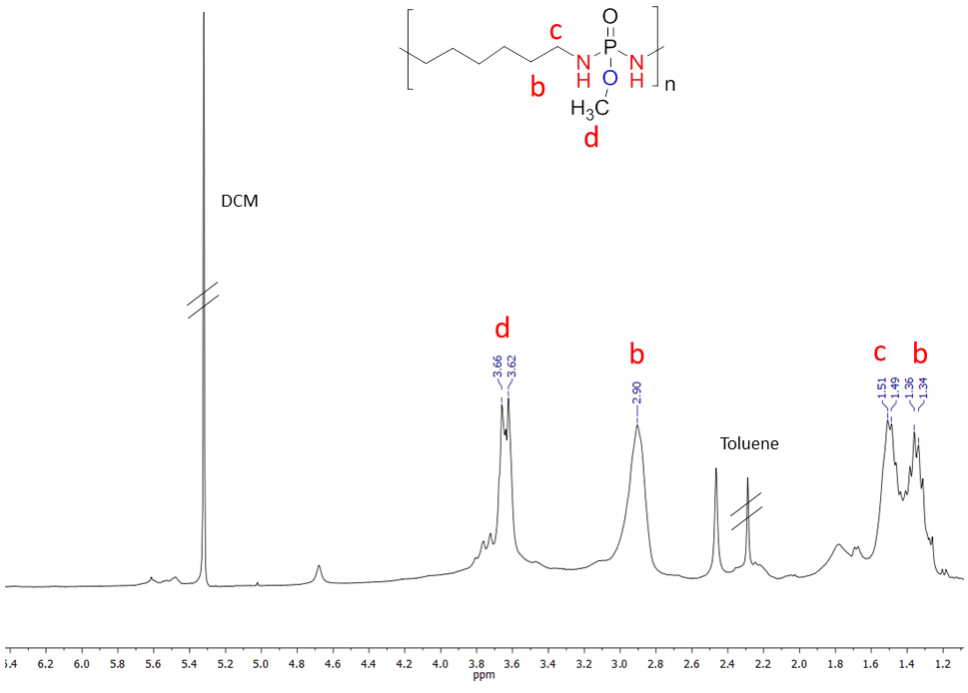

Figure S82: ^{1}H NMR of **poly-H(13)** (300 MHz, 298 K, $CDCl_3$).

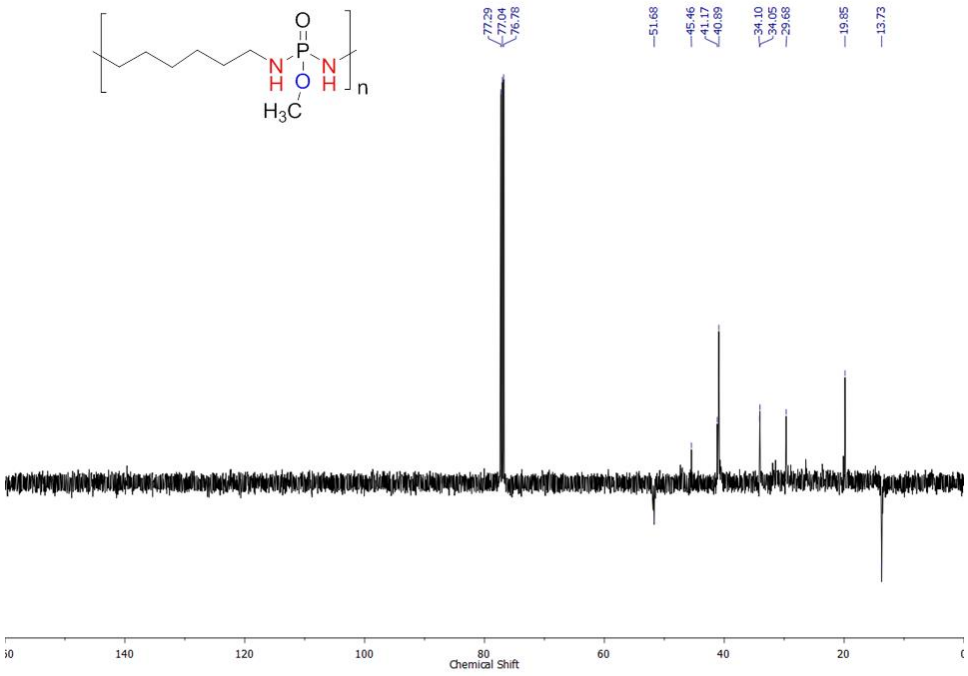

Figure S83: DEPT-135 $^{13}C\{H\}$ NMR of **poly-H(13)** (126 MHz, 298 K, $CDCl_3$).

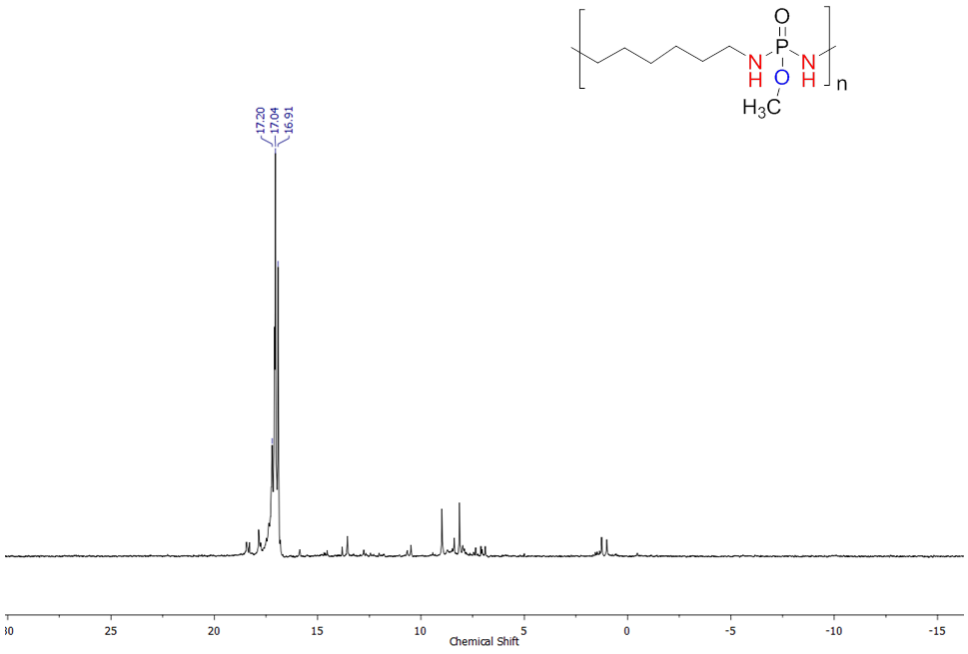

Figure S84: $^{31}P\{H\}$ NMR of **poly-H(13)** (202 MHz, 298 K, $CDCl_3$).

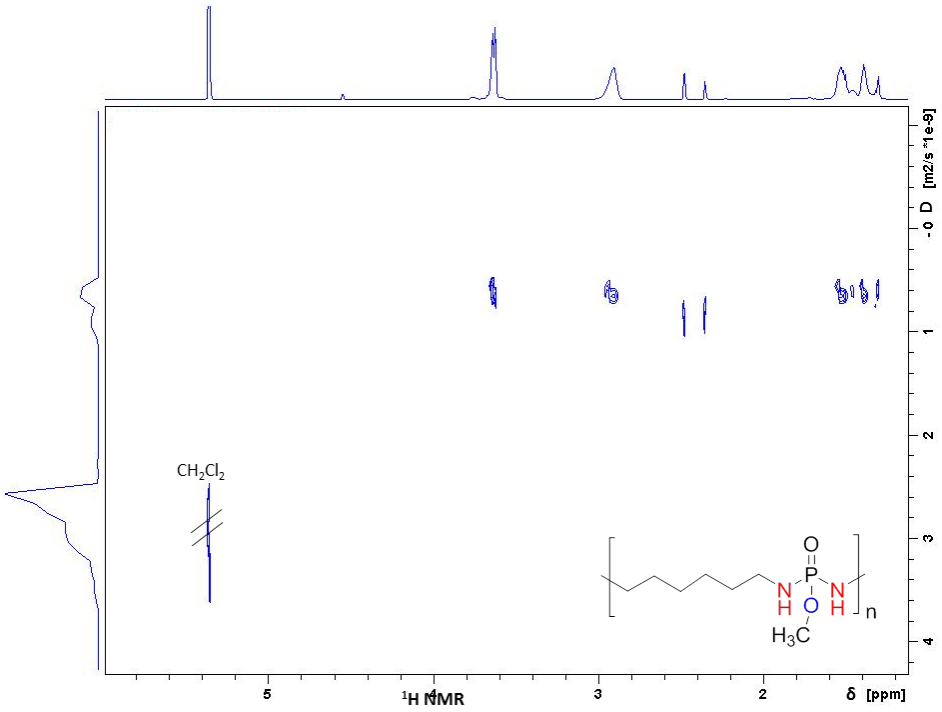

Figure S85: ^{1}H DOSY of **poly-H(13)** (700 MHz, 298 K, $CDCl_3$).

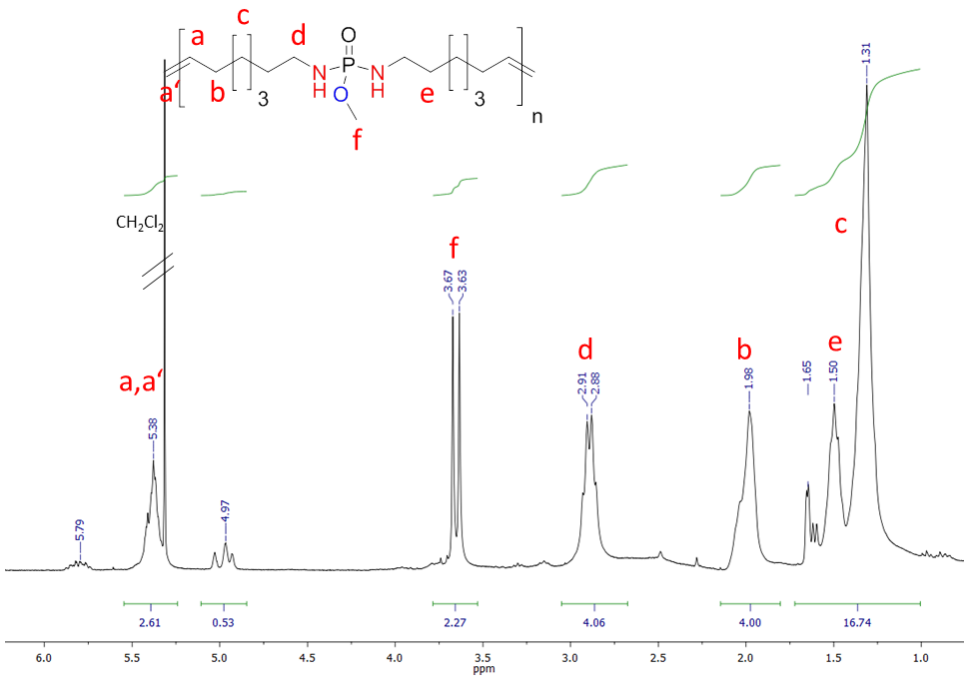

Figure S86: ^{1}H NMR of **poly(14)** (300 MHz, 298 K, $CDCl_3$).

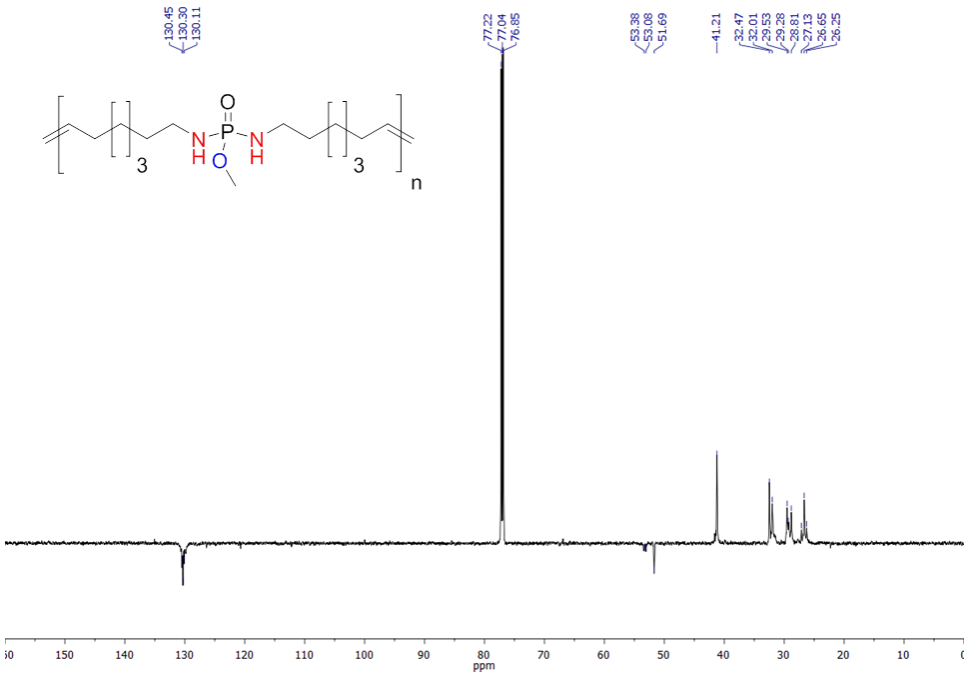

Figure S87: DEPT-135 $^{13}C\{H\}$ NMR of **poly(14)** (176 MHz, 298 K, $CDCl_3$).

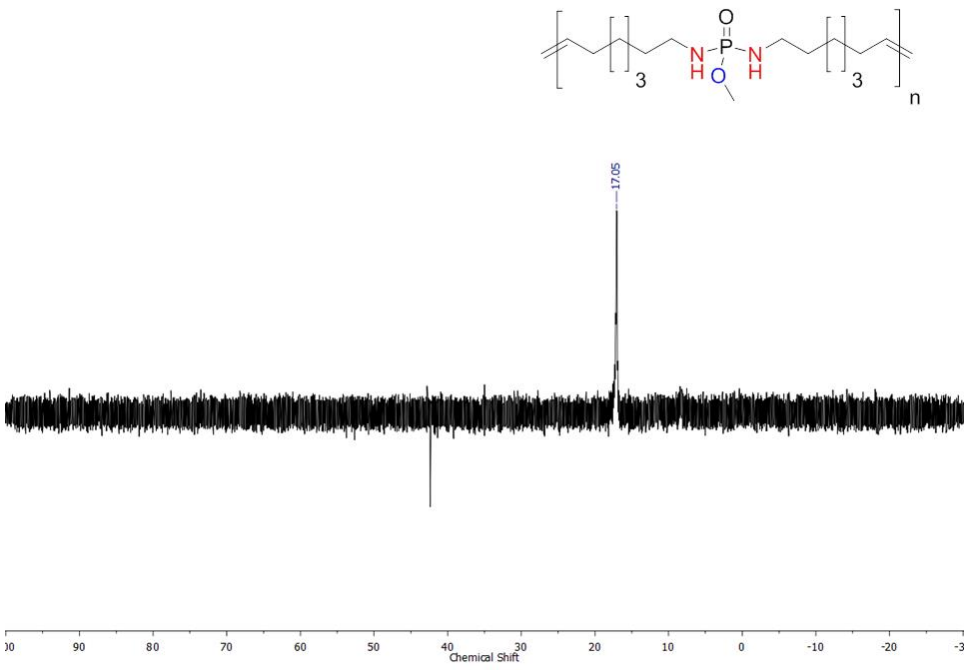

Figure S88: $^{31}P\{H\}$ NMR of **poly(14)** (121.5 MHz, 298 K, $CDCl_3$).

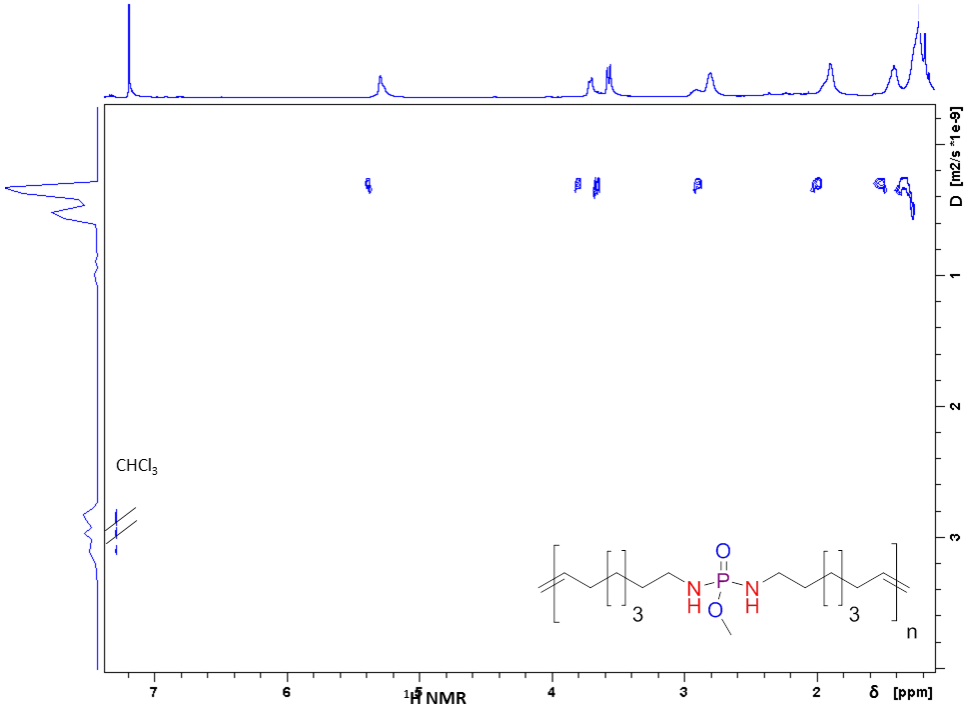

Figure S89: ^{1}H DOSY of **poly(14)** (500 MHz, 298 K, $CDCl_3$).

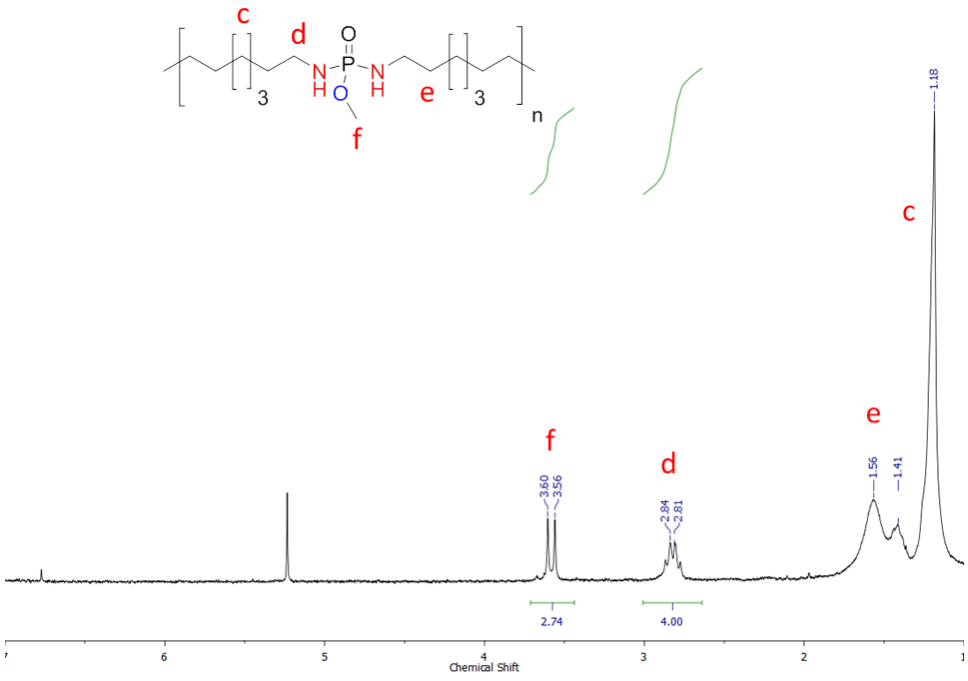

Figure S90: ^{1}H NMR of **poly-H(14)** (300 MHz, 298 K, $CDCl_3$).

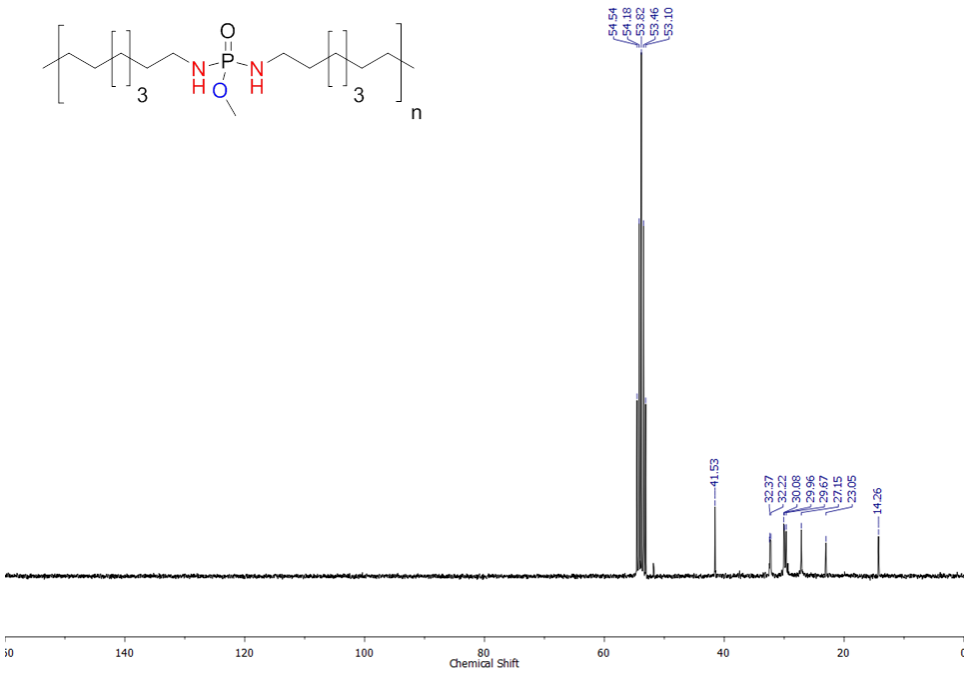

Figure S91: $^{13}C\{H\}$ NMR of **poly-H(14)** (75 MHz, 298 K, CD_2Cl_2).

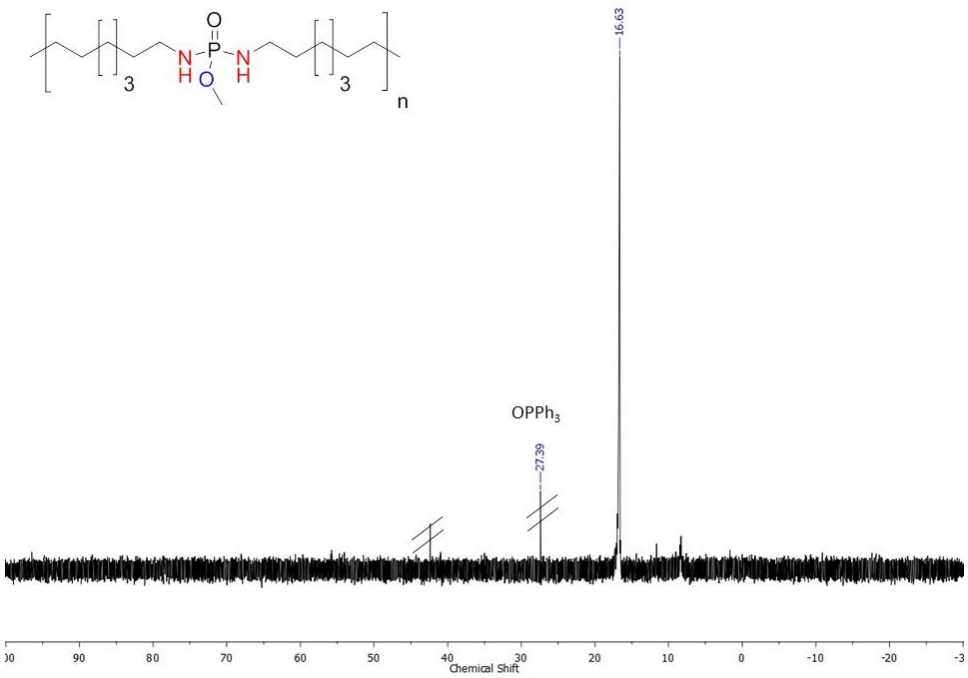

Figure S92: $^{31}P\{H\}$ NMR of **poly-H(14)** (121.5 MHz, 298 K, $CDCl_3$).

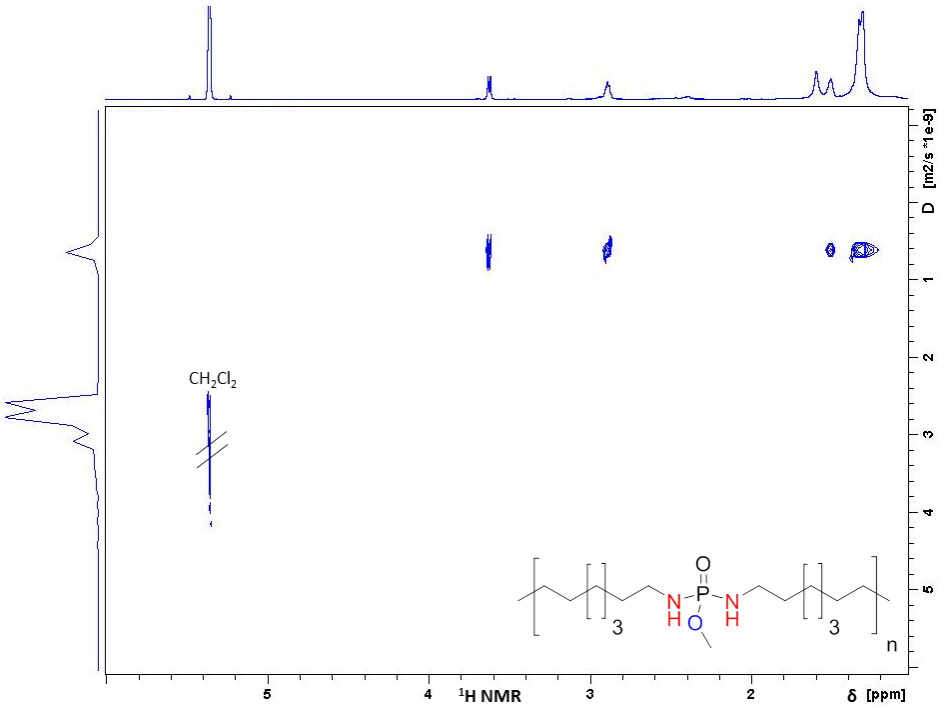

Figure S93: ^{1}H DOSY of **poly-H(14)** (700 MHz, 298 K, $CDCl_3$).

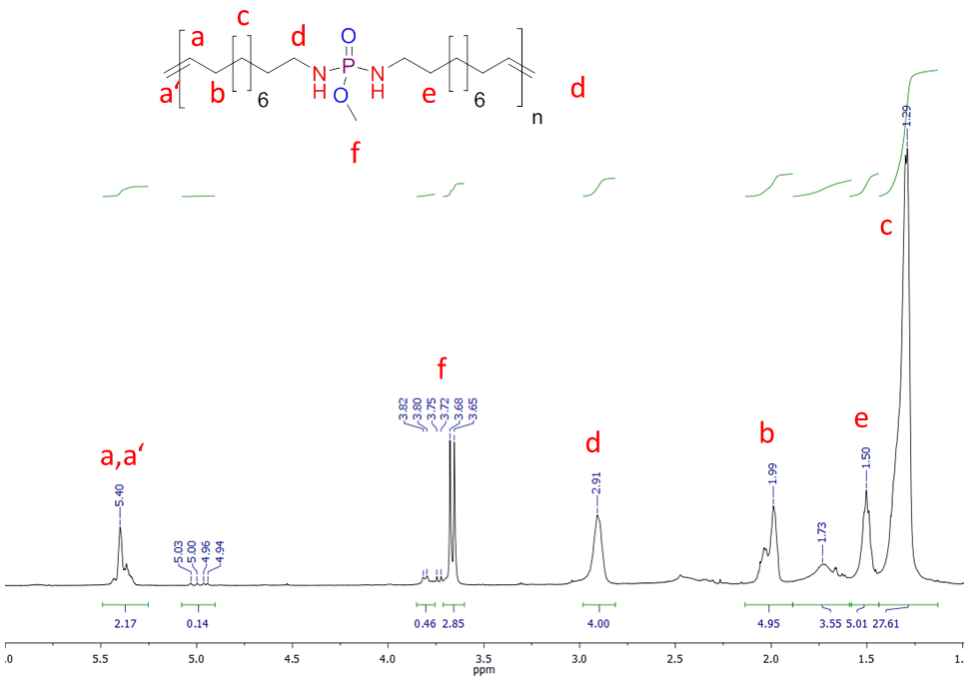

Figure S94: ^{1}H NMR of **poly(15)** (500 MHz, 298 K, $CDCl_3$).

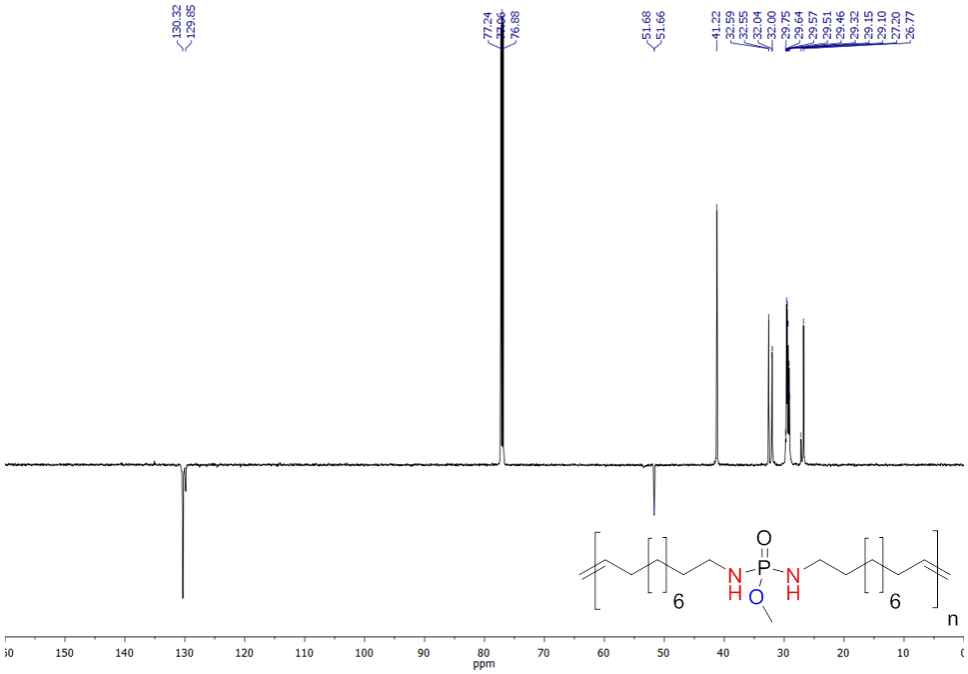

Figure S95: DEPT-135 $^{13}C\{H\}$ NMR of **poly(15)** (176 MHz, 298 K, $CDCl_3$).

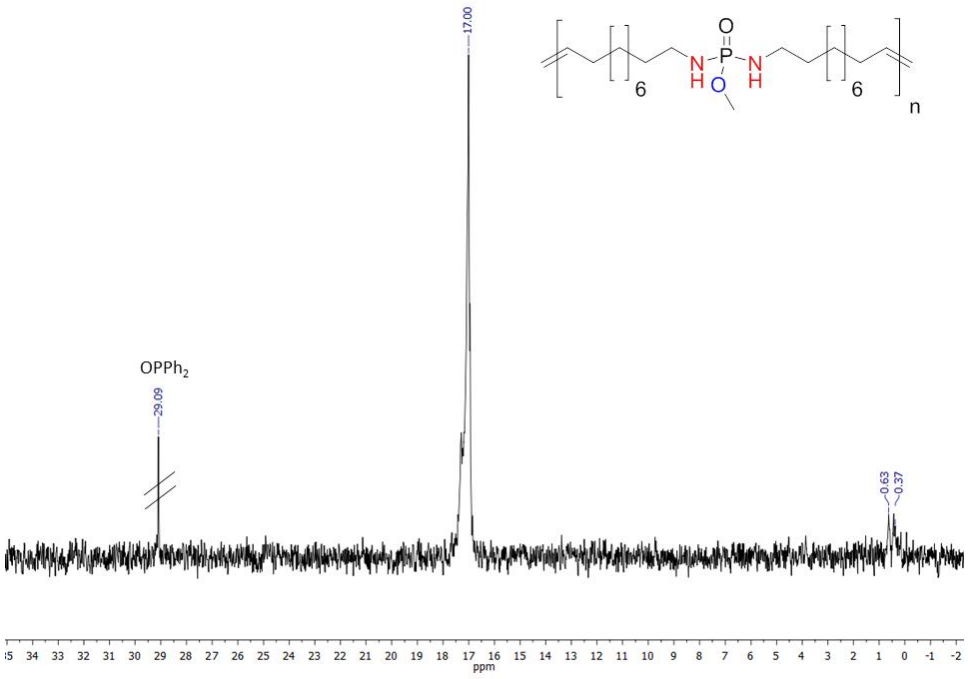

Figure S96: $^{31}P\{H\}$ NMR of **poly(15)** (202 MHz, 298 K, $CDCl_3$).

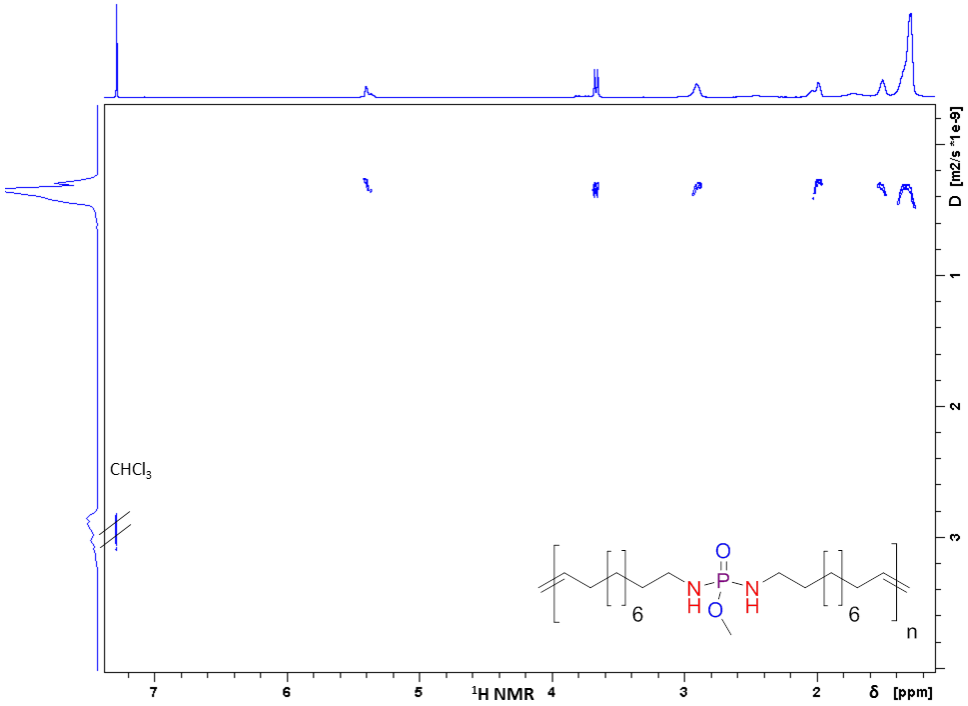

Figure S97: ^{1}H DOSY of **poly(15)** (500 MHz, 298 K, $CDCl_3$).

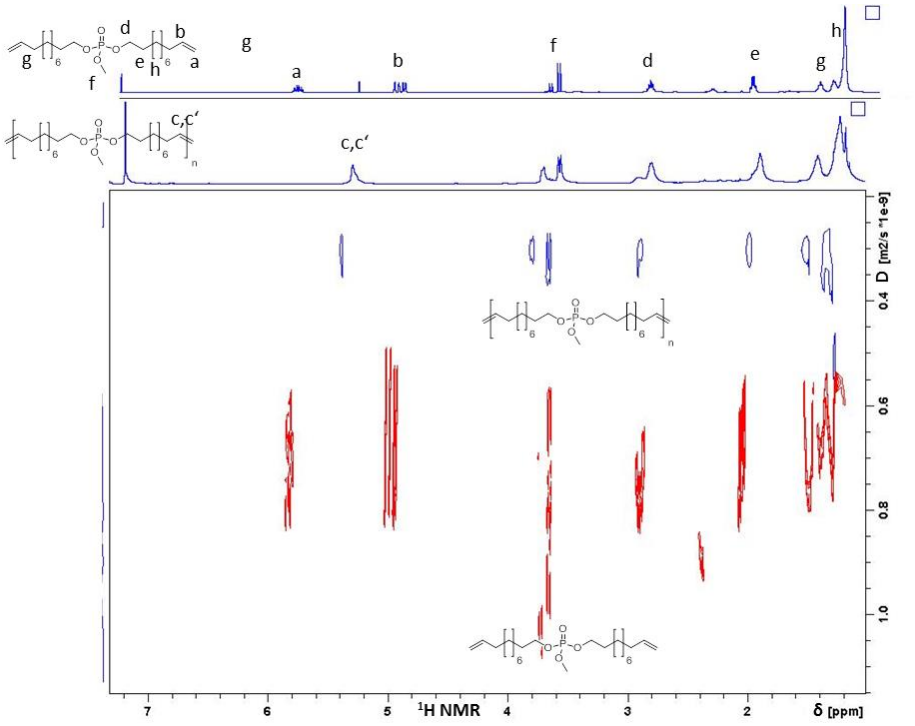

Figure S98: ^{1}H NMR spectrum of monomer **15** (top spectrum of ^{1}H NMR spectra; red signals of DOSY spectrum) and the respective polymer **poly(15)** (bottom spectrum of ^{1}H NMR spectra; blue signals of DOSY spectrum), proving the formation of internal double bonds at 5.4 ppm and the diffusion coefficient shift (500 MHz, 298 K, $CDCl_3$).

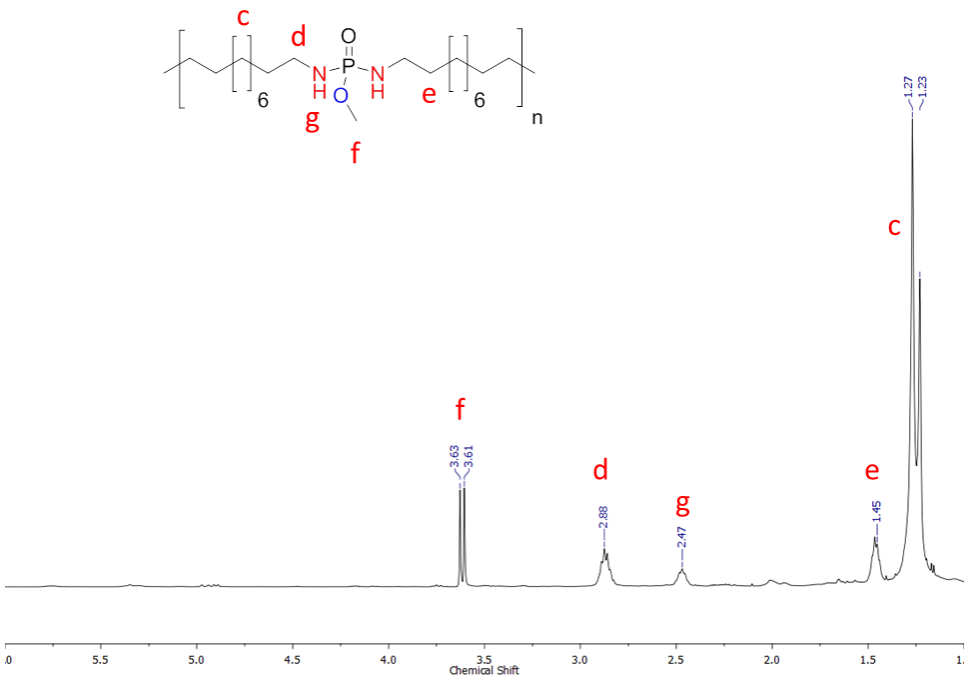

Figure S99: ^{1}H NMR of **poly-H(15)** (500 MHz, 298 K, $CDCl_3$).

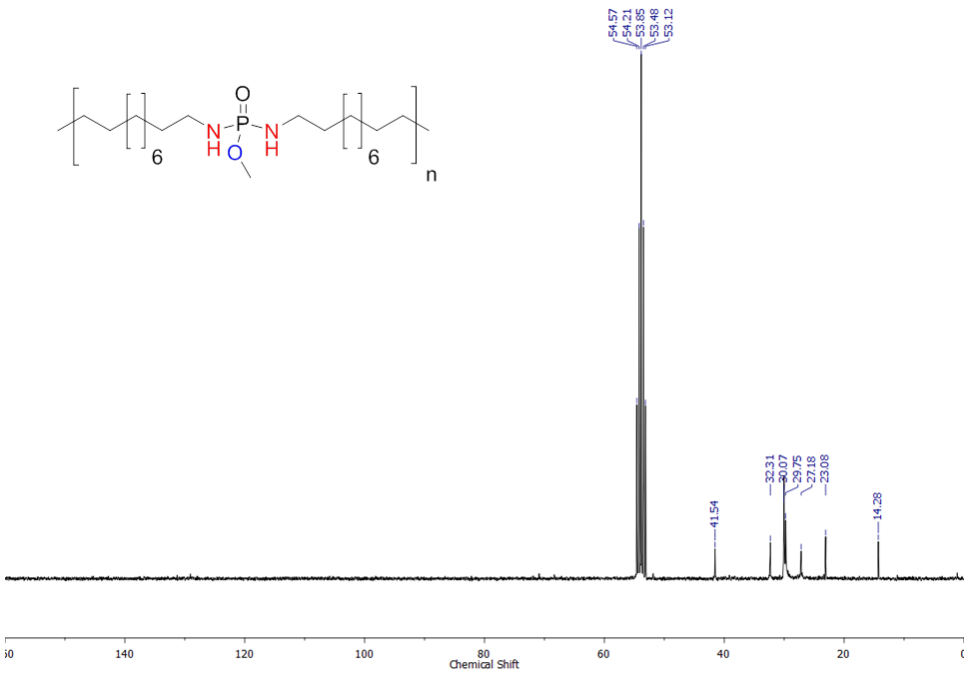

Figure S100: ^{13}C{H} NMR of **poly-H(15)** (75 MHz, 298 K, CD_2Cl_2).

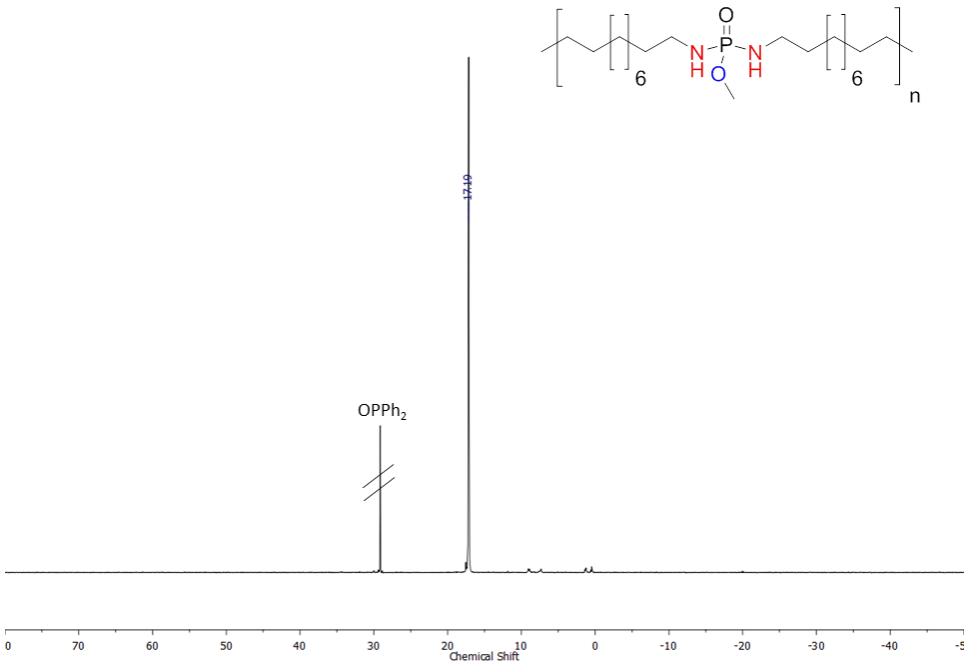

Figure S101: $^{31}P\{H\}$ NMR of **poly-H(15)** (202 MHz, 298 K, $CDCl_3$).

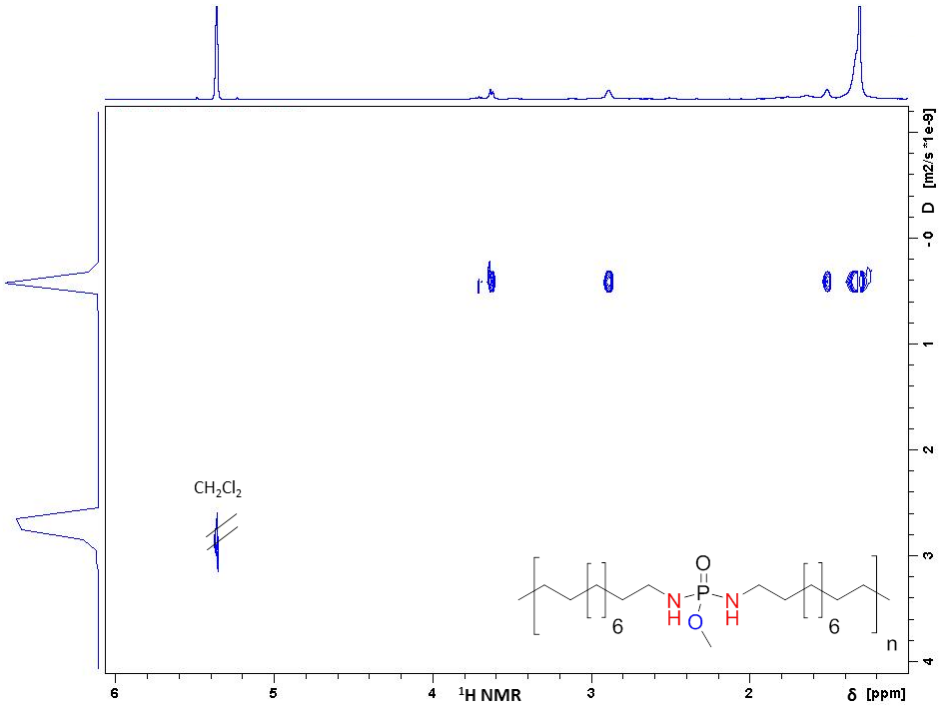

Figure S102: ^{1}H DOSY of **poly-H(15)** (700 MHz, 298 K, $CDCl_3$).

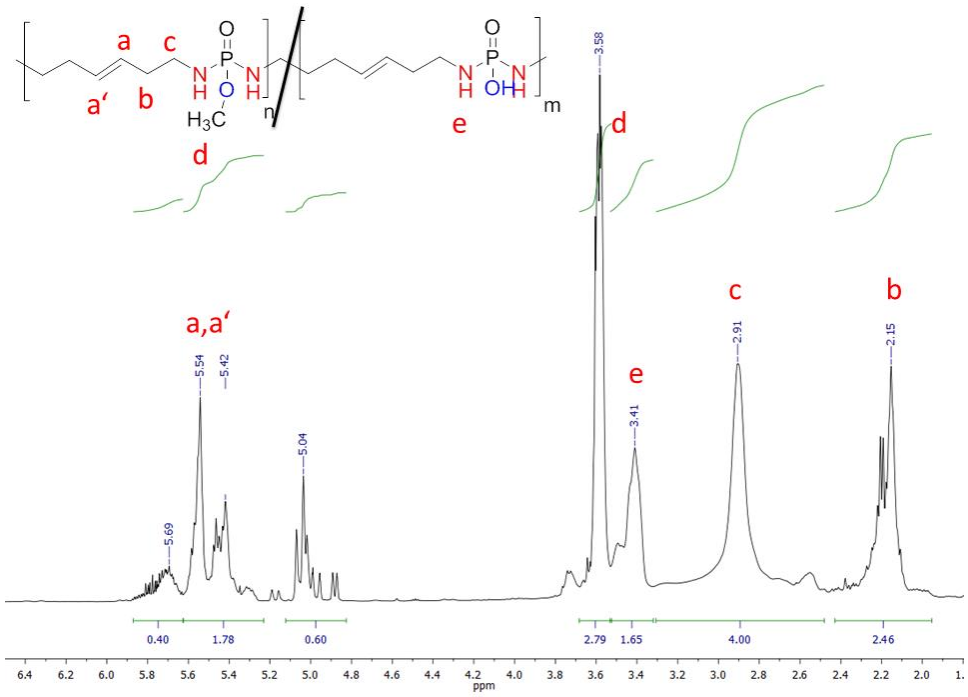

Figure S103: ^{1}H NMR of copolymer **poly(11-13)** (300 MHz, 298 K, $CDCl_3$).

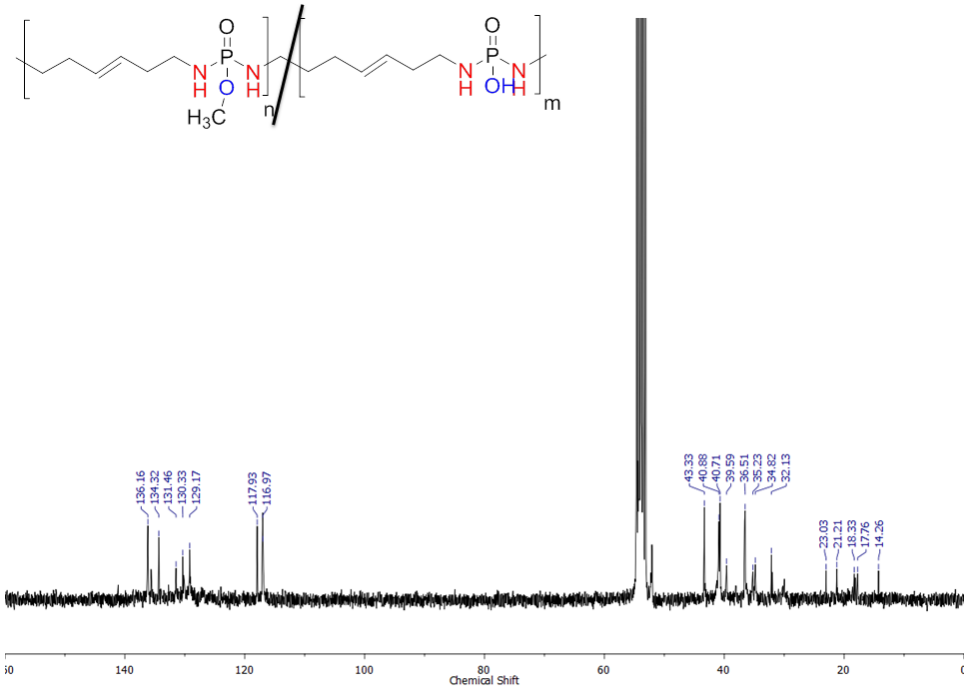

Figure S104: ^{13}C{H} NMR of copolymer **poly(11-13)** (75 MHz, 298 K, $CDCl_3$).

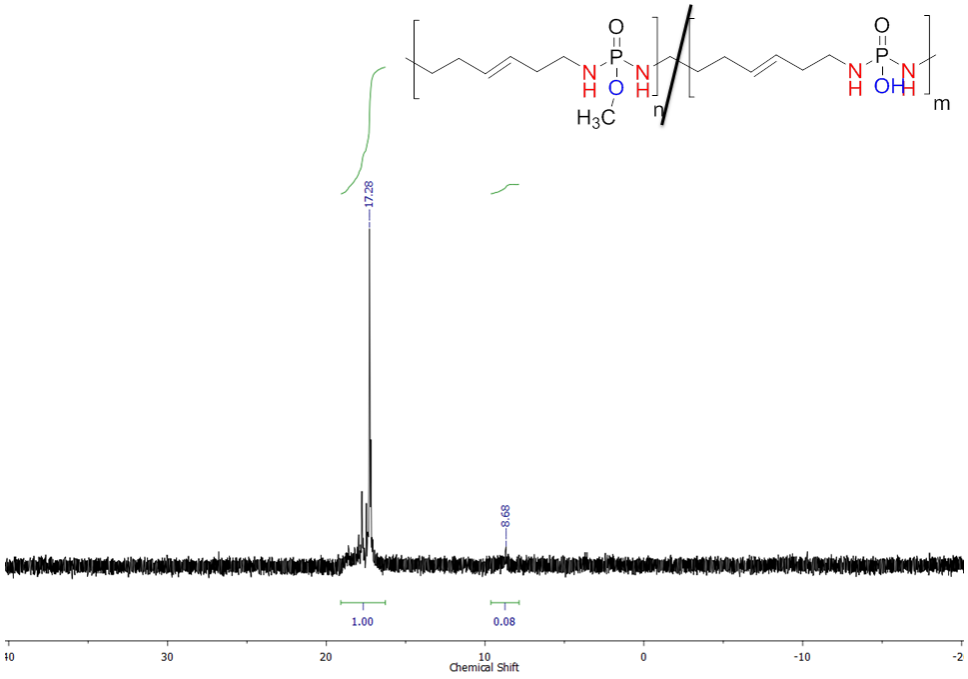

Figure S105: $^{31}P\{H\}$ NMR of copolymer **poly(11-13)** (121.5 MHz, 298 K, $CDCl_3$).

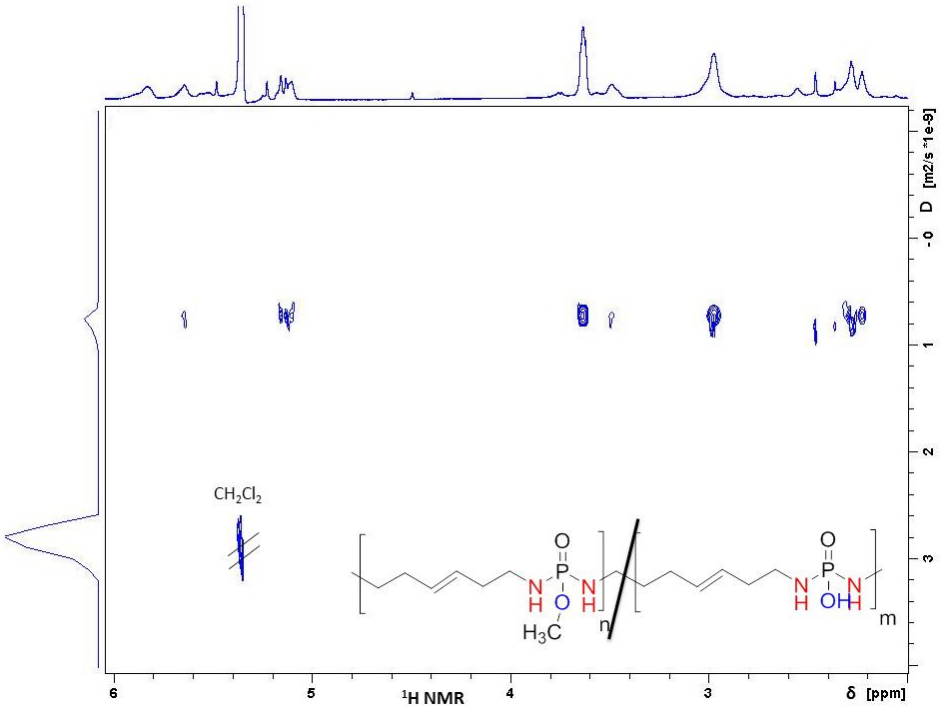

Figure S106: ^{1}H DOSY of copolymer **poly(11-13)** (700 MHz, 298 K, $CDCl_3$).

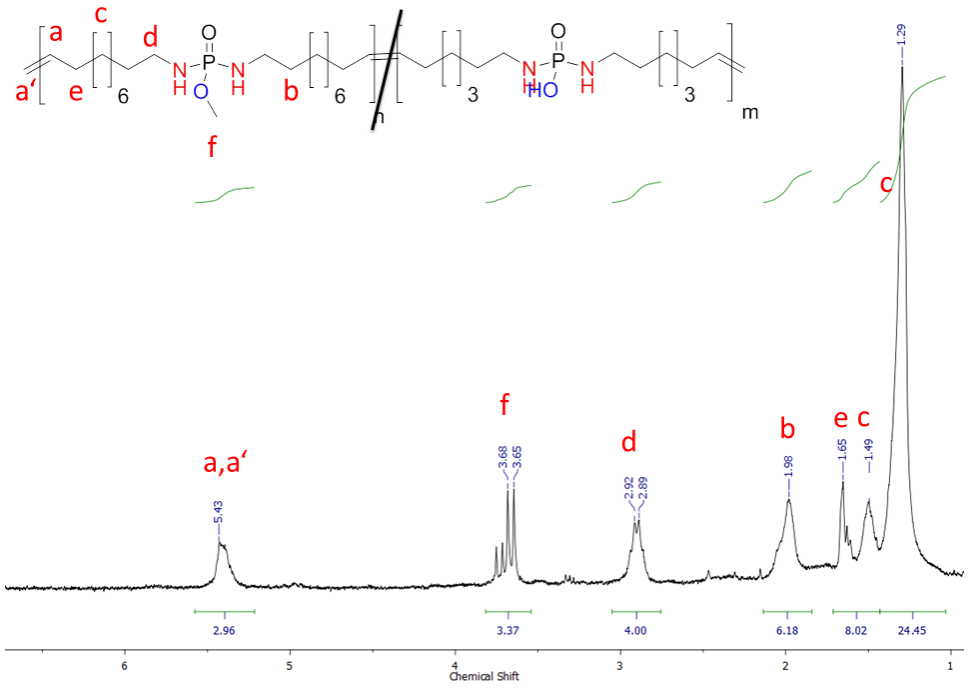

Figure S107: ^{1}H NMR of copolymer **poly(12-15)** (300 MHz, 298 K, $CDCl_3$).

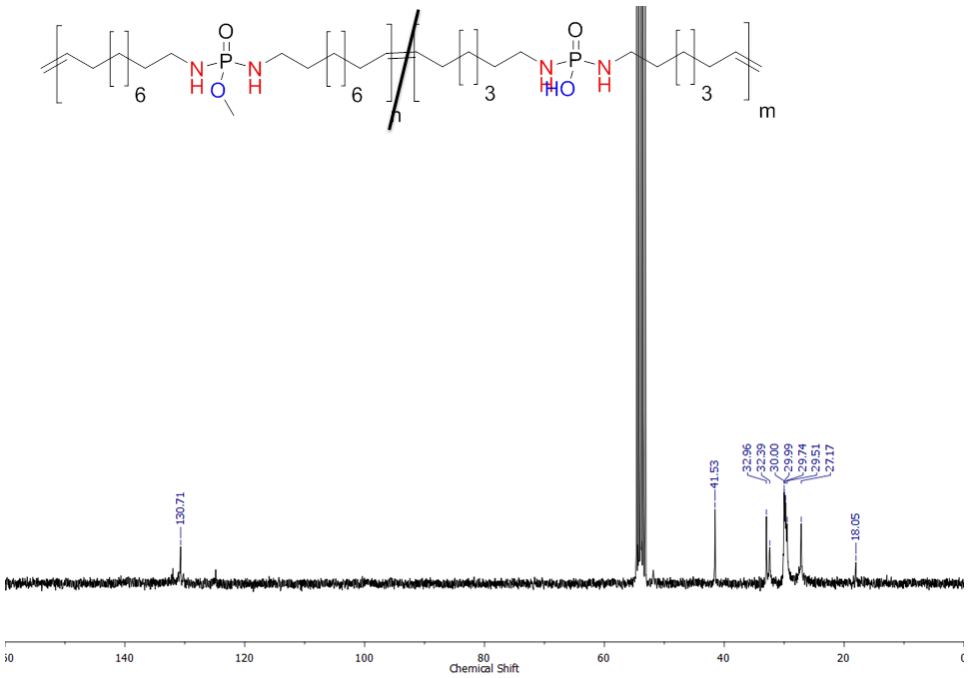

Figure S108: ^{13}C{H} NMR of copolymer **poly(12-15)** (75 MHz, 298 K, $CDCl_3$).

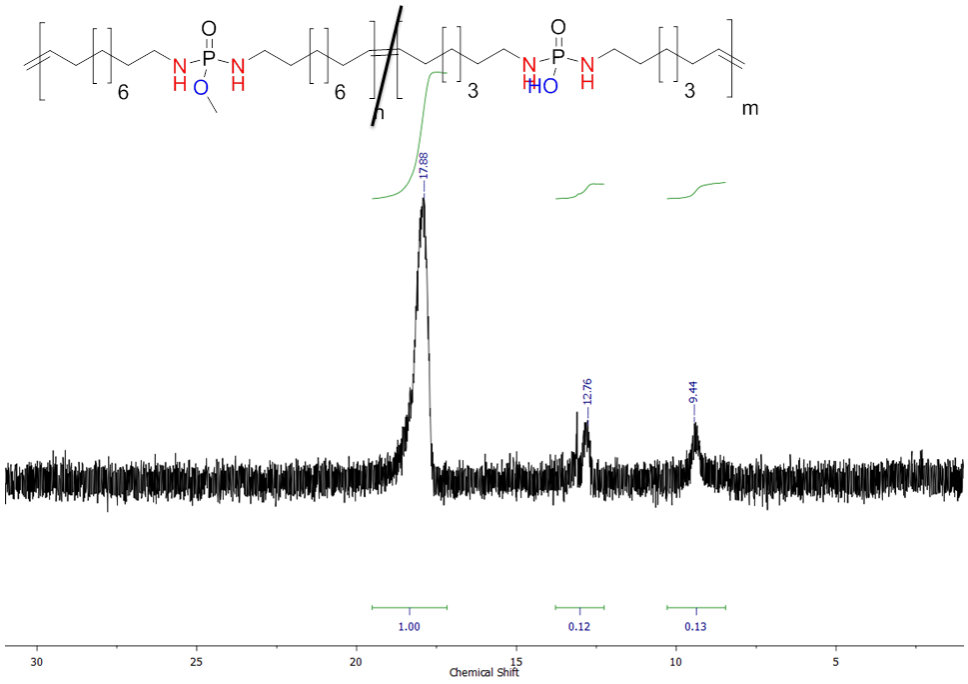

Figure S109: $^{31}P\{H\}$ NMR of copolymer **poly(12-15)** (121.5 MHz, 298 K, $CDCl_3$).

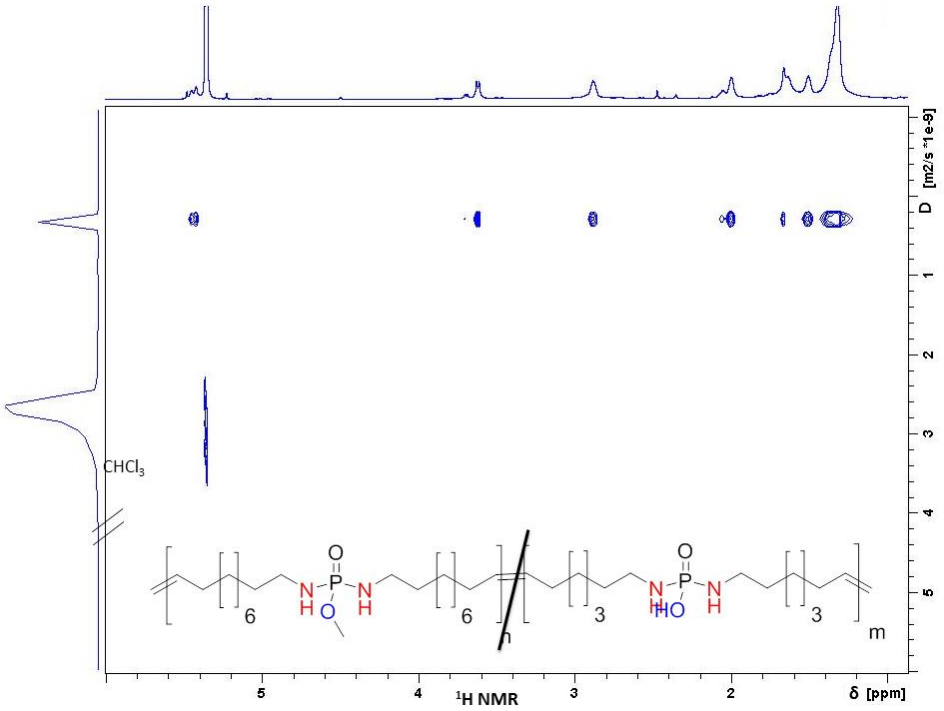

Figure S110: ^{1}H DOSY of copolymer **poly(12-15)** (700 MHz, 298 K, CD_2Cl_2).

3.3 Poly(phosphorodiamidate)s and Poly(phosphate)s via Thiol-ene Polyaddition

Thiol-ene polyadditions are attractive for many applications because of their high efficiency (**Chapter 1.2.6.1**). These reactions tolerate many functional groups due to mild reaction conditions. Furthermore, thiol-ene polyadditions are simple to execute with no side products due to the fact that they are radical step-growth reactions. The yields are usually high and the reactions are carried out in short timeframes. This makes thiol-ene polyadditions a versatile tool for many classes of polymers. New materials for optical components, adhesives, or high-impact energy absorbing materials are just a few examples for the broad range of applications of thiol-ene polyadditions.[48] Moreover, no metal based catalyst is needed. This is a great advantage in order to avoid metals which are known to be toxic to organisms. Surprisingly, the thiol-ene approach has never been conducted for phosphorus-based polymers thus far.

Herein is a discussion on preparing the first water-soluble PPDAs via thiol-ene polymerization. The possibility of subsequent oxidation of thioether functionalities to sulfone groups ensures completely water-soluble material. Potential applications such as protecting groups of hydroxyl moieties are imaginable. Specific degradation could lead to controlled release of an active agent release. Possible fields of applications are drug delivery, tissue engineering, biodegradable scaffolds, and flame retardant additives.

3.3.1 Water-soluble and degradable polyphosphorodiamidates via radical polyaddition

*Mark Steinmann, Frederik R. Wurm**

Max-Planck-Institut für Polymerforschung, Ackermannweg 10, 55128 Mainz, Germany.

Contact address: wurm@mpip-mainz.mpg.de

Abstract

Water-soluble poly(phosphorodiamidate)s (PPDAs) and structural analogues polyphosphates (PPEs) are synthesized by the metal-free radical thiol-ene polyaddition. PDAs or PEs are investigated within the main-chain. Further variations have been achieved by the third pedant group. Either hydroxyl groups or methoxy moieties affect hydrolytic stability. Thioether and ethylene oxide functionalities form the second part of the main-chain besides aliphatic hydrocarbons. Those groups make the material softer as just aliphatic hydrocarbons. To ensure complete water-solubility the thioether functionalities have been transformed to sulfons by oxidation. Different stability against hydrolytic degradation has been occurred by exchanging the binding motive of phosphorus and the third pedant group. For comparison reasons all synthesized polymers are structural analogue except the binding motive of phosphorus. Degradation experiments under acidic and basic conditions have been conducted. Controlled as well as uncontrolled degradation could be observed by adjusting the binding motive of phosphorus. It has been observed that P-N bonds are labile at acidic conditions and the other way around for PE based systems. It could be shown that the usage of (bio)orthogonal thiol-ene polyadditions, where no metal-based catalyst is needed, introduces completely adjustable polymers. Properties as hydrophilicity or degradability have been modified as desired by changing the monomers, the side chain or by oxidation.

Introduction

The demand for water-soluble polymers with adjustable degradation rates is important for many applications especially in drug delivery. Poly(phosphoesters and -amide)s are promising novel materials due to the high chemical versatility around the central phosphorus. Here, we prepare the first library of water-soluble poly(phosphorodiamidate)s (PPDAs) and compare them to their "ester-analogues". Besides poly(phosphoester)s (PPEs) with hydrolytically labile P-O-linkages in the main and the pendant chain, the far more labile P-N-bonds are found scarcely in the current literature. Polymers with P-N-linkages, such as polyphosphazenes or PPDAs exhibit high thermo-oxidative stability (up to 450 °C) and fire resistant behavior.[95, 99, 117, 156, 183] They are studied as flame retardant additives, while other potential applications have not been investigated.[102, 117-118] Initial investigations of the hydrolytic degradation of phosphoramidate side-chains were carried out by Wooley and coworkers and more recently also by our group.[90, 110]

But never before structurally diverse water-soluble, main-chain PPDAs with controlled degradation behavior were reported. We prepared phosphoester (PE) and phosphorodiamidate (PDA) monomers that were polymerized by the metal-free thiol-ene polyaddition. The prepared polymers were water-soluble after oxidation of the thioether functionality to sulfon groups by a green chemistry protocol using hydrogen peroxide and boric acid. For their preparation only azobisisobutyronitrile (AIBN) and boric acid were used as the catalysts avoiding metals and other toxic reagents.[184] The hydrolytic degradation of the polymers was studied and was found to be precisely controlled by the binding pattern around the central phosphorus (P-O vs. P-N).

Results and Discussion

Thiol-ene polyadditions are tolerant to many functional groups. The radical thiol-ene polyaddition allows us the preparation of PPDAs and PPEs in a straightforward manner. The choice of the dithiol comonomer has a tremendous influence on the final material properties. We chose 2-(2-methoxyethoxy)ethanethiol to produce perfectly alternating copolymers with hydrophilic ethylene glycol segments in the polymer backbone, besides thioethers and the phosphoesters or –amides. The thioethers can be used for further modification, i.e. to increase their hydrophilicity by the oxidation of the thioethers to sulfones or potentially to react with other nucleophiles. Recent studies in our group used olefin metathesis for the preparation of PPEs, PPAs, and PPDAs (**Chapter 3**).[110, 164] This precise chemistry however, depends on the use of metal catalysts which can be omitted by radical polymerization.[48]

We chose two monomers with a pendant P-OH group, namely a phosphodiester (bis-(but-3-en-1-yl)-phosphate (**1**)) and a phosphorodiamidate *N,N`*-bis-(but-3-en-1-yl)-phosphoro-diamidate (**3**). In addition, monomers with a pendant methyl-ester have been prepared, i.e. the phosphotriester (bis-(but-3-en-1-yl)-methylphosphate (**2**)) and *N,N`*-bis-(but-3-en-1-yl)-methylphosphorodiamidate (**4**) (**Scheme 1**). **1** and **3** carry a pH-responsive P-OH as pendant group, while **2** and **4** carry a pendant ester P-OR. Adjusting the hydrolytic degradation should be feasible with such structures.

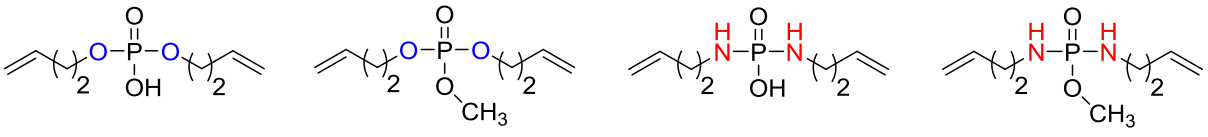

Scheme 1: Chemical structures of monomers for the radical polyaddition.

The thiol-ene polyaddition of the P-monomers (**1, 2, 3,** and **4**) with the comonomer **5** was carried out at 65 °C in the presence of azobisisobutyronitrile (AIBN; **Scheme 2**). For monomers **1, 2** and **4** the reaction was carried out in the bulk, as those monomers are liquids and miscible with **5**. As monomer **3** is solid and insoluble in **5**, the polymerization was carried

out in water at 65 °C. Both materials are not water soluble itself but addition of triethylamine (TEA) and heating the dispersion at 65 °C until the scent of TEA is vaporized deliver completely dissolved monomers. Afterwards the reaction mixture was purged with argon and AIBN was added to start the polymerization. The polymerization time was usually 4-5 h until the reaction mixture was too viscous to adequately stirring.

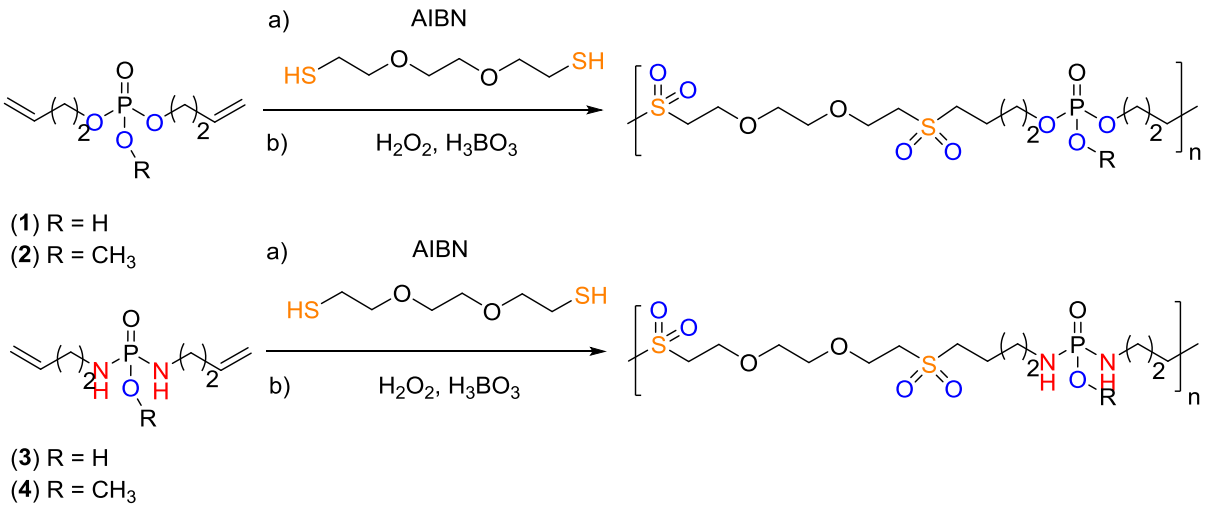

Scheme 2: Preparation of PPEs and PPDAs via thiol-ene polyaddition and subsequent oxidation by hydrogen peroxide.

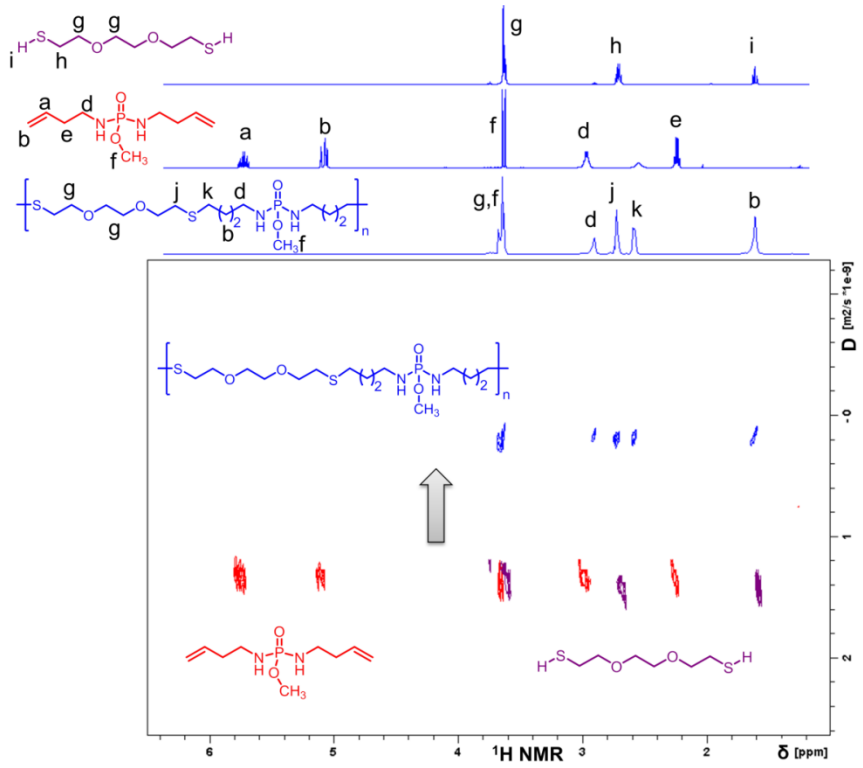

Figure 1: Overlay of the ^{1}H DOSY NMR spectra of monomer **4** (red), comonomer **5** (purple) and the respective polymer **poly(4)** (blue) (500 MHz, 298 K, $CDCl_3$).

All resonances of both monomers and the polymer are clearly detectable and assigned to the structure. All main-chain resonances have shifted in the spectrum of the polymer compared to the monomers after polymerization, accordingly. the signals of the olefinic groups **a + b** and the thiol protons **i** are disappeared due to the thiol-ene polyaddition and new resonances **j + h** have appeared to indicate the thioether linkage of the polymer backbone.

Table 1 lists the polymerization results, reaction conditions and molecular weights measured by GPC in water or dimethylformamide (DMF); molecular are located between ca. 2,000 and 6,000 g/mol.

Table 1: Molecular weight results for the thiol-ene polyaddition of phosphates and phosphorodiamidates as well as polymers after oxidation.

Polymer	M_{nGPC} (g/mol)	M_{wGPC} (g/mol)	$Đ$
Poly(1)[a]	1,500	2,800	1.81
Poly(2)[b]	6,500	13,000	1.85
Poly(3)[a]	1,700	2,000	1.18
Poly(4)[b]	2,900	7,600	2.63
Poly-Ox(1)[a]	2,200	7,800	3.47
Poly-Ox(2)[b]	6,100	12,400	2.02
Poly-Ox(4)[b]	3,000	5,300	1.77

Conditions: a) Determined by GPC in H_2O vs. PEG standards measured by RI-detector; b) Determined by GPC in DMF with polystyrene standard measured by RI-detector

Also the PPDA exhibit lower molecular weights compared to the PPEs because the monomers have higher viscosity (**4**) or are solids **(3**) and needed to be polymerized in solution. The molecular weights of the polymers remain unchanged after the oxidation to the sulfons. Furthermore the molecular weight dispersities of **poly(3)** and **poly-Ox(1)** are rather low for step-growth polymerization. As a consequence it should be noted that molecular weights and molecular weight distribution with different solvents, columns, and standards are problematic to compare with one another and the results should be considered with care as interactions with the column material is a typical obstacle with P-containing polymers.

To increase the hydrophilicity of such polymers further, they were oxidized to the sulfons. Only **poly(3)** was directly water soluble and used as received by polymerization. Hydrogen peroxide in either water or DMF was used for the oxidation of polymers **poly(1), poly(2)**, and **poly(4)**. After two hours of stirring at room temperature all thioether functionalities were transformed into sulfon groups (**Scheme 2** and **Figure 2)**.

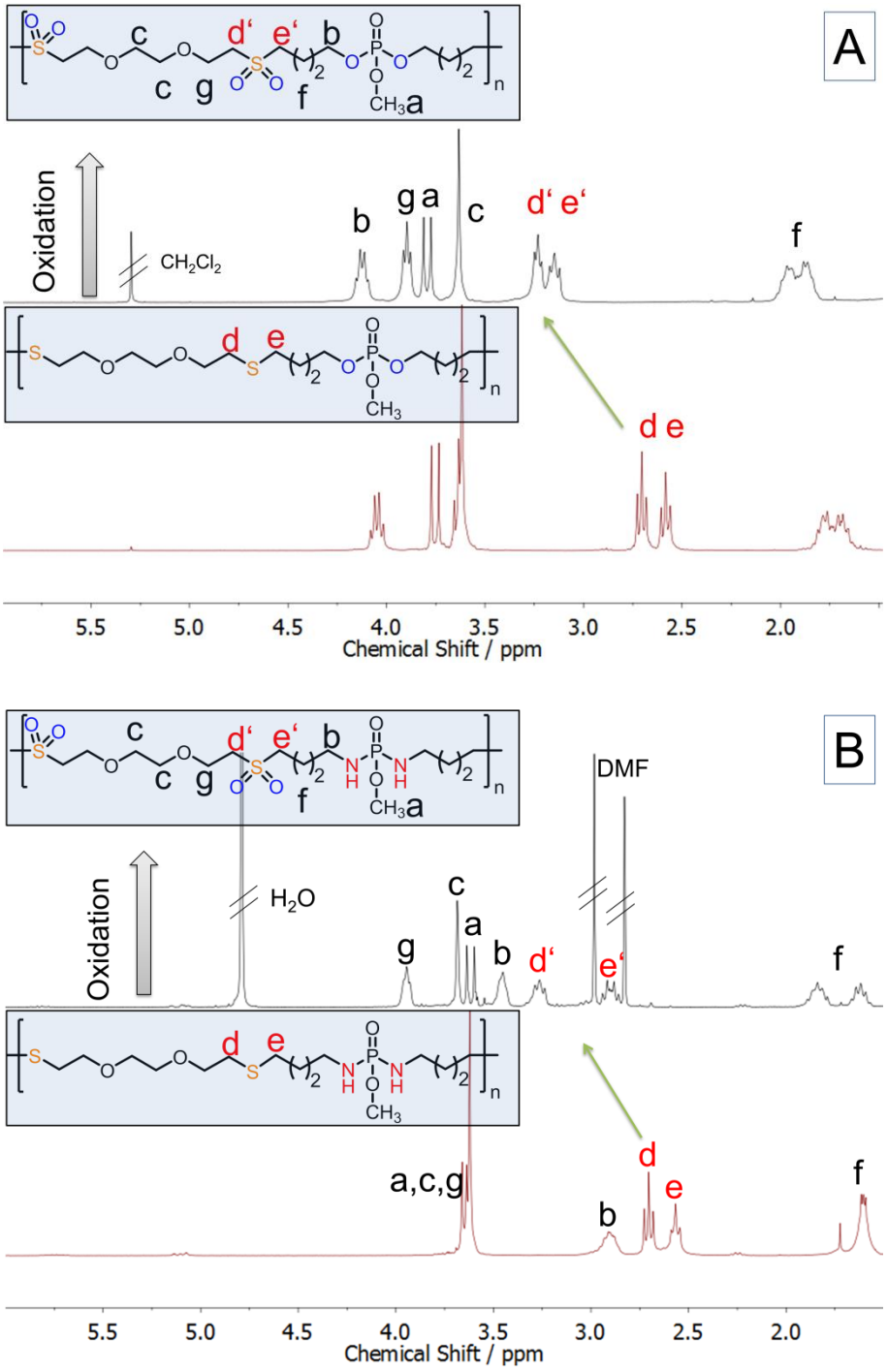

Figure 2: Comparison of ^{1}H NMR spectra of **poly-(2)** (bottom; 300 MHz, 298 K, $CDCl_3$) and oxidized **poly-ox(2)** (top; 300 MHz, 298 K, $CDCl_3$) and **poly-(4)** (bottom; 300 MHz, 298 K, $CDCl_3$) and oxidized **poly-ox(4)** (top; 300 MHz, 298 K, H_2O).

The ^{1}H NMR spectra in **Figure 2** show the change of the resonances of **poly(2)** after oxidation to **poly-ox(2)** (top). The green arrow is pointing out the shift of the methylene groups next to either thioether (Figure 2 bottom) or sulfon (Figure 2 top) functionality. For the phosphorodiamidate-based polymer **poly(4)** the resonances can be assigned accordingly; also in this case the successful oxidation to **poly-ox(4)** can be clearly seen from the spectrum (Figure 2 bottom) from the shift to lower field for the methylene hydrogens next to the sulfon group. This is in accordance with the stronger electron withdrawing sulfon group.

Hydrolytic stability. The degradation behavior of PPEs and PPDAs under acidic and basic conditions differ strongly.[90] In contrast to carboxylic acid based amides, the P-N bonds within phosphoramidates and phosphorodiamidates are more labile to acidic hydrolysis.[108] Phosphotriesters instead are relatively stable in acidic conditions but degradable in neutral and basic settings.[88] The hydrolytic degradation of the water-soluble PPEs and PPDAs were studied at different pH-values by NMR spectroscopy in D_2O. The experimental relationship pD = pH + 0.4 was applied to convert pDs into pH values.[179] Consistent to previous reports, poly(phosphodiester)s, such as (**poly-ox(1)**), are resilient to hydrolysis. In contrast, **poly-ox(2)**, a poly(phosphotriester), hydrolyzes at neutral and basic conditions (pH = 7.0, 9.0 and 13.0). The PPE is hydrolyzed either along the polymer backbone or the pendant chain is released producing very stable phosphodiesters. ^{31}P{H} NMR spectroscopy reveals two different phosphates after degradation (δ 1.87 ppm and 0.75 ppm, while the polymer resonance at 0.60 ppm disappeared (**Figure S6**). The PPDAs are much more prone to hydrolysis: the backbone of **poly(3)** degrades at acidic conditions (^{31}P{H} NMR signal shifts from 3.58 ppm to 0.00 ppm; **Figure S7, S11**). Contrary at basic conditions (pH = 13.0) no degradation of **poly(3)** occurred, as it is deprotonated with the anionic charge hindering nucleophilic attack on the phosphorus.

The PPDA **poly-ox(4)** with a pendant methylester degrades at similar rates under acidic conditions (^{31}P{H} NMR signal shifts from 20.51 ppm to 1.52 ppm, **Figure S8**), but under basic conditions, the side-chain is released selectively and the backbone remains intact (^{31}P{H} NMR signal shifts from 20.61 ppm to 14.33 ppm; example **Figure S9**).

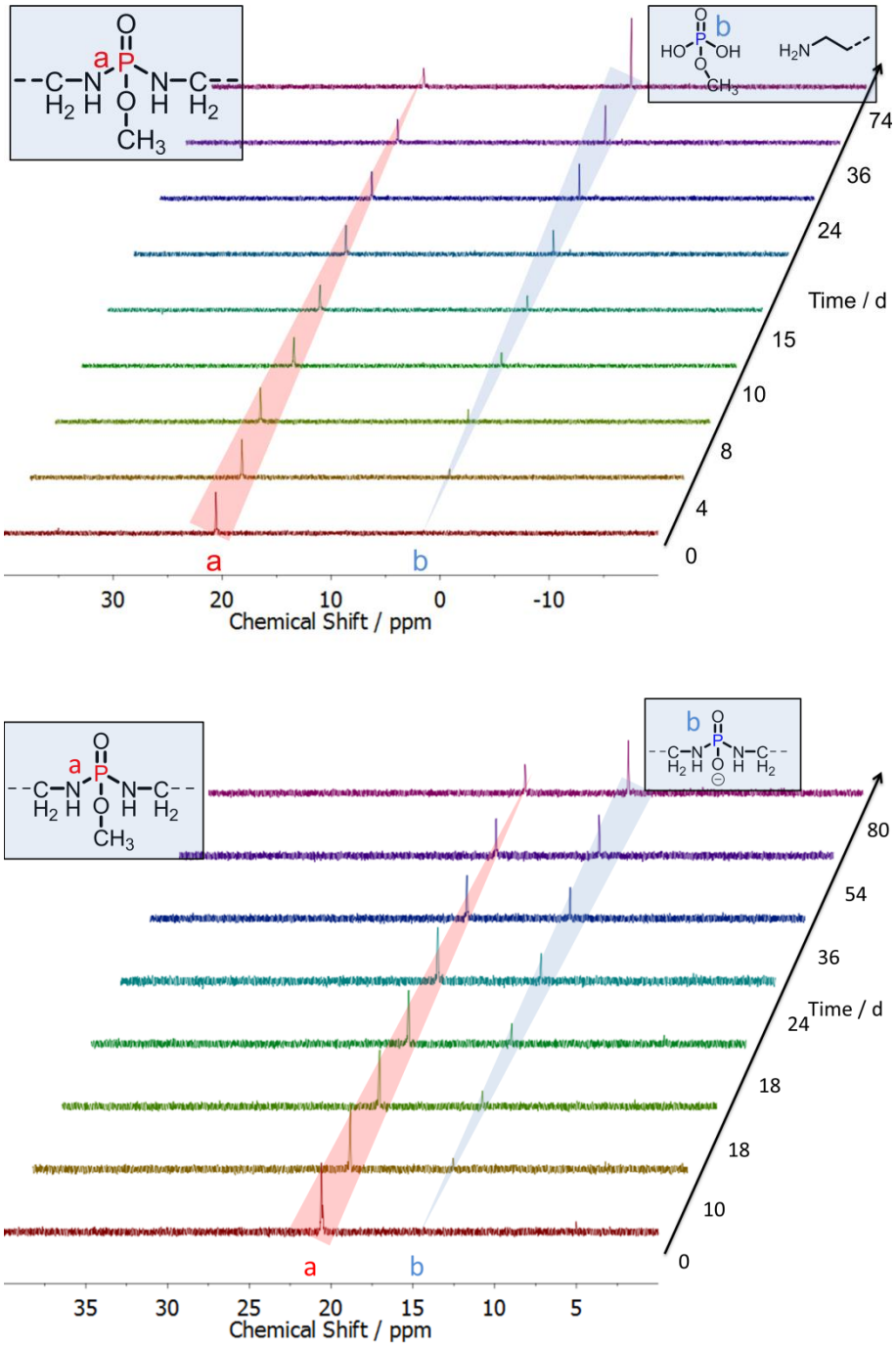

Figure 3: Controlled Degradation of **poly-ox(4)** of either the main-chain cleavage at pH = 3.0 (top) or the side-chain cleavage at pH = 13.0 (bottom) plotted versus degradation time monitored by ^{31}P NMR (121.5 MHz, 298 °C, D2O).

In **Figure 3** the degradation of **poly-ox(4)** is monitored at pH = 3.0 and pH = 13.0. At pH = 3.0 (**Figure 3**; top) the degradation kinetics of the phosphoramidate bonds is indicated. The ^{31}P NMR resonance signal of the phosphoramidate linkage (a) is decreasing and the emerging

phosphoric acid signal (b) is increasing. At pH = 13.0 (**Figure 3**; bottom) the cleavage of the methoxy side-chain is indicated. Here the changed resonance signal for the phosphoramidate linkage is displayed. The uncontrolled degradation of **poly-ox(2)** at basic conditions is shown in **Figure S5 + S6** in Supp. Info.).

In **Figure S10 - S13** are plotted the decreasing $^{31}P\{H\}$ resonance signal of polymer in comparison with the emerging $^{31}P\{H\}$ peak of degradation products of degradable polymers **poly-ox(2)**, **poly(3)** and **poly-ox(4)** over a range of at least 30 days. **Figure S12** specifically displays the backbone degradation of **poly-ox(4)** at pH = 3.0 and 5.0. As expected the degradation at pH = 5.0 is slower compare to degradation at pH = 3.0. Whereas, **Figure S10** and **Figure S13** exhibits the degradation of **poly-ox(2) and poly-ox(4)** at neutral and basic pH values. After 30 days at pH = 13.0 **poly-ox(2)** was already completely degraded into phosphorodiester fragments. pH = 7.0 and 9.0 feature slower degradation times as anticipated. The side-chain cleavage of the PPDA counterpart with the same methyl side-chain takes much more time as displayed in **Figure S13** in comparison to **Figure S10**. Here, pH 7.0 and pH = 9.0 do not even show degradation until 40 days of treatment. This is in due to the probability of cleaving. There are three possible bonds to cleave for the PPE but only one for the PPDA. In **Figure 11** can be seen the degradation rates of the **poly(3)** main-chain at pH = 1.0, 3.0 and 5.0. As expected the backbone cleavage at pH = 1.0 is much faster as at pH = 3.0 and even slower for 5.0. For comparison reasons all water soluble monomers and polymers and their degradation behavior are shown in the previous paper about the phosphorodiamidate binding motive (**Chapter 3**).

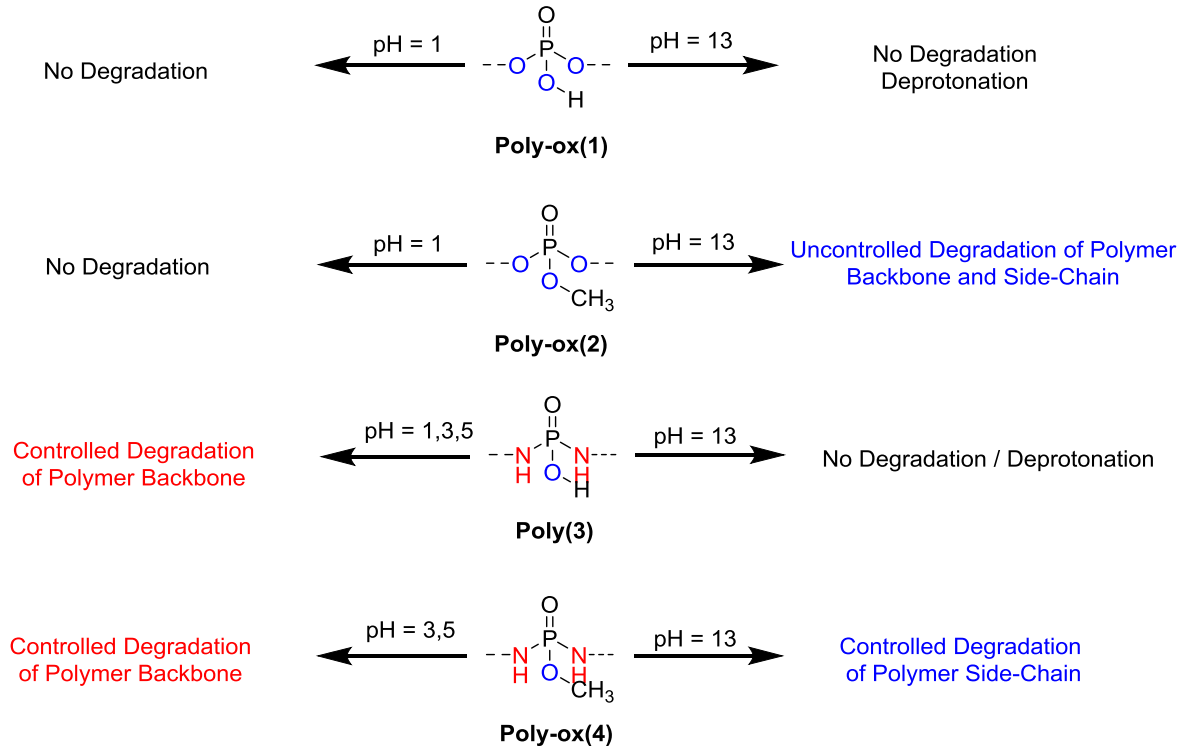

Scheme 3: Controlled and uncontrolled hydrolytic degradation of polymers under acidic and basic conditions (monitored over a period of 80 days).

Biological Compatibility. The cytotoxicity of **poly-ox(1), poly-ox(2), poly(3)** and **poly-ox(4)** was investigated *in vitro* against HeLa cells at a concentration of 0.75 µg mL^{-1} after 24 h of incubation at 37 °C in EMEM Medium (10% FBS, 1% Penistrep, 1% Glutamine. CellTiter 96® Aqueous One Solution Reagent was used as proliferation assay. The quantity of formazan product as measured by the amount of the 570 nm absorbance is directly proportional to the number of living cells in the culture. 10 % DMSO was used as the positive benchmark, and just cell media was used as negative control. All polymers (**Figure 3**) showed no toxicity toward HeLa cells at the tested concentration. The overall nontoxicity of the presented polymers was observed.

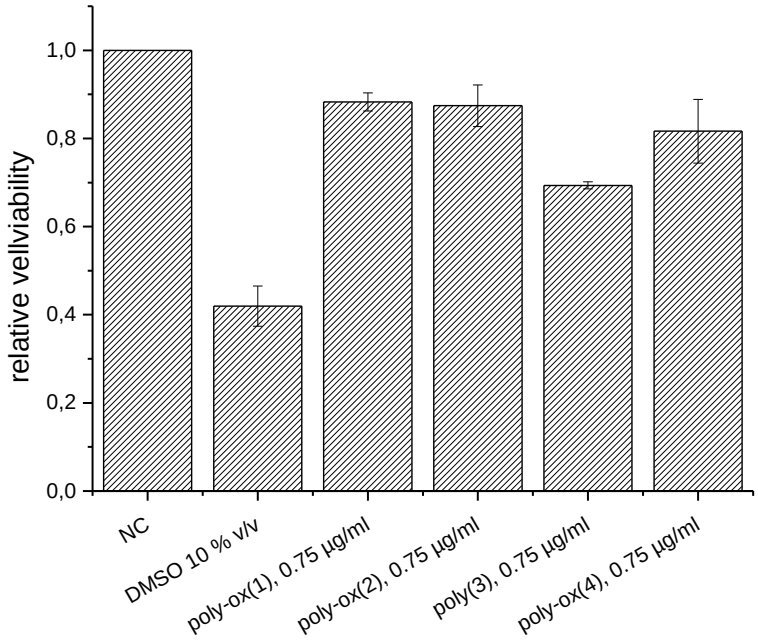

Figure 3: *In vitro* cell viability of HeLa cells treated with **poly-ox(1), poly-ox(2), poly(3)** and **poly-ox(4)** after 24 h of incubation. The experiments were carried repeated twice.

Conclusion

The first water-soluble main-chain poly(phosphorodiamidate)s and also water-soluble poly(phosphate)s were prepared by a metal-free radical polyaddition strategy. The polymers were designed to have the same backbone except of the binding motive around the phosphorus center. Polymers carrying a pendant P-OH or a P-OCH_3 group were prepared, carrying either esters or amides along the backbone. The resulting hydrophilic polymers can further be adjusted with respect to hydrophilicity by oxidation with peroxide in the presence of boric acid. All polymers have been investigated regarding their hydrolytic stability and their toxicity. PPEs and PPDAs show different behavior in hydrolytic stability. PPEs degrade faster than PPDAs under basic conditions by a statistical cleavage of one of the ester linkages. They are rather stable under acidic conditions. PPDAs, in contrast, are acid-labile compounds allowing a precise adjustment of the backbone degradation profile of all polymers. The PPDA backbone is stable under basic conditions, but the pendant methyl group is selectively cleaved.

Hydrolytic degradable, biocompatible, watersoluble and oxidizable polymers which are nontoxic could be added to the interesting class of phosphorus containing polymers. Potentially fields of applications may be drug delivery by controlled release of side-chain modifications, tissue engineering by phosphate groups with inherent bone adhesion ability, or the generation of biodegradable scaffolds, which can be already degenerated by small variations of pH.

Experimental section

Chemicals. Phosphate buffered saline (BioPerformance Certified, pH 7.4; PBS buffer), 2,2'-(ethylenedioxy)diethanethiol 95 %, trimethylamine >99.5 %, AIBN 98 %, DMF (analytical grade), potassium chloride >99 %, sodium acetate >99 %, sodium hydroxide p.a., sodium chloride p.a., magnesium chloride >98 %, tris base >99.9 %, Phosphatase (Alkaline from bovine intestinal mucosa), and Lipase from Pseudomonas cepacia were purchased from Sigma Aldrich and used as received. Acetic acid glacial (analytical grade) was purchased from fisher chemical. Potassium hydrogen phthalate was purchased from Merck Millipore. H_2O_2 30 % was purchased from Roth. Phosphodiesterase I (E.C. 3.1.4.1) from *Crotalus adamanteus* venom was purchased from affymetrix.

Methods. Gel-permeation chromatography (GPC) measurements were carried out in DMF, with samples of the concentration of 2 g L^{-1}. Sample injection was performed by a 1260-ALS auto sampler (Waters) at 60 °C (DMF). The flow was 1 mL min^{-1}. In DMF (+ LiBr 1g/L), two GRAM 100 and one GRAM 1000 columns (PSS) with dimensions of 300 × 80 mm, 10 µm particle size and pore sizes of 10000, 1000 und 100 Å were employed. Detection was accomplished with a DRI Shodex RI 1260-RID detector (ERC) and UV-Vis 1260-VWD detector (Agilent). Calibration was achieved using poly(styrene) standards provided by Polymer Standards Service. Gel-permeation chromatography (GPC) measurements were carried out in H_2O, with samples of the concentration of 1 g L^{-1}. Sample injection was performed by a 1260-ALS auto sampler (Waters) at 25 °C (H_2O). The flow was 1 mL min^{-1}. In DMF (+ $NaNO_3$ 0.1g/L), Suprema Linear M column (PSS) with dimensions of 300 × 80 mm, 10 µm particle size was employed. Detection was accomplished with a DRI Shodex RI 101-RID detector (ERC) and UV/VIS Dual 2487-VWD detector (Agilent). Calibration was achieved using poly(ethylene oxide) standards provided by Polymer Standards Service.

^{1}H NMR, ^{13}C NMR, and ^{31}P NMR spectra were either recorded on a Bruker Avance 250 MHz or 300 MHz or 500 MHz or 700 MHz spectrometer (Details of several measurements by different spectrometers see below). The proton, carbon and phosphorous spectra were measured in $CDCl_3$, D2O and CD_2Cl_2 at 298.3K and the spectra were referenced as follows:

for the residual $CHCl_3$ at $\delta(^1H)$ = 7.26 ppm, CH_2Cl_2 at $\delta(^1H)$ = 5.28 ppm, H_2O (^1H) = 4.79 ppm, $CHCl_3$ $\delta(^{13}C$ triplett) = 77,0 ppm and triphenylphosphine (TPP) $\delta(^{31}P)$ = - 6.00 ppm.

^1H, ^{13}C,^{31}P NMR and ^1H DOSY experiments were recorded with a 5 mm BBI 1H/X z-gradient on the 700 MHz spectrometer with an Bruker Avance III system. For a ^1H NMR spectrum 64 transients were used with an 11 µs long 90° pulse and a 12600 Hz spectral width together with a recycling delay of 5 s. The ^1H NMR (700 MHz), ^{13}C NMR (176 MHz), and ^{31}P NMR (283 MHz) measurements were obtained with an ^1H powergate decoupling method using 30° degree flip angle, which had a 14,5 µs long 90° pulse for carbon and an 27,5 µs long 90° pulse for phosphor. Additionally carbon spectra were kept with a J-modulated spin-echo for ^{13}C-nuclei coupled to ^1H to determine number of attached protons with decoupling during acquisition. The spectral widths were 41660 Hz (236 ppm) for ^{13}C and 56818 Hz (200 ppm) for ^{31}P, both nuclei with a relaxation delay of 2s.

Monomers

Bis-(but-3-en-1-yl)-phosphate (1), bis-(but-3-en-1-yl)-methylphosphate (2), *N,N`*-Bis-(but-3-en-1-yl)-phosphorodiamidate (3), and *N,N`*-Bis-(but-3-en-1-yl)-methylphosphorodiamidate (4) were synthesized corresponding to the literature procedure by Steinmann et al (**Chapter 3.2.1**).

*Representative procedure for the thiol-ene bulk polymerization of monomer **1,2,4,** and **5***

Poly(1). Bis-(but-3-en-1-yl)-methylphosphate **1** (200.0 mg, 0.908 mmol, 1.0 eq), 2,2'-(Ethylenedioxy)diethanethiol (165.6 mg, 147.8 µl, 0.908 mmol, 1.0 eq) and AIBN (9.0 mg, 0.0545 mmol, 6 mol%) were placed in a glass Schlenk tube equipped with a magnetic stir bar under an argon atmosphere. After three freeze-pump-thaw cycles to degas the system, the reaction was carried out at a temperature of 65 °C for 16 h. **Poly(1-5)** was obtained as colorless viscous oil in quantitative yield. The following spectral properties were observed: ^1H NMR (500 MHz, 298 K, $CDCl_3$, δ/ ppm): 4.11 – 3.97 (m), 3.79 – 3.68 (m), 3.68 – 3.53 (m), 2.79 – 2.63 (m), 2.63 – 2.47 (m), 1.84 – 1.72 (m), 1.72 – 1.61 (m). $^{13}C\{H\}$ NMR (126 MHz, $CDCl_3$, δ/ ppm): 73.0, 71.2, 71.1, 70.4, 70.4, 70.4, 67.4, 67.3, 54.3, 54.3, 32.1, 32.1, 31.6, 31.6, 29.5, 29.4, 25.8, 24.4. $^{31}P\{H\}$ NMR (202 MHz, 298 K, $CDCl_3$, δ/ ppm): 0.30.

Poly(2). The reaction was carried out following the general procedure above with bis-(but-3-en-1-yl)-phosphate **2** (200.0 mg, 0.970 mmol, 1.0 eq) as monomer 1 and 2,2'-(Ethylenedioxy)diethanethiol (176.8 mg, 158.0 µl, 0.970 mmol, 1.0 eq) as monomer 2. The following spectral properties were observed: ^{1}H NMR (500 MHz, 298 K, DMSO, δ / ppm): 3.97 – 3.70 (m), 3.58 – 3.54 (m), 2.72 – 2.59 (m), 2.59 – 2.52 (m), 1.75 – 1.49 (m). ^{13}C{H} NMR (126 MHz, 298 K, $CDCl_3$, δ / ppm): 75.6, 75.5, 75.5, 75.0, 74.8, 74.7, 74.7, 74.6, 70.4, 70.2, 48.6, 47.3, 45.3, 45.1, 45.0, 44.8, 44.6, 44.5, 44.3, 36.4, 36.0, 35.9, 34.4, 34.3, 33.3, 30.8. ^{31}P{H} NMR (202 MHz, 298 K, DMSO, δ/ ppm): 0.30.

Poly(4). The reaction was carried out following the general procedure above *N,N`*-bis-(but-3-en-1-yl)-methylphosphorodiamidate **4** (100.0 mg, 0.458 mmol, 1.0 eq) as monomer 1 and 2,2'-(Ethylenedioxy)diethanethiol (83.5 mg, 74.6 µl, 0.458 mmol, 1.0 eq) as monomer 2. The following spectral properties were observed: ^{1}H NMR (500 MHz, 298 K, $CDCl_3$, δ/ ppm): 3.80 – 3.43 (m), 3.05 – 2.80 (m), 2.80 – 2.41 m), 1.79 – 1.44 (m). ^{13}C{H} NMR (126 MHz, $CDCl_3$, δ/ ppm): 71.2, 70.5, 51.9, 41.0, 32.3, 31.6, 31.2, 27.0. ^{31}P{H} NMR (202 MHz, 298 K, $CDCl_3$, δ/ ppm): 16.94.

Procedure for the thiol-ene solution polymerization of monomer 3 and 5

Poly(3). A dispersion of *N,N`*-Bis-(but-3-en-1-yl)-phosphorodiamidate **3** (50.0 mg, 0.245 mmol, 1.0 eq), 2,2'-(Ethylenedioxy)diethanethiol (45.0 mg, 40.0 µl, 0.245 mmol, 1.0 eq) in water (100µl) were placed in a glass Schlenk tube equipped with a magnetic stir bar under an argon atmosphere. The dispersion was treated with triethylamine (TEA; 20 mg) at 60 °C until the dispersion transformed to a solution (ca. 1 h). Afterwards AIBN (2.5 mg, 0.0147 mmol, 3.0 mol%) was added. The reaction was carried out at a temperature of 60 °C for 16 h. **Poly(3)** was obtained as colorless viscous oil in quantitative yield. The following spectral properties were observed: ^{1}H NMR (250 MHz, 298 K, D_2O, δ/ ppm): 3.83 – 3.53 (m), 3.08 – 2.83 (m), 2.83 – 2.68 (m), 2.68 – 2.49 (m), 1.86 – 1.41 (m). ^{13}C{H} NMR (75 MHz, D_2O, δ/ ppm): 133.0, 118.8, 69.5, 69.3, 46.6, 40.9, 39.0, 30.6, 30.4, 25.9, 25.7, 8.2. ^{31}P{H} NMR (121.5 MHz, 298 K, D_2O (acidic), δ/ ppm): 3.56. ^{31}P{H} NMR (121.5 MHz, 298 K, D_2O (basic), δ/ ppm): 14.45 (anion); 8.29, 8.11 (neutral); -0.91, -0.07 (cation).

Representative procedure for the oxidation of the thiol-ene polymers

The thioether polymer (1 eq.) was added to a solution of 30% H_2O_2 (10 equiv.) and boric acid (0.2 mol%) in either DMF or water (dependent of the solubility of the polymer). The solution was stirred at room temperature for 24 h. Afterwards the solution was freeze dried to observe pure product in quantitative yield. All oxidized polymers were characterized by ^{1}H NMR, ^{13}C{H} NMR, ^{31}P{H} NMR and by GPC (see Supp. Info.).

Poly-ox(1). ^{1}H NMR (300 MHz, 298 K, DMSO, δ/ ppm): 4.08 – 3.79 (m), 3.79 – 3.64 (m), 3.55 – 3.40 (m), 3.39 – 3.24 (m), 2.42 – 2.14 (m), 2.00 – 1.68 (m). ^{13}C{H} NMR (126 MHz, DMSO, δ / ppm): 70.1, 70.1, 69.9, 69.6, 67.6, 65.6, 64.5, 53.6, 53.5, 52.5, 51.7, 43.8, 42.5, 36.2, 34.8, 31.2, 29.2, 29.2, 28.5, 18.4. ^{31}P{H} NMR (121.5 MHz, 298 K, D_2O, δ/ ppm): 0.50.

Poly-ox(2). ^{1}H NMR (300 MHz, 298 K, D_2O, δ/ ppm): 4.23 – 4.03 (m), 4.03 – 3.84 (m), 3.84 – 3.72 (m), 3.72 – 3.58 (m), 3.53 – 3.36 (m), 3.36 – 3.18 (m), 2.01 – 1.66 (m). ^{13}C{H} NMR (126 MHz, DMSO, δ/ ppm): 69.9, 67.0, 67.0, 64.5, 54.5, 54.4, 53.3, 52.6, 36.2, 29.0, 28.9, 18.1. ^{31}P{H} NMR (121.5 MHz, 298 K, DMSO, δ/ ppm): 0.25, 0.10.

Poly-ox(4). ^{1}H NMR (300 MHz, 298 K, D_2O, δ/ ppm): 3.97 – 3.80 (m), 3.67 – 3.59 (m), 3.59 – 3.51 (m), 3.47 – 3.31 (m), 3.31 – 3.10 (m), 2.90 – 2.78 (m), 1.92 – 1.44 (m). ^{13}C{H} NMR (126 MHz, DMSO, δ/ ppm): 136.9, 116.5, 69.9, 64.5, 53.6, 52.5, 51.6, 36.4, 31.2, 30.6, 26.4, 19.1. ^{31}P{H} NMR (121.5 MHz, 298 K, DMSO, δ/ ppm): 17.58, 17.41. ^{31}P{H} NMR (121.5 MHz, 298 K, D_2O, δ/ ppm): 20.57.

Procedure for the degradation by pH

Poly-ox(1), Poly-ox(2), Poly(3), or **Poly-ox(4)** (6.0 mg) were dissolved into 0.6 ml deuterated buffer solution (pH = 1.0: 0.136 mM hydrogen chloride - potassium chloride solution, pH = 3.0: 0.088 mM hydrogen chloride - potassium hydrogen phthalate solution, pH = 5.0: 0.100 mM sodium acetate - acetic acid solution, pH = 7.0: 0.01 mM PBS buffer solution, pH = 9.0: 0.05 M Tris - hydrogen chloride solution with 49 mM magnesium chloride, pH = 13: 0.145 mM sodium hydroxide - potassium chloride solution). The mixtures were poured in NMR tubes and measured during the degradation.

The CellTiter 96® AQueous One Solution Cell Proliferation Assay

Hela cells (5x10^4 cells/well) were incubated for 4 h with Nanoparticles at 75 ug/mL in EMEM Medium (10% FBS, 1% Penistrep, 1% Glutamine). After the incubation time, the cells were washed with PBS and fresh medium was added. For Positive Control, 10% of DMSO was added in the culture well. Negative control was only cells in fresh medium. The cells were incubated overnight at 37°C, 5% CO2. In the next day, 20 uL of the CellTiter 96® AQueous One Solution Reagent was directly added to culture wells and incubated for 4h and then recording absorbance at 570nm with a 96-well plate reader. The quantity of formazan product as measured by the amount of 570nm absorbance is directly proportional to the number of living cells in culture.

Polymer Characterization of "Water-soluble and degradable polyphosphorodiamidates via radical polyaddition"

PDA functionalities introduce higher thermal stability and crystallinity when compared to the PE-based polymers. Hydroxyl groups and methoxy moieties affect thermal behavior, as well. The introduced polymers do not show melting points. Thioether and ethylene oxide groups make the material softer, similar to aliphatic hydrocarbons. To improve the flame retardant properties, thioether functionalities have been transformed to sulfones by oxidation. For comparison reasons, all synthesized polymers are structural analogues except for the binding motif of phosphorus. Properties such as crystallinity or thermal degradability have been modified as desired by changing the monomers or the side chain, or by oxidation.

Thermal properties. Phosphoesters are well-known for their flame retardant properties.[185] Nitrogen is used for improving flame retardant material properties, as well. Together, these materials can even show synergistic effects of P and N.[103] If the content is high enough of these elements, the charcoal residue is unusual high, leading to a reduction of pyrolysis-able gases.[104] Different (P)PEs and (P)PA polymers are already known.[186-187] However, examples of PPDAs are very rare.[102, 117-118] This work shows potential candidates which have these interesting properties.

Table 2: Thermal properties of polymers and oxidized polymers measured by DSC and TGA.

Polymer	T_g / °C	ΔC_p / $Jg^{-1}K^{-1}$	T_{on} / °C	$T_{50\%}$ / °C	Char yield / %
poly(1)	-50.6	0.572	209	256	19.5
poly-ox(1)	-17.63	0.621	188	313	25.2
poly(2)	-72.1	0.590	204	247	14.1
poly-ox(2)	-26.0	0.575	213	308	28.0
poly(3)	-9.08	0.413	284	327	22.6
poly(4)	-34.5	0.445	138	318	18.3
poly-ox(4)	-26.38	0.591	158	354	39.1

a = T_{on} was determined at a weight loss of 5 %

Table 2 exhibits the differential scanning calorimetry (DSC) values of polymers, including oxidized polymers. Furthermore, the thermogravimetric analysis (TGA) results are displayed in **Table 2** and Supplementary Info. It has been shown that the polymers are not able to crystallize or do not show melting points due to the soft system by using **5** as second

monomer and short alkyl chains. The polymers exhibit low glass transition temperatures (T_g) as expected for this soft system. However, after oxidation, the T_g's are significant increased. For both samples of PPEs by thiolene polymerization, the T_g is ca. 35 °C higher for the oxidized polymer. Here, the strong influence of the more rigid sulfone group is indicated. The polymers based on PDAs present continually higher T_g's when compared to the PPEs. The phosphoramidate groups can interact with other polymer chains more effectively due to the hydrogen atom connected to the nitrogen. However the difference of T_g's between the polymer and the oxidized counterpart is ca 10 °C less than for PPEs because the interactions between the chains are determined by strong interactions between the PDA groups and not by the introduced sulfone functionalities. **Poly(3-5)** displays already a high T_g of -9.1 °C, which can be explained by the additional hydroxyl functionality at the phosphorus atom. It is likely that the phosphoramidate unit and the hydroxyl group on the phosphorus are working synergistically.

A difference of $T_{50\%}$ from 40 to 50 °C between the polymer and its oxidized version can be investigated by TGA measurements. Both PPEs and the PPDAs show this effect. The PPEs present continuously lower degradation, about 50 °C below the PPDAs. In addition, the oxidized PPDA shows a very high charcoal residue of ca. 40 % and a degradation range starting already from ca. 100 °C to very high temperatures (ca. 400 °C). These properties indicate excellent flame retardant behavior. Applications in the context of flame retardant materials are promising for the future.

Conclusion

Oxidization increases the degradation and glass transition temperatures, as well as the charcoal residue. Due to high thermal stabilities and charcoal residues, possible applications of these polymers are as novel flame retardant materials.

Methods. The glass transition temperature was measured by differential scanning calorimetry (DSC) on a Mettler Toledo DSC 823 calorimeter. Three scanning cycles of heating–cooling were performed (in a N_2 atmosphere 30 mL min^{-1}) with a heating rate of 10 °C min^{-1}. Thermogravimetric analysis (TGA) measurements were performed on a Mettler-

Toledo 851 (Mettler-Toledo, USA) thermobalance with temperatures ranging from 35 °C to 600 °C at a heating rate of 10 °C min^{-1} under nitrogen flow (30 mL min^{-1}).

3.3.2 Polyphosphorodiamidates via Radical Polyaddition

Besides good water-solubility and degradation properties in **Chapter 3.3.1**, poly(phosphorodiamidate)s and poly(phosphate)s synthesized via thiol-ene polyaddition exhibit other interesting features. In thiol-ene polyadditions, a comonomer is required. By exchanging the comonomer, a far greater scope of possibilities is imaginable. 1,2-ethanedithiol (**1**) and 2,2'-(ethylenedioxy)diethanethiol (**2**) (chosen for improvement of water solubility) were introduced as monomers beside the phosphates or phosphorodiamidates, respectively. These are selected depending on the length of the unsaturated alkyl chain in order to have the same length of backbone in each case. Therefore, bis-(but-3-en-1-yl)-phenylphosphate (**3**), bis-(undec-10-en-1-yl)-phenylphosphate (**4**), bis-(oct-7-en-1-yl)-methylphosphate (**5**), bis-(undec-10-en-1-yl)-methylphosphate (**6**), *N*,*N*`-bis-(oct-7-en-1-yl)-methylphosphorodiamidate (**8**), and *N*,*N*`-bis-(undec-10-en-1-yl)-methylphosphorodiamidate (**9**) were chosen as appropriate amines or alcohols for the synthesis of phosphor-based monomers. The synthesis of PPEs and PPDAs were accomplished by thiol-ene polymerizations of monomers containing two double bonds as introduced in **Chapter 3.3.1.** Crystallinity and thermal degradability have been modified by changing the monomers, the side chain, or the comonomer. All synthesized polymers are introduced in **Figure 1**, and molecular weights and distributions are listed in **Table 1.**

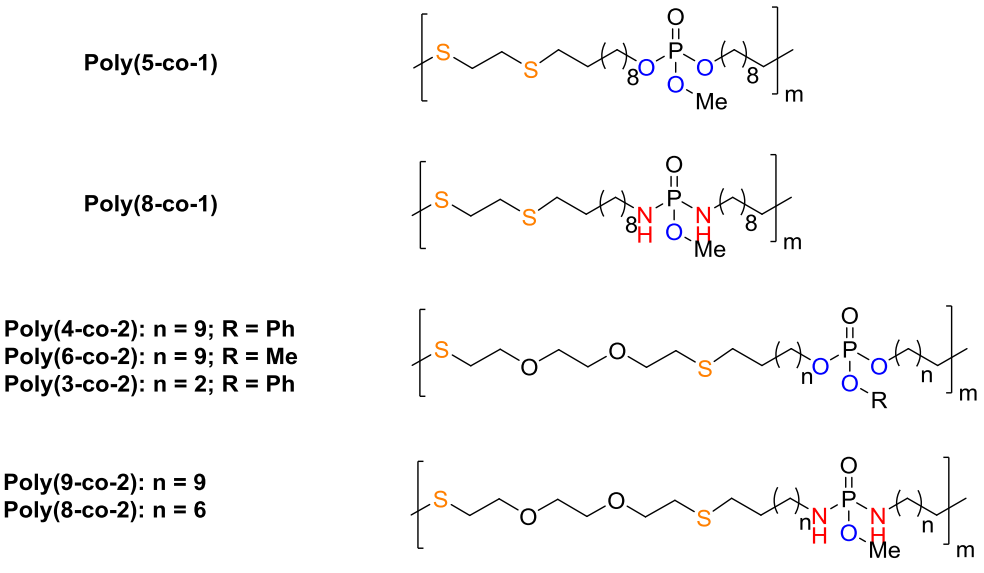

Figure 1: Synthesized PPEs and PPDAs via thiol-ene polyaddition.

Table 1: Molecular weight results for the thiol-ene polyaddition of phosphates and phosphorodiamidates polymers.

Polymer	M_{nGPC} (g/mol)	M_{wGPC} (g/mol)	M_{wNMR} (g/mol)	Đ
Poly(5-co-1)[b]	8,900	23,100	19,300	2.58
Poly(8-co-1)[c]	-	-	4,500	-
Poly(4-co-2)[a]	11,600	19,000	-	1.97
Poly(6-co-2)[a]	12,700	27,100	-	1.65
Poly(3-co-2)[a]	10,700	17,300	-	1.62
Poly(8-co-2)[c]	-	-	6,000	-
Poly(9-co-2)[c]	-	-	12,800	-

Conditions: a) Determined by GPC in THF vs. polystyrene standards measured by RI-detector; b) Determined by GPC in DMF with polystyrene standard measured by RI-detector, c) Determined by ^{1}H DOSY NMR.

Poly(5-co-1) and **Poly(8-co-1)** have been synthesized because they exhibit the same number of atoms within the backbone as PPE **poly-H(10) (poly(10))** and PPDA **poly-H(15) (poly(15))** synthesized by ADMET in **Chapter 3.2.1**. The only difference is that two carbon atoms are replaced by two sulfur atoms. Thermal behavior between those similar polymers is discussed later.

Table 1 indicates generally high molecular weights and PDIs around two as expected. The same problem with PPDAs via thiol-ene polyaddition occurred that no reasonable GPC measurements have been successfully accomplished. Therefore ^{1}H DOSY measurements can be used after calibration to determine molecular weights as explained in **Chapter 3.2.1**.

Thermal properties.

The polymers with comonomer **2** and longer alkyl-chain in the phosphorus-containing monomer are partly crystalline and exhibit T_m's. In contrast to the polymers with the same comonomer **2** introduced in **Chapter 3.3.1**. **Poly(9-co-2)** shows already a high T_m with 57 °C. **poly(8-co-2)** exhibit two melting points at ca. 9 °C and 44 °C. In both cases the T_g's are similar to the polymers in **Chapter 3.3.1**.

Comonomer **1** and either monomer **5** or **8** leads to almost structural analogous of **poly-H(10) (poly(10))** or **poly-H(15) (poly(15))** in **Chapter 3.2.1**. The only difference is that the alkyl-

chain with double bond (**poly(10) + poly(15)**) or just alkyl-chain (**poly-H(10) + poly-H(15)**) is replaced with two thioether functionalities in **poly(5-co-1)** (PPE) and **poly(8-co-1)** (PPDA). Interestingly, **poly(5-co-1)** shows similar behavior regarding T_m with **poly(10)** as **poly-H(10).** The T_m's are almost identical, but the enthalpy is half for **poly(10)** and therefore rather similar to the enthalpy of **poly-H(10).** This confirms the comparison of **poly-H(15)** and **poly(9-co-2)**. Here, both the enthalpy and T_m values are similar. The T_m of **poly(9-co-2)** is almost as high as the T_m of **poly-H(15)**.

Table 2: Thermal properties of polymers measured by DSC and TGA.

Polymer	T_g / °C	ΔC_p / $Jg^{-1}K^{-1}$	T_m / °C	ΔH_m / Jg^{-1}	$T_{50\%}$ / °C	Char yield / %
Poly(5-co-1)	-	-	15.8	-50.1	312	18.3
Poly(8-co-1)	-	-	69.2	-35.5	387	18.4
Poly(4-co-2)	-49.1	0.443	-15.7	-28.9	301	12.8
Poly(6-co-2)	-62.0	0.351	-16.5	-33.3	301	15.4
Poly(3-co-2)	-57.0	0.416	-	-	248	22.0
Poly(8-co-2)	-63.9	0.261	8.7/44.6	-13.1/-24.9	372	18.3
Poly(9-co-2)	-49.4	0.373	57.3	-43.1	368	15.6

a = T_{on} was determined at a weight loss of 5 %

The comparison of the degradation temperature ($T_{50\%}$) and the charcoal residue are as high as the polymers with the shorter alkyl-chain in **Chapter 3.3.1**. The $T_{50\%}$'s are around 300 °C for PPEs and around 350 °C for the PPDAs. The charcoal residue is ca. 20 % in all cases.

TGA data reveals for both PPEs and PPDAs with comonomer **1** similar degradation temperatures and charcoal residues between 18 and 30 %. The thermal properties might be improved by oxidation.

Conclusion

The use of a more rigid comonomer resulted in polymers with already high T_m's as the hydrogenated ADMET polymers in **Chapter 3.2.1.** However, as known from **Chapter 3.3.1**, the oxidation of thioether groups increases the degradation temperature, the T_g's, the charcoal residue, and especially the T_m's. Therefore, T_m's of over 100 °C are reasonable for the oxidized PPDA. Many applications are imaginable for a polymer with that high of a T_m as a biocompatible and biodegradable alternative for commonly-used plastics.

Experimental Section

Chemicals. AIBN 98 %, 1,2-Ethanedithiol 98%, and 2,2'-(Ethylenedioxy)diethanethiol 95% were purchased from Sigma Aldrich and used as received.

Methods see Chapter 3.1.1.

Monomers

1,2-Ethanedithiol (**1**) and 2,2'-(Ethylenedioxy)diethanethiol (**2**) as comonomers.

Bis-(oct-7-en-1-yl)-methylphosphate (**5**), bis-(undec-10-en-1-yl)-methylphosphate (**6**), *N,N`*-bis-(oct-7-en-1-yl)-phosphorodiamidate (**7**), *N,N`*-bis-(oct-7-en-1-yl)-methylphosphoro-diamidate (**8**), and *N,N`*-bis-(undec-10-en-1-yl)-methylphosphorodiamidate (**9**) were synthesized as described in **Chapter 3.2.1**.

Bis-(but-3-en-1-yl) phenylphosphate 3 was synthesized as reported earlier.[153] **3** was obtained as a clear oil (yield: 70 %; Rf: 0.3 (CH_2Cl_2)).

^{1}H NMR (250 MHz, $CDCl_3$, δ / ppm): 7.40 – 7.28 (t, J = 7.8 Hz, 2H), 7.25 – 7.10 (dd, J = 13.7, 7.2 Hz, 3H), 5.92 – 5.62 (td, J = 17.0, 6.7 Hz, 2H), 5.22 – 4.99 (m, 4H), 4.29 – 4.05 (q, J = 7.1 Hz, 4H), 2.56 – 2.32 (q, J = 6.7 Hz, 4H). ^{13}C NMR (176 MHz, $CDCl_3$, δ / ppm): 150.7, 133.1, 129.7, 125.1, 120.0, 117.9, 67.5, 34.6, 15.3. ^{31}P NMR (283 MHz, $CDCl_3$, δ / ppm): -6.40. ESI-MS m/z 305.07 $[M+Na]^+$, 587.18.30 $[2M+Na]^+$ (Calculated for $C_{14}H_{19}O_4P$: 282.10).

Bis-(undec-10-en-1-yl) phenylphosphate 4 was synthesized as reported earlier.[153] **4** was obtained as a clear oil (yield: 80 %; Rf: 0.5 (CH_2Cl_2)).

^{1}H NMR (250 MHz, $CDCl_3$, δ / ppm): 7.38 – 7.28 (m, 2H), 7.25 – 7.11 (m, 3H), 5.95 – 5.68 (td, J = 16.9, 6.7 Hz, 2H), 5.07 – 4.86 (m, 4H), 4.22 – 4.03 (q, J = 7.0 Hz, 4H), 2.14 – 1.92 (q, J = 6.8 Hz, 4H), 1.79 – 1.56 (t, J = 7.0 Hz, 5H), 1.48 – 1.12 (m, 25H). ^{13}C NMR (176 MHz, $CDCl_3$, δ / ppm): 151.0, 139.3, 129.8, 125.0, 120.1, 114.3, 68.7, 33.9, 30.4, 29.5, 29.0, 25.5. ^{31}P NMR (283 MHz, $CDCl_3$, δ / ppm): -6.11. ESI-MS m/z 501.33 $[M+Na]^+$, 979.67 $[2M+Na]^+$, 1458.00 $[3M+Na]^+$ (Calculated for $C_{28}H_{47}O_4P$: 478.32).

Representative procedure for the thiol-ene bulk polymerization

Poly(5-co-1). Bis-(oct-7-en-1-yl)-methylphosphate (**9**) (100.0 mg, 0.301 mmol, 1.0 eq), 1,2-ethanedithiol (**1**) (28.3 mg, 25.2 µl, 0.301 mmol, 1.0 eq) and AIBN (3.0 mg, 0.0181 mmol, 6 mol%) were placed in a glass Schlenk tube equipped with a magnetic stir bar under an argon atmosphere. After three freeze-pump-thaw cycles to degas the system, the reaction was carried out at a temperature of 65 °C for 16 h. **Poly (9-co-1)** was obtained as yellowish viscous oil in quantitative yield. ^{1}H NMR (500 MHz, 298 K, $CDCl_3$, δ/ ppm): 4.10 – 3.91 (m), 3.84 – 3.66 (m), 2.77 – 2.61 (m), 2.59 – 2.44 (m), 1.72 – 1.62 (m), 1.62 – 1.49 (m), 1.44 – 1.15 (m). ^{13}C NMR (126 MHz, 298 K, $CDCl_3$, δ/ ppm): 68.0, 67.9, 54.2, 32.4, 32.3, 30.4, 30.4, 30.4, 30.3, 29.8, 29.3, 29.2, 29.2, 29.2, 28.9, 28.9, 25.5, 25.5. ^{31}P NMR (202 MHz, 298 K, $CDCl_3$, δ/ ppm): 0.37.

Poly(8-co-1). The reaction was carried out following the general procedure above with *N,N`*-bis-(oct-7-en-1-yl)-methylphosphorodiamidate (**14**) (200.0 mg, 0.605 mmol, 1.0 eq) as monomer 1 and 1,2-Ethandithiol (**1**) (57.0 mg, 50.8 µl, 0.605 mmol, 1.0 eq) as monomer 2. The following spectral properties were observed: ^{1}H NMR (300 MHz, 298 K, $CDCl_3$, δ/ ppm): 5.90 – 5.70 (m), 5.17 – 4.80 (m), 3.95 – 3.48 (m), 3.07 – 2.81 (m), 2.81 – 2.64 (m), 2.64 – 2.19 (m), 1.89 – 0.98 (m). ^{13}C NMR (126 MHz, 298 K, $CDCl_3$, δ/ ppm): 138.94, 138.76, 132.12, 132.04, 128.54, 128.44, 114.44, 114.32, 53.47, 53.42, 51.73, 51.69, 41.41, 41.20, 41.18, 39.67, 33.73, 33.68, 33.65, 32.20, 32.10, 32.03, 31.98, 31.92, 31.53, 29.75, 29.69, 29.66, 29.19, 28.87, 28.84, 28.80, 28.75, 28.71, 28.68, 27.63, 26.70, 26.58, 25.17. ^{31}P NMR (202 MHz, 298 K, $CDCl_3$, δ/ ppm): 16.88 (m), 14.95 -14.81 (m), 0.54 - 0.35 (m).

Poly(4-co-2). The reaction was carried out following the general procedure above with bis-(undec-10-en-1-yl)-phenylphosphate (**4)** (200.0 mg, 0.418 mmol, 1.0 eq) as monomer 1 and 2,2'-(ethylenedioxy)diethanethiol (**2**) (76.2 mg, 68.0 µl, 0.418 mmol, 1.0 eq) as monomer 2. The following spectral properties were observed: ^{1}H NMR (500 MHz, 298 K, $CDCl_3$, δ/ ppm): 7.38 – 7.28 (m), 7.24 – 7.08 (m), 4.22 – 4.02 (m), 3.80 – 3.46 m), 2.78 – 2.61 (m), 2.61 – 2.43 (m), 1.78 – 1.62 (m), 1.62 – 1.46 (m), 1.46 – 1.08 (m). ^{13}C NMR (126 MHz, $CDCl_3$, δ/ ppm): 151.0, 151.0, 129.8, 125.0, 120.1, 120.1, 71.2, 70.4, 68.7, 68.7, 33.9, 32.8, 31.6, 30.4, 30.3, 30.0, 29.6, 29.6, 29.6, 29.6, 29.5, 29.4, 29.2, 29.2, 29.0, 29.0, 25.5. ^{31}P NMR (202 MHz, 298 K, $CDCl_3$, δ/ ppm): -6.12.

Poly(6-co-2). The reaction was carried out following the general procedure above with bis-(undec-10-en-1-yl)-methylphosphate (**10)** (200.0 mg, 0.480 mmol, 1.0 eq) as monomer 1 and 2,2′-(ethylenedioxy)diethanethiol (**2**) (87.6 mg, 78.2 µl, 0.480 mmol, 1.0 eq) as monomer 2. The following spectral properties were observed: ^{1}H NMR (500 MHz, 298 K, $CDCl_3$, δ/ ppm): 4.07 – 3.94 (m), 3.81 – 3.69 (m), 3.69 – 3.54 (m), 2.79 – 2.61 (m), 2.61 – 2.43 (m), 1.76 – 1.61 (m), 1.61 – 1.46 (m), 1.46 – 1.00 (m). ^{13}C NMR (126 MHz, $CDCl_3$, δ/ ppm): 139.3, 114.3, 71.2, 70.4, 68.0, 68.0, 54.2, 54.2, 33.9, 32.8, 31.6, 30.5, 30.4, 30.3, 30.3, 30.0, 29.8, 29.7, 29.6, 29.6, 29.5, 29.4, 29.3, 29.3, 29.2, 29.0, 29.0, 25.6, 25.5. ^{31}P NMR (202 MHz, 298 K, $CDCl_3$, δ/ ppm): 0.38.

Poly(3-co-2). The reaction was carried out following the general procedure above with bis-(but-3-en-1-yl)-phenylphosphate (**3)** (200.0 mg, 0.709 mmol, 1.0 eq) as monomer 1 and 2,2′-(ethylenedioxy)diethanethiol (**2**) (129.2 mg, 115.3 µl, 0.709 mmol, 1.0 eq) as monomer 2. The following spectral properties were observed: ^{1}H NMR (500 MHz, 298 K, $CDCl_3$, δ/ ppm): 7.40 – 7.29 (m), 7.23 – 7.08 (m), 4.25 – 4.04 (m), 3.75 – 3.44 (m), 2.80 – 2.59 (m), 2.60 – 2.42 (m), 1.87 – 1.71 (m), 1.71 – 1.55 (m). ^{13}C NMR (126 MHz, 298 K, $CDCl_3$, δ/ ppm): 150.9, 150.8, 129.9, 129.9, 125.2, 120.1, 120.1, 77.4, 77.4, 77.2, 76.9, 71.1, 70.4, 70.4, 68.1, 68.1, 32.1, 31.6, 31.6, 29.4, 29.4, 27. ^{31}P NMR (202 MHz, 298 K, $CDCl_3$, δ/ ppm): -6.19.

Poly(9-co-2). The reaction was carried out following the general procedure above *N,N`*-bis-(undec-10-en-1-yl)-methylphosphorodiamidate (**15)** (100.0 mg, 0.241 mmol, 1.0 eq) as monomer 1 and 2,2′-(ethylenedioxy)diethanethiol (**2**) (44.0 mg, 39,3 µl, 0.241 mmol, 1.0 eq) as monomer 2. The following spectral properties were observed: ^{1}H NMR (300 MHz, 298 K, $CDCl_3$, δ/ ppm): 3.90 – 3.43 (m), 3.07 – 2.79 (m), 2.80 – 2.62 (m), 2.62 – 2.48 (m), 1.67 – 1.42 (m, 8H), 1.42 – 1.14 (m). ^{13}C NMR (176 MHz, $CDCl_3$, δ/ ppm): 71.1, 70.3, 51.7, 51.7, 41.2, 32.6, 32.1, 32.0, 31.4, 29.8, 29.6, 29.5, 29.5, 29.3, 29.3, 28.9, 26.8. ^{31}P NMR (202 MHz, 298 K, $CDCl_3$, δ/ ppm): 16.97 (m), 0.59 – 0.38 (m).

Poly(7-co-2). The reaction was carried out following the general procedure above *N,N`*-bis-(oct-7-en-1-yl)-methylphosphorodiamidate (**12)** (200.0 mg, 0.605 mmol, 1.0 eq) as monomer 1 and 2,2′-(ethylenedioxy)diethanethiol (**2**) (110.3 mg, 98.5 µl, 0.605 mmol, 1.0 eq) as monomer 2. The following spectral properties were observed: ^{1}H NMR (250 MHz, 298 K,

$CDCl_3$, δ/ ppm): 3.84 – 3.43 (m), 3.03 – 2.72 (m), 2.73 – 2.56 (m), 2.56 – 2.37 (m), 1.61 – 1.37 (m), 1.37 – 0.99 (m). ^{13}C NMR (126 MHz, $CDCl_3$, δ/ ppm): 72.9, 71.3, 71.1, 70.5, 70.4, 70.3, 70.3, 70.3, 69.7, 41.4, 41.2, 39.7, 32.6, 32.6, 32.1, 32.0, 31.5, 31.4, 29.9, 29.8, 29.8, 29.7, 29.6, 29.5, 29.5, 29.4, 29.3, 29.3, 28.9, 28.9, 27.7, 26.9, 26.8, 26.8, 24.3. ^{31}P NMR (202 MHz, 298 K, $CDCl_3$, δ/ ppm): 17.01 (m), 14.96-14.83 (m), 2.00 (m), 0.59-0.40 (m), 9.40 (m).

Supporting Information for

Water-soluble and degradable polyphosphorodiamidates via radical polyaddition

*Mark Steinmann, Frederik R. Wurm**

Max Planck Institut für Polymerforschung, Ackermannweg 10, 55128 Mainz, Germany.

Contact address: wurm@mpip-mainz.mpg.de

GPC

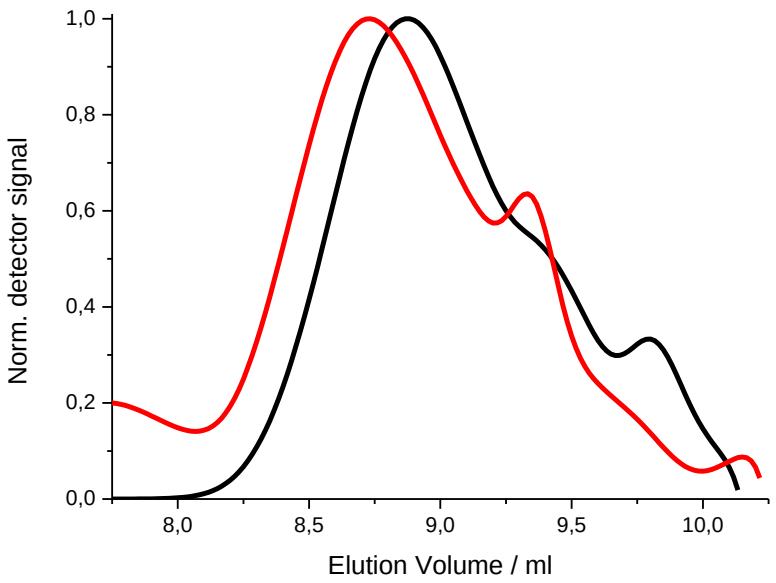

Figure S1: GPC-elugram of polymer **poly(1)** (M_n = 1,500 g·mol^{-1}; black curve) and **poly-ox(1)** (M_n = 2,200 g·mol^{-1}; red curve) vs. polystyrene standards in DMF measured by RI-detector.

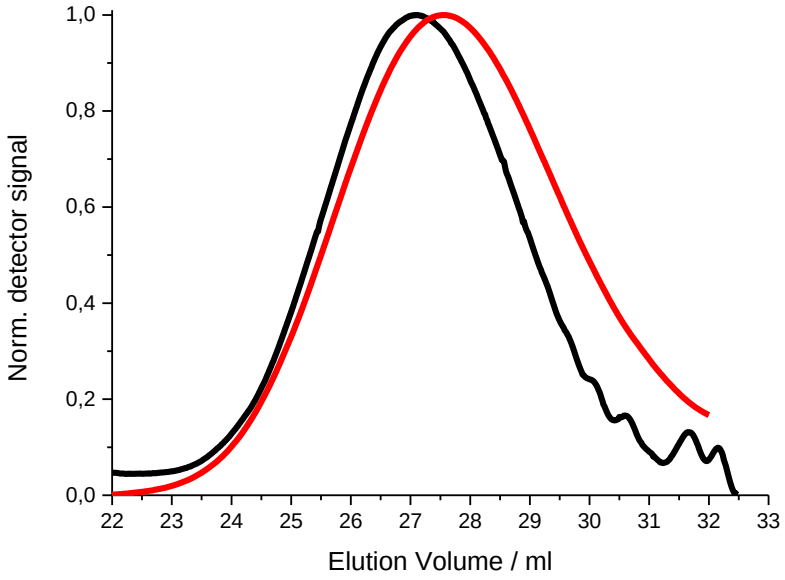

Figure S2: GPC-elugram of polymer **poly(2)** (M_n = 6,500 g·mol^{-1}; black curve) and **poly-ox(2)** (M_n = 6,100 g·mol^{-1}; red curve) vs. PEG standards in H_2O measured by RI-detector.

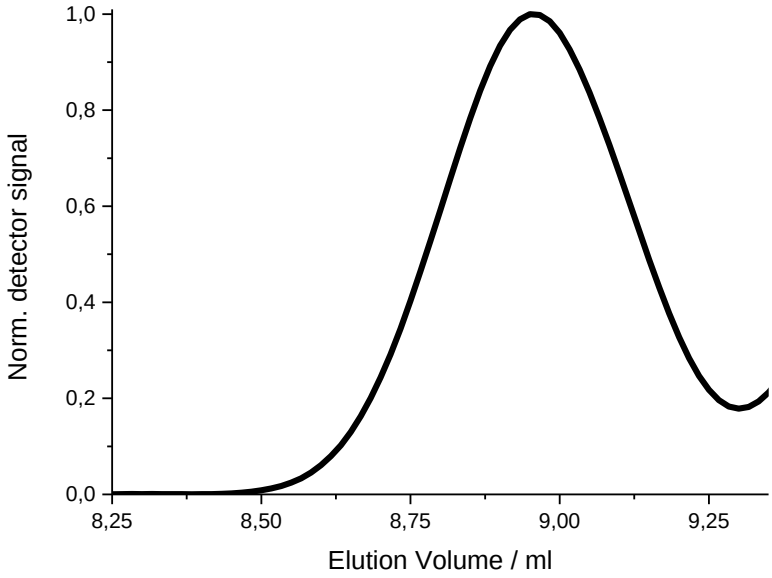

Figure S3: GPC-elugram of polymer **poly(3)** (M_n = 1,700 g·mol^{-1}) vs. PEG standards in H_2O measured by RI-detector.

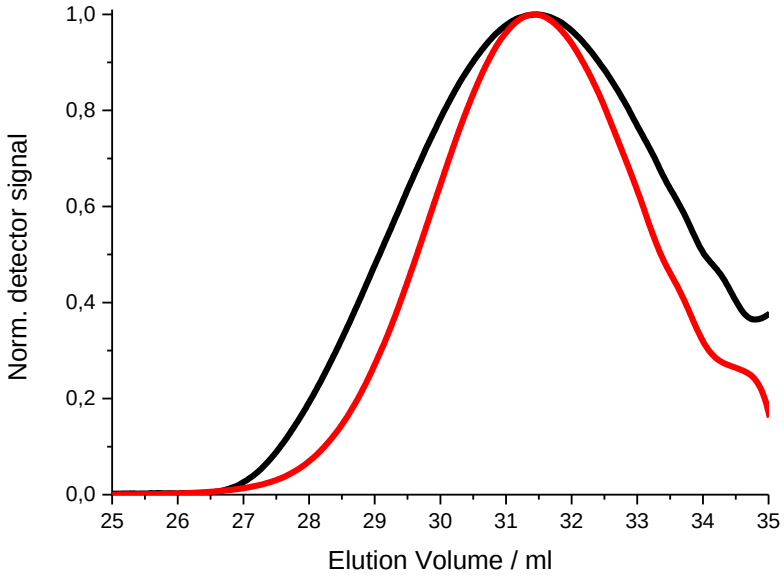

Figure S4: GPC-elugram of polymer **poly(4)** (M_n = 2,900 g·mol^{-1}; black curve) and **poly-ox(4)** (M_n = 3,000 g·mol^{-1}; red curve) vs. polystyrene standards in DMF measured by RI-detector.

Degradation

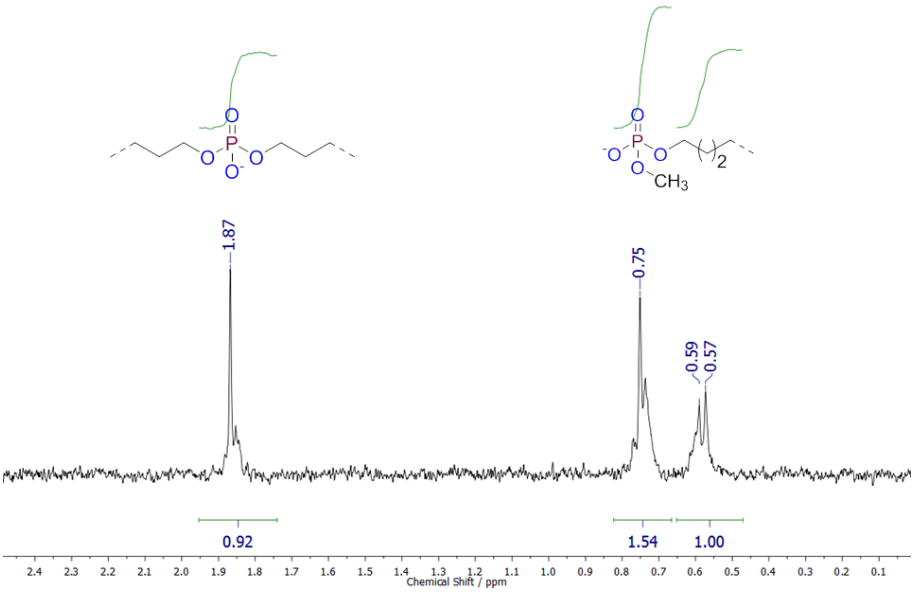

Figure S6: $^{31}P\{H\}$ NMR example of uncontrolled cleavage of phosphotriester to phosphodiester by degradation of the side-chain (1.87 ppm) or main-chain (0.75 ppm) of **poly-ox(2)** at pH = 13.0 after 7 days (121.5 MHz, 298 K, D_2O).

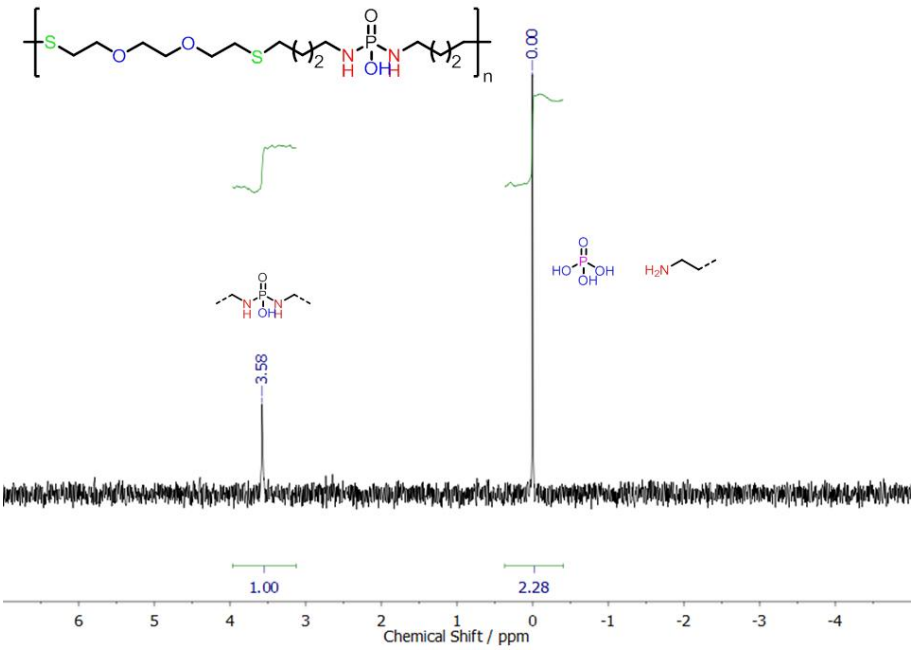

Figure S7: $^{31}P\{H\}$ NMR example of controlled degradation of polymer main-chain of **poly(3)** at pH = 3.0 after 16 days (121.5 MHz, 298 K, D_2O).

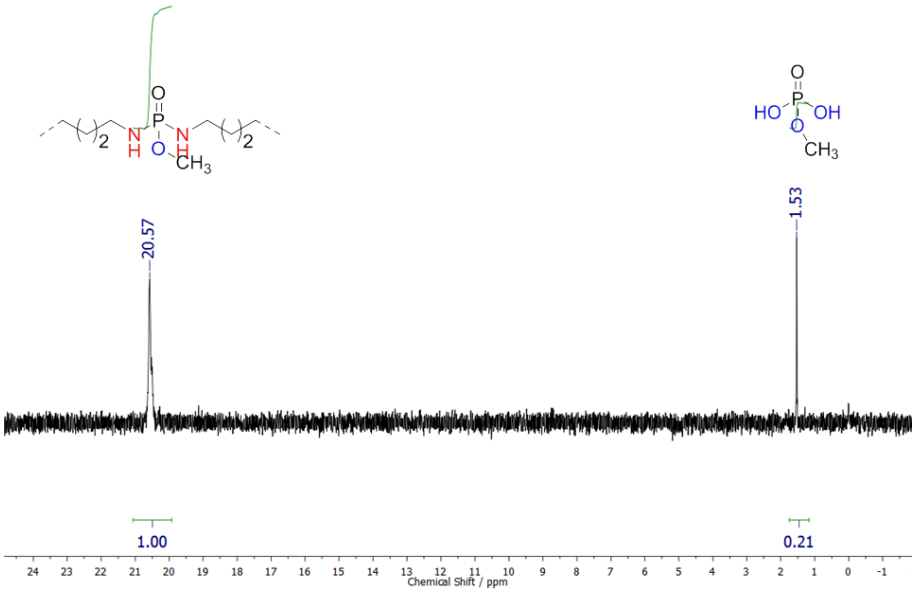

Figure S8: $^{31}P\{H\}$ NMR example of controlled degradation of polymer main-chain of **poly-ox(4)** at pH = 3.0 after 24 days (121.5 MHz, 298 K, D_2O).

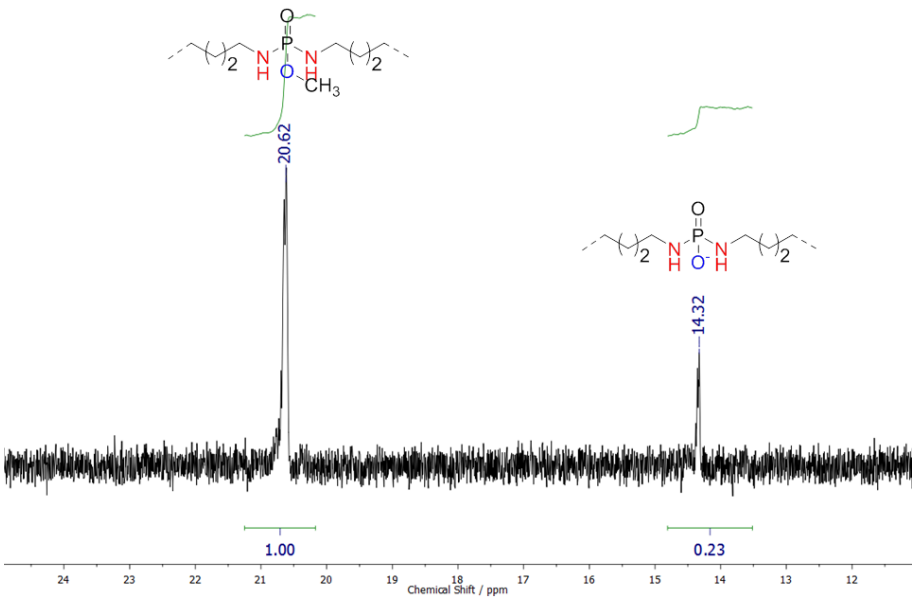

Figure S9: $^{31}P\{H\}$ NMR example of controlled degradation of polymer side-chain of **poly-ox(4)** at pH = 13.0 after 18 days (121.5 MHz, 298 K, D_2O).

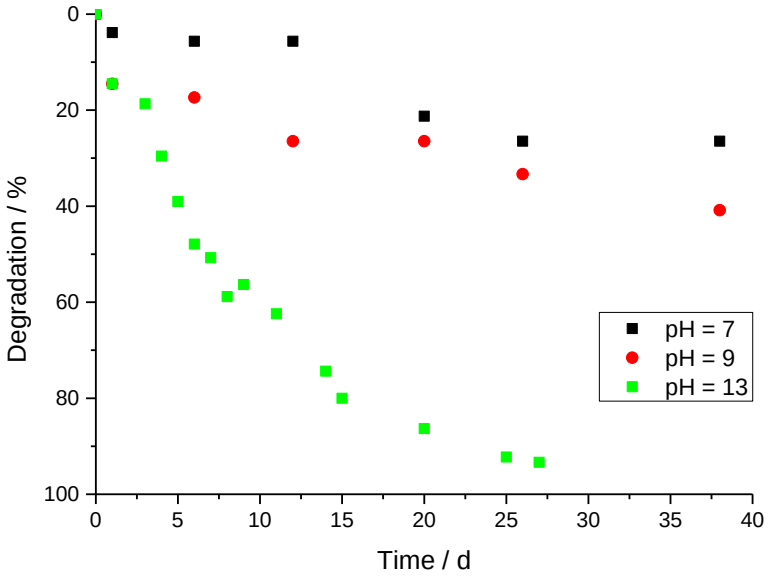

Figure S10: Degradation monitored by $^{31}P\{H\}$ NMR**:** Uncontrolled cleavage of phosphotriester to phosphodiester by degradation of the side-chain or main-chain of **poly-ox(2)** at different pH values. The ratio of decreasing ^{31}P NMR signal of **poly-ox(2)** and increasing signal of degradation product is plotted (121.5 MHz, 298 K, D_2O).

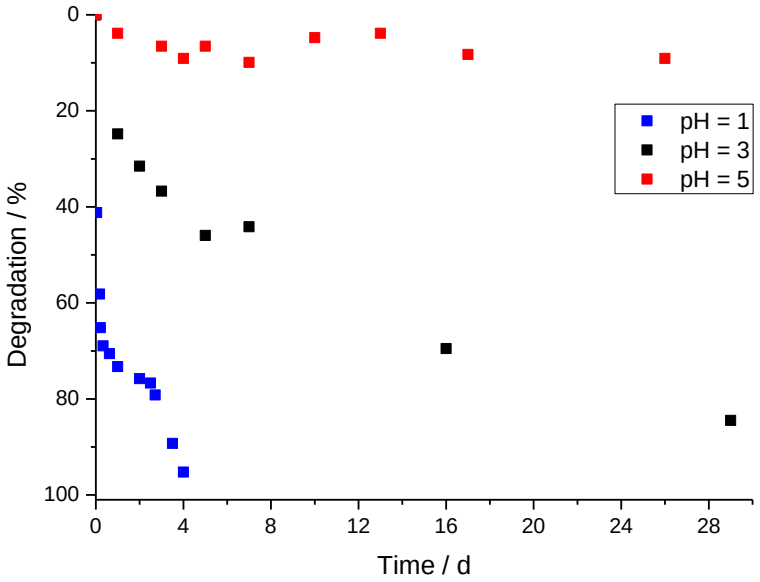

Figure S11: Degradation monitored by $^{31}P\{H\}$ NMR**:** Controlled degradation of phosphorodiamidate linkages as degradation of the polymer main-chain of **poly(3)** at different pH values (121.5 MHz, 298 K, D_2O).

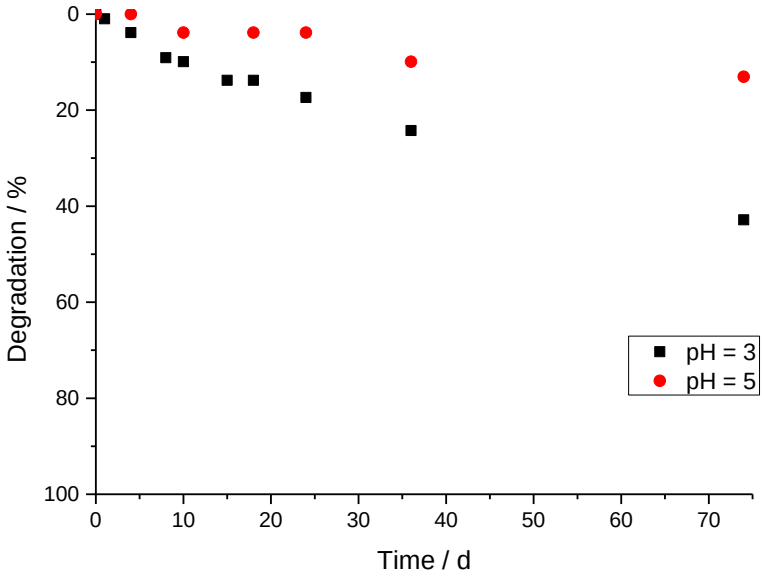

Figure S12: Degradation monitored by $^{31}P\{H\}$ NMR**:** Controlled degradation of phosphorodiamidate linkages as degradation of the polymer main-chain of **poly-ox(4)** at different pH values (121.5 MHz, 298 K, D_2O).

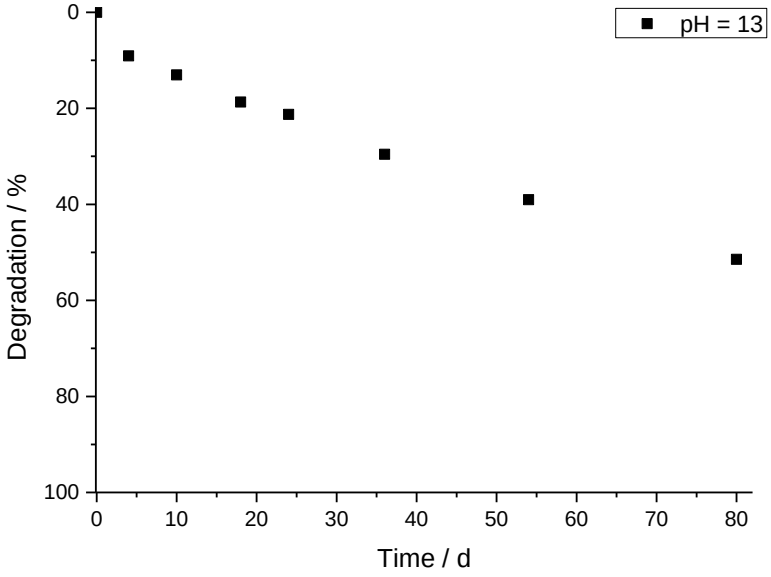

Figure S13: Degradation monitored by $^{31}P\{H\}$ NMR**:** Controlled degradation of polymer methyl side-chain of **poly-ox(4)** at pH = 13 (121.5 MHz, 298 K, D_2O).

NMR
Polymers

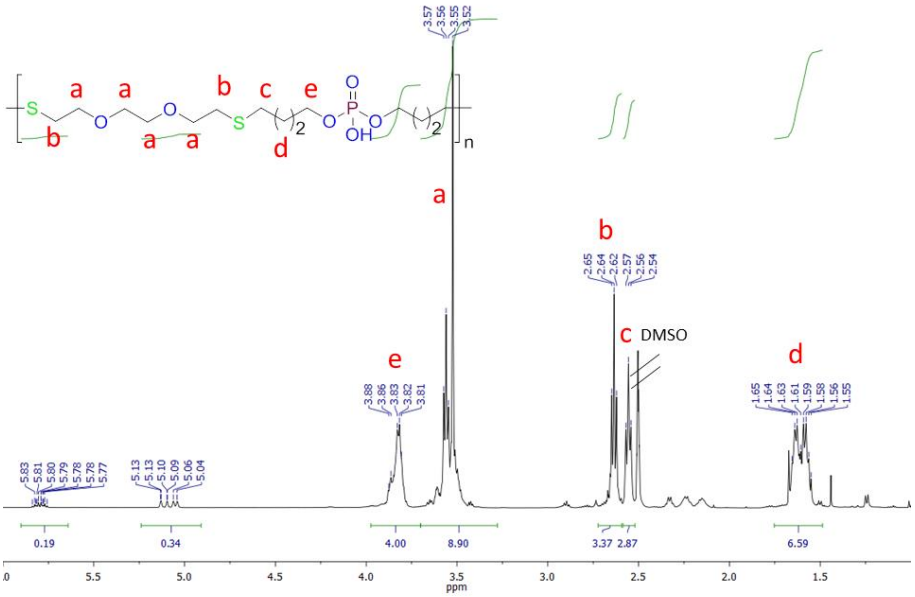

Figure S14: ^{1}H NMR of **poly(1)** (500 MHz, 298 K, DMSO).

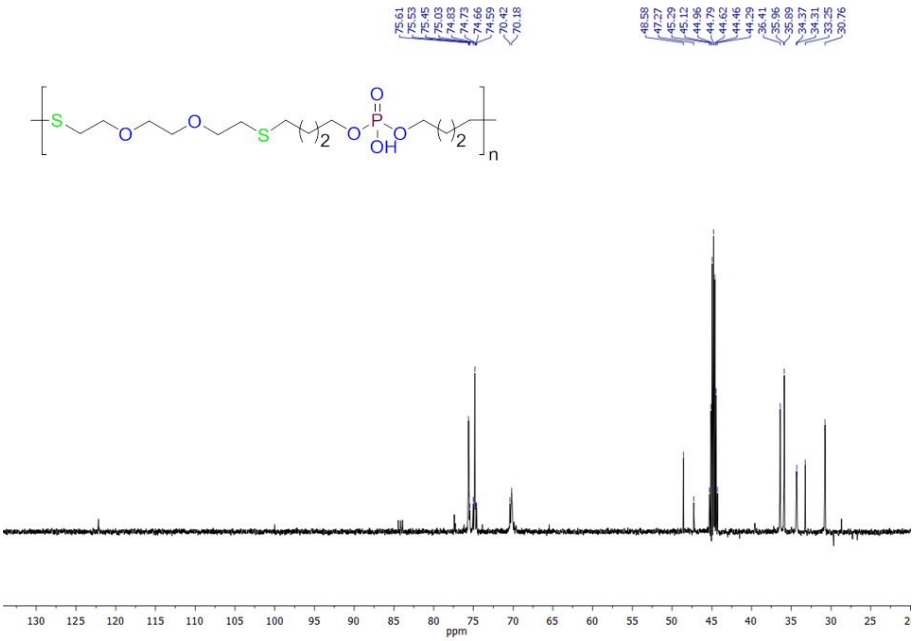

Figure S15: ^{13}C{H} NMR of **poly(1)** (126 MHz, 298 K, DMSO).

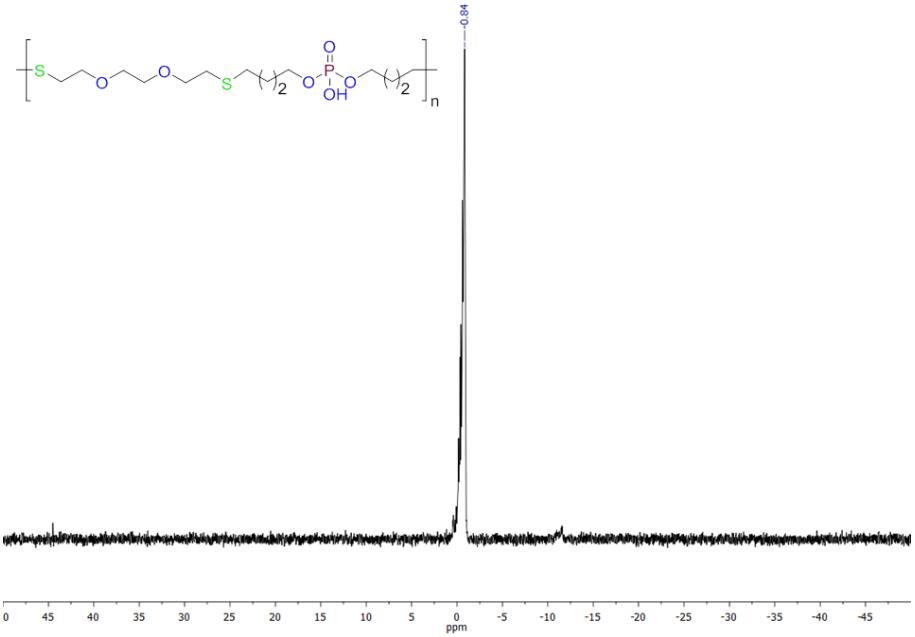

Figure S16: $^{31}P\{H\}$ NMR of **poly(1)** (202 MHz, 298 K, DMSO).

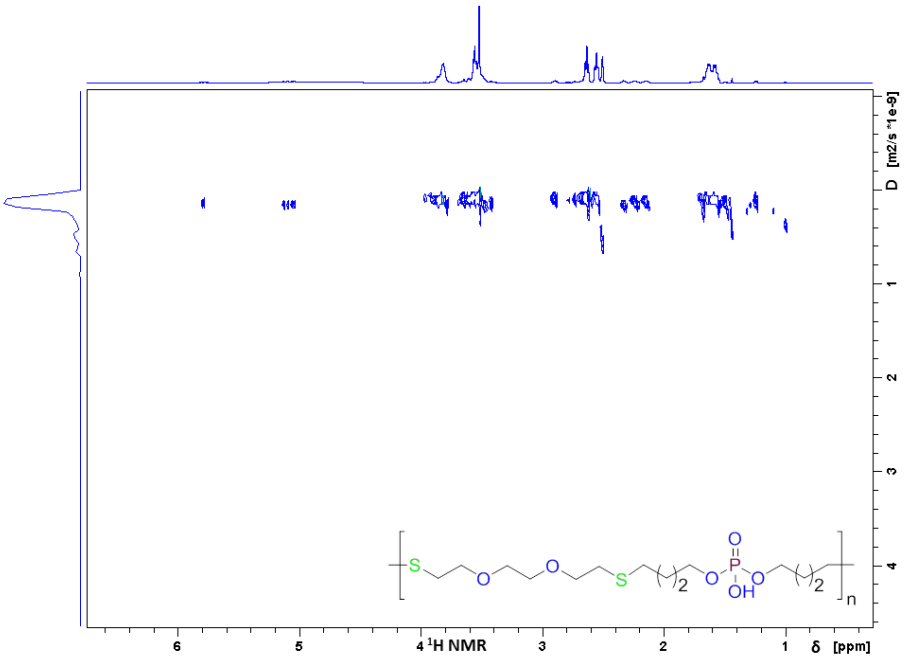

Figure S17: ^{1}H DOSY of **poly(1)** (500 MHz, 298 K, $CDCl_3$).

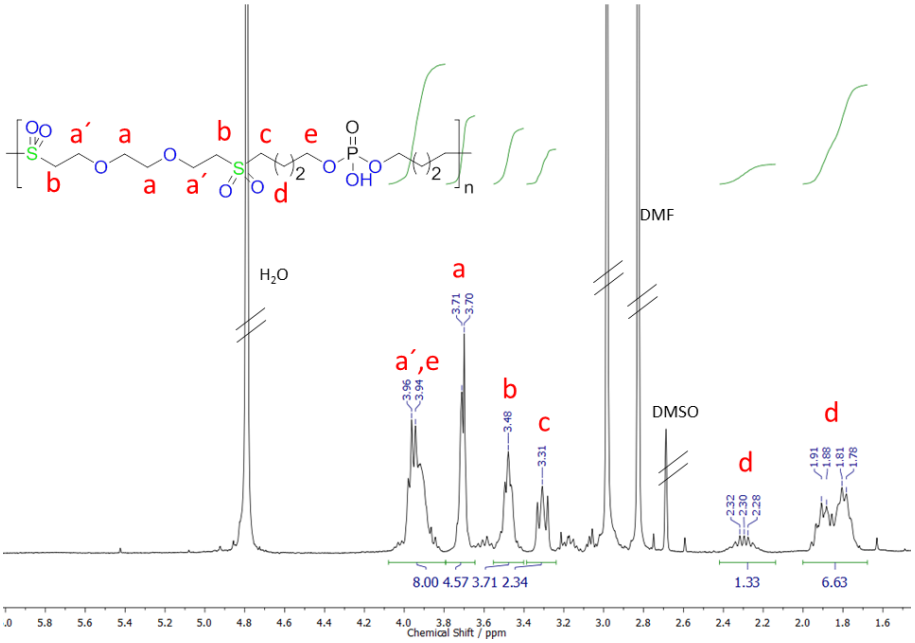

Figure S18: ^{1}H NMR of **poly-ox(1)** (300 MHz, 298 K, DMSO).

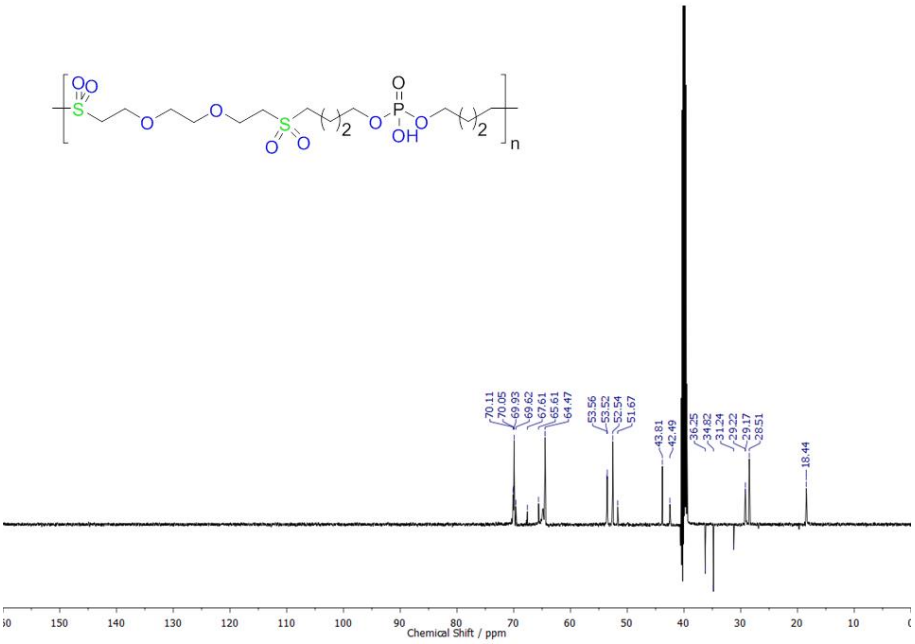

Figure S19: ^{13}C{H} NMR of **poly-ox(1)** (126 MHz, 298 K, DMSO).

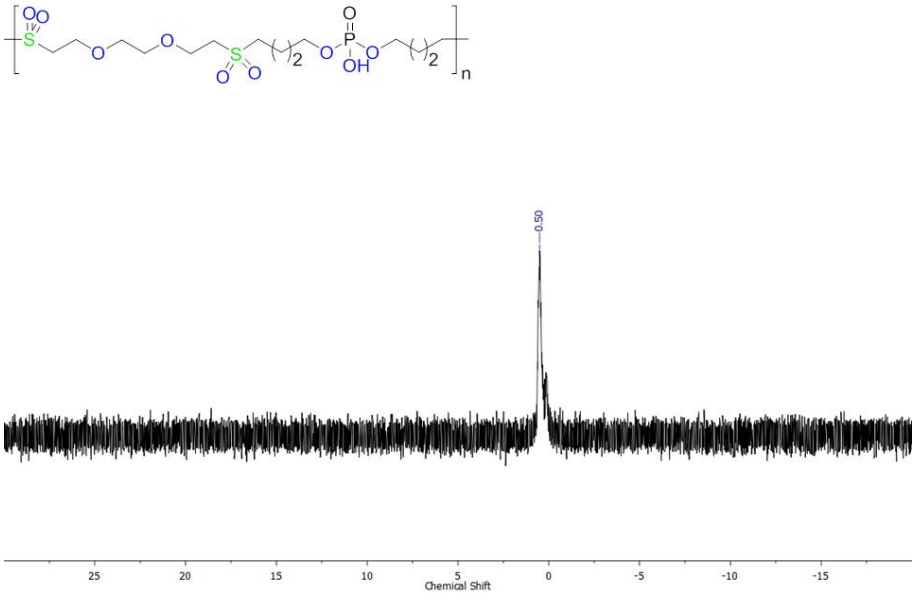

Figure S20: $^{31}P\{H\}$ NMR of **poly-ox(1)** (121.5 MHz, 298 K, D_2O).

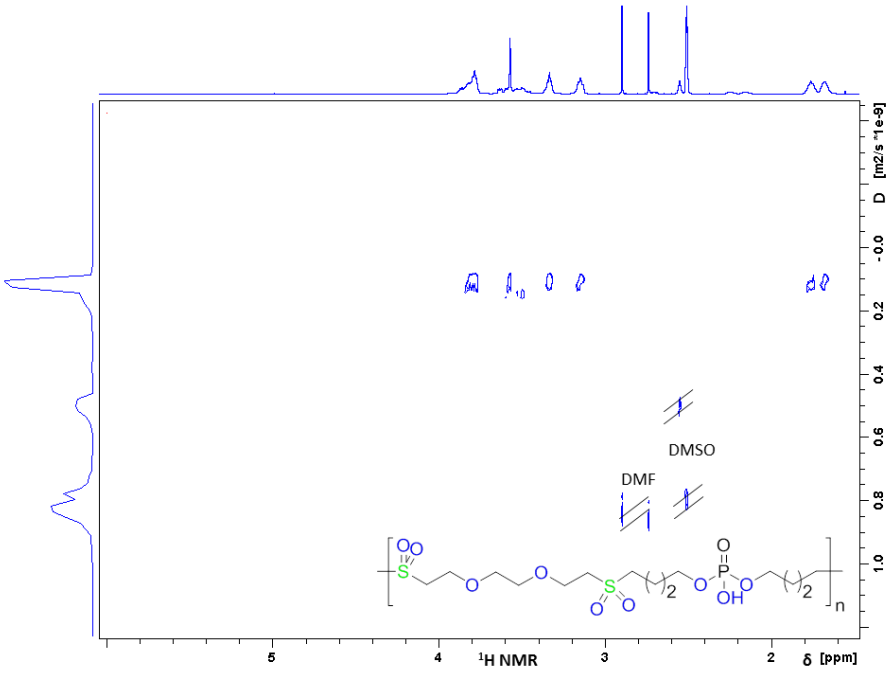

Figure S21: ^{1}H DOSY of **poly-ox(1)** (500 MHz, 298 K, DMSO).

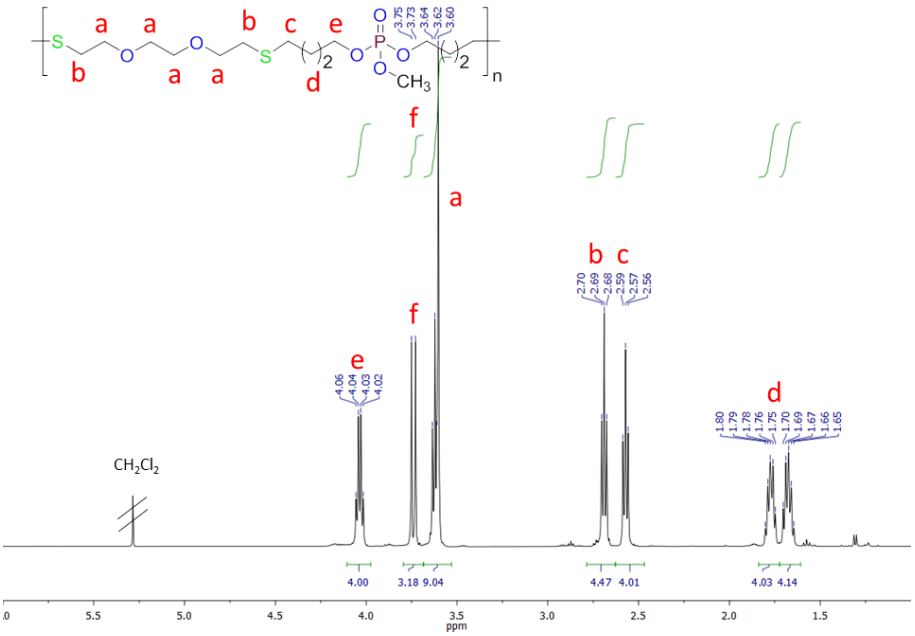

Figure S22: ^{1}H NMR of **poly(2)** (500 MHz, 298 K, $CDCl_3$).

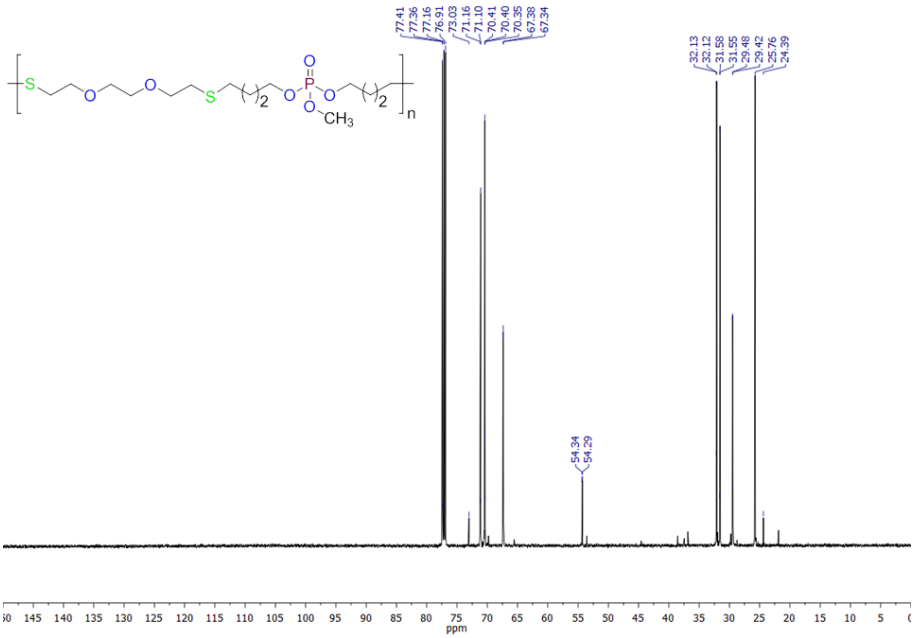

Figure S23: ^{13}C{H} NMR of **poly(2)** (126 MHz, 298 K, $CDCl_3$).

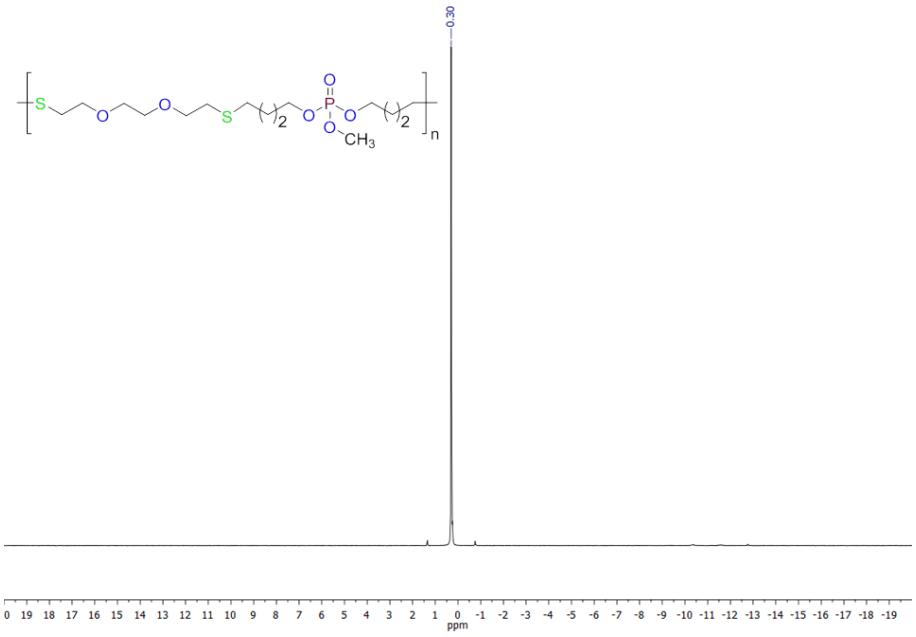

Figure S24: $^{31}P\{H\}$ NMR of **poly(2)** (202 MHz, 298 K, $CDCl_3$).

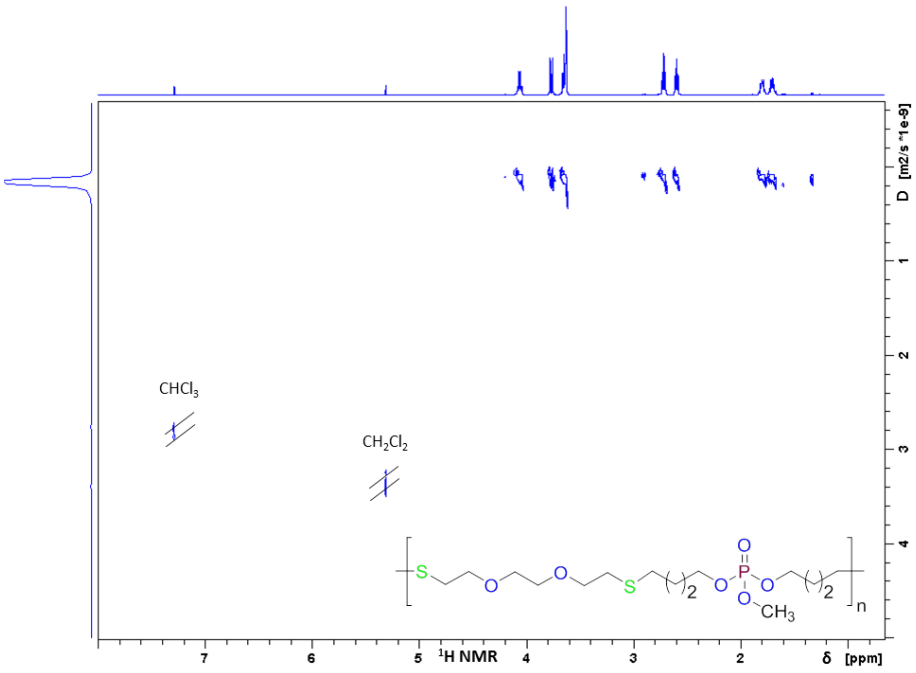

Figure S25: ^{1}H DOSY of **poly(2)** (500 MHz, 298 K, $CDCl_3$).

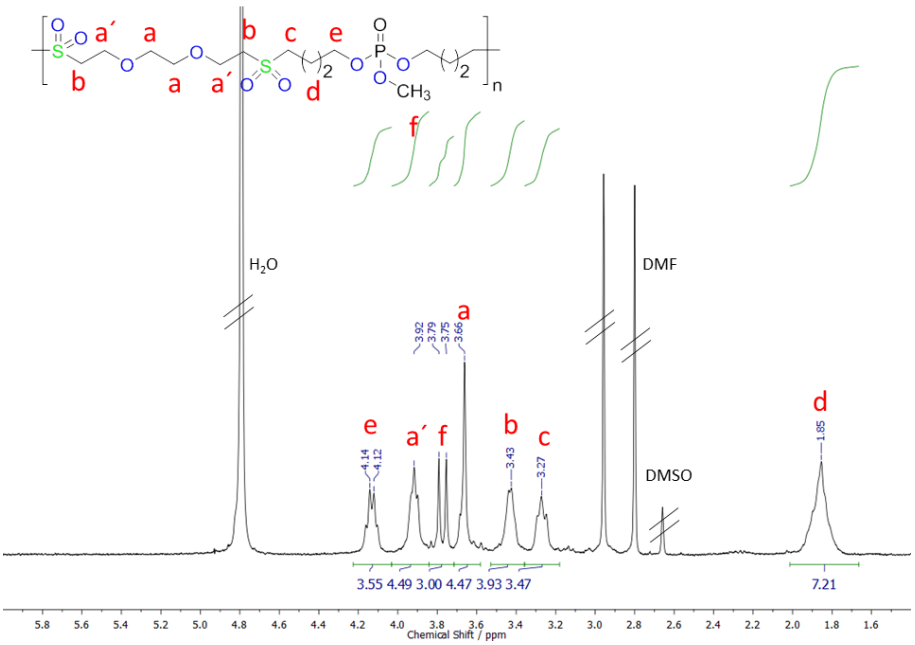

Figure S26: ^{1}H NMR of **poly-ox(2)** (300 MHz, 298 K, D_2O).

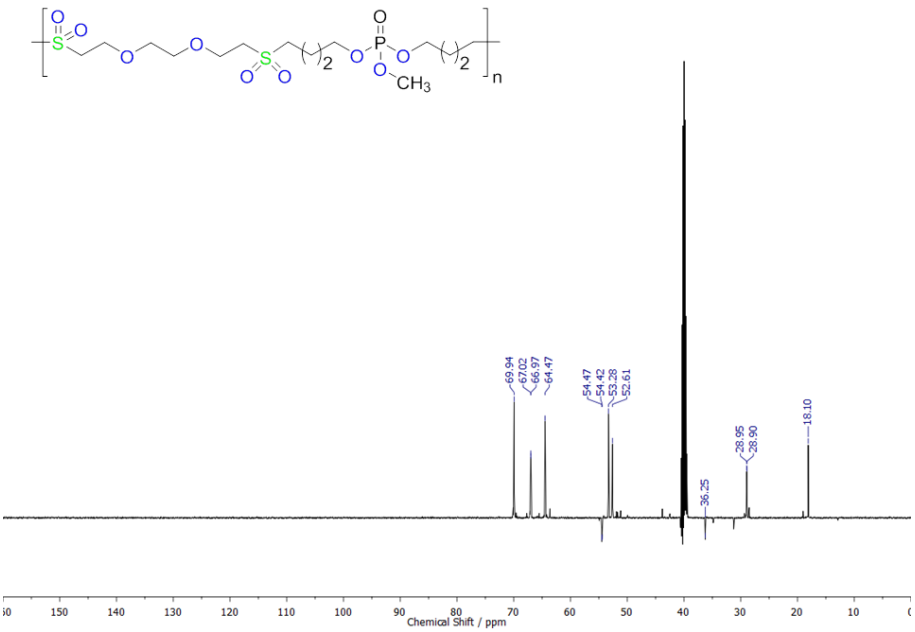

Figure S27: ^{13}C{H} NMR of **poly-ox(2)** (126 MHz, 298 K, DMSO).

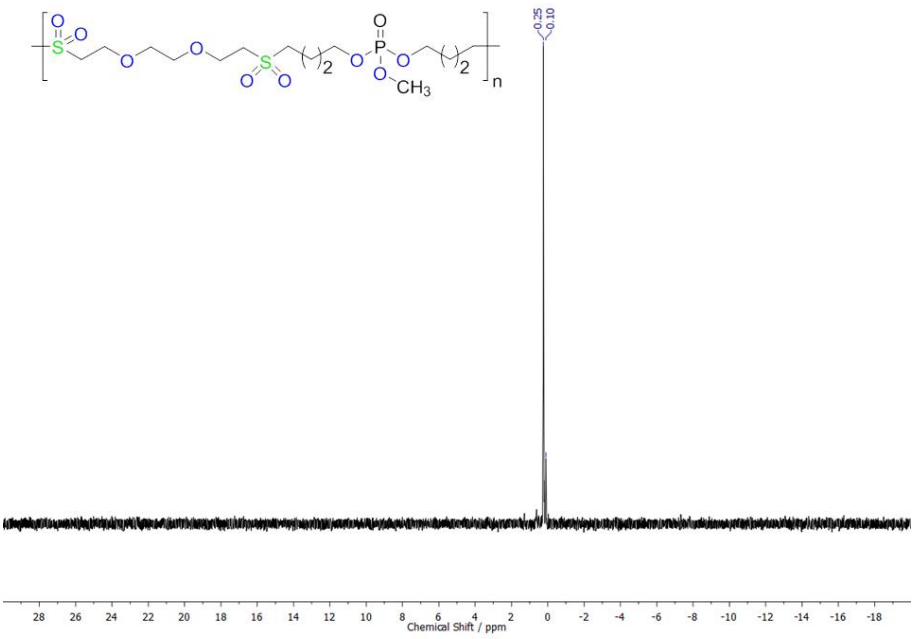

Figure S28: $^{31}P\{H\}$ NMR of **poly-ox(2)** (121 MHz, 298 K, DMSO).

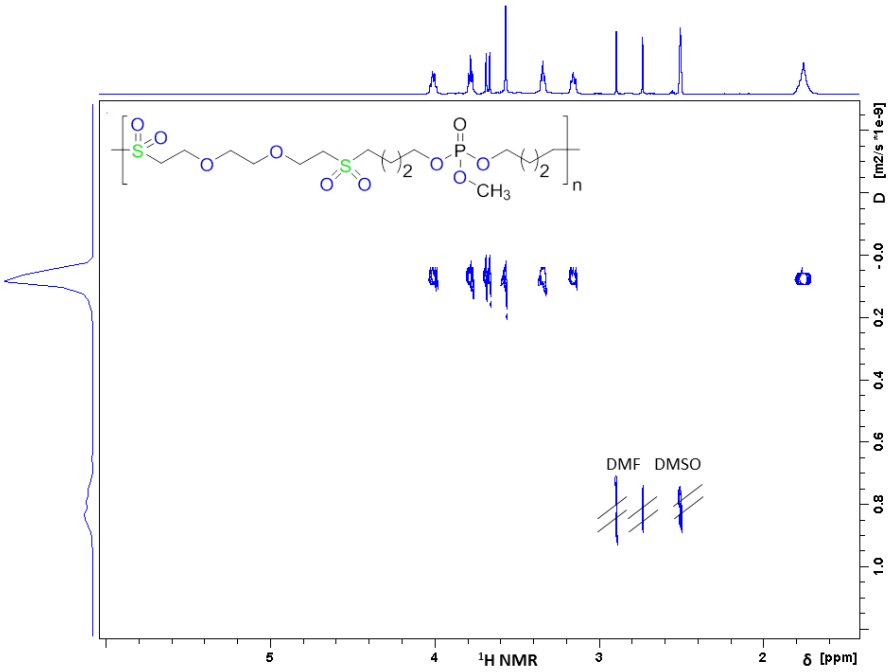

Figure S29: ^{1}H DOSY of **poly-ox(2)** (500 MHz, 298 K, DMSO).

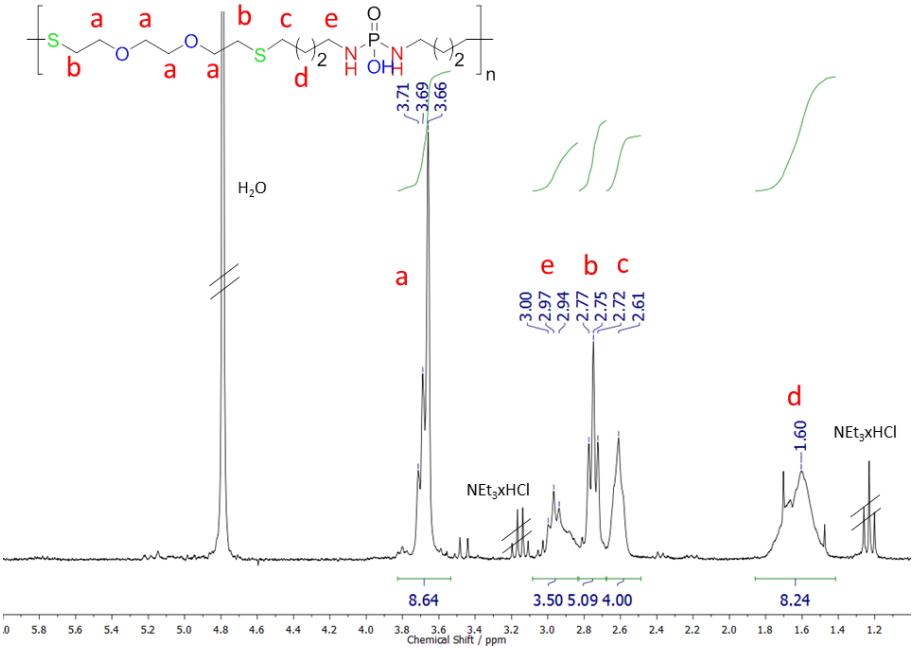

Figure S30: ^{1}H NMR of **poly(3)** (500 MHz, 298 K, $CDCl_3$).

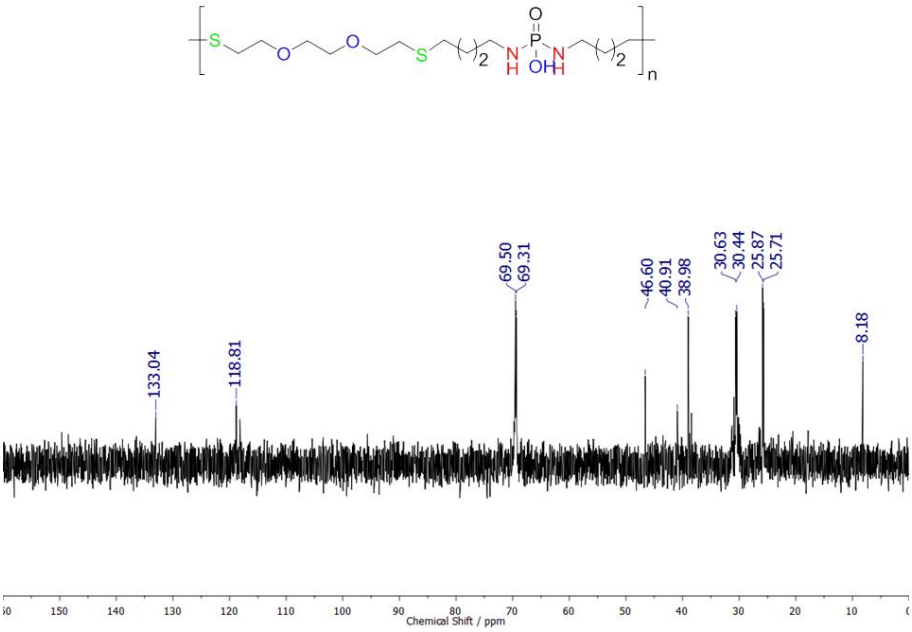

Figure S31: ^{13}C{H} NMR of **poly(3)** (126 MHz, 298 K, $CDCl_3$).

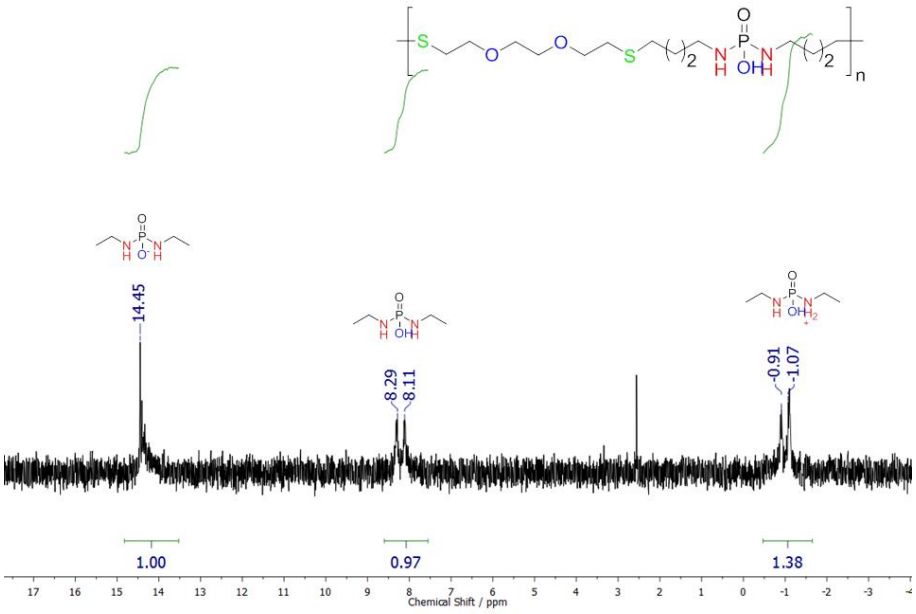

Figure S32: $^{31}P\{H\}$ NMR of **poly(3)** (202 MHz, 298 K, $CDCl_3$).

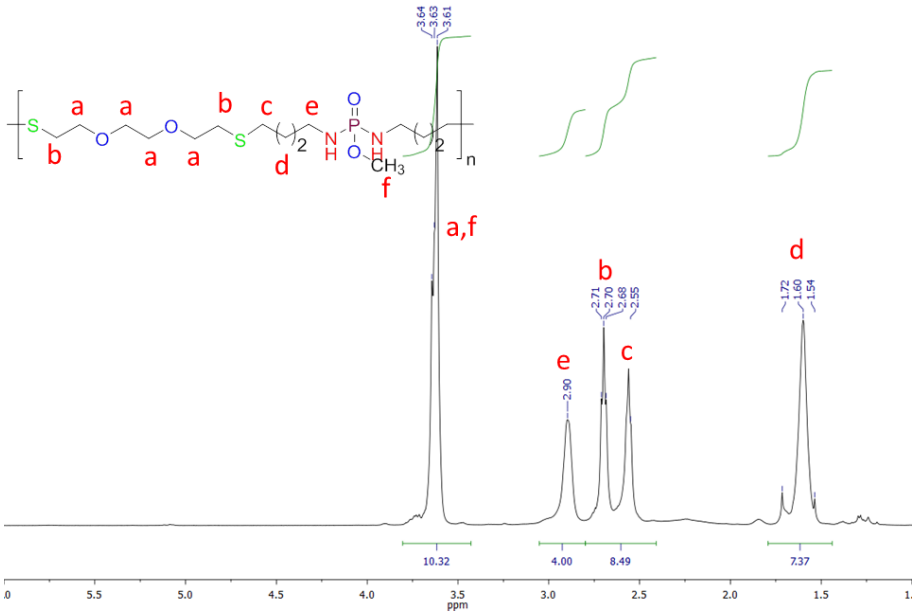

Figure S33: ^{1}H NMR of **poly(4)** (500 MHz, 298 K, $CDCl_3$).

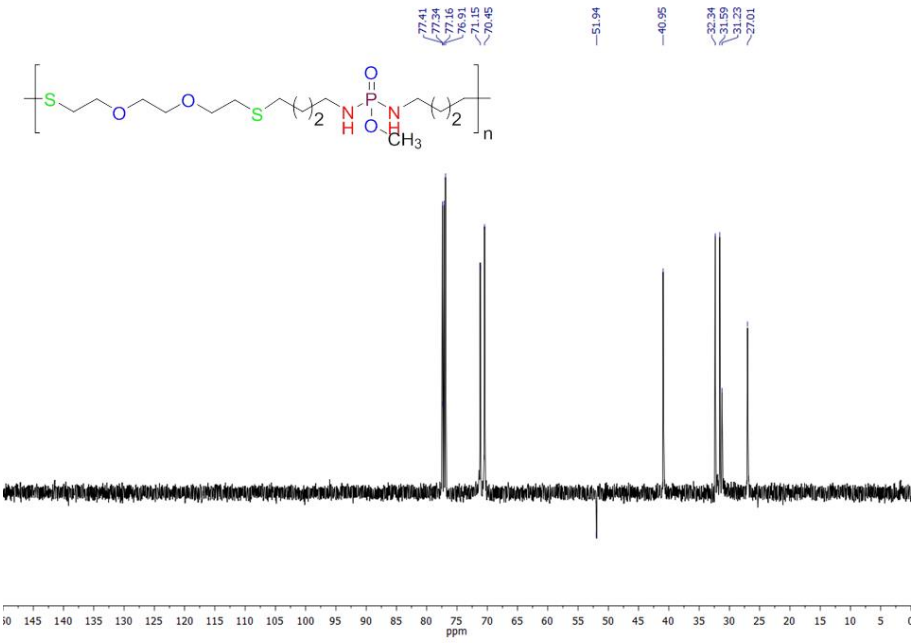

Figure S34: $^{13}C\{H\}$ NMR of **poly(4)** (126 MHz, 298 K, $CDCl_3$).

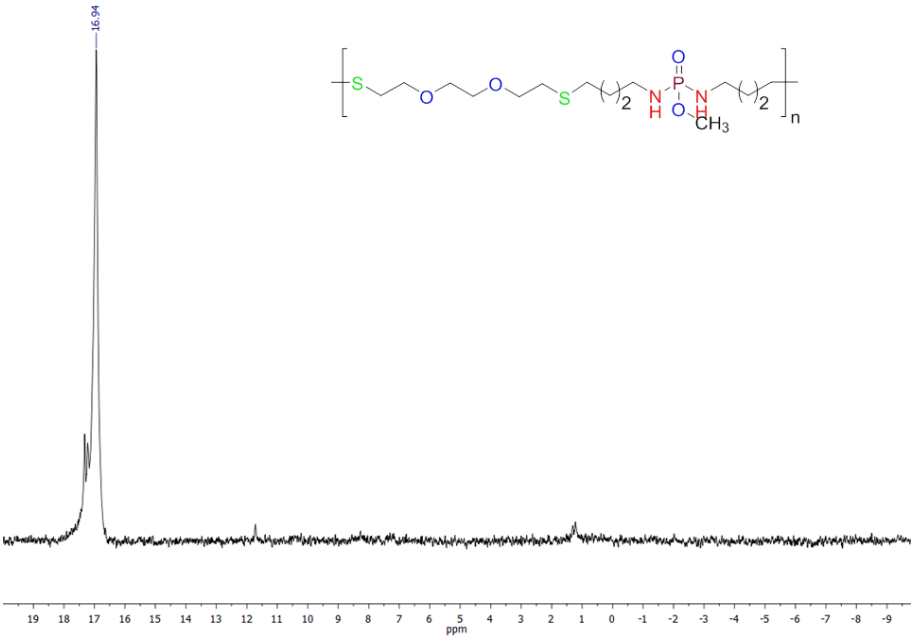

Figure S35: $^{31}P\{H\}$ NMR of **poly(4)** (202 MHz, 298 K, $CDCl_3$).

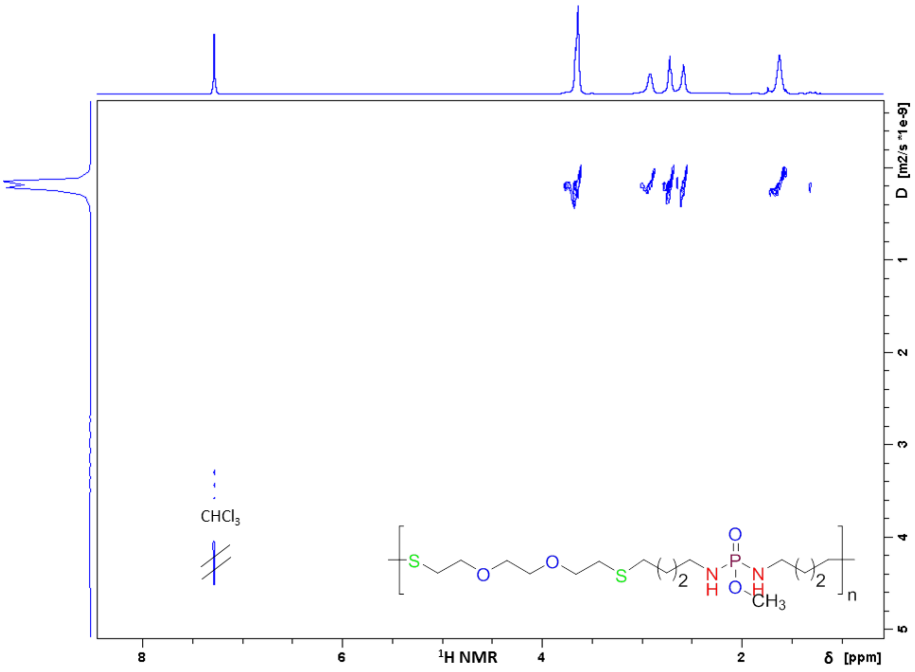

Figure S36: ^{1}H DOSY of **poly(4)** (500 MHz, 298 K, $CDCl_3$).

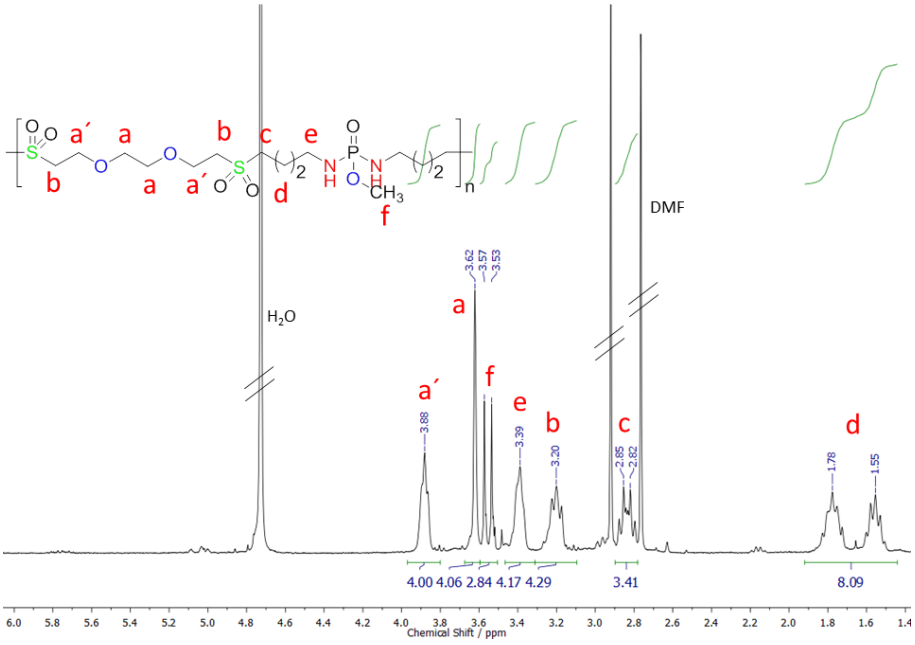

Figure S37: ^{1}H NMR of **poly-ox(4)** (300 MHz, 298 K, D_2O).

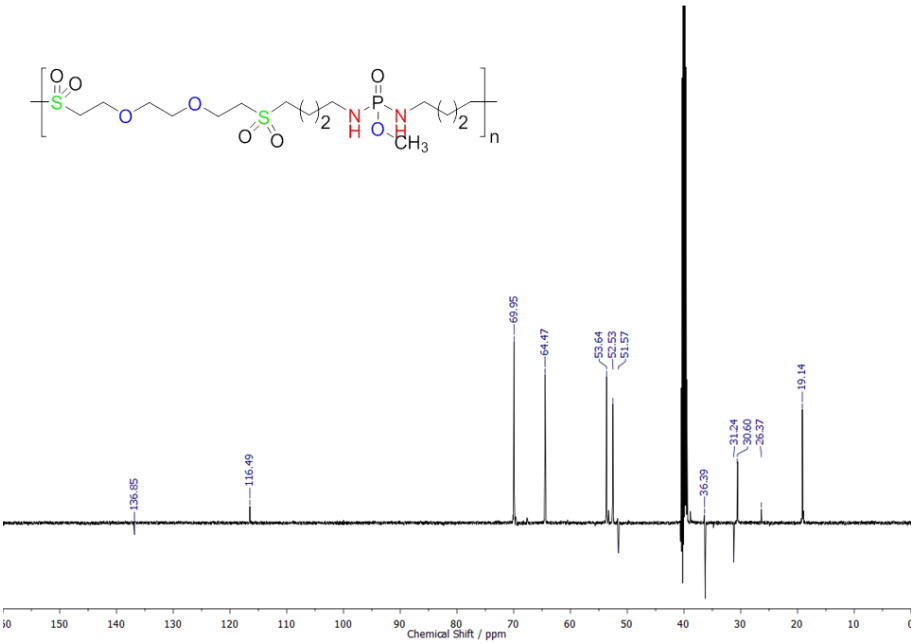

Figure S38: $^{13}C\{H\}$ NMR of **poly-ox(4)** (126 MHz, 298 K, $CDCl_3$).

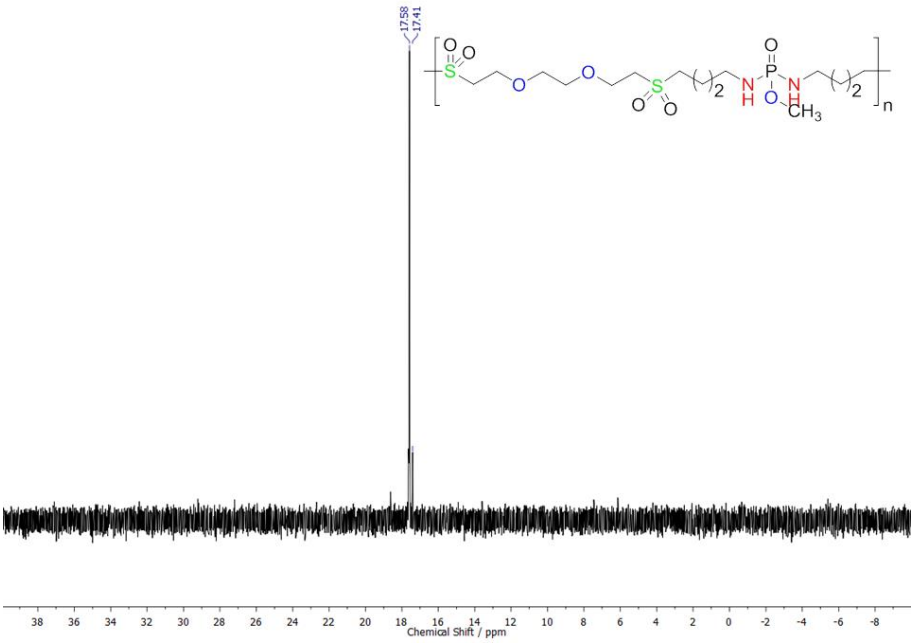

Figure S39: $^{31}P\{H\}$ NMR of **poly-ox(4)** (121.5 MHz, 298 K, DMSO).

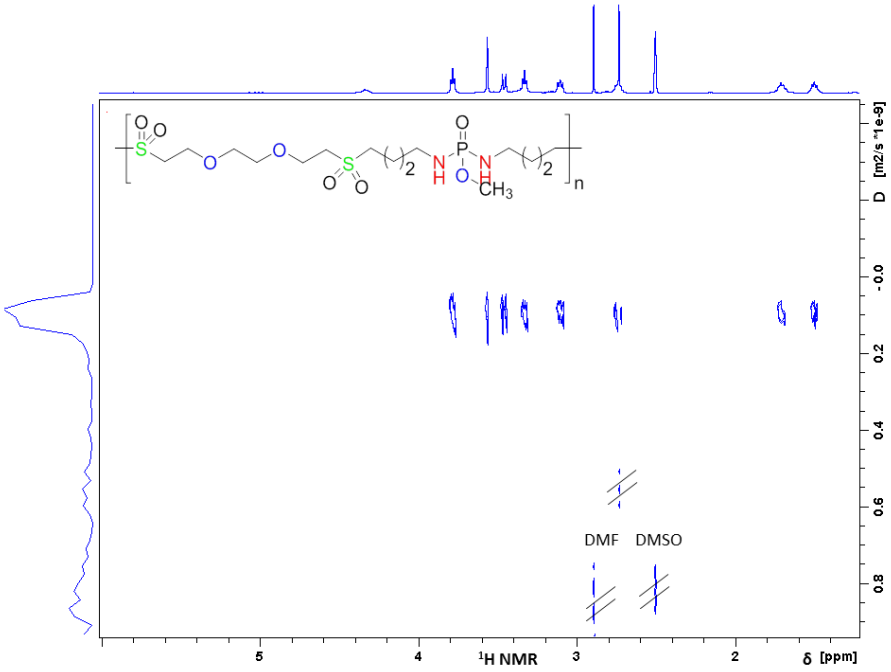

Figure S40: ^{1}H DOSY of **poly-ox(4)** (500 MHz, 298 K, DMSO).

Supporting Information for: Water-soluble and degradable polyphosphorodiamidates via radical polyaddition

Thermal Analysis: DSC

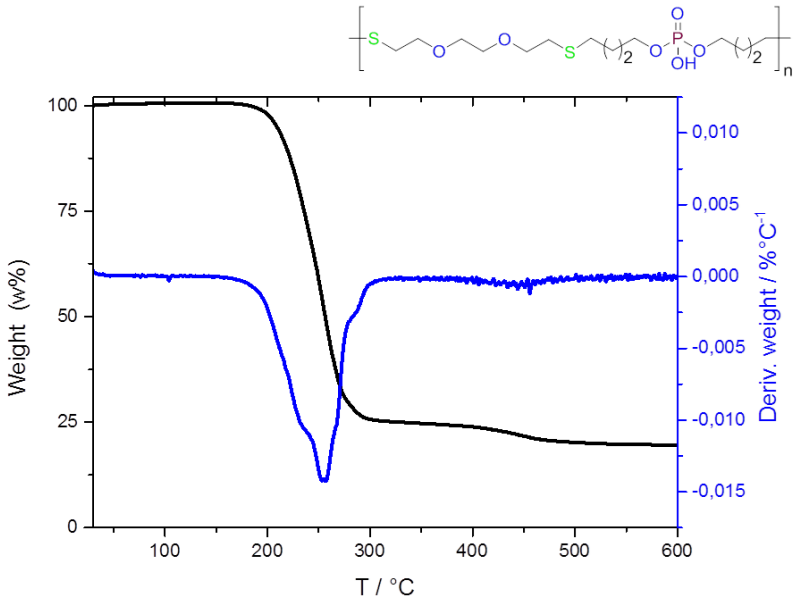

Figure S41: Thermogravimetric analyses (TGA) and derived TGA of **poly(1).**

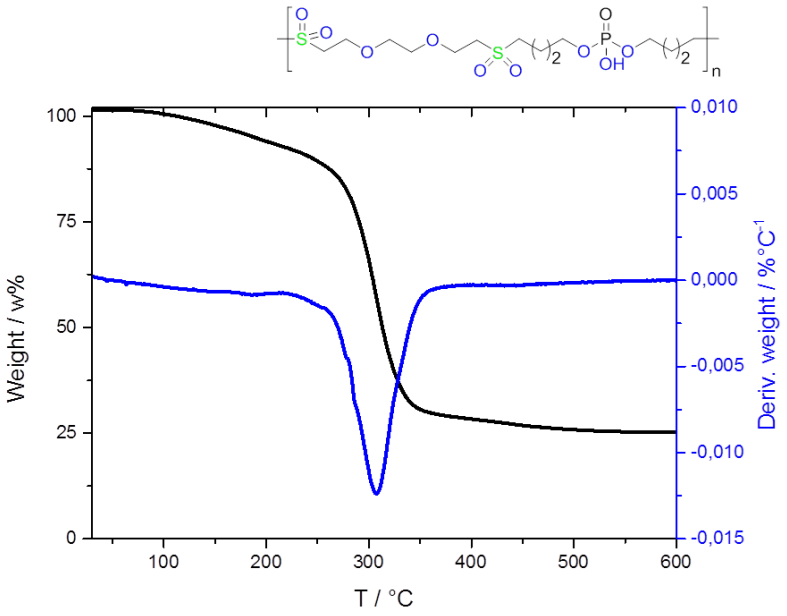

Figure S42: Thermogravimetric analyses (TGA) and derived TGA of **poly-ox(1).**

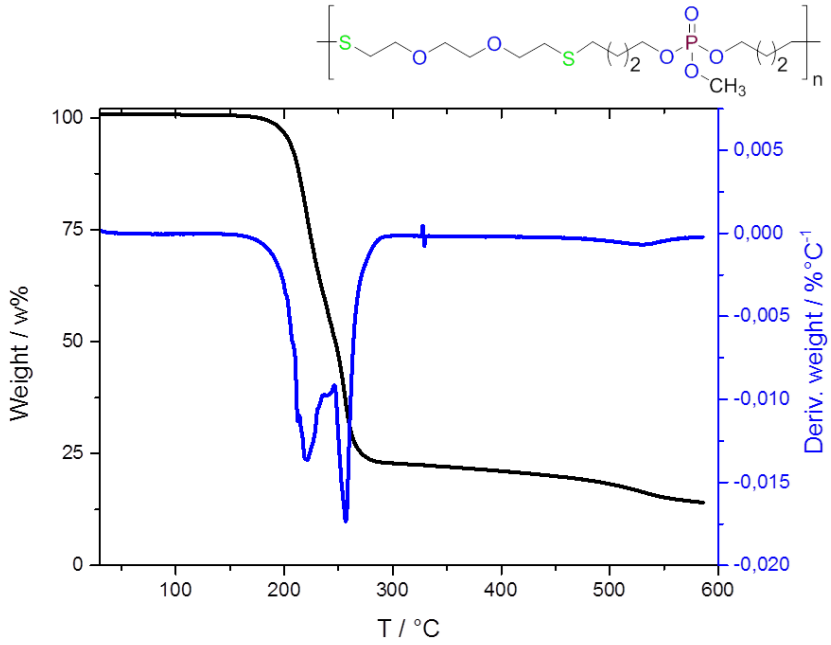

Figure S43: Thermogravimetric analyses (TGA) and derived TGA of **poly(2).**

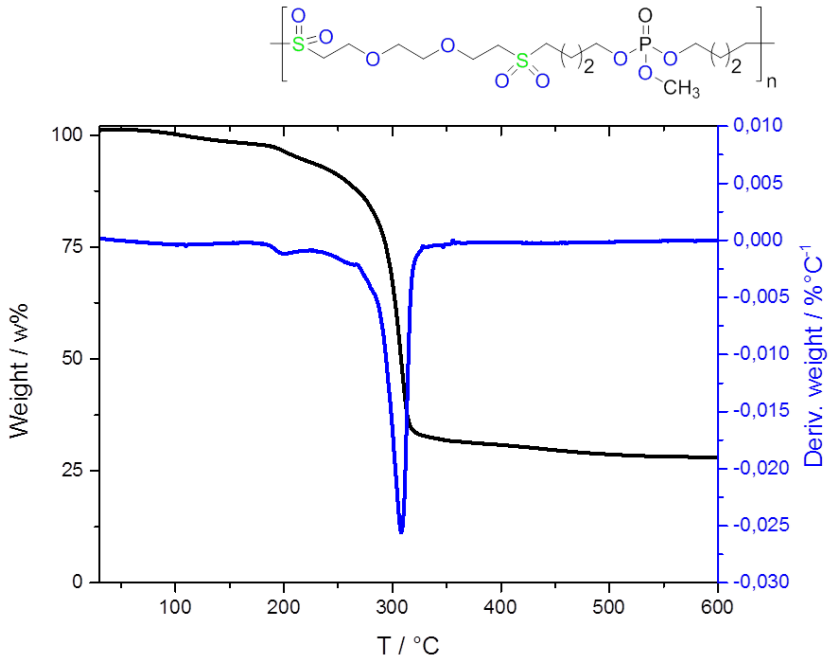

Figure S44: Thermogravimetric analyses (TGA) and derived TGA of **poly-ox(2).**

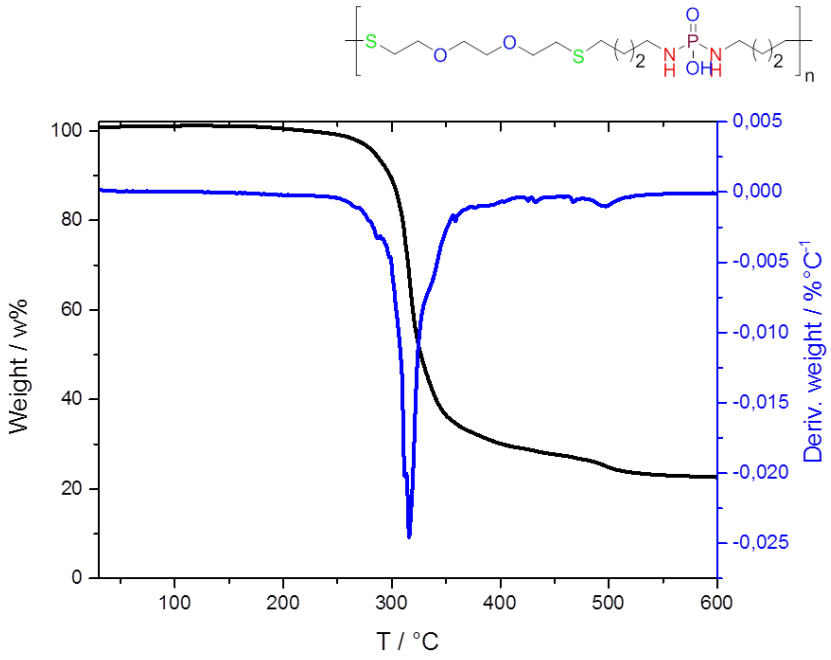

Figure S45: Thermogravimetric analyses (TGA) and derived TGA of **poly(3).**

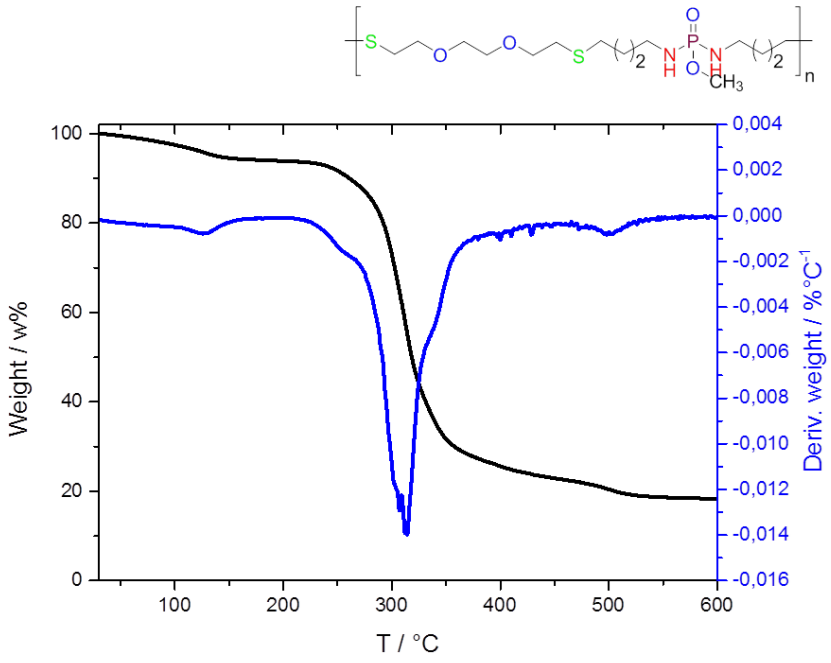

Figure S46: Thermogravimetric analyses (TGA) and derived TGA of **poly(4).**

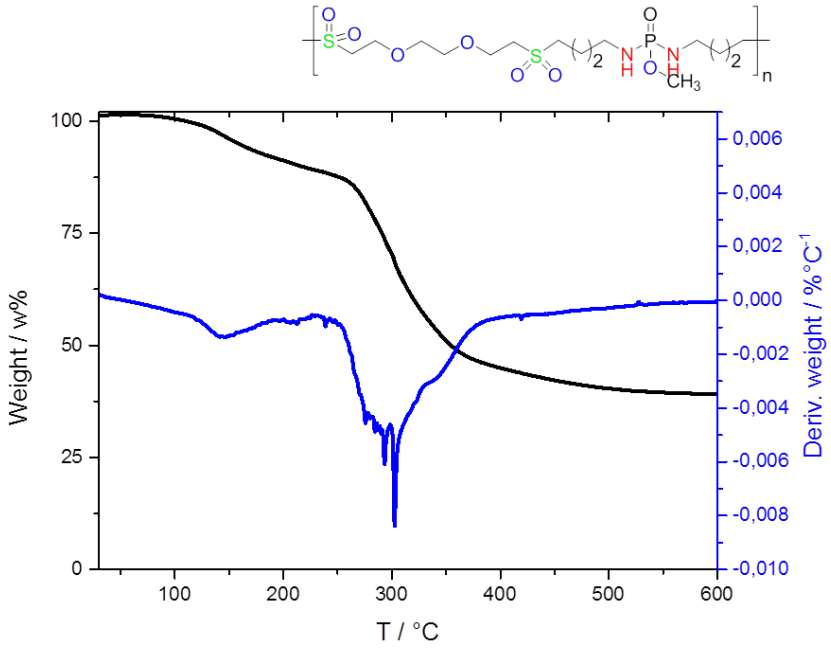

Figure S47: Thermogravimetric analyses (TGA) and derived TGA of **poly-ox(4).**

Supporting Information for: Polyphosphorodiamidates via Radical Polyaddition

GPC

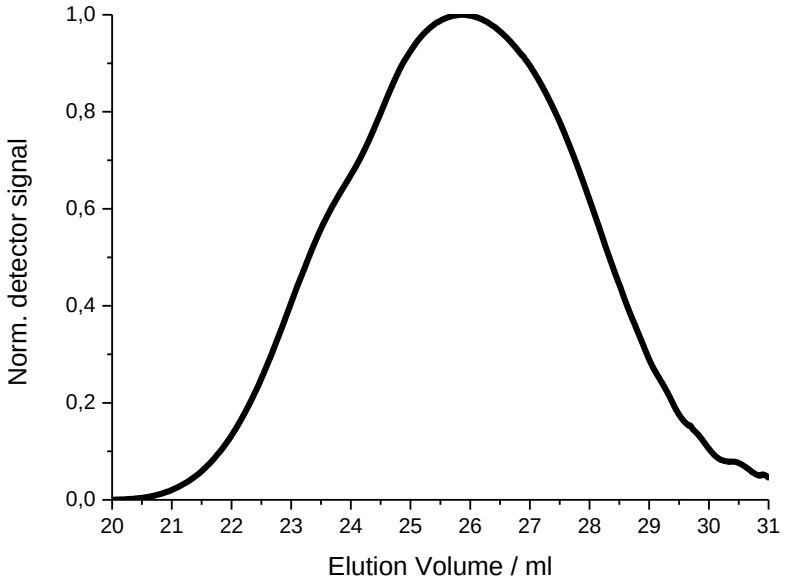

Figure S1: GPC-elugram of polymer **Poly(5-co-1)** (M_n = 8,900 g·mol^{-1}) vs. polystyrene standards in THF measured by RI-detector.

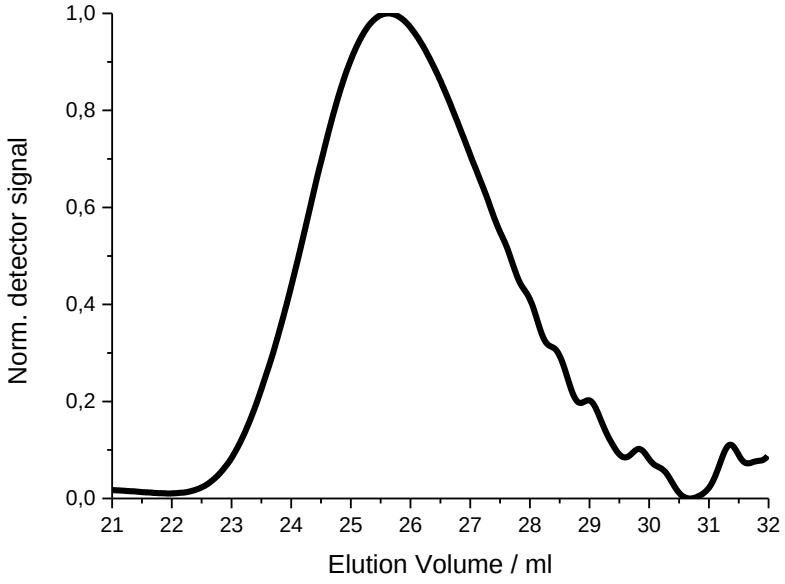

Figure S2: GPC-elugram of polymer **Poly(4-co-2)** (M_n = 8,300 g·mol^{-1}) vs. polystyrene standards in THF measured by RI-detector.

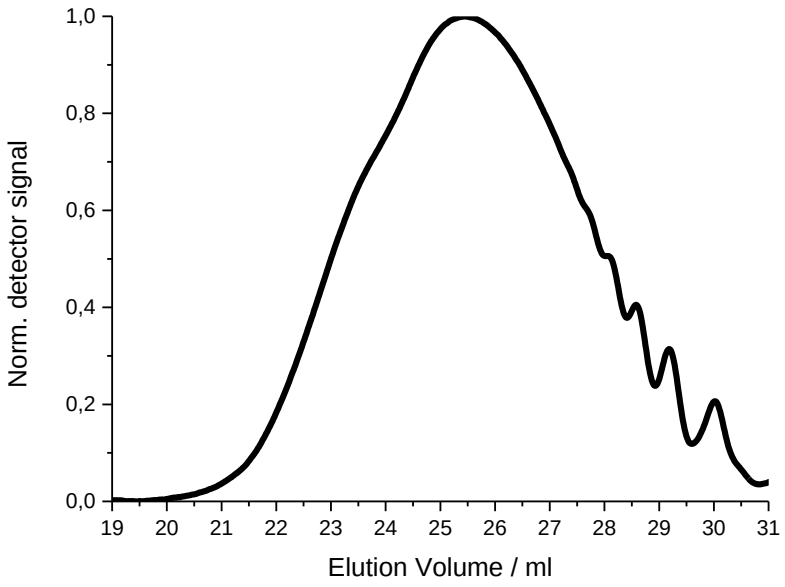

Figure S3: GPC-elugram of polymer **Poly(6-co-2)** (M_n = 8,300 g·mol^{-1}) vs. polystyrene standards in THF measured by RI-detector.

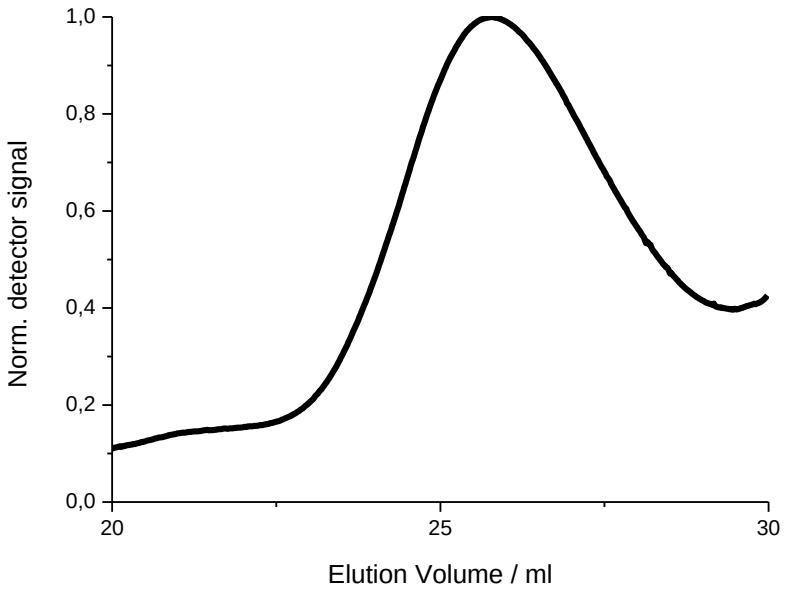

Figure S4: GPC-elugram of polymer **Poly(3-co-2)** (M_n = 10,700 g·mol^{-1}) vs. polystyrene standards in THF measured by RI-detector.

NMR spectra: Polymers

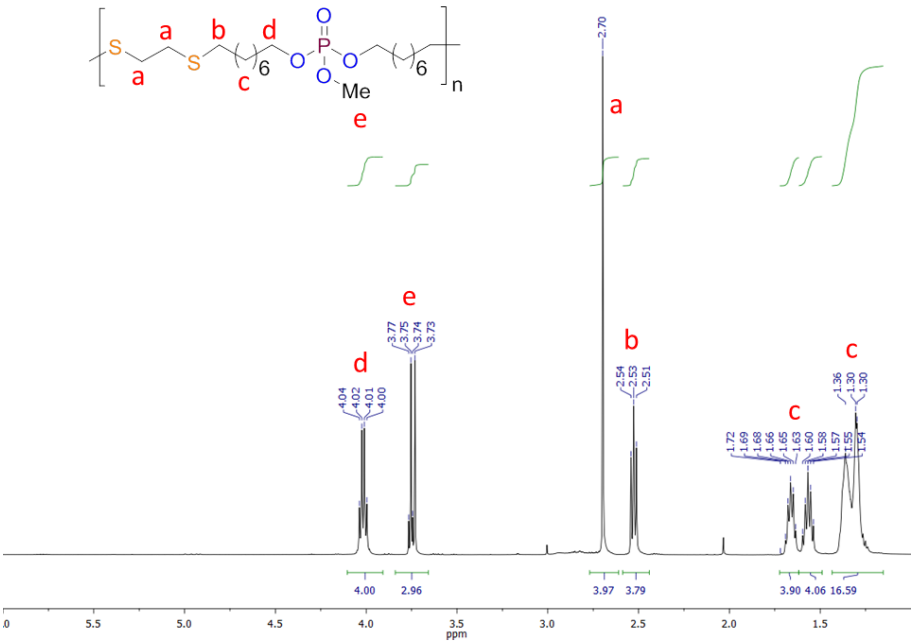

Figure S5: ^{1}H NMR of **Poly(5-co-1)** (500 MHz, 298 K, $CDCl_3$).

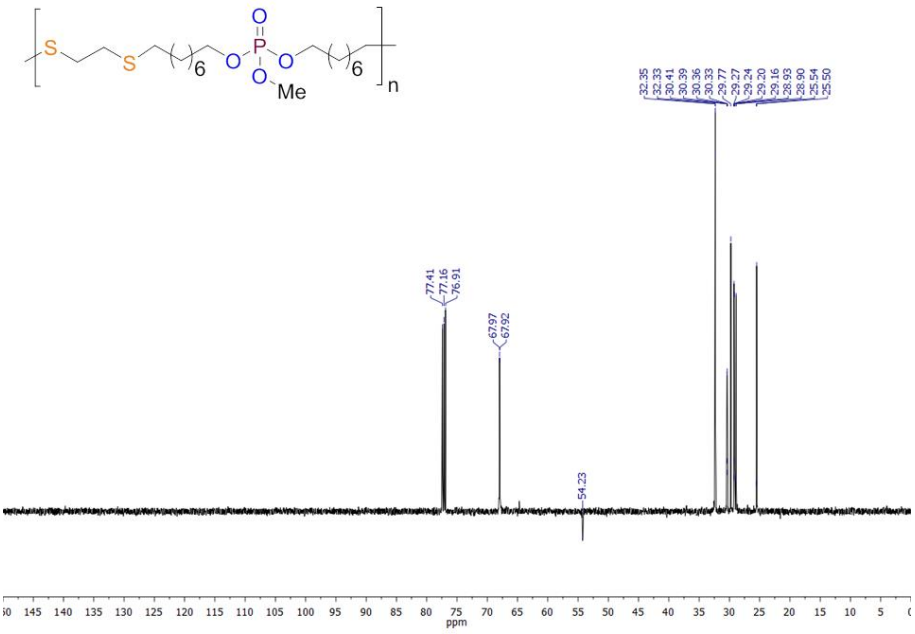

Figure S6: ^{13}C NMR of **Poly(5-co-1)** (126 MHz, 298 K, $CDCl_3$).

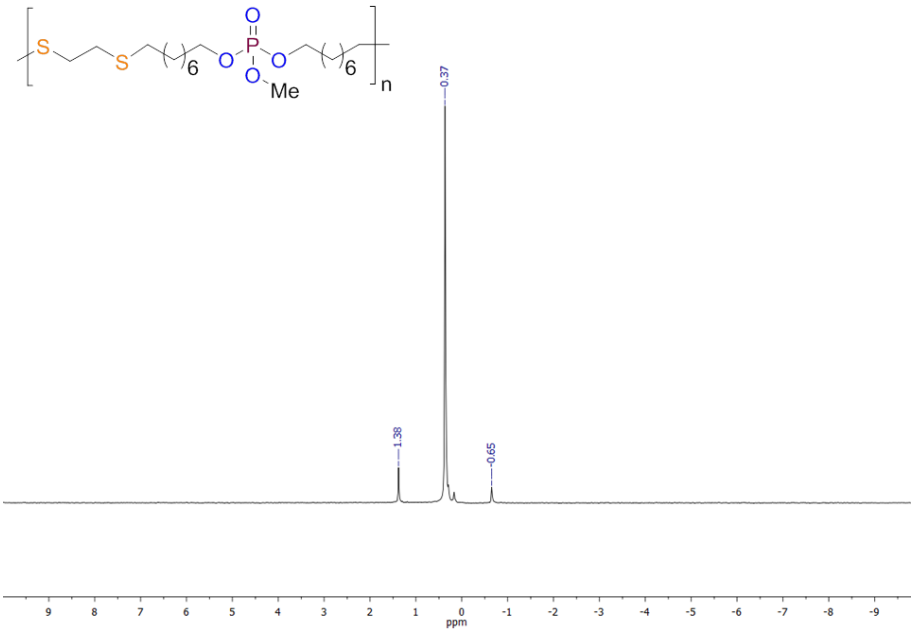

Figure S7: ^{31}P NMR of **Poly(5-co-1)** (202 MHz, 298 K, $CDCl_3$).

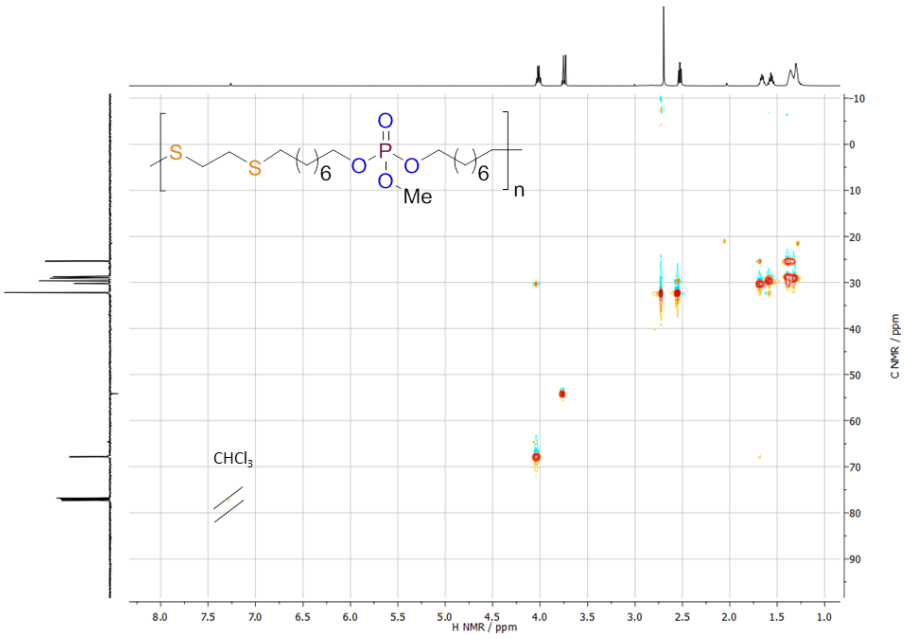

Figure S8: ^{1}H, ^{13}C HSQC NMR of **Poly(5-co-1)** (500 MHz, 298 K, $CDCl_3$).

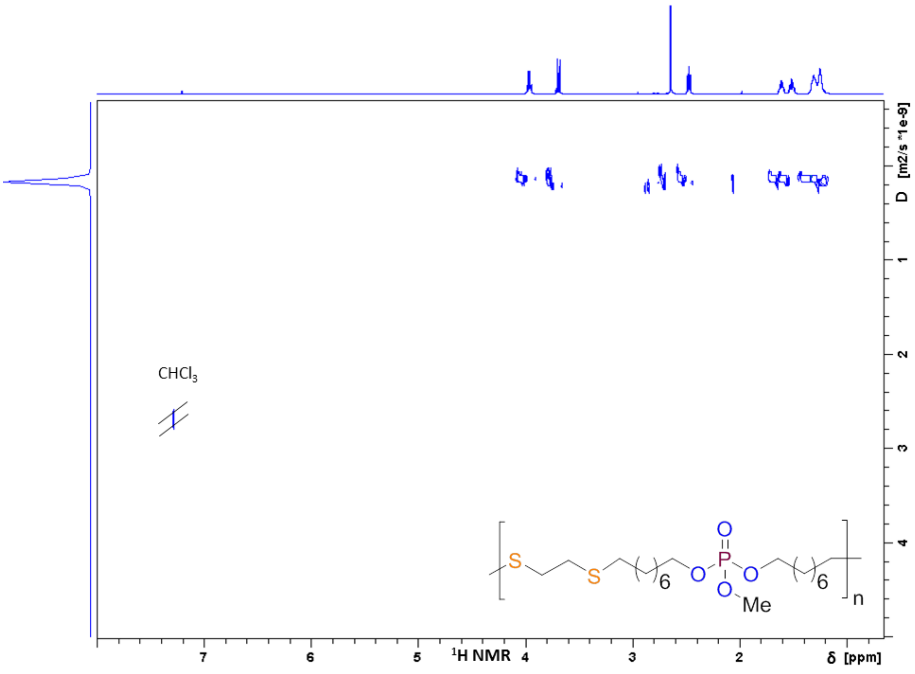

Figure S9: ^{1}H DOSY of **Poly(5-co-1)** (500 MHz, 298 K, $CDCl_3$).

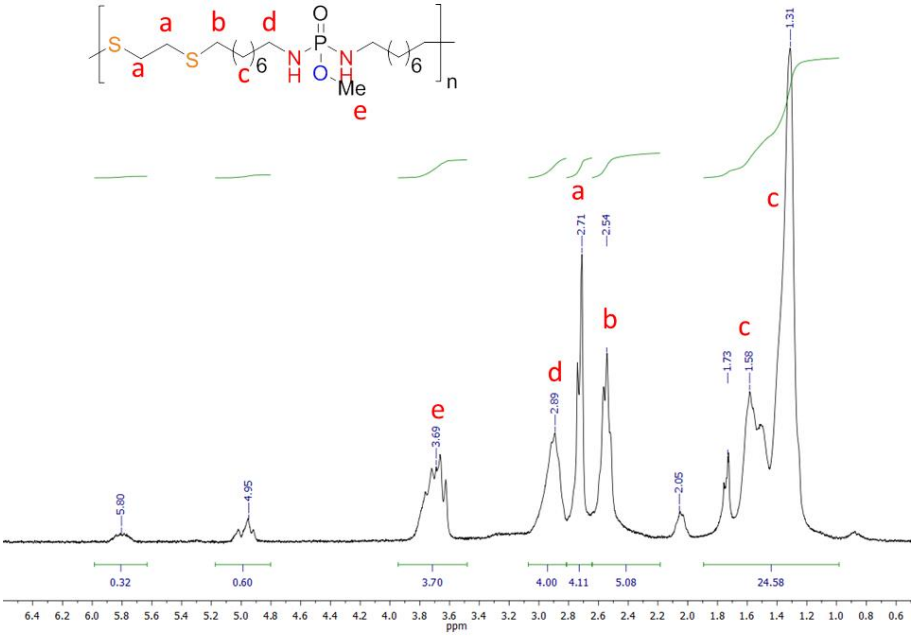

Figure S10: ^{1}H NMR of **Poly(8-co-1)** (500 MHz, 298 K, $CDCl_3$).

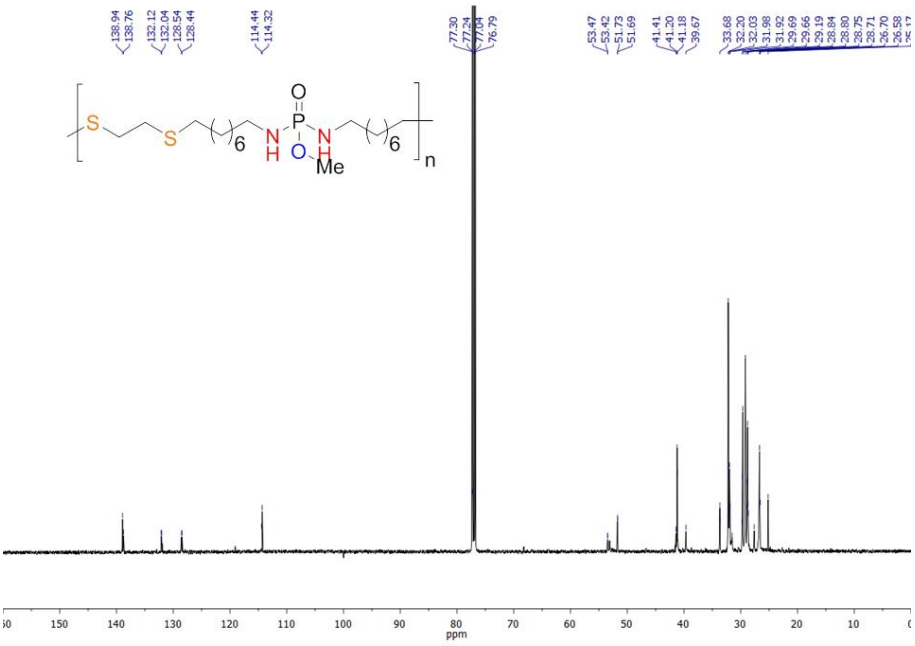

Figure S11: ^{13}C NMR of **Poly(8-co-1)** (126 MHz, 298 K, $CDCl_3$).

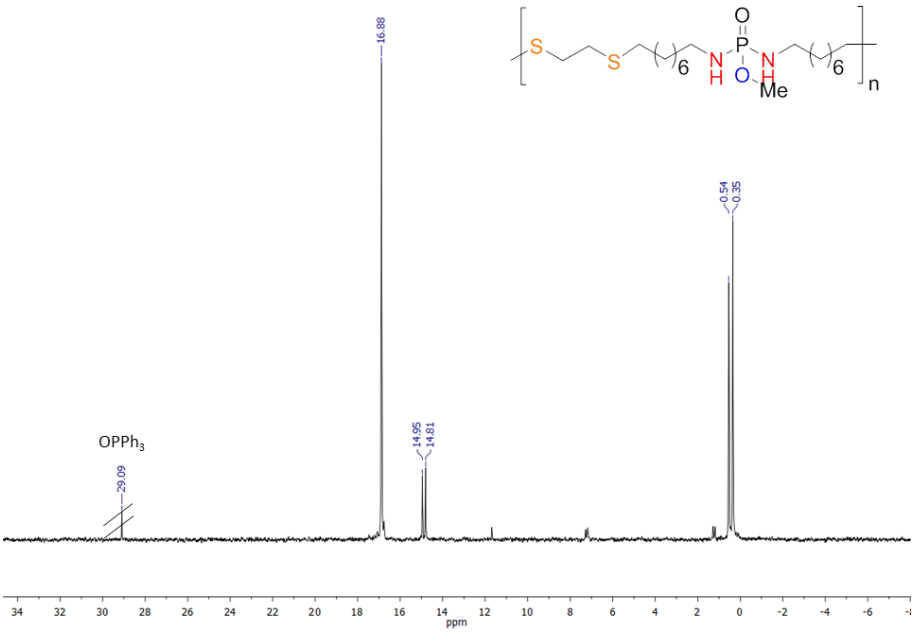

Figure S12: ^{31}P NMR of **Poly(8-co-1)** (202 MHz, 298 K, $CDCl_3$).

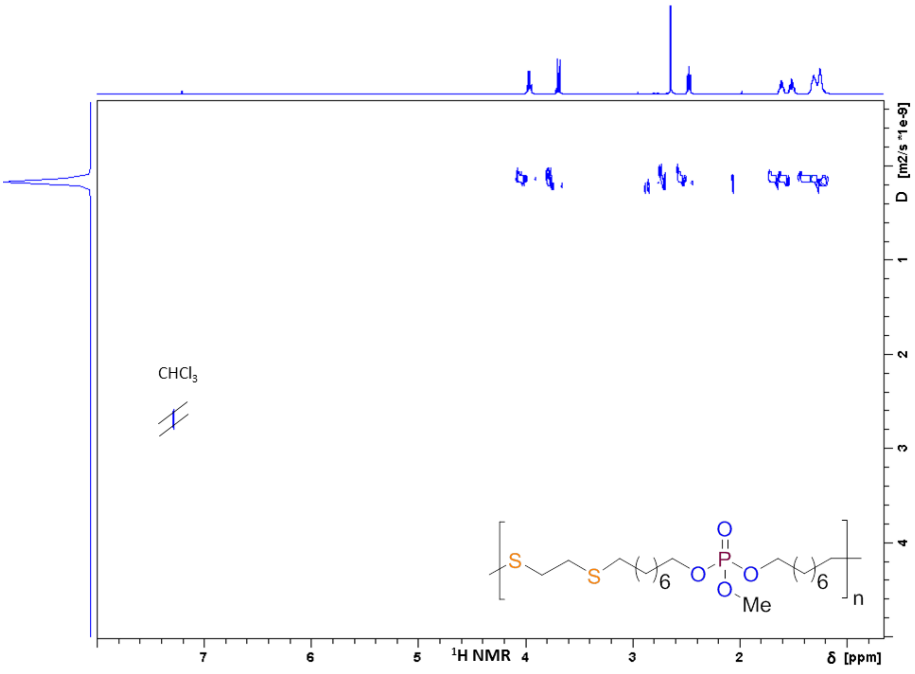

Figure S13: ^{1}H DOSY of **Poly(8-co-1)** (700 MHz, 298 K, $CDCl_3$).

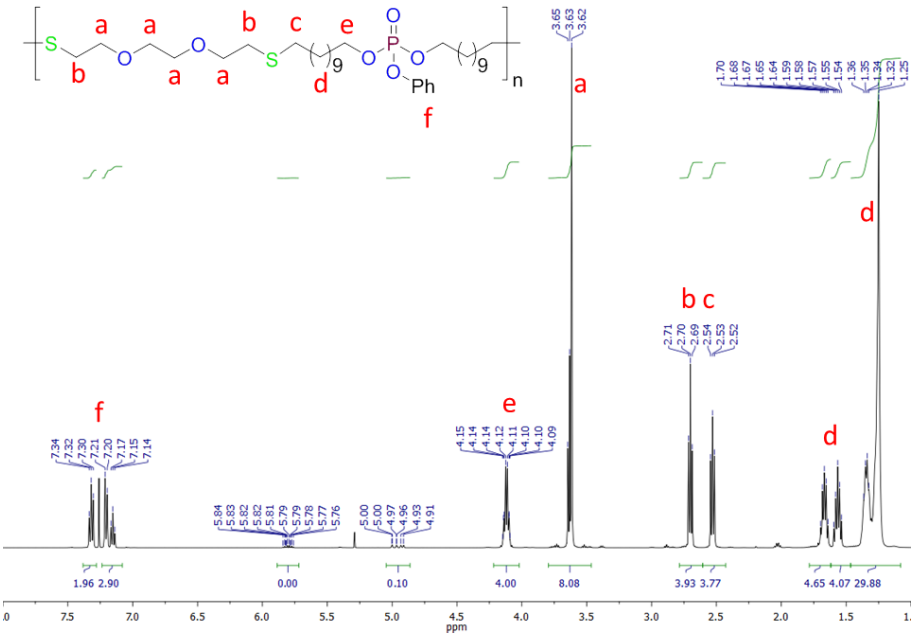

Figure S14: ^{1}H NMR of **Poly(4-co-2)** (500 MHz, 298 K, $CDCl_3$).

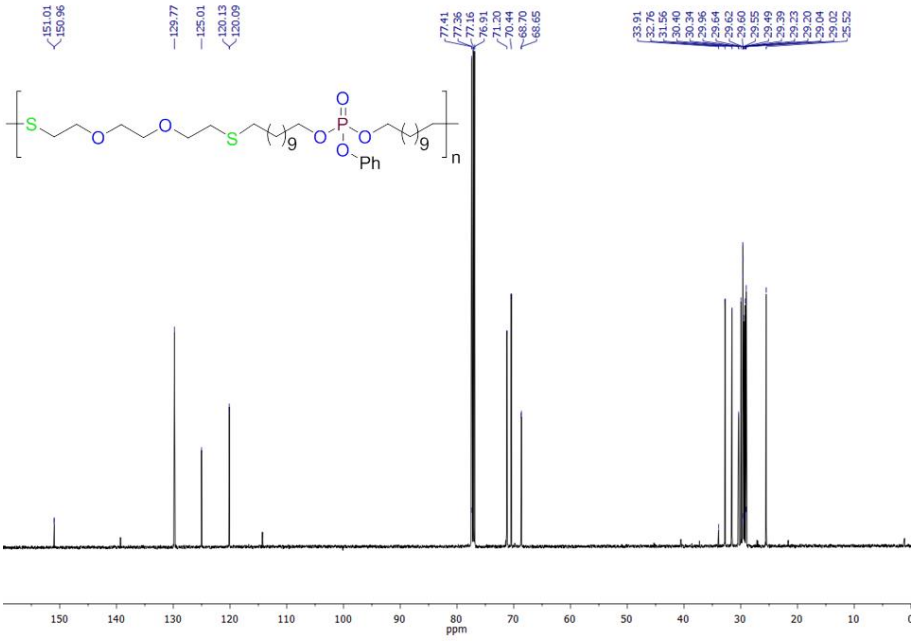

Figure S15: ^{13}C NMR of **Poly(4-co-2)** (126 MHz, 298 K, $CDCl_3$).

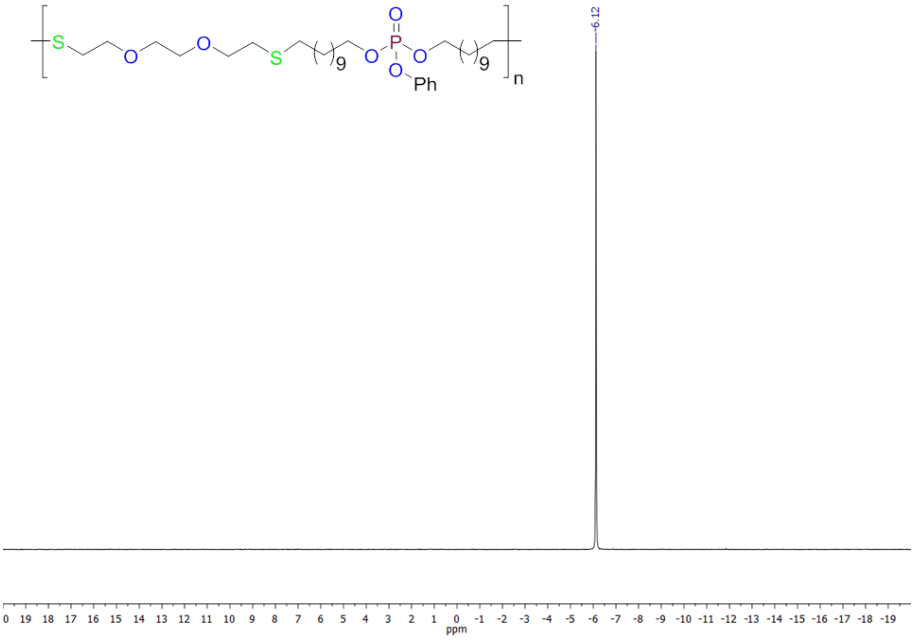

Figure S16: ^{31}P NMR of **Poly(4-co-2)** (202 MHz, 298 K, $CDCl_3$).

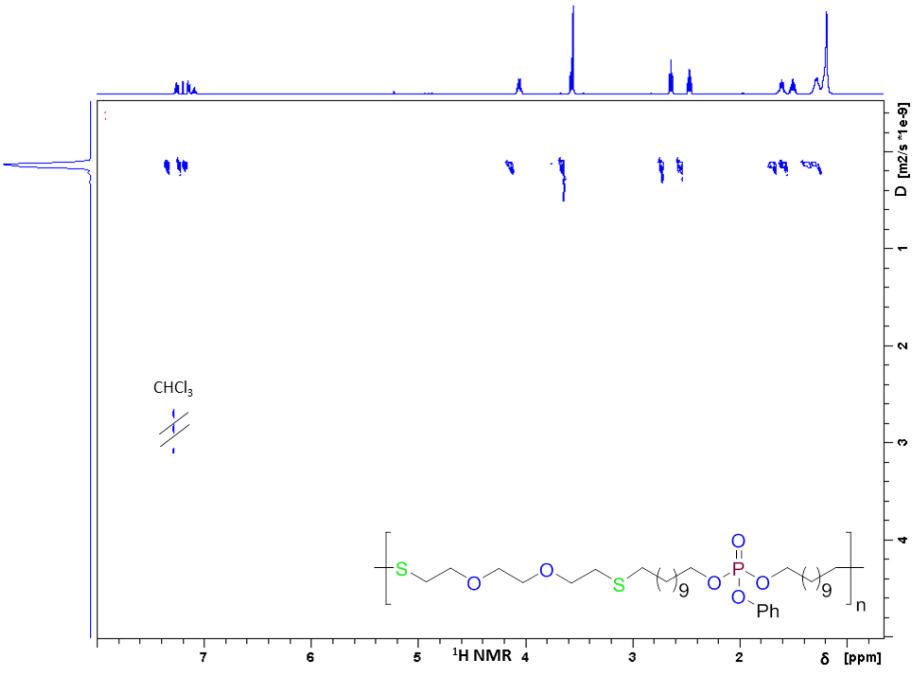

Figure S17: ^{1}H DOSY of **Poly(4-co-2)** (500 MHz, 298 K, $CDCl_3$).

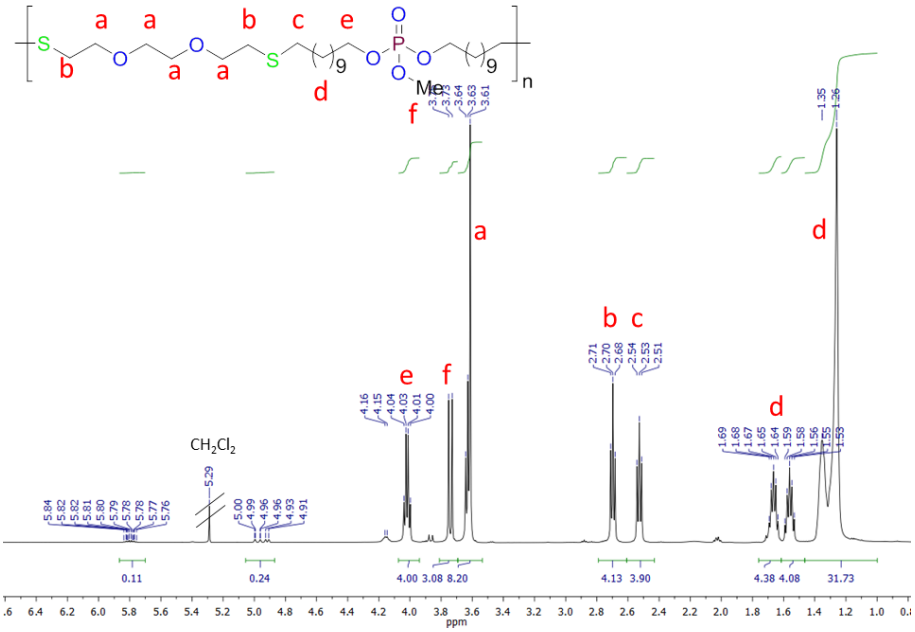

Figure S18: ^{1}H NMR of **Poly(6-co-2)** (500 MHz, 298 K, $CDCl_3$).

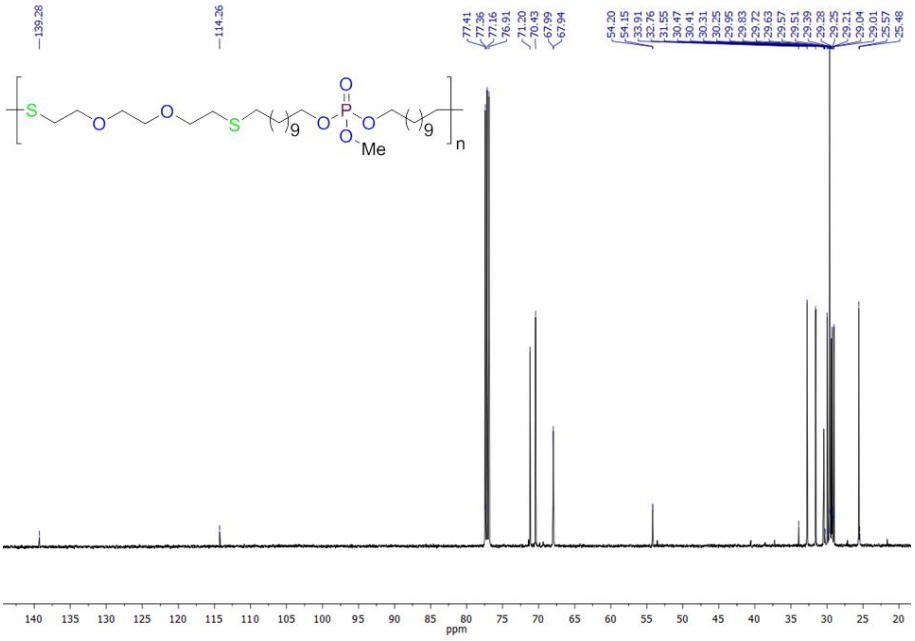

Figure S19: ^{13}C NMR of **Poly(6-co-2)** (126 MHz, 298 K, $CDCl_3$).

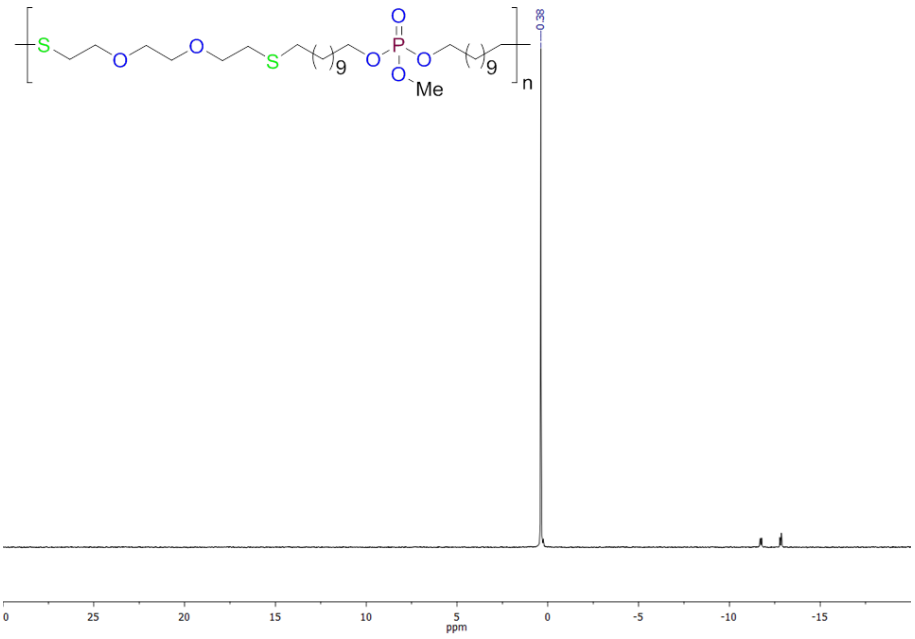

Figure S20: ^{31}P NMR of **Poly(6-co-2)** (202 MHz, 298 K, $CDCl_3$).

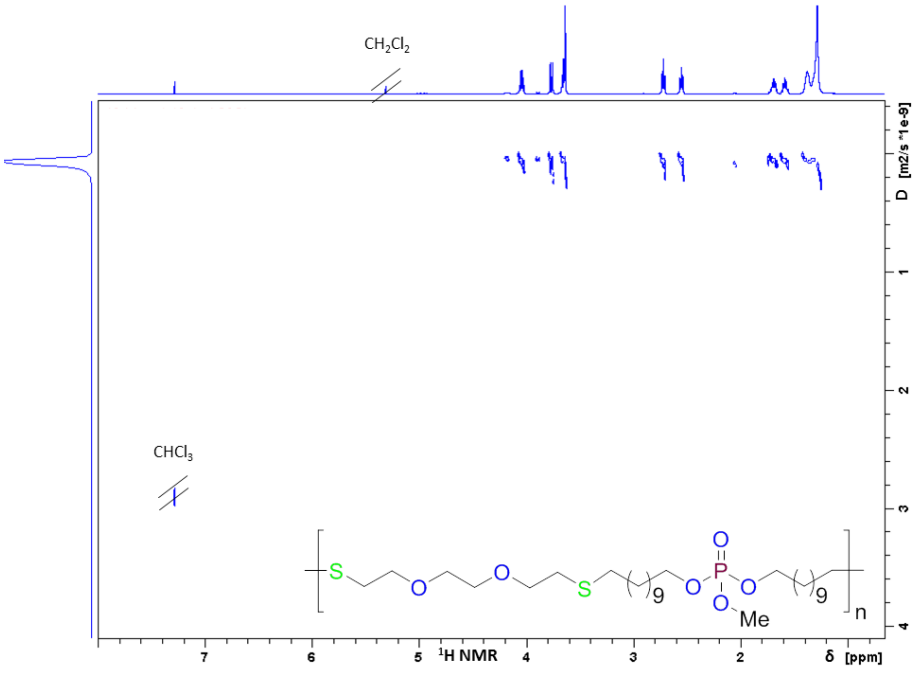

Figure S21: ^{1}H DOSY of **Poly(6-co-2)** (500 MHz, 298 K, $CDCl_3$).

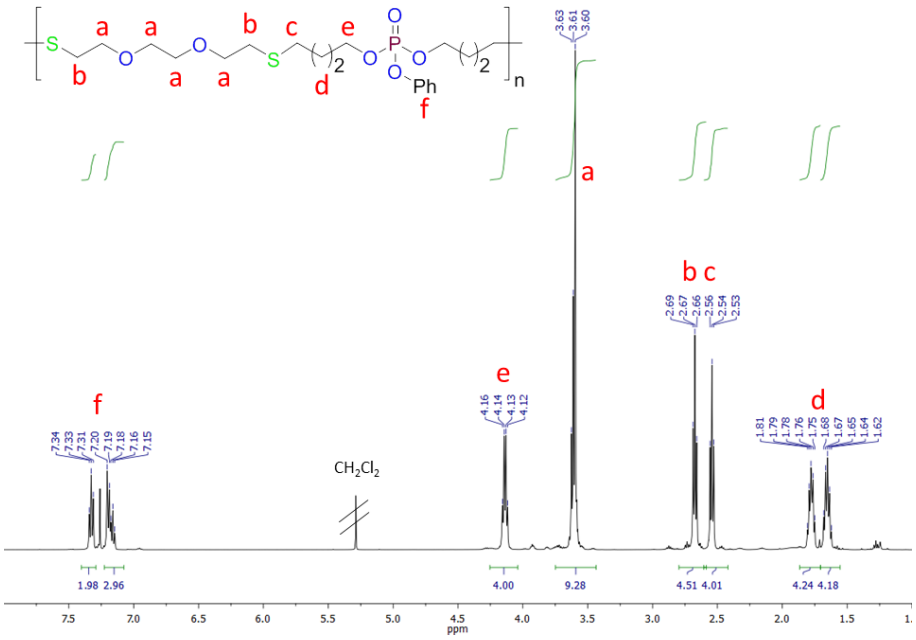

Figure S22: ^{1}H NMR of **Poly(3-co-2)** (500 MHz, 298 K, $CDCl_3$).

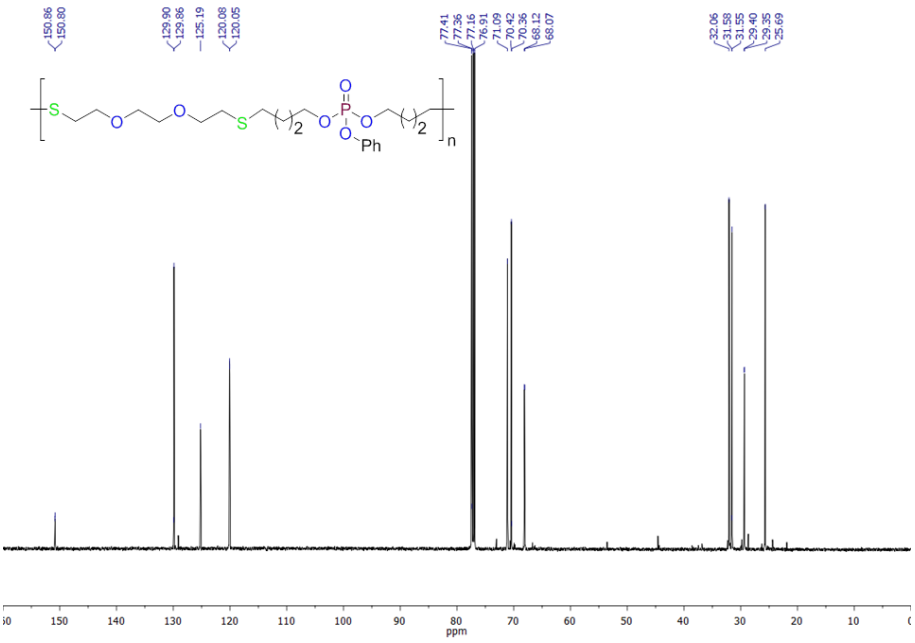

Figure S23: ^{13}C NMR of **Poly(3-co-2)** (126 MHz, 298 K, $CDCl_3$).

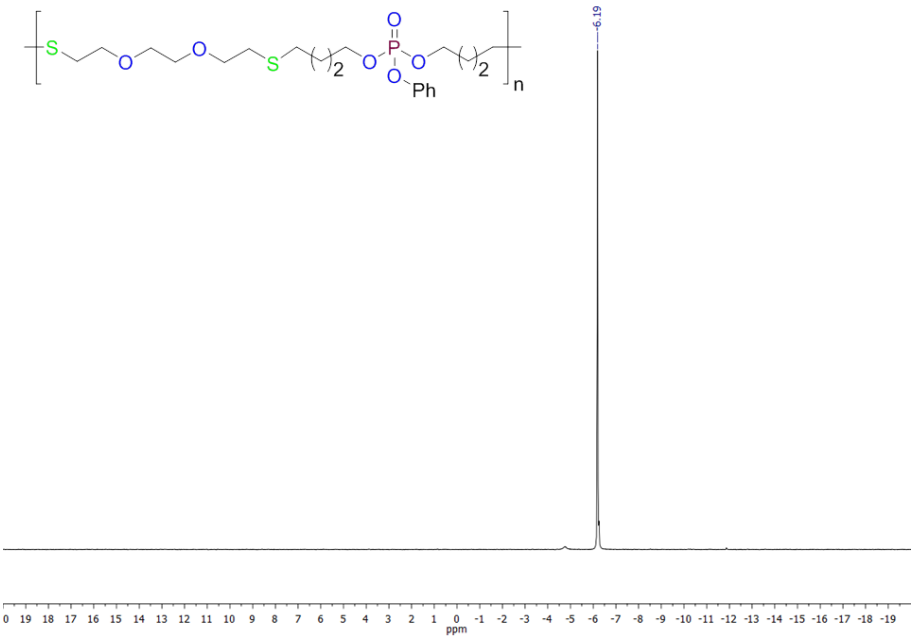

Figure S24: ^{31}P NMR of **Poly(3-co-2)** (202 MHz, 298 K, $CDCl_3$).

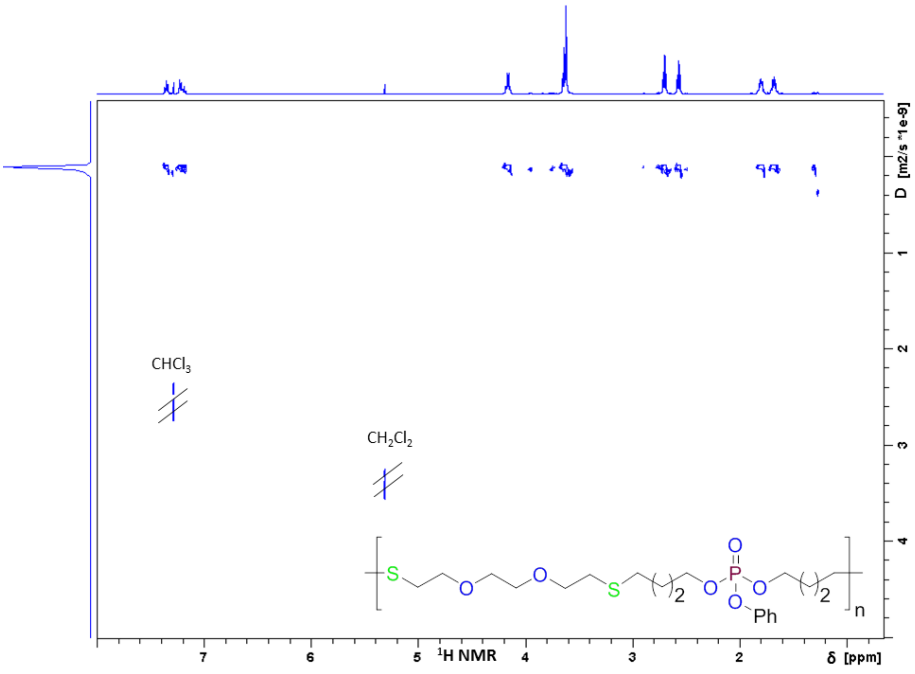

Figure S25: ^{1}H DOSY of **Poly(3-co-2)** (500 MHz, 298 K, $CDCl_3$).

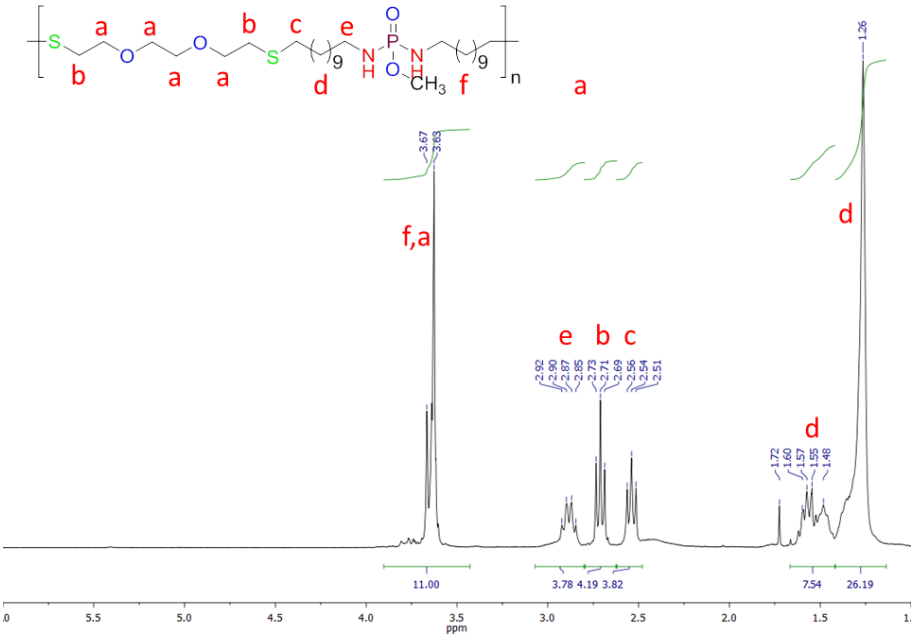

Figure S26: ^{1}H NMR of **Poly(9-co-2)** (300 MHz, 298 K, $CDCl_3$).

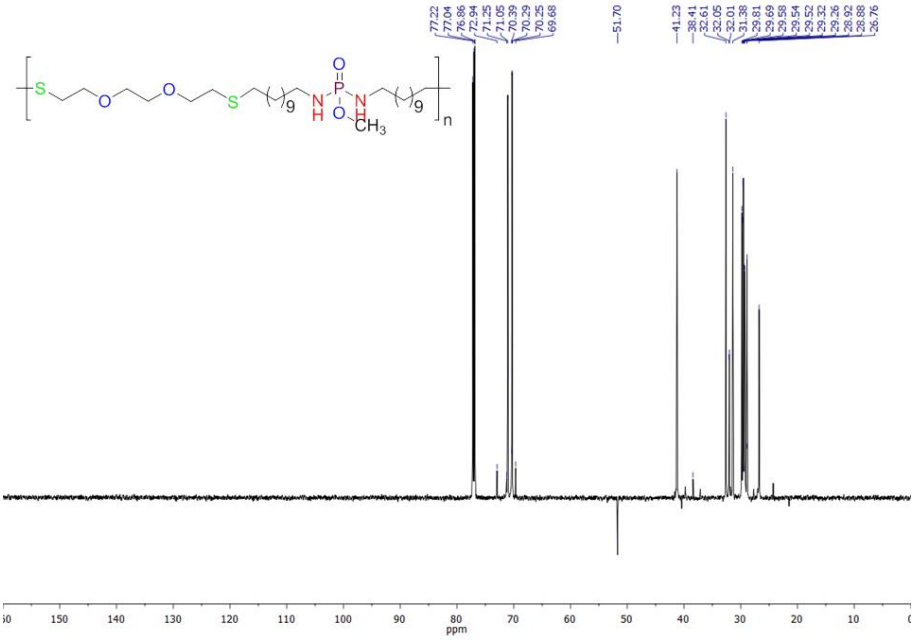

Figure S27: ^{13}C NMR of **Poly(9-co-2)** (176 MHz, 298 K, $CDCl_3$).

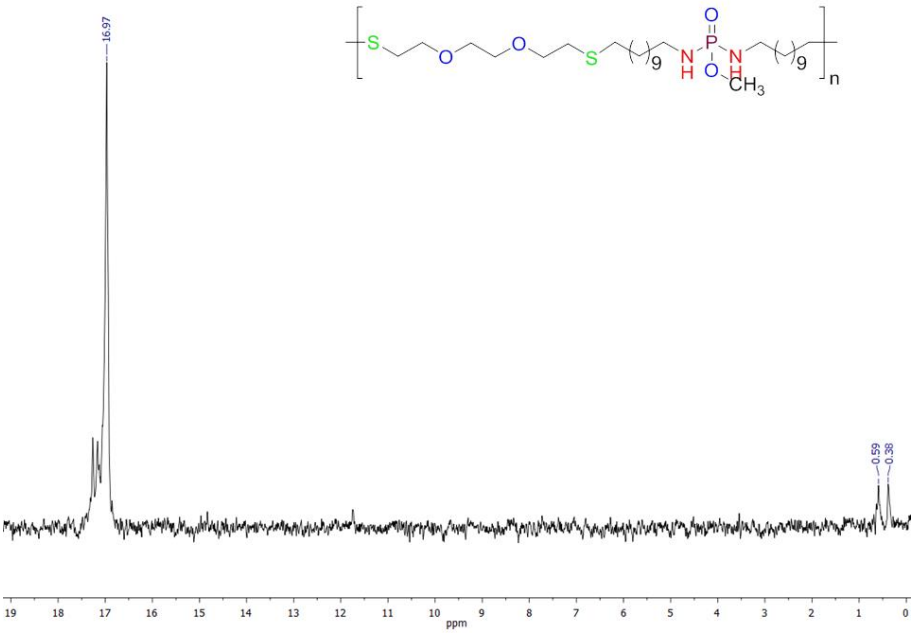

Figure S28: ^{31}P NMR of **Poly(9-co-2)** (202 MHz, 298 K, $CDCl_3$).

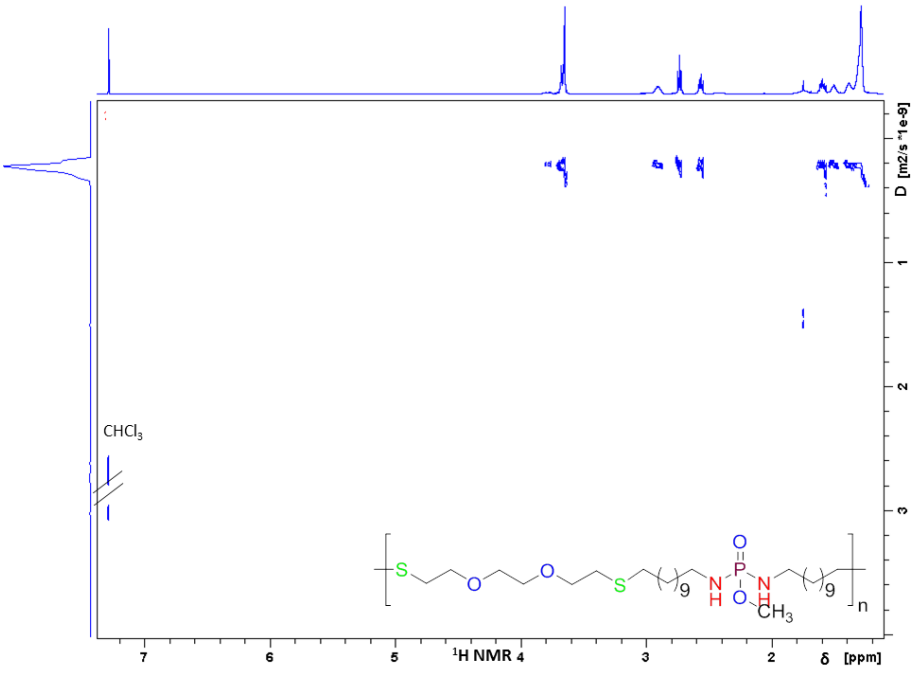

Figure S29: ^{1}H DOSY of **Poly(9-co-2)** (500 MHz, 298 K, $CDCl_3$).

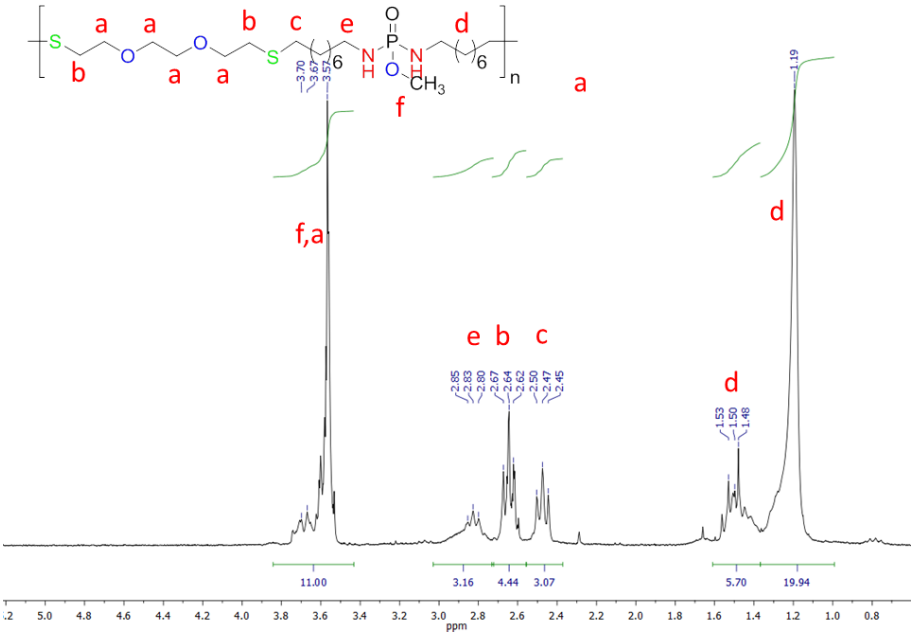

Figure S30: ^{1}H NMR of **Poly(7-co-2)** (250 MHz, 298 K, $CDCl_3$).

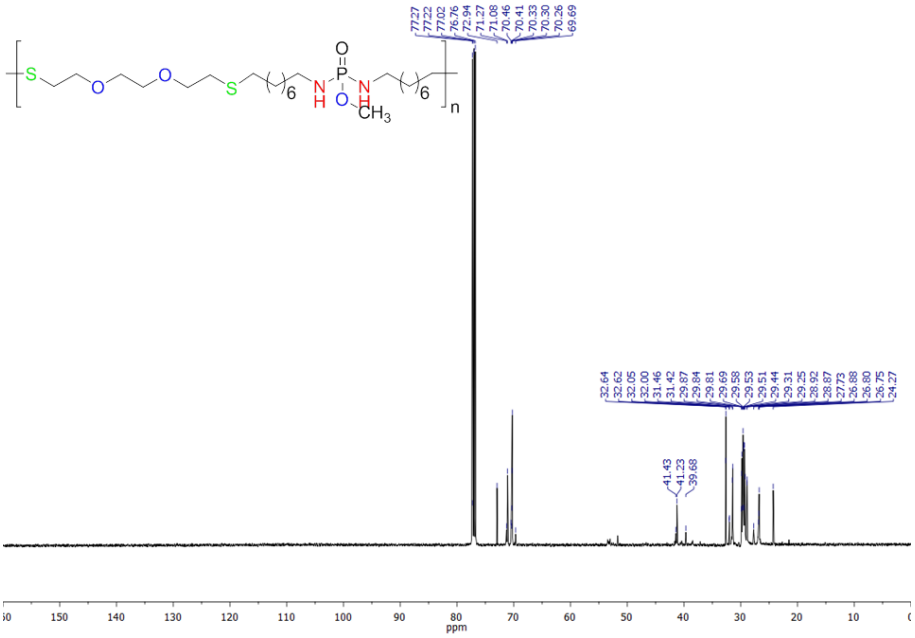

Figure S31: ^{13}C NMR of **Poly(7-co-2)** (126 MHz, 298 K, $CDCl_3$).

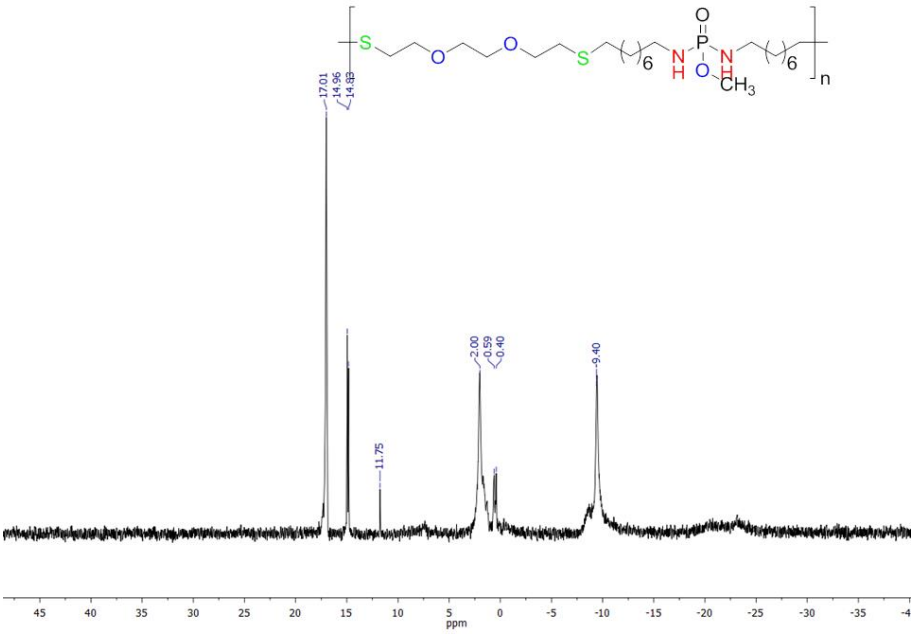

Figure S32: ^{31}P NMR of **Poly(7-co-2)** (202 MHz, 298 K, $CDCl_3$).

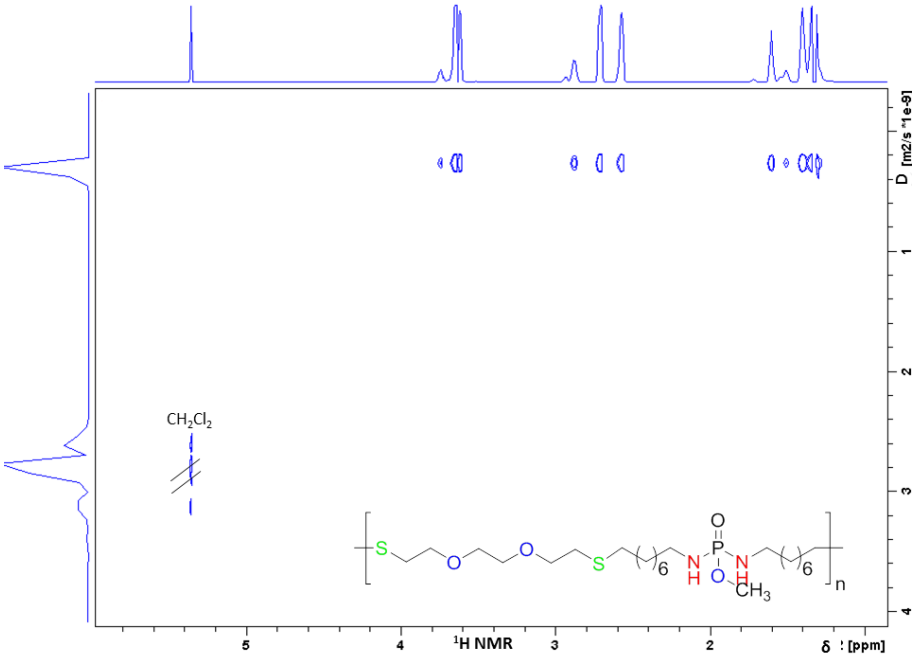

Figure S33: ^{1}H DOSY of **Poly(7-co-2)** (700 MHz, 298 K, CD_2Cl_2).

Thermal Analysis: DSC

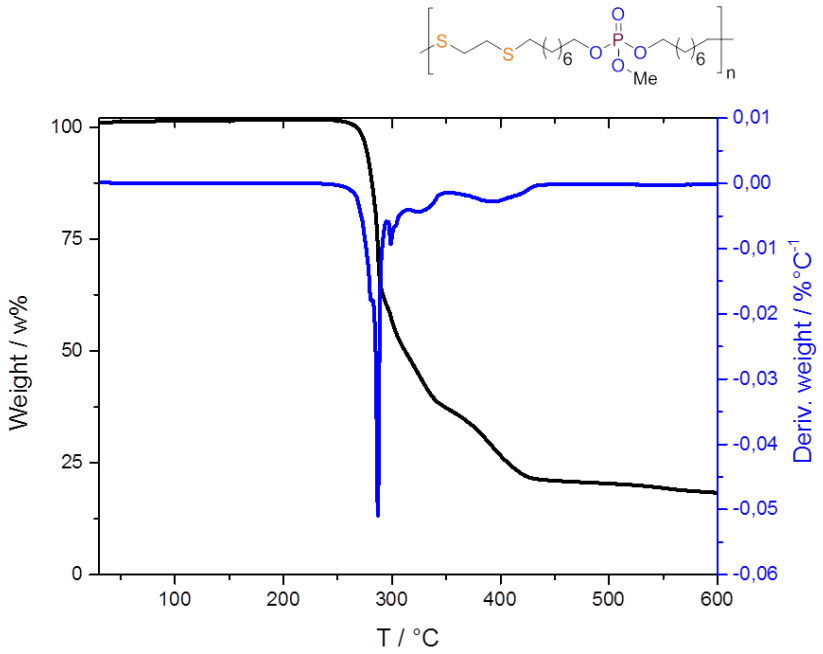

Figure S34: Thermogravimetric analyses (TGA) and derived TGA of **Poly(5-co-1).**

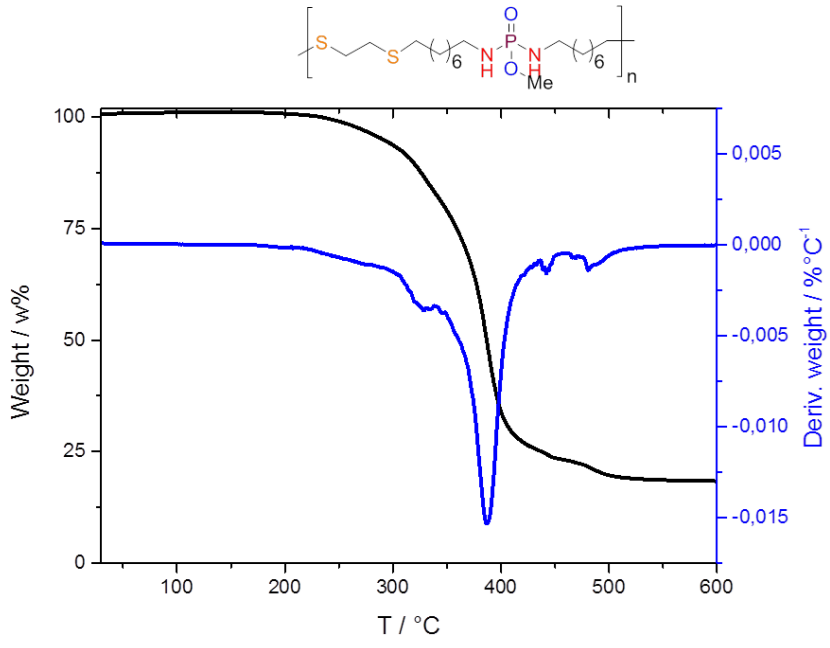

Figure S35: Thermogravimetric analyses (TGA) and derived TGA of **Poly(8-co-1).**

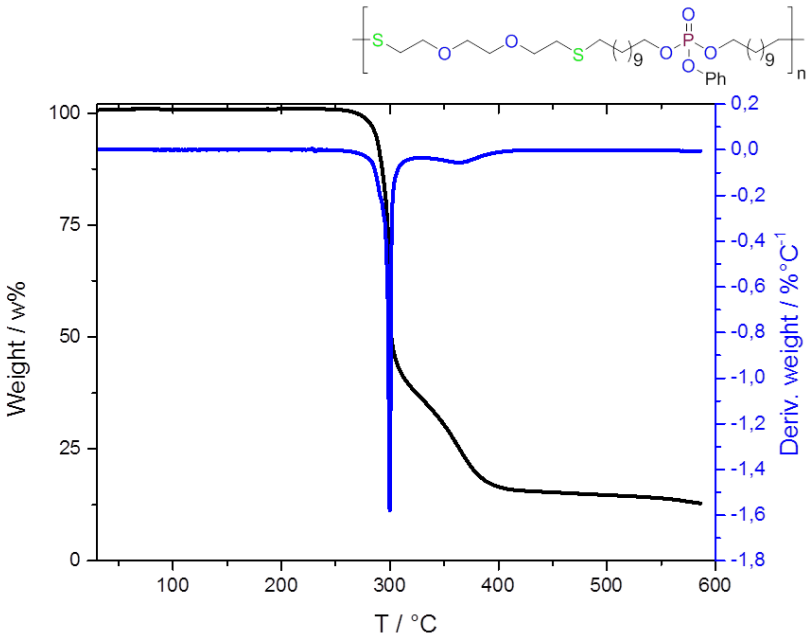

Figure S36: Thermogravimetric analyses (TGA) and derived TGA of **Poly(4-co-2).**

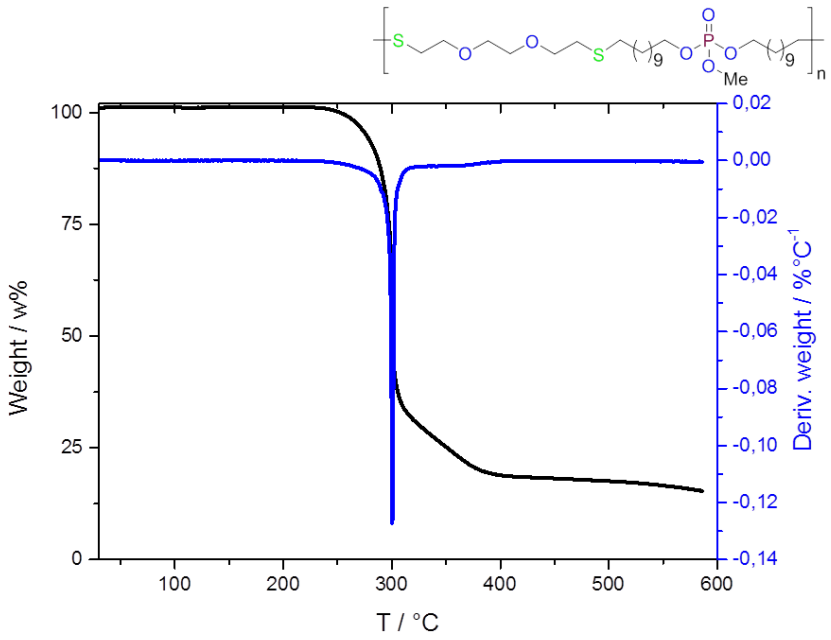

Figure S37: Thermogravimetric analyses (TGA) and derived TGA of **Poly(6-co-2).**

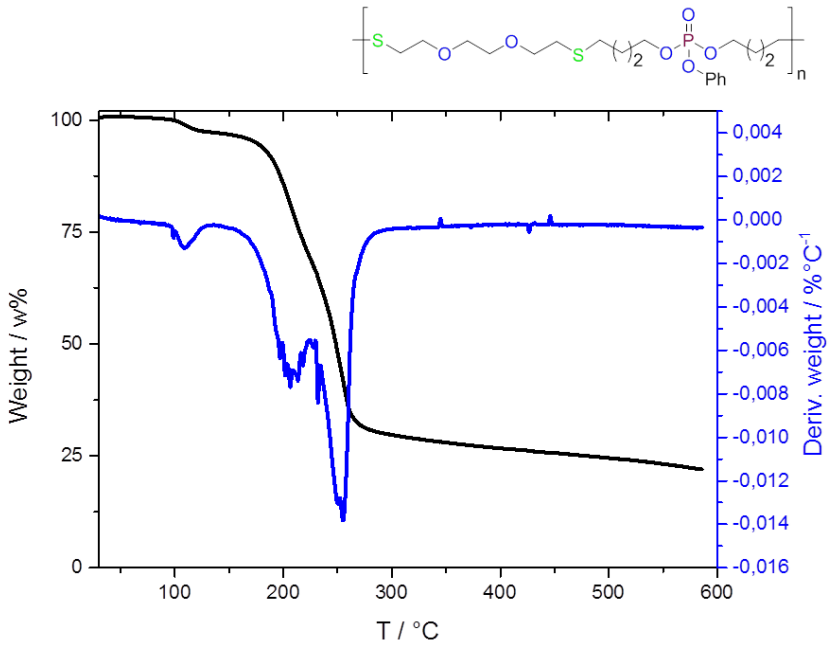

Figure S38: Thermogravimetric analyses (TGA) and derived TGA of **Poly(3-co-2).**

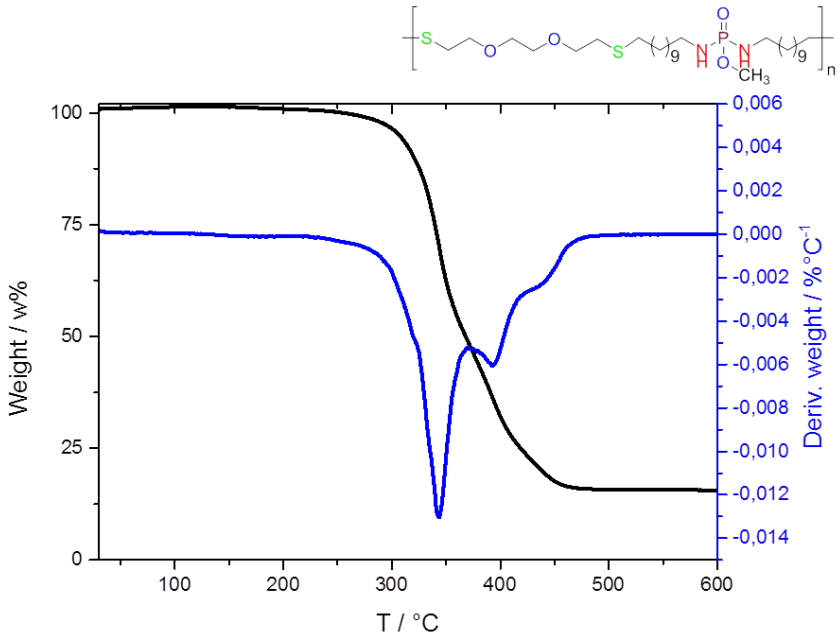

Figure S39: Thermogravimetric analyses (TGA) and derived TGA of **Poly(9-co-2).**

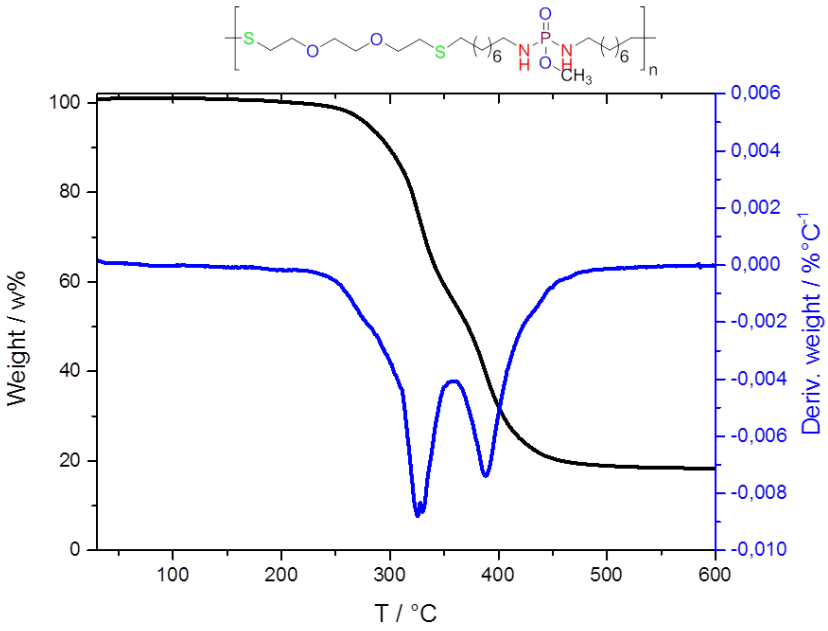

Figure S40: Thermogravimetric analyses (TGA) and derived TGA of **Poly(7-co-2).**

3.4 Poly(phosphorodithiolate)s via ADMET and Thiol-ene Polyaddition

Motivation

Phosphorodithiolates (PDTs) are used as pesticides today.[188] Common examples are Ethoprophos, an insecticide, or Cadusafos, a nematicide.[189-190] (**Figure 1)**.

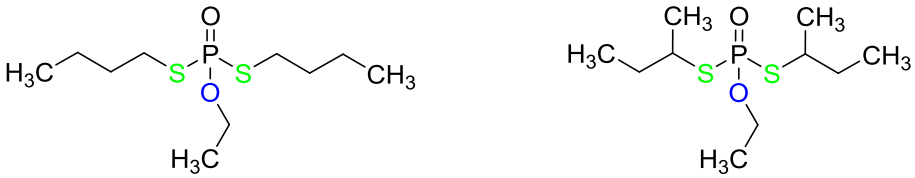

Ethoprophos **Cadusafos**

Figure 1: Commonly used phosphorodithiolate pesticides Ethoprophos (left) and Cadusafos (right).

The mechanism of action of PDTs is the inhibition of acetylcholinesterase in nerve cells, which consequently leads to the eventual death of the organism.[191-192] Other phosphorus-containing organic chemicals act in the same way. The best known class is nerve agents such as sarin or venomous agent X (VX). They were used as chemical warfare agents until an international convention prohibited the production, storage, and use because of potential danger to humankind.[193] This is why pesticides are also considered to be harmful to humans. A lot of research has been done to investigate the potential danger of these compounds.[194] PDTs are suspected to trigger diseases,[195] affect the central nervous system,[196] and pollute the environment,[197] to name a few. Ethoprophos is classified as very toxic and dangerous for the environment.[198] Studies have shown that Ethoprophos is highly toxic to amphibians[199] and rats.[200] Nevertheless, Ethoprophos is approved as pesticide in the EU. In contrast, cadusafos, also declared as very toxic, is not even permitted in the EU.[201]

A potentially safer method of dealing with PDTs may be reached by polymerization. Acute toxicity is usually lower for molecules with high molecular weights. Further imaginable is a longer-term effect of polymerized PDTs as compared to individual PDT molecules. However, prior literature on polymerizing PDTs does not exist. Therefore, this work explores novel

studies in polymerizing PDTs and characterizing these promising materials by using modern synthesis techniques consisting of ADMET polymerization.

Results and Discussion

For the preparation of phosphothioester monomers, unsaturated thiols were prepared. The first experiment was carried out with alkyl bromides and thiourea as a sulfur reagent. After thiourea and undecenyl bromide were dissolved in ethanol, the mixture was heated at reflux for 5 hours (**Scheme 1 (a)**). Afterwards an aqueous sodium hydroxide solution (10 %) was added and additional 2 hours were refluxed to cleave the thioacetate compound. However, the cleavage of the thiouronium bromide was not complete and the already formed thiols were reacting to thioethers and disulfides as a side reaction. The main side product was the formation of disulfides by oxidation, although oxidizing agents were carefully excluded from the experimental setup. Thioethers were also present as minor side products from the harsh conditions for deprotecting the thiol. The resulting ^{1}H NMR spectrum is displayed in **Figure 2 (a):** the triplet at 2.68 ppm belongs to the methylene group next to a disulfide bond and the multiplet at 2.50 ppm belongs to either thioether or thiol functionalities instead of only thiol groups. A triplet of doublets (quartet) at ca. 2.5 ppm had been expected because of splitting from sulfur. Therefore, another method was introduced, this time as an S_N2 reaction of the alkyl bromide with sodium hydrosulfide in *N*-Methyl-2-pyrrolidone (NMP) (**Scheme 1 (b)**). The mixture of sodium hydrosulfide and undecenyl bromide in NMP was heated at 60 °C and stirred overnight. An excess amount of sodium hydrosulfide needed to be used since the resulting thiol may have reacted with one of the remaining alkyl bromides to give thioethers. However, this approach also did not produce the unsaturated thiol successfully. The same side reaction occurred after transforming the bromide into a thiol, and thioethers and disulfides were obtained (**Figure 2 (b)**). To avoid the side reactions, a third experiment was conducted. An α,ω-diene was reacted with thioacetic acid to form an unsaturated thioacetate compound in the first step. To obtain the thioacetate compound, thioacetic acid was added dropwise into a solution of the diene and azobisisobutyronitrile (AIBN) at 60 °C. After 2 hours of vigorous stirring, the thioacetic acid was used up. Purification was accomplished by distillation. To unprotect the thiol, the pure unsaturated thioacetate intermediate was dissolved in a suspension of potassium carbonate and methanol. The reaction mixture was stirred for one hour and then quenched with acid. After purification, the desired product was pure 7-octen-1-thiol (**Scheme 1** and **Figure 2 (c)**).

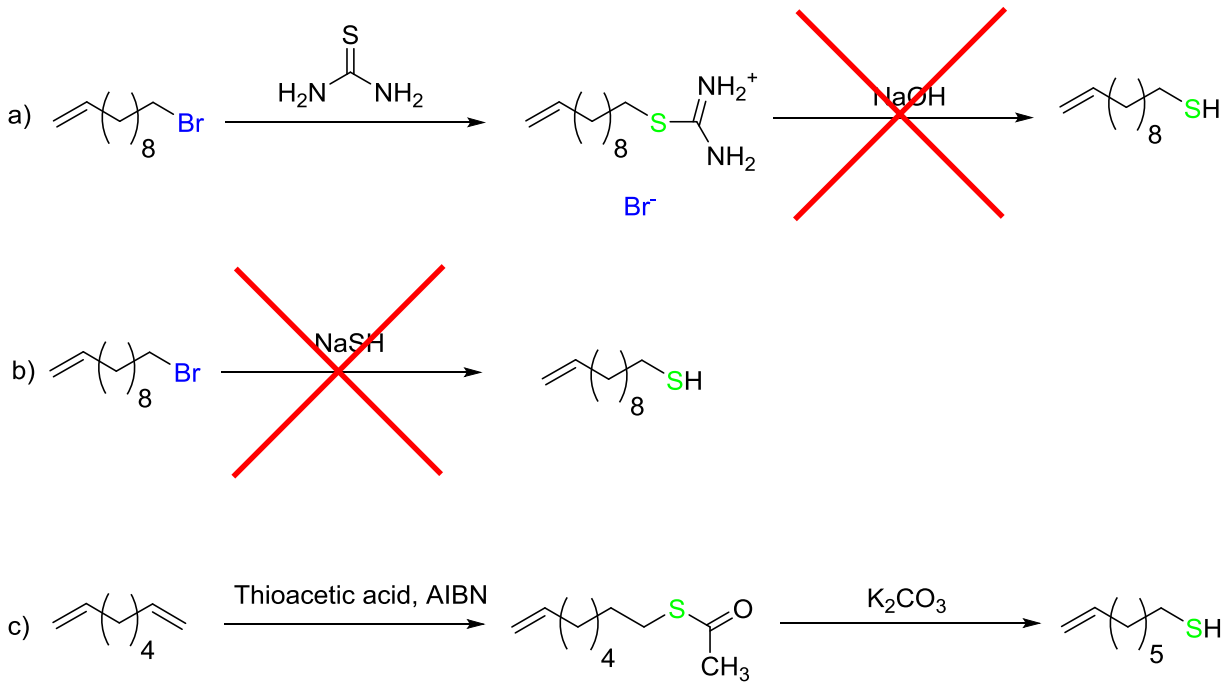

Scheme 1: Different synthesis methods to produce unsaturated thiols. a) thiourea approach; b) sodium hydrosulfide approach; c) thioacetic acid approach.

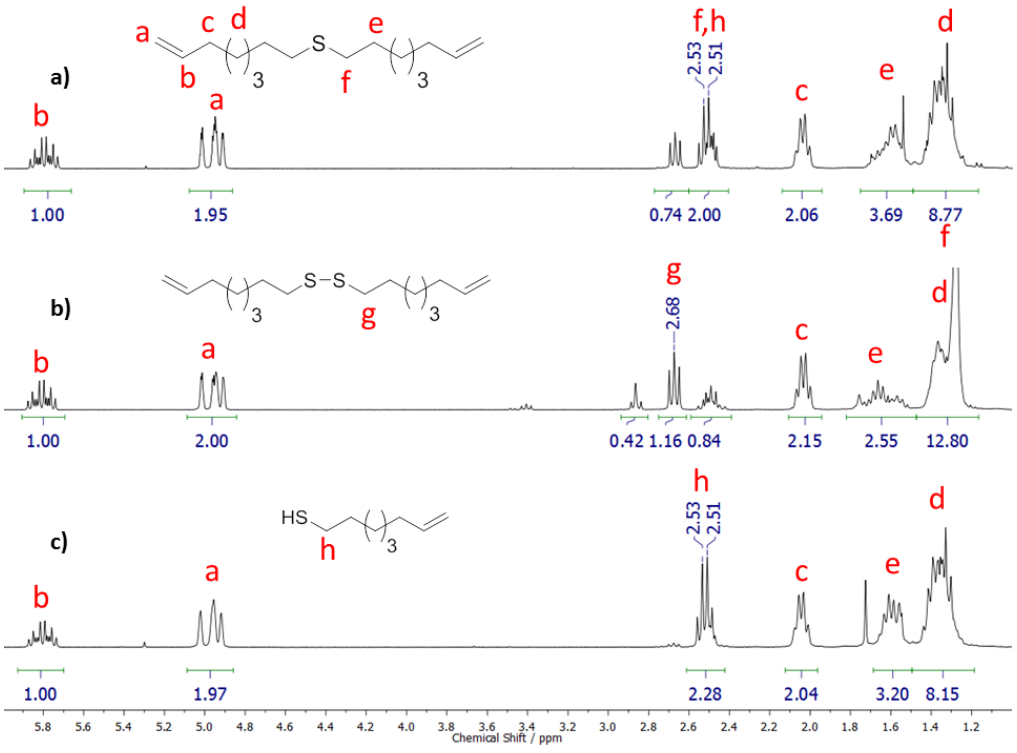

Figure 2: ^{1}H NMR spectra of the products of different attempts to generate unsaturated thiols. a) thiourea approach; b) sodium hydrosulfide approach; c) thioacetic acid approach (300 MHz, 298 K, $CDCl_3$).

Commercially available allyl thiol and the synthesized 7-octen-1-thiol were used to react with methyl dichlorophosphate to give methyl PDTs. First attempts with procedures similar to those discussed above could not produce the desired PDT.[153] Therefore, another synthesis method was adapted from literature.[202] In order to obtain the desired PDT, the thiol was mixed with sodium hydride in dry tetrahydrofuran (THF) until the gas evolution stopped. Afterwards, methyl dichlorophosphate in dry THF was added dropwise to the suspension of sodium hydride and thiol at 0 °C. After stirring at room temperature overnight, the mixture was worked up and crude product was observed. The dissolved monomer in hexane was purified by washing with sodium hydrogencarbonate solution. The reaction is displayed in **Scheme 2**. The monomer synthesis with ally thiol led to the desired *S,S*-bis-(prop-2-en-1-yl)-methylphosphorodithiolate and with 7-octen-1-thiol resulted *S,S*-bis-(oct-7-en-1-yl)-methylphosphorodithiolate (see **Scheme 2**). Additionally, the latter spectrum exhibits beside the monomer the unsaturated disulfide of 7-octen-1-thiol. However it reacts equally as the actual monomer and was also used for polymerization. The resultant ^{1}H NMR spectra of the monomers are shown in **Figure 3** and **Figure 4**. ^{31}P{H} NMR reveals low field phosphorus signals at ca. 65 ppm as expected from literature.[188] For ^{13}C{H} NMR and ^{31}P{H} NMR spectra, see the Supplemental Information section.

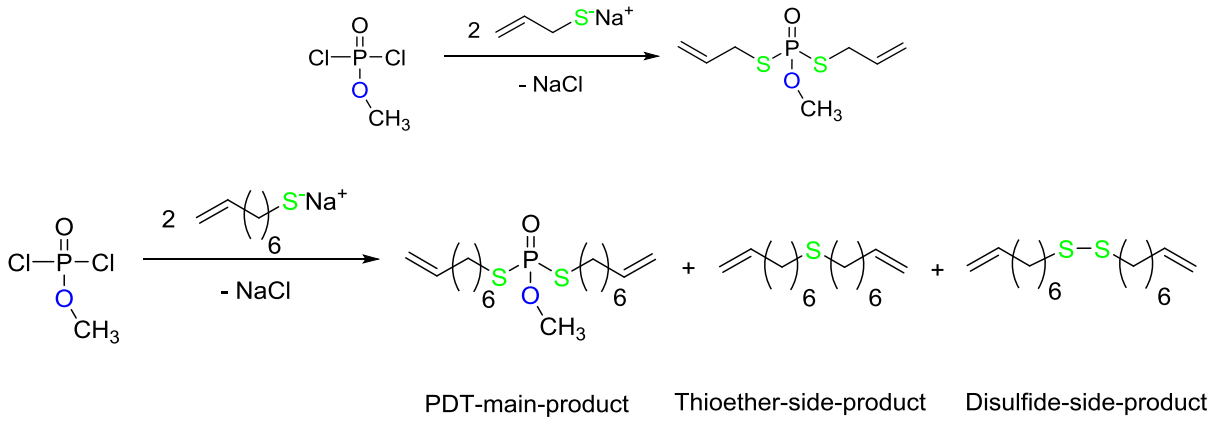

Scheme 2: Unsaturated PDT monomer synthesis including side-products.

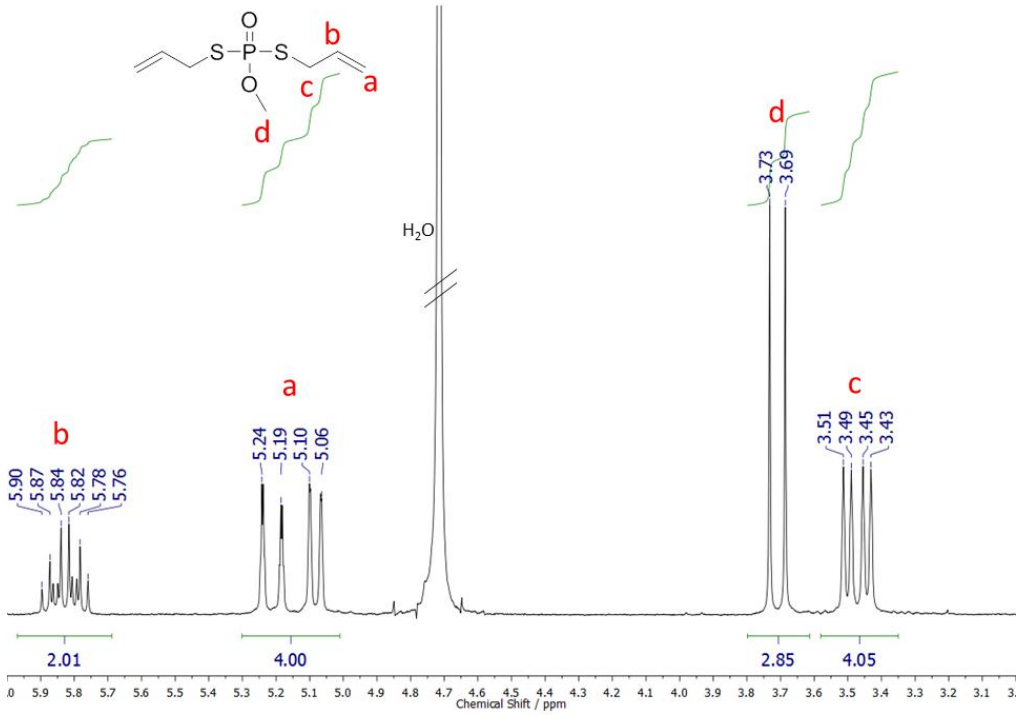

Figure 3: ^{1}H NMR spectrum of *S,S*-bis-(prop-2-en-1-yl)-methylphosphorodithiolate (300 MHz, 298 K, D_2O).

The resonance of the methoxy group from *S,S*-bis-(prop-2-en-1-yl)-methylphosphoro-dithiolate is detected as the typical doublet (3.71 ppm, *J* = 11,2 Hz) due to coupling with the NMR-active phosphorus. The characteristic methylene group next to the phosphorthiolate (at 3.47 ppm) is detected as a doublet of a doublet (c) also due to coupling with phosphorus and the coupling to the acrylate group.

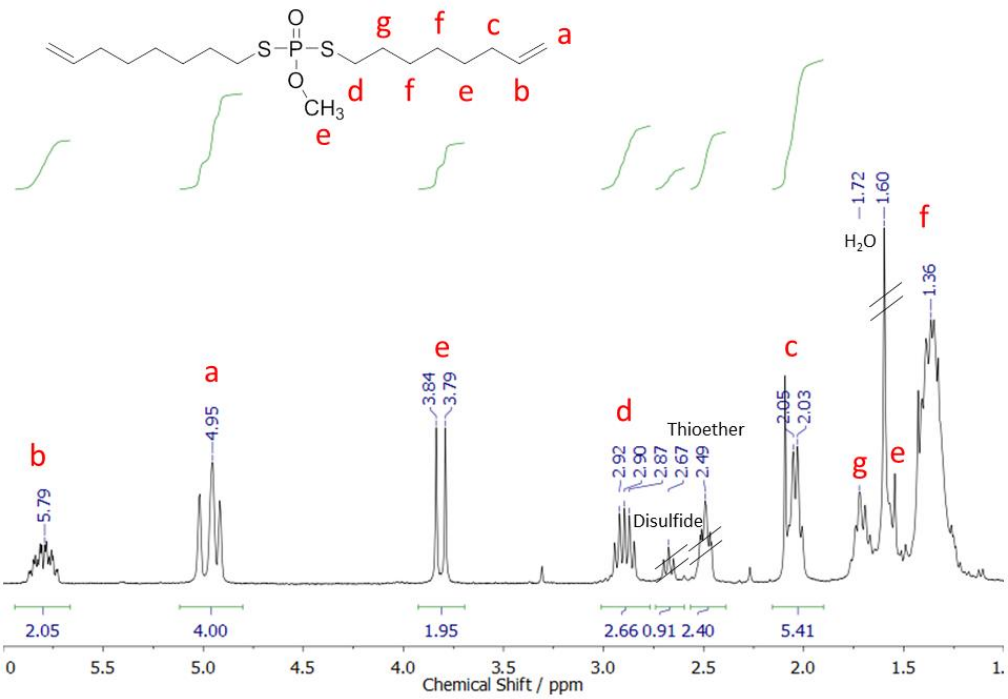

Figure 4: ^{1}H NMR spectrum of *S,S*-bis-(oct-7-en-1-yl)-methylphosphorodithiolate (300 MHz, 298 K, $CDCl_3$).

The ^{1}H NMR spectrum of *S,S*-bis-(oct-7-en-1-yl)-methylphosphorodithiolate (**Figure 4**) shows the characteristic methylene group next to the phosphorthioester which splits into a doublet of triplet (d) due to coupling with phosphorus and the methylene group. Purification was conducted by washing the crude product with hydrochloride acid (10 %), sodium hydrogen carbonate solution and brine. After purification the side products di(oct-7-en-1-yl)sulfane (Thioether at 2.49 ppm) and 1,2-di(oct-7-en-1-yl)disulfane (Disulfide at 2.67 ppm) have not been removed. However both side products are able to polymerize in the same manner and therefore do not have to be removed for the first polymerization approach.

The *S,S*-bis-(prop-2-en-1-yl)-methylphosphorodithiolate monomer is soluble in water. Degradation studies in water were accomplished at pH = 1.0, pH = 9.0, and pH = 13.0. It was observed that the monomer is stable at pH = 1.0 for at least for 30 days. However, in a basic setting, the monomer is easily degradable. 3 hours in a pH = 13.0 environment is enough to completely cleave a phosphorthiolate bond into the *S*-(prop-2-en-1-yl)-methylphosphor-thiolate degradation product (**Scheme 3**; For ^{1}H NMR and ^{31}P{H} NMR spectra of *S*-(prop-2-

en-1-yl)-methylphosphorthiolate, see the Supplemental Information). Only one thiol has been split off of the monomer due to protection from a nucleophilic attack by the anionic nature of the monomer.

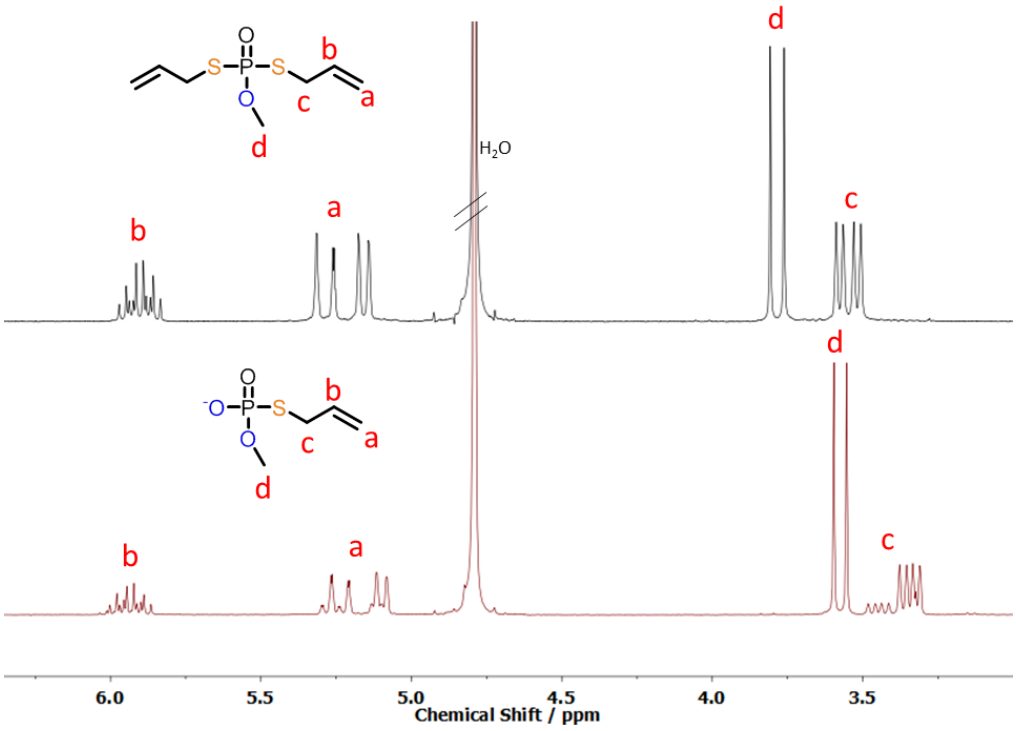

Figure 5: Comparison of ^{1}H NMR spectra of *S,S*-bis-(prop-2-en-1-yl)-methylphosphorodithiolate (top) and degradation product *S*-(prop-2-en-1-yl)-methylphosphorthiolate (bottom) (300 MHz, D_2O, 298K).

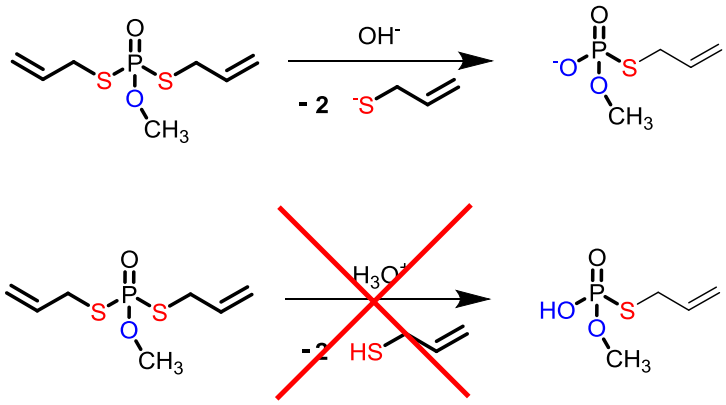

Scheme 3: Degradation process of *S,S*-bis-(prop-2-en-1-yl)-methylphosphorodithiolate by acidic and basic conditions.

At pH = 9.0, PDT degradation is faster. In **Figure 6**, the degradation over time is plotted as a function of the decreasing monomer signal in comparison with *N,N*-bis-(But-3-en-1-yl)-methylphosphorodiamidate as a phosphorodiamidate equivalent monitored by $^{31}P\{H\}$ NMR spectroscopy. After 25 days of treatment, the PDT monomer has almost 70 % of one the phosphorthiolate bonds split off at pH = 9.0. The degradation in acidic conditions of the phosphorothiolate group could not be observed by $^{31}P\{H\}$ NMR spectroscopy after 40 days. In contrast, the phosphoramidate bond of the PDA monomer is cleaved in acidic conditions but not in basic milieus as shown for pH = 8.0. However, even at pH = 9.0, the degradation of the phosphorthiolate bond is faster than at pH = 3.0 for the phosphoramidate equivalent. This behavior of P-N bonds when compared to P-S linkages is an interesting feature for controlled degradation. Experimental data can be found in the Supplemental Information.

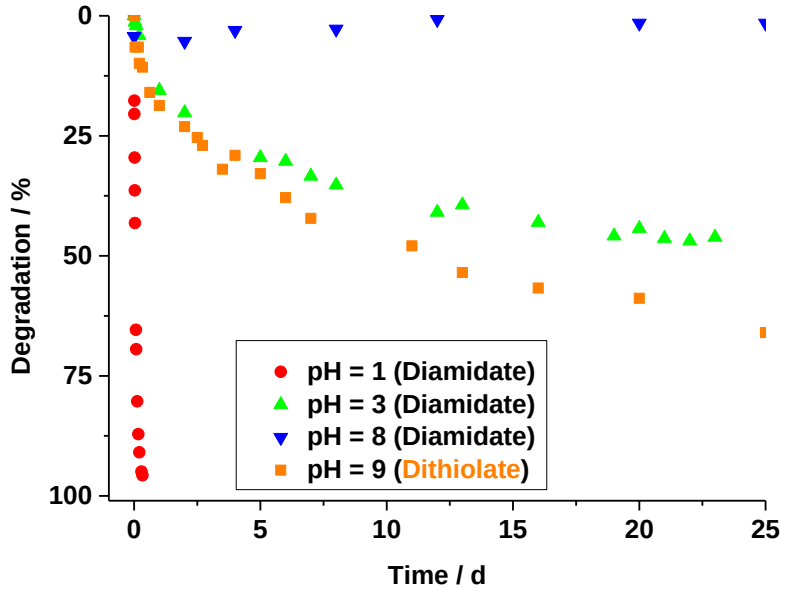

Figure 6: Degradation of *N,N*-bis-(But-3-en-1-yl)-methylphosphorodiamidate (Diamidate) and *S,S*-bis-(prop-2-en-1-yl)-methylphosphorodithiolate (Dithiolate) monitored by $^{31}P\{H\}$ NMR spectroscopy (121.5 MHz, 298 K, D_2O).

Afterwards the new monomers were polymerized via ADMET to obtain PPDTs. The *S,S*-bis-(prop-2-en-1-yl)-methylphosphorodithiolate monomer was not able to polymerize by using ADMET. That result was expected due to the negative neighboring effect as observed before.[153] The expected polymer synthesis via ADMET polymerization is shown in **Scheme 4**.

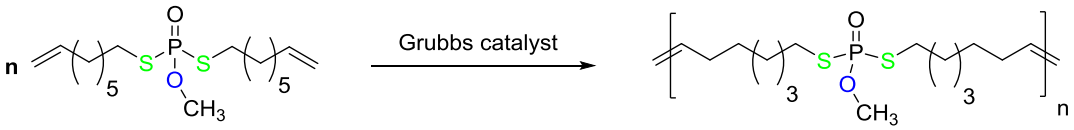

Scheme 4: Polymerization of *S,S*-bis-(oct-7-en-1-yl)-methylphosphorodithiolate by ADMET approach.

The ADMET polymerization of *S,S*-bis-(oct-7-en-1-yl)-methylphosphorodithiolate was successfully conducted. The resulting polymer was measured by ^{1}H NMR and ^{1}H DOSY NMR and is shown in **Figure 7** and **Figure 8,** respectively. NMR spectroscopy allows the calculation of the absolute molecular weight by integration of the terminal olefinic resonances in comparison with the internal double bonds (see **chapter 2**). The polymer exhibits a molecular weight of 2,600 g · mol^{-1} by integration of ^{1}H NMR signals. By the ^{1}H DOSY NMR molecular weight determination method (see **chapter 3**) the weight average molecular weight is 6,200 g · mol^{-1}. GPC data reveals a molecular weight of 4,500 g · mol^{-1}. Unfortunately all methods show different molecular weights. However it can be used as prove of polymerization for PDTs to PPDTs for the first time. ^{31}P{H} NMR, ^{13}C{H} NMR as well as GPC data and ^{1}H DOSY experiments, are provided in the Supplemental Information.

In **Figure 7** the copolymer of the PDT and the side-products of the monomer synthesis are displayed. The thioether (h) and the disulfide (g) resonance signal together with only one signal in ^{1}H DOSY NMR (**Figure 8**) confirm the successful polymerization and the integration of thioether and disulfide groups into the polymer.

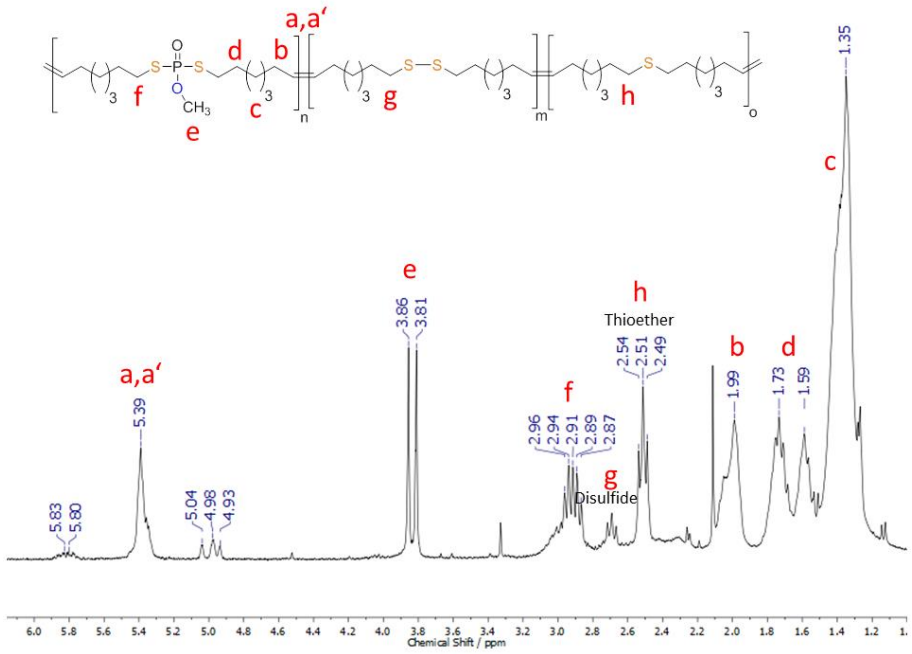

Figure 7: ^{1}H NMR polymer spectrum of *S,S*-bis-(oct-7-en-1-yl)-methylphosphorodithiolate by ADMET approach (300 MHz, 298 K, $CDCl_3$).

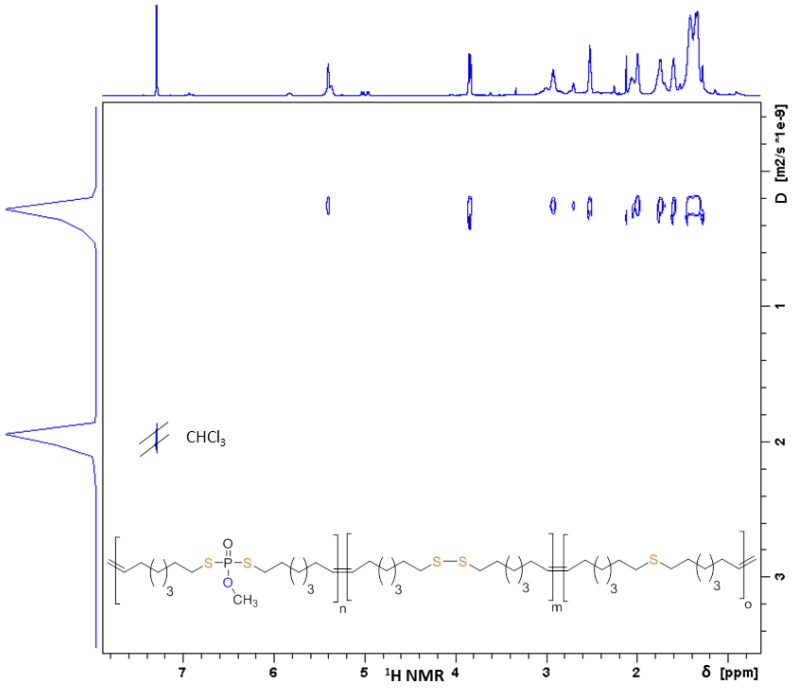

Figure 8: ^{1}H DOSY NMR polymer spectrum of *S,S*-bis-(oct-7-en-1-yl)-methylphosphorodithiolate by ADMET approach (700 MHz, 298 K, $CDCl_3$).

Thermal properties

Differential scanning calorimetry (DSC) reveals a glass transitions temperature (T_g) of -73.5 °C (0.633 $Jg^{-1}K^{-1}$) and a crystallization point of -33 °C (-3.27 Jg^{-1}; **Figure 9**). These values indicate a similar behavior to PPEs by comparing T_g's. PPDA instead show usually higher T_g's. The melting point of -33 °C exhibits an unusual low melting enthalpy (ΔH_m). This could be due to the different monomers within the polymer, which probably exhibit different crystallite structures. Moreover the polymer is behaving as a rubber-like material at room temperature, which was not observed for PPEs and PPDAs. This indicates that the PPDT has few crystalline areas which are transform into an amorphous state at -33 °C. Degradation temperatures around 300 °C and charcoal residues of ca. 20 % monitored by thermogravimetric analysis (TGA) are similar to PPEs but exhibit lower degradation temperatures and charcoal residues as PPDAs (**Figure 10**).

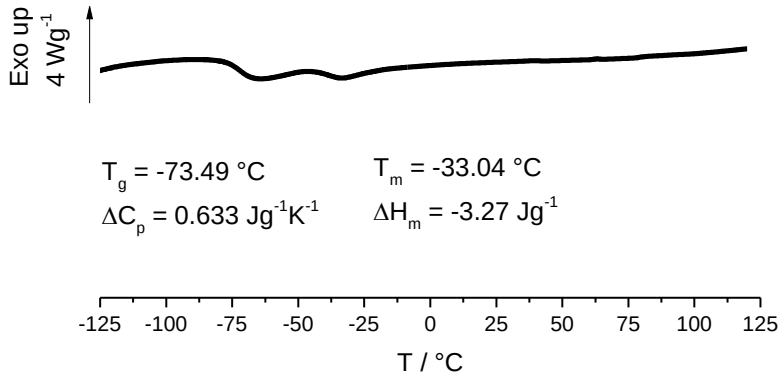

Figure 9: DSC thermogram of ADMET polymer of *S,S*-bis-(oct-7-en-1-yl)-phosphorodithiolate.

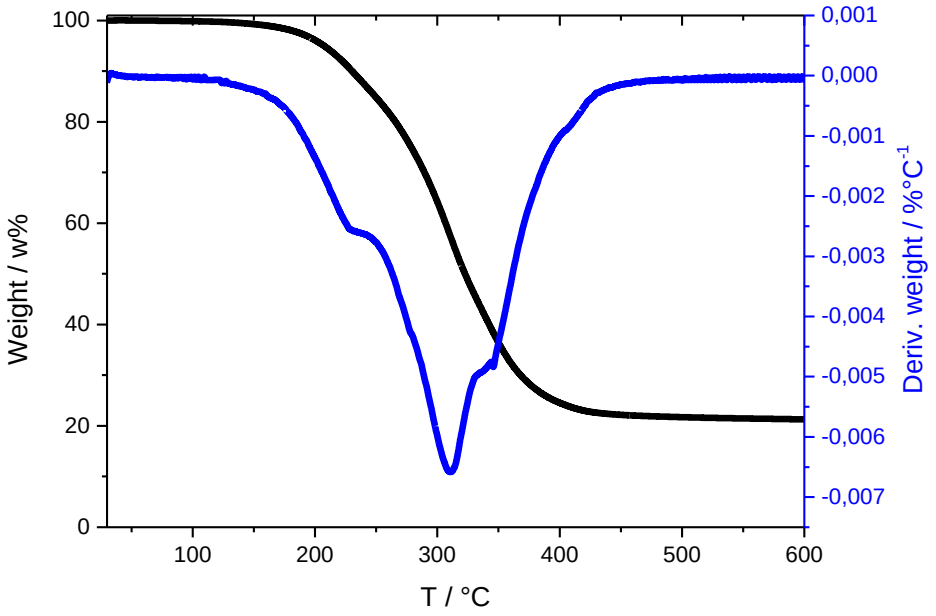

Figure 10: Thermogravimetric analyses (TGA) and derived TGA of ADMET polymer consisting of *S,S*-bis-(oct-7-en-1-yl)-methylphosphorodithiolate.

Conclusion

In summary, this novel unsaturated phosphodithiolates have been prepared and polymerized by ADMET. Two new monomers, namely *S,S*-bis-(prop-2-en-1-yl)-methylphosphorodithiolate and *S,S*-bis-(oct-7-en-1-yl)-phosphorodithiolate. *S,S*-bis-(prop-2-en-1-yl)-methylphosphorodithiolate could not be polymerized. Instead, degradation experiments were done to show that the compound is stable at lower pH values (pH < 7.0) for at least 30 days. In comparison, the PDT monomer was relatively labile in basic conditions. At pH = 13.0, the monomer was completely degraded after 3 hours. However, the cleavage of phosphorthiolate groups was slower at lower pH values, at pH = 9.0. Here degradation occurred up to 70 % in 25 days. It features only one phosphorthiolate bond cleavage in basic conditions instead of both functionalities as the phosphorodiamidates in acidic media. This is due to the stabilization of the remaining phosphorthiolate bond by negatively charged oxygen. Nucleophilic attack is inhibited. This inverse behavior of P-N bonds compare to P-S linkages can be used for biomedical applications as for controlled drug release etc. Furthermore, the polymerization of *S,S*-bis-(oct-7-en-1-yl)-methyl-phosphorodithiolate was successfully introduced via ADMET reaction for the first time, whereas thiol-ene polyaddition do not provide polymers.

Experimental Section

Chemicals. Phosphate buffered saline (BioPerformance Certified, pH 7.4; PBS buffer), 2,2'-(ethylenedioxy)diethanethiol 95 %, sodium hydride 95 %, potassium chloride >99 %, AIBN 98 %, sodium hydroxide p.a., tris base >99,9 % were purchased from Sigma Aldrich and used as received. Diethylether, Dichloromethane (CH_2Cl_2), thioacetic acid 98 %, and tetrahydrofuran (THF) were purchased from Acros and used as received. Methyl dichlorophosphate 85% was purchased from Sigma Aldrich and purified by distillation before use. Hoveyda-Grubbs Catalyst 2nd Generation 97% was purchased from Sigma Aldrich and stored under argon. 1,7-Octadiene >98 % was purchased from Merck. Methanol (HPLC grade was purchased from VWR. Potassium carbonate 99.5 % was purchased from WTL Laborbedarf.

Methods. See methods of publications used in this thesis.

Synthesis of 7-octen-1-thiol

Thioacetic acid (5.18 g, 4.9 ml, 0.0681 mol, 1.0 eq.) was added dropwise to a stirred solution of AIBN (0.67 g, 0.409 mmol, 0.03 eq.) in 1,7-octadiene (7.50 g, 10.0 ml, 0.0681 mol, 1.0 eq.) at 60 °C. Afterwards the resulting suspension was clearing up and stirred for 2 h at 60 °C. Subsequently, the desired unsaturated thioacetate was purified by distillation (100 °C at 5 · 10^{-2} mbar; yield: 5.0 g, 43 %). The pure intermediate was added to a suspension of K_2CO_3 (10.35 g, 0.0749 mol, 1.1 eq.) in MeOH (80 ml) which was stirred at room temperature for half an hour. After 1 h of stirring the reaction was quenched by diluted HCl (0.03 M). The thiol was extracted with CH_2Cl_2 (3x50 ml). The CH_2Cl_2 phase was washed with brine and dried over Na_2SO_4, filtered, and concentrated at reduced pressure. The crude unsaturated thiol was used without further purification. (Yield: 4.10 g, 0.0293 mmol; 95 %). ^{1}H NMR (250 MHz, 298 K, $CDCl_3$, δ / ppm): 5.90 – 5.59 (m, 1H), 5.03 – 4.78 (m, 2H), 2.54 – 2.30 (td, J = 7.4 Hz, 2H), 2.12 – 1.84 (m, J = 6.7 Hz, 2H), 1.63 – 1.42 (m, 3H), 1.42 – 1.04 (m, 7H). ^{13}C{H} NMR (176 MHz, 298 K, $CDCl_3$, δ / ppm): 139.0, 139.0, 114.3, 114.2, 39.2, 34.0, 34.0, 33.7, 33.7, 32.2, 29.7, 29.1, 29.1, 29.0, 28.9, 28.9, 28.8, 28.7, 28.5, 28.3, 28.2, 25.2, 24.6. ESI-MS m/z 432.33 $[3M+H]^+$, 577.44 $[4M+H]^+$, (Calculated for $C_8H_{16}S$: 144.10). Calcd C 66.60. H 11.18. S 22.22; found C 66.44. H 11.27. S 22.29.

Monomer syntheses:

Representative procedure for synthesis of the phosphorodithiolate monomers

***S,S*-Bis-(prop-2-en-1-yl)-methylphosphorodithiolate.** Methyl dichlorophosphate (1.00 g, 0.67 ml, 6.715 mmol, 1.0 eq.) in dry THF (20 ml) was added dropwise to a stirred suspension of ally thiol (1.00 g, 1,11 ml, 13.431 mmol, 2.0 eq.) and sodium hydride ((387 mg, 16.116 mmol, 2.4 eq.) in dry THF (50 ml) at 0 °C after the gas evolution was completed (10 min). After stirring overnight at room temperature the resulting suspension was diluted by diethyl ether (80 ml), washed with saturated NH_4Cl solution, water, and brine. The organic layer dried over Na_2SO_4, filtered, and concentrated at reduced pressure. The crude product was dissolved in hexane and washed with sodium hydrogen carbonate solution to observe pure *S,S*-bis-(prop-2-en-1-yl)-methylphosphorodithiolate (Yield: 620 mg, 2.855 mmol; 41 %). ^{1}H NMR (300 MHz, 298 K, D_2O, δ / ppm): 5.97 – 5.69 (td, J = 17.0, 7.1 Hz, 2H), 5.30 – 5.01 (m, 4H), 3.80 – 3.61 (d, J = 13.9 Hz, 3H), 3.58 – 3.35 (dd, J = 17.5, 7.1 Hz, 4H). ^{13}C{H} NMR (75 MHz, 298 K, $CDCl_3$, δ / ppm): 133.0, 133.0, 132.9, 132.8, 119.1, 118.8, 53.7, 53.6, 42.3, 35.6, 35.5, 34.5, 34.5, 30.3. ^{31}P{H} NMR (121.5 MHz, 298 K, D_2O, δ / ppm): 65.24. ESI-MS m/z 225.03 $[M+H]^+$, 247.00 $[M+Na]^+$, (Calculated for $C_7H_{13}O_2PS_2$: 224.01). Calcd C 37.49. H 5.84. S 28.59; found C 37.37. H 5.68. S 28.77.

***S,S*-Bis-(oct-7-en-1-yl)-methylphosphorodithiolate.** Following the representative procedure described above using 7-octen-1-thiol, *S,S*-bis-(oct-7-en-1-yl)-methylphosphorodithiolate was obtained as colorless oil (Yield: 40 %). ^{1}H NMR (300 MHz, 298 K, $CDCl_3$, δ / ppm): 5.94 – 5.66 (s, 2H), 5.12 – 4.80 (s, 4H), 3.93 – 3.69 (d, J = 13.6 Hz, 2H), 3.01 – 2.77 (m, 3H), 2.74 – 2.60 (s, 1H), 2.16 – 1.90 (d, J = 6.6 Hz, 5H). ^{13}C{H} NMR (75 MHz, 298 K, $CDCl_3$, δ / ppm): 139.0, 138.9, 138.8, 114.4, 114.3, 114.2, 53.4, 53.3, 39.1, 34.3, 33.7, 33.6, 32.1, 31.9, 31.9, 30.4, 30.3, 29.6, 29.1, 29.1, 28.8, 28.7, 28.4, 28.4, 15.5. ^{31}P{H} NMR (121.5 MHz, 298 K, $CDCl_3$, δ / ppm): 59.03.

Procedure for the ADMET copolymerization of methylphosphate monomers and phosphorodithiolate monomers

Polymer of *S,S*-Bis-(oct-7-en-1-yl)-methylphosphorodithiolate. *S,S*-Bis-(oct-7-en-1-yl)-phosphorodithiolate (100 mg, 0.274 mmol, 1 eq) Hoveyda-Grubbs catalyst 2st generation (5.2 mg, 0.0082 mmol, 3 mol% and 3 mol% after 24 h) were placed in a glass Schlenk tube equipped with a magnetic stir bar under an argon atmosphere. The reaction was carried out at reduced pressure at a temperature of 60 °C for 48 h. The polymer was obtained as brownish rubber-like substance in quantitative yield. ^{1}H NMR (300 MHz, 298 K, $CDCl_3$, δ / ppm): 5.94 – 5.70 (m), 5.54 – 5.26 (m), 5.12 – 4.87 (m), 3.98 – 3.66 (m), 3.13 – 2.79 (m), 2.15 – 1.89 (m), 1.82 – 1.66 (m), 1.66 – 1.50 (m), 1.52 – 1.02 (m). ^{13}C{H} NMR (176 MHz, 298 K, $CDCl_3$, δ/ ppm): 130.4, 130.3, 130.1, 114.4, 32.5, 32.2, 31.9, 30.4, 29.7, 29.4, 29.2, 28.9, 28.6, 27.9, 27.2, 26.5. ^{31}P{H} NMR (121.5 MHz, 298 K, $CDCl_3$, δ/ ppm): 59.01.

Procedure for the degradation by pH

S,S-Bis-(prop-2-en-1-yl)-methylphosphorodithiolate (6.0 mg) were dissolved into 0.6 ml deuterated buffer solution (pH = 1.0: 0.136 mM hydrogen chloride - potassium chloride solution, pH = 9.0: 0.100 mM tris - hydrogen chloride solution, pH = 13: 0.145 mM sodium hydroxide - potassium chloride solution). The mixtures were poured in NMR tubes and measured during the degradation.

Supporting Information for

Phosphorodithiolates Polymers

*Mark Steinmann, Frederik R. Wurm**

Max-Planck-Institut für Polymerforschung, Ackermannweg 10, 55128 Mainz, Germany.

Contact address: wurm@mpip-mainz.mpg.de

GPC

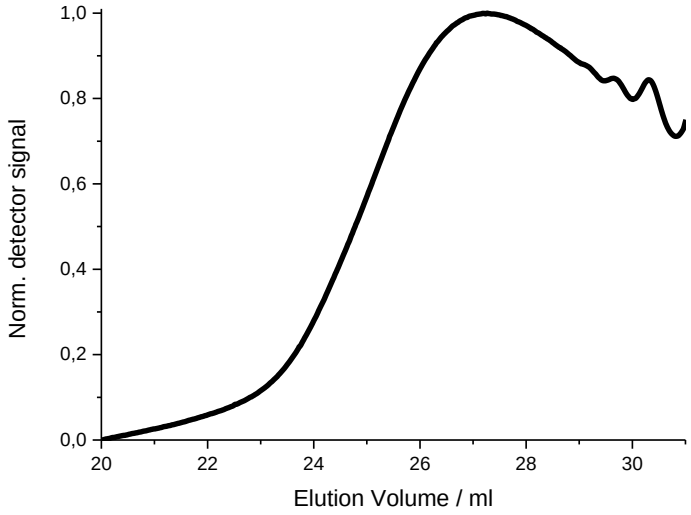

Figure S1: GPC-elugram of ADMET polymer of S,S-bis-(oct-7-en-1-yl)-methylphosphorodithiolate (M_n = 4,500 g·mol^{-1}) in THF measured by RI-detector.

Degradation

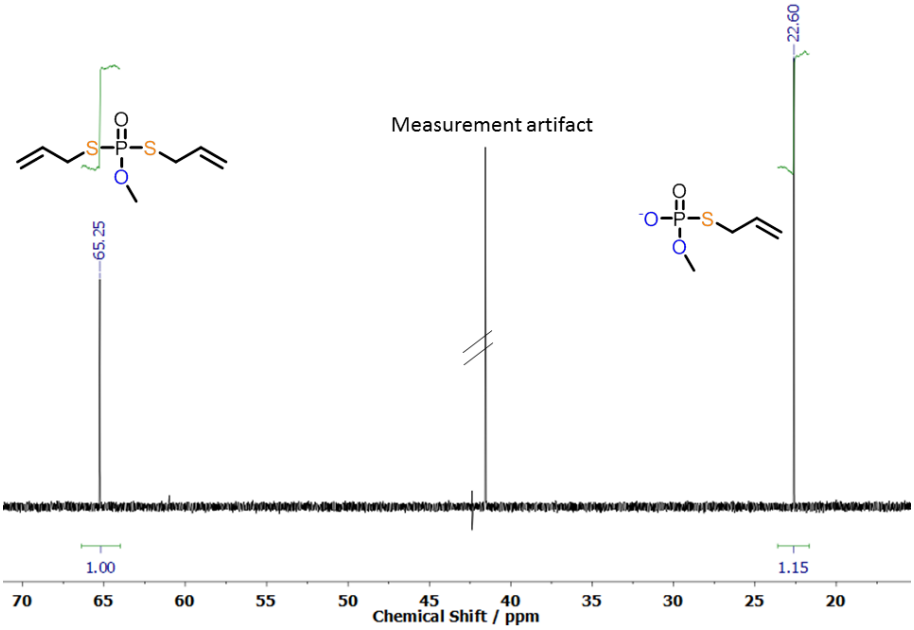

Figure S2: $^{31}P\{H\}$ NMR spectra of *S,S*-bis-(prop-2-en-1-yl)-methylphosphorodithiolate (left) and degradation product *S*-(prop-2-en-1-yl)-methylphosphorthiolate (right) after 13 days (121.5 MHz, D_2O, 298K).

NMR spectra: Monomers:

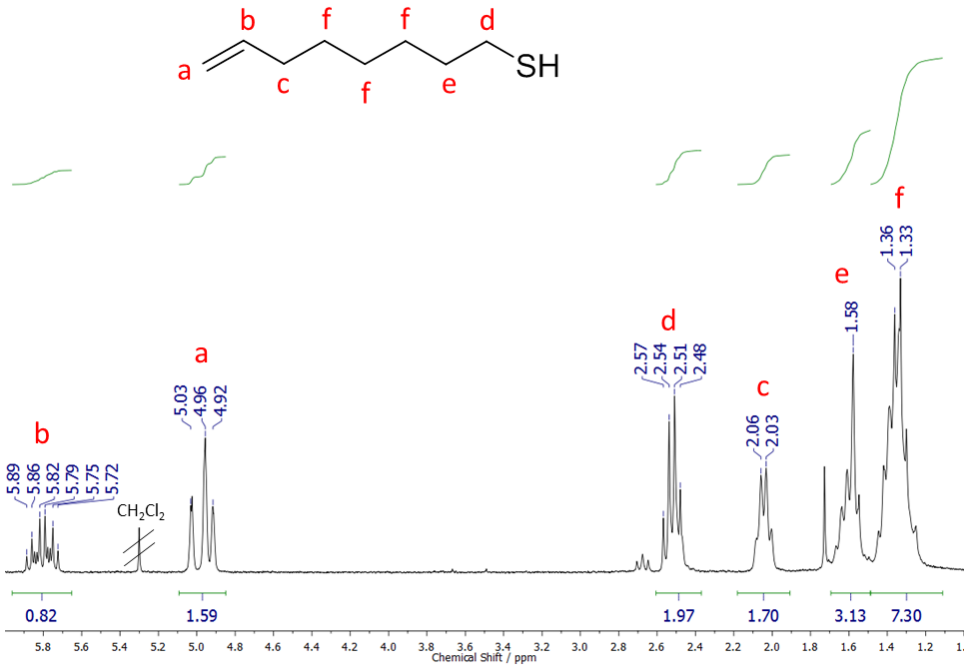

Figure S3: ^{1}H NMR of 7-octen-1-thiol (250 MHz, 298 K, $CDCl_3$).

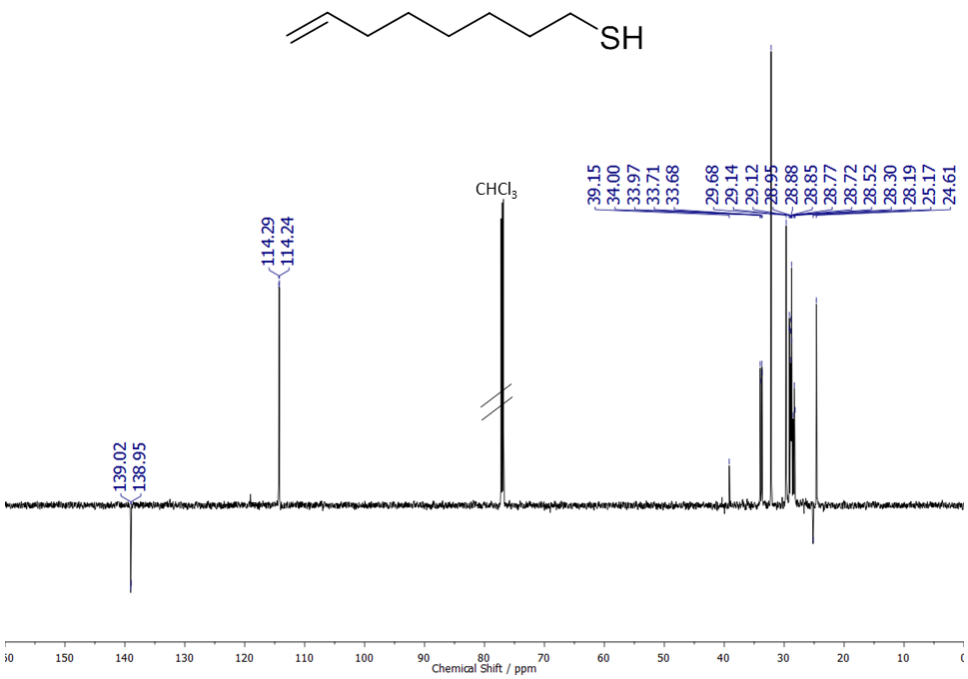

Figure S4: DEPT-135 ^{13}C{H} NMR of 7-octen-1-thiol (176 MHz, 298 K, $CDCl_3$).

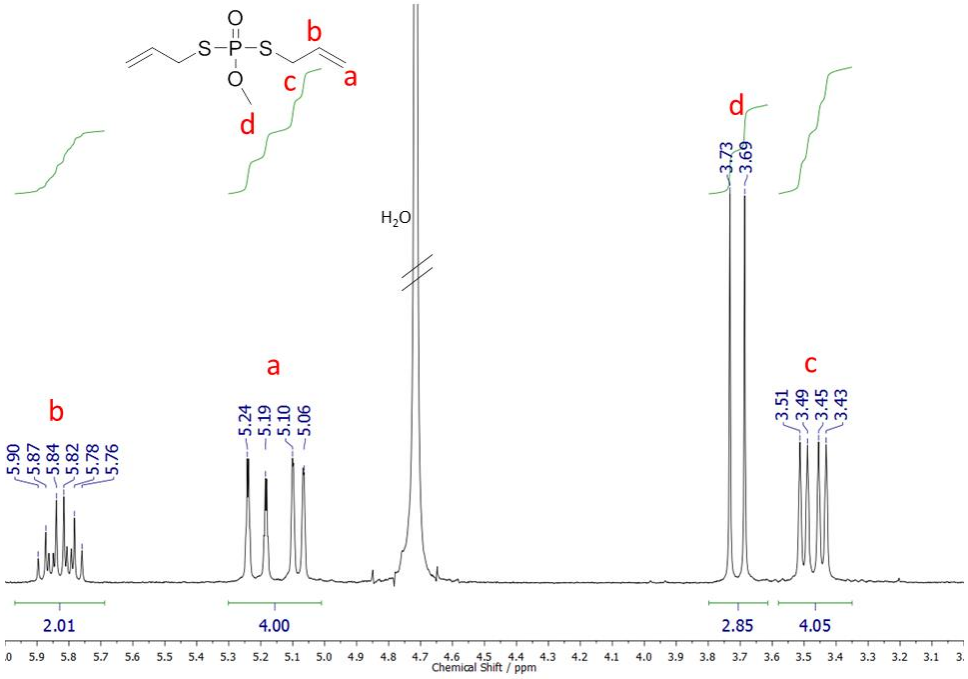

Figure S5: ^{1}H NMR of *S,S*-bis-(prop-2-en-1-yl)-methylphosphorodithiolate (300 MHz, 298 K, D_2O).

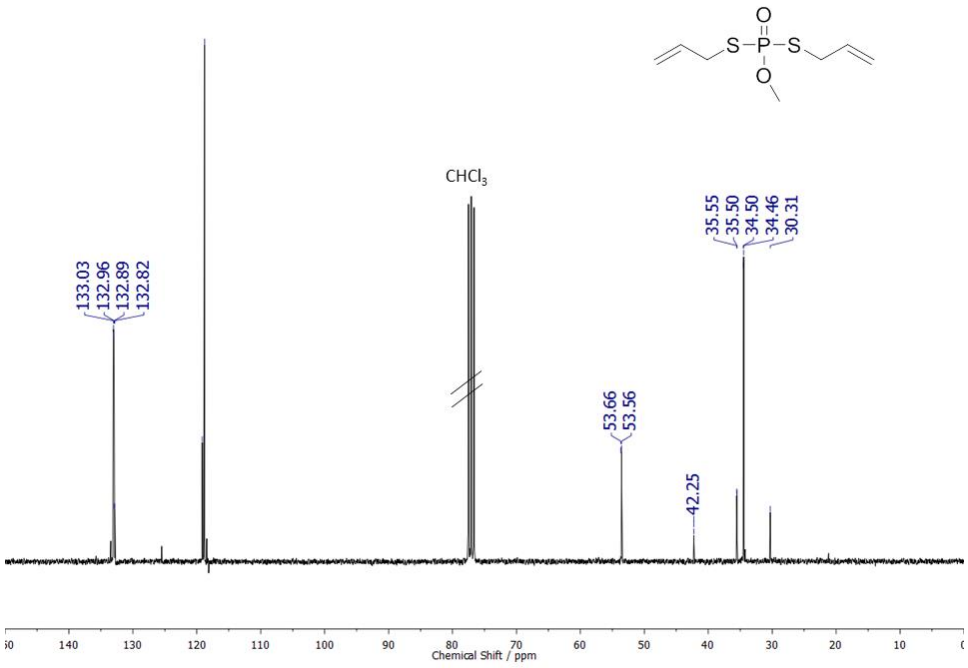

Figure S6: ^{13}C{H} of *S,S*-bis-(prop-2-en-1-yl)-methylphosphorodithiolate (75 MHz, 298 K, $CDCl_3$).

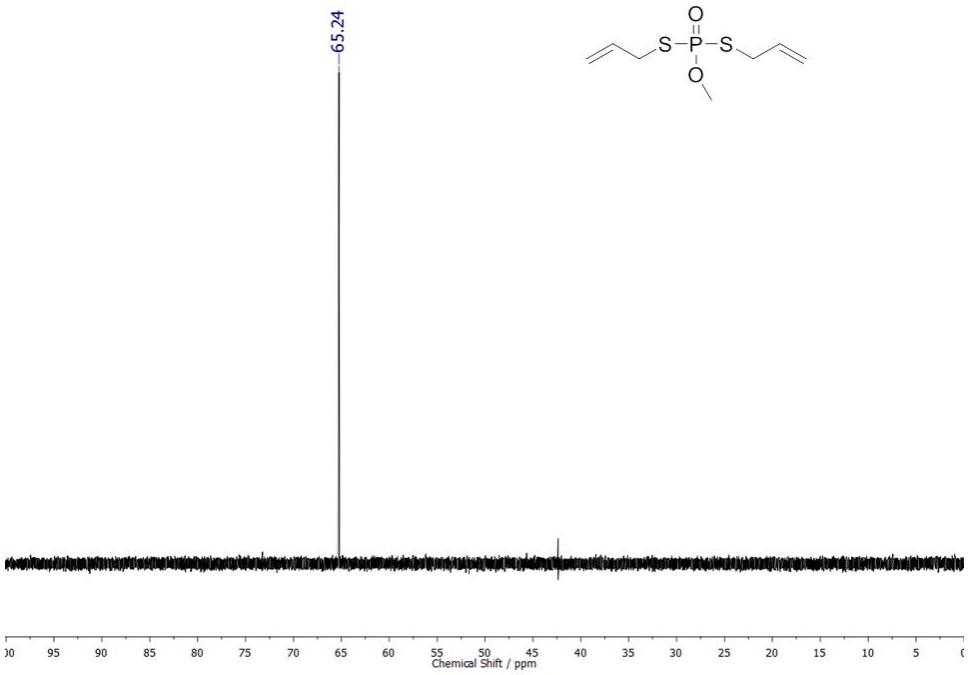

Figure S7: $^{31}P\{H\}$ NMR of *S,S*-bis-(prop-2-en-1-yl)-methylphosphorodithiolate (121.5 MHz, 298 K, D_2O).

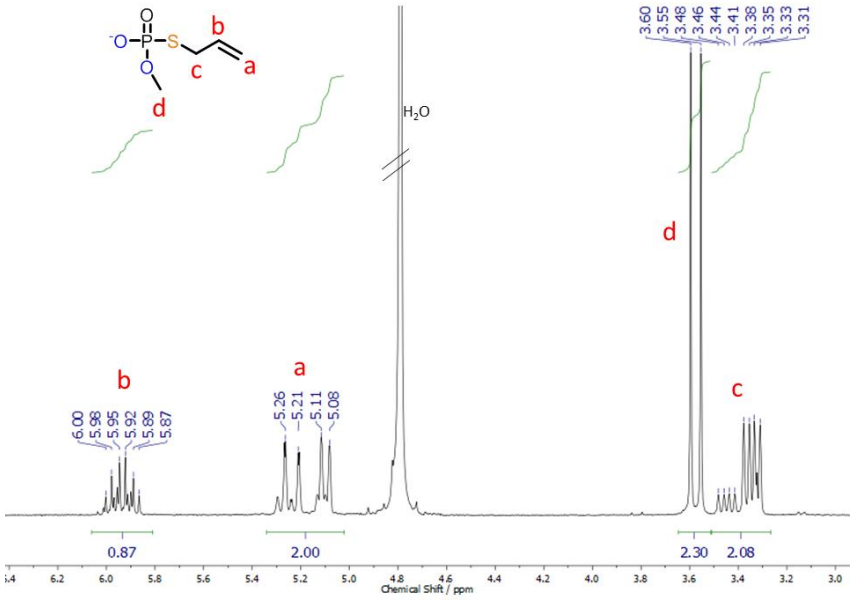

Figure S8: ^{1}H NMR spectrum of degradation product *S*-(prop-2-en-1-yl)-methylphosphorthiolate after 3 hours at pH = 13 (300 MHz, 298 K, D_2O).

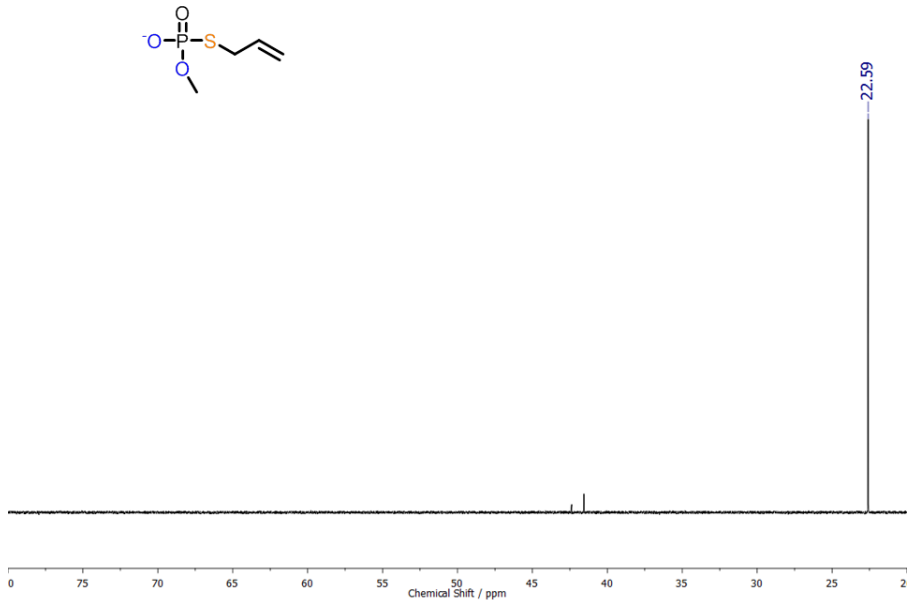

Figure S9: $^{31}P\{H\}$ NMR spectrum of degradation product *S*-(prop-2-en-1-yl)-methylphosphorthiolate after 3 hours at pH = 13 (121.5 MHz, 298 K, D_2O).

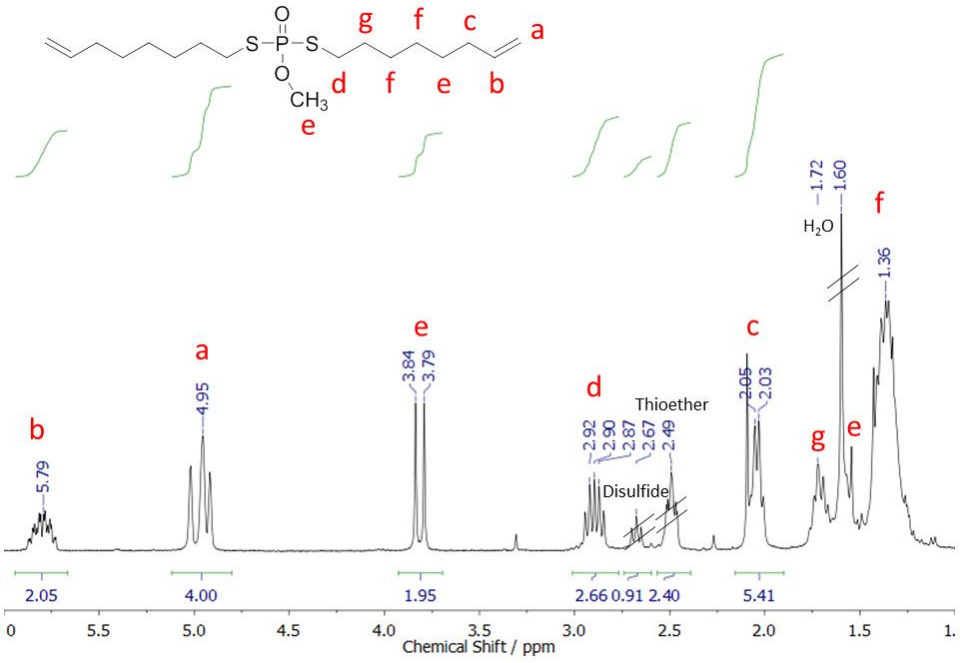

Figure S10: ^{1}H NMR of *S,S*-bis-(oct-7-en-1-yl)-methylphosphorodithiolate (300 MHz, 298 K, $CDCl_3$).

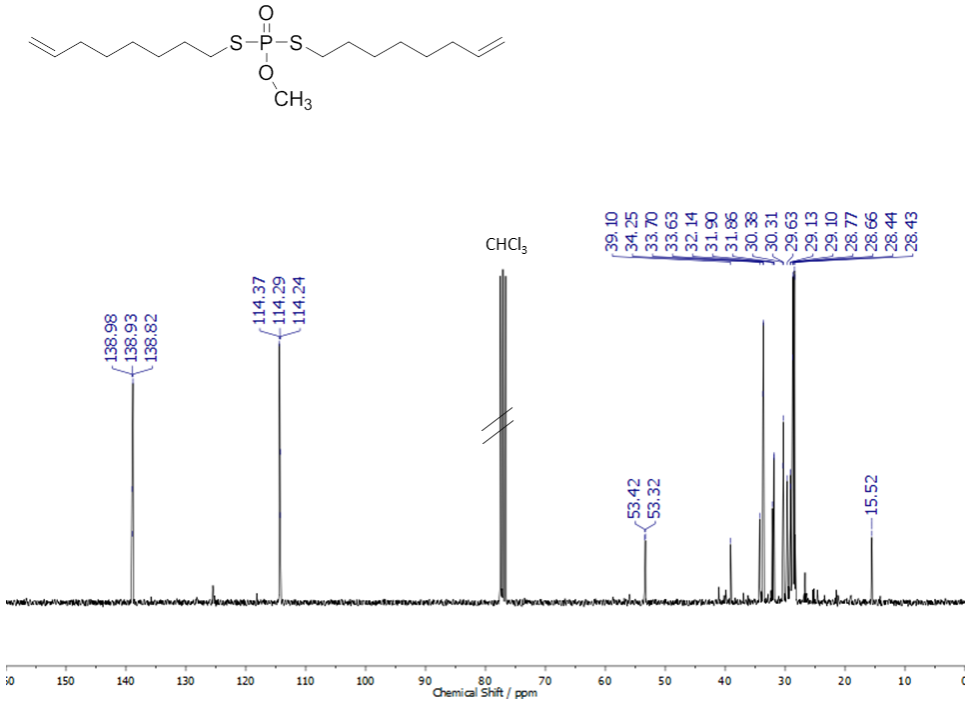

Figure S11: $^{13}C\{H\}$ NMR of *S,S*-bis-(oct-7-en-1-yl)-methylphosphorodithiolate (75 MHz, 298 K, $CDCl_3$).

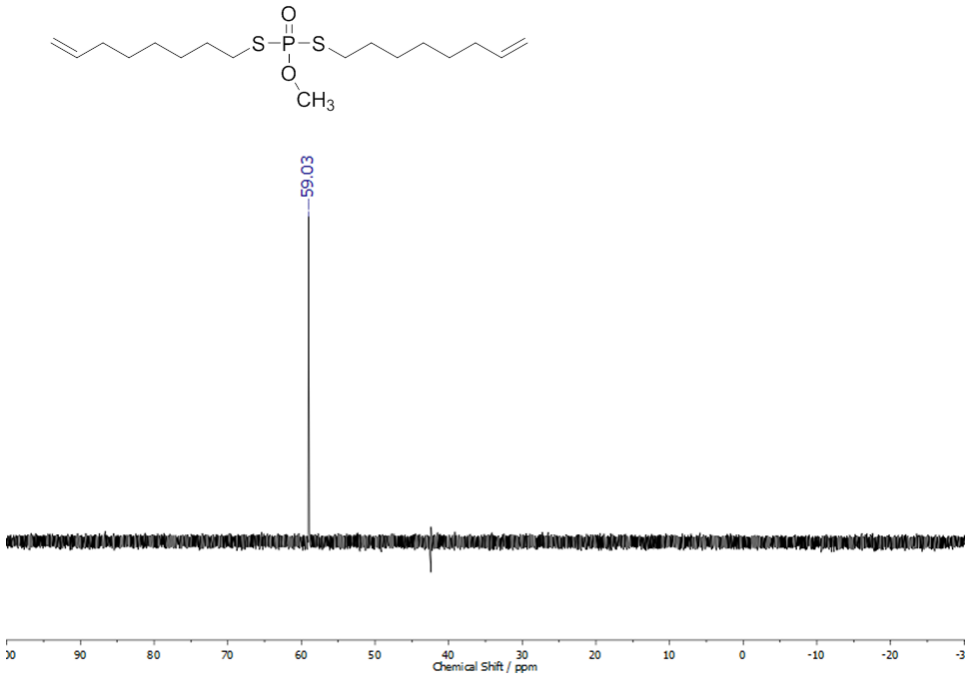

Figure S12: $^{31}P\{H\}$ NMR of *S,S*-bis-(oct-7-en-1-yl)-methylphosphorodithiolate (121.5 MHz, 298 K, $CDCl_3$).

Polymers

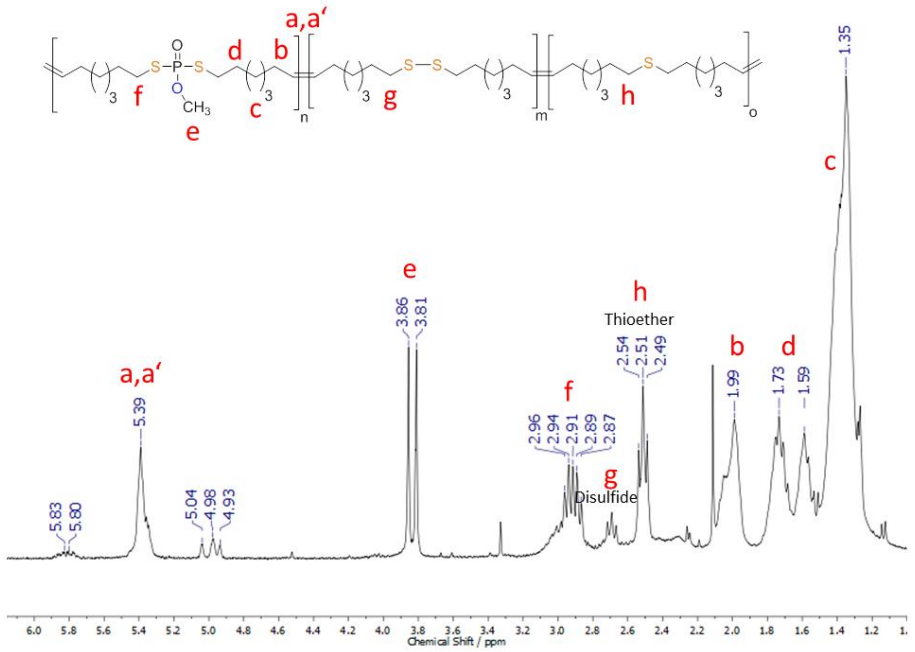

Figure S13: ^{1}H NMR polymer spectrum of *S,S*-bis-(oct-7-en-1-yl)-methylphosphorodithiolate via ADMET polymerization (300 MHz, 298 K, $CDCl_3$).

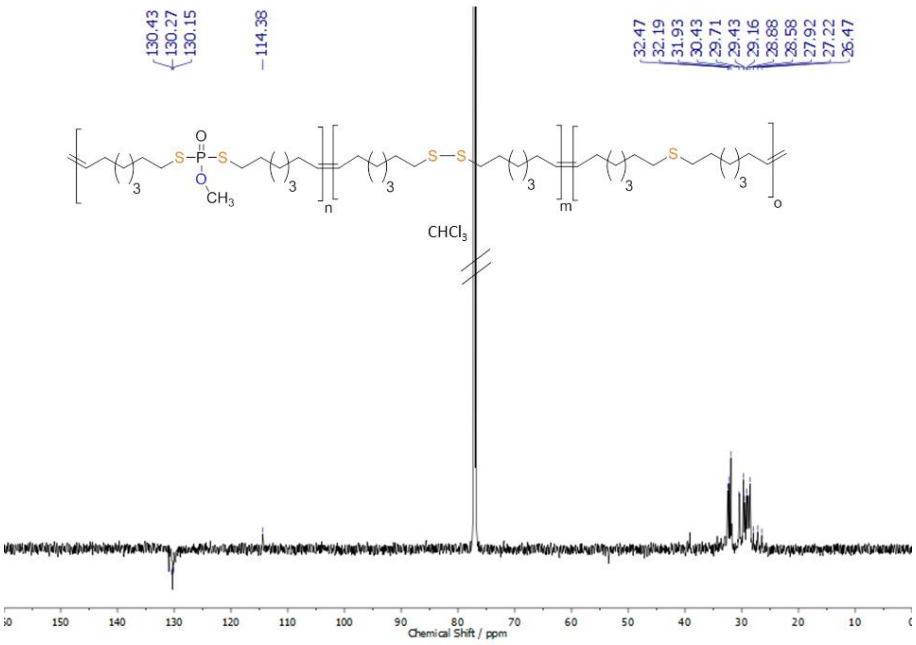

Figure S14: DEPT-135 ^{13}C{H} NMR polymer spectrum of *S,S*-bis-(oct-7-en-1-yl)-methylphosphorodithiolate via ADMET polymerization (176 MHz, 298 K, $CDCl_3$).

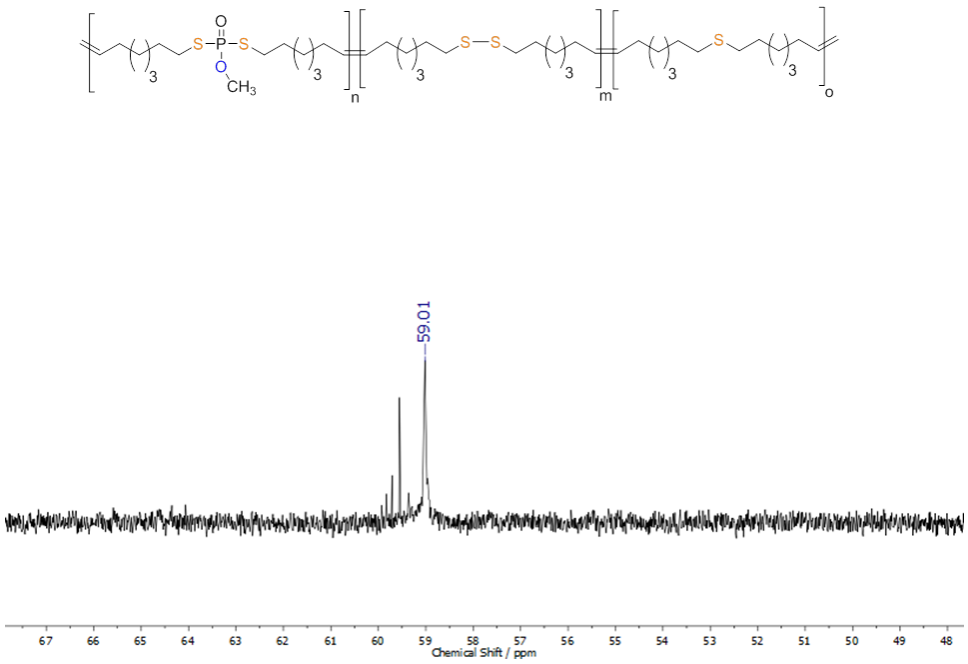

Figure S15: $^{31}P\{H\}$ NMR polymer spectrum of *S,S*-bis-(oct-7-en-1-yl)-methylphosphorodithiolate via ADMET polymerization (121.5 MHz, 298 K, $CDCl_3$).

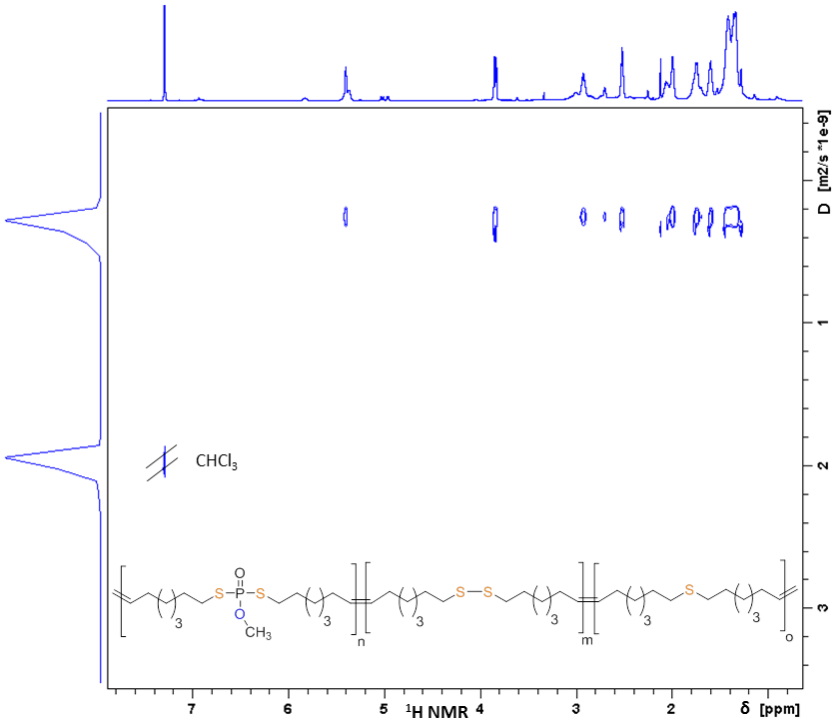

Figure S16: ^{1}H DOSY polymer spectrum of *S,S*-bis-(oct-7-en-1-yl)-methylphosphorodithiolate via ADMET polymerization (700 MHz, 298 K, $CDCl_3$).

4 Conclusion and Outlook

Phosphorus-containing polymers have been known for a long time ago. However, only the recent development of modern synthetic approaches such as olefin metathesis polymerization have made it possible to extend the scope of phosphorus-containing polymers for applications beyond flame retardancy. The introduction of thiol-ene polyaddition as a polymerization technique in Chapter 1 and further investigations in the Wurm research group have shown that thiol-ene polyadditions are another versatile tool in the construction kit of modern synthesis methods of polymers. Olefin metathesis polymerization is already established for PPEs, and the thiol-ene polyaddition has the opportunity to catch up in the next few years. Novel systems based on various binding motifs of phosphorus have been introduced to the scientific world in Chapters 2 - 5. Chapter 2 presents a new class of reactive PPEs which can easily be post-modified by various functional nucleophiles. Presented PPDAs, PPEs, and PPTs in Chapters 3 - 5 can also be manufactured as desired by the synthesis of appropriate monomers. Controlled degradation of specific binding motifs of phosphorus has been evaluated. It has been shown that P-N linkages are acid labile, P-O bonds are cleavable under both acidic and basic conditions, and P-S connections only base labile. These fascinating properties enable the introduction of many applications into the scientific world. Examples are given in this thesis by excellent flame retardancy and adhesive properties, and countless applications in the biomedical field (see Chapters 1 - 5).

Many applications can be promoted by several binding motifs around the phosphorus atom which dedicated scientists have developed, many of which are not present in nature. Unlike polymers found in nature, these synthetic polymers feature more elements linked to the phosphorus atom in order to observe a greater variety of properties. This makes phosphorus one of the most versatile groups in modern chemistry. Phosphorus-containing polymers have been evaluated for appropriateness as materials for modern applications. Biocompatibility and degradability, as well as adjustable properties, have made this class of polymers a promising area of interest.

However, limited resources and energy-intensive synthesis have thus far prevented phosphorus-containing polymers from being commercially available and serving as sustainable alternatives to commonly used polymers. Nevertheless, achievements and developments in recent years have shown that phosphorus-containing polymers are a promising field for the future of material science and the biomedical sector.

5 Appendix

5.1 Side-Chain Poly(phosphoramidate)s via Acyclic Diene Metathesis Polycondensation

*Alper Cankaya, Mark Steinmann, Yagmur Bülbül, Ingo Lieberwirth, and Frederik R. Wurm**

Max-Planck-Institut für Polymerforschung, Ackermannweg 10, 55128 Mainz, Germany.

wurm@mpip-mainz.mpg.de

KEYWORDS poly(phosphoramidate), poly(phosphoester), acyclic diene metathesis, biodegradable polymer, polyphos-phate.

A. Cankaya, M. Steinmann, Y. Bülbül, I. Lieberwirth and F. R. Wurm, *Polym. Chem.*, 2016, **7**, 5004 - Published by The Royal Society of Chemistry.

Abstract

Poly(phosphoester)s (PPEs) are interesting degradable multi-functional polymers. Here, we present the first synthesis of poly(phosphoramidate)s (PPAs) via acyclic diene metathesis polycondensation (ADMET) with the amidate linkage in the side chain. Two novel α,ω-dienes, i.e. bis-(undecen-10-yl)-*n*-butyl-phosphoramidate (1) and bis-(undecen-10-yl)-*n*-butyl-phosphate (2) have been polymerized by Grubbs-type catalysts to compare unsaturated PPAs with structural analogues PPEs. After hydrogenation of the polymers polyethylene-like structures were obtained. PPAs were compared to their PPE analogues with respect to their thermal behavior and stability by differential scanning calorimetry (DSC) and thermogravimetric analysis (TGA), showing similar crystallization behavior for the saturated materials, but significant differences for unsaturated PPA vs. PPE. This synthesis of PPAs via ADMET polymerization offers an interesting approach to various PPAs. The hydrolytically labile pendant phosphoramidate further offers the possibility for the development of hydrolytically degradable materials or as processable intermediates for poly(phosphodiester)s which often show limited solubility.

Introduction

Biodegradable polymers with precise properties and structure are a field of research with increasing attention ranging from plastics to for biomedical implants or drug delivery, for example. Polyesters and -amides lead the field in current literature due to established syntheses and proven biocompatibility.[203,204] However, as polyesters degrade, the pH may drop due to the release of carboxylic acids; also the chemical versatility of polyesters is limited or may demand several reaction steps to introduce functionality.[205]

Poly(phosphoester)s (PPEs), with a backbone of repeating phosphoester bonds, are biodegradable and (typically) biocompatible polymers with a high degree of chemical versatility.[163] Due to the formation of three ester-bonds, PPEs can be tailored along their main and side chain,[145] offering a variety of possible polymer structures, rendering PPEs interesting for diverse applications like for drug[27, 206-207] and gene delivery[82] and tissue engineering.[208] The stability of the phosphorus-containing polymers is directly influenced by the first binding sphere around the central phosphorus: the development of poly(phosphonate)s with stable P-C-bond as main[209] or side chain elements[210] or poly(phosphoramidate)s (PPAs) with a hydrolysis-labile P-N bond in the side chain[90] has a direct influence on the polymers' degradation profile.

Side-chain PPAs have been only scarcely studied; their classical synthesis relies on the post-polymerization modification of poly(H-phosphonate)s by the versatile Atherton-Todd reaction.[211-213] More recently, the Wooley lab presented an elegant approach by ring-opening polymerization[90] of a cyclic dioxaphospholane. PPAs been studied for delivery of nucleic acids or as flame-retardant polymers.[204, 214, 211, 215-216]

Our group developed several protocols based on olefin metathesis polymerization (either as acyclic diene metathesis (ADMET) or ring-opening metathesis polymerization) for phosphorus-containing materials.[40-41, 217]

Herein, we use the robust ADMET protocol[154] to present the first strategy to aliphatic saturated and unsaturated PPAs with the phosphoramidate bond as side chain. The labile P-N bond can be used to release the pendant chain (e.g. for pH-senstitive drug delivery) or can be regarded as soluble precursor for poly(phosphodiester)s after acidic hydrolysis, which

typically are hardly soluble and are interesting materials for bone targeting, for example.[218] Such polymers may find also useful application as novel polymeric flame retardant additives.[219] In addition, we compare the PPA to a structurally identical PPE (a single oxygen is exchanged by "NH", cf. Scheme 1).

Experimental

Materials

Solvents were purchased from Acros Organics and Sigma Aldrich and used as received, unless otherwise stated.

Phosphoroxychloride, 10-undecen-1-ol, triethylamine, tris(hydroxymethyl)phosphine and butan-1-ol were used as received from Sigma-Aldrich (Germany). Grubbs catalyst 1st generation was purchased from Sigma-Aldrich and stored under argon atmosphere. *n*-butyl amine was purchased from TCI chemicals and used without further purification.

Deuterated solvents were purchased from Acros Organics and Carl Roth Chemicals.

Instrumentation

Gel-permeation chromatography (GPC) measurements were carried out in THF, with samples of the concentration of 1 g L^{-1}. Sample injection was performed by a 1260-ALS auto sampler (Waters) at 30 °C (THF). The flow was 1 mL min^{-1}. In THF, three SDV columns (PSS) with dimensions of 300 × 80 mm, 10 µm particle size and pore sizes of 106, 104 und 500 Å were employed. Detection was accomplished with a DRI Shodex RI-101 detector (ERC) and UV-Vis 1260-VWD detector (Agilent). Calibration was achieved vs. poly(styrene) standards provided by Polymer Standards Service. ^{1}H-NMR spectra were recorded on a Bruker Avance 300 MHz spectrometer, ^{13}C-NMR and ^{31}P- spectra were recorded on a Bruker Avance 500 MHz spectrometer. ^{1}H^{15}N-NMR spectra were recorded on a Bruker Avance 700 MHz spectrometer. The ^{13}C-NMR (176 MHz) and ^{31}P-NMR (283 MHz) measurements were obtained with a ^{1}H powergate decoupling method using 30° degree flip angle.

^{1}H-DOSY experiments were recorded with a 5 mm BBI 1H/X z-gradient on the 700 MHz spectrometer with an Bruker Avance III system. For a ^{1}H NMR spectrum 64 transients were used with an 11 µs long 90° pulse and a 12600 Hz spectral width together with a recycling

delay of 5 s. The temperature for all experiments was kept at 298.3 K. The proton, carbon and phosphorous spectra were measured in $CDCl_3$ or DMSO-d_6. The spectra were referenced to the residual proton signals of the deuterated solvent ($CDCl_3$ (^1H) = 7.26 ppm; DMSO-d_6 (^1H) = 2.50 ppm). All spectra were processed with MestReNova 6.1.1-6384 software. Differential Scanning Calorimetry (DSC) measurements were performed using a Perkin-Elmer 7 series thermal analysis system and a Perkin Elmer Thermal Analysis Controller TAC 7/DX in the temperature range from –150 to 130 °C. Three scanning cycles of heating–cooling were performed (in a N2 atmosphere 30 mL min^{-1}) with a heating rate of 10 °C min^{-1}.

Thermogravimetric analysis (TGA) was measured on a Mettler Toledo ThermoSTAR TGA/SDTA 851-Thermowaage in the range of temperature between 25°C and 600 °C, with a heating rate of 10 °C min-1. For wide-angle X-ray scattering (WAXS) and small-angle X-ray scattering (SAXS) experiments samples were prepared by hot pressing an approximately 200−400 µm thick film on a hot stage. A sufficient amount of the sample was placed on a

preheated glass slide and allowed to melt. Subsequently, another hot glass slide was pressed on the melt. This sandwich was kept above melting point for another 5 min before cooling it down to room temperature in order to eliminate any shear-induced orientation in the sample.

SAXS was recorded using Cu Kα radiation (wavelength 1.54 Å) from a rotating anode source (Rigaku MicroMax 007 X-ray generator) with curved multilayer optics (Osmic Confocal Max-Flux). The scattered intensity was recorded on a 2D detector (Mar345 image plate) with a sample−detector distance of 2 m. For WAXS measurements the sample−detector distance was set to 20 cm. Transmission Electron Microscopy (TEM). A FEI Tecnai F20 transmission electron microscope operated at an acceleration voltage of 200 kV was used to determine the crystal morphology, thickness, and crystal structure.

Synthesis of bis-(undecen-10-yl) chlorophosphate. To a dried two-necked, 500 mL round bottom flask, 5g (32.61 mmol) phosphoroxychloride dissolved in 100 mL of dry CH_2Cl_2 were added under argon atmosphere. After cooling down the solution to 0°C, 1.8 equiv. (58.70 mmol) of 10-undecen-1-ol and 1 equiv. (3.3 g, 32.61 mmol) of triethylamine dissolved in 50

mL CH_2Cl_2 were added drop-wise to the solution at 0°C. The reaction was stirred overnight at room temperature. The precipitated $Et_3N{\cdot}HCl$ was removed as a white solid by filtration, the filtrate was reduced at reduced pressure. The residue was dissolved in diethylether and further precipitated $Et_3N{\cdot}HCl$ was removed again. This procedure was repeated until no salt precipitated no more. After removal of the solvent under reduced pressure a colorless, viscous liquid was obtained and used for further reactions without purification (Yield: 65%, 21.4 g).

^{1}H-NMR (300 MHz, $CDCl_3$, ppm): δ 5.81 (ddt, J_1 = 18Hz, J_2 = 9 Hz, J_3 = 6Hz, 2H, CH_2=C<u>H</u>-), δ 4.96-4.82 (m, 4H, C<u>H_2</u>=CH-), δ 4.20-3.90 (m, 4H,- O-C<u>H_2</u>-), δ 2.03 (q, J = 6Hz, 4H, CH_2=CH-C<u>H_2</u>-), δ 1.81-1.71 (m, 4H, -O-CH_2-C<u>H_2</u>-), δ 1.44-1.28 (m, 24H, -C<u>H_2</u>-).

*Synthesis of bis-(undecen-10-yl) butylphosphoramidate (**1**).* To a dried two-necked, 250 mL round-bottom flask 8.94g (21.24 mmol) of bis-(undecen-10-yl) chlorophosphate dissolved in 100 mL of dry CH2Cl2 with stirring was added under an argon atmosphere. The solution was cooled to 0 °C, then 1 equiv. of n-butylamine (1.55 g, 21.24 mmol)and 1 equiv. of triethylamine (2.15 g, 21.24 mmol) were added drop-wise under cooling to the solution. The reaction was stirred overnight at room temperature. The precipitated $Et_3N{\cdot}HCl$ was removed as a white solid by filtration, the filtrate was reduced under vacuum. The residue was dissolved in diethylether and further precipitated $Et_3N{\cdot}HCl$ was removed again. This procedure was repeated until no salt precipitated no more. The reduced product is dissolved in CH_2Cl_2 and was8,94hed once with aqueous 10% HCl and twice with brine. The organic layer was dried over magnesium sulfate filtered and concentrated in vacuum. The product was obtained as a yellow oil after column chromatography over silica using toluene:acetone (8:1) as eluents (R_f: 0.58, yield: 63%, 3.5 g).

^{1}H-NMR (298K, 300 MHz, DMSO-d_6, ppm): δ 5.81 (ddt, J_1 = 12 Hz, J_2 = 6 Hz, J_3 = 3 Hz 2H, CH_2=C<u>H</u>-), δ 5.02-4.90 (m, 4H, C<u>H_2</u>=CH-), δ 4.79-4.74 (dt, 1H, -N<u>H</u>-), δ 3.97 (qd, 4H,-O-C<u>H_2</u>-), δ 2.92-2.84 (m, 2H, -NH-C<u>H_2</u>-), δ 2.03 (m, =CH-C<u>H_2</u>-), δ 1.65 (q, J = 9 Hz, 4H, -O-CH2-C<u>H_2</u>-), δ 1.31 (m, 28H, -C<u>H_2</u>-, -C<u>H_2</u>-CH3), δ 0.91 (t, J = 6 Hz, 3H, -CH2-C<u>H_3</u>). ^{13}C-NMR (298K, 75 MHz, DMSO-d_6, ppm): δ 139.06 (CH_2=<u>C</u>H-), 114.04 (<u>C</u>H_2=CH-), 66.21 (-O-<u>C</u>H_2-), 41.06 (-NH-<u>C</u>H_2-), 33.71 (=CH-<u>C</u>H_2-), 30.31 (-O-CH2-<u>C</u>H_2-), 29.01 (-<u>C</u>H_2-), 25.44 (-NH-CH_2-<u>C</u>H_2-), 19.56 (-<u>C</u>H_2-CH3), 13.69 (-<u>C</u>H_3). ^{31}P-NMR (298K, 125 MHz DMSO-d_6, ppm): δ 10.00.

*Synthesis of bis-(undec-10-en-1-yl)butylphosphate (**2**).* In a dry three-necked 500 mL round-bottom flask a stirred solution of phosphoroxychloride (6.57 g, 4.00 mL, 42.78 mmol) in 100 mL dry CH_2Cl_2 under argon atmosphere was cooled down to 0 °C. A mixture of n-butanol (5.7 g, 77.01 mmol) and triethylamine (7.79 g, 10.74 mL, 77.01 mmol) in 50 mL dry CH_2Cl_2 was added drop-wise under cooling und stirred overnight at room temperature. In a next step, the reaction mixture is cooled down to 0°C again and 10-undecen-1-ol (3.17 g, 42.78 mmol) and triethylamine (4.33 g, 42.78 mmol) in 50 mL dry CH_2Cl_2 were added drop-wise to the reaction. The mixture was stirred overnight and $Et_3N{\cdot}HCl$ was removed as a white solid by filtration. The filtrate was reduced under vacuum. The residue was dissolved in diethylether and further precipitated $Et_3N{\cdot}HCl$ was removed again. This procedure was repeated until no further salt precipitated. The filtrate is reduced under pressure and dissolved in CH_2Cl_2, washed once with aqueous 10% HCl and twice with brine. The organic layer was dried over magnesium sulfate filtered and concentrated at reduced pressure. The product was obtained as a yellow oil after column chromatography over silica using dichlormethane:ethylacetate (8:1) as eluents (R_f: 0.8, yield: 37%, 7.4 g).

^{1}H-NMR (298K, 300 MHz, $CDCl_3$, ppm): δ 5.74 (ddt, J_1 = 12 Hz, J_2 = 9 Hz, J_3 = 3 Hz, 2H, CH2=C<u>H</u>-), δ 4.96-4.84 (m, 4H, C<u>H</u>$_2$=CH-), δ 4.00-3.92 (m, 6H, -O-C<u>H</u>$_2$-), δ 2.01-1.93 (m, 4H, CH2=CH-C<u>H</u>$_2$-), δ 1.65-1.55 (m, 6H, -O-C<u>H</u>$_2$-), δ 1.36-1.17 (m, 26H, -C<u>H</u>$_2$-), δ 0.87 (t, *J* = 6 Hz, 3H, -C<u>H</u>$_3$). ^{13}C-NMR (298K, 75 MHz, $CDCl_3$, ppm): δ 139.09 (CH$_2$=<u>C</u>H-), 113.93 (<u>C</u>H$_2$=CH-), 67.45 (-O-<u>C</u>H$_2$-), 33.66 (=CH-<u>C</u>H$_2$-), 30.35 (-O-CH$_2$-<u>C</u>H$_2$-), 29.15 (-<u>C</u>H$_2$-), 25.32 (-<u>C</u>H$_2$-<u>C</u>H$_2$-CH3), 18.49 (-<u>C</u>H$_2$-CH3), 13.38 (-<u>C</u>H$_3$). ^{31}P-NMR (298K, 125MHz, $CDCl_3$, ppm): δ -0.65.

Representative procedure for ADMET bulk polycondensation for UPPEs. In a glass Schlenk tube, the monomer (600 mg) and the Grubbs catalyst 1st generation (1-3 mol%) were mixed under an argon atmosphere. The polycondensation was carried out at reduced pressure to remove ethylene gas evolving during the metathesis reaction, at temperatures between 70°C and 80 °C over a period of 16-18 h. The crude mixture was dissolved in CH_2Cl_2, treated with tris (hydroxymethyl) phosphine (50 eq with respect to the catalyst) and washed twice with aqueous 10% HCl and water. The organic layer was dried over sodium sulfate, filtered, concentrated at reduced pressure, and precipitated into hexane. Yields were typically between 90-95 % (after drying).

P1:

^{1}H-NMR (298K, 300 MHz, $CDCl_3$, ppm): δ 5.33-5.25 (m, 2H, -C<u>H</u>=C<u>H</u>-), δ 3.90 (qq, 4H, -O-C<u>H</u>$_2$-), δ 2.81 (dt, J_1 = 9 Hz, J_2 = 6 Hz, 2H, -NH-C<u>H</u>$_2$-), δ 1.89 (q, J = 6 Hz, 4H, =CH-C<u>H</u>$_2$-), δ 1.58 (q, J = 6 Hz, 4H, -O-CH$_2$-C<u>H</u>$_2$-), δ 1.42-1.20 (m, 28H, -C<u>H</u>$_2$-), δ 0.84 (t, J = 6 Hz 3H, -C<u>H</u>$_3$). ^{13}C-NMR (298K, 75 MHz, $CDCl_3$, ppm): δ 130.21 (-C<u>H</u>=C<u>H</u>-), 66.14 (-O-C<u>H</u>$_2$-), 41.00 (-NH-C<u>H</u>$_2$-), 33.88 (-CH=CH-C<u>H</u>$_2$-), 32.61 (-O-CH$_2$-C<u>H</u>$_2$-), 30.43 (-C<u>H</u>$_2$-), 25.60 (-NH-CH$_2$-C<u>H</u>$_2$-), 19.74 (-C<u>H</u>$_2$-CH$_3$), 13.69 (-C<u>H</u>$_3$). ^{31}P-NMR (298K, 125 MHz, $CDCl_3$, ppm): δ 10.02

P2:

^{1}H-NMR (298K, 300 MHz, $CDCl_3$, ppm): δ 5.33-5.26 (m, 2H, -C<u>H</u>=C<u>H</u>-), δ 3.96 (qd, 6H, -O-C<u>H</u>$_2$-), δ 1.88 (q, J = 6 Hz, 4H, =CH-C<u>H</u>$_2$-), δ 1.59 (dtt, 6H, -O-CH$_2$-C<u>H</u>$_2$-), δ 1.40-1.20 (m, 26H, -C<u>H</u>$_2$-), δ 0.87 (t, J = 6 Hz, 3H, -C<u>H</u>$_3$). ^{13}C-NMR (298K, 75 MHz, $CDCl_3$, ppm): δ 130.70 (-C<u>H</u>=C<u>H</u>-), 68.15 (-O-C<u>H</u>$_2$-), 33.14 (-CH=CH-C<u>H</u>$_2$-), 30.78 (-O-CH$_2$-C<u>H</u>$_2$-), 30.01 (-C<u>H</u>$_2$-), 25.95 (-C<u>H</u>$_2$-CH$_3$), 19.15 (-C<u>H</u>$_2$-CH$_3$), 14.05 (-C<u>H</u>$_3$). ^{31}P-NMR (298K, 125 MHz, $CDCl_3$, ppm): δ – 0.84

Procedure for the catalytic hydrogenation. In a dried two-necked, 250 mL round-bottom flask, 200 mg of unsaturated polymer in 50 mL toluene and 5% Pd/C (25mg, 12.5 wt%) were placed and flushed with argon. The mixture was then flushed thoroughly with hydrogen and a hydrogen balloon as a reservoir was connected to the flask. After complete hydrogenation (typically after 36 h) of the polymer the solution was filtered over celite and the polymer was obtained a solid after solvent evaporation in quantitative yield.

P1-H:

^{1}H-NMR (298K, 300 MHz, $CDCl_3$, ppm): δ 3.93 (qq, 4H, -O-C<u>H</u>$_2$-), δ 2.84 (dt, J_1 = 9 Hz, J_2 = 6 Hz, 2H, -NH-C<u>H</u>$_2$-), δ 1.58 (q, J = 7 Hz, 4H, -O-CH$_2$-C<u>H</u>$_2$-), δ 1.42-1.20 (m, 28H, -C<u>H</u>$_2$-), δ 0.84 (t, J = 5 Hz 3H, -C<u>H</u>$_3$). ^{13}C-NMR (298K, 75 MHz, $CDCl_3$, ppm): δ 66.14 (-O-C<u>H</u>$_2$-), 41.00 (-NH-C<u>H</u>$_2$-), 32.01 (-O-CH$_2$-C<u>H</u>$_2$-), 30.43 (-C<u>H</u>$_2$-), 26.20 (-NH-CH$_2$-C<u>H</u>$_2$-), 19.53 (-C<u>H</u>$_2$-CH$_3$), 13.71 (-C<u>H</u>$_3$). ^{31}P-NMR (298K, 125 MHz, $CDCl_3$, ppm): δ 10.02

P2-H:

^{1}H-NMR (298K, 300 MHz, $CDCl_3$, ppm): δ 3.96 (qd, 6H, -O-C$\underline{H}_2$-), δ 1.66 (dtt, 6H, -O-CH_2-C$\underline{H}_2$-), δ 1.40-1.20 (m, 26H, -C$\underline{H}_2$-), δ 0.93 (t, *J* = 6 Hz, 3H, -C$\underline{H}_3$). ^{13}C-NMR (298K, 75 MHz, $CDCl_3$, ppm): δ 67.15 (-O-C$\underline{H}_2$-), 38.18 (-O-CH_2-$\underline{C}H_2$-), 29.91 (-$\underline{C}H_2$-), 25.95 (-$\underline{C}H_2$-CH_3), 19.15 (-$\underline{C}H_2$-CH_3), 14.31 (-$\underline{C}H_3$). ^{31}P-NMR (298K, 125 MHz, $CDCl_3$, ppm): δ – 0.84

Procedure for the selective degradation of amidate side chain. A NMR tube was equipped with 5 mg of **poly(1)** and 5 mg of p-toluenesulfonic acid in a mixture of deuterated chloroform and deuterated methanol (6:4). The degradation was measured every day over the duration of 1.5 weeks by ^{1}H NMR and ^{31}P NMR spectroscopy.

Results and Discussion

For the comparison of PPEs with PPAs, we designed two novel α,ω-dienes, i.e. bis-(undecen-10-yl) butylphosphoramidate (**1**) and its phosphoester equivalent (**2**) (characterization data can be found in the Supp. Info.). Both monomers can be synthesized starting from phosphoroxychloride with sequential substitution of the chlorides with alcohols (undecenol and/or *n*-butanol) and/or the amine (*n*-butylamine) (Scheme 1). Due to its high nucleophilicity, the amine is attached after the incorporation of the polymerizable groups, while for the phosphoester side chain (**2**) butanol can be also added in a first step. Both monomers were purified by column chromatography and are stable at room temperature over a period of at least several months (^{1}H, ^{13}C, ^{31}P, ^{1}H^{15}N HMBC NMR spectra can be found in the Supporting Information). The ^{15}N NMR chemical shift for the amidate-N is detected at 42.3 ppm (Figure S4), while the ^{31}P NMR spectra show distinct resonances for the phosphoramidate at ca. 10 ppm and the phosphoester at -0.65 ppm (Scheme 1).

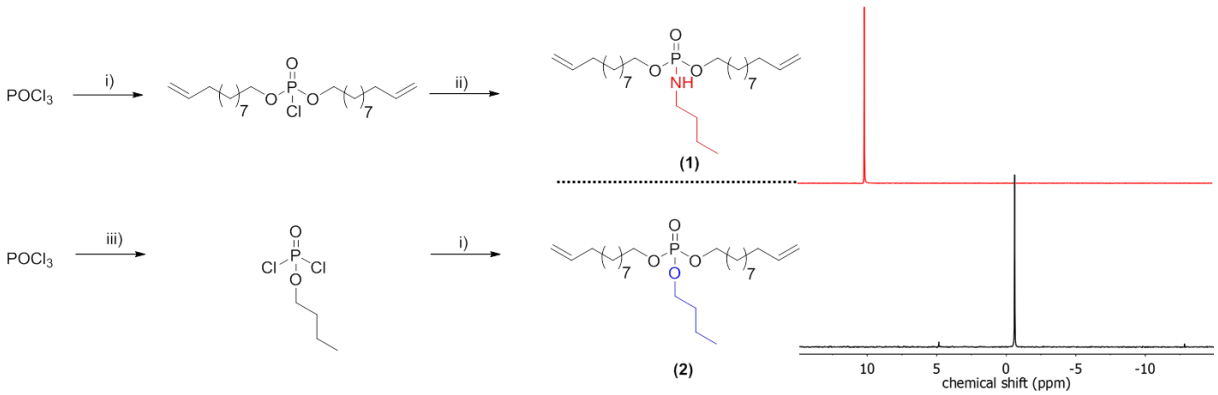

Scheme 1. a) Synthesis of the ADMET monomers bis-(undecen-10-yl) butylphosphoramidate (**1**) and bis-(undec-10-en-1-yl)butylphosphate (**2**) and their ^{31}P NMR spectra. (i) 10-undecen-1-ol, triethylamine, dichloromethane; ii) butylamine, triethylamine, dichloromethane; iii) butanol, triethylamine, dichloromethane.)

Both α,ω-dienes (phosphoramidate/-ester) monomers were polymerized by ADMET polycondensation using Grubbs 1st generation catalyst or Hoveyda-Grubbs catalyst 2nd generation. The reaction was carried out in bulk at 80°C for 12h at reduced pressure in order to remove arising ethylene during this reaction (Scheme 2). For the poly(phosphoramidate)s polymerization by Grubbs 1st generation catalyst (3mol%) produced polymers with apparent M_n's of up to 4,800 g /mol. The polymerization of **1** was also investigated with the typically more active Grubbs Hoveyda 2nd generation catalyst. 1, 3, 5, and 10 mol% were used and the apparent M_n were increased to ca. 9,000 g/mol for 5mol% catalyst loading. 10 mol% of catalyst loading changed the molar mass only slightly (Table 1 & Figure S14). In addition to SEC, apparent molecular weights have been determined by ^{1}H DOSY NMR spectroscopy for two examples: ^{1}H-DOSY NMR. In order to determine M_w of the polymers, poly(styrene) samples with known absolute molecular weights (GPC standards) were measured via DOSY and used as a calibration.[176, 220] The determined Mws from the H-DOSY NMR spectra are in a range between 9,400 g/mol and 11,000 g/mol for the PPAs P1-b and P1-d, respectively.

Table 1. Characterization data for poly(phosphoramidate)s **P1** and poly(phosphoester)s **P2**.

Code	conditions[a]	M_n[b]	M_w/M_n[b]	T_g/°C[c]	T_m/°C[c]
P1-a	A	3,100	1.25	n.d.	n.d.
P1-b	A	4,800	2.19	-72	-8
P1-c	B	4,400	1.82	n.d.	n.d.
P1-d	C	6,500	1.70	-71	8
P1-e	D	9,000	1.72	n.d.	n.d.
P1-f	E	9,500	1.66	n.d.	n.d.
P2-a	A	9,000	2.70	-84	0
P2-b	A	9,600	2.71	n.d.	n.d.
P2-c	D	19,600	1.81	n.d.	n.d.
P1-d-H	--	7,000	1.60	-50	51
P2-b-H	--	10,000	2.55	-80	47

[a] A: Grubbs 1st generation, 3mol%. Grubbs Hoveyda 2nd gen. 1mol%=B, 3mol%=C, 5mol%=D, 10mol%=E

[b] determined via SEC in THF (vs. PS standards).

[c] determined by differential scanning calorimetry (10K/min).

n.d. = not determined

The poly(phosphoester) based on **2** was not reported in literature, however similar polymers with phenoxy side chains have been prepared and GPC indicates for **P2**s a M_n of ca. 9,000 g/mol in this case (which is probably not the upper limit). Successful polymerization of both monomers can be easily detected from the ^{1}H NMR spectra, as the terminal olefin resonances change into internal alkenes after the polymerization (end groups may be detected, but isomerization is known to shift the end groups also to internal alkenes, spectra can be found in the Supp. Info.). These unsaturated PPAs/ PPEs converted by catalytic hydrogenation with Pd/C into their saturated counterparts. The ^{1}H NMR spectra show the disappearance of any alkene resonances after successful hydrogenation (Figures S11 & S12) and SEC proves the stability of the polymer under these conditions (Figure 16).

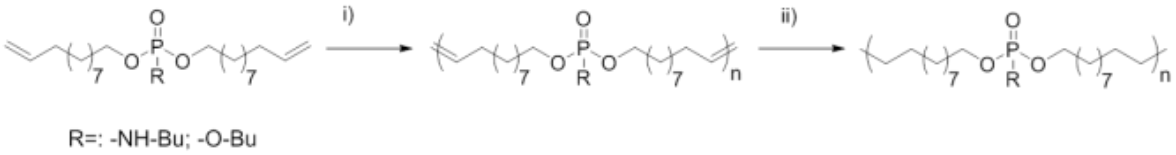

Scheme 2. ADMET polymerization of **1** and **2** and subsequent hydrogenation (i) Grubbs catalyst, vaccuum, 60-80°C; ii) Pd/H_2, toluene).

As possible flame-retardant materials phosphoramidates typically exhibit different thermal behavior compared to their ester analogues.[219] The thermal properties of the unsaturated and saturated poly(phosphoramidate)s and poly(phosphoester)s were studied by differential scanning calorimetry (DSC) and thermogravimetric analysis (TGA) (Figures S17 & S18). **P2** was studied by TGA and a single thermal decomposition at ca. 310°C (10% weight loss: $T_{10\%}$ = 311°C) with a char residue at 450°C of 9% was identified. The thermal degradation of phosphoramidates is different compared to phosphoresters and was already studied for various flame retardant additives or modified polymers (typically with low molecular weight additives or modification of a common polymer matrix).[104, 221] **P1** shows a more complex degradation profile than the corresponding polyester: a first mass loss of ca. 23% mass up to ca. 298°C, followed by a second process until ca 325°C and 60% weight loss. This char slowly degrades under further heating to ca. 15% remaining at 440°C. Compared to low molecular weight flame retardant phosphoramidates, this TGA profile also renders PPAs interesting candidates for flame retardants additives.[219]

The hydrogenated samples (**P1-H** and **P2-H**) can also be regarded as a defect poly(ethylene) (PE) with the phosphate/-amidate acting as defects, spaced by 20 methylene groups. The unsaturated PPE (**P2**) shows a low T_g of ca. -84°C and a melting endotherm at ca. 0°C with a melting enthalpy of ΔH_m=-31 J/g. After hydrogenation (**P2-H**), the T_g remains rather unchanged (-80°C) and the melting temperature is increased to ca. 47°C (ΔH_m=-59 J/g), similar to previously reported PPEs.[40, 153] Interestingly, a second melting endotherm is detected after hydrogenation at ca. -1°C with a very low ΔH_m=-8 J/g, indicating another crystalline structure, maybe due to side chain crystallinity (Figure S18). For the unsaturated PPAs **P1** a different behavior is detected: The T_g is with -72°C higher than for the corresponding PPE; in addition above T_g the polymer crystallizes at T_c = -40°C, before the melting is detected at -8°C. Also in the cooling curve of the **P1**-series, no recrystallization is observed under these conditions (10°C/min), leaving a completely amorphous polymer after cooling. In contrast, **P2** recrystallizes during the same cooling procedure. The hydrogenated PPA (**P1-H)** exhibits a similar thermal behavior as its PPE-analog with a melting endotherm at ca. 51°C with a similar melting enthalpy of ΔH_m=-45 J/g.

The solid state properties of **P1H** and **P2H** were analyzed by WAXS and SAXS measurements. The small angle x-ray scattering diagram (Fig. 1) shows a dominant peak at q = 0.2368 $Å^{-1}$, corresponding to a long period of 2.7 nm. This peak is found in the wide angle x-ray scattering (WAXS) as well at 2 Θ = 3.6 °. Accordingly, the lamellar thickness of **P1-H** crystals corresponds to the length of the 20 CH_2 groups in all-trans conformation. P1H and P2H were dissolved in hot *n*-octane and crystallized slowly during the cooling process from solution. Drop-cast TEM (cf. Fig. S19 & S20) shows the resulting crystals for both polymers. The electron diffraction pattern (inset Fig. S19, S20)) indicates that the crystal packing is similar to the pseudohexagonal crystal phase of polyethylene.[222] For P1H a lattice spacing of 4.1 Å was measured from TEM diffraction and also the WAXS measurement yields a lattice spacing of 4.1 Å. Interestingly, the structural analogue PPE, i.e. **P2-H**, behaves similar in the bulk phase: the SAXS diagram (Fig. S21) shows a major signal at q = 0.2808 Å-1, corresponding to a long period of 2.2 nm, similar to **P1-H**. The WAXS shows a small peak at 2 Θ = 6.8 ° which corresponds to a spacing of 1.3 nm. The dominant peak in the WAXS data corresponds to a lattice spacing of 4.2 Å, indicating again the pseudo-hexagonal crystal structure. Fig. S20 shows a TEM micrograph of **P2-H** crystals with the corresponding diffraction pattern yielding a lattice spacing of 4.2 Å (compare above 4.1 Å for **P1-H**). From these structural examinations the **P2-H** crystallizes in a pseudo-hexagonal crystal structure with a lamellar long period of 2.2 nm as P1-H. As reported previously for other defect-PEs, the pendant groups are located outside of the crystalline lamellae[223] and thus for P1-H the amidate side chains are located outside of the crystals. Due to the easy cleavage of P-N bonds (see below), this might be a handle for future tuning of crystal surfaces and currently studied in our department.

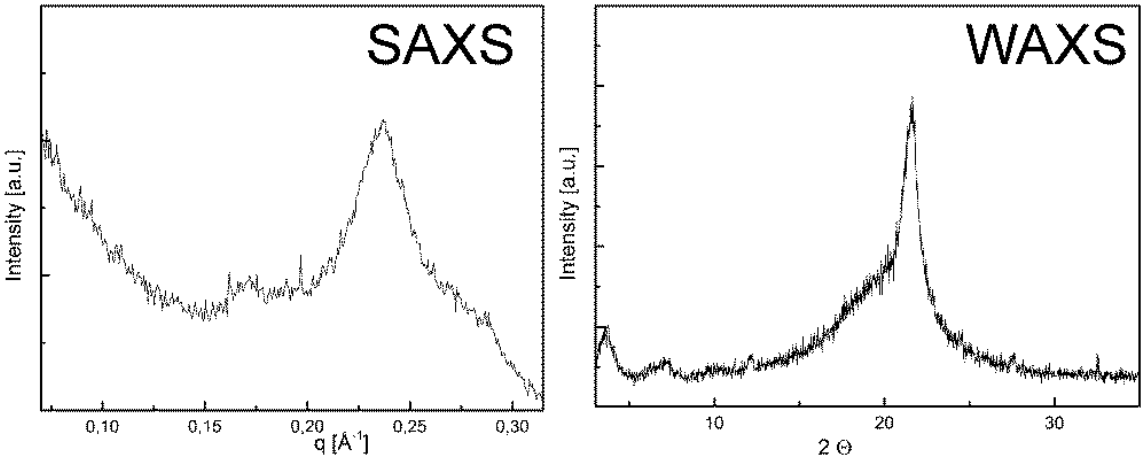

Figure 1: Small- and wide angle x-ray scattering of **P1-H**. Prior to the x-ray measurement the sample was annealed at 42 °C for 24 hours.

The P-N-bond in phosphoramidates is known to be hydrolytically labile in contrast to the stronger P-O bond.[90] Thus, PPAs can be used to release the pendant groups in an acidic environment; while at neutral pH PPAs are stable. This behavior makes PPAs advantageous for using in a low pH-triggered release of side chain-bound material, e.g. for drug release.

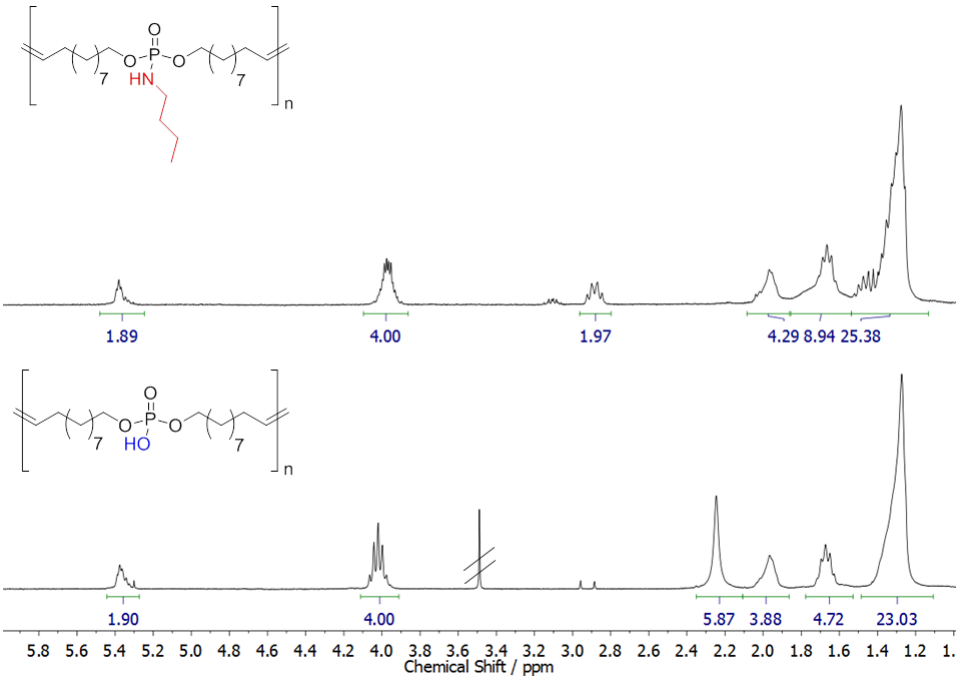

Figure 2. Degradation of **P1** and preparation of a poly(phosphodiester). Top: ^{1}H of **P1.** Bottom: ^{1}H NMR of degraded **P1.**

The cleavability of the phosphoramidate bond with *p*-toluenesulfonic acid was investigated by ^{1}H NMR (Figure 2) and ^{31}P NMR (Figure S13): the complete conversion of the phosphoramidate (9.78 ppm) into a phosphate group (0.40 ppm) is detected after 7 days. No scission of the main chain was observed under these conditions from the NMR spectra. It has to be noted, that the polyphosphodiester exhibit low solubility in common solvents either (methanol/ chloroform mixtures or basic conditions, e.g. pyridine, can be used), and thus SEC analysis was not possible. However, literature reports that phosphodiesters have a very high stability under acidic conditions.[224] This renders the pendant amidate also a potential protective group for the P-OH group, which allows easy handling due to higher solubility as the resulting polyphosphodiester.

Conclusions

In summary, this work presented the first synthesis of poly(phosphoramidate)s via acyclic diene metathesis polycondensation. In addition the comparison of structurally analogues saturated and unsaturated poly(phosphoester)s was performed. Distinct differences for both classes of materials have been identified in their thermal behavior, thermal stability, and hydrolytic stability. Their crystallization behavior was found to be very similar and rather independent of the binding motif of the pendant chain. The pendant amidate was selectively hydrolyzed under acidic conditions, producing a poly(phosphodiester) with a very high stability towards acids. This selective degradation profile renders the phosphoramidates a powerful protective group for the P-OH groups, which in general exhibit strong hydrogen bonding and low solubility. These materials extend the class of degradable P-containing polymers that may find applications ranging from fire retardant additives to biodegradable scaffolds for tissue engineering or drug delivery.

Acknowledgments

The authors thank the Deutsche Forschungsgemeinschaft (WU 750/5-1) for funding. The authors thank Prof. Dr. Katharina Landfester (MPIP) for continuous support. We thank Dr. Manfred Wagner (MPIP) for support in NMR spectroscopy.

Supporting Information

for

Side-Chain Poly(phosphoamidate)s via Acyclic Diene Metathesis Polycondensation

*Alper Cankaya, Mark Steinmann, Yagmur Bülbül, Ingo Lieberwirth, and Frederik R. Wurm**

Max-Planck-Institut für Polymerforschung, Ackermannweg 10, 55128 Mainz, Germany. E-mail: wurm@mpip-mainz.mpg.de, Fax: +49 6131 370 330; Tel: +49 6131 379 581

Table of content

NMR-spectra

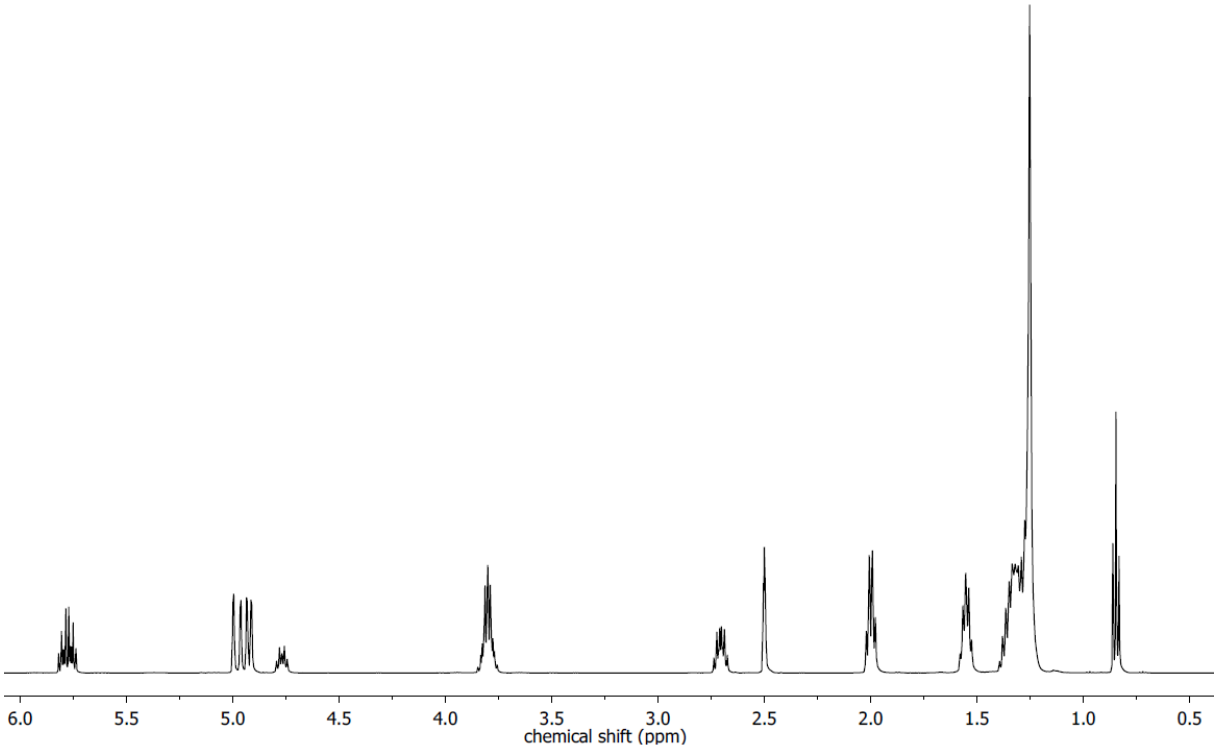

Fig. S1: ^{1}H NMR spectrum of **1** (298K, 300 MHz in DMSO-d_6).

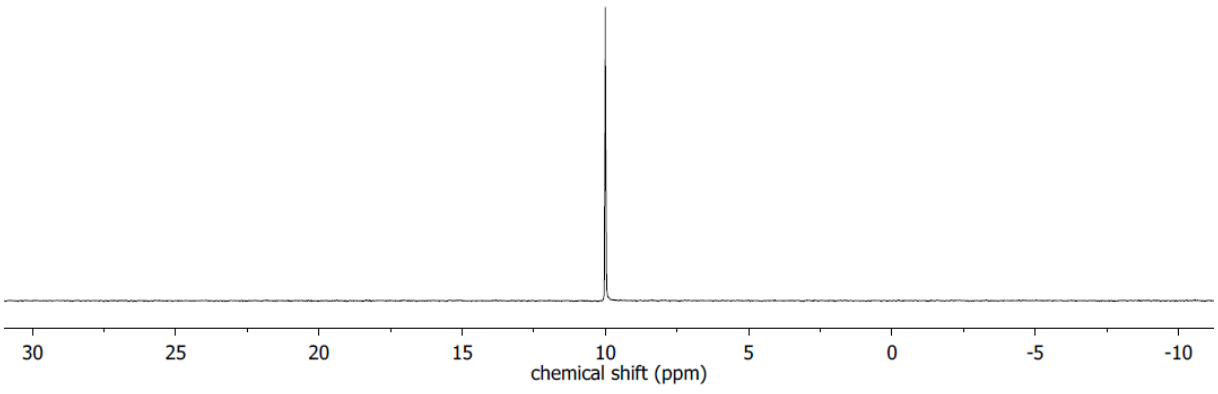

Fig. S2. ^{31}P NMR spectrum of **1** (298K, 202 MHz in DMSO-d_6).

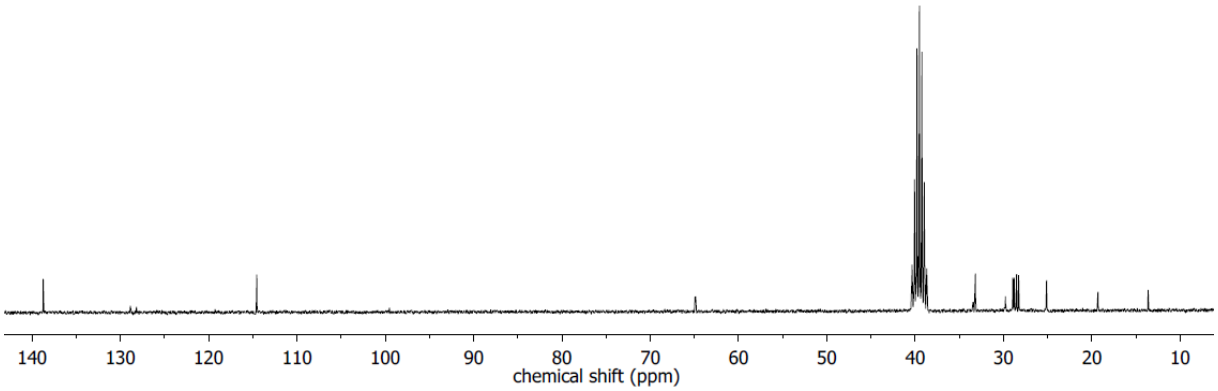

Fig. S3. ^{13}C NMR spectrum of **1** at (298 K, 125 MHz in DMSO-d_6).

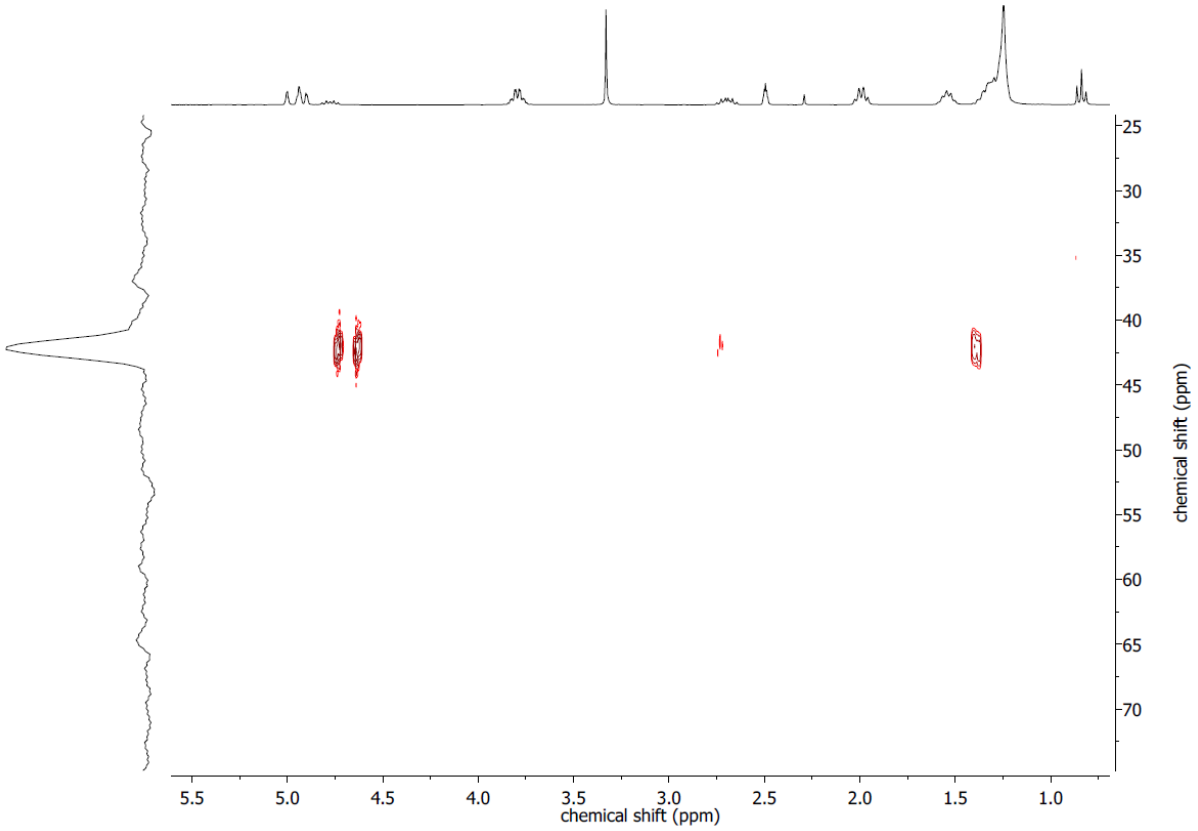

Fig. S4. $^{1}H^{15}N$ HMBC spectrum of **1** (298K, 710 MHz in DMSO-d_6). Cross relaxation between the ^{15}N signal at 42.29 ppm with the neighboring protons can be observed. Cross relaxation is displayed between the ^{15}N signal and the proton bound to the nitrogen atom at 4.75 ppm. The alpha (2.71 ppm) and beta (1.37 ppm) methylene groups to the amidate group show also cross relaxation.

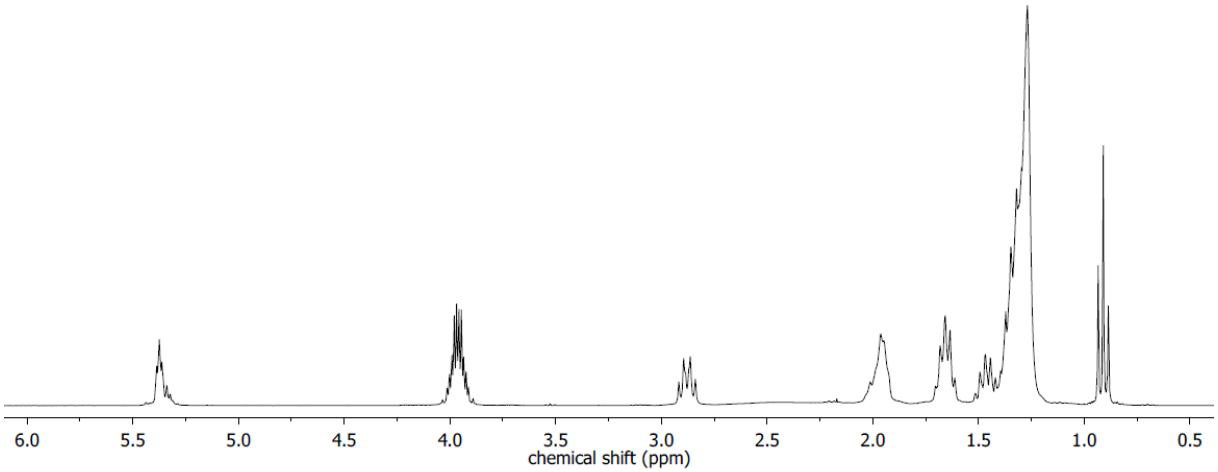

Fig. S5. ^{1}H NMR spectrum of **Poly1** (298 K, 300 MHz in $CDCl_3$).

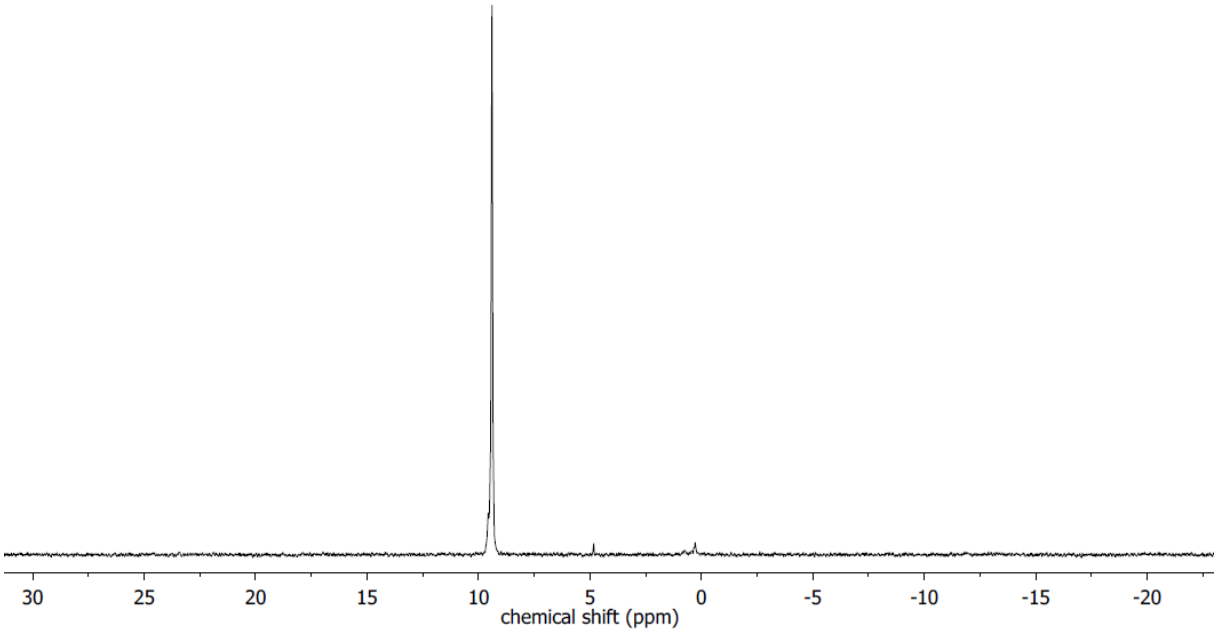

Fig. S6. ^{31}P NMR spectrum of **Poly1** (298 K, 202 MHz in $CDCl_3$).

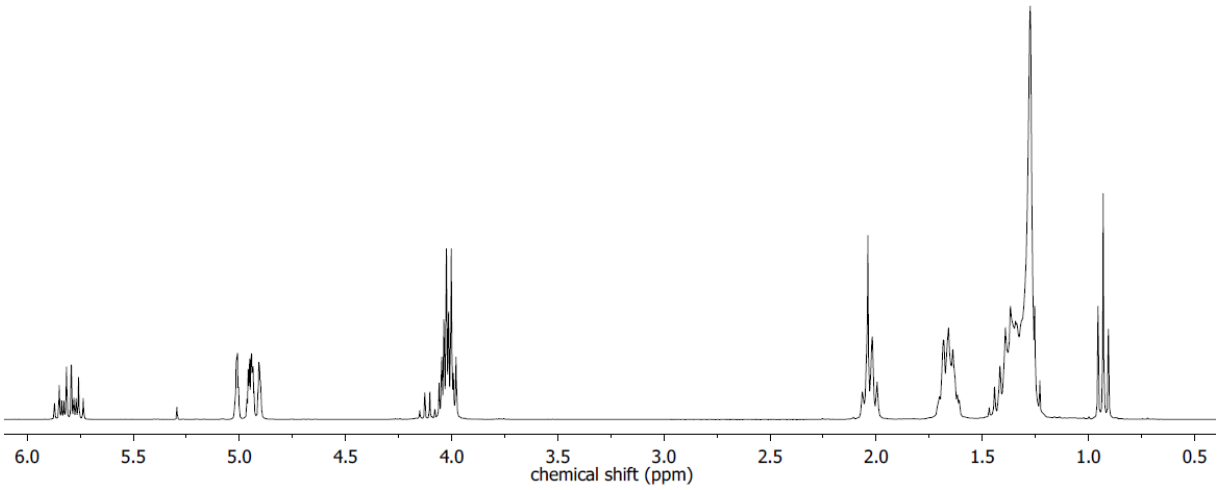

Fig. S7. ^{1}H NMR spectrum of **2** at (298 K, 300 MHz in $CDCl_3$).

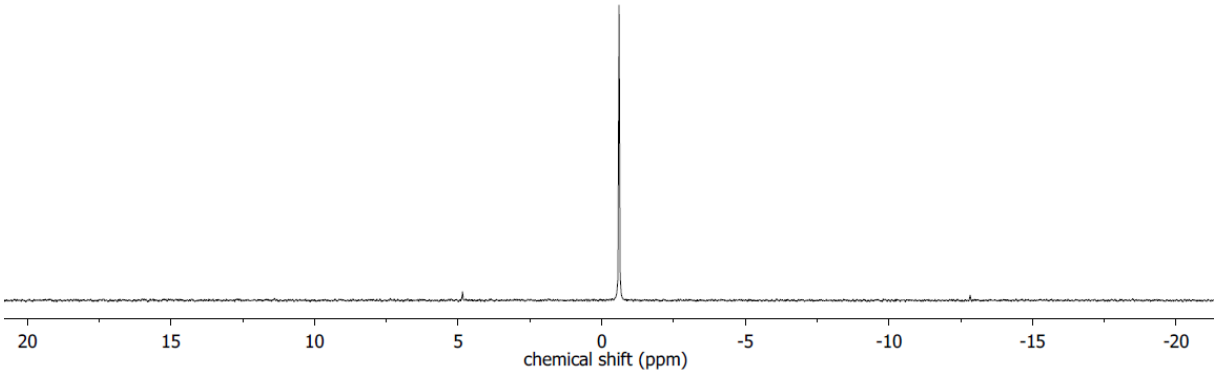

Fig. S8. ^{31}P NMR spectrum of **2** (298 K, 202 MHz in $CDCl_3$)

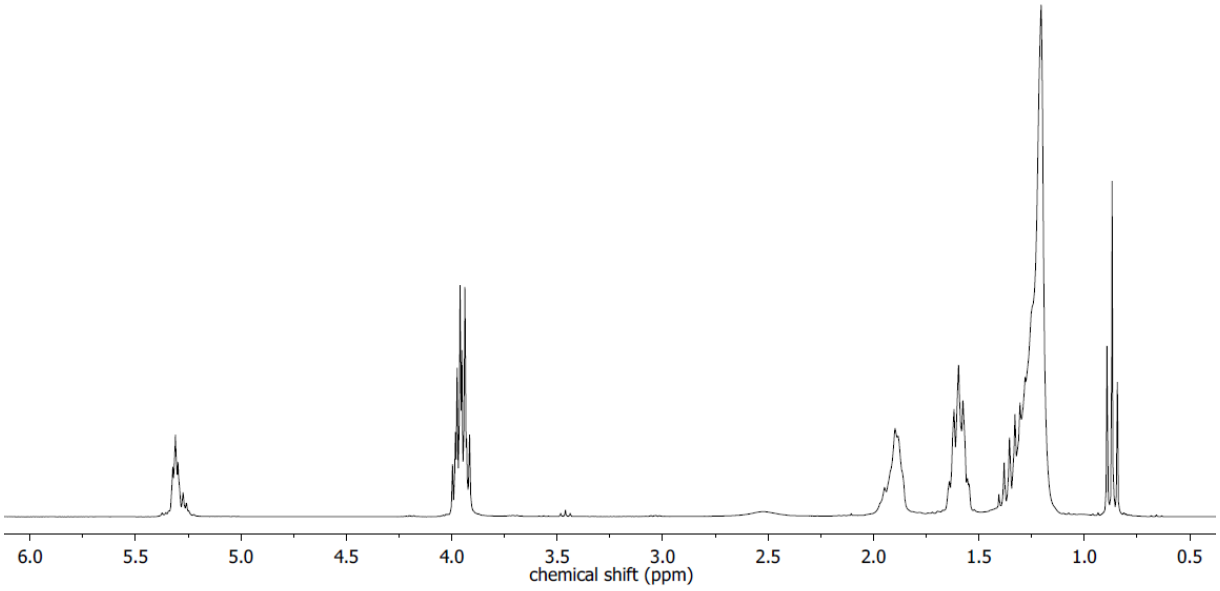

Fig. S 9. ^{1}H NMR spectrum of Poly2 at (298 K, 300 MHz in $CDCl_3$).

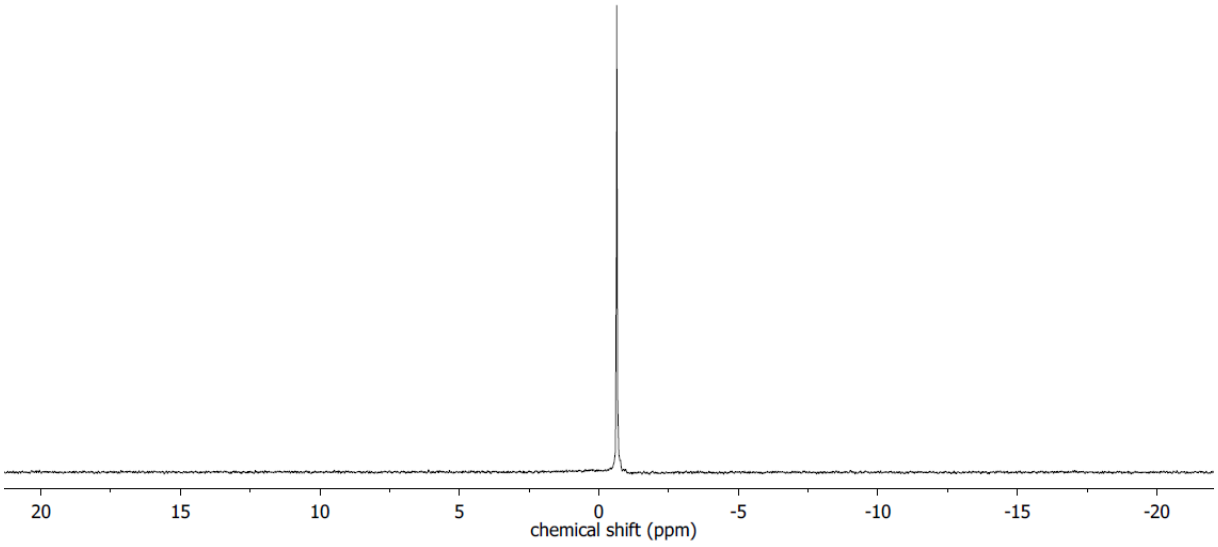

Fig. S 10. ^{31}P NMR spectrum of Poly2 at (298 K, 202 MHz in $CDCl_3$).

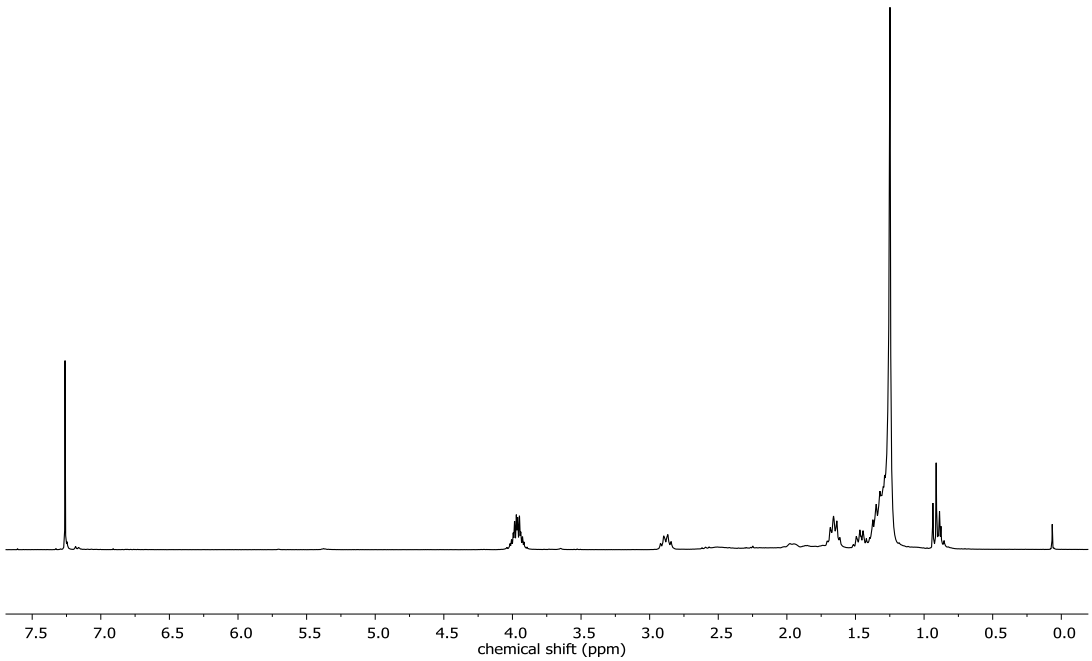

Fig. S11. ^{1}H NMR spectrum of **P1-H** at (298 K, 300 MHz in $CDCl_3$).

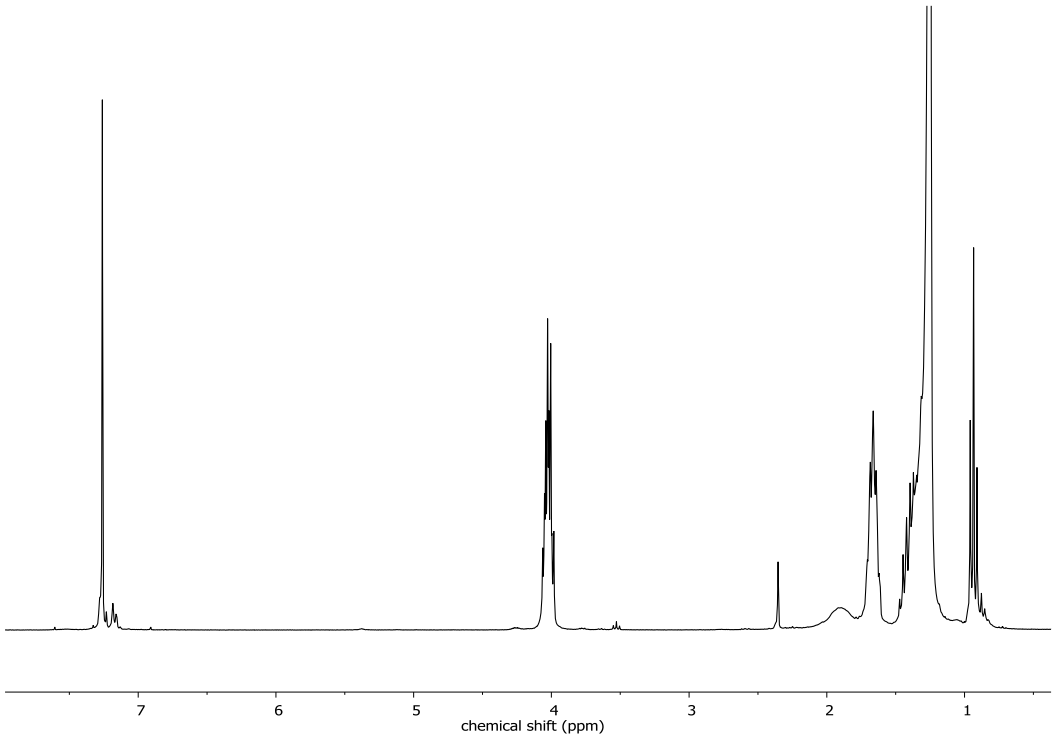

Fig. S12. ^{1}H NMR spectrum of **P2-H** at (298 K, 300 MHz in $CDCl_3$).

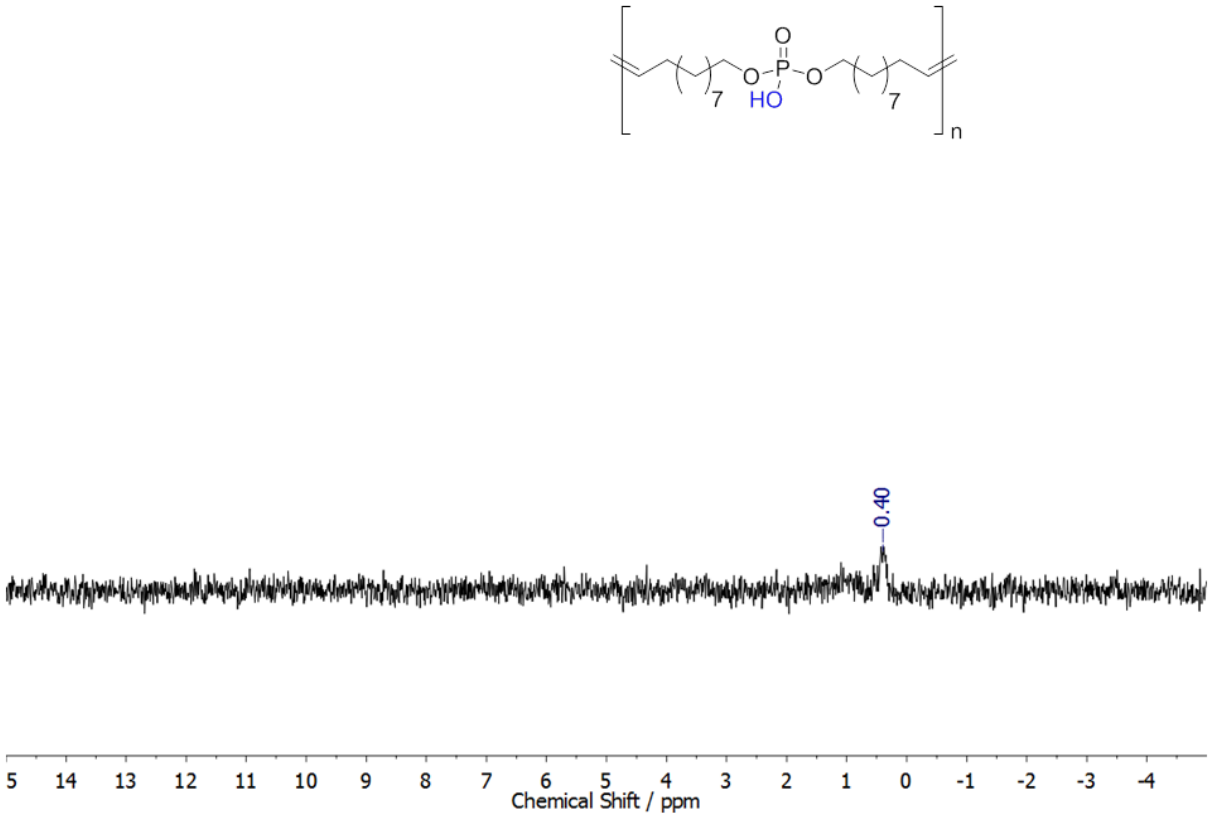

Fig. S13. ^{31}P NMR spectrum after side-chain cleavage of **P1** at (298 K, 121.5 MHz in $CDCl_3$).

GPC-data

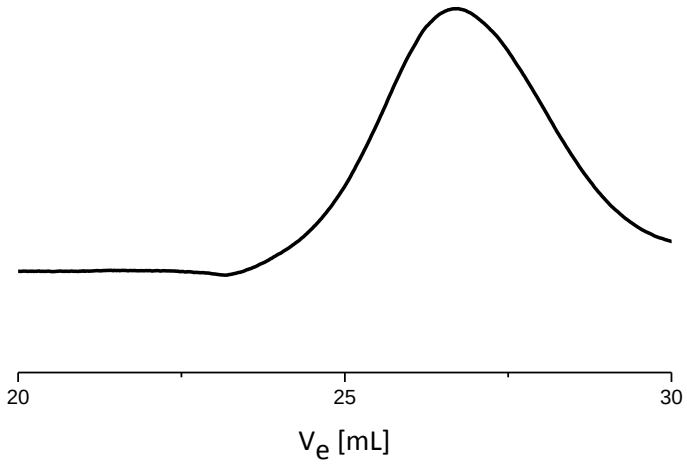

Fig. S 114. Representative GPC elugram of Poly1-c prepared by ADMET polycondensation.

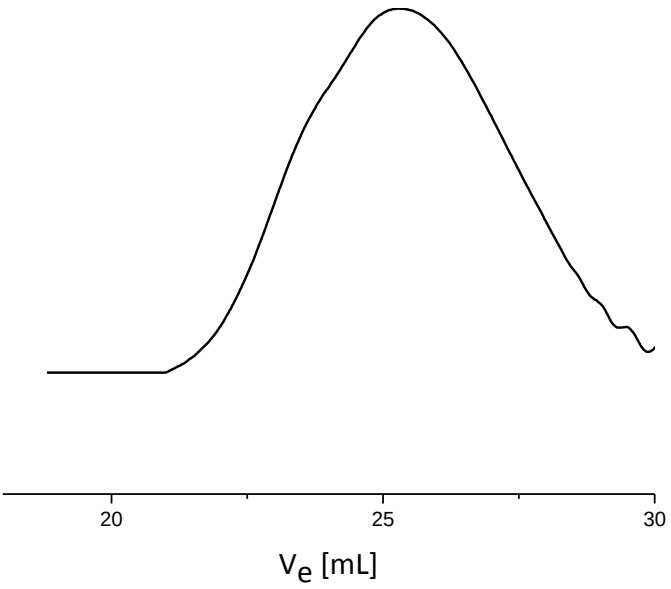

Fig. S125. Representative GPC elugram of Poly2 prepared by ADMET polycondensation.

Bulk properties

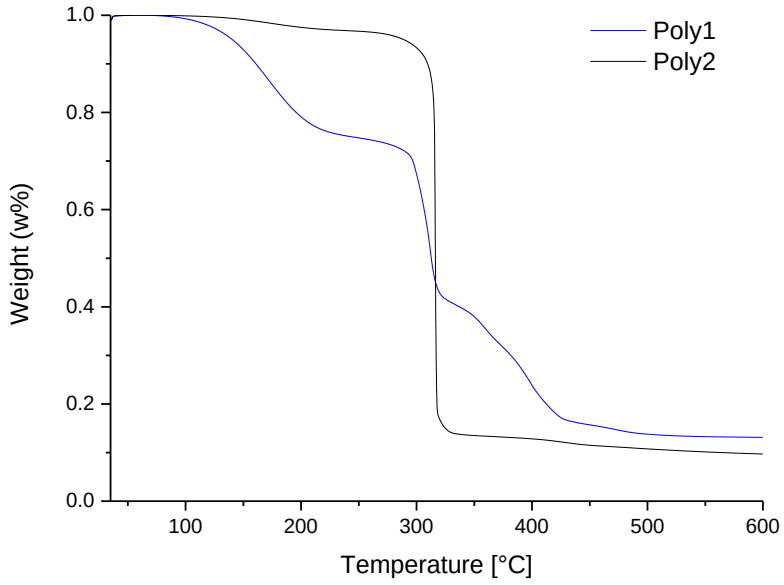

Fig. S136. TGA thermograms of Poly1 and Poly2.

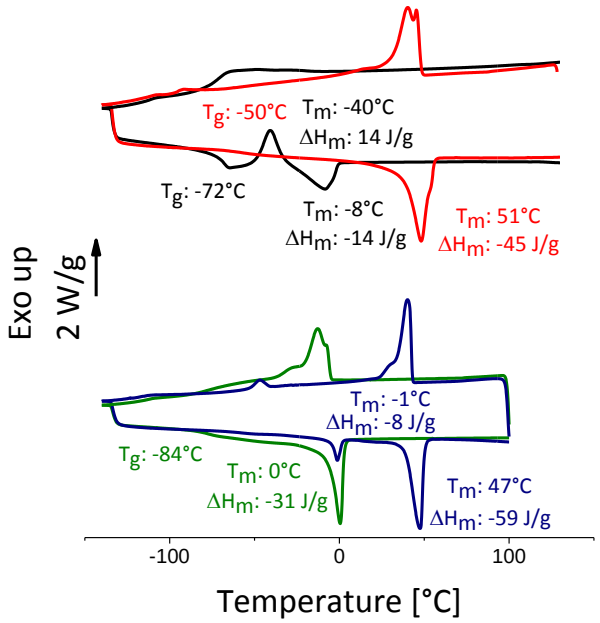

Figure S17. DSC thermograms of (a) P1 (black) and P1-H (red). (b) P2 (green) and P2-H (blue). Both experiments were performed at a heating/cooling rate of 10°C/min.

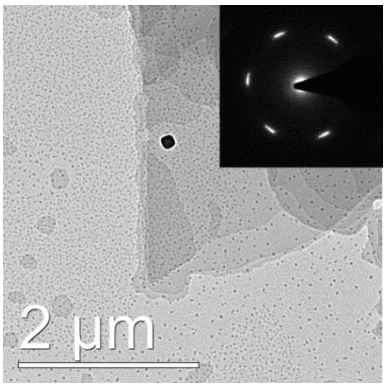

Figure S18: TEM micrograph and the corresponding diffraction pattern of solution crystallized P1-H.

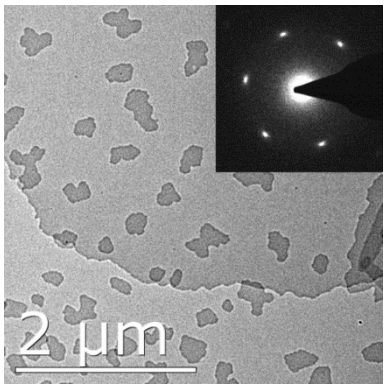

Figure S19: TEM micrograph and the corresponding diffraction pattern (inset) of solution crystallized P2-H.

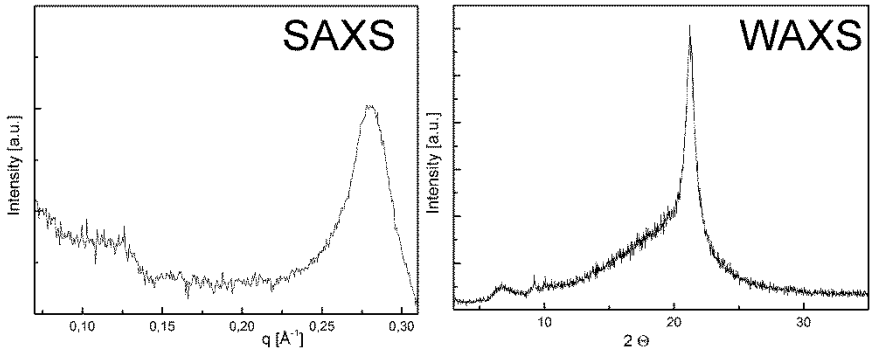

Figure S20: SAXS and WAXS measurements of P2-H samples. Prior to the x-ray measurement the sample was annealed at 42 °C for 24 hours.

6 Literature

1. Wachiralarpphaithoon, C.; Iwasaki, Y.; Akiyoshi, K., Enzyme-degradable phosphorylcholine porous hydrogels cross-linked with polyphosphoesters for cell matrices. *Biomaterials* **2007,** *28* (6), 984-993.
2. Wang, Y.-C.; Tang, L.-Y.; Sun, T.-M.; Li, C.-H.; Xiong, M.-H.; Wang, J., Self-assembled micelles of biodegradable triblock copolymers based on poly (ethyl ethylene phosphate) and poly (ϵ-caprolactone) as drug carriers. *Biomacromolecules* **2007,** *9* (1), 388-395.
3. Schlattner, U.; Tokarska-Schlattner, M.; Wallimann, T., Mitochondrial creatine kinase in human health and disease. *Biochimica et Biophysica Acta (BBA) - Molecular Basis of Disease* **2006,** *1762* (2), 164-180.
4. Marina, A.; Waldburger, C. D.; Hendrickson, W. A., Structure of the entire cytoplasmic portion of a sensor histidine-kinase protein. *The EMBO Journal* **2005,** *24* (24), 4247-4259.
5. Metcalf, W. W.; van der Donk, W. A., Biosynthesis of phosphonic and phosphinic acid natural products. *Annual review of biochemistry* **2009,** *78* (1), 65-94.
6. L. L. Clark, E. D. I., R. Benner, Marine organic phosphorous cycling; novel insights from nuclear magnetic resonance. *Am. J. Sci* **1999,** *299* (1), 724-737.
7. Alberts, B., *Molecular biology of the cell*. 2015.
8. Garrett, R. H.; Grisham, C. M., *Biochemistry*. Brooks/Cole: Boston, 2010.
9. Campbell, N. A.; Williamson, B.; Heyden, R. J.; Pearson/Prentice, H., *Biology : exploring life*. Pearson/Prentice Hall: Boston, Mass., 2006.
10. Castellana, E. T.; Cremer, P. S., Solid supported lipid bilayers: From biophysical studies to sensor design. *Surf. Sci. Rep.* **2006,** *61* (10), 429-444.
11. Monge, S.; David, G., *Phosphorus-based Polymers: From Synthesis to Applications*. Royal Society of Chemistry: 2014; Vol. 11.
12. James, A. A., Resinous compositions. Google Patents: 1936.
13. Maiboroda, V. D.; Datskevich, L. A., Polycondensation of phenylphosphoryl dichloride with diethylene glycol. *Polymer Science U.S.S.R.* **1964,** *6* (10), 2113-2117.
14. E, C. W., Organo-phosphorus resinous compositions. Google Patents: 1952.
15. Kemmlein, S.; Herzke, D.; Law, R. J., Brominated flame retardants in the European chemicals policy of REACH—Regulation and determination in materials. *J. Chromatogr. A* **2009,** *1216* (3), 320-333.
16. Hendriks, H. S.; Antunes Fernandes, E. C.; Bergman, Å.; van den Berg, M.; Westerink, R. H. S., PCB-47, PBDE-47, and 6-OH-PBDE-47 Differentially Modulate Human GABAA and α4β2 Nicotinic Acetylcholine Receptors. *Toxicol. Sci.* **2010,** *118* (2), 635-642.
17. Carraher, C. E.; Winthers, D. O.; Millich, F., Importance of the diamine reactant in the production of polyphosphonamides by the interfacial technique. *Journal of Polymer Science Part A-1: Polymer Chemistry* **1969,** *7* (10), 2763-2773.
18. Kishore, K.; Kannan, P., Synthesis of Novel Flame-Retardant Polyamidophosphate Esters from Aromatic Diols and N-Arylphosphoramidic Dichlorides. *Polym. Bull.* **1990,** *24* (5), 481-486.
19. Kishore, K.; Kannan, P., Synthesis, Spectral, Thermal, and Flammability Studies of Phenolphthalein Polyphosphate Esters. *J. Polym. Sci. Pol. Chem.* **1990,** *28* (12), 3481-3486.
20. Libiszowski, J.; Kałużynski, K.; Penczek, S., Polymerization of cyclic esters of phosphoric acid. VI. Poly(alkyl ethylene phosphates). Polymerization of 2-alkoxy-2-oxo-1,3,2-dioxaphospholans and structure of polymers. *Journal of Polymer Science: Polymer Chemistry Edition* **1978,** *16* (6), 1275-1283.
21. Zhai, X.; Huang, W.; Liu, J.; Pang, Y.; Zhu, X.; Zhou, Y.; Yan, D., Micelles from Amphiphilic Block Copolyphosphates for Drug Delivery. *Macromolecular Bioscience* **2011,** *11* (11), 1603-1610.

22. Steinbach, T.; Wurm, F. R., Poly(phosphoester)s: A New Platform for Degradable Polymers. *Angew. Chem. Int. Ed.* **2015,** *54* (21), 6098-6108.
23. Halasa, A. F., Recent Advances in Anionic Polymerization. *Rubber Chem. Technol.* **1981,** *54* (3), 627-640.
24. Biela, T.; Kłosiński, P.; Penczek, S., Microstructure of poly(alkylene phosphates) related to biopolymers (teichoic acids). *J. Polym. Sci., Part A: Polym. Chem.* **1989,** *27* (3), 763-774.
25. Yuan, Y.-Y.; Du, J.-Z.; Song, W.-J.; Wang, F.; Yang, X.-Z.; Xiong, M.-H.; Wang, J., Biocompatible and functionalizable polyphosphate nanogel with a branched structure. *J. Mater. Chem.* **2012,** *22* (18), 9322-9329.
26. Liu, J.; Huang, W.; Zhou, Y.; Yan, D., Synthesis of hyperbranched polyphosphates by self-condensing ring-opening polymerization of HEEP without catalyst. *Macromolecules* **2009,** *42* (13), 4394-4399.
27. Zhang, F.; Zhang, S.; Pollack, S. F.; Li, R.; Gonzalez, A. M.; Fan, J.; Zou, J.; Leininger, S. E.; Pavía-Sanders, A.; Johnson, R.; Nelson, L. D.; Raymond, J. E.; Elsabahy, M.; Hughes, D. M. P.; Lenox, M. W.; Gustafson, T. P.; Wooley, K. L., Improving Paclitaxel Delivery: In Vitro and In Vivo Characterization of PEGylated Polyphosphoester-Based Nanocarriers. *J. Am. Chem. Soc.* **2015,** *137* (5), 2056-2066.
28. Xiong, M.-H.; Wu, J.; Wang, Y.-C.; Li, L.-S.; Liu, X.-B.; Zhang, G.-Z.; Yan, L.-F.; Wang, J., Synthesis of PEG-armed and polyphosphoester core-cross-linked nanogel by one-step ring-opening polymerization. *Macromolecules* **2009,** *42* (4), 893-896.
29. Kobayashi, S.; Hashimoto, T.; Saegusa, T., Alcoholysis Polymerization of Cyclic Acyloxyphosphorane to Polyphosphate Triesters: Polyphosphorylation of Alcohol. *Macromolecules* **1980,** *13* (6), 1650-1654.
30. Kobayashi, S.; Suzuki, M.; Saegusa, T., Cationic ring-opening polymerization of 2-phenyl-1,2-oxaphospholane (deoxophostone). *Polymer Bulletin* **1981,** *4* (6), 315-321.
31. Kobayashi, S.; Tokunoh, M.; Saegusa, T., Cationic ring-opening polymerization of 2-phenyl-1,3,2-dioxaphosphepane, a seven-membered cyclic phosphonite. *Macromolecules* **1986,** *19* (2), 466-469.
32. Lucas, H. J.; Mitchell, F. W.; Scully, C. N., Cyclic Phosphites of Some Aliphatic Glycols. *J. Am. Chem. Soc.* **1950,** *72* (12), 5491-5497.
33. Lapienis, G.; Penczek, S., Cationic Polymerization of 2-Alkoxy-2-oxo-1,3,2-dioxaphosphorinanes (1,3-Propylene Alkyl Phosphates). *Macromolecules* **1977,** *10* (6), 1301-1306.
34. Xiao, C.-S.; Wang, Y.-C.; Du, J.-Z.; Chen, X.-S.; Wang, J., Kinetics and Mechanism of 2-Ethoxy-2-oxo-1,3,2-dioxaphospholane Polymerization Initiated by Stannous Octoate. *Macromolecules* **2006,** *39* (20), 6825-6831.
35. Nederberg, F.; Connor, E. F.; Möller, M.; Glauser, T.; Hedrick, J. L., New Paradigms for Organic Catalysts: The First Organocatalytic Living Polymerization. *Angew. Chem. Int. Ed.* **2001,** *40* (14), 2712-2715.
36. Pratt, R. C.; Lohmeijer, B. G. G.; Long, D. A.; Waymouth, R. M.; Hedrick, J. L., Triazabicyclodecene: A Simple Bifunctional Organocatalyst for Acyl Transfer and Ring-Opening Polymerization of Cyclic Esters. *Journal of the American Chemical Society* **2006,** *128* (14), 4556-4557.
37. Penczek, S.; Pretula, J., High-molecular-weight poly(alkylene phosphates) and preparation of amphiphilic polymers thereof. *Macromolecules* **1993,** *26* (9), 2228-2233.
38. Vogt, W.; Balasubramanian, S., Über die polykondensation von diäthylphosphit mit aliphastischen diolen. *Die Makromolekulare Chemie* **1973,** *163* (1), 111-134.
39. Nagarkar, A. A.; Crochet, A.; Fromm, K. M.; Kilbinger, A. F. M., Efficient Amine End-Functionalization of Living Ring-Opening Metathesis Polymers. *Macromolecules* **2012,** *45* (11), 4447-4453.

40. Steinbach, T.; Alexandrino, E. M.; Wahlen, C.; Landfester, K.; Wurm, F. R., Poly(phosphonate)s via Olefin Metathesis: Adjusting Hydrophobicity and Morphology. *Macromolecules* **2014,** *47* (15), 4884-4893.
41. Steinbach, T.; Alexandrino, E. M.; Wurm, F. R., Unsaturated poly(phosphoester)s via ring-opening metathesis polymerization. *Polymer Chemistry* **2013,** *4* (13), 3800-3806.
42. Wagener, K. B.; Brzezinska, K.; Anderson, J. D.; Younkin, T. R.; Steppe, K.; DeBoer, W., Kinetics of Acyclic Diene Metathesis (ADMET) Polymerization. Influence of the Negative Neighboring Group Effect. *Macromolecules* **1997,** *30* (24), 7363-7369.
43. Marsico, F.; Turshatov, A.; Pekoz, R.; Avlasevich, Y.; Wagner, M.; Weber, K.; Donadio, D.; Landfester, K.; Baluschev, S.; Wurm, F. R., Hyperbranched unsaturated polyphosphates as a protective matrix for long-term photon upconversion in air. *Journal of the American Chemical Society* **2014,** *136* (31), 11057-64.
44. Taeuber, K.; Marsico, F.; Wurm, F. R.; Schartel, B., Hyperbranched poly(phosphoester)s as flame retardants for technical and high performance polymers. *Polymer Chemistry* **2014,** *5* (24), 7042-7053.
45. Minegishi, S.; Komatsu, S.; Kameyama, A.; Nishikubo, T., Novel synthesis of polyphosphonates by the polyaddition of bis(epoxide) with diaryl phosphonates. *J. Polym. Sci., Part A: Polym. Chem.* **1999,** *37* (7), 959-965.
46. Minegishi, S.; Tsuchida, S.; Sasaki, M.; Kameyama, A.; Kudo, H.; Nishikubo, T., Synthesis of polyphosphonates containing pendant chloromethyl groups by the polyaddition of bis(oxetane)s with phosphonic dichlorides. *J. Polym. Sci., Part A: Polym. Chem.* **2002,** *40* (21), 3835-3846.
47. Posner, T., Beiträge zur Kenntniss der ungesättigten Verbindungen. II. Ueber die Addition von Mercaptanen an ungesättigte Kohlenwasserstoffe. *Berichte der deutschen chemischen Gesellschaft* **1905,** *38* (1), 646-657.
48. Hoyle, C. E.; Bowman, C. N., Thiol–Ene Click Chemistry. *Angew. Chem. Int. Ed.* **2010,** *49* (9), 1540-1573.
49. Senyurt, A. F.; Wei, H.; Phillips, B.; Cole, M.; Nazarenko, S.; Hoyle, C. E.; Piland, S. G.; Gould, T. E., Physical and Mechanical Properties of Photopolymerized Thiol−Ene/Acrylates. *Macromolecules* **2006,** *39* (19), 6315-6317.
50. Kade, M. J.; Burke, D. J.; Hawker, C. J., The power of thiol-ene chemistry. *J. Polym. Sci., Part A: Polym. Chem.* **2010,** *48* (4), 743-750.
51. Ding, L.; Qiu, J.; Zhu, Z., Facile Synthesis of Thiol-Functionalized Long-Chain Highly Branched ROMP Polymers and Surface-Decorated with Gold Nanoparticles. *Macromol. Rapid Commun.* **2013,** *34* (20), 1635-1641.
52. Maiti, S.; Banerjee, S.; Palit, S. K., Phosphorus-containing polymers. *Prog. Polym. Sci.* **1993,** *18* (2), 227-261.
53. Kiefer, R. L., Handbook of Engineering Polymeric Materials Edited by Nicholas P. Cheremisinoff. Marcel Dekker: New York. 1997. xii + 881 pp. $225.00. ISBN 0-8247-9799-X. *J. Am. Chem. Soc.* **1998,** *120* (16), 4053-4054.
54. Kondo, H.; Sato, M.; Yokoyama, M., Phenothiaphosphine-containing polyamides and polyesters. *Journal of Polymer Science: Polymer Chemistry Edition* **1984,** *22* (5), 1055-1064.
55. Kondo, H.; Sato, M.; Yokoyama, M., Preparation of phosphorus-containing polymers—XXVI. *Eur. Polym. J.* **1981,** *17* (6), 583-588.
56. Melissaris, A. P.; Mikroyannidis, J. A., Phosphorus-containing crosslinkable polymers for fire- and heat-resistant applications. *Eur. Polym. J.* **1989,** *25* (3), 275-280.
57. Sato, M.; Yokoyama, M., Preparation of phosphorus-containing polymers—XX. Synthesis of phenoxaphosphine-containing polyesters. *Eur. Polym. J.* **1980,** *16* (1), 79-83.

58. Sato, M.; Yokoyama, M., Preparation of phosphorus-containing polymers. XXII. Phenoxaphosphine-containing poly- 1,3,4-oxadiazoles. *Journal of Polymer Science: Polymer Chemistry Edition* **1980,** *18* (8), 2751-2754.
59. Brehme, S.; Schartel, B.; Goebbels, J.; Fischer, O.; Pospiech, D.; Bykov, Y.; Döring, M., Phosphorus polyester versus aluminium phosphinate in poly(butylene terephthalate) (PBT): Flame retardancy performance and mechanisms. *Polym. Degrad. Stab.* **2011,** *96* (5), 875-884.
60. Balabanovich, A. I.; Pospiech, D.; Häußler, L.; Harnisch, C.; Döring, M., Pyrolysis behavior of phosphorus polyesters. *J. Anal. Appl. Pyrolysis* **2009,** *86* (1), 99-107.
61. Pretula, J.; Kaluzynski, K.; Szymanski, R.; Penczek, S., Transesterification of oligomeric dialkyl phosphonates, leading to the high-molecular-weight poly-H-phosphonates. *Journal of Polymer Science Part A: Polymer Chemistry* **1999,** *37* (9), 1365-1381.
62. Frechet, J., Functional polymers and dendrimers: reactivity, molecular architecture, and interfacial energy. *Science* **1994,** *263* (5154), 1710-1715.
63. Kałużynski, K.; Libiszowski, J.; Penczek, S., Poly(2-hydro-2-oxo-1,3,2-dioxaphosphorinane). Preparation and NMR spectra. *Die Makromolekulare Chemie* **1977,** *178* (10), 2943-2947.
64. Pretula, J.; Kaluzynski, K.; Szymanski, R.; Penczek, S., Preparation of Poly(alkylene H-phosphonate)s and Their Derivatives by Polycondensation of Diphenyl H-Phosphonate with Diols and Subsequent Transformations. *Macromolecules* **1997,** *30* (26), 8172-8176.
65. Troev, K.; Tsatcheva, I.; Koseva, N.; Georgieva, R.; Gitsov, I., Immobilization of aminothiols on poly (oxyethylene H-phosphonate) s and poly (oxyethylene phosphate) s—An approach to polymeric protective agents for radiotherapy of cancer. *J. Polym. Sci., Part A: Polym. Chem.* **2007,** *45* (7), 1349-1363.
66. Le Corre, S. S.; Berchel, M.; Couthon-Gourvès, H.; Haelters, J.-P.; Jaffrès, P.-A., Atherton–Todd reaction: mechanism, scope and applications. *Beilstein Journal of Organic Chemistry* **2014,** *10*, 1166-1196.
67. Bogomilova, A.; Höhn, M.; Günther, M.; Herrmann, A.; Troev, K.; Wagner, E.; Schreiner, L., A polyphosphoester conjugate of melphalan as antitumoral agent. *European Journal of Pharmaceutical Sciences* **2013,** *50* (3–4), 410-419.
68. Schmidt, M.; Freitag, D.; Bottenbruch, L.; Reinking, K., Aromatische polyphosphonate: Thermoplastische polymere von extremer brandwidrigkeit. *Die Angewandte Makromolekulare Chemie* **1985,** *132* (1), 1-18.
69. Nishikubo, T.; Kameyama, A.; Minegishi, S., Novel Syntheses of Poly(phosphonate)s and Poly(phosphate)s by Addition Reactions of Bisepoxides with Phosphonic Dichlorides and Dichlorophosphates. *Macromolecules* **1995,** *28* (14), 4810-4814.
70. Steinbach, T.; Ritz, S.; Wurm, F. R., Water-Soluble Poly(phosphonate)s via Living Ring-Opening Polymerization. *ACS Macro Letters* **2014,** *3* (3), 244-248.
71. Wolf, T.; Steinbach, T.; Wurm, F. R., A Library of Well-Defined and Water-Soluble Poly(alkyl phosphonate)s with Adjustable Hydrolysis. *Macromolecules* **2015,** *48* (12), 3853-3863.
72. Steinbach, T.; Wahlen, C.; Wurm, F. R., Poly (phosphonate)-mediated Horner–Wadsworth–Emmons reactions. *Polymer Chemistry* **2015**.
73. Bauer, K.; Tee, H. T. C.; Lieberwirth, I.; Wurm, F. R., In-Chain Poly(phosphonate)s by Acyclic Diene Metathesis Polycondensation. *Macromolecules (Washington, DC, United States)* **2016**.
74. Steinmann, M.; Markwart, J.; Wurm, F. R., Poly(alkylidene chlorophosphate)s via Acyclic Diene Metathesis Polymerization: A General Platform for the Postpolymerization Modification of Poly(phosphoester)s. *Macromolecules* **2014,** *47* (24), 8506-8513.
75. Huang, S.-W.; Wang, J.; Zhang, P.-C.; Mao, H.-Q.; Zhuo, R.-X.; Leong, K. W., Water-Soluble and Nonionic Polyphosphoester: Synthesis, Degradation, Biocompatibility and Enhancement of Gene Expression in Mouse Muscle. *Biomacromolecules* **2004,** *5* (2), 306-311.
76. Chen, S.; Zhang, D.; Cheng, X.; Li, T.; Zhang, A.; Li, J., Preparation and characterization of a novel hyperbranched polyphosphate ester. *Mater. Chem. Phys.* **2012,** *137* (1), 154-159.

77. Koseva, N.; Bogomilova, A.; Atkova, K.; Troev, K., New functional polyphosphoesters: Design and characterization. *Reactive & Functional Polymers* **2008,** *68* (5), 954-966.
78. Marsico, F.; Turshatov, A.; Weber, K.; Wurm, F. R., A Metathesis Route for BODIPY Labeled Polyolefins. *Org. Lett.* **2013,** *15* (15), 3844-3847.
79. Alexandrino, E. M.; Ritz, S.; Marsico, F.; Baier, G.; Mailänder, V.; Landfester, K.; Wurm, F. R., Paclitaxel-loaded polyphosphate nanoparticles: a potential strategy for bone cancer treatment. *Journal of Materials Chemistry B* **2014,** *2* (10), 1298.
80. Iwasaki, Y.; Akiyoshi, K., Synthesis and Characterization of Amphiphilic Polyphosphates with Hydrophilic Graft Chains and Cholesteryl Groups as Nanocarriers. *Biomacromolecules* **2006,** *7* (5), 1433-1438.
81. Kristin N. Bauer, H. T. Tee., Evandro M. Alexandrino, Frederik R. Wurm, Main-chain degradable and biomimetic poly(phosphoester)s: from synthesis to applications. submitted 2016.
82. Wang, J.; Mao, H.-Q.; Leong, K. W., A Novel Biodegradable Gene Carrier Based on Polyphosphoester. *J. Am. Chem. Soc.* **2001,** *123* (38), 9480-9481.
83. Huang, S.-W.; Wang, J.; Zhang, P.-C.; Mao, H.-Q.; Zhuo, R.-X.; Leong, K. W., Water-soluble and nonionic polyphosphoester: synthesis, degradation, biocompatibility and enhancement of gene expression in mouse muscle. *Biomacromolecules* **2004,** *5* (2), 306-311.
84. Wen, J.; Mao, H. Q.; Li, W.; Lin, K. Y.; Leong, K. W., Biodegradable polyphosphoester micelles for gene delivery. *J. Pharm. Sci.* **2004,** *93* (8), 2142-2157.
85. Xu, X.; Yu, H.; Gao, S.; Mao, H.-Q.; Leong, K. W.; Wang, S., Polyphosphoester microspheres for sustained release of biologically active nerve growth factor. *Biomaterials* **2002,** *23* (17), 3765-3772.
86. Wang, Y.-C.; Yuan, Y.-Y.; Du, J.-Z.; Yang, X.-Z.; Wang, J., Recent Progress in Polyphosphoesters: From Controlled Synthesis to Biomedical Applications. *Macromol Biosci* **2009,** *9*, 1154-1164.
87. Huang, S.-W.; Zhuo, R.-X., Recent Advances in Polyphosphoester and Polyphosphoramidate-Based Biomaterials. *Phosphorus, Sulfur, and Silicon and the Related Elements* **2008,** *183* (2-3), 340-348.
88. Baran, J.; Penczek, S., Hydrolysis of Polyesters of Phosphoric Acid. 1. Kinetics and the pH Profile. *Macromolecules* **1995,** *28* (15), 5167-5176.
89. Kugel, L.; Halmann, M., Solvolysis of phosphoric acid esters. Hydrolysis of methyl, ethyl, isopropyl, and tert-butyl dihydrogen phosphates. *The Journal of Organic Chemistry* **1967,** *32* (3), 642-647.
90. Zhang, S.; Wang, H.; Shen, Y.; Zhang, F.; Seetho, K.; Zou, J.; Taylor, J.-S. A.; Dove, A. P.; Wooley, K. L., A Simple and Efficient Synthesis of an Acid-Labile Polyphosphoramidate by Organobase-Catalyzed Ring-Opening Polymerization and Transformation to Polyphosphoester Ionomers by Acid Treatment. *Macromolecules* **2013,** *46* (13), 5141-5149.
91. Du, J.-Z.; Sun, T.-M.; Weng, S.-Q.; Chen, X.-S.; Wang, J., Synthesis and characterization of photo-cross-linked hydrogels based on biodegradable polyphosphoesters and poly (ethylene glycol) copolymers. *Biomacromolecules* **2007,** *8* (11), 3375-3381.
92. Iwasaki, Y.; Nakagawa, C.; Ohtomi, M.; Ishihara, K.; Akiyoshi, K., Novel biodegradable polyphosphate cross-linker for making biocompatible hydrogel. *Biomacromolecules* **2004,** *5* (3), 1110-1115.
93. Wang, Y.-C.; Tang, L.-Y.; Li, Y.; Wang, J., Thermoresponsive Block Copolymers of Poly(ethylene glycol) and Polyphosphoester: Thermo-Induced Self-Assembly, Biocompatibility, and Hydrolytic Degradation. *Biomacromolecules* **2009,** *10* (1), 66-73.
94. Xiang, D. F.; Bigley, A. N.; Ren, Z.; Xue, H.; Hull, K. G.; Romo, D.; Raushel, F. M., Interrogation of the Substrate Profile and Catalytic Properties of the Phosphotriesterase from Sphingobium sp. Strain TCM1: An Enzyme Capable of Hydrolyzing Organophosphate Flame Retardants and Plasticizers. *Biochemistry* **2015**.

95. Allcock, H. R., Recent advances in phosphazene (phosphonitrilic) chemistry. *Chemical Reviews* **1972,** *72* (4), 315-356.
96. Sohn, Y. S.; Cho, Y. H.; Baek, H.; Jung, O.-S., Synthesis and Properties of Low Molecular Weight Polyphosphazenes. *Macromolecules* **1995,** *28* (22), 7566-7568.
97. Honeyman, C. H.; Manners, I.; Morrissey, C. T.; Allcock, H. R., Ambient Temperature Synthesis of Poly(dichlorophosphazene) with Molecular Weight Control. *Journal of the American Chemical Society* **1995,** *117* (26), 7035-7036.
98. Simon, J., Inorganic and organometallic polymers (ACS symposium series 360). Edited by M. Zeldin, K. J. Wynne and H. R. Allcock. American Chemical Society, Washington 1988. xii, 512 pp., bound, US $ 119.95.—ISBN 0-8412-1442-5. *Adv. Mater.* **1989,** *1* (4), 132-133.
99. Allcock, H. R.; Crane, C. A.; Morrissey, C. T.; Nelson, J. M.; Reeves, S. D.; Honeyman, C. H.; Manners, I., "Living" Cationic Polymerization of Phosphoranimines as an Ambient Temperature Route to Polyphosphazenes with Controlled Molecular Weights. *Macromolecules* **1996,** *29* (24), 7740-7747.
100. Zhu, J. L.; Chen, G. J.; Jow, J.; Su, K. C. H.; Wei, P.; Wang, C., Intumescent, Halogen-Free, Silicon-Phosphorus-Nitrogen Based Polymeric Flame Retardant. Google Patents: 2010.
101. Kannan, P.; Kishore, K., Novel Flame-Retardant Polyphosphoramide Esters. *Polymer* **1992,** *33* (2), 418-422.
102. Zhao, W.; Liu, J.; Peng, H.; Liao, J.; Wang, X., Synthesis of a novel PEPA-substituted polyphosphoramide with high char residues and its performance as an intumescent flame retardant for epoxy resins. *Polym. Degrad. Stab.* **2015,** *118*, 120-129.
103. Tai, Q.; Hu, Y.; Yuen, R. K. K.; Song, L.; Lu, H., Synthesis, structure-property relationships of polyphosphoramides with high char residues. *J. Mater. Chem.* **2011,** *21* (18), 6621-6627.
104. Gaan, S.; Rupper, P.; Salimova, V.; Heuberger, M.; Rabe, S.; Vogel, F., Thermal decomposition and burning behavior of cellulose treated with ethyl ester phosphoramidates: Effect of alkyl substituent on nitrogen atom. *Polym. Degrad. Stab.* **2009,** *94* (7), 1125-1134.
105. Lu, S.-Y.; Hamerton, I., Recent developments in the chemistry of halogen-free flame retardant polymers. *Progress in Polymer Science* **2002,** *27* (8), 1661-1712.
106. Łapienis, G.; Penczek, S.; Aleksiuk, G. P.; Kropachev, V. A., Synthesis of poly(alkylene phosphate)s with N-containing bases in the side chains. II. 9-N-oxoethyleneadenine on the poly(trimethylene phosphate) chain. *J. Polym. Sci., Part A: Polym. Chem.* **1987,** *25* (7), 1729-1736.
107. Pretula, J.; Kaluzynski, K.; Penczek, S., Synthesis of poly(alkylene phosphates) with nitrogen-containing bases in the side chains. 1. Nitrogen- and carbon-substituted imidazoles. *Macromolecules* **1986,** *19* (7), 1797-1799.
108. Rahil, J.; Haake, P., Reactivity and mechanism of hydrolysis of phosphonamides. *Journal of the American Chemical Society* **1981,** *103* (7), 1723-1734.
109. Benkovic, S. J.; Sampson, E. J., Structure-reactivity correlation for the hydrolysis of phosphoramidate monoanions. *J. Am. Chem. Soc.* **1971,** *93* (16), 4009-4016.
110. Cankaya, A.; Steinmann, M.; Bulbul, Y.; Lieberwirth, I.; Wurm, F. R., Side-chain poly(phosphoramidate)s via acyclic diene metathesis polycondensation. *Polymer Chemistry* **2016**.
111. Gutmann, V.; Hagen, D. E.; Utvary, K., Umsetzungen des Phenylphosphoroxydichlorids mit aromatischen Diaminen. *Monatshefte für Chemie und verwandte Teile anderer Wissenschaften* **1962,** *93* (3), 627-631.
112. Greenley, R. Z., Method of preparing polymeric heterocyclic amides. Google Patents: 1966.
113. Carraher, C. E.; Winthers, D. O., Interfacial synthesis of polyiminocarbonylimino(phenylphosphinylidene) and polyiminocarbonylmethylenecarbonylimino-(phenylphosphinylidene). *Journal of Polymer Science Part A-1: Polymer Chemistry* **1969,** *7* (8), 2417-2420.

114. John, F., Polyphosphonamide polymers and copolymers. Google Patents: 1963.
115. Sivaram, S.; Laboratory, N. C., *Polymer Science: Contemporary Themes*. Tata McGraw-Hill Publishing Company: 1991.
116. Lyu, W.; Cui, Y.; Zhang, X.; Yuan, J.; Zhang, W., Fire and thermal properties of PA 66 resin treated with poly-N-aniline-phenyl phosphamide as a flame retardant. *Fire and Materials* **2016**, n/a-n/a.
117. Kannan, P.; Umamaheshwari, N.; Kishore, K., Synthesis and characterization of new flame-retardant polyaryl phosphoramide esters containing furan and thiophene units. *J. Appl. Polym. Sci.* **1995,** *56* (1), 113-118.
118. Li, Z.; Wei, P.; Yang, Y.; Yan, Y.; Shi, D., Synthesis of a hyperbranched poly(phosphamide ester) oligomer and its high-effective flame retardancy and accelerated nucleation effect in polylactide composites. *Polym. Degrad. Stab.* **2014,** *110*, 104-112.
119. Gordon, K. L.; Thompson, C. M.; Lyon, R. E., Flame Retardant Epoxy Resins containing Aromatic Poly(phosphonamides). *High Perform. Polym.* **2010,** *22* (8), 945-958.
120. Vyle, J. S.; Li, X.; Cosstick, R., New methods for the synthesis of 3′-S-phosphorothiolate internucleoside linkages. *Tetrahedron Lett.* **1992,** *33* (21), 3017-3020.
121. Bentley, J.; Brazier, J. A.; Fisher, J.; Cosstick, R., Duplex stability of DNA[middle dot]DNA and DNA[middle dot]RNA duplexes containing 3[prime or minute]-S-phosphorothiolate linkages. *Organic & Biomolecular Chemistry* **2007,** *5* (22), 3698-3702.
122. Jayakumar, H. K.; Buckingham, J. L.; Brazier, J. A.; Berry, N. G.; Cosstick, R.; Fisher, J., NMR studies of the conformational effect of single and double 3′-S-phosphorothiolate substitutions within deoxythymidine trinucleotides. *Magn. Reson. Chem.* **2007,** *45* (4), 340-345.
123. Li, N.-S.; Frederiksen, J. K.; Piccirilli, J. A., Synthesis, Properties, and Applications of Oligonucleotides Containing an RNA Dinucleotide Phosphorothiolate Linkage. *Acc. Chem. Res.* **2011,** *44* (12), 1257-1269.
124. Mileson, B. E.; Chambers, J. E.; Chen, W. L.; Dettbarn, W.; Ehrich, M.; Eldefrawi, A. T.; Gaylor, D. W.; Hamernik, K.; Hodgson, E.; Karczmar, A. G.; Padilla, S.; Pope, C. N.; Richardson, R. J.; Saunders, D. R.; Sheets, L. P.; Sultatos, L. G.; Wallace, K. B., Common Mechanism of Toxicity: A Case Study of Organophosphorus Pesticides. *Toxicol. Sci.* **1998,** *41* (1), 8-20.
125. Schönbein, C. F., *Phil. Mag.* **1847,** *31*.
126. Schönbein, C. F., *Prog. Ann.* **1846,** *70*.
127. James E. Mark, B. E., Frederick R. Eirich, *From Science and Technology of Rubber, Third Edition*. 3 ed.; ELSEVIER ACADEMIC PRESS 2005.
128. Matyjaszewski, K., Macromolecular engineering: From rational design through precise macromolecular synthesis and processing to targeted macroscopic material properties. *Prog. Polym. Sci.* **2005,** *30* (8–9), 858-875.
129. Wurm, F.; Frey, H., Linear-dendritic block copolymers: The state of the art and exciting perspectives. *Progress in Polymer Science* **2011,** *36* (1), 1-52.
130. Wang, J.-S.; Matyjaszewski, K., Controlled/"living" radical polymerization. atom transfer radical polymerization in the presence of transition-metal complexes. *J. Am. Chem. Soc.* **1995,** *117* (20), 5614-5615.
131. Kricheldorf, H., *Polycondensation; History and new Results*. Springer-Verlag: 2014; p 216.
132. Hadjichristidis, N.; Iatrou, H.; Pitsikalis, M.; Mays, J., Macromolecular architectures by living and controlled/living polymerizations. *Prog. Polym. Sci.* **2006,** *31* (12), 1068-1132.
133. Obermeier, B.; Wurm, F.; Mangold, C.; Frey, H., Multifunctional Poly(ethylene glycol)s. *Angewandte Chemie-International Edition* **2011,** *50* (35), 7988-7997.
134. Günay, K. A.; Theato, P.; Klok, H.-A., Standing on the shoulders of Hermann Staudinger: Post-polymerization modification from past to present. *J. Polym. Sci., Part A: Polym. Chem.* **2013,** *51* (1), 1-28.

135. Theato, P.; Klok, H.-A., *Functional Polymers by Post-Polymerization Modification; Concepts, Guidelines, and Applications*. 1 ed.; Wiley-VCH: Weinheim, 2012.
136. Gauthier, M. A.; Gibson, M. I.; Klok, H.-A., Synthesis of Functional Polymers by Post-Polymerization Modification. *Angew. Chem. Int. Ed.* **2009,** *48* (1), 48-58.
137. Seyednejad, H.; Ghassemi, A. H.; van Nostrum, C. F.; Vermonden, T.; Hennink, W. E., Functional aliphatic polyesters for biomedical and pharmaceutical applications. *J. Controlled Release* **2011,** *152* (1), 168-176.
138. Bezdushna, E.; Ritter, H.; Troev, K., Microwave-assisted single-step synthesis of poly(alkylene hydrogen phosphonate)s by transesterification of dimethyl hydrogen phosphonate with poly(ethylene glycol). *Macromol. Rapid Commun.* **2005,** *26* (6), 471-476.
139. Pretula, J.; Kaluzynski, K.; Wisniewski, B.; Szymanski, R.; Loontjens, T.; Penczek, S., Formation of poly(ethylene phosphates) in polycondensation of H3PO4 with ethylene glycol. Kinetic and mechanistic study. *J. Polym. Sci. Pol. Chem.* **2008,** *46* (3), 830-843.
140. Pretula, J.; Kaluzynski, K.; Wisniewski, B.; Szymanski, R.; Loontjen, T.; Penczek, S., H3PO4 in a direct synthesis of oligo-poly(ethylene phosphate) from ethylene glycol. *J. Polym. Sci. Pol. Chem.* **2006,** *44* (7), 2358-2362.
141. Iwasaki, Y.; Yamaguchi, E., Synthesis of Well-Defined Thermoresponsive Polyphosphoester Macroinitiators Using Organocatalysts. *Macromolecules* **2010,** *43* (6), 2664-2666.
142. Zhang, S.; Zou, J.; Elsabahy, M.; Karwa, A.; Li, A.; Moore, D. A.; Dorshow, R. B.; Wooley, K. L., Poly(ethylene oxide)-block-polyphosphester-based paclitaxel conjugates as a platform for ultra-high paclitaxel-loaded multifunctional nanoparticles. *Chemical Science* **2013**.
143. Zhang, S.; Zou, J.; Zhang, F.; Elsabahy, M.; Felder, S. E.; Zhu, J.; Pochan, D. J.; Wooley, K. L., Rapid and Versatile Construction of Diverse and Functional Nanostructures Derived from a Polyphosphoester-Based Biomimetic Block Copolymer System. *J. Am. Chem. Soc.* **2012,** *134* (44), 18467-18474.
144. Zhang, S.; Li, A.; Zou, J.; Lin, L. Y.; Wooley, K. L., Facile Synthesis of Clickable, Water-Soluble, and Degradable Polyphosphoesters. *ACS Macro Letters* **2012,** *1* (2), 328-333.
145. Lim, Y. H.; Heo, G. S.; Rezenom, Y. H.; Pollack, S.; Raymond, J. E.; Elsabahy, M.; Wooley, K. L., Development of a Vinyl Ether-Functionalized Polyphosphoester as a Template for Multiple Postpolymerization Conjugation Chemistries and Study of Core Degradable Polymeric Nanoparticles. *Macromolecules* **2014,** *47* (14), 4634-4644.
146. Troev, K. D.; Troev, K. D., *Poly(alkylene H-phosphonate)s*. Elsevier Science Bv: Amsterdam, 2012; p 1-127.
147. Mitova, V.; Slavcheva, S.; Shestakova, P.; Momekova, D.; Stoyanov, N.; Momekov, G.; Troev, K.; Koseva, N., Polyphosphoester conjugates of dinuclear platinum complex: Synthesis and evaluation of cytotoxic and the proapoptotic activity. *Eur. J. Med. Chem.* **2014,** *72*, 127-136.
148. Castner, K. F.; Calderon, N., Ring-opening polymerization of cyclic olefins substituted with polar groups. 5-Norbornene-2,3-dicarboxy anhydride (CPD-MA). *J. Mol. Catal.* **1982,** *15* (1–2), 47-59.
149. Tallon, M. A.; Rogan, Y.; Marie, B.; Clark, R.; Musa, O. M.; Khosravi, E., Monomer sequencing and microstructural analysis on polymers of dimethyl norbornene dicarboxylate and 7-oxanorbornene dicarboxylic derivatives employing ruthenium catalysts by ring-opening metathesis polymerization. *J. Polym. Sci., Part A: Polym. Chem.* **2014,** *52* (17), 2477-2501.
150. Grela, K., *Olefin Metathesis: Theory and Practice*. Wiley: 2014; p 608.
151. Tonhauser, C.; Alkan, A.; Schömer, M.; Dingels, C.; Ritz, S.; Mailänder, V.; Frey, H.; Wurm, F. R., Ferrocenyl Glycidyl Ether: A Versatile Ferrocene Monomer for Copolymerization with Ethylene Oxide to Water-Soluble, Thermoresponsive Copolymers. *Macromolecules* **2013,** *46* (3), 647-655.
152. Maynard, H. D.; Grubbs, R. H., Purification technique for the removal of ruthenium from olefin metathesis reaction products. *Tetrahedron Lett.* **1999,** *40* (22), 4137-4140.

153. Marsico, F.; Wagner, M.; Landfester, K.; Wurm, F. R., Unsaturated Polyphosphoesters via Acyclic Diene Metathesis Polymerization. *Macromolecules* **2012,** *45* (21), 8511-8518.
154. Mutlu, H.; de Espinosa, L. M.; Meier, M. A. R., Acyclic diene metathesis: a versatile tool for the construction of defined polymer architectures. *Chem. Soc. Rev.* **2011,** *40* (3), 1404-1445.
155. Thomas, A.; Niederer, K.; Wurm, F.; Frey, H., Combining oxyanionic polymerization and click-chemistry: a general strategy for the synthesis of polyether polyol macromonomers. *Polymer Chemistry* **2014,** *5* (3), 899-909.
156. Allcock, H. R.; Kugel, R. L., Synthesis of High Polymeric Alkoxy- and Aryloxyphosphonitriles. *Journal of the American Chemical Society* **1965,** *87* (18), 4216-4217.
157. Allcock, H. R., Generation of structural diversity in polyphosphazenes. *Appl. Organomet. Chem.* **2013,** *27* (11), 620-629.
158. Täuber, K.; Marsico, F.; Wurm, F. R.; Schartel, B., Hyperbranched poly(phosphoester)s as flame retardants for technical and high performance polymers. *Polym. Chem.* **2014,** *5* (24), 7042-7053.
159. Liu, J.; Huang, W.; Pang, Y.; Zhu, X.; Zhou, Y.; Yan, D., Hyperbranched Polyphosphates for Drug Delivery Application: Design, Synthesis, and In Vitro Evaluation. *Biomacromolecules* **2010,** *11* (6), 1564-1570.
160. Hagnauer, G. L., Polydichlorophosphazene Polymerization Studies. *Journal of Macromolecular Science: Part A - Chemistry* **1981,** *16* (1), 385-408.
161. Potin, P.; De Jaeger, R., Polyphosphazenes: Synthesis, structures, properties, applications. *Eur. Polym. J.* **1991,** *27* (4–5), 341-348.
162. Neilson, R. H.; Wisian-Neilson, P., Poly(alkyl/arylphosphazenes) and their precursors. *Chem. Rev.* **1988,** *88* (3), 541-562.
163. Steinbach, T.; Wurm, F. R., Poly(phosphoester)s: A new platform for degradable polymers. *Angew. Chem. Int. Ed.* **2015,** *54*, 6098-6108.
164. Marsico, F.; Wagner, M.; Landfester, K.; Wurm, F. R., Unsaturated Polyphosphoesters via Acyclic Diene Metathesis. *Macromolecules* **2012,** *45* (21), 8511-8518.
165. Steinbach, T.; Alexandrino, E. M.; Wurm, F. R., Unsaturated poly(phosphoester)s via ring-opening metathesis polymerization. *Polym. Chem.* **2013,** *4*, 3800-3806.
166. Tauber, K.; Marsico, F.; Wurm, F. R.; Schartel, B., Hyperbranched poly(phosphoester)s as flame retardants for technical and high performance polymers. *Polymer Chemistry* **2014,** *5* (24), 7042-7053.
167. Shaw, S. D.; Blum, A.; Weber, R.; Kannan, K.; Rich, D.; Lucas, D.; Koshland, C. P.; Dobraca, D.; Hanson, S.; Birnbaum, L. S., Halogenated flame retardants: Do the fire safety benefits justify the risks? *Reviews on Environmental Health* **2010,** *25* (4), 261-305.
168. Chen, Y.; Li, J.; Liu, L.; Zhao, N., Polybrominated diphenyl ethers fate in China: A review with an emphasis on environmental contamination levels, human exposure and regulation. *Journal of Environmental Management* **2012,** *113*, 22-30.
169. Klinkowski, C.; Wagner, S.; Ciesielski, M.; Döring, M., Bridged phosphorylated diamines: Synthesis, thermal stability and flame retarding properties in epoxy resins. *Polym. Degrad. Stab.* **2014,** *106*, 122-128.
170. W, Z.; Y, L.; C, H.; W, C.; J, H.; L, Z.; W, Y.; Y, W., Hyperiid amphipod communities and the seasonal distribution of water masses in eastern Beibu Gulf, South China Sea. *Aquatic Biology* **2014,** *20* (3), 209-217.
171. Li, H.; Fahrenbach, A. C.; Coskun, A.; Zhu, Z.; Barin, G.; Zhao, Y.-L.; Botros, Y. Y.; Sauvage, J.-P.; Stoddart, J. F., A Light-Stimulated Molecular Switch Driven by Radical–Radical Interactions in Water. *Angew. Chem. Int. Ed.* **2011,** *50* (30), 6782-6788.
172. Tsai, S.-C.; Fu, Y.-S.; Liao, J.-H.; Yu, S. J., Versatile and Efficient Synthesis of a New Class of Aza-Based Phosphinic Amide Ligands via Unusual P□C Cleavage. *Helv. Chim. Acta* **2006,** *89* (12), 3007-3017.

173. Wallace, K. J.; Hanes, R.; Anslyn, E.; Morey, J.; Kilway, K. V.; Siegel, J., Preparation of 1,3,5-Tris(aminomethyl)-2,4,6-triethylbenzene from Two Versatile 1,3,5-Tri(halosubstituted) 2,4,6-Triethylbenzene Derivatives. *Synthesis* **2005,** *2005* (12), 2080-2083.
174. Yoshino, T.; Imori, S.; Togo, H., Efficient esterification of carboxylic acids and phosphonic acids with trialkyl orthoacetate in ionic liquid. *Tetrahedron* **2006,** *62* (6), 1309-1317.
175. Steinmann, M.; Marsico, F.; Wurm, F., Reactive poly(phosphoester)-telechelics. *J Polym Res* **2015,** *22* (7), 1-9.
176. Li, W.; Chung, H.; Daeffler, C.; Johnson, J. A.; Grubbs, R. H., Application of 1H DOSY for Facile Measurement of Polymer Molecular Weights. *Macromolecules* **2012,** *45* (24), 9595-9603.
177. Yu, Y.; Fu, S.; Song, P. a.; Luo, X.; Jin, Y.; Lu, F.; Wu, Q.; Ye, J., Functionalized lignin by grafting phosphorus-nitrogen improves the thermal stability and flame retardancy of polypropylene. *Polym. Degrad. Stab.* **2012,** *97* (4), 541-546.
178. Ma, H.; Wang, J.; Fang, Z., Cross-linking of a novel reactive polymeric intumescent flame retardant to ABS copolymer and its flame retardancy properties. *Polym. Degrad. Stab.* **2012,** *97* (9), 1596-1605.
179. Glasoe, P. K.; Long, F. A., USE OF GLASS ELECTRODES TO MEASURE ACIDITIES IN DEUTERIUM OXIDE1,2. *The Journal of Physical Chemistry* **1960,** *64* (1), 188-190.
180. Wang, Y.-C.; Tang, L.-Y.; Sun, T.-M.; Li, C.-H.; Xiong, M.-H.; Wang, J., Self-Assembled Micelles of Biodegradable Triblock Copolymers Based on Poly(ethyl ethylene phosphate) and Poly(ϵ-caprolactone) as Drug Carriers. *Biomacromolecules* **2008,** *9* (1), 388-395.
181. Stejskal, E. O.; Tanner, J. E., Spin Diffusion Measurements: Spin Echoes in the Presence of a Time-Dependent Field Gradient. *The Journal of Chemical Physics* **1965,** *42* (1), 288-292.
182. Jerschow, A.; Müller, N., 3D Diffusion-Ordered TOCSY for Slowly Diffusing Molecules. *Journal of Magnetic Resonance, Series A* **1996,** *123* (2), 222-225.
183. Z, G. R.; L, N. M., Phosphinic amides. Google Patents: 1967.
184. Singh, R.; Gautam, N.; Mishra, A.; Gupta, R., Heavy metals and living systems: An overview. *Indian Journal of Pharmacology* **2011,** *43* (3), 246-253.
185. Chao, P.; Li, Y.; Gu, X.; Han, D.; Jia, X.; Wang, M.; Zhou, T.; Wang, T., Novel phosphorus-nitrogen-silicon flame retardants and their application in cycloaliphatic epoxy systems. *Polymer Chemistry* **2015,** *6* (15), 2977-2985.
186. Nguyen, C.; Kim, J., Synthesis of a novel nitrogen-phosphorus flame retardant based on phosphoramidate and its application to PC, PBT, EVA, and ABS. *Macromol. Res.* **2008,** *16* (7), 620-625.
187. Edwards, B.; Rudolf, S.; Hauser, P.; El-Shafei, A., Preparation, Polymerization, and Performance Evaluation of Halogen-Free Radiation Curable Flame Retardant Monomers for Cotton Substrates. *Industrial & Engineering Chemistry Research* **2015,** *54* (2), 577-584.
188. Xiang, D. F.; Bigley, A. N.; Ren, Z.; Xue, H.; Hull, K. G.; Romo, D.; Raushel, F. M., Interrogation of the Substrate Profile and Catalytic Properties of the Phosphotriesterase from Sphingobium sp. Strain TCM1: An Enzyme Capable of Hydrolyzing Organophosphate Flame Retardants and Plasticizers. *Biochemistry* **2015,** *54* (51), 7539-7549.
189. European Food Safety, A., Conclusion regarding the peer review of the pesticide risk assessment of the active substance cadusafos. *EFSA Journal* **2009,** *7* (5), n/a-n/a.
190. European Food Safety, A., Conclusion regarding the peer review of the pesticide risk assessment of the active substance ethoprophos. *EFSA Journal* **2006,** *4* (4), n/a-n/a.
191. Fukuto, T. R., Mechanism of Action of Organophosphorus and Carbamate Insecticides. *Environ. Health Perspect.* **1990,** *87*, 245-254.
192. Pope, C. N., ORGANOPHOSPHORUS PESTICIDES: DO THEY ALL HAVE THE SAME MECHANISM OF TOXICITY? *Journal of Toxicology and Environmental Health, Part B* **1999,** *2* (2), 161-181.
193. Schwetlick, K., *Organikum Organisch-chemisches Grundpraktikum*. Wiley-VCH: Weinheim, 2015.

194. Damalas, C. A.; Eleftherohorinos, I. G., Pesticide Exposure, Safety Issues, and Risk Assessment Indicators. *International Journal of Environmental Research and Public Health* **2011,** *8* (5), 1402-1419.
195. Betarbet, R.; Sherer, T. B.; MacKenzie, G.; Garcia-Osuna, M.; Panov, A. V.; Greenamyre, J. T., Chronic systemic pesticide exposure reproduces features of Parkinson's disease. *Nat Neurosci* **2000,** *3* (12), 1301-1306.
196. Rosenstock, L.; Keifer, M.; Daniell, W. E.; McConnell, R.; Claypoole, K., Originally published as Volume 2, Issue 8761Chronic central nervous system effects of acute organophosphate pesticide intoxication. *The Lancet* **1991,** *338* (8761), 223-227.
197. Wauchope, R. D., The Pesticide Content of Surface Water Draining from Agricultural Fields—A Review1. *Journal of Environmental Quality* **1978,** *7* (4), 459-472.
198. Wesseling, C.; McConnell, R.; Partanen, T.; Hogstedt, C., Agricultural Pesticide Use in Developing Countries: Health Effects and Research Needs. *International Journal of Health Services* **1997,** *27* (2), 273-308.
199. Ghose, S. L.; Donnelly, M. A.; Kerby, J.; Whitfield, S. M., Acute toxicity tests and meta-analysis identify gaps in tropical ecotoxicology for amphibians. *Environ. Toxicol. Chem.* **2014,** *33* (9), 2114-2119.
200. Verschoyle, R. D.; Cabral, J. R. P., Investigation of the acute toxicity of some trimethyl and triethyl phosphorothioates with particular reference to those causing lung damage. *Arch. Toxicol.* **1982,** *51* (3), 221-231.
201. Gemeinschaften, D. K. d. E. 2007/428/EG. http://eur-lex.europa.eu/eli/dec/2007/428/oj (accessed 03.09.2016).
202. Carta, P.; Puljic, N.; Robert, C.; Dhimane, A.-L.; Ollivier, C.; Fensterbank, L.; Lacôte, E.; Malacria, M., Intramolecular homolytic substitution at the sulfur atom: an alternative way to generate phosphorus- and sulfur-centered radicals. *Tetrahedron* **2008,** *64* (52), 11865-11875.
203. Wang, J.; Zhang, P.; Mao, H.; Leong, K., Enhanced gene expression in mouse muscle by sustained release of plasmid DNA using PPE-EA as a carrier. *Gene therapy* **2002,** *9* (18), 1254-1261.
204. Huang, S.-W. Z., Ren-Xi, Recent Advances in Polyphosphoester and Polyphosphoramidate-Based Biomaterials. *Phosphorus, Sulfur, and Silicon* **2008,** *183*, 340-348.
205. Ikada, Y.; Tsuji, H., Biodegradable polyesters for medical and ecological applications. *Macromolecular Rapid Communications* **2000,** *21* (3), 117-132.
206. Zhao, Z.; Wang, J.; Mao, H.-Q.; Leong, K. W., Polyphosphoesters in drug and gene delivery. *Advanced Drug Delivery Reviews* **2003,** *55* (4), 483-499.
207. Zhang, F.; Smolen, J. A.; Zhang, S.; Li, R.; Shah, P. N.; Cho, S.; Wang, H.; Raymond, J. E.; Cannon, C. L.; Wooley, K. L., Degradable polyphosphoester-based silver-loaded nanoparticles as therapeutics for bacterial lung infections. *Nanoscale* **2015,** *7* (6), 2265-2270.
208. Qiu, J.-J.; Liu, C.-M.; Hu, F.; Guo, X.-D.; Zheng, Q.-X., Synthesis of unsaturated polyphosphoester as a potential injectable tissue engineering scaffold materials. *Journal of Applied Polymer Science* **2006,** *102* (4), 3095-3101.
209. Bauer, K. N.; Tee, H. T.; Lieberwirth, I.; Wurm, F. R., In-Chain Poly(phosphonate)s via Acyclic Diene Metathesis Polycondensation. *Macromolecules* **2016,** *49* (10), 3761-3768.
210. Wolf, T.; Steinbach, T.; Wurm, F. R., A Library of Well-Defined and Water-Soluble Poly(alkyl phosphonate)s with Adjustable Hydrolysis. *Macromolecules* **2015,** *48* 3853–3863.
211. Wang, J.; Gao, S. J.; Zhang, P. C.; Wang, S.; Mao, H. Q.; Leong, K. W., Polyphosphoramidate gene carriers: effect of charge group on gene transfer efficiency. *Gene Ther* **2004,** *11* (12), 1001-1010.
212. Troev, K.; Tsatcheva, I.; Koseva, N.; Georgieva, R.; Gitsov, I., Immobilization of aminothiols on poly(oxyethylene H-phosphonate)s and poly(oxyethylene phosphate)s—An approach to

polymeric protective agents for radiotherapy of cancer. *J. Polym. Sci., Part A: Polym. Chem.* **2007,** *45* (7), 1349-1363.

213. Mitova, V.; Koseva, N.; Troev, K., Study on the Atherton-Todd reaction mechanism. *RSC Advances* **2014,** *4* (110), 64733-64736.
214. Zhang, X.-Q.; Wang, X.-L.; Huang, S.-W.; Zhuo, R.-X.; Liu, Z.-L.; Mao, H.-Q.; Leong, K. W., In Vitro Gene Delivery Using Polyamidoamine Dendrimers with a Trimesyl Core†. *Biomacromolecules* **2005,** *6* (1), 341-350.
215. Jiang, X.; Qu, W.; Pan, D.; Ren, Y.; Williford, J.-M.; Cui, H.; Luijten, E.; Mao, H.-Q., Plasmid-Templated Shape Control of Condensed DNA–Block Copolymer Nanoparticles. *Advanced Materials* **2013,** *25* (2), 227-232.
216. Chang, Y. L.; Wang, Y. Z.; Ban, D. M.; Yang, B.; Zhao, G. M., A novel phosphorus-containing polymer as a highly effective flame retardant. *Macromolecular Materials and Engineering* **2004,** *289* (8), 703-707.
217. Steinbach, T.; Wahlen, C.; Wurm, F. R., Poly(phosphonate)-mediated Horner-Wadsworth-Emmons reactions. *Polymer Chemistry* **2015,** *6* (7), 1192-1202.
218. Low, S. A.; Kopeček, J., Targeting polymer therapeutics to bone. *Adv. Drug Delivery Rev.* **2012,** *64* (12), 1189-1204.
219. Neisius, M.; Liang, S.; Mispreuve, H.; Gaan, S., Phosphoramidate-Containing Flame-Retardant Flexible Polyurethane Foams. *Industrial & Engineering Chemistry Research* **2013,** *52* (29), 9752-9762.
220. Mazarin, M.; Viel, S.; Allard-Breton, B.; Thévand, A.; Charles, L., Use of Pulsed Gradient Spin−Echo NMR as a Tool in MALDI Method Development for Polymer Molecular Weight Determination. *Anal. Chem.* **2006,** *78* (8), 2758-2764.
221. Nguyen, T.-M.; Chang, S.; Condon, B.; Slopek, R.; Graves, E.; Yoshioka-Tarver, M., Structural Effect of Phosphoramidate Derivatives on the Thermal and Flame Retardant Behaviors of Treated Cotton Cellulose. *Ind. Eng. Chem. Res.* **2013,** *52* (13), 4715-4724.
222. Qiu, W.; Sworen, J.; Pyda, M.; Nowak-Pyda, E.; Habenschuss, A.; Wagener, K. B.; Wunderlich, B., Effect of the Precise Branching of Polyethylene at Each 21st CH2 Group on Its Phase Transitions, Crystal Structure, and Morphology. *Macromolecules* **2006,** *39* (1), 204-217.
223. Zheng, Y. R.; Tee, H. T.; Wei, Y.; Wu, X. L.; Mezger, M.; Yan, S.; Landfester, K.; Wagener, K.; Wurm, F. R.; Lieberwirth, I., Morphology and Thermal Properties of Precision Polymers: The Crystallization of Butyl Branched Polyethylene and Polyphosphoesters. *Macromolecules* **2016,** *49* (4), 1321-1330.
224. Kirby, A. J.; Younas, M., The reactivity of phosphate esters. Diester hydrolysis. *Journal of the Chemical Society B: Physical Organic* **1970,** (0), 510-513.